DEVELOPMENT AND APPLICATION OF IMPRINTED POLYMERS FOR SELECTIVE ADSORPTION OF METAL IONS AND FLAVONOLS IN COMPLEX SAMPLES

Vusumzi Emmanuel Pakade

A Thesis submitted to the Faculty of Science, University of the Witwatersrand, Johannesburg, in fulfilment of the requirements for the degree of Doctor of Philosophy

MAY 2012

DECLARATION

I declare that this Thesis is my own, unaided work. It is being submitted for the Degree of Doctor of Philosophy at the University of the Witwatersrand, Johannesburg. It has not been submitted before for any degree or examination at any other University.

(Signature of Candidate)

----------10th----------Day of--------MAY----------2012

Supervisor:

Prof Luke Chimuka (WITS, School of Chemistry)

Co-supervisor:

Prof Ewa Cukrowska (WITS, School of Chemistry)

ABSTRACT

Presence of heavy metals in the environment is a worldwide known contamination problem. Depending on their chemistries and level of contamination, these heavy metals can have severe effects on the ecosystem, aquatic life and eventually humans. Researchers have been particularly interested in finding methods for the removal of these pollutants from the environment. Several methods have been proposed and some have been used with some degree of success. Methods used for trace metal removal include, chemical precipitation, chemical reduction, solvent extraction, micellar ultrafiltration, organic and inorganic ion exchange, adsorption processes, *etc*. However, the matrix in which these heavy metals are present in is sometimes very complex and some of these heavy metals are present in the environment at very low concentrations, say ppb levels. However, they can have adverse effects even at such low-level concentrations. The above-mentioned methods usually suffer from the effects of the matrix and by-products produced after treatment such as sludge in the case of precipitation. Hence, in this study molecularly imprinted polymers (MIPs) were used. MIPs are highly cross-linked polymers prepared with the presence of template molecule. Once the template has been removed it leaves behind a cavity that can only fit the template, hence MIPs are very selective for the template molecule. Metals of interest in this study were uranium (VI) and chromium (VI). Therefore, two separate imprinted polymers were prepared using chromium and uranium as template molecules for selective extraction of these oxy-ions from aqueous samples. Beside removal of heavy metals, the study also focussed on developing MIPs for selective recovery of high value compounds from plant materials (onion and *Moringa oleifera*).

Three separate imprinted polymers using chromium, uranium or quercetin templates were prepared by bulk polymerization method. Functional monomers used were 4-vinylpyridine; 1-(prop-2-en-1-yl)-4-(pyridin-2-ylmethyl)piperazine (PPMP) and methacrylic acid; and 4-vinylpyridine for chromium, uranium and quercetin imprinted polymers, respectively. For all imprinted polymers, ethylene glycol dimethacrylate (EDMA) and 1,1’-azobis(cyclohexanecarbonitrile) (ACCN)

were used as the cross-linking monomer and initiator, respectively. Control polymers (CP) or non-imprinted polymers (NIP) for each imprinted polymer were prepared and treated exactly the same as imprinted polymers but with omission of respective templates. Following removal of respective templates with appropriate solutions, various parameters that affect selective adsorption such as solution pH, initial concentration, aqueous phase volume, sorbent dosage, contact time, breakthrough volumes etc., were optimized to get optimal adsorption of the imprinted polymers.

Optimal parameters for Cr (VI) adsorption were as follows: solution pH, 3; contact time, 120 min; eluent, 20 mL of 0.1 M NaOH; and sorbent amount, 125 mg. Maximum retention capacity of IIP and CP was 37.58 and 25.44 mg g^{-1}, respectively. The observed selectivity order was as follows, Cr (VI) > SO_4^{2-} > F^- > PO_4^{3-} > NO_2^- > NO_3^- > Cl^-. However, in the presence of high concentrations of sulphate ions, the selectivity on the CP completely collapsed. For uranium VI removal, the optimal pH was 4.0-8.0, sorbent amount was 20 mg, contact time was 20 min and the retention capacity was 120 mg of uranyl ion per g of IIP. The selectivity order observed was as follows, UO_2^{2+} > Fe^{3+} >> Cu^{2+} > Co^{2+} > Mn^{2+} > Zn^{2+} ~ Ni^{2+}.

The binding capacity of quercetin MIPs was investigated at 25 and 84°C, respectively, in batch mode. The slopes for the effect of extraction time revealed that the mass transfer of the analytes was higher at 84°C than at 25°C. Also, the binding capacity for the most promising MIP and its corresponding NIP increased at 84°C but the MIP had higher binding capacity. The increase in binding capacity for the MIP was from ~30 µmol g^{-1} at 25°C to ~120 µmol g^{-1} at 84°C. For the corresponding NIP, the binding capacity values were ~15 and ~90 µmol g^{-1}, at 25 and 84°C, respectively. A demonstration of MIP selectivity at higher temperature using standard solutions of selected flavonols showed that the MIP still retained its selectivity for quercetin. Similar selectivity was observed when preliminary application studies on aqueous yellow onion extracts were investigated. The study clearly demonstrated the suitability of the developed imprinted polymers (for

chromium, uranium and quercetin) for selective adsorption of Cr (VI), UO_2^{2+} and quercetin from their respective complex matrices.

Breakthrough volume of molecular imprinted polymer solid-phase extraction (MISPE) was investigated using a mixture of myricetin, quercetin and kaempferol. The breakthrough volumes for quercetin, kaempferol and myricetin were 22, 27 and 8 mL, respectively. The number of theoretical plates (*N*) for the MISPE column corresponding to these volumes were 18, 47 and 4 for quercetin, kaempferol and myricetin, respectively. Using these results, selectivity of MIP and its retention capacity was evaluated. The extractions of *Moringa* leaves and flowers were carried out using a MISPE cartridge and various solvents were investigated for the selective elution of quercetin from the MIP sorbents. For identification and quantification of quercetin and other flavonols, a high performance liquid chromatography (HPLC) was used. Recoveries of quercetin from different *Moringa* extracts ranged from 87 – 92% and this demonstrated that the MISPE method can be used for the recovery of quercetin and kaempferol from the *Moringa* extracts. Amount of quercetin found in *Moringa* leaves was 1555 mg kg^{-1}.

All the imprinted and non-imprinted polymers prepared in the study were characterized with Fourier Transform Infrared (FTIR) spectroscopy. Scanning electron microscopy (SEM) was used for recording surface morphology of all the polymers. Surface area and pore size analysis were recorded on Micromeritic Tristar BET. For quercetin MIP, thermogravimetric analysis (TGA) was also used in addition to the mentioned techniques.

In additional studies, the concentrations of metals in the soil and, in the leaves and flowers of *Moringa* plant grown in South Africa were examined. The investigation included heavy metals, major and trace nutrient elements. The analysis of metals was achieved after total digestion of soils or leaves using a microwave, and the concentrations of metals were determined using inductively coupled plasma-optical emission spectroscopy (ICP-OES). These results were

compared to those obtained from some selected vegetables like spinach, cabbage, cauliflower, broccoli, and peas. No toxic heavy metals were detected in the leaves and flowers of *Moringa*. On average *Moringa* contained higher concentration of Ca (18500 mg kg^{-1}) and Mg (5500 mg kg^{-1}) than other vegetables compared with in the study. Other major nutrients contained in *Moringa* were much similar to other vegetables. Besides metals, the concentrations of flavonols (myricetin, quercetin, kaempferol) determined from *Moringa* leaves and flowers were also compared to selected vegetables. Plant and vegetable materials were extracted under reflux using acidified methanol (1% HCl) solution. Following which, the flavonols were identified and quantified using reverse phased-high performance liquid chromatography method equipped with UV detection. *Moringa* leaves exhibited highest concentrations of myricetin (1296.6 mg kg^{-1}), quercetin (1362.6 mg kg^{-1}), kaempferol (1933.7 mg kg^{-1}) than vegetables (spinach: myricetin 620.0 mg kg^{-1}, quercetin 17.9 mg kg^{-1}, kaempferol 215.3 mg kg^{-1}).

Lastly, the antioxidant activity of *Moringa* flowers and leaves were compared to that of the aforementioned selected vegetables. The antioxidant activity was studies by analyzing the total phenolic content (TPC), total flavonoid content (TFC), reducing power, radical scavenging activity, and the 2,2-diphenyl-1-picrylhydrazyl free radical (DPPH) method. Moring contained almost twice the TPC and thrice the TFC than the vegetables. Also, *Moringa* demonstrated higher reducing power and lower percentage of free radicals remaining (DPPH method). Hence, *Moringa* showed to be a good antioxidant source than the selected vegetables compared with.

To my grandmother

Nomatshaka Pakade

and my mother

Nomkhitha Pakade

ACKNOWLEDGEMENTS

Foremost, I'm deeply grateful to my supervisors Prof. L. Chimuka and Prof. E. Cukrowska for their continued encouragement, guidance and support throughout this project. Without you this project wouldn't have been possible. I feel both honoured and privileged to have worked under your supervision. I also want to acknowledge Dr. H. Tutu for his insightful discussions and professional guidance.

I am indebted to Prof. C. Turner and Dr. B. Vrana for their inspiration and support during the time I spent in Sweden and Slovakia, respectively. To Green Tech Group, of Sofia, Irene, Jaing, Abdol, and Aruwah, you made my time in Lund very special, thank you. Peter and the crew in Bratislava, you were also great. Also, I would like to acknowledge my fellow colleagues of the Environmental Analytical Chemistry Research Group who have contributed immensely to my personal and professional time at Wits University: N. Tavengwa, P. Sibiya, R. Lokhothwayo, J. G. Lusilao, E. Bakatula, T. Mabaso, Y. Asiedu, D. Saad, T. Mavunganidze, R. Amdany, B. Yalala, and A. Sharifi. Not forgetting my former colleague H. Nyoni as well as T. Phadi for the BET samples, thank you guys.

Last but not least, the financial support of National Research Foundation Scarce Skills and Equity, NRF grant holder linked, the Bradlow Foundation Award, the Swedish Foundation for International Cooperation in Research and Higher Education (STINT, YR2009-7015) for sponsoring my visit to Sweden, and Water Research Commission for financing author's visit to Slovakia are all gratefully appreciated.

Lest I forget the ONE who makes all things possible....the Almighty God.

TABLE OF CONTENTS

LIST OF FIGURES

LIST OF TABLES

LIST OF ABREVIATIONS

% RSD	Percentage relative standard deviation
AA	Acrylic acid
AAm	Acrylamide
ACCN	1,1'-Azobis(cyclohexane carbonitrile)
AIBN	2,2'-Azobis(2-isobutyronitrile)
C_{18}	Octadecylsilane-bonded silica
CRM	Certified reference material
Cr (VI)	Chromium VI
CP	Control polymers
DEAEM	2 2-(diethylamino) ethyl methacrylate
DLLME	Dispersive liquid–liquid microextraction
DVB	Divinylbenzene
ECD	Electron capture detector
EDMA	Ethylene glycol dimethacrylate
ELM	Emulsion liquid membrane
EPA	Environmental Protection Agency
FID	Flame ionisation detector
FI–ICPMS	Injection–inductively coupled plasma mass spectrometry
FT-IR	Fourier Transform InfraRed
GC	Gas chromatograph
HEMA	2-Hydroxyethyl methacrylate
HPLC	High performance liquid chromatograph
HPLC-DAD-MSn/ESI	Liquid chromatography-tandem mass spectrometry
HPLC–ESI-QTOF	Liquid chromatography/electrospray ionisation-time of flight-mass spectrometry
HPTLC	High performance thin layer chromatography
IC	Ion chromatograph
IIP	Ion imprinted polymers
ILs	Ionic liquids
LC	Liquid Chromatography

LC–MS	Liquid Chromatography–Mass Spectrometry
LLE	Liquid liquid extraction
LPME	Liquid phase microextraction
MAA	Methacrylic acid
MAAm	Methacrylamide
MAE	Microwave assisted extraction
MEMO	γ-methacryloxypropyltrimethoxysilane
MHG	Microwave hydrodiffusion and gravity extraction
MIPs	Molecularly imprinted polymers
MISPE	Molecularly imprinted solid phase extraction
MSPD	Matrix solid phase dispersion
M1, M2,	Quercetin imprinted polymers
M3, M4	Quercetin imprinted polymers
NIP	Non-imprinted polymer
N1 & N2	Quercetin non-imprinted polymers
PDMS	Polydimethylsiloxane
PLE	Pressurised liquid extraction
PMME	Polymer monolith microextraction
PP	Precipitation polymerization
PSFME	Pressurised solvent-free microwave assisted extraction
P1, P2	Chromium ion imprinted polymer
P3	Chromium ion non-imprinted polymer
P4	Uranium ion-imprinted polymer
P5	Uranium non-imprinted polymer
RAM	Restricted access membrane
SBSE	Stir bar sorptive extraction
SFE	Supercritical water extraction
SLE	Solid–liquid extraction
SPE	Solid phase extraction
SPMD	Semi-permeable membrane devices
SPME	Solid phase microextraction

SWE	Subcritical water extraction
TEOS	Tetraethoxysilane
TRIM	Trimethylopropane
TP	Bulk polymerization
USE	Ultrasonic extraction
UV	Ultra violet
U (VI)	Uranium VI
VP	Vinylpyridine

The Thesis consists of 7 Chapters. Chapters 1 to 5 form the basis of the study where the emphasis was on production and use of molecularly imprinted polymers for selective extraction of chromium, uranium, and quercetin from different complex matrices. Chapter 6 deals with some additional work on *Moringa* plant and in this section, no imprinted polymers were used. Chapter 7 gives detailed conclusion remarks that cover Chapter 1 to 6, and the references are cited in alphabetical order.

Chapter 1: Introduction

1.1. The focus of study

The following study focuses on development of MIPs for three target compounds, chromium VI, uranium VI, and quercetin (3,3',4',5,7-pentahydroxylflavone). The MIPs for each of the three mentioned target compounds were used for different purposes. For example, chromium VI and uranium VI are toxic whereas quercetin is a high value antioxidant organic compound. Therefore, MIPs were used for toxic metal removal as well as for the recovery of high value compounds from plant waste material. Non-covalent imprinting technique was used to generate MIPs for the three specified compounds.

1.1.1. Background on chromium

Chromium, a hard metal, was first discovered from Crocoite pigment in 1797 by Louis Nicolas Vauquelin and latter found in mineral chromite (Britannica encyclopaedia). Industries such as electroplating, mining operations, leather tanning, metal plating, water cooling, and pigment manufacturing are the main sources where chromium is used (Katz and Salem, 1994). Unfortunately, this use introduces chromium into the environment where it can have detrimental effects depending on the state in which it is present. Chromium can exist in several oxidation states ranging from -2 to +6 depending on the pH and oxidative properties of the location, the trivalent and the hexavalent are the most predominant states (Goyal et al., 2003). Chromium in the +6 oxidation state is regarded as a genotoxic, mutagenic and carcinogen to humans and ecosystem (Chakraborty and Kumar, 2009) due to its solubility, mobility which is 500 times (Sarin and Pant, 2006) and a toxicity 100 times more than that of Cr (III) (Unnithan et al., 2001). Furthermore, Cr (VI) is declared as Group one carcinogenic (meaning that it can cause cancer) by EPA (US EPA, 1999), while Cr (III) is known to be important for mammalian functions as it helps to maintain

glucose, lipid and protein metabolism (Ramnani and Sabharwal, 2006). Due to its toxicity, hexavalent chromium has to be regulated by strict regulations and as such the maximum permissible levels set out by US EPA in both drinking water and wastewater are 0.05 mg L^{-1} for Cr (VI), and 5 mg L^{-1} of Cr (III), respectively (Acar and Malkoc, 2004). Furthermore, the hexavalent chromium Cr (VI), can exist in most aquatic environments as water soluble oxyanions, $HCrO_4^{1-}$ or CrO_4^{2-} depending on pH and concentration. Pulmonary congestions, liver damage, vomiting, and severe diarrhea are some of the known health problems associated with Cr (VI) (Raji and Anirudhan, 1998).

1.1.2. Background on uranium

Uranium is a weakly radioactive toxic metal with three natural isotopes ^{238}U, ^{235}U and ^{234}U belonging to the actinide series and was discovered in 1789 by German Chemist Martin Heinarich Klaproth (www.epa.gov/radiation/radionuclides/uranium.html). The ^{238}U isotope is the most abundant (99%) in nature. Uranium, particularly ^{235}U, is used in military sector as high density penetrators and in the civilian sector to fuel nuclear power plants (www.epa.gov/radiation/radionuclides/uranium.html) and it is through these usage, as well as seepages from mining, that the metal can end up in the environment where it can have undesirable effects human and the ecosystem. Similar to chromium, uranium can exist in several oxidation states, ranging from +2 to +6, depending on pH, concentration and the presence of carbonates (Pavel et al., 2009; Langmuir, 1978; Mason et al., 1997).

Uranium VI is the most toxic form of uranium. Uranium (VI) is a ‘hard” Lewis acid meaning it is capable of forming strong complexes with with “hard” Lewis bases such as chlorides, inorganic oxygen donor ligands like sulphates, nitrates, carbonates and phosphates as well as organic ligands such as amines and amides (Diallo et al., 2008). Uranium is a pollutant capable of causing irreversible renal injuries or even death if consumed at high concentrations. Due to its radioactivity, uranium can cause bone cancer, liver cancer and leukaemia if swallowed, however, when inhaled in high concentrations can increase risk to lung cancer (www.epa.gov/radiation/radionuclides/uranium.html). Due to toxicity of uranium

in the environment, regulations were set. US EPA set tolerance level of 30 μg L^{-1} of this contaminant in drinking water (Anirudhan et al., 2009) whereas the WHO, Health Canada and Australian drinking water guidelines have set 20 μg L^{-1} as the maximum allowable concentration of uranium in drinking water (Gilman et al., 1998; WHO, 1998). The uranyl ion (UO_2^{2+}), where uranium is in +6 oxidation state, is the most toxic of the uranium species. Both groundwater and surface water can be polluted by uranium that is seeped from the mining and milling leachates as well as from the normal run-off associated with mining sites (www.pembina.org/pub/1503).

1.1.3. Background on quercetin

Quercetin, a polyphenol aglycone from the flavone family, has been regarded to possess anti-inflammatory and antioxidant properties of the flavone family, and is present in vegetables and fruits, such as onions, apples and grapes in low amounts (Hollman and Arts, 2001; Davis et al., 2009). Besides antioxidant properties, quercetin possesses some antitumor and antiviral properties as well as aiding in adjusting the immune system (Russo et al., 2000). In fruits and vegetables, quercetin is present as glycosides, where glucose and rhamnose are two most common sugar groups (Biesaga and Pyrznska, 2009). Hence, adequate dietary intake of vegetables and fruits may reduce the risk of cancer (US, Food and Drug Administration). In some other plants like citrus fruits and buckwheat, quercetin might exist as glycosides such as rutin and quercitrin. However, in yellow onion, quercetin-3,4´-diglucoside and quercetin-4´-glucoside are the main abundant glucosides (Biesaga and Pyrznska, 2009). Nonetheless, the aglycone and other quercetin glucosides are also present but in lower concentrations. Quercetin can be extracted from onion using a solid-liquid extraction with aqueous methanol which normally involves the use of high concentrations of HCl to catalyze the hydrolysis of glucosides to aglycones (Price and Rhodes, 1997; Nuutila et al., 2002). However, a more sustainable alternative method to methanol-HCl extraction has been proposed and it involves the use of pressurised hot water as solvent and the hydrolysis is enzyme catalyzed (Turner et al., 2006; Lindahl et al.,

2010). Contrary to uranium and chromium, quercetin is classified by International Agency for Research on Cancer (IARC) as Group 3, meaning no evidence of carcinogenicity has been associated with quercetin.

1.2. The technique of molecular imprinting

The technique of molecular imprinting dates back to 1931 when the first imprinted polymer for benzene was prepared by M V Polyakov (Alexander et al., 2003). This technique involves fabrication of polymer material with specific recognition sites for the target analyte, *i.e*., mimicking the enzyme-receptor principle (Alexander et al., 2003). One of the advantages of the molecularly imprinted polymers is that, they can be easily prepared by polymerization of functional monomers with cross-linking agent and a template molecule (target) in a one-pot synthesis. Highly cross-linked three-dimensional network polymer is achieved. After polymerization, the template molecule is removed leaving behind binding sites with shape, size and functionalities complementary to the target analyte (Tamayo et al., 2007).

Molecularly imprinted polymers (MIPs) have already been used in a broad range of applications from structural studies of ligand-receptor interactions to selective binding-matrices in detection, separation, and purification (Mosbach, 1994; Andersson et al., 1995a). The ability of MIPs to selectively bind the target analyte is based on the theory that after removal of the template molecule the interactions between complementary functionalities present in the imprint molecule and the monomer(s) prior to the initiation of polymerization are conserved in the product polymer (Sieman et al., 1996). The general scheme showing how the imprinting technique is fabricated is illustrated below, Figure 1.1. Although bulk polymerization that usually involve radical polymerization has been the most widely used approach but several other approaches such as suspension and precipitation have also enjoyed wide use.

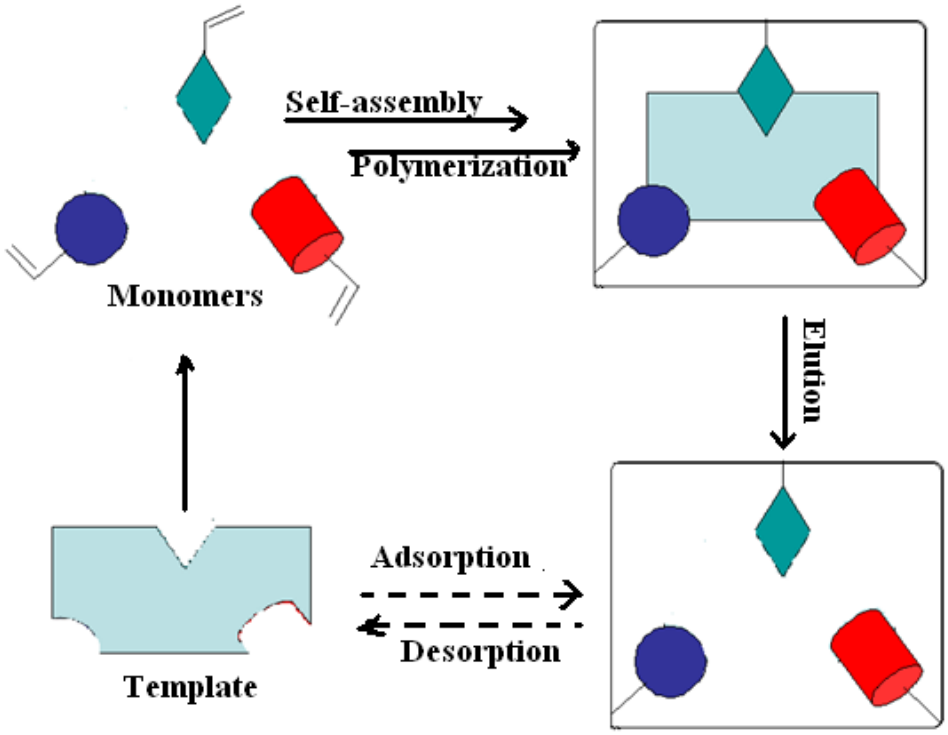

Figure 1.1: Principle of preparation of MIPs.

1.3. Different polymerization methods

The scope of the MIPs allows different polymerization techniques such as suspension, emulsion, seed polymerization to be used depending on the desired perceived outcome of particle size and shape. In this study two polymerization methods were used, *i.e.*, bulk and precipitation polymerization. The polymer fabrication for bulk and precipitation methods is the same except that in precipitation almost 10 times the volume of solvent/ porogen is used compared to bulk polymerization. Due to the fact that the polymer is neither soluble in its monomer or monomer-solvent combination as a result the polymer precipitates as small particles in the solvent rather than forming bulk monoliths which will require crushing and sieving to bring to particular desirable particle size. This is the advantage of the precipitation method over bulk. Advantage of precipitation over suspension polymerization is that precipitation involves no addition of stabilizers or surfactants as this interfere with the interaction of monomer and template. However, the particle size produced by precipitation can be

polydesperse although some authors claim that fine tuning is possible to achieve monodisperse polymer particle size (Takekoh et al., 2006; Croll et al., 2005).

1.4. Plant materials (Onions and *Moringa oleifera*)

In plants parts such as leaves, quercetin occurs mainly as aglycones and glycosides. Glucose, galactose and rhamnose are the most common sugar groups usually attached to phenolic groups by glycosidic bond at the 3-position (Wach et al., 2007). Onion exists in three different colours, red, yellow and white, and all these belong in the genus *Allium*, specifically *Allium cepa L.* It is known that onion contains some flavonoids for an example red onion contains about 1910 mg kg^{-1} of quercetin where higher concentrations are found in the outermost ring (Smith et al., 2003). In fact, quercetin 4'-O- β-glucoside and quercetin 3,4'-O-β-diglucoside account for about 80% of the total content of flavonoids (Bonaccorsi et al., 2005).

The plant *Moringa oleifera* has many different names by different countries. The plant is known for its exceptional nutritional value and healing purposes hence has been used for different purposes (Shindano and Kasase, 2009). The tree itself is rather slender, with drooping branches that grow to approximately 10 m in height. In cultivation, it is often cut back annually to 1 meter or less and allowed to regrow so that pods and leaves remain within arm's reach. The plant contains a range of polyphenol compounds including 46 antioxidants where quercetin is part of them (Ezeike et al., 2011). Contrary to onion, *Moringa* contains much higher amounts of quercetin and kaempferol as it was found that freeze-dried leaf samples contained both quercetin and kaempferol in concentration ranges between 633.5 and 926 mg per 100 g and between 104.7 and 225.4 mg per 100 g, respectively (Siddhuraju and Becker, 2003).

Chapter 2: Literature review

Chapter 2 focuses on the literature review and the following topics are discussed in detail: the technique of molecular imprinting; different polymerization approaches; literature on MIPs for chromium, uranium and quercetin; the fate of chromium and uranium; extraction methods; analytical method used for determination and analytical techniques used for characterization.

2.1. Molecularly Imprinted Polymers

Molecularly imprinted polymers (MIPs) are polymer materials which are produced by a process of molecular imprinting technology (MIT) where chemically selective binding sites are introduced on the surface of an adsorbent. These binding sites are produced by incorporating the analyte molecule (template) in the polymerization solution during polymer/ sorbent fabrication. The functional monomer and the cross-linking monomer then fix the template molecule in place through pre-defined bonding interactions depending on the functional groups on the template and monomer (Ye and Mosbach, 2001a). Removal of the template after the polymer has formed lead to creation of predefined binding cavities specific for the removed template molecule.

Since its inception (Polyakov 1931), molecular imprinting technique has gained a lot of attention as shown by its applications in biology, chemistry, and in other various fields. This is reflected in Figure 2.1 which shows the growth in numbers of publications. The examples of fields where MIPs have been applied on include, biosensors (Ebarvia et al., 2004), antibody simulation (Ye and Mosbach, 2001b), chiral resolution (Quaglia et al., 2001), enzyme catalysis simulation (Wulff, 2002) and biochemical separation (Zhang et al., 2003). MIPs are macromolecules that possess high affinity and selectivity for the imprint/target molecule. This high affinity for template comes from formation of predefined interaction between the template molecule and functional groups on the monomer. Therefore, it can be said that the molecular imprinting technique (MIT) is a mimic of natural molecular recognition (Shea, 1994; Mosbach and Ramström, 1996; Zhang and Mosbach, 2006).

Besides, MIPs are mostly used as sorbents for the solid-phase extraction (MISPE) technique, as this offers both pre-concentration and removal of interferences (Caro et al., 2006). Our group has also demonstrated the potential of combining MIPs with liquid membrane for the extraction of β-estradiol from aqueous samples (Nemulenzi et al., 2009). Due to their selectivity, MIPs have been used in environmental assays for toxic heavy metal removal, a technique called ion imprinted polymers (IIPs). This is the same reason that MIPs were used in the

present study, that is, selective removal of uranyl ion and chromium (VI) in contaminated environmental samples. Furthermore, in the same study the MIPs were used for selective recovery of high value compounds from plant waste materials such as onion peels and *Moringa oleifera* plant.

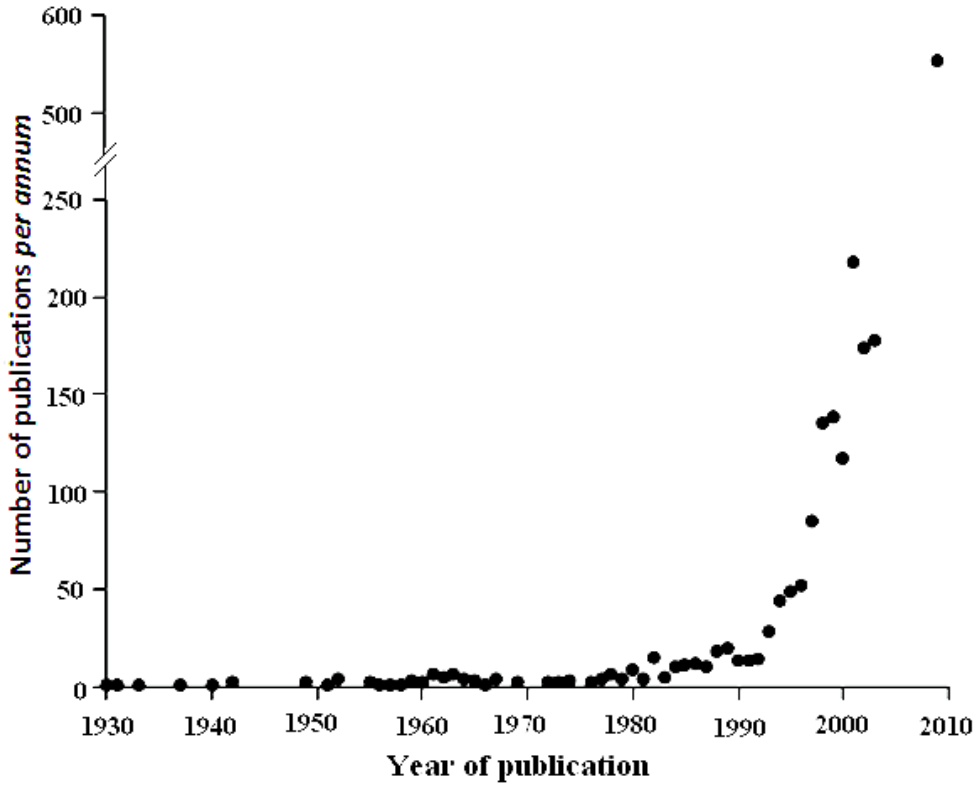

Figure 2.1: The number of publications within the field of MIP technology per annum for the period 1931–2003 (Alexander et al., 2006). Data for 2010 added by author after search from MIP database.com. 28 October 2011.

The technique of molecular imprinting offers several advantages such as; cost-effective alternative to biomolecule-based recognition; easy to prepare and handle; good thermal and chemical stability of the resulting polymer; polymers can be reused with excellent reproducibility (Gallego-Gallegos et al., 2009).

2.1.1. Monomers and templates; and their interactions

Figure 2.2 lists some of the most commonly used functional monomers since the introduction of molecularly imprinting technique. An ideal situation in MIP technology is that, a functional monomer should be able to form strong interactions with the template either through covalent or non-covalent bonding. During MIP synthesis, especially non-covalent imprinting, excess of monomer-to-template ratio is used. This is done to achieve monomer-template complexes. The strength of these interactions has a profound factor on the performance of MIPs including selectivity (Zhang et al., 2008a) and binding capacity for the target compound (Koohpaei et al., 2008; Shamsipur et al., 2007). It is believed that, the stability of the monomer-template complex during pre-polymerization depends on how strong the monomer-template interactions are, and this has a direct effect on the binding capacity of the MIPs. Meaning that the stronger are these interactions, the better the molecular recognition of the resulting MIP is (Suqin Wu et al., 2011). Hence, UV-vis (Li, et al., 2008; Luo et al., 2008), FTIR (Molinelli et al., 2005; Lv et al., 2007), NMR (Courtois et al., 2006; Sun et al., 2008; Malosse et al., 2008; Ansell and Wang, 2009) and computer simulation methods such as the density functional theory (DFT) (Becke, 1993), as well as trial-and-error methods have all been used for the selection of a functional monomer that will produce the most stable monomer-template interactions. DFT uses the Gaussian 03 software (Frisch et al., 2003) to calculate the binding energy (ΔE) of the template molecule and the monomer (Suqin Wu et al., 2011).

A more comprehensive review on the methods used for selection of appropriate functional monomers was published by Karim et al. (2005). Other readings on computer-aided MIP study for the selection of best optimum conditions such as functional monomer and porogen can also be found in the following articles (Piletsky et al., 2001; Wu et al., 2003; Meng et al., 2004; Diňeiro et al., 2005; Diňeiro et al., 2006; Farrington and Regan, 2007; Azenha et al., 2008; Yao et al., 2008). On the other hand, molecular dynamics have been recommended as a more faster and reliable method for searching for optimal imprinting conditions, including screening for functional monomers (Molinelli et al., 2005; Pavel and

Lagowski, 2005; Piletska et al., 2005; Chianella et al., 2006; Pavel et al., 2006; Breton et al., 2007; Wei et al., 2007). Nevertheless, the excess of monomer used can lead to different configurations of monomer-template equilibria giving rise to polymer with heterogeneous binding sites. Therefore, a balance has to be struck.

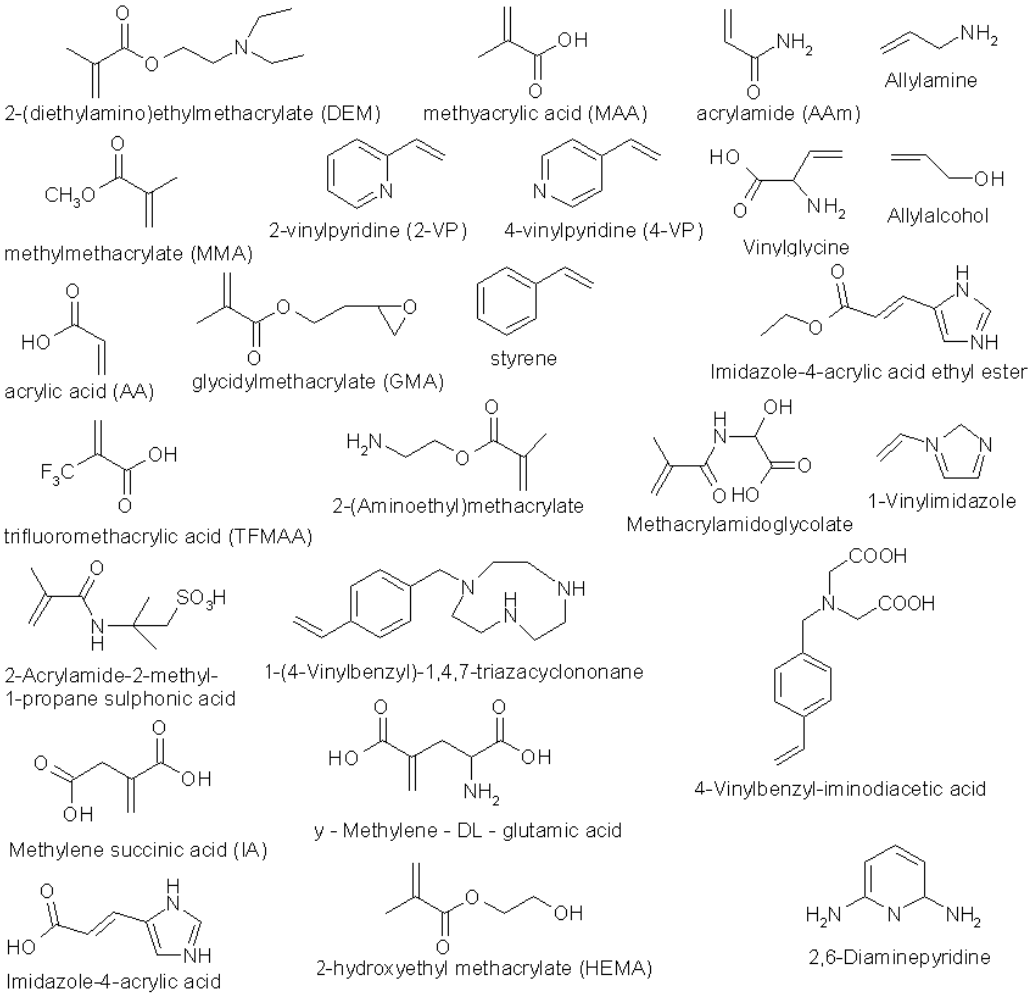

Figure 2.2: Selection of the most commonly used monomers**.**

2.1.2. Cross-linkers

Choosing appropriate cross-linkers is equally important as choosing functional monomers. This is because of the role these cross-linkers play in MIP synthesis. Typically, 90% of the amount of cross-linker to functional monomer is used. Cross-linkers bring about the mechanical stability of the polymer, control the morphology of the MIP matrix and stabilize the imprinted binding sites in order to

retain the recognition binding sites (Sellergren, 1999). However, too much of the cross-linker used can impede the binding sites because it might be difficult to remove the template completely, resulting in polymers with low binding capacity. Also, the cross-linker should have less interactions with the template in order to prevent formation of non-specific binding sites. Amongst the many cross-linkers used, ethylene glycol dimethacrylate (EDMA) and trimethalolpropane trimethacrylate (TRIM) are the most commonly utilized and TRIM is viewed to give more rigid and effective binding sites than EDMA (Vasapollo et al., 2011). TRIM is more suitable when precipitation polymerization is used (Yoshimatsu et al., 2007). Nonetheless, EDMA is mostly used in bulk polymerization. Figure 2.3 lists some of those common cross-linkers used.

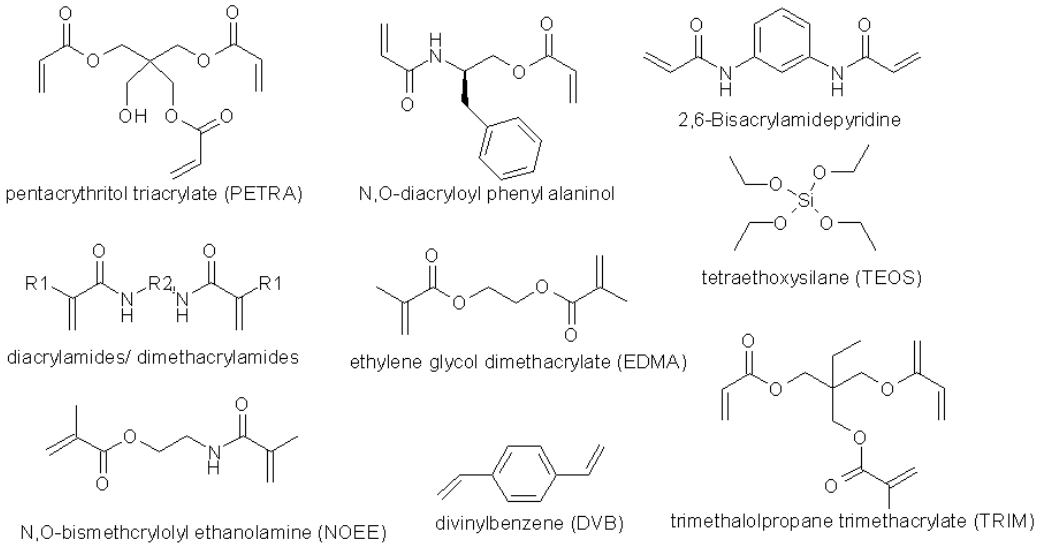

Figure 2.3: Typical cross-linkers used in MIP/ IIP synthesis**.**

2.1.3. Porogens

Of further importance in these interactions is the role of a solvent (which in MIP terms is called a porogen) because it not only acts as a solvent but also a pore forming agent. The rule of thumb is that, the monomer, template, cross-linker and initiator should all be soluble in the porogen. However, the porogen should have minimal interactions with both the template and the monomer as this will weaken the strength of the pre-polymerization complex (Mayes and Whitcombe, 2005).

For an example, in non-covalent imprinting approach, if the desired recognition of monomer and template is due to hydrogen bonding, then the use of protic solvents is not encouraged. In such case aprotic solvents such as acetonitrile, toluene, dichloromethane and chloroform are used. Some common solvents used in MIP synthesis are listed in Table 2.1.

Table 2.1: Most commonly used porogens

Solvent	Mw ($g\ mol^{-1}$)	Boiling point (°C)	Density ($g\ mL^{-1}$)	Polarity index	Dielectric constant*	H-bond strength
Acetone	58.08	56.2	0.786	21.0	20.7 (25)	7.0
Acetonitrile	41.05	81.6	0.786	5.8	37.5	6.1
Carbon tetrachloride	153.82	76.7	1.587 (liquid)	1.6	-	-
Chloroform	119.38	61.7	0.795	4.1	4.81	5.7
Dichloromethane	84.93	39.8	1.326	3.1	9.08	7.1
Dimethylformamide	73.09	189	0.944	6.4	36.7	11.3
DMSO-acetonitrile	-	-	-	-	-	-
Ethanol	46.07	78.5	0.789	5.2	24.6	19.4
Ethanol-water	-	-	-	-	-	-
Methanol	32.04	64.6	0.791	5.1	32.6 (25)	22.3
Methanol-water	-	-	-	-	-	-
2-Methoxy ethanol	76.09	125.0	0.965	-	16.9	-
Tetrahydrofuran	72.11	66.0	0.886	4.0	7.6	8.0
Toluene	92.14	110.6	0.867	2.4	2.38 (25)	2.0

* T = 20°C, unless specified

2.1.4. Initiators

Literature reveals that the most commonly used method for preparing MIPs is the free radical polymerization where in most cases the azo-initiators are used (Vasapollo et al., 2011). The most commonly used of these azo-initiators is the azo-*N*-*N*'-bis isobutyronitrile (AIBN). AIBN has a decomposition temperature of around 60ºC. Other than azo-initiators, polymerization reaction can be initiated thermally or by photochemical initiation. Generally mild reaction conditions with temperatures less than 80ºC are used. In MIP synthesis, the choice of initiator is equally important as other parameters as it can influence the morphology and

binding capacity of MIPs. Therefore, one has to choose accordingly and the stability of the monomers and templates under such initiation has to be taken care of. Figure 2.4 shows some of the available initiators.

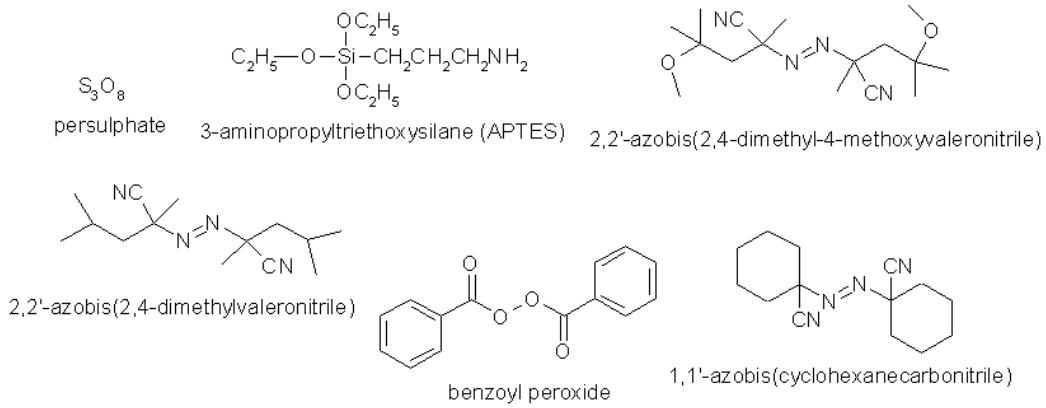

Figure 2.4: Some common initiators used in IIP/MIP synthesis.

2.2. Different imprinting approaches

Ever since the pioneering work by Polyakov (1931), several imprinting methods have emerged and been used for making MIPs for different purposes. One such method is the one involving the use of a pre-organised arrangement of monomer and template termed as covalent imprinting approach mainly developed by Wulff and Sarhan (Wulff and Sarhan, 1972). Another method of imprinting is the non-covalent imprinting approach which is by far the most widely used. This method is based on self-assembly approach (that is, it is based on physical interactions of the template molecule and the functional monomer through, for an example, hydrogen bonding, electrostatic interaction and/or weak van der Waals forces) and was advocated mainly by Mosbach and co-workers (Arshady and Mosbach, 1981). In this method since the template and monomer(s) are arranged together by non-covalent interactions hence, the subsequent recognition is also dependent on these interactions (Sellergren, 1997). Non-covalent imprinting is the most widely used method in MIPs owing to its simplicity, wide range of polymerizable units which possess various functional groups that may interact with the template, and limited organic synthesis required. Semi-covalent imprinting is another method

which is used and is based on the use of sacrificial spacer methodology (Whitcombe et al., 1995). This method can be viewed as a combination of covalent and non-covalent imprinting approaches. In fact, the template is covalently bonded to the polymer whilst the rebinding is through non-covalent interactions (Cacho et al., 2006) as shown in the Figure 2.5 below with point B on the template. Noteworthy mentioning is that, semi-covalent imprinting is most particularly used with templates lacking binding sites (functional groups). Figure 2.5 below shows the illustration of these methods together with the ligand exchange imprinting method.

Recently, sophisticated techniques like controlled/living free radical polymerization (CLRP) have been developed. CLRP techniques include reversible addition-fragmentation chain transfer (RAFT) polymerization, metal-catalyzed atom transfer radical polymerization (ATRP), nitroxide-mediated polymerization (NMP) (An et al., 2007). However, only few articles have been reported using the block copolymer self-assembly technique due to the complicated procedure involved (Chen et al., 2010).

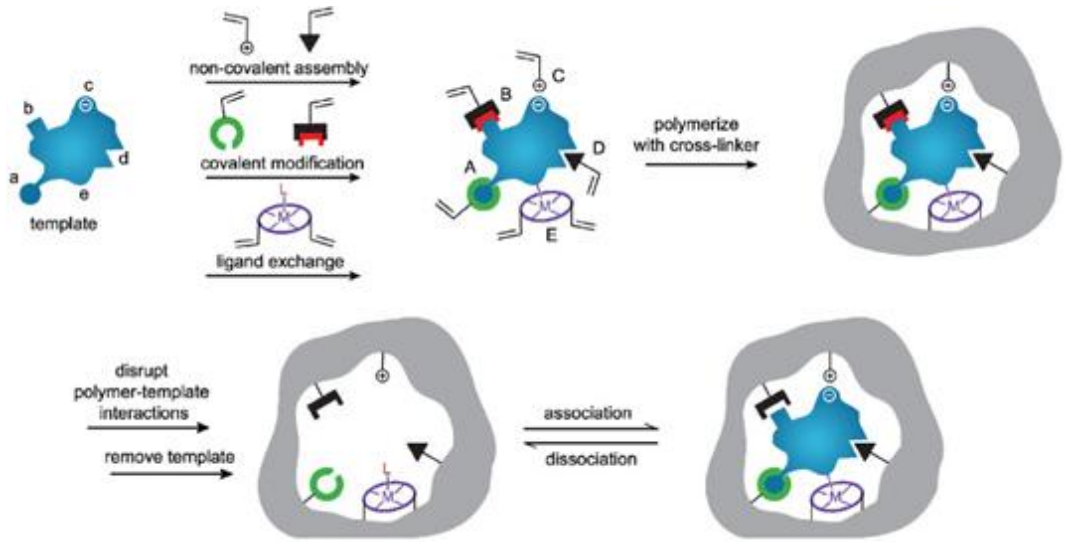

Figure 2.5: Molecularly imprinting representation showing different types of imprinting methods*;* (a) reversible covalent bonds, (b) activated non-covalent bonding, (c) electrostatic interactions, (d) van der Waals or hydrophobic interactions, (e) co-ordination with metal centre, taken from Alexander et al. (2006).

The way the template molecule is fixed within a polymeric matrix can vary depending on the method of choice used for polymerization and this has an impact on the quality of the binding sites produced. When covalent imprinting is used, the template molecule and the monomer are fixed by strongly covalent bonds. This method produces well defined binding sites where the template is fixed at a particular arrangement or position. No unspecific binding is generated with this method but its downfall is that it has lower binding capacity than the non-covalent imprinting and also there's a bottleneck of binding polymerizable functional units with reversible covalent bonds (Kim and Spivak, 2003; O'Mahony et al., 2006). Hence, this limits the use of covalent imprinting approach. In contrast, when non-covalent imprinting approach is used, no carbon-carbon bond formation is required but rather physical interactions between the monomer and the template through weak van der Waals forces, electrostatic interaction, hydrogen bonding and/ or hydrophobic bonding in case of organic analytes. In the case of inorganics, the physical interactions can be through electrostatic, coordination ion pairing, and complexation as the method of recognition. Non-covalent imprinting will be looked at in more detail in the next paragraph as is the method that was used in the current study.

2.2.1. The non-covalent imprinting approach on organics

As mentioned earlier, when the pre-polymer complex is formed through non-covalent imprinting, greater numbers of high affinity sites are produced as opposed to covalent methods. In non-covalent imprinting, the aim is to maximize the pre-polymer complex concentration either by increasing the amount of functional monomer or increase the amount of template (Kim and Spivak, 2003). Studies have shown that the template can, in principle, be increased indefinitely without compromising the final formulation of the polymer, and this is because the template is all removed at the end of the imprinting process (Andersson et al., 1999). The theory behind using high volumes of template is that, the pre-polymer complex can eventually be driven to its full complex state while a desired cross-linker to functional monomer ratio is maintained (Kim and Spivak, 2003).

However, the use of large volumes of template can lead to formation of non-specific binding sites (single or double point attachments) which will compromise the performance of the polymer/ sorbent. In fact, Andersson et al. (1999) also found out in their studies that the increased amounts of template did not optimize the MIP performance rather the peak performance was found to be closer to a 4:1 monomer:template ratio, which was the theoretical value of binding sites. The distribution of binding affinities and number of binding sites may be obtained by using results acquired from equilibrium batch experiments and fitting the data into suitable models. The template rebind to the MIP using the same types of interactions it used during polymer formation. Listed below in Table 2.2 are some examples were non-covalent imprinting approach was used.

In order to produce MIPs with good affinity for the template molecule using non-covalent imprinting, the template should possess one or more functional groups that can either donate or accept protons, or can form electrostatic interactions through groups such as tertiary amines. Templates such as dichlorodiphenyltrichloroethane (DDT) and polycyclic aromatic hydrocarbons (PAHs) for example which do not possess any of these functional groups are difficult to imprint using non-covalent imprinting as their mode of recognition whould be the hydrophobic interactions and shape recognition. However, there are cases where hydrophobic interactions were used as sole modes of recognition in non-covalent imprinting more especially for application in aqueous environments (Yu, Ramström, Mosbach, 1997). However, due to non-specific nature of hydrophobic bonding, most authors prefer to combine hydrophobic interactions with say electrostatic interaction or metal-ion coordination (Piletsky, Andersson, Nicholls, 1999; Xu et al., 2007). Generally, due to the strength of the bonds, the order in which MIPs with good imprintability can be produced using non-covalent bonding is, electrostatic > hydrogen > hydrophobic. Table 2.2 shows the versatility of the non-covalent imprinting approach for some selected organic templates. Factors that can influence the strength of electrostatic interactions include the size and charge of the template ion, type of ligands *etc*. Whereas hydrophobic interactions can, for example, be influenced by the size and shape of the template molecules.

Table 2.2: Non-covalent imprinting approach for selected templates

Sample	Analyte	Template	Monomer	Cross linker	Preparation method	Application method	Reference
Salicornia *herbacea* L.	protocatechuic acid, caffeic acid, and ferulic acid	caffeic acid	AAm	EDMA	Monolithic column	Online, LC	Zhu et al., 2011b
Catharanthus *roseus*	indole alkaloids	catharanthine	MAA	EDMA	Bulk	MISPE, LC	Lopez et al., 2011
Catharanthus *roseus*	indole alkaloids	vindoline	Itaconic acid	EDMA	Bulk	MISPE, LC	Lopez et al., 2011
Catharanthus *roseus*	vinblastine	vinblastine	MAA	EDMA	Bulk	MISPE, LC	Zhu et al., 2007; Zhu et al., 2010
Chamaecyparis *obtusa*	quercitrin, myricetin, and amentoflavone	quercetrin	AAm	EDMA	Bulk	MISPE, LC	Tian et al., 2011
Citrus fruits and orange juice samples	thiabendazole	thiabendazole	MAA	DVB	Precipitation	Online, LC	Barahona et al., 2011
Spiked corn and soybean samples	metolachlor, propisochlor and butachlor	metolachlor	MAA	TRIM	Coated fiber	SPME-HPLC	Hu et al., 2011
Tomato and pear	pirimicarb	pirimicarb	MAA	EDMA	Micropipette tip	PMME, LC	Zhou et al., 2010
Immature embryos of pea, rice and wheat	Auxins	indole-3-butyric acid	4-VP and β-cyclodextrin	TRIM	Suspension	Offline, LC	Zhang et al., 2010a
Fresh cole and breaking-wall rape pollen	24-epibrassinolide	24-epibrassinolide	4-VP and styrene	TRIM	Suspension	Offline, LC	Zhang et al., 2010b
Soybean and corn	chloroacetanilide herbicides	metolachlor	MAA	TRIM	Coated fiber	SPME-HPLC	Hu et al., 2010
Herbal medicine	(E)-Piceatannol, butein	quercetin	AA	EDMA	Bulk	Offline, LC	Zhu and Xu, 2003
TCM honeysuckle	chlorogenic acid	chlorogenic acid	MAA	TRIM	Surface imprinting	Offline, LC	Gu et al., 2010
Maize samples	sulfonylurea herbicides	chlorsulfuron	DEAMA	TRIM	Precipitation	Offline, LC-MS/MS	She et al., 2010
Saffron (*Crocus sativus*)	crocin	gentiobiose	MAAm	EDMA	Bulk	Offline, LC	Mohajeri et al., 2010
Onion	triazines	cytisine	MAA	EGGE	Surface imprinting	Batch, UV/vis	Djozan and Ibrahimi, 2008
Licorice Root	glabridin	glabridin	HEMA	EDMA	Bulk	MISPE, LC	Yan et al., 2009
Liquorice roots extract	triterpene acid	18-β-glycyrrhetinic acid	MAA	EDMA	Bulk	Offline, LC	Claude et al., 2008
Tomato	fenitrothion	fenitrothion	MAA	EDMA	Bulk	Batch, LC	de Barros et al., 2010

2.2.2. The non-covalent imprinting approach on inorganics

IIPs are similar to MIPs in that they keep all the qualities of MIPs only that the template is an inorganic (Araki et al., 2005; Singh and Mishra; 2009a; Su et al., 2008; Rao et al., 2006). Four techniques are used for the imprinting of metal ions and these involve trapping of the vinylated and/or non-vinylated chelating ligand (a), chemical immobilization (b), surface imprinting (c), and cross-linking of bifunctional reagent with linear chain polymers (d). Examples of surface imprinting and trapping of non-vinylated ligands are shown in Figures 2.6 and 2.7.

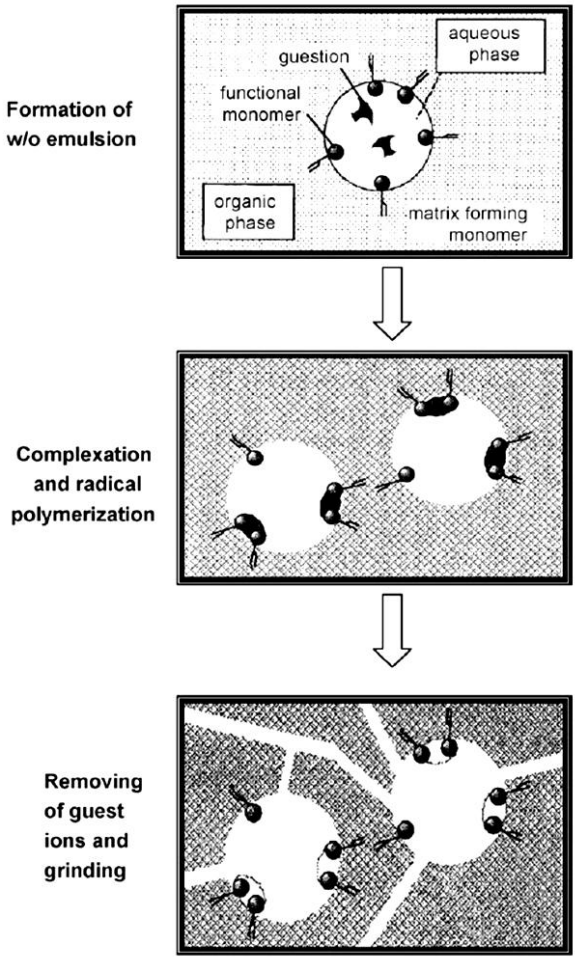

Figure 2.6: Surface imprinting technique (Uezu et al., 1994).

Chemical immobilization is similar to trapping method except that binary complexes of metal ions with ligands having vinyl groups are sometimes isolated and then polymerized with matrix-forming monomers (Rao et al., 2006). Typical examples of this method are those by Gupta and Neckers (1982), Rosatzin et al. (1991), Kuchen and Schram (1988), Say et al. (2003), and Ersöz et al. (2004).

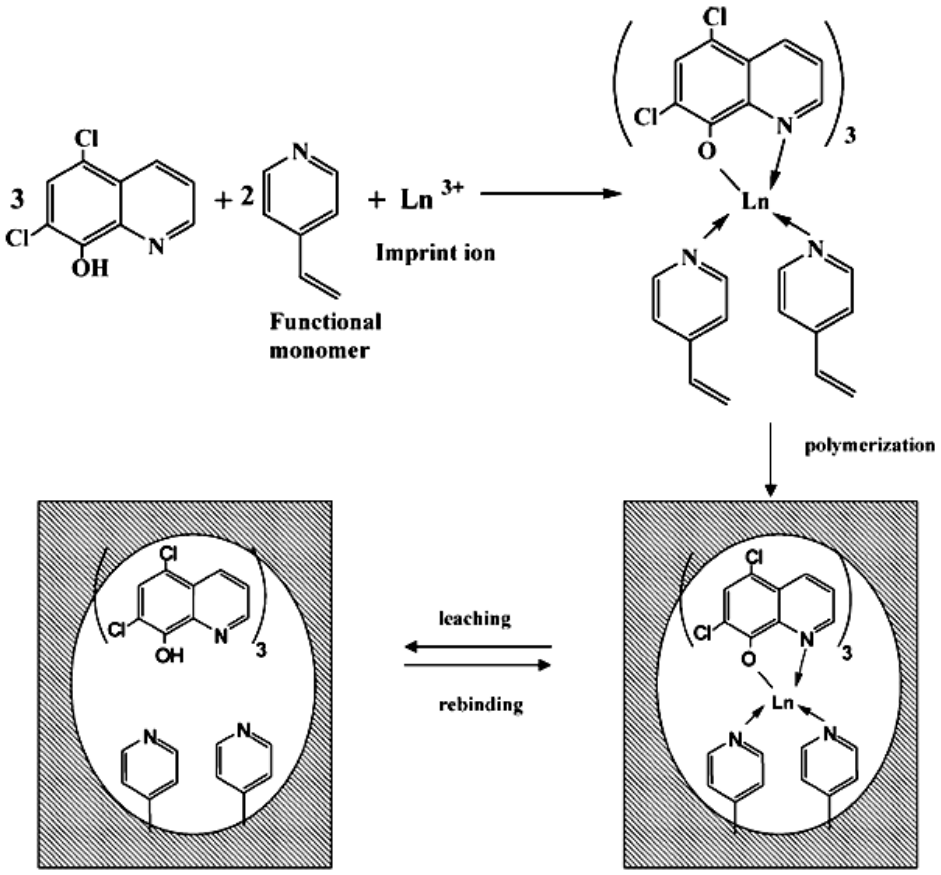

Figure 2.7: Schematic representation of IIP preparation via trapping of 5,7-dichloroquinoline-8-ol (Rao et al., 2006).

Examples of these methods include the earlier work of Nishide and Deguchi (1976) who cross-linked poly(4vinylpyridine) with 1,4-dibromobutane in presence of metal ions, such as Cu^{2+}, Zn^{2+}, Co^{2+}, Ni^{2+}, Hg^{2+} and Cd^{2+} as templates. Similarly, a cross-linked copolymer of diethylvinylphosphonate and acrylic acid with *N*,*N*'-methylene diacrylamide was later produced using metal ions as templates (Kabanov et al., 1979).

As in the case of MIPs, the shape of the template, the rigidity of the monomer-template, and the number and type of interaction sites determines the quality of the binding sites produced during imprinting (Rao et al., 2006). However, other methods such as the sol-gel process (Dai et al. 1997) and a combination of sol-gel and surface imprinting have also been used (Fang et al. 2005) for developing IIPs with selective removal of uranyl ion and cadmium, respectively. Prasada Rao has been advocating for the method which involves trapping of non-vinylated chelate during the polymer synthesis (Biju et al., 2003a; Kala et al., 2004; Krishna et al., 2005; Kala et al., 2005; Biju et al., 2003b; Kala et al., 2006; Gladis and Prasada Rao, 2003; Gladis and Prasada Rao, 2004; Metilda et al., 2004; Preetha et al., 2006; Daniel et al., 2003; Daniel et al., 2005a; Daniel et al., 2005b) for removal of lanthanide, actinide and noble metal using SPE IIPs. Novel Cd^{2+} IIP with hierarchical structures has also been prepared using the double imprinting methodology being advocated by Dai, (2001), and Lu and Yan (2004). Similar to MIPs, different IIPs configurations such as beads, microspheres or irregular particles can also be produced using different polymerization methods. Applications of IIPs are in solid phase extractions, detoxification of toxic inorganics from actual industrial effluents, membranes and metal ion sensors (selectrodes and optrodes) (Rao et al., 2006). Comparing the number of publications in Figures 2.1 and 2.8, one may say IIP is still at its infancy.

During imprinting of inorganics, no carbon-carbon bond formation is required and this generally makes the imprinting approach to follow non-covalent bonding. In fact, ion-imprinting is based on complexation, ionic bonding and ion pairing. The selectivity of a polymeric adsorbent is based on the coordination geometry, coordination number of the ions, on their charges and sizes (Su et al., 2008; Hoai et al., 2010; Liu et al., 2006). Meaning that, less conformational changes (less entropy loss) lead to production of polymers with high selectivity and the affinity for the template. Although IIPs are still considered to be at infancy by some compared to MIPs but the over the past decade there has been some considerable interest on the IIP technology. IIPs for trace removal of UO_2^{2+} (Singh and Mishra; 2009b), Cr^{3+} (Zhang et al., 2008b), Pd^{2+} (Zheng et al., 2007), Ni^{2+} (Jiang et al.,

2006; Ersóz et al., 2004), Fe^{3+} (Chang et al., 2007), Cd^{2+} (Fang et al., 2005; Li et al., 2007), Zn^{2+} (He et al., 2006), Cu^{2+} (Fujiwara et al., 2003; Ren et al., 2008) and Dy^{3+} (Zhang et al., 2007), have been prepared mostly by using surface imprinting technique.

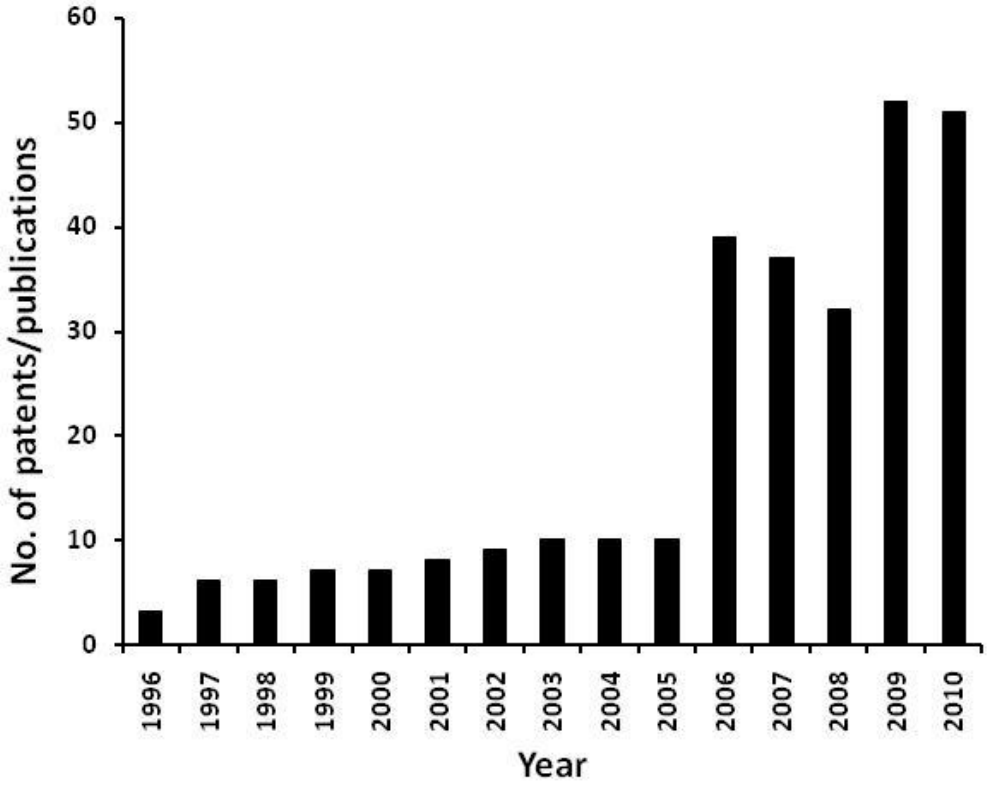

Figure 2.8: Approximated number of publication of IIPs. Data up to 2005 taken from (Prasada Rao et al., 2006) and 2006 – 2010 compiled by author after a search from Society of Molecular Imprinting Database (http://mipdatabase.com/ accessed 28 October 2010).

Although the molecular imprinting technique has shown to have some interesting advantages, however, it is not immune to drawbacks. Some of these shortfalls will be looked at in detail in the next paragraphs.

2.2.3. The challenges of molecular imprinted polymers

2.2.3.1. Template bleeding

Template bleeding resulting from incomplete template removal still remains the biggest challenge in MIP synthesis. This incomplete removal of the template is

largely due to the fact that some template might be fused deeper in the polymer matrix where it becomes difficult to be accessible by solvents. Hence, after washing of the polymer some template remains trapped and might start moving forward during polymer application which might lead to incorrect determination of the amount of analyte adsorbed. This is particularly more prone when trace levels of the target compound need to be determined, for an example, using molecularly imprinted solid-phase extraction (MISPE). Among the various methods that have been proposed by researchers to rectify this problem, the use of "dummy" template still remains the most popular and effective. Only the dummy template will bleed out and this will not interfere with the analysis as one will be absolutely sure that the analyte of interest was never added during the polymer fabrication.

MIPs for 2,4,6-trinitrotoluene (Walker et al., 2007), dopamine (Suedee et al., 2006), cyproheptadine (Feas et al., 2009) and organophosphorous nerve agents (Moullec et al., 2006) were all prepared using the dummy template method. Isotope molecular imprinting (Kawaguchi et al., 2005), post polymerization treatment methods such as thermal annealing, microwave assisted extraction and supercritical fluid extraction (Ellwanger et al., 2001), parallel extraction on blank samples (Berggren et al., 2000) have all been suggested as approaches to reduce template bleeding. However, they have less impact as compared to "dummy" template method. Imprinting with a dummy template also helps when the analyte of interest is too expensive or involves safety consideration when being handled and when the template is susceptible to degradation under polymerization conditions or has just limited solubility in the medium used (Kuginiya and Takei, 2008). In preparing MIPs using a dummy template two procedures are used, that is, fragment imprinting (Nemoto et al., 2007; Kubo et al., 2007; Kubo et al., 2005a) and interval immobilization (Kubo et al.,2004; Kubo et al., 2005b; Tominaga et al., 2009).

Basically, fragment imprinting refers to a scenario where a part of the target molecule is used as a pseudo-template for the fabrication of MIPs. This method can be used for analytes with both flexible and rigid chemical structure as well as for imprinting proteins (Chen et al., 2010). On the other hand, interval

immobilization refers to the use of a "dummy" compound with similar distances between two functional groups as the template (Chen et al., 2010). Nonetheless, the search for molecules to be used as dummy templates is never straightforward. However, it is clear that further work still needs to be undertaken in order to improve template leaking. For instance, in imprinting of organic compounds, Soxhlet extraction is used mostly for template removal. Therefore, more work on optimizing elution of template is needed. Having said that, substantial work has already being done in this regard like using surface imprinting technique which is believed to position the imprinting sites on the surface or near the proximity of the surface thereby allowing easy removal of the template (Li et al., 2006a).

Another interesting method in this regard is the use of semi-covalent imprinting technique which also limits template leakage. This is because the template would be covalently bound to the polymer and the condition used for template removal during rebinding exercises are less harsher than those used for template removal during polymer formation. This will mean the small amounts of template that might be still trapped in the polymer will remain there during polymer use without leaking out (Wang et al., 2009b).

2.2.3.2. Heterogeneous binding sites

Another challenge is batch-to-batch reproducibility of the production of MIPs. This includes surface area, particle size distribution, number and quality of binding sites. These drawbacks are true for all methods of MIP polymerization *e.g*., bulk, precipitation, emulsion and suspension. To account for particle size distribution, precipitation polymerization is preferred over bulk polymerization. However, proper selection of sieves can narrow the particle size distribution in bulk polymerization. Use of materials with known surface area as in surface imprinting also solves the surface area problem. However, even the methods of recognition especially where non-covalent imprinting is used contribute to the formation of heterogeneous binding sites. This is because during pre-polymerization step the reactions/ interactions are not well controlled and this is sometimes referred to as the "blackbox" of molecular imprinting (Allender, 2005).

During this step, a monomer and the template can form a number of interactions with differing ratios of attachment *e.g*., single point, two-point attachments and multiple point attachments. An ideal situation is to form as many interactions on the monomer with the template as possible in order to keep the template in a fixed position to limit unspecific rebinding. It has been postulated that during polymerization, it is possible that the polymer might "spit out" the template from those well-defined multiple interaction sites leading to an occurrence of more non-specific or heterogeneous binding sites (Mayes and Whitcombe, 2005).

Excess of either a monomer or template in the polymerization mixture also yields to production of more heterogeneous binding sites (Caro et al., 2002). Cross-linker backbone could also contribute to non-specific binding. Similarly, to the problem of template bleeding, the semi-covalent imprinting method was proposed for use in order to rectify the heterogeneous binding sites challenges (Cacho et al., 2006). Since the template in this method is bonded with covalent bonds to the monomer, therefore, well defined binding cavities are formed due to rigid control of functional group location and this eliminates non-specific binding of the template onto the polymer matrix (Klein et al., 1999; Kirsch et al., 2004). The template is removed together with the sacrificial spacer allowing the rebinding of the template to be through non-covalent bonding hence, there will be reduced kinetic restriction during rebinding (Klein et al., 1999; Kirsch et al., 2004).

Although the use of semi-covalent method is also limited by the presence of polymerizable functional ligands that can be readily cleaved from the template and also covalent bonds that can withstand polymerization conditions, the method has been used successfully to introduce homogenous binding sites (Chen et al., 2010). Besides, this method offers an opportunity to re-functionalize binding sites after template removal a process which led to more selective binding as was demonstrated by Ki et al. (2002), He et al. (2008) and Wang et al. (2009b). Zimmerman and Lemcoff (2004) reviewed other possible methods which have been suggested to reduce the formation of heterogeneous binding sites. These methods include selective modification of low affinity sites, and stoichiometric non-covalent imprinting through using stronger binding interactions.

2.2.3.3. Incompatibility with aqueous conditions

Preparation of MIPs in polar protic solvents such as water still remains a challenge in imprinting technology particularly if non-covalent imprinting is used. This is because non-covalent imprinting is based on the physical interaction of the template and monomer in order to generate the recognition sites for the template molecule. Hence, presence of water in non-covalent imprinting can disrupt these recognition sites particularly if these are based on hydrogen bonding as water can act both as a hydrogen donor and acceptor. In this instance water will get in-between template and monomer preventing them from interacting with each other. Presence of water favours hydrophobic bonding which in most cases leads to formation of unspecific binding sites by both MIP and NIP, a process that results in both MIP and NIP having similar performance in terms of selectivity. For electrostatic interactions water has less influence.

Preparation of MIPs with high recognition for organic analytes in pure aqueous environment solutions is also a challenge and recently much research has been dedicated on this topic (Qiao and Sun, 2010; Caro et al., 2006; Turiel et al., 2007; Yan et al., 2008). Although there have been advances made on this topic but it has become apparent that it is a template specific problem (*i.e.*, template can offer specific solutions, Piletska et al., 2009). Hence, this is less of a problem for templates with ionic interactions for an example. Several strategies have been proposed for the synthesis of MIPs with higher recognition in aqueous environments. These include a two-step extraction method advocated by Hu et al. (2009) where, hydrophobic bonding is more pronounced in aqueous solutions. MIPs relying on hydrogen bonding for interaction with the template tend to suffer from unspecific binding in this instance leading to a situation where NIP and MIP have similar recoveries of the template thereby defying the effect of imprinting. One other example was reported where the template was lipophilic and aromatic, and in this case both hydrophobic interactions and the electron-poor character of the molecule provided targeted interactions for recognition (Das et al., 2003). However, aqueous solutions are not a problem for inorganics as the recognition mechanism is based ionic interactions. Ionic interactions are generally much stronger than hydrogen bonding.

As mentioned before that several studies have focussed on improving performance of MIPs in pure aqueous environments (Pileska et al., 2008; Qiao and Sun 2010; Pan et al., 2010; Piletsky et al., 1999; Piletska et al., 2005; Das et al., 2003; Dirion et al., 2003; Sellergren, 2001). A water-compatible MIP was synthesized using trimethylolpropane trimethacrylate as cross-linker and methacryclic acid (MAA) as functional monomer (Yan et al., 2007). Although the polymer worked, it was evident that more fine-tuning needs to be done in order to improve the selectivity and suppress the nonspecific binding (Qiao and Sun, 2010). Few other groups have reported preparation of water-compatible MIPs where 2-hydroxyethyl methacrylate (2-HEMA) was used as a hydrophilic monomer in some cases in a water-methanol system (Qiao and Sun, 2010; Yan et al., 2008). In an attempt to fabricate synthetic receptor with high recognition for drugs of abuse cocaine, deoxyphedrine and methadone, problems relating to water-compatibility were addressed (Pileska et al., 2008). It was reported that MIPs prepared using 2-trifluoromethacrylic acid (TFMAA) in combination with toluene as porogen were highly effective for the recognition of the template in water with imprinting factors between 2.6 and 1.4. Corresponding NIPs were unable to differentiate between the various analytes (Piletska et al., 2008). Dzygiel et al. (2007) investigated the recognition ability of sildenafil and desmethyl sildenafil from aqueous and organic media employing MIP-solid phase extraction (MISPE). They reported that MIPs demonstrated superior selectivity of sildenafil template among its analogues from plasma samples than in organic solvents. Similarly to the work done by Qiao and Sun (2010) and Yan et al. (2008), it was also found that in this particular case addition of a hydrophilic functional comonomer HEMA also improved the polymer compatibility to aqueous solutions by reducing non-specific binding.

Another water-compatible MIP for cipropfloxacin was prepared using trimethylolpropane trimethacrylate as cross-linker and methacryclic acid (MAA) as functional monomer was synthesized (Yan et al., 2007). More recently, Shen and Ye (2011) reported a new technique for producing water-compatible MIPs for propranolol. Their method is based on Pickering emulsion polymerization and in this case a combination of hydrophobic and electrostatic interactions was used for

the recognition of the analyte in water. However, it is clear from this example and others mentioned here that templates / analytes that possess ionic interactions are much easier to imprint for water-compatibility purposes. Interestingly, there are no reports on preparing water compatible MIPs for quercetin recognition. The reason could be also due to poor solubility of quercetin in aqueous system (< 0.1 g L^{-1} in water at 20-100°C, Srinivas et al., 2010). Hence, its extraction is mainly done using organic solvents like ethanol or methanol. In this regard, there is no need for water-compatible MIP for quercetin. However, inspired by the green chemistry concept (green chemistry advocate for use of less harsh and toxic

Table 2.3: Solutions to existing MIPs challenges (Chen et al., 2010)

Problem	Possible solutions
Protein imprinting	(1) Surface imprinting (immobilized template) (2) Epitope-mediated imprinting (3) Metal coordination procedure (4) Polyacrylamide soft gel imprinting
Incompatibility with aqueous media	(1)Two-step extraction (2) Polymerization in aqueous phase using hydrophilic monomers or non-hydrogen interaction (metal chelate or hydrophobic interactions) (3) Surface modification of MIPs (RAM-MIP)
Leakage of template molecules	(1) Dummy molecular imprinting (2) Nanostructeured imprinted polymer (3) Porous imprinted polymer
Heterogeneous binding sites	(1) Semi-covalent imprinting or covalent imprinting (2) Selective chemical modification of low affinity sites
Hydrophylic compound impinting	(1) Dummy molecular imprinting (ion-pair as template) (2) Imprinting in aqueous media

solvents such as water), a method for extracting quercetin from onion waste using pressurised hot water extraction was proposed (Turner et al., 2006; Lindahl et al., 2010). In such case, the extract is in aqueous environment. Hence, the present study looked at developing MIP to be used for extraction of quercetin and other related compounds in such environments. In the review by Chen et al. (2010),

several possible solutions to MIP challenges, including incompatibility with water, are detailed (Table 2.3). Moreover, use of different polymerization can also offer some remedies to MIP challenges.

2.3. Different polymerization techniques

There are several ways in which MIPs can be prepared. However, free-radical polymerization and sol-gel process have enjoyed a lot of attention in this regard. Particularly, bulk polymerization, which is by far the most widely used method due to its simplicity and robustness in preparation as this method involves no expensive or complicated instruments. This section deals with different polymerization strategies that are employed to produce MIPs. Critical review on their merits and demerits will be looked into as well as their applications.

2.3.1. Bulk polymerization in MIPs

Bulk polymerization is the most widely used method of polymerization in MIP synthesis. Simplicity in preparation, compatibility with many types of templates and the fact that only limited organic chemistry is required give this technique the edge over others (Gallego-Gallegos et al., 2009; Chen et al., 2010; Beltran et al., 2010). This method is sometimes referred to as traditional polymerization (TP) (Beltran et al., 2010). Although MIP synthesis started much earlier but it is the work in early 1970s that really introduced bulk polymerization (Wulff and Sarhan 1972). Numerous reports have since then surfaced in literature where bulk polymerization was used during MIP synthesis. In brief, MIP synthesis using bulk polymerization often is carried out in a single reaction vessel where a functional monomer, template, cross-linker and initiator are dissolved in an appropriate porogenic solvent. This solution mixture is usually cooled to 0°C to prevent unwanted polymerization followed with purging with nitrogen to remove dissolved air. Several methods can be used to initiate polymerization. These

include, use of heat as in free radical polymerization, by means of UV radiations or photochemically to produce a bulk monolith.

During making of MIPs with this method, a minimum porogen (about 10 mL of solvent) is used and because of this the growing polymer chains will precipitate in bulk forming a single monolith solid. The monolith is usually crushed, ground and sieved to obtain a useful particle size range to be used for adsorption of the target analyte. Characteristics of particles produced this way are irregularity in shape and size. Although the method is easy to perform but there has been drawbacks that are associated with this technique of imprinting such as longer time of post-treatment during the crushing, grinding and sieving process. This process not only produces irregular particle size but may also destroy some high affinity binding sites on the surface of the MIPs during crushing leading to the formation of low affinity binding sites thereby compromising the efficiency of the prepared polymers (Sellergren, 1997; Bartsch and Maeda, 1998; Sellergren, 2001; Ramström, 2005). Also, a lot of the MIP is wasted as only 30-40% of the MIP is recovered as usable material after crushing, grinding and sieving.

Nevertheless, the method has been successfully applied for the synthesis of MIP and IIPs for various purposes including removal of selected substances from polluted environments, plasma samples and extracting of certain compounds from plant materials. Specific examples include, recovery of quercetin (Xie et al., 2001; Weiss et al., 2002; Molinelli et al., 2002; Zhu et al., 2003; Mahony et al., 2006; Song et al., 2009a), removal of uranyl ion (Rao et al., 2006; Bae et al., 1999; Metilda et al., 2004; James et al., 2009; Singh and Mishra 2009b; Ahmadia et al., 2010; Gladis and Rao, 2003) and hexavalent chromium (Bayramoglu and Arica, 2011).

Although bulk polymerization is viewed as the traditional method for MIP synthesis due to its advantages mentioned earlier. However, it also has disadvantages. Consequently, a lot of effort has been put on addressing the challenges of the bulk polymerization process and few methods have been used. These include, suspension polymerization (Jing et al., 2009), emulsion polymerization (Tan and Tong, 2007; Tan et al., 2008), seed polymerization

(Hoshina et al., 2009) and precipitation polymerization (Liu et al., 2010a). These investigations were aimed at eliminating crushing and grinding, hence producing spherical particles which will in turn improve polymerization yield, mass transfer of the analyte as well as packing of cartridges (Beltran et al., 2010). Because there is no crushing and grinding in the above-mentioned methods, therefore the quality of binding sites produced should be homogeneous (Zimmerman and Lemcoff, 2004). Other than the above-mentioned methods, some other techniques have also been used in pursuit of trying to overcome the bulk polymerization process challenges. One such technique is the formation of the thin layer of imprinted polymer on the surface of organic polymer (Glad et al., 1995) and the other is where the thin layer is formed on inorganic material such as silica (Norrlrw et al., 1984; Plunkett and Arnold, 1995). However, both these methods produce polymers with low rebinding capacity (Ansell and Mosbach, 1997).

2.3.2. Precipitation polymerization in MIPs

After bulk polymerization, precipitation polymerization (PP) is the second mostly used polymerization technique. PP method produces pre-polymerization mixtures that are similar to the ones used in bulk polymerization, except that higher amount of solvent is employed in precipitation polymerization resulting in diluted system (Gallego-Gallegos et al., 2009). PP uses about 10 times the volume of solvent (100 mL) used in bulk polymerization. The distinguishing feature between PP and bulk polymerization method is that when the growing polymeric chains reach a critical mass they precipitate producing microspheres or aggregates particles which are typically 10 µm as compared to the monoliths formed in bulk polymerization (Cacho et al., 2009; Ye et al., 1999, 2001). These polymeric chains are no longer soluble in the solvent. No sieving and grinding is required as particles were directly placed, for an example, on Soxhlet extraction system for template removal after polymerization has ceased.

One other advantage of using PP is that it involves no use of stabilizers and/ or surfactants, and particles of controlled size and size distribution can be produced

(Beltran et al., 2009; Takekoh et al., 2006; Croll et al., 2005). Sometimes the particle size range produced can be below the sub-µm range and this is a disadvantage for use in MISPE (Beltran et al., 2010). Another notable limitation of the PP method is that it is not robust as bulk polymerization, it has been shown that the particle size produced depends on the template used. The 'imprintability'' (that is, the possibility of imprinting any given template molecule) of this method has remained the subject of concern as some authors showed that the presence of template can either increase the particle size (Beltran et al., 2009a), or decrease polymerization yield (Sambe et al., 2006) or have no effect at all (Wang et al., 2003). Nevertheless, PP method is regarded as a more simpler and better method than emulsion, multistep swelling or grafting as it involves the no use of stabilizers and surfactants which can contaminate the final product.

Particle products obtained from PP method have been widely used in affinity chromatograph separations as well as SPE sorbents (Yoshimatsu et al., 2007). Beltran et al. (2009) demonstrated the use of precipitation polymerization for the synthesis of two different MIPs in the form of imprinted microspheres with well-defined particle size and particle size distribution, and their subsequent use in MISPE protocols for the selective extraction of carbamazepine (CBZ) and its main metabolite, oxcarbazepine (OCBZ), from human urine. The MIPs were synthesised using MAA functional monomer, DVB cross-linker, AIBN and porogen mixture of acetonitrile:toluene (75/25, *v/v*). Similarly, PP particles for recognition of chinconidine (CD) were produced using HEMA as a co-monomer (Liu et al., 2010a).

Yoshimatsu et al. (2007) , instead of using simple precipitation polymerization technique that leads to the aforementioned challenges, studied new synthetic conditions that will lead to controllable particle size in the range of nano- to micrometers. The authors reported that varying the amount of cross-linker could produce monodisperse particles in the size range of 130 nm to 204 µm. It was further reported that the polymer prepared under such conditions performed better than irregular particles from bulk polymerization for the selective binding of (S)-

propranolol enantiomer over (R)-propranolol enantiomer by 7 folds (Yoshimatsu et al., 2007). Interestingly, Xia et al. (2006) is reported to have prepared the first quercetin MIP by precipitation polymerization. Chitosan and MAA were used as functional monomers and the MIPs demonstrated higher selectivity and capacity compared to MIPs prepared from MAA or chitosan alone as a functional monomer.

Another modified approach for preparation of MIPs with precipitation method was proposed by Jin et al. (2008). In their work, instead of using the usual 95 wt.% of porogen which is associated with cost and environmental concerns, 50 wt.% porogen of alkane:toluene mixture was used. Monodispersed MIPs of the size range 2-3 μm diameter with high recognition for bisphenol A, estradiol and tebunazoleas were prepared. MIPs prepared from this modified method were found to perform better than the MIPs prepared from conventional precipitation. The group of Tamayo et al. (2005) prepared three different MIPs by precipitation polymerization where linuron (LIN) or isoproturon (IPN) (phenylureaherbicides) were used as templates and MAA or trifluormethacrylic acid (TFMAA) as functional monomers. During the evaluation of the rebinding characteristics it was observed that TFMAA-based polymer where IPN was used as template presented the best properties to be used as a selective sorbent for the extraction of phenylurea herbicides.

2.3.3. Suspension polymerization in MIPs

In suspension polymerization water is mainly used as a dispersing medium (Hosoya et al., 1994) although liquid paraffin and perfluorocarbon liquid can also be used. The continuous phase of water is used to suspend a droplet of the pre-polymerization mixtures in the presence of a stabilizer or surfactants (Sellergren, 2001; Perez-Moral and Mayes, 2001). Although there have been sound reports (Sellergren, 2001; Perez-Moral and Mayes, 2001; Ozcan et al., 2006; Lai et al., 2004) on the use of conventional suspension polymerization in both covalent and non-covalent imprinting approaches the particles produced are still of wide size

range. Moreover, the use of water as a dispersing solvent is the downfall of this technique since water can interrupt template-monomer bonding more especially if the non-covalent imprinting method is used (Nicholls, 1995). Suspension polymerization has been used to produce MIPs with good recognition and chromatographic properties but with perfluorocarbon liquid as a dispersing medium not water (Mayes and Mosbach, 1996; Hantash et al., 2006). The advantage of these liquids is their immiscibility with most organic solvents and that they are chemically inert. This means that they do not interfere with non-covalent interactions during imprinting hence the recognition sites formed will be of good quality (specific). However, perfluoro polymeric surfactant is needed in this method. Surfactants just like stabilizers in the conventional suspension polymerization interfere with monomer-template interactions. Nevertheless, another more modified suspension method is the use of mineral oil (liquid paraffin) for the formation of pre-polymerization droplets (Kempe and Kempe, 2006).

Although the use of these liquids addresses the water interference problem, however, the particles produced in all three methods are still polydispersed with a range of few to hundreds micrometers. With mineral oil, no surfactants or stabilizers are required (Kempe and Kempe, 2006) but the downfall is that some porogenic solvents like chloroform and toluene cannot be used with the method as there are miscible with mineral oil (Chen et al., 2010). In an interesting study by Hu et al. (2005), it was reported that MIPs prepared by bulk polymerization demonstrated higher retention capacity and selectivity than MIPs prepared from suspension polymerization a property that was related to larger pore size and number of active sites on MIPs prepared by bulk polymerization methods (Hu et al., 2005).

2.3.4. Emulsion polymerization in MIPs/ Surface graft polymerization in MIPs

Although rarely used, emulsion polymerization is employed when "surface imprinting" is used more especially for protein imprinting (Tan and Tong, 2007; Tan et al., 2008). In this case, microsphere particles are produced by emulsion polymerization using water/oil medium. This method requires an oil-soluble functional host molecule, a water-soluble template, an emulsion stabilizer, and a polymer matrix forming monomer. Molecules self-assemble at the oil–water interface forming recognition sites on the polymer surface (Yu et al., 1992). Contrary to suspension and precipitation, particles with monodisperse particle size range are produced (Tan and Tong, 2007). However, it also suffers from the interference caused by the added surfactants.

Although the method is suitable for imprinting of high molecular weight compounds, it can be used for imprinting of small analytes, peptides and sugars (Bossi et al., 2001). Generally, two approaches are used for the proteins, the first approach is based on the proper placement of few functional groups able to form strong interactions with the template (Mallik et al., 1994). Template recognition may be achieved by metal-chelating or strong electrostatic interactions (Mallik et al., 1994; Kempe et al., 1995; Kempe and Mosbach, 1995). The second approach is based on MIP's ability to recognize a template by using a combination of shape complimentarity and multipoint weak interactions provided by the monomers able to form hydrophobic interactions or hydrogen bonds (Hjertén et al., 1997). The major problem with imprinting of large templates, such as proteins, lies in the restricted mobility of those molecules within highly cross-linked polymer networks and the poor reversibility and efficiency in binding. MIPs selective for protein templates with differing mass and charge such as horseradish, peroxidises, lactoperoxidase, haemoglobin, microperoxidase were produced using surface coating on polystyrene microtiter plates (Bossi et al., 2001). Grafting method can also be used to produce composite materials (Tamayo and Martín-Esteban, 2005), where the polymer is grafted on the surface of a silica material which is etched away after polymerization to reveal more binding sites (Yilmaz et al., 2007).

However, this technique requires use of corrosive solvents and demands for more synthetic skill (Beltran et al., 2010). Nevertheless, the method has been successfully used for imprinting different target compounds (Gallego-Gallegos et al., 2009).

2.3.5. Dispersion polymerization in MIPs

Dispersion polymerization is viewed as a modified precipitation polymerization where a monomer is soluble in the dispersion medium but not the polymer and where well-defined polymer particles are formed. The required use of stabilizer differentiates this method from the precipitation polymerization (Winnik et al., 1987; Shen et al., 1993). Similar to emulsion polymerization, dispersion polymerization may be used to address some of the shortfalls of the bulk polymerization method (Li et al., 2010). These shortfalls include irregular particle size particularly if the polymer is to be used as sorbents in chromatographic analysis (Sellergren, 1994). Dispersion polymerization procedure was developed for *in situ* preparation of imprinted affinity phases in aqueous or polar media. This method usually produces agglomerates of micron-sized globular particles with a microporous or mesoporous morphology (Sellergren, 1994). Similarly, Li et al. (2010) prepared MIPs for extraction of melanine from milk samples using dispersion polymerization. In this method, microsphere particles with high selectivity with controlled particle size and shape were produced by using large volumes of acetonitrile as a dispersion medium. Dispersion polymerization can also be used for production of IIP microsphere as was demonstrated by Say et al. (2003). In their study, Cu^{2+}-imprinted poly(ethylene glycol dimethacrylate–methacryloyl amidohistidine/Cu^{2+}) microbeads were produced by a dispersion polymerization of EDMA and methacryloyl amido histidine MAH/Cu^{2+}. The recognition point of the prepared imprinted polymer was through the interaction between Cu^{2+}) ion and imidazoyl group. The imprinted microbeads obtained were of the size range of 150-200 µm and they demonstrated superior selectivity and binding capacity when compared to Zn^{2+}, Ni^{2+} and Co^{2+} competing ions.

2.3.6. Seed polymerization/ Multi-step swelling polymerization

In multi-step swelling polymerization procedure, preformed seed particles of identical size are suspended in water and, after several additions of suitable organic solvents, the initial particles swell to a final size in the range 5–10 μm (Beltran et al., 2010). The first step is to get particle to swell to a desired size thereafter, other components required for polymerization are added to the solution and finally polymerization is initiated. Similarly to dispersion method, particles of monodispersed size range are produced but the method is elaborate and time consuming as it involves multi-step swelling and polymerization (Hoshina et al., 2009; Hantash et al., 2006). Also, the presence of water which is used as a continuous phase interferes with non-covalent interactions between the template and the functional monomer. Furthermore, multi-step swelling polymerization has not been used as TP or PP has, much owing to its complexity. Imprinted polymers for selective extraction of triazine herbicides (Sambe et al., 2007) and barbiturates (Hoshina et al., 2009) from river samples have been reported by Haginaka group. Also extraction of domoic acid from blue mussels using MIPs fabricated from the multi-step swelling polymerization is reported (Kubo et al., 2007). Haginaka (2008) has written a more comprehensive review on different polymerization techniques used in MIPs.

2.4. MIPs for chromium (quaternization)

Various technologies for the removal of hexavalent chromium from contaminated environments have been reported. These include reduction of Cr (VI) to Cr (III), followed by Cr (III) precipitation under the alkaline conditions (Kratochvil et al., 1998), membrane separation, extraction, and sorption (Patterson, 1985), sorption by activated carbon (Huang and Wu, 1977), ion exchangers (Santiago et al., 1992) and biosorbents (Brower et al., 1997) all have been used for the removal of chromium (VI). However, adsorption and ion exchange are the most common techniques used for the removal of chromium (VI) from aqueous environments (Neagu and Mikhalovsky, 2010). A range of natural and synthetic sorbents have

been used (Srinivasan et al., 1988; Fang et al., 2007; Qian et al., 2000; Ramnani and Sabharwal, 2006; Deng and Bai, 2004; Raji and Anirudhan, 1998). Similarly, the use of ion exchangers for the removal of chromium (VI) has been reported in literature including the use of the commercial Aliquat 336 (Vincent and Guibalf, 2001) and Lewatit-anion exchanger (Pehlivan and Cetin, 2009). Incomplete metal removal, expense, swelling (in case of resins) etc are some of the drawbacks associated with some of the techniques. MIPs offer several advantages including high thermal stability and mechanical strength over other polymeric materials.

The use of quaternized poly-(4-vinylpyridine) polymers for the removal of anionic species such as chromate, arsenate and perchlorate has been known (Mitchell et al., 2004; Cannon et al., 2005). The quaternized polymeric molecules are known to possess both the hydrophobic groups and ionic moieties capable of undergoing ion exchange and ion pairing reaction in aqueous environments with the anionic species present (Fang et al., 2007). The reason for this is that after quaternization, the electron-deficient pyridine ring renders the pyridyl-N more attractive to anions than amine-N (Fang et al., 2007). However, although quaternization is closest to classical "cross-linking of ligand system" advocated by Nishide (1976), the above cannot be regarded as imprinting as the "print/ template" molecule was not involved in the synthesis of the materials.

Use of the IIP method for the removal of chromium has been reported but it was mostly for the removal of Cr^{3+} where Cr^{3+} was used as a template (Zhang et al., 2008b; Birlik et al., 2007; An and Gao, 2009; Chen et al., 2010). Recently, Bayramoglu and Arica (2011) developed an IIP specific for Cr (VI) using Cr (VI) anion solution for template. Polymers were produced using the traditional bulk polymerization. Prepared IIP demonstrated higher selectivity when compared to Ni^{2+} ions and the binding capacity of the prepared IIPs was reported at 3.31 mmol g^{-1} at pH 4. 4-Vinyl pyridine was used as functional monomer units and EDMA was the cross-linker. Although there is a patent for production of cationic IIPs for inorganic anions (Southard, 2009), in the patent there are no examples of results to prove that the IIPs were prepared and that they work for all anions. This clearly

shows there still a gap as far as development of chromium IIPs. Up to this far only one Cr (VI) IIP has been reported (Bayramoglu and Arica, 2011).

2.5. MIPs for uranium

In contrast to the application of IIP technology for selective removal of toxic chromium, a lot has been done on the uses of IIPs for the removal of uranyl ion from environmental samples such as aqueous and seawater solutions. The pioneers in this work include a group by Bae et al. (1999) who synthesized ion exchange resins by copolymerization of styrenic monomers with uranyl ion complexes possessing polymerizable ligands. This group reported that the polymer prepared in this manner showed remarkable concentration efficiency and good selectivity for the uranyl ion. IIPs were formulated from 5 wt.% uranium vinylbenzoate complex and 4 wt.% divinylbenzene in styrene using chemical initiation by 1 wt.% azobisisobutyronitrile (AIBN). Therefore, in this case polymer cavities specific for uranium were created using complexing ligands arranged to match the charge, coordination number, coordination geometry, and size of UO_2^{2+}. The unique shape of the uranyl ion may be expected to lead to much greater selectivity for the uranyl ion by molecular imprinting than for other metal ions.

Following these studies were patents by Dai et al. (2001) and John et al. (2002) on the use of IIPs for uranium recovery. The imprinted mesoporous sorbents prepared by Dai et al. (2001) were based on the use of bifunctional ligands such as amines, sulphonic acids, and phosphonic acids for the separation of uranium from aqueous solutions. On the other hand, John et al. (2002) relates to the detection and extraction of uranyl ion by polymer imprinting where in the complexable functionality is of the formula CTCOOH where, T is a hydrogen or any halogen (preferably chlorine) methyl and halogen substituted forms there of or CCOOH or PhCOOH. However, both these inventions do not allude to the selectivity of the prepared IIPs for uranium over other metal ions (Gladis and Rao, 2003). In another study, IIPs selective for uranium over other 2+, 3+ and 4+ competitor

metal ions was synthesized from a copolymer with chloroacrylic acid and ethylene glycol dimethacrylate, and applied on the selective removal of uranium from dilute aqueous solutions (Saunders et al., 2000). Following these studies were reports from the Rao group who synthesized uranium IIPs by trapping vinylated and/ or non-vinylated functional monomers in the polymer structure (Gladis and Rao, 2003; Gladis and Rao, 2004; Metilda et al., 2004; Prasada Rao et al., 2006). Uranium IIPs were prepared by using UO_2^{2+} template, 5,7-dichloroquinoline-8-ol/ succinic acid/ salicylaldoxime/ catechol, and vinylpyridine ternary complex as template in presence of styrene, divinyl benzene, and 2,2'-azo-bis-isobutyronitrile. The prepared polymers demonstrated high selectivity of uranyl ion from dilute aqueous and seawater solutions as well as on soils and sediment samples. From there, several other uranyl ion IIP synthesis reports appeared in literature (Say et al., 2003; Kimaro et al., 2005; Preetha et al., 2006; Metilda et al., 2007a; Sadeghi and Mofrad, 2007; Metilda et al., 2007b; James et al., 2009; Singh and Mishra, 2009b; Ahmadi et al., 2010). Application of these were for removal of uranium from synthetic nuclear power reactor effluents with weakly acidic solutions (Preetha et al., 2006), inland and seawater (Metilda et al., 2007b), synthetic seawater and groundwater (Sadeghi and Mofrad, 2007), mining industry feed stimulant and natural water solutions (James et al., 2009). Various chelating ligands such as methacryloylamidoglutamic acid (MAGA) (Say et al., 2003), salicylaldoxime (Preetha et al., 2006), amidoxime ligand (James et al., 2009) and *N,N'*-ethylenebis(pyridoxylideneiminato) ligand (Ahmadi et al., 2010) were all used for different IIP synthesis.

Application of IIPs on U (VI)

Almost all applications of IIPs have focused on removal of toxic uranyl ion from some kind of wastewater (Table 2.4). Also, a lot has been done using batch mode of extraction. This clearly points to further developments in this area since the batch method is more manual. The use of IIPs as sorbents in solid-phase extraction cartridges is still very rare. Only one study showed IIP sensors (Metilda et al., 2007b).

Table 2.4: Summary of the applications of IIP for UO_2^{2+} ion

Sample	pH range	Imprinting method	Mode of extraction	References
Sambhar salt lake and groundwater	5-7	Modified precipitation	Batch	Milja et al., 2011
Ground, river and seawater	3.5-5.5	Bulk polymerization	Batch	Singh and Mishra, 2009
Uranium mining industry feed simulant	8-9	Bulk polymerization	Batch	James et al., 2009
Groundwater and synthetic seawater	5	Bulk polymerization	Batch and SPE	Sadeghi and Mofrad, 2007
Natural and synthetic seawater	7	Bulk polymerization	Batch	Metilda et al., 2007a
Seawater	7	Bulk polymerization	Membrane based sensor	Metilda et al., 2007b
Synthetic nuclear power reactor effluents	3.5-5.0	Bulk polymerization	Batch	Preetha et al., 2006
Complex environmental samples	3.5	Bulk polymerization	Batch	Kimaro et al., 2005
Dilute aqueous solutions	4.5-7.5	Bulk polymerization	Batch	Metilda et al., 2004
Seawater	3.5	Bulk polymerization	Resin in syringe	Bae et al., 1999
Aqueous systems	7	Bulk polymerization	Batch	Ahmadi et al., 2010
Dilute aqueous solutions and synthetic seawater	5-7	Bulk polymerization	Batch	Gladis and Rao, 2003
Soil and sediments	4.5-7.0	Surface grafting	Batch and SPE	Liu et al., 2010b
Aqueous solutions	5	Dispersion polymerization	Batch	Liu et al., 2010c

Note: Uranium ion imprinted articles with no application are omitted from the Table.

2.6. MIPs for quercetin

From a biological point of view, quercetin is one of the most active compound amongst the flavonoids and hence its selective extraction using MIPs which can be fine tuned for a specific target is justified (Xie et al., 2001; Weiss et al., 2002). The antioxidant activity of quercetin is attributed to the hydroxyl groups attached to the aromatic rings as well as with the electronic delocalization (Russo et al., 2000). There has been a growing interest in development of quercetin MIPs from the past decade or so (Xie et al., 2001; Weiss et al., 2002; Molinelli et al., 2002; Zhu et al., 2003; Xia et al., 2006; Mahony et al., 2006; Song et al., 2009a). For an example, Weiss et al. (2002), demonstrated the feasibility of preparing quercetin imprinted polymers and the utilization of these selective membranes as advanced separation phase. The polymer was made from 4-VP functional monomer, EDMA cross-linker and the AIBN initiator. The MIPs were used as stationary phase during HPLC measurements as well as sorbents in MISPE formats for wine analysis. The selectivity of quercetin among other related compounds using the MIPs was said to be good (Weiss et al., 2002).

Quercetin is a polyphenol consisting of a benzene ring and hydroxy groups, meaning that quercetin can form very strong hydrogen bonding and hydrophobic bonding depending on the functional monomer used for the imprinting. This explains the variation in type of monomers used in Table 2.5. The work of O'Mahony (2006) focussed on studying the nature and structure of pre-polymerization complexes for the quercetin MIPs. From the work of Baggiani et al. (2004) and Nicholls et al. (2004), it emerged that the inclusion of a polymerizable derivative of the template molecule in the polymerization mixture may increase MIP affinity for the template molecule. This is an indication of the formation of template clusters within the binding sites as rebinding takes place. O'Mahony et al. (2002, 2006) have previously prepared quercetin MIPs with remarkable specificity from 4-vinylpyridine functional monomer. Therefore, the quercetin-4-vinylpyridine system of the MIPs was examined in order to understand the mechanism of this remarkable specificity. A combination of ^{1}H NMR, FTIR, spectroscopy and X-ray crystallography were employed in order to

determine with the greatest possible accuracy the nature and structure of the complexes that exist in the pre-polymerization solution prior to the actual initiation of the polymerization reaction (O'Mahony et al., 2006; Shea and Sasaki, 1989, 1991). Computational quantum chemical analysis (CQCA) was used for the calculations of stabilization energy in an investigation of the influence of porogenic solvents, functional monomers and cross-linker on adsorption specificity of the MIPs to quercetin (Song et al., 2009a). MIPs have been used for selective recovery of quercetin from wine, Chinese traditional medicinal plants, and Ginkgo leaves (Molinelli et al., 2002; Zhu and Xu, 2003; Xie et al., 2001).

Table 2.5: Some of the literature on quercetin MIPs

Functional monomer	Cross-linker	Initatior	Porogen	Reference
AAm	EDMA	AIBN	THF/1,4-dioxane/ acetone/acetonitrile	Song et al., 2009a
AAm	EDMA	AIBN	THF	Song et al., 2009b
4-VP	EDMA	AIBN	Acetone	Molinelli et al., 2002
4-VP	EDMA	AIBN	Acetonitrile-THF (3:1)	Zhu et al., 2003*
4-VP	EDMA	AIBN	Acetone	O'Mahony et al., 2006a
4-VP	EDMA	AIBN	Acetone	O'Mahony et al., 2006b
AA	EDMA	AIBN	THF	Xie et al., 2001
4-VP	EDMA	AIBN	Acetone	Weiss et al., 2002
MAA	DEGDA	AIBN	DMF	Xia et al., 2006
AA	TRIM	AIBN	THF	Xie et al., 2003
MAA/ 4-VP	EDMA	AIBN	DMSO & ACN/ DMSO & DMF	Theodoris et al., 2006
AA	EDMA	AIBN	THF	Zhu and Xu, 2003
AAm	EDMA	AIBN	THF	Tian et al., 2011
4-VP	EDMA	AIBN	Acetone	Krska et al., 2005
AAm or DAEM	EDMA	AIBN	Acetone	Kudrinskaya et al., 2009
4-VP	EDMA	ATRP	Acetonitrile	Gam-Derouich et al., 2010
MAA	EDMA	AIBN	THF or ethanol	Batlokwa et al., 2011
MAA	EDMA	AIBN	THF:MeOH (1:3)	Shan and Wang, 2011
AAm	EDMA	AIBN	Acetone	Ding et al., 2006**

*template: piceatannol
**template: epicatechin
2-(dimethylamino)-ethylmethacrylate (DAEM)
atom transfer radical polymerization (ATRP)

2.7. Fate of chromium in the environment

As mentioned earlier, chromium can exist in several oxidation states ranging from -2 to +6. Of these, largely the +3 and +6 oxidation states are most common in soil and groundwater ecosystems. Cr (III) is responsible for metabolism while Cr (VI) is toxic. Hexavalent chromium is considered as a genotoxic, mutagenic and carcinogen to humans and web-biota (Chakraborty and Kumar, 2009) due to its solubility and mobility (Sarin and Pant, 2006). On the other hand, trivalent chromium Cr (III) is considered to be the most thermodynamically stable form of chromium in soil as it can readily precipitate into hydroxides such as iron–chromium hydroxide ($(Fe,Cr)(OH)_3$) and chromium hydroxide ($Cr(OH)_3$) or gets immobilized to soil colloids. The mechanism for the precipitation and adsorption into colloids is governed by the cation exchange capacity, pH conditions, presence, quality and amount of clay-oxides–hydroxides and inorganic carbon (Covelo et al., 2007).

Chromium (VI) is an oxyanion meaning that it is complexed with oxygen ligands and the possible forms are chromate CrO_4^{2-}, bichromate $HCrO_4^-$, and dichromate $Cr_2O_7^{2-}$. Since these oxyanions are not sorbed onto soil colloids under alkaline and sub-neutral conditions Cr (VI) is much more mobile in soils than Cr (III) and therefore Cr (VI) will remain thermodynamically metastable in the pore solution (Leita et al., 2009). It has been known that Cr (VI) can be reduced to Cr (III) by soil organic matter (Bartlett and Kimble, 1976; Banks et al., 2006; Jardine et al., 1999) as well as in the presence of various electron donors (Nakayasu et al., 1999; Palmer and Wittbrodt, 1991). The speciation of chromium is summarized in the Eh-pH diagram (Figure 2.9). The Eh-pH diagrams are very useful for visualizing the stability fields of species and this helps in understanding the chemistry controlling any wastewater environment (Kumar et al., 2011). It can be observed that Cr (VI) exists in almost the entire pH range, particularly at higher oxidising conditions. The existence of Cr (VI) species at higher Eh potential makes it more bioavailable for aquatic life and because of its toxicity, it is a course for concern. Hence, there has been a lot of research directed to the developments of methods for the removal of this toxic substance. However, there are also natural causes or

substances that in a way help for the removal of toxic substances in various complex environments. One particular example of these substances is humic acids (HAs).

Although the subject deducing defined structure of humic acids is still an ongoing debate but it has generally been agreed to that these materials contain aromatic rings, alcohol, amide, amine, carboxylic, carbonyl, phenolic, hydroxyl and quinone functional groups which are all interlinked by flexible carbon chains (Leita et al., 2009). Due to the presence of these multifunctional groups HAs can complex with a range of metals as well as bonding with organic in the environment through various interactions such as hydrophobic, hydrogen, electrostatic and coordination bonding. Depending on the pH of electron donors/acceptors several organic and inorganic contaminants can be reduced either making them more soluble or labile. This clearly demonstrates the influence of HAs on solubility and chemical and biochemical stability of pollutants (Borges et al., 2005; Campitelli et al., 2006; Lubal et al., 1998; Lieta et al., 2009).

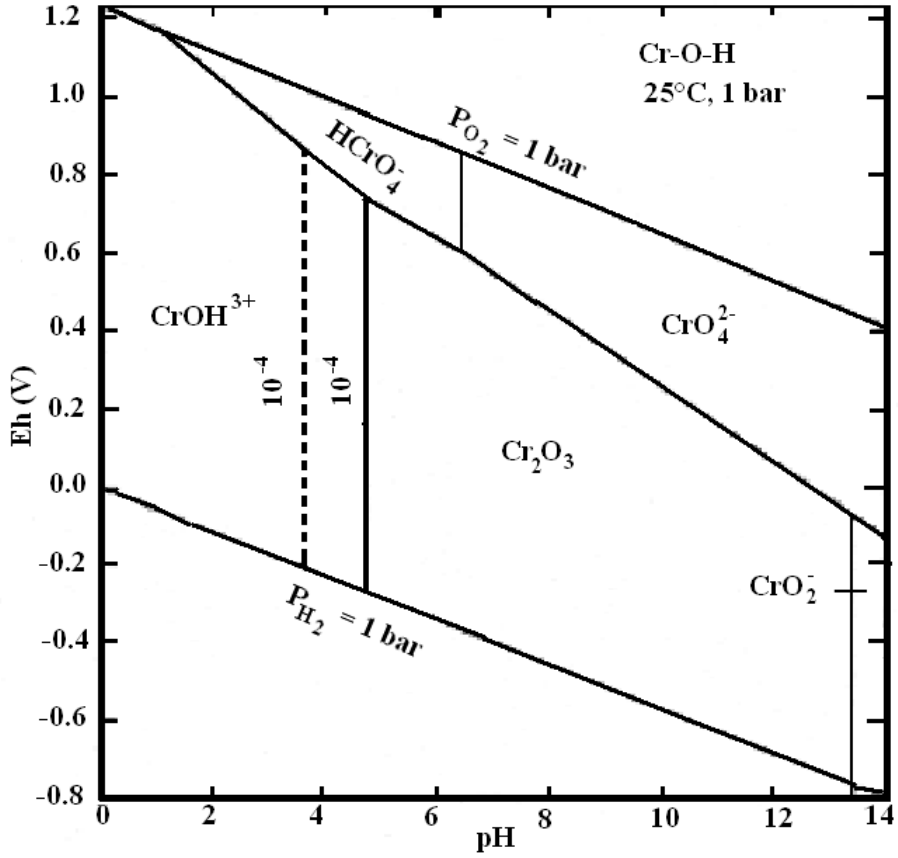

Figure 2.9: Eh-pH diagram of chromium (Brookins, 1988).

2.8. Fate of uranium in the environment

Uranium is a toxic radioactive metal which is generally present in all soil, rock, and water. Human activities such as mining as well as wind, rain and geologic processes are responsible for distribution of uranium in the environment (EPA radionuclides). Uranium may enter human bodies by ingestion of contaminated food or drinking contaminated water or by inhalation; however, most of the ingested uranium is being excreted from the body in the form of faeces and urine (EPA radionuclides). Uranium does not absorb through the skin and alpha particles released by uranium during radioactive decay cannot penetrate the skin (EPA radionuclides). However, some of it might remain in the body, specifically will deposit on the bones and this is because bones contain phosphorus and uranium has high affinity for phosphates (EPA radionuclides; Rufyikiri et al., 2006). As mentioned before, once radionuclides are released into the environment they can accumulate on the upper layer of soils, they can also accumulate of the aquatic systems (Gavrilescu et al., 2009). Figure 2.10 shows a scheme proposed for tracing the movement of radionuclides in soil (Igwe et al., 2005). Uranium in soil can exist in various forms, it can be sorbed both on soil particles and pore water, complexed, precipitated and reduced forms, all of which have various impacts on mobility and fate in the soil environment (Gavrilescu et al., 2009).

Environmental contamination by depleted uranium can occur in soil, water, biota, and as airborne particles. It is known that chemical behaviour of uranium isotopes is relatively similar although their radiological properties differ considerably. Therefore, knowledge about the transformation, transport and fate of natural uranium in the environment can be applied to depleted uranium. In swamps and wetlands where conditions are reducing, U (IV) is the most stable chemical form because it does not readily dissolve in water, hence it remains immobile. However, under oxidizing conditions, such as in shallow water or on the surface of the ground, depleted uranium oxidizes to a form in which it can dissolve and become mobile in water.

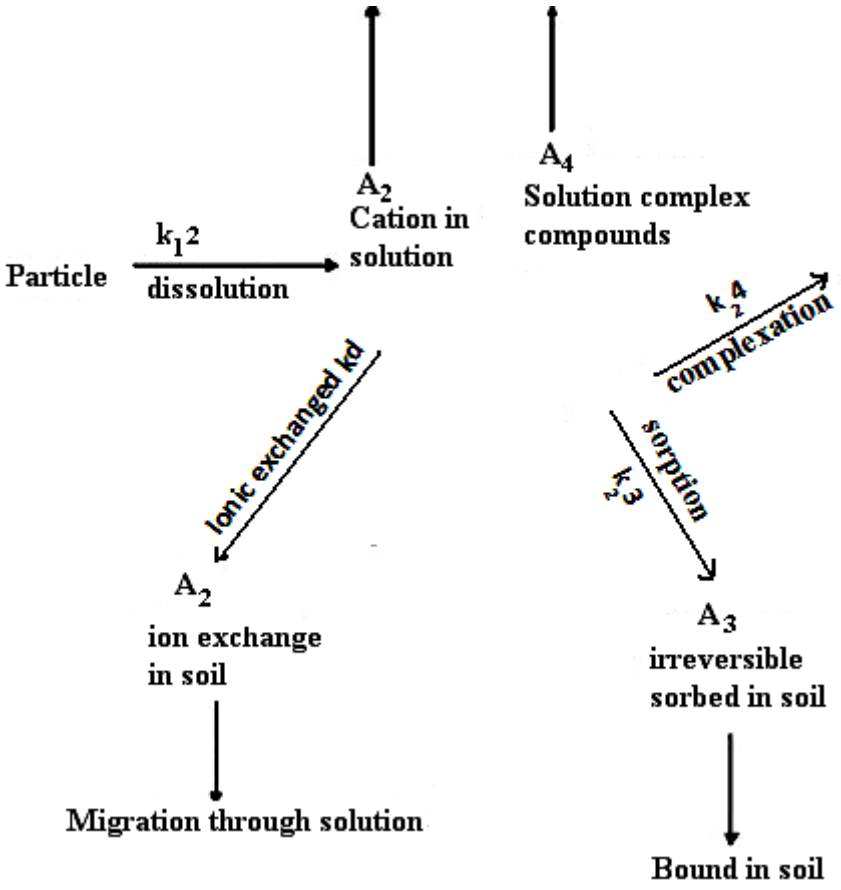

Figure 2.10: Radionuclide transformation processes in soil (ki – reaction rate) (Igwe et al., 2005).

As it was alluded to before that uranium can exist in different oxidation states, hence its speciation in the environment largely depends on pH, concentration, amount of organic and inorganic particularly the presence of carbonates, fluorides, sulphates, phosphates, as well as dissolved carbon and humic acids, soil texture, redox potential and temperature (Gavrilescu et al., 2009; Pavel et al., 2009; Langmuir, 1978). Most soils have a pH of 4-7.5, hence uranium under these conditions will exist in hydrolysed forms and can be uptaken by plants. However, the plants can accumulate very little amount of the soluble forms of uranium, the uranium carbonate complexes and uranyl ion, and these remain the most mobile forms of uranium in the environment (Deutsch and Serne, 1984). Due to its longer half-life of million to billion years, uranium can remain in soluble and exchangeable forms in the environment for a very long time (EPA radionuclides;

Zhu and Chen, 2009; Sheppard and Thibault, 1992; Luo and Gu 2009). On the other hand, part of uranium might remain bound or immobilised in soil and this can be naturally occurring or as a result of remediation technologies such as phytoremediation or use of sorbent materials like polymers including MIPs (Gavrilescu et al., 2009; Huang et al., 1998; James et al., 2009). Three different mechanisms by which uranium can be retained in soils have been outlined as through precipitation reactions, complexation with humous in organic particles and adsorption onto the surface of mineral particles (Gavrilescu et al., 2009; Pavel et al., 2009; Luo and Gu, 2009). The +4 and +6 oxidation states of uranium are the two most common and the stability between these two major oxidation states is influence by redox reactions. For an example, the presence of oxidants such as dissolved oxygen (Gu et al., 2005; Sani et al., 2005; Senko et al., 2002), intermediates of denitrification (nitrite, nitrous oxide, and nitric oxide) (Senko et al., 2002), and/or iron oxyhydroxides (Sani et al., 2005; Zhong et al., 2005) oxidizes U (IV) to U (VI) resulting in mobile uranium whereas the reduction of U (VI) to U (IV) immobilizes uranium (Gavrilescu et al., 2009) although partial oxidation still do occur under these conditions as well (Wan et al., 2005).

pH-Eh diagram showing a typical uranium speciation in groundwater is depicted in Figure 2.11. Like chromium, it is known that uranium contents and its mobility are governed by the oxidation reduction potential (ORP), pH, and the type of complexing agents presents (Langmuir, 1978). These complexing agents can be carbonates, phosphates, vanadates, fluorides, sulphates and silicates. Below is an Eh-pH uranium speciation diagram for U-SO_4^{2-}-H_2O systems as modelled by Tutu et al. (2009). This modelling was based on acid mine surface water with sulphates concentration of about 1000 mg L^{-1}. Also, in the present study sulphate concentrations in the wastewater were found to be around 700 mg L^{-1}. Understanding the processes and the chemistry of uranium species in different environment system allows for remediation of toxic uranium.

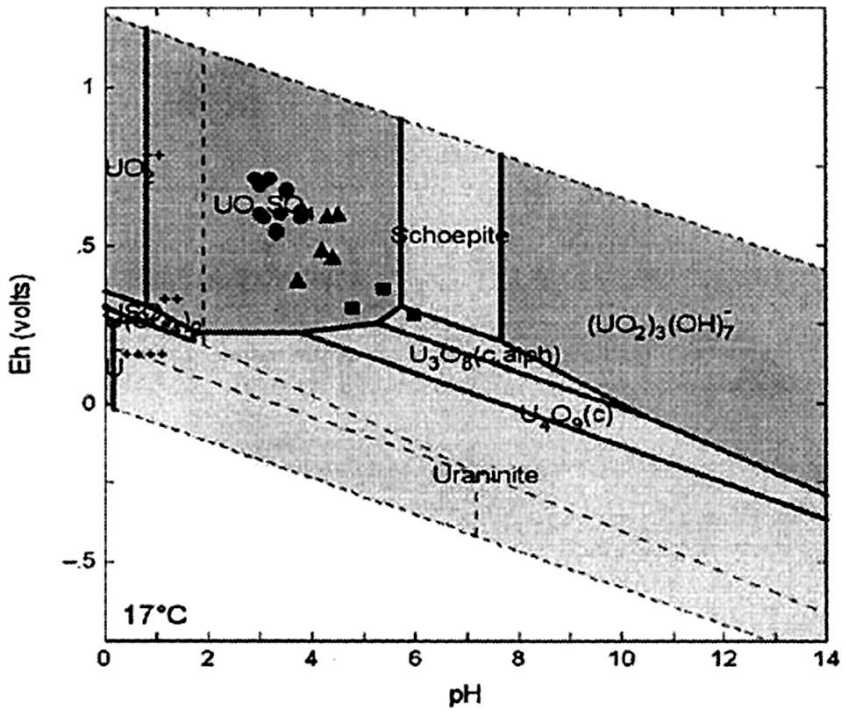

Figure 2.11: Eh-pH diagram showing U-SO_4^{2-}-H_2O system (Tutu et al., 2009).

Figure 2.12 outlines three basic process that can be followed for remediation, namely, separation, concentration, and immobilization or sequestration (Pavel et al., 2009). However, each of the aforementioned fundamental techniques involves a multidisciplinary approach as chemistry, engineering and non-engineering factors such as socio-economic issues have to be taken into consideration before remediation is done (Pavel et al., 2009). Literature has reported numerous groundwater and soil remediation methodologies using *in situ* or *ex situ* technologies (Pavel et al., 2009). *In situ* technologies involve less disturbance of the contaminated area and these are mostly less complicated but more economical. *Ex situ* on the other hand are not very popular for radionuclides such as uranium because of radionuclides are undegradable. This is because *ex situ* requires waste disposal.

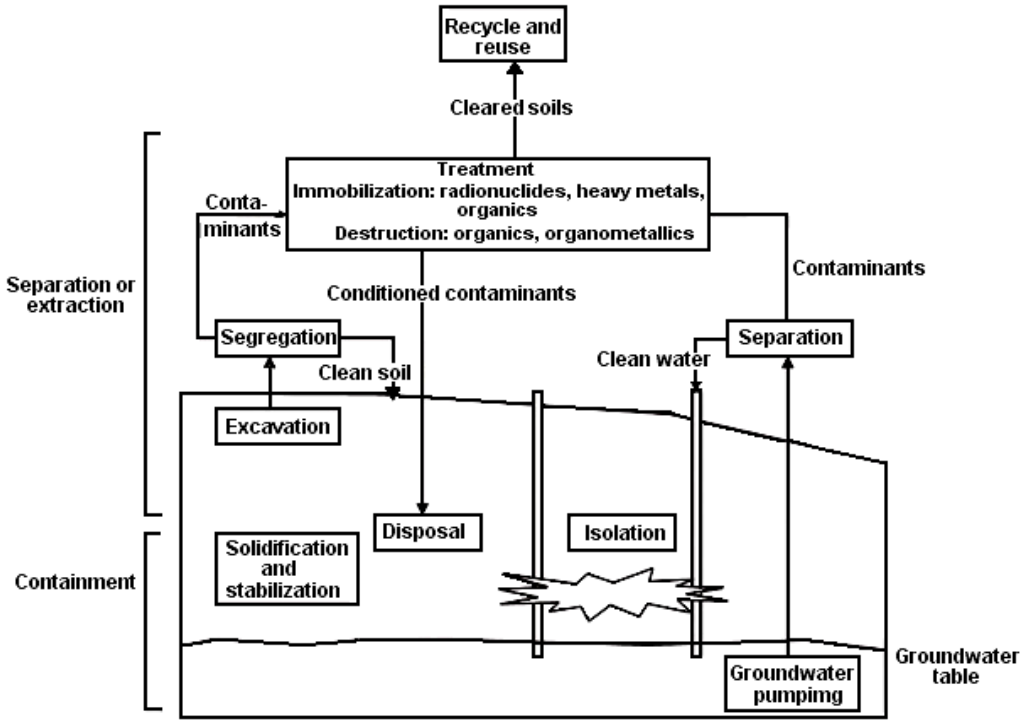

Figure 2.12: Classification of remediation techniques by function (Pavel et al., 2009; Johnson et al., 1999).

2.9. Fate of quercetin in the environment (and in human and animals)

Quercetin, unlike chromium and uranium, its fate and transport in the environment has not received much attention. However, there have been numerous studies on the study of quercetin fate in human and animals following its consumption (Walle et al., 2001). These studies have shown that quercetin is extensively metabolized, with carbon dioxide being the major metabolite (Walle et al., 2001). Other resultant metabolites from microbial degradation in the gastrointestinal tract are excreted in the faeces and urine. It has been established in *in vitro* assays that quercetin is a mutagen, whereas numerous studies on carcinogenicity, genotoxicity and anti-carcinogenicity have not been confirmed quercetin mutagenic properties for *in vivo* assays (Day and Williamson, 1999). Studies by Moon et al. (2008) investigated the stability of quercetin at three different pH's (2.7, 7 and 10) at 4°C, and -20°C. It was generally found that, the stability of quercetin depend on both pH and temperature. Low temperatures and acidic conditions were identified as more conducive to quercetin stability with

protocatechuic acid, phloroglucinic acid, and phloroglucinol identified as primary oxidative degradation products. Similar findings were reported by Schmalhausen et al. (2007), that quercetin auto-oxidized under neutral pH (pH 7.5) aqueous solutions. In addition, these primary degradation products are not expected to result in any adverse effects on human health since these metabolic products results from colonic microbial degradation (Day and Williamson, 1999). Figure 2.13 shows the absorption, metabolism, and excretion of quercetin in mammals.

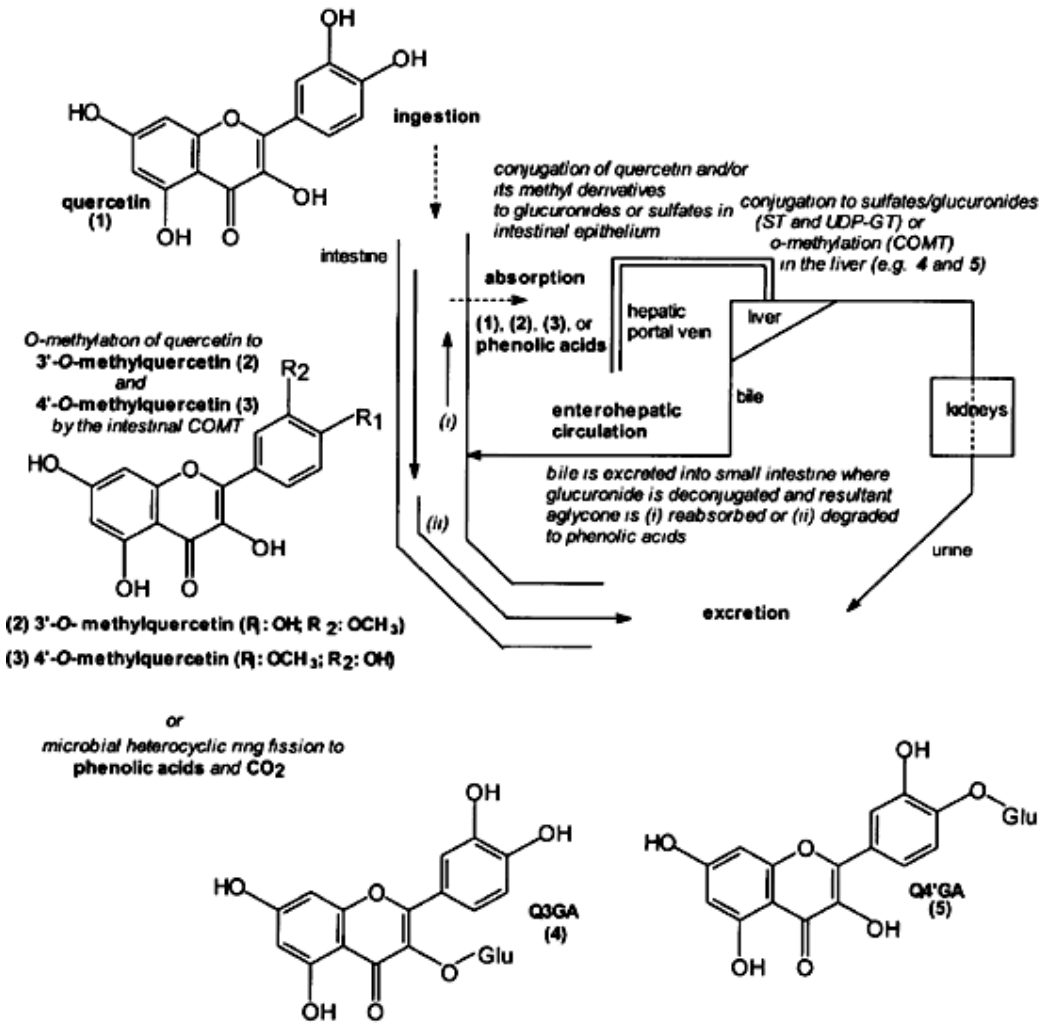

Figure 2.13: Schematic representation of the absorption, metabolism, and excretion of quercetin in mammals (Day and Williamson, 1999).

2.10. Extraction methods

The scope of extraction methods for both organics and metal ions is relatively wide. Listed below are some of the extraction techniques used in analytical sciences (Table 2.6). Liquid-liquid extraction (LLE) is a classical technique which by now forms the basis to which other new techniques are compared. In this technique the sample is partitioned/ distributed between two immiscible liquids or phases in which the compound and matrix have different solubilities. However, depending on the properties of the analyte and the sample matrix, various methods can be used. Table 2.6 shows some of the options available today.

Table 2.6: Classification of extraction techniques

Extraction technique	Type of analyte	Type of sample	Example of analyte	Reference
LLE	organic/metal ion	aqueous	Am(III) and Eu(III)	Bhattacharyya et al., 2011
SPE	organic/metal ion	aqueous	pesticides	Rubio et al., 2008
SPME	organic	aqueous	volatiles	Bianchi et al., 2011
SBSE	organic	aqueous	PPCPs*	Bratkowska et al., 2011
SDME or LPME	organic	aqueous	pesticides	Lambropoulou and Albanis, 2007
PFE or PLE or ASE or PSE	organic	solid	sulfonamide antibiotics	Stoob et al., 2006
MAE	organic	solid	theobromine and caffeine	Gonzalez-Nunez and Canizares-Macias, 2011
MSPD	organic	solid	polychlorinated biphenyls (PCBs)	Criado et al., 2004
SFE	organic	solid	flavanoids	Peng et al., 2006

* polar pharmaceuticals and personal care products (PPCPs)

Recent literature relating to Cr (VI), U (VI) and quercetin extraction from various samples are listed in Table 2.7. It is important to note that although the interest in using adsorption methods for extraction of the mentioned analytes has increased, but other methods are still popular as well. Adsorbents are also not of the same class as others like natural polymers have shown to process very large surface area, which act in their advantage. However, use of IIP/ MIP adsorbents is forever

gaining momentum. This is due to the selectivity and stability of such polymers. Unfortunately, when IIP/ MIPs are used the analyte must be in liquid phase. Meaning that another extraction method is often required to extract the analyte from solid sample into liquid phase before the application of MIP/ IIP. Therefore, in our studies PHWE and Soxhlet extraction were used to achieve that and these will be discussed in more detail below together with the SPE technique.

Table 2.7: Extraction techniques for Cr (VI), U (VI) and quercetin from various complex matrixes

	Type of sample	Extraction technique	Analytical tool	Reference
Cr (VI)	Solid soil-like matrix	SFE	ICP AES	Foy and Pacey, 2000
	Plastics	Organic-assisted alkaline extraction	UV-vis	Kim et al., 2011
	Wastewater	Ion pairing	Spectrofluorimeter	El-Shahawi et al., 2011
	Black, green and herbal teas	Na_2CO_3 leaching	AA	Mandiwana et al., 2011
	Wastewater	SPE	UV-vis	Rajesh et al., 2007
	Sediments	Cloud-point extraction	HPLC-UV	Wang et al., 2010
	Wastewater	ELM	AA	Kumbasar, 2010
	Wastewater	Ionic liquid	HPLC-UV	Ying et al., 2011
U (VI	Groundwater and seawater	DLLME	FI–ICPMS and ICP OES	Chandrasekaran et al., 2011
	Aqueous solution	LLE	UV-vis	Madane et al., 2011
	Aqueous solution	LLE in ILs or chloroform	UV-vis	Shen et al., 2011
	Wastewater	SPE	ICP AES	Zhao et al., 2010a
	Nuclear waste	SFE	-	Zhu et al., 2011a
	Aqueous solution	Biosorption	UV-vis	Liu et al., 2011
	Sediments	Carbonate–bicarbonate extraction	ICP MS	Um et al., 2010
	Sediments	Isotope exchange	Liquid scintillation counter and ICP-MS	Um et al., 2010
Quecetin	Seabuckthorn (Hippophae rhamnoides) leaves	SWE	HPLC-UV	Kumar et al., 2011b
	Leaves of *Rhododendron* species	USE	HPTLC	Sharma et al., 2010
	Hippophaë rhamnoides L. berries	PSFME	LC–MS	Michel et al., 2011
	Oldenlandia diffusa	SPE	HPLC-UV	Zhu and Row, 2011
	Tomato	SPE	HPLC–ESI-QTOF	Vallverdu-Queralt et al., 2011
	Onions	MHG	HPLC-UV	Zill-e-Huma et al., 2011
	Onions	SLE	HPLC-UV	Zill-e-Huma et al., 2011
	Onions	SFE	HPLC-UV	Martino and Guyer, 2004
	Onion, cabbage, carrot, potato	PLE	HPLC-UV	Søltoft et al., 2009
	Onion	SWE	HPLC-UV	Turner et al., 2006

2.10.1. Pressurised hot water extraction (PHWE)

Pressurized Hot Water Extraction (PHWE) is viewed as an assortment of the Pressurized Fluid Extraction (PFE) which is an attractive extraction technique as

it allows fast extraction, small solvent consumption, and automated extraction procedures (Petersson et al., 2010). PFE trade in different names such as Pressurized Liquid Extraction (PLE®), Pressurized Solvent Extraction (PSE®) and Accelerated Solvent Extraction (ASE®) (Petersson et al., 2010). The technique is mostly developed for extraction of organic compounds from solid samples (Table 2.6). Pressurised hot water extraction uses a combination of high water pressure for agitation, and hot water to increase reaction rate. The most important parameters to control are temperature, pressure, effect of additives or modifiers, effect of static (using Dionex ASE 200 unit) or dynamic (using home build oven, Figure 2.14) mode of extraction. Pioneering work on use of PHWE for extraction for polar and some non-polar analytes from soils was first reported by Hawthorne and co-workers in 1994 (Hawthorne et al., 1994), and recently a comprehensive reviews on the technique were published (Kronholm et al., 2007; Teo et al., 2009; Ong et al., 2006). During PHWE the density of water remains almost constant over the temperature range used and this helps to maintain the effects of the pressure on the properties of water to a minimal (Meyer, 1993). During the extraction, superheated water steam may form when there is a drop in pressure while the temperature is above the boiling point, an undesirable effect that has to be guarded against (Teo et al., 2010). One of the interesting features of the PHWE is its feasibility as a green solvent extraction method to extract organic and non-polar compounds from various kinds of matrices (Kronholm et al., 2007; Smith, 2002; Schantz, 2006; Ong et al., 2006; Beek et al., 2009). Fundamental principles for the PHWE to understand are the physicochemical properties of water, the instrumentation and extraction mechanism. Some of the properties of water that are manipulated in PHWE are summarised in Figure 2.14 below.

Water is regarded as the most polar solvent with a high dielectric constant (ε) at room temperature (about 80 at 25°C, Kronholm et al., 2007) and atmospheric pressure due to the presence of extensive hydrogen-bonded structure. However, when the temperature of water is increased, a steady decrease in its viscosity, permittivity and surface tension is observed while its diffusivity characteristic properties increase. Enough pressure is needed to maintain water in the liquid phase at elevated temperature as a result water will start behaving like an organic

solvent. For an example, water at 25°C has a dielectric constant of 80, at 250°C and 50 bar the dielectric constant decreases to 27 which falls in the range between those of ethanol (ε=24) and methanol (ε=33) at 25°C (Teo et al 2009; Zaibunnisa et al., 2009; Roudsari et al., 2009; Zbiral and Nemec, 2009).

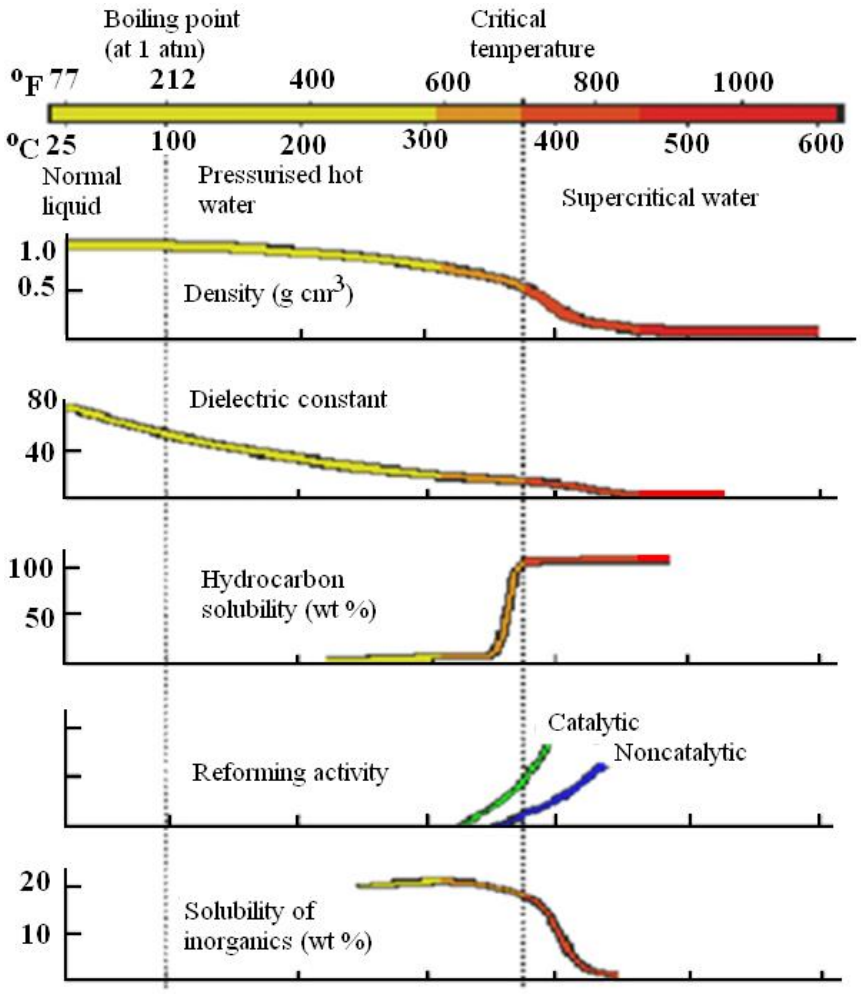

Figure 2.14: Properties of water (Kronholm et al., 2007).

The instrumentation used in PHWE is illustrated in Figure 2.15 which normally consists of stainless steel extraction cells with varying dimensions, GC oven for temperature programming, pump system, sometimes a restrictor to generate backpressure, and the sample collection cell.

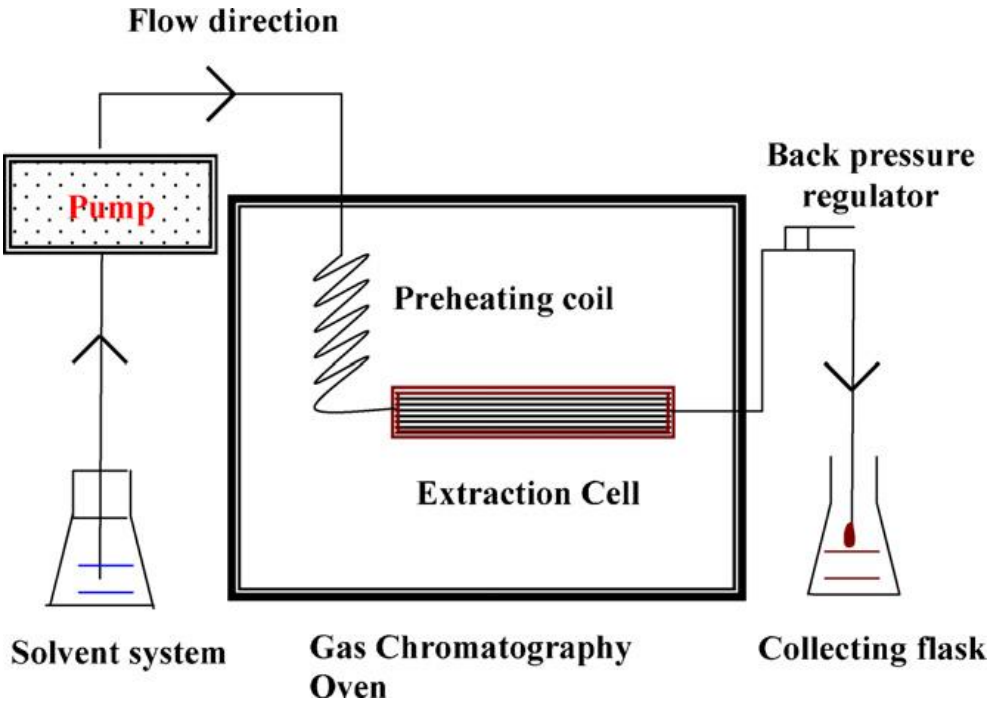

Figure 2.15: Pressurised Hot Water Extraction system setup (Ong et al., 2000).

The mechanism of extraction is postulated to follow four sequential steps (illustrated in Figure 2.16). "The first step is desorption of solutes from the various active sites in the sample matrix under the pressurized and elevated temperature conditions. The second step may involve the diffusion of extraction fluid into the matrix. Next, depending on the sample matrix, the solutes may partition themselves from the sample matrix into the extraction fluid and finally be chromatographically eluted out of the extraction cell to the collection vial" (Kronholm et al., 2007; Ong et al., 2006; Hawthorne et al., 1994).

Two main factors which are attributed to the enhanced extraction efficiencies achieved with PHWE compared to other methods are: (i) due to improved solubility and mass transfer effects and (ii) an increased disruption of surface equilibria at elevated temperatures (Ong et al., 2006). At elevated temperatures, the properties of water are modified resulting in faster diffusion rates due to reduced viscosity and increased capacity of the fluid to solubilize analytes. Under these conditions, better penetration through the matrix particles by water molecules is achieved. Similarly to traditional methods of extraction like Soxhlet,

introduction of fresh water into the system during extraction leads to increased in extraction rates due to improved mass transfer. Surface equilibria is disordered by both temperature and pressure because at increased temperatures the solute–matrix interaction caused by van der Waals forces, hydrogen bonding, dipole attraction of the solutes molecules and active sites in the matrix are disrupted. As a consequence, the thermal energy supplied can dislocate cohesive (solute–solute) and adhesive (solute–matrix) interaction by decreasing the activation energy required for desorption process. The diffusion and convection processes are the driving forces for the transfer of the analytes from matrix to pressurized hot water (Smith, 2002). Nonetheless, degradation of thermally labile compounds at elevated temperatures is another concern. If liquid is used above its boiling point, a sufficient pressure is required to be exerted on it to keep the fluid in its liquid state. An advantage on the use of pressure is that it forces the liquid even to pores that would inaccessible without the use of elevated pressure providing better extraction for those analytes trapped in matrix pores (Richter et al., 1996).

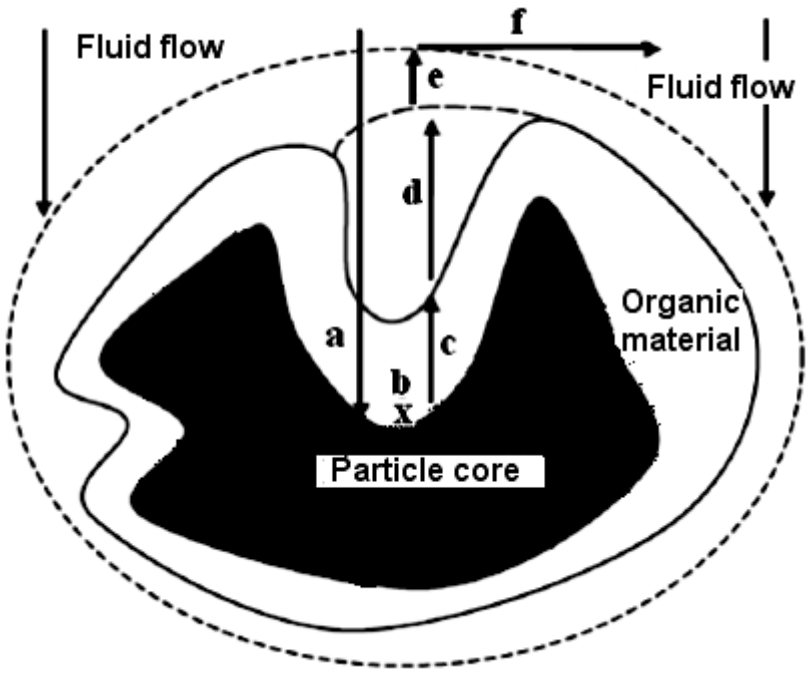

Figure 2.16: Schematic representation showing proposed extraction steps in PHWE: (a) rapid fluid entry; (b) desorption of solutes from matrix active sites; (c) diffusion of solutes through organic materials; (d) diffusion of solutes through static fluid in porous materials; (e) diffusion of solutes through layer of stagnant

fluid outside particles; and (f) elution of solutes by the flowing bulk of fluid (Ong et al., 2006).

Extraction steps for PHWE

PHWE experiments can either be performed in a dynamic mode at a constant flow or static extraction with the Dionex ASE 200 unit. Both systems consist of an extraction cell and a collection cell. Pre-treatment of the plant samples including either plain air- or freeze-drying is sometimes desirable. After drying, the samples are ground to a certain sample size range usually 100–1000 μm or just sieved through a 2 mm sieve. Plant materials ground to smaller sizes are advantageous in that, shorter diffusion paths can give rise to easier and faster transportation of analytes to the surface of the particle (Ong et al., 2006).

During extraction of plant materials in PHWE, the following steps are taken into consideration:-

• Due to the tendency of plant materials to adsorb water, precautionary measure like mixing the plant material with sand before extraction is needed. This is achieved by thoroughly mixing high portion of sand with plant material to be extracted in a glass tube followed by transferring these contents to an extraction cell and filling up any voids with more sand. This setup helps to prevent blockages of the system (Ong and Len, 2003a; Ong and Len, 2003b; Ong and Len, 2004). Nevertheless, when organic solvent such as methanol is used for extraction, mixing of the plant material with sand is not required. The following are the steps used in PHWE:

• Plant materials are loaded into the extraction cell.

• Extraction cell is filled with the water and the cell is set to certain values.

• Extraction cell is heated in an oven to the set values.

• Extracting the plant materials for a certain time with dynamic or static extraction. For dynamic extraction, the pump will be set at a constant flow rate of 0.5–2.0 mL min^{-1}.

• In dynamic extraction, the fluid coming out of the extraction cell is collected in the collection vial as shown in Figure 2.15. However, using Dionex ASE 200 unit

(static extraction), the fluid is flushed out from the extraction cell to the collection vial using a suitable gas.

• Appropriate pre-concentration and clean-up procedures are sometimes needed for the aqueous extract from PHWE (Ong et al., 2006).

Turner group has been advocating for use of PHWE method for extraction of quercetin from food and plant material such as onion (Turner et al., 2006, Lindahl et al., 2010). Ko et al. (2011) have also demonstrated the used of SWE for the extraction of quercetin from onion waste.

2.10.2. Solid phase extraction

2.10.2.1. General introduction

As described by Poole (2003), solid phase extraction (SPE) basically involves the partitioning of selected analytes between the sample matrix into a solid sorbent. The sample matrix can be a gas, fluid or liquid phase. SPE is used primarily when matrix removal (separation), trace enrichment (pre-concentration) and medium exchange (transfer from the sample matrix to a different solvent or gas phase) are desired (Camel, 2003; Liska, 2000). A typical application is when SPE is used as a clean-up procedure before a chromatographic or other analytical method is used for quantification of the analyte(s) in the sample. Hence, the advantages of SPE over other conventional extraction methods include use of low volumes of solvent; high recoveries and good reproducibility; applicability to a wide variety of sample matrices; automation; fine tuning selectivity. Nonetheless, it also has disadvantages like greater cost per sample; method development can be time consuming; wide range of chemistries (*i.e.*, many choices to manipulate the solvent and pH conditions).

2.10.2.2. Principles and theory

The major trait of SPE is that analytes are transferred from the matrix to the sorbent. Once in the sorbent, the analytes get trapped/ retained for the duration of the sampling process. After the sampling process has lapsed, the analytes are recovered/ isolated from the solid phase by elution using a liquid or fluid, or by

thermal desorption into the gas phase (Poole, 2003). However, the elution can be carried out in 3 different phases depending on the goal of the extraction. These phases are:

(i) Bind-elute strategy

This is the most commonly used strategy. In this case analytes bind to the sorbent together with matrix components. Firstly, the matrix components are washed off with a suitable solvent or mixture of solvents leaving behind the analyte molecules. The last step is the elution of analytes using a proper solvent. In some cases, pre-concentration of elute solution by evaporation is required before HPLC or GC analysis.

(ii) Interference removal strategy

In this case all the unwanted matrix components are retained on the sorbent and only the analytes pass through during the sample loading stage. This is much quicker than the above method as it eliminates the matrix washing step but the selectivity can be compromised.

(iii) Fractionation strategy

This is a much longer process than the above two but very similar to the first method only that after the analytes have been retained, different classes of compounds are sequentially eluted by modifying eluant pH or the concentration of organic solvent.

Understanding the retention mechanism can also help in terms of choosing the right elution strategy for particular analytes. Generally, the sorbents are classified into 4 main categories, *viz.*, reversed-phase, normal-phase, ion-exchange, and adsorption.

Reversed phase involves use of non-polar modified solid phase and polar liquid phase. The types of interactions that can exist between the analyte and solid phase-liquid phase are hydrophobic interactions which could be due to nonpolar-nonpolar interactions or dispersion forces.

Normal Phase involves use of polar modified solid phase and nonpolar liquid phase. Hydrophilic interactions of the analyte with the sorbent and liquid phase could be due to polar-polar interactions, hydrogen bonding, pi-pi interactions, dipole-dipole interactions, and dipole-induced dipole interactions.

Ion Exchange is a result of electrostatic attraction of charged group on compound to a charged group on the surface of the sorbent.

A***dsorption*** is generally due to hydrophobic and hydrophilic interactions which may be a result of interactions of compounds with unmodified materials.

It is also desired that the type of sorbent to be used for analysis be chosen such that it does not have strong interactions with the analyte of interest. This is because, the stronger are these interactions the larger volumes of elution solvent will be required. Figure 2.17 gives some suggested solid sorbent materials to use when facing a problem of extracting analytes with known log P values from complicated matrices (Agilent Technologies). These are just general guidelines from which one can improve upon. The sorbents used are described below as they are only given in market names in the figure. SampliQ WAX (weak anion exchange) – is a polymeric resin with neutral primary amine modified divinylbenzene polymer. This is suitable for retention of acids, neutral and most importantly strong acidic compounds like sulphonates. SampliQ SCX (strong cation exchange) – is a sulphonic acid modified divinylbenzene polymer suitable for retention of weak bases.

SampliQ OPT (optimized polymer technology) – is an amide modified divinyl benzene polymer resin suitable for retaining chemicals with a wide range of properties *e.g.*, basic, acidic, neutral, hydrophilic and organic soluble compounds. SampliQ WCX (weak cation exchange) – has a carboxylic acid functionality in hydrogen form designed to retain and release strong bases such as quaternary amines. SampliQ SAX (strong anion exchange) – is a tertiary amine modified divinylbenzene polymer resin suitable for retaining both acidic and neutral compounds on a wide range of hydrophobicity (log P). Besides these, other stationary phases are known, *e.g.*, those based on C_{18} (capped or uncapped), cyano products, amines, silica, unfunctionalized divinylbenzene *etc*.

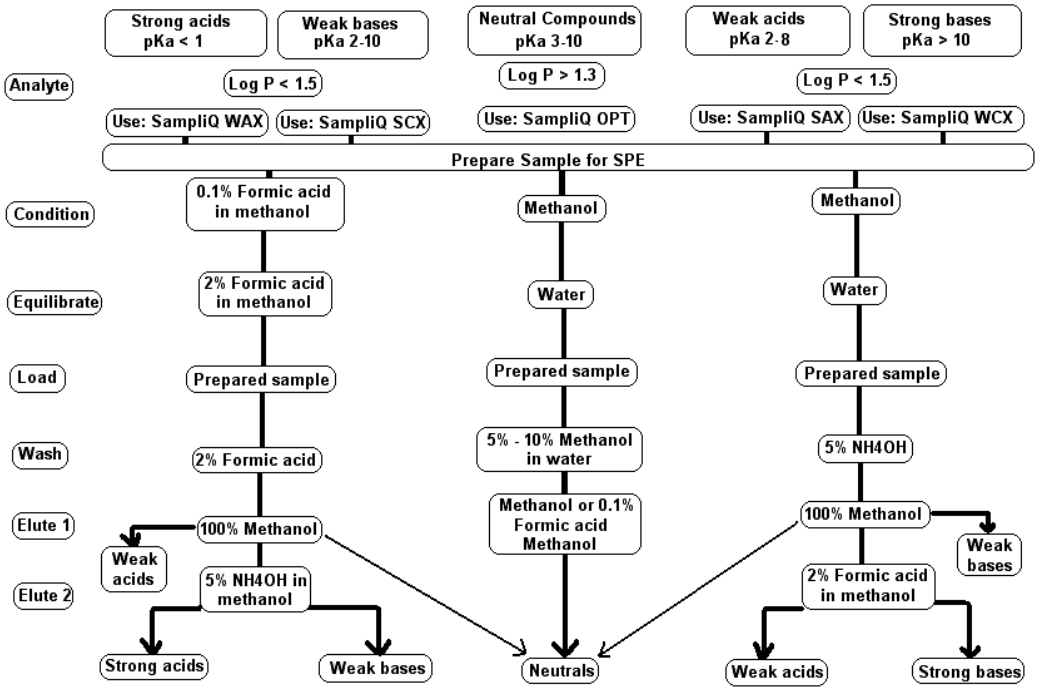

Figure 2.17: Some suggested guidelines for SPE method development (Majors, 2009).

2.10.2.3. SPE steps

SPE method is generally composed of five steps, namely, wetting of sorbent, precondition/equilibration, loading of sample, washing off of interferences, and elution of analyte (Figure 2.18). For optimum performance of the technique each step offers an opportunity to be manipulated.

(i) Sample pre-treatment

The pre-treatment of the sample depends on the analyte of interest, sample matrix, and nature of retention chemistry perceived to be used. These could involve adjustment of pH, dilution, filtration, addition of buffers, *etc*. In some cases the analyte of interest is in solid sample, then in that case extraction into liquid phase, centrifugation *etc* might be required.

(ii) Conditioning/ equilibration

The conditioning is achieved by passing a suitable solvent through the SPE material to *wet* the bonded functional groups on the sorbent. Proper *wetting* ensures consistent interaction of the analytes with sorbent. Equilibration refers to

treating the sorbent with a solution that is similar to the sample matrix in terms of polarity and pH. This also maximizes the retention of analytes.

(iii) Sample load

A certain volume of the sample is introduced into the SPE format. Depending on the strategy chosen as detailed in Section 2.10.2.2., otherwise during this step the analytes of interest are bound/ extracted onto the sorbent/ liquid phase, respectively.

(iv) Washing

Washing involves using a suitable solvent to selectively remove unwanted matrix interferences which were co-extracted with the analyte. This solvent should be chosen so that the analytes are not extracted during this stage.

(v) Elution

The analytes of interest are extracted from the solid phase using an appropriate solvent, in many cases a much stronger one than that used for washing. This is to ensure that the primary and secondary retention interactions between sorbent and analytes of interest are disrupted. It is best to choose a solvent that can allow direct injection of elute into an analytical technique. However, if required evaporation and reconstitution of the eluant with mobile phase can be done prior to analysis (optional).

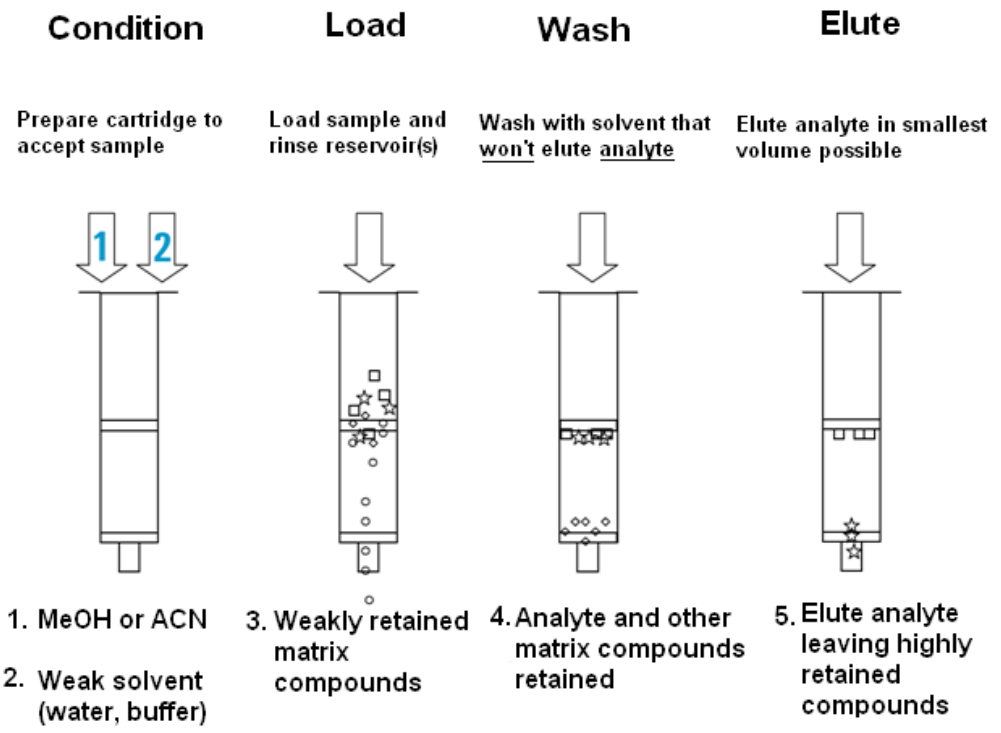

Figure 2.18: Diagram showing SPE procedure (Agilent Technologies).

2.10.2.4. Breakthrough volume

One of the problems of SPE is the analyte passing through the SPE sorbent during loading stage unnoticed. The causes of this sample-processing problem could be attributed to the limited sorption capacity of sorbents as well as analyte displacement or plugging of sorbent pores by matrix components (Poole, 2003). Overloading of sorbent with sample can also lead to this problem. In chemistry terms, the point referred above is called breakthrough volume. Breakthrough volume has been defined by many authors in different ways. Some of these definitions are quoted below.

Poole (2003) defined breakthrough volume as "the sample volume which can be loaded on the sorbent bed without the loss of the analytes; or the sample volume over which the analytes are eluted by the sample matrix". Other researchers defined it as "the sample volume that can be loaded onto an SPE bed providing a given ratio of outlet to inlet analyte concentration at a given temperature" (López, et al., 2007; Ortega et al., 2001). Hennion (1999) defined it as the maximum sample volume which can be applied with a theoretical 100% recovery. "The

volume of sample which has to flow through the sorbent in order to obtain a percent of retention of 99–95%" (Ferrer et al., 1997).

Besides the parameters mentioned above, flow rate applied during sample percolation can also affect how the analyte bond to the sorbent, that is, breakthrough volume. Too fast a flow rate might result in analytes not binding to the solid phase, hence low recoveries. An ideal optimized method will have as high breakthrough volume as possible. Therefore, proper control of the flow rate during sample load is equally important as controlling the flow rate for the other stages. This is because during sample loading you want to give the analytes enough time to interact with the sorbent. However, faster flow rates during matrix removal step can lead to dirty extracts as the matrix will be incompletely removed. While faster flow rates during elution step might result in inadequate elution of analyte. Therefore, flow rates should be specified in all SPE protocols inorder to ensure reproducibility of experiment from one analyst to analyst or between laboratories.

Breakthrough volume curves are plotted as a relationship between the concentration in the effluents and total volume of sample passed through the sorbent. In frontal chromatography breakthrough occurs when the capacity of the sorbent has been exhausted. From the breakthrough volume curves plotted, the breakthrough volume (V_B) and number of theoretical plates (N) can be calculated as expressed in equations 2.1 and 2.2, respectively.

$$\boldsymbol{V_B = V_R - 2\sigma_V} \qquad \textbf{(2.1)}$$

where, V_R is the retention volume and can be determined graphically from the breakthrough curve diagram as well as the σ_V value (Figure 2.19). V_R corresponds to 0.5 of the average value of maximum analyte concentration in the effluent (C_E).

$$\boldsymbol{N = \frac{V_R(V_R - \sigma_V)}{\sigma_V^2}} \qquad \textbf{(2.2)}$$

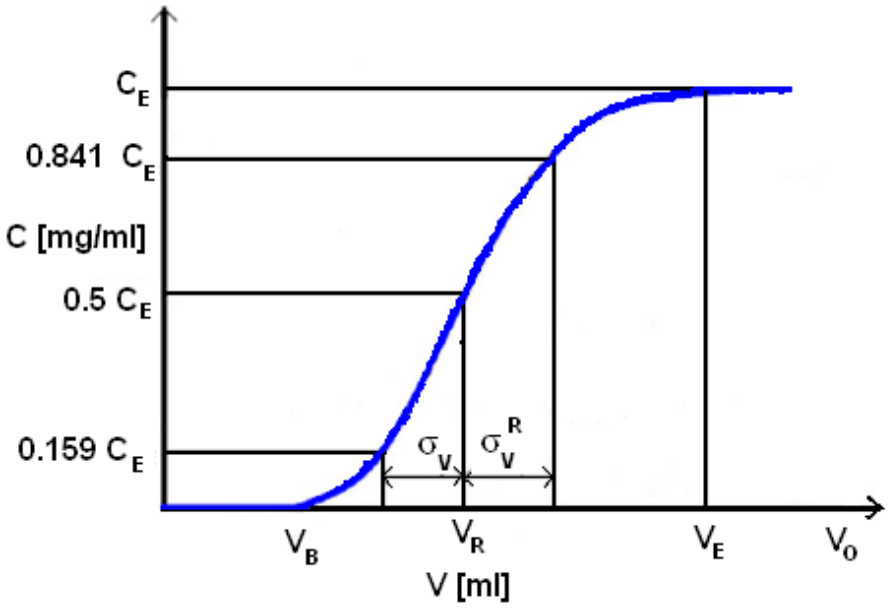

Figure 2.19: Typical breakthrough curve (Bielicka-Daszkiewicz and Voelkel 2009).

2.10.2.5. Types of formats

Ever since the inception of the SPE technique various formats have emerged. These are SPE tubes in the form of cartridges, SPE disks, pre-column, batch, SPE funnel, and pipette tips. Among these, cartridges are the most popular maybe because they are easy to handle. All these are available commercially with different packing matrices. Pictures of these formats are shown in Figure 2.20.

Figure 2.20: Various SPE formats (Supelco; Sigma-Aldrich).

The technique can be applied in both online and offline mode where the solid sorbent is packed in a cartridge or just pipette needles. The online flow injection approach offers advantages such as high sample throughput, improved precision, low sample and reagent consumption, reusability and green concept (Prasada Rao et al., 2006).

A typical SPE vacuum manifold instrumentation that can take up to twenty samples simultaneously is shown in Figure 2.21.

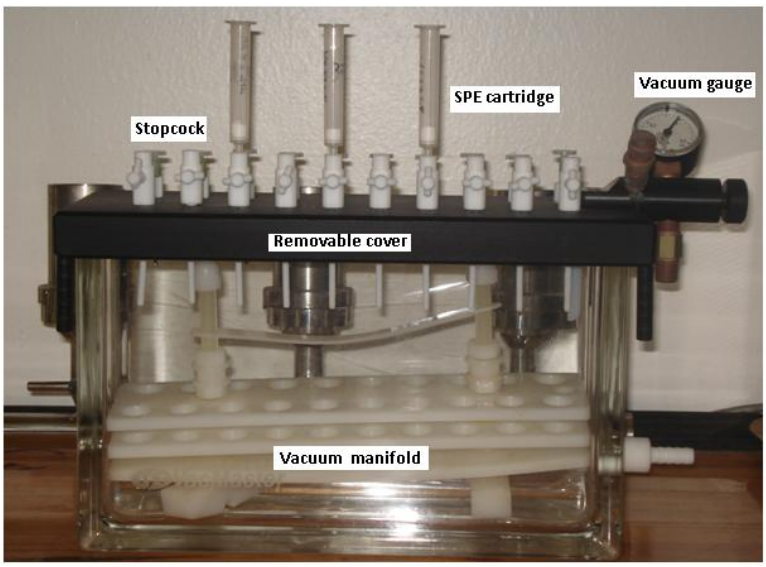

Figure 2.21: Twenty port vacuum manifold for SPE extraction unit**.**

2.10.2.6. Types of sorbents

Solid sorbents used with SPE can be grouped into three categories; (i) inorganic-based ones, these include silica gel (SiO_2), alumina (Al_2O_3), magnesia (MgO) and other oxide species, (ii) organic based ones these are natural polymers, synthetic polymers such as ion-imprinted polymers, and (iii) inorganic–organic hybrid materials *e.g*., C_{18}-silica (Rao et al., 2006) (Figure 2.22).

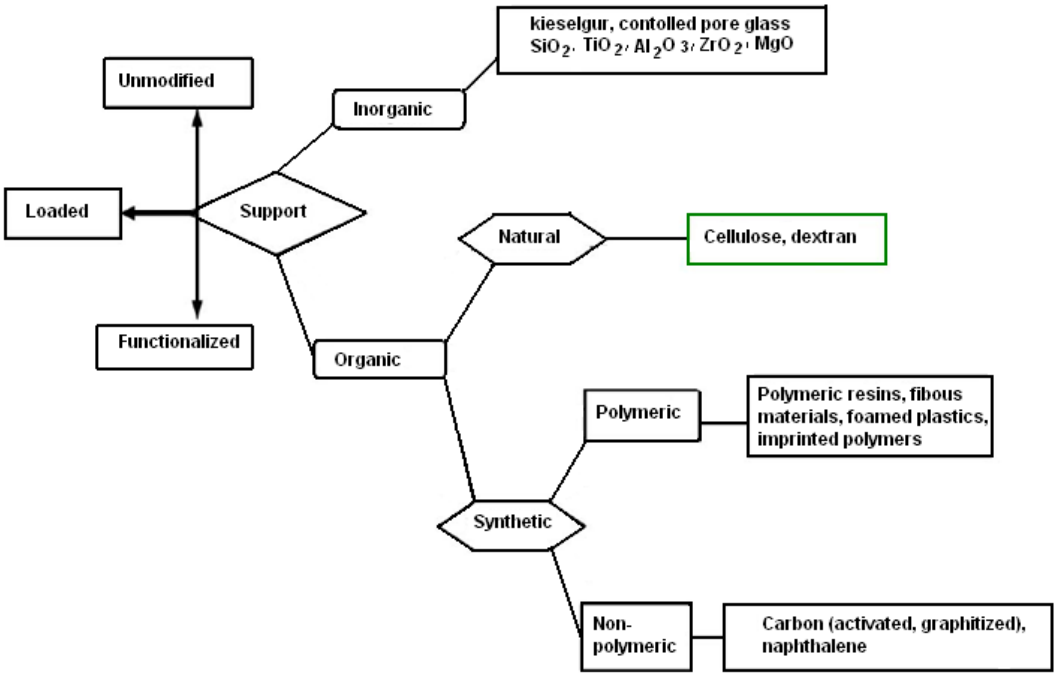

Figure 2.22: Types of solid-phase extraction sorbents (Rao et al., 2006).

Commercially, numerous sorbents are available and this provides the SPE with its high selectivity compared to traditional methods like LLE. Below is an example of sorbents marketed by Supelco and some details as to for which analytes and sample matrix can they be used (Table 2.8).

Table 2.8: More details on the types of organic SPE sorbents commercialized by Supelco (Supelco, Bulletin 910)

Reversed Phase	**Silica-Based Packing – 40µm particles, 60Å pores (unless otherwise noted).**		
	LC-18	octadecyl bonded, endcapped silica	For reversed phase extraction of nonpolar to moderately polar compounds, such as antibiotics, barbiturates, benzodiazepines, caffeine, drugs, dyes, essential oils, fat soluble vitamins, fungicides, herbicides, pesticides, hydrocarbons, parabens,
	ENVITM-18	octadecyl bonded, endcapped silica	Higher phase coverage and carbon content than LC-18, greater resistance to extreme pH conditions, and slightly higher capacity for nonpolar compounds. For reversed phase extraction of nonpolar to moderately polar compounds, such as antibiotics, caffeine, drugs, dyes, essential oils, fat soluble vitamins, fungicides, herbicides, pesticides, PNAs, hydrocarbons, parabens, phenols, phthalate esters, steroids, surfactants, water soluble vitamins. Also available in
	LC-8	octyl bonded, endcapped silica	For reversed phase extraction of nonpolar to moderately polar compounds, such as antibiotics, barbiturates, benzodiazepines, caffeine, drugs, dyes, essential oils, fat soluble vitamins, fungicides, herbicides, pesticides, hydrocarbons, parabens, phenols, phthalate esters, steroids, surfactants, theophylline, and water soluble vitamins. Also
	ENVI-8	octyl bonded, endcapped silica	Higher phase coverage and carbon content than LC-8, greater resistance to extreme pH conditions, and slightly higher capacity for nonpolar compounds. For reversed phase extraction of barbiturates, benzodiazepines, caffeine, drugs, dyes, essential oils, fat soluble vitamins, fungicides, herbicides, pesticides, PNAs, hydrocarbons,
	LC-4	butyldimethyl bonded, end-capped silica (500Å pores)	Less hydrophobic than LC-8 or LC-18. For extraction of peptides and proteins.
	LC-Ph	phenyl bonded silica	extraction of nonpolar to moderately polar compounds, especially aromatic compounds.
	HisepTM	hydrophobic surface enclaved by a hydrophilic network	For exclusion of proteins in biological samples; retains small molecules such as drugs under reversed phase conditions.
Normal Phase	LC-CN	cyanopropyl bonded, endcapped silica	For reversed phase extraction of moderately polar compounds, normal phase extraction of polar compounds, such as aflatoxins, antibiotics, dyes, herbicides, pesticides,
	LC-Diol	diol bonded silica	For normal phase extraction of polar compounds.
Ion Exchange	LC-NH_2	aminopropyl bonded silica	For normal phase extraction of polar compounds, weak anion exchange for carbohydrates, weak anions, and organic acids.
	LC-SAX	quaternary amine bonded silica with Cl- counterion	For strong anion exchange for anions, organic acids, nucleic acids, nucleotides, and surfactants. Capacity: 0.2meq/g.
	LC-SCX	sulfonic acid bonded silica with Na+ counterion	For strong cation exchange for cations, antibiotics, drugs, organic bases, amino acids, catecholamines, herbicides, nucleic acid bases, nucleosides, and surfactants.
	LC-WCX	carboxylic acid bonded silica with Na+ counterion	For weak cation exchange of cations, amines, antibiotics, drugs, amino acids, catecholamines, nucleic acid bases, nucleosides, and surfactants.
Adsorption	LC-Si	silica gel with no bonded phase	For extraction of polar compounds, such as alcohols, aldehydes, amines, drugs, dyes, herbicides, pesticides, ketones, nitro compounds, organic acids, phenols,
	Alumina-Based Packing – Crystalline, chromatographic grade alumina, irregular particles, 60/325 mesh.		
	LC-Alumina-A	acidic pH ~5	For anion exchange and adsorption extraction of polar compounds, such as
	LC-Alumina-B	basic pH ~8.5	For adsorption extraction of polar compounds, and cation exchange.
	LC-Alumina-N	neutral pH ~6.5	For adsorption extraction of polar compounds. With pH adjustment, cation or anion exchange. For extraction of vitamins, antibiotics, essential oils, enzymes, glycosides, and hormones.
	Florisil®-Based Packing – Magnesium silicate, 100/120 mesh particles.		
	LC-Florisil		For adsorption extraction of polar compounds, such as alcohols, aldehydes, amines, drugs, dyes, herbicides, pesticides, PCBs, ketones, nitro compounds, organic acids, phenols, and steroids.
	ENVI-Florisil*		For adsorption extraction of polar compounds, such as alcohols, aldehydes, amines,drugs, dyes, herbicides, pesticides, PCBs, ketones, nitro compounds, organic acids, phenols, and steroids.
	Graphitized Carbon-Based Packing – Nonbonded carbon phase.		
	ENVI-Carb	nonporous, surface area 100m2/g, 120/400 mesh	For adsorption extraction of polar and nonpolar compounds.
	ENVI-Carb C	nonporous, surface area 100m2/g, 120/400 mesh	For adsorption extraction of polar and nonpolar compounds.
	Resin-Based Packing – 80-160µm spherical particles		
	ENVI-Chrom P**		For extraction of polar aromatic compounds such as phenols from aqueous samples. Also for adsorption extraction of nonpolar to midpolar aromatic

* SPE tubes that are packed with this material contain stainless steel or Teflon® frits, required by US Environmental Protection Agency Contract Laboratory Program (CLP) pesticide methods.

** Highly crosslinked, neutral, specially cleaned styrene-divinylbenzene resin. Very high surface area, mean pore size 110-

2.10.2.7. Method development strategies for SPE

Method development is crucial for optimum performance of any SPE technique. Few pointers need to be addressed before any method development is carried out. These include knowledge about the sample matrix, analyte Log Po/w, pKa(s), and functional groups on analyte and sorbent to be used. Therefore, after all these investigation, an appropriate SPE phase should be chosen based on an understanding of the sample matrix and influence that the analyte(s) functional groups might have on solubility, ionization state and polarity. Also, the understanding of how the analyte(s) might behave on the sorbent in response to changing extraction conditions. The analyst must manipulate the above conditions in order to meet the defined sample preparation objectives. A correct sorbent has to be chosen in accordance with the matrix and analyte. Below is also a summary of the sorbent materials and sample matrices on which the sorbents have better performance (Table 2.9). These might help in choosing the right sorbent. Figure 2.23 gives a pattern that can be followed for method development strategies in SPE.

Table 2.9: Sorbent to help with method development (Supelco-Aldrich)

	Reversed phase	Normal phase	Ion exchange
Retention mechanism	**Non-polar hydrophobic interactions** * van der Waals dispersion forces	**Polar interactions** * Hydrogen bonding, pi-pi, dipole-dipole, and induced dipole-dipole	Electrastatic attraction of charged functional groups of the analyte(s) to oppositely charged functional groups on the sorbent. Combination of reversed-phase and ion-exchange for mixed-mode
Sample Matrix	**Aqueous samples** * Biological fluids (serum, plasma, urine) * Aqueous extracts of tissues * Environmental water samples * Wine, beer and other aqueous samples	**Non-polar samples** * Organic extracts of solids * Very non-polar solvents * Fatty oils, hydrocarbons	Aqueous or organic samples of low salt concentration (<0.1 M) * Bological fluids * Solution phase synthesis reactions
Analyte characteristics	**Analytes exhibiting non-polear functionalities** * Most organic analytes * Alkyl, aromatic, alicyclic functional groups	**Analytes exhibiting polar functionalities** * Hydroxyl groups, carbonyls, amines, double bonds * Hetero atoms (O, N, S, P) * Functional groups with resonance properties	* Use cation-exchange for isolating basic compounds: primary, secondary, tertiary, and quartenary amines * Use anion-exchange for isolating acidic compounds: carboxylic acids, sulphonic acids, and phosphates
Elution scheme	**Disrupt reversed-phase interaction with solvent or solvent mixture of adequate non-polar character** * Methanol, acetonitrile, dichloromethane * Buffer/ solvent mixtures	**Polar interactions disrupted with a more polar solvent or solution** * Acetonitrile, methanol, isopropanol * Combinations of buffer/ solvent or solvent/solvent mixtures	Electrostatic interactions disrupted via: * pH modification to neutralize compound and / or sorbent functioal groups * Increase salt concentration (>1 M); or use a more selective counter-ion to compete for ion exchange binding sites
Common applications	* Drugs and metabolites in biological fluids * Environmental pollutants in water * Aqueous extracts of tissues and solids	* Clean-up of organic extracts of soils and sludge * Fractionation of petroleum hydrocarbons * PCBs in tranformer oil * Isolation of compounds in cosmetics	* Drugs of abuse and pharmaceutical compounds in biological fluids * Fatty acids removal in food/ agricultural compounds * Clean-up of synthetic reactions * Organic acids from urine * Herbicides in soil

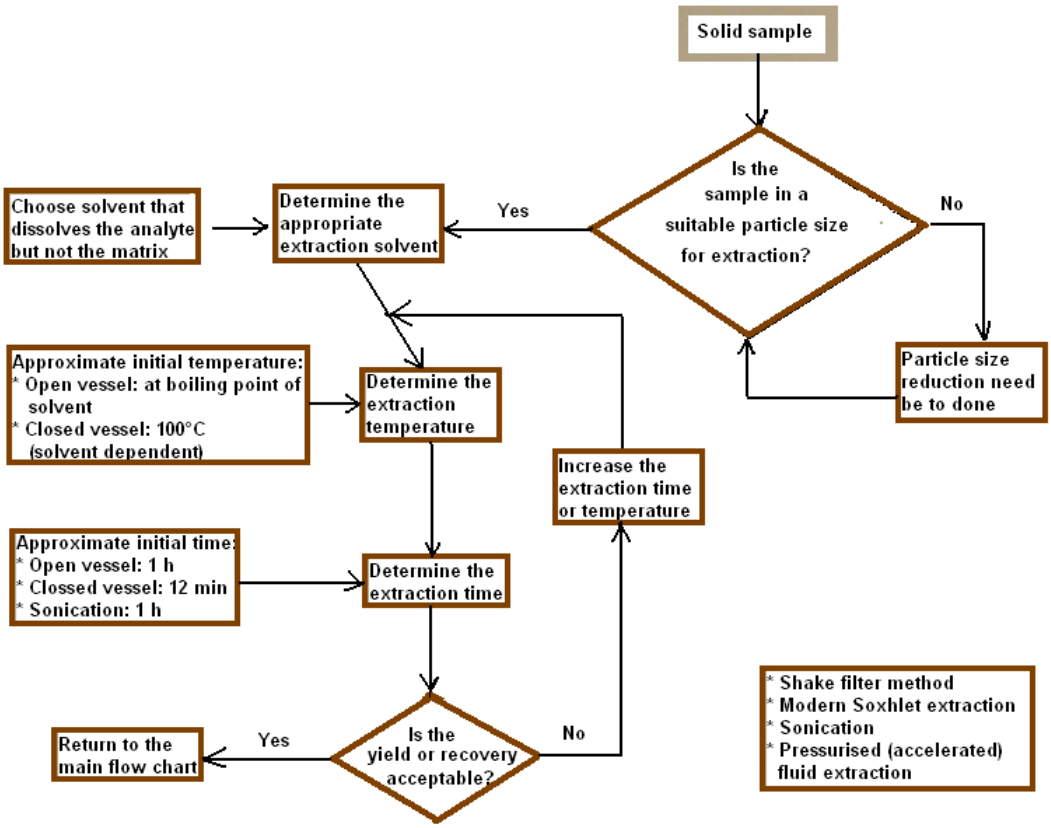

Figure 2.23: SPE method development strategies.

Besides the sorbents listed above, other sorbents that might be used with SPE include immunoassays, restricted access memory and molecularly imprinted polymers. More details on the application of MIPs in SPE, a technique referred to as molecularly imprinted solid-phase extraction (MISPE), are given below.

2.10.2.8. Molecularly imprinted solid-phase extraction (MISPE)

Molecular imprinted polymers (MIPs), sometimes referred to as plastic antibodies are also used as packed sorbents for extraction of a variety of analytes. As discussed previously, these polymers offer high selectivity due to the memory effects they possess for the target/ imprint molecule. MIPs can be used with a variety of SPE formats, *e.g.*, cartridge, batch or column. In Table 2.10 below are some of the examples for the application of SPE technique for the extraction of flavonoids from different samples.

Table 2.10: Applications of SPE on extraction of flavonols

Sample	Analyte	Sorbent	Analytical method	Reference
Wine	Quercetin	MIP*	HPLC-UV	Theodoridis et al., 2006
Wine	Rutin	MIP	HPLC-UV	Theodoridis et al., 2006
Bee honey	Glycocyl flavonoids	C18	HPLC-DAD-MSn/ESI	Truchado et al., 2011
Bee honey	Rutin, quercetin, kaempferol	C18, Oasis HLB, Strata X, Amberlite XAD-2	HPLC-DAD	Michalkiewicz et al., 2008
Grape	Kaempferol, quercetin	C18	HPLC-UV	Dopico-García et al., 2007
Human plasma and urine	Quercetin, kaempferol	Oasis HLB	HPLC-UV	Ishii et al., 2003

* more other examples are on Table 2.5

2.10.2.9. Batch extractions

Batch extraction is one of the oldest SPE extraction techniques known. By batch extraction we refer to the case where extraction is carried out in small reaction vessels where the solid adsorbent is stirred/shaked/swirled with extraction liquid, containing the analytes to be adsorbed, at room temperature or at controlled temperature for a specified time. Filtration is required to separate the liquid and solid materials. Un-adsorbed analytes can be measured from the liquid and adsorbed analytes are obtained by leaching or washing out the sorbent with appropriate solutions followed by measurement of analytes in solution using a suitable analytical tool.

2.10.3. Soxhlet extraction

Soxhlet extractor, first invented in 1879 by Franz von Soxhlet, is a piece of laboratory apparatus that can be used for extraction of solid samples. Soxhlet is among the oldest extraction techniques such that it has become a *de facto* standard to which newly developed solvent extraction techniques are compared against. In Soxhlet extraction the sample to be extracted is placed inside a thimble made from thick filter paper. The extraction solvent is contained in a flask which is placed on a heating source. The solvent is heated to reflux and the hot vapours are condensed to liquid dripping back into the thimble. This process continues until

the Soxhlet chamber is almost full, then the chamber is automatically emptied by a siphon side arm, with the solvent running back down to the distillation flask. The cycle may be allowed to repeat over hours or days. This technique is more appropriate to use when the desired compound of interest has a limited solubility in a solvent, and the impurity is insoluble in that solvent such that only the compound of interest is extracted leaving impurities with the solid samples. The process is simple, effective and inexpensive but can be very unselective and needs longer extraction times. If desired, the solvent can be removed after extraction by using a rotary evaporator to yield the extracted compound.

However, in some cases the technique may be used to remove some impurities from the solid materials (an example is the extraction of templates in MIP synthesis). Hence, in this particular case the solid material will be the desired product. A more modified version of Soxhlet extraction is the automated Soxtec^{TM} extractor (FOSS, 2006). Its advantage is that the sample is in contact with the boiling liquid during extraction giving higher extraction efficiency and shorter extraction times. Also, many samples can be processed simultaneously. However, the amount of organic solvent used is still much higher compared to other sample preparation techniques. A diagram of a classical Soxhlet extraction tool and a schematic representation of the modified Soxtec version are shown in Figure 2.24.

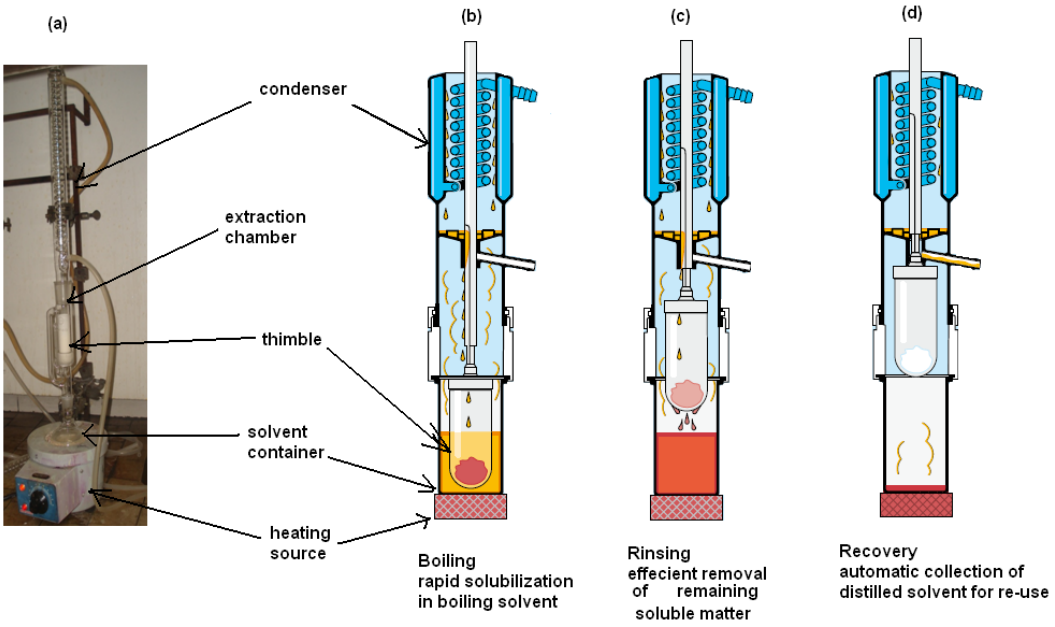

Figure 2.24: Typical Soxhlet apparatus setup used in our laboratory (a), and an automated Soxtec apparatus, (b), (c), (d) (FOSS, 2006).

2.11. Determination techniques

2.11.1. Liquid chromatography

The use of chromatographic methods dates back to early 1900. Although Michael Tswett is largely credited with the invention of chromatographic methods as he used chromatography for the separation of leaf pigments on a polar solid phase, Robinson (1959) demonstrated that chromatographic methods were used even before Tswett's time. Interestingly, during this time the technique was only limited to applications where the distribution was only between a solid stationary and a liquid mobile phase (Liquid Solid Chromatography, LSC). It was only after 1958 that the technique was refined by Stahl and developed into the technique that is being used today (Stahl, 1959). The term chromatography is used as an inclusive term to refer to a set of laboratory techniques used for the separation of mixtures. A range of chromatographic methods are known but the major classification is that of liquid chromatography, ion chromatography, gas chromatography, capillary electrophoresis chromatography and supercritical fluid

chromatography. This classification is based on the type of mobile phase in chromatographic technique. Only high-performance liquid chromatography or high-pressure liquid chromatography (HPLC) and ion chromatography will be detailed because they were used in this study. HPLC is a chromatographic technique that allows separation of a mixture of compounds based on their solubilities and idiosyncratic polarities on the stationary phase and mobile phase. This technique is mostly used in analytical chemistry and biochemistry to identify, quantify and purify the individual components of the mixture. An HPLC system is normally composed of the following compartments; a column packed with stationary phase inside, a pump that moves the mobile phase(s) and analyte through the column, and a detector that provides a characteristic retention time for the analyte. A data projector like computer collects the chromatogram where identification and quantification are made. Usually analytes have specific retention times depending on the strength of their interactions with the stationary phase, the ratio or composition of mobile phase solvent(s) used, and the flow rate of the mobile phase. Therefore, retention times are used for analyte identification. Depending on the type of material packed inside the column as a stationary phase, HPLC can be regarded as normal-phase chromatography and reversed-phase chromatography.

2.11.1.1. Normal-phase chromatography

In normal-phase HPLC, the stationary phase is made from polar materials with functional groups such as amino, cyano or silica while the mobile phase is non-polar (*e.g.,* dichloromethane or hexane). The idea in HPLC is that the analyte should be more soluble in the mobile phase than in the stationary phase. In normal-phase chromatography, usually the least polar component is eluted first and hence if the polarity of the mobile phase is increased results in shorter elution time as the analyte would be more soluble in the mobile phase ("like dissolves like principle"). Normal-phase chromatography is normally used for fairly polar analytes (non-ionic water-soluble analytes) and the interactions are based on electrostatic attractions. Most applications in liquid chromatography are now

performed in reversed-phase mode. This is because normal liquid chromatography has slow equilibration times and therefore, seen as tedious.

2.11.1.2. Reversed-phase chromatography

In reversed-phase chromatography, the stationary phase is non-polar usually made from siliceous material bonded to long-chain hydrocarbons *e.g.*, C_{18} or C_8 which can be capped or endcapped. The mobile phase is polar *e.g.*, methanol–water mixture, acetonitrile-water system or tetrahydrofuran. Contrary to normal-phase, in reversed-phase the most polar component is eluted first and it is used when an analyte of interest is non-polar. Hence, increasing the polarity of the mobile phase increases the elution time. Reversed phase operates on the principle of hydrophobic interactions which results from the repulsive forces between a relatively polar solvent, the relatively non-polar analyte, and the non-polar stationary phase (used for non-polar, water-insoluble analytes). Reversed-phase chromatography has been widely used in analytical separations including in the separation of a range of polyphenols such as quercetin from a mixture of other flavonoids (Olszewska, 2008; Zu et al., 2006).

2.11.1.3. Mobile phase

Modern HPLC systems allow for a use of one or more solvent reservoirs. When one solvent reservoir is used, the system is said to be isocratic as the mobile phase composition is kept constant. Isocratic elution is also achieved even if two solvent reservoirs are used. The only requirement is that, the ratio of the two solvents should be kept constant. Nevertheless, the use of two reservoirs allows for gradient elution where two or more solvent systems with differing polarities are used. Gradient elution allows for a variation of the composition of mobile phase periodically. Addition of small percentage of volatile acids such as acetic acid, formic acid or trifluoric acid to the mobile phase as well as buffers can improve the selectivity of certain analytes as these will play a significant role on the analyte retention due to the pH effect. The composition of the solvents can be

changed gradually during the experimental run. In both methods, it is important that the solvent is purged and filtered before the analysis. This process can be carried out manually or online during runs.

2.11.1.4. Pumping system

High pressure pumps are required in HPLC for the pumping of mobile phase through the column for traversing of analytes. Reciprocating, pneumatic or peristaltic pumps can all be used in HPLC systems. The pump should be able to generate up to 6000 psi (approximately 414 bar) of pressure, flow rates between 0.1 – 10 mL min^{-1} and resist corrosion by a variety of solvents.

2.11.1.5. Sample injection system

The use of sample loop for the introduction of sample is the most common and is the integral part of liquid chromatography. Loops come in sizes ranging from 5-500 µL. The sample loop is connected to two ports of the three-way valve injector. One port is connected to the mobile phase while the other is connected to the column and two ports for sample loop waste during loading and injection. During loading the sample *i.e*., when the injection valve is on ”load” the sample loop is in suspension for the mobile phase. Meaning that, the mobile phase is not passing through the loop but rather goes straight to the column. However, when the injection is switched to “inject” position the mobile phase goes through the loop and transports the sample to the column for separation. System should be able to achieve some degree of reproducibility of injections and some systems may have autosamplers incorporated in them. Figure 2.25 below depicts how the valves are interchangeable during loading and injection of sample in HPLC.

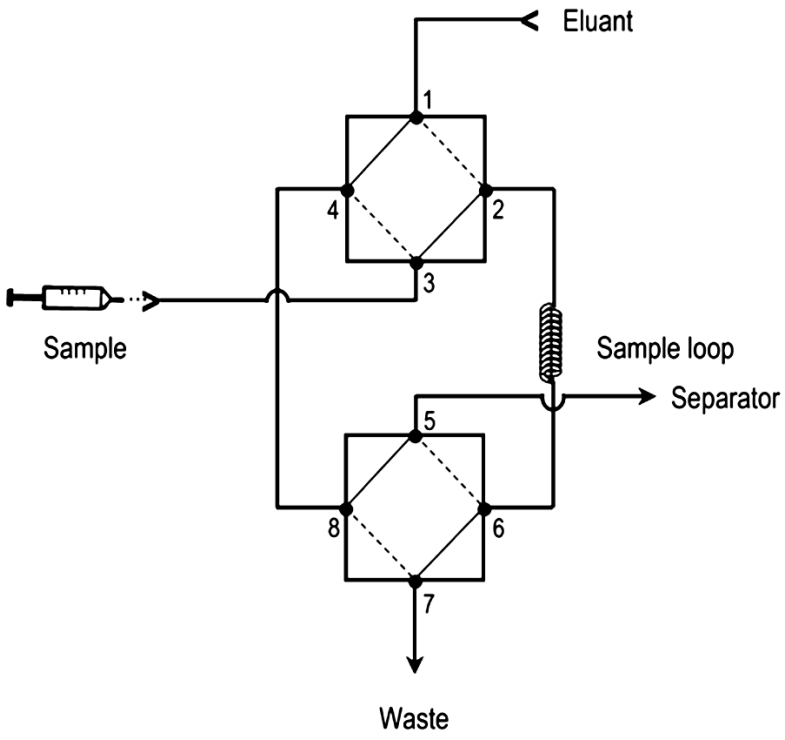

Figure 2.25: Loading position of sample loop (Weiss and Weis, 2005).

2.11.1.6. Columns and guard columns

Columns come in different sizes and different packing materials normally in the range of 3-10 µm. Columns with minimal solvent consumption are desired due to higher costs of high purity solvents used. The finnier the particle size the more pressure will be needed to push the analytes through the column. Guard column is placed between the sample introduction port and the analytical column in order to improve the life of the analytical column by trapping particulate matter before it reaches the column. One other important factor is that both the guard column and analytical column should be of the same stationary phase otherwise lose of analyte due to adsorption might occur. Some HPLCs are fitted with column thermostats for the adjustment of the column temperature during analysis.

2.11.1.7. HPLC detectors

In HPLC analysis, a detector, which is connected to the end of the column, is a very important component as it provides the response signal due to the eluting sample. Detector should be small and compatible with the liquid flow. There are several detectors that are compatible with HPLC but the choice to use depends on the nature of the analyte of interest. Possible detectors that can be used with HPLC are listed in Table 2.11.

Table 2.11: Showing possible detectors for an HPLC system (Settle, 1997; Yeung and Synovec, 1986)

HPLC detector	Mass LOD (typical)	Linear range (decades)
Absorbance	10 pg	3-4
Conductivity	100 pg - 1 ng	5
Electrochemical	100 pg	4-5
Element selective	1 ng	4-5
Fluorescence	10 fg	5
FTIR	1 μg	3
Light scattering	1 μg	5
Mass spectrometry	<1 pg	5
Optical activity	1 ng	4
Photoionization	<1 pg	4
Refractive index	1 ng	3

Among the listed detectors, ultraviolet (UV) detectors which measure the ability of a sample to absorb light at one or more wavelengths are the most commonly used and these will be discussed in detail. UV detectors can be used for both organic and inorganic compounds. Specifically for organic compounds wavelengths of 254 nm and 280 nm are most commonly used as these are the lines where most organic functional groups absorb light. However, some organic compounds like quercetin absorb at two different wavelengths, that is, 250 and 350 nm (Lindahl et al., 2010), where the bands at 250 nm and 350 nm are attributed to the presence of the benzoyl chromophore and the cinnamoyl chromophore, respectively, of the quercetin molecule (Shan and Wang, 2011). The diagram illustrates how a typical HPLC system is allied (Figure 2.26). The mechanism of how a UV-vis detector works are discussed below in the form of UV-vis spectrophotometers.

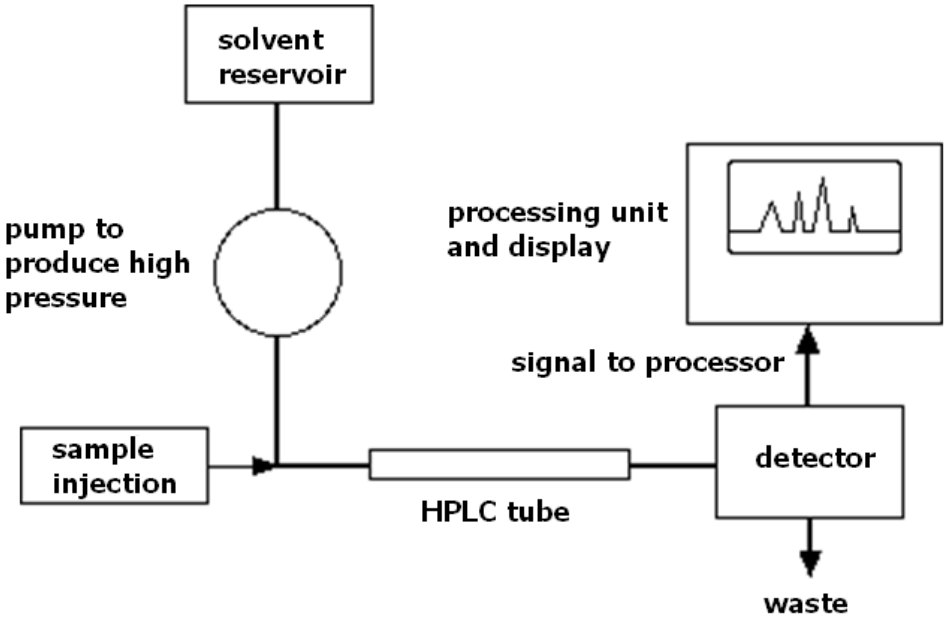

Figure 2.26: Schematic representation of an HPLC system (Clark, 2007).

(i) Ultra violet-visible range detection

A UV/vis spectrophotometer can itself be used as a detector for HPLC. In such case, the response given by the presence of an analyte is assumed to be proportional to the concentration. However, for more accurate results, the instrument's response to the analyte in the unknown should be compared with the response to a standard; an approach similar to the use of calibration curves. The response (*e.g.*, peak height) for a particular concentration is known as the response factor. For organic molecules, valuable information as to determining the types of functional groups on the molecule can be obtained through correlation of the wavelengths of absorption peaks with the types of bonds in a given molecule (Misra et al., 2002).

During UV/vis spectrophotometer determinations, the intensity of light passing through a sample (I) is measured and compared to the intensity of light before it passes through the sample (I_o). The ratio I/I_o is called the *transmittance*, and is usually expressed as a percentage (%T). The absorbance, A, is the measure of the transmittance as illustrated in the equation 2.3 below:

$$A = -\log_{10}(\%T / 100\%) \quad (2.3)$$

A configuration to them UV-visible spectrophotometer to measure the reflectance is also possible. In this case, the intensity of light reflected from a sample (I) is measure and compared to the intensity of light reflected from a reference material (I_o) (such as a white tile). Similarly, the ratio I/I_o will be called the *reflectance* in this case, and is usually expressed as a percentage (%R).

More commonly, a photodiode detector or a charge-coupled device (CCD) is used in UV-visible spectrophotometer as detection devices. The use of monochromators with photodiodes allows for the filtration of the light so that only light of a single wavelength reaches the detector. However, the diffraction gratings used with CCDs allow for the collection of light of different wavelengths on different pixels. Commercial UV-vis absorption spectrometers use one of the three overall optical designs; (i) a fixed or scanning spectrometer with a single light beam and sample holder, (ii) scanning spectrometers with dual light beams and dual sample holders for simultaneous measurement of P and Po, (iii) non-scanning spectrometer with an array detector for simultaneous measurement of multiple wavelengths. In an array-detector instrument, all wavelengths pass through the sample and the dispersing element is between the sample and the array detector.

(ii) Absorption of light by UV-Vis spectroscopy

In UV-vis absorption spectrometry, a beam of light from a suitable source passes through the prism then through the sample to the detector (in case of single-beam instrument). However, in case of double-beam the light gets reflected to the sample cell then pass through to the detector. In the ultraviolet-visible spectroscopy region (uv = 200-400 nm, visible = 400-800 nm) molecules undergo electronic transitions. Of particular interest are the transitions which involve π-orbitals and lone pairs (n = non-bonding). The lowest energy transition is the one that is between the **h**ighest **o**ccupied **m**olecular **o**rbital (HOMO) and the **l**owest

unoccupied **m**olecular **o**rbital (LUMO) in the ground state. EM radiation absorbed by the sample excites an electron in the outer orbital to the LUMO thereby creating an excited state. In Figure 2.27, the gap between HOMO and LUMO, ΔE, is dependent on the degree of conjugation of the system analyzed. That is, the more highly conjugated the system is, the smaller the ΔE, hence the lower the frequency and longer the wavelength, λ. In organic molecules, the part of the compound responsible for absorption for a certain colour is called a chromophore and these are most commonly due to C=C (π-π*) and C=O (n-π*) systems (Hunt, University of Calgary). Importantly, when dealing with organic compounds, proper choice of solvent is required as not all organic solvents are suitable for use in UV spectroscopy due to their tendency to absorb light at most wavelength and the fact that the polarity and pH of the solvent can affect the absorption spectrum of an organic compound under investigation. A typical example is the observed increase in absorption maxima and molar extinction coefficient of tyrosine when pH is increased from 6 to 13 or when polarity of the solvent is decreased.

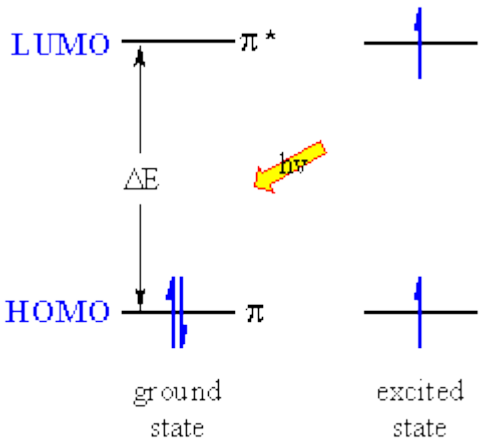

Figure 2.27: Showing excitation of electron (Hunt, University of Calgary).

Hence, UV-vis spectroscopy is used for identifying conjugated systems which tend to have stronger absorptions (Hunt, University of Calgary). Nevertheless, UV/vis spectroscopy is also used in routine quantitative determination of solutions of transition metal ions and biological macromolecules. In contrast to fluorescence spectroscopy which deals with transitions from the excited state to

the ground state, in ultraviolet-visible spectroscopy transitions due absorption of the molecules from the ground state to the excited state are measured (Skoog et al., 2007). The UV/vis technique is generally more suitable for quantitative measurements rather than sample identification.

In transition metal ion solutions, the *d* electrons within the metal atoms are accessible for excitation from one electronic state to another. In such case, the colour of metal ion solutions is strongly affected by the presence of other species, such as certain anions or ligands. Typical example is the intensification of the light blue copper sulphate solution colour and the shift in wavelength of maximum absorption (λ_{max}) due to addition ammonia. Interestingly, the colours generated by charge transfer complexes are often too intense to be used for quantitative measurement.

For quantitation purposes, the Beer-Lambert law which relates the concentration of an analyte in solution to the absorbance at a certain wavelength is applied (Ingle and Crouch, 1988). The Beer-Lambert law states that the absorbance of a solution is directly proportional to the path length and the concentration of the absorbing species in the solution. This means that, if the path length of the cell is known then, the concentration of the absorber in a solution can be determined by UV/vis spectroscopy. However, more importantly is the knowledge of understanding how quickly the absorbance changes with concentration. References of molar extinction coefficients tables as well as the use of calibration curves (which are more accurate) can be used as indicators for the changes of absorption with concentration.

The Beer-Lambert law is given by the following equation:-

$$A = \log_{10}(I_0/I) = \varepsilon.c.L \qquad (2.4)$$

where A is the measured absorbance, I_0 is the intensity of the incident light at a given wavelength, I is the transmitted intensity, L the path length through the

sample, and *c* the concentration of the absorbing species. For each species and wavelength, ε is a constant known as the molar absorptivity or extinction coefficient. This constant is a fundamental molecular property in a given solvent, at a particular temperature and pressure, and has units of 1/*M*cm* or often *AU*/*M*cm*. Although the Beer-Lambert Law is useful for characterization of many compounds but it does not hold as a universal relationship for the concentration and absorption of all substances.

(iii) Instrumentation

Spectrophotometers generally consist of a light source from which a given wavelength or wavelength range is selected by using a selection device. The radiation selected is then directed to the analytical sample to be analysed and the transmitted light is monitored by a detector. The intensity of the light measured by the detector is then compared with that transmitted by the reference sample. The ratio of these transmissions is recorded on the readout device usually as % transmittance. Typical layout of the single-beam and double-beam spectrophotometer is illustrated in Figure 2.28 and 2.29. In a single beam instrument all of the light passes through the sample cell and the I_o is measured by removing the sample. This was the earlier of the two designs, however, it is still very much common use in both teaching and industrial labs. In a double-beam instrument, the light is split into two beams before it reaches the sample (Figure 2.29). One beam is used as the reference while the other beam passes through the sample. The intensity of the reference beam is taken as 100% Transmission (or 0 Absorbance), and the measurement displayed is the ratio of the two beam intensities. Several arrangements of double-beam instruments are possible, such as having two photodiodes detectors where the sample and reference beam are measured at the same time. Whilst in other instruments, the two beams pass through a beam chopper where one beam is blocked at a time. The detector alternates between measuring the sample beam and the reference beam at the same rate with chopper (Skoog et al., 2007). The dual-beam instruments have largely superseded the single-beam instruments because in the double beam instrument it is possible to eliminate the instability and drift resulting from temporal differences in scanning the reference and the sample.

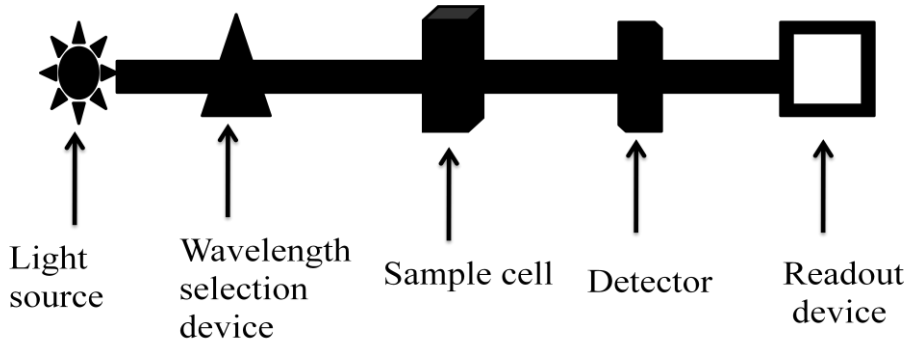

Figure 2.28: Typical layout of single-beam spectrophotometer.

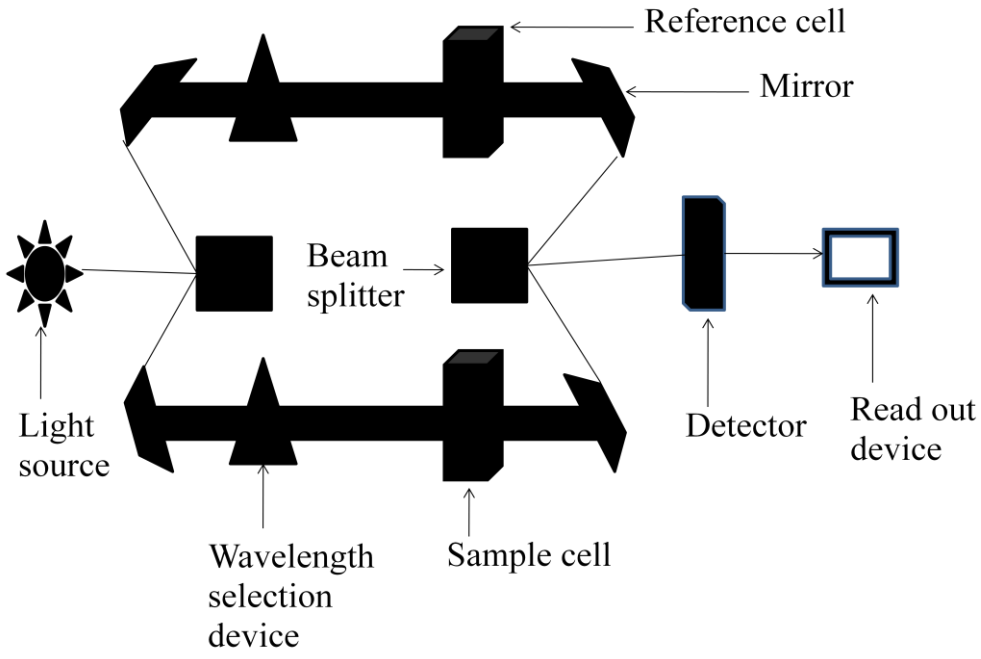

Figure 2.29: Typical layout of double-beam spectrophotometer.

2.11.2. Ion chromatography

Ion chromatography (IC), sometimes referred to as ion-exchange chromatography is a chromatographic process where ions and polar molecules can be separated based on their charge. The technique is applicable for almost any kind of charged molecule including large proteins, amino acids and small nucleotides. Contrary to

HPLC which retains analytes based on the solubilities between the stationary phase and the mobile phase, the IC retains analytes on the column based on coulombic (ionic) interactions. That is, the ionic interactions between the ions of the solute and counter ions that are situated in, or on the stationary phase.

Small, Stevens, and Bauman are credited for introducing ion chromatography (IC) as a new analytical method around 1975 (Willis, 2002). As from then, the technique has evolved from being used as a new detection scheme for a few selected inorganic anions and cations to a versatile analytical technique for ionic species in general (Weiss and Weiss, 2005). IC is equipped with a "suppressor" column which is connected between the analytical column and the conductivity detector. The function of the suppressor column is to chemically reduce the conductivity of the eluant background (mobile phase), while at the same time increasing the electrical conductance of the analyte ions (Weiss and Weiss, 2005).

The column is usually packed with a stationary phase containing ionic functional groups (R-X) on the surface that interact with analyte ions of opposite charge. These functional groups on the surface can either be positively charged or negatively charged, in such case the technique will be called anion exchange chromatography and cation exchange chromatography, respectively. In essence, cation exchange chromatography retains positively charged cations because the stationary phase displays a negatively charged functional group. An example of the process taking place is given below:

$$\text{R-X}^{-}\text{C}^{+} + \text{M}^{+}\text{B}^{-} \rightleftarrows \text{R-X}^{-}\text{M}^{+} + \text{C}^{+} + \text{B}^{-}$$

Likewise, anions are retained on an anion exchange chromatography as the stationary phase consists of positively charged functional groups. The principle is demonstrated below:

$$\text{R-X}^{+}\text{A}^{-} + \text{M}^{+}\text{B}^{-} \rightleftarrows \text{R-X}^{+}\text{B}^{-} + \text{M}^{+} + \text{A}^{-}$$

It is important to understand that the equilibrium position as well as the retention time can be shifted by adjusting the ion strength of either C^+ or A^- in the mobile phase. Figure 2.30 below depicts how a typical IC system is allied.

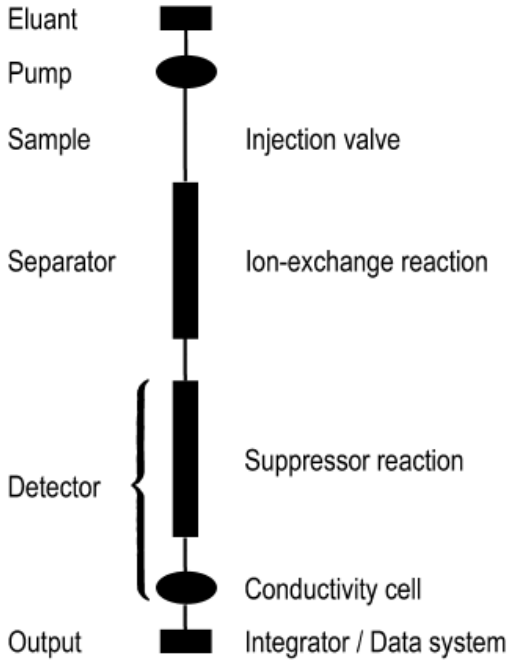

Figure 2.30: Schematic representation of an IC system (Weiss and Weiss, 2005).

Ion chromatography-high performance liquid chromatography with post-column derivatization

IC-HPLC is a hyphated technique which combines HPLC and IC. This technique differs from IC in that no suppressor is used instead post-column derivatization is carried out. The method can be used for chromate analysis where 1,5-diphenylcarbazide is employed as a post-derivatization reagent as the dye is more specific for the chromate anion (Thomas et al., 2002). Analysis for polyphosphonate, polyphosphate, and transition metals using IC post-column derivatization in combination with photometric detection are also known. These analyses provide a powerful extension to conventional titrimetric and atomic spectrometry methods (Weiss and Weiss, 2005). When this method was employed for Cr (VI) analysis, a UV-vis detector was used (Pakade et al., 2011). However, in most cases ion chromatograph employs conductivity detection.

Conductivity detectors (Scott, 2008)

Electrical conductivity detectors measure the conductivity of the mobile phase. This is because electrical conductivity detector is a bulk property detector. Meaning that it detects any ions present in solution be it from a solute or from the mobile phase. Therefore, some suitable adjustments need to be done in order to avoid these incorrect measurements or inability to do any measurements just because the detector is overwhelmed by the buffer ions. Normally to make these measurements possible, a suitable suppressor liquid phase is pumped together with the mobile phase to suppress the mobile phase ions. Electrical conductivity measures the resistance of the electrode system rather than the impedance, therefore the polarization of the sensing electrodes should be avoided by using AC voltages (Scott, 2008). However, the conductivity of a solution is related to its resistance by equations 2.5; 2.6 and 2.7 (Scott, 2008). The resistance (R) of any conductor can be obtained by using equation 2.5.

$$R = \frac{\rho L}{a} \qquad (2.5)$$

where, (L) is the length of a conductor, (a) is the cross sectional area of the conductor. The specific conductance (k) of a solute, which is the resistance across two opposite faces of a 1 cm cube made of the conductor material, is given in equation 2.6 as a reciprocal of the specific resistance.

$$K = \frac{1}{\rho} \qquad (2.6)$$

Hence, the conductance (C, ohm^{-1}) of any given solution is given by,

$$C = \frac{1}{R} = \frac{K\,a}{L} \qquad (2.7)$$

where all the terms have been previously described.

2.11.3. Inductively coupled plasma-optical emission spectroscopy

Inductively coupled plasma optical emission spectrometry (ICP-OES), sometimes referred to as inductively coupled plasma atomic emission spectroscopy (ICP-

AES), is an analytical technique which can be used for determination of all elements with the exception of argon and helium. However, with that being said, optimization of the instrument might be required for certain elements. Inductively coupled plasma (ICP) which is a very high temperature (7000-8000K) excitation source is used to produce excited atoms and ions that emit electromagnetic radiation at wavelengths characteristic of a particular element as the excited species return to ground state (Mermet, 2005; Stefánsson et al., 2007). The emission is brought about by the fact that atoms like to be in ground state as opposed to excited state hence the emission of energy as they fall back. An element can have more than one characteristic emission line and depending on possible interferences and other factors such as sensitivity, best line(s) is selected for each element (Skoog and Leary, 1992; Smith, 1990). Due to higher temperature needed for excitation, this leads to reduction of molecular interferences however, not complete elimination of interferences. The concentration of the element within the sample is related to the intensity of the emission using the Planck's equation:

$$\mathbf{E = hc/\lambda} \qquad \mathbf{(2.8)}$$

where **E** is the energy difference between two levels, **h** is Planck's constant, **c** is the speed of light, and **λ** is wavelength. Planck's equation relates energy difference and wavelength.

Instrument components and the process

The main components of ICP-OES are the sample introduction system comprising of a peristaltic pump, nebulizer, spray chamber and drain assembly; the gas supply, ICP torch and the plasma; a source for production of stable radio frequency; transfer optics and optical spectrometer; detectors; computer (Smith, 1990) (Figure 2.31). The sample is transported into the instrument as a stream of liquid but its gets converted into an aerosol once inside the instrument, a process which is called nebulization. Briefly, the sample is pumped from a sample container by the peristaltic pump to the nebulizer where the sample is nebulized

and entrained in the flow of plasma support gas, which is typically Ar. As soon as the sample reaches the plasma, it immediately collides with the electrons and charged ions in the plasma and is itself broken down into charged ions (Figure 2.32). This is followed by the break-up of the various molecules in the sample into their respective atoms which then lose electrons and recombine repeatedly in the plasma, giving off radiation at the characteristic wavelengths of the elements involved. A specific device sorts out these radiation by wavelength and the electronic signal of these radiations is converted into concentration information that the analyst can use. Only smaller droplets with diameter in the region of few microns pass through the spray chamber otherwise bigger droplets fall down and eventually go to waste (Boss and Fredeen, 1997).

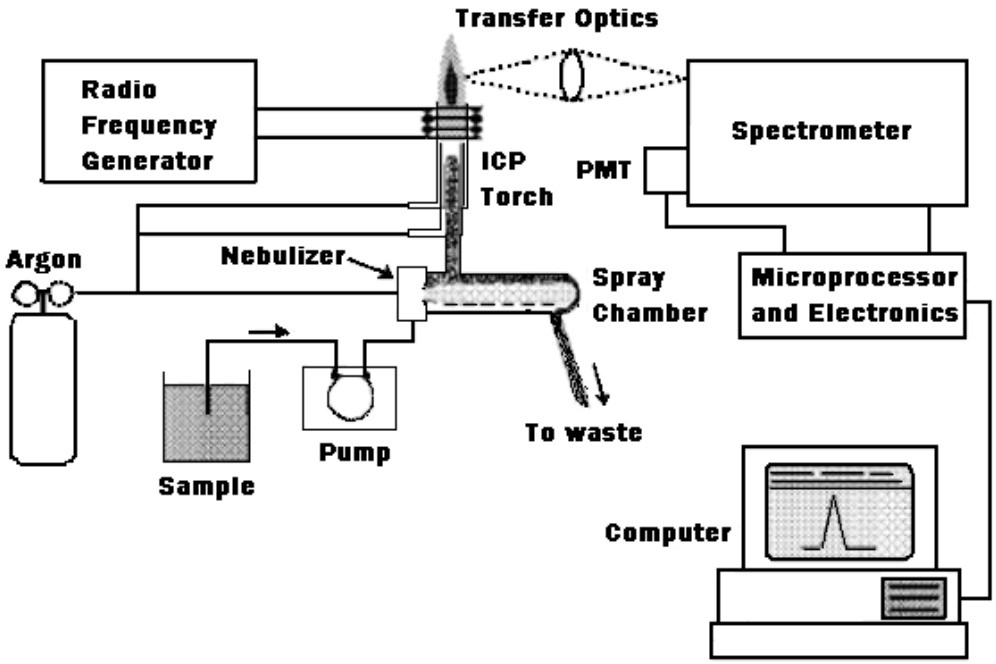

Figure 2.31: Schematic diagram showing major components and layout of a conventional ICP OES instrument (Boss and Fredeen, 1997).

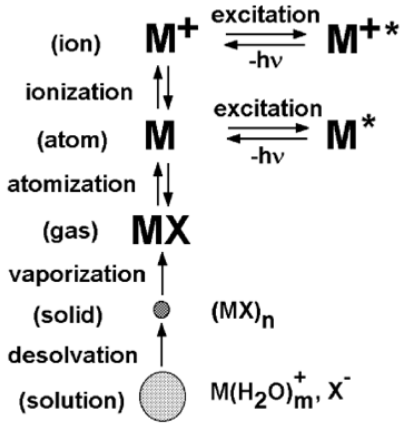

Figure 2.32: Process taking place when a sample is introduced into an ICP discharge (Boss and Fredeen, 1997).

In the sample introduction component, nebulizers are critical devices because the ability of nebulizers to produce small droplets (aerosol) for many different samples determines the utility of an ICP-OES nebulizer (Boss and Fredeen, 1997). Pneumatic forces and ultrasonic mechanical forces are the most typically used forces to break-up samples particles into an aerosol. However, most commercial ICP uses pneumatic forces, with the most commonly used pneumatic nebulizers being the concentric nebulizer, cross-flow nebulizer and the Babington nebulizer (Boss and Fredeen, 1997).

Spray chambers are situated between the torch and the plasma. Among the functions of the spray chamber, removal of large droplets (typically larger than 10 µm) from the aerosol is the most important. That is, only droplets with diameter less than 10 µm pass through to the plasma, this is typically less than 5% of the sample introduced, meaning that the remaining 95% goes to waste. Then the other function is to smooth out the pulses occurring during nebulization mostly due to pumping of the solution. The drains are, in many cases, taken as not important features of the ICP-OES but they can have a significant influence on the performance of the ICP in that, if the drain is not working properly, *e.g.*, it allows bubbles to pass through it, this may cause disruption of the sample introduction to the plasma resulting in noisy emission signals (hence, interfering with detection)

(Boss and Fredeen, 1997). It also provides the back-pressure required to push the sample aerosol-carrying nebulizer gas flow through the injector of the torch tube and into the plasma discharge.

The plasma torch consists of three concentric quartz tubes. The central or inner tube carries the sample aerosol, the next tube is for an auxiliary gas flow (usually argon) and the outer tube contains flowing gas to keep the tubes cool (referred to as *outer gas flow*). It is important that the spacing between the two outer tubes is kept narrow, this will cause the gas introduced between them to be at high velocity. The outer gas flow travels spirally around the chamber as it proceeds upward cooling the quartz walls of the torch (Figure 2.33(a)). A radio frequency (RF) generator, device that provides the power for generating and sustaining the plasma discharge, (typically 1-5 kW @ 27 MHz) produces an oscillating current in a load coil (usually a copper coil) which surrounds the top of the torch (Figure 2.33(b)). An oscillating magnetic field is created by the RF oscillation of the current in the coil. This magnetic field will in turn sets up an oscillating current in the ions and electrons of the support gas (argon). Application of a spark causes stripping of some of the electrons from their argon atoms (Figure 2.33(c)). When more energy is added to these electrons using the coil, a process known as *inductive coupling* is yielded. These high-energy electrons collide with other argon atoms further stripping more electrons and this process continues in a chain reaction breaking down the gas into a plasma consisting of argon atoms, electrons, and argon ions, leading to the formation of what is known as an inductively coupled plasma (ICP) discharge (Boss and Fredeen, 1997) (Figure 2.33(e)).

When a sample aerosol is introduced into this ICP discharge, vaporization, atomization, ionization and excitation processes occur. The analyte emission is measured at the normal analytical zone (NAZ). For the detection of the emitted light, several devises such as photo-multiplier tube (PMT) detectors; advanced detector techniques such as a charge-injection device (CID) or a charge-coupled device (CCD) can be utilized. External calibration curves which plot the emission

intensity versus concentration of standards are used to obtain quantitative information about the analyte.

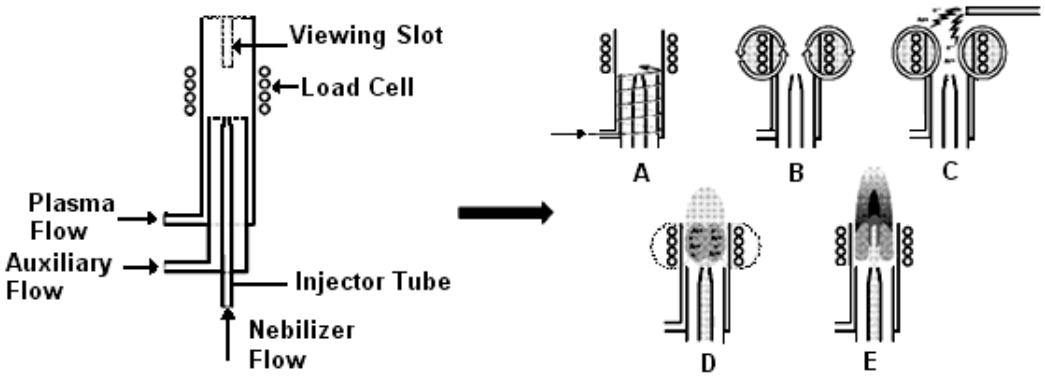

Figure 2.33: A typical ICP-OES torch, next to it is its cross-sectional area and a load cell showing the ignition sequence. A – argon gas is swirled through the torch; B – RF power is applied to the load cell; C – a spark produces some free electrons in the argon; D – the free electrons are accelerated by the RF fields causing further ionization and forming a plasma; E – the sample aerosol-carrying nebulizer flow punches a hole in the plasma (adapted from Boss and Fredeen, 1997).

2.12. Characterization techniques

Instrumental techniques used for the characterization of the synthesized functional monomers and the prepared polymers are detailed below.

2.12.1. Scanning electron microscope (SEM)

In scanning electron microscope (SEM), a high-energy beam of electrons in a raster scan pattern is used for imaging sample. Signals containing information about the sample's chemical composition, surface morphology (texture), crystalline structure as well as orientation of materials making up the sample can be obtained through interactions of electrons with the atoms at or near the surface of the sample. Signals produced include secondary electrons, back-scattered electrons (BSE), characteristic X-rays, light (cathodoluminescence), specimen current and transmitted electrons. Beam electrons that are reflected from the sample by elastic scattering are called back-scattered electrons (BSE).

Characteristic X-rays are X-rays emitted when an inner shell electron is removed from the sample due to application of electron beam on the surface. This process results in higher energy electron filling up the shell and in the process releasing energy. These characteristic X-rays are used to identify the elemental analysis and measure the abundance of elements in the sample (Goldstein et al., 1981). Although secondary electron detectors are the most common in all SEMs machines, however, it is rare that a single machine would have detectors for all possible signals. Very high-resolution images of the surface of a sample capable of showing details about less than 1-5 nm can be obtained with secondary electron imaging (SEI). Data is mostly collected over a selected area of the sample and two-dimensional image displaying spatial variations in the aforementioned properties is obtained. Various magnifications ranging from 10 times to more than 500,000 times, are possible. (Goldstein et al., 1981). The same sample can be analysed for a number of repeated times during SEM analysis the X-rays generated by electron interactions do not lead to volume loss of the sample, hence, the technique is said to be "non-destructive".

A typical SEM instrument has the following essential components:

- Electron Source ("Gun")
- Electron Lenses
- Sample Stage
- Detectors for all signals of interest
- Display / Data output devices
- Infrastructure Requirements:
    - Power Supply
    - Vacuum System
    - Cooling system
    - Vibration-free floor
    - Room free of ambient magnetic and electric fields

All SEMs have at least one detector (usually a secondary electron detector) but can also have additional detectors. The detectors that the instrument

accommodates are the determining factors for its specific capabilities. A Figure showing an illustration of the instrument is supplied below (Figure 2.34).

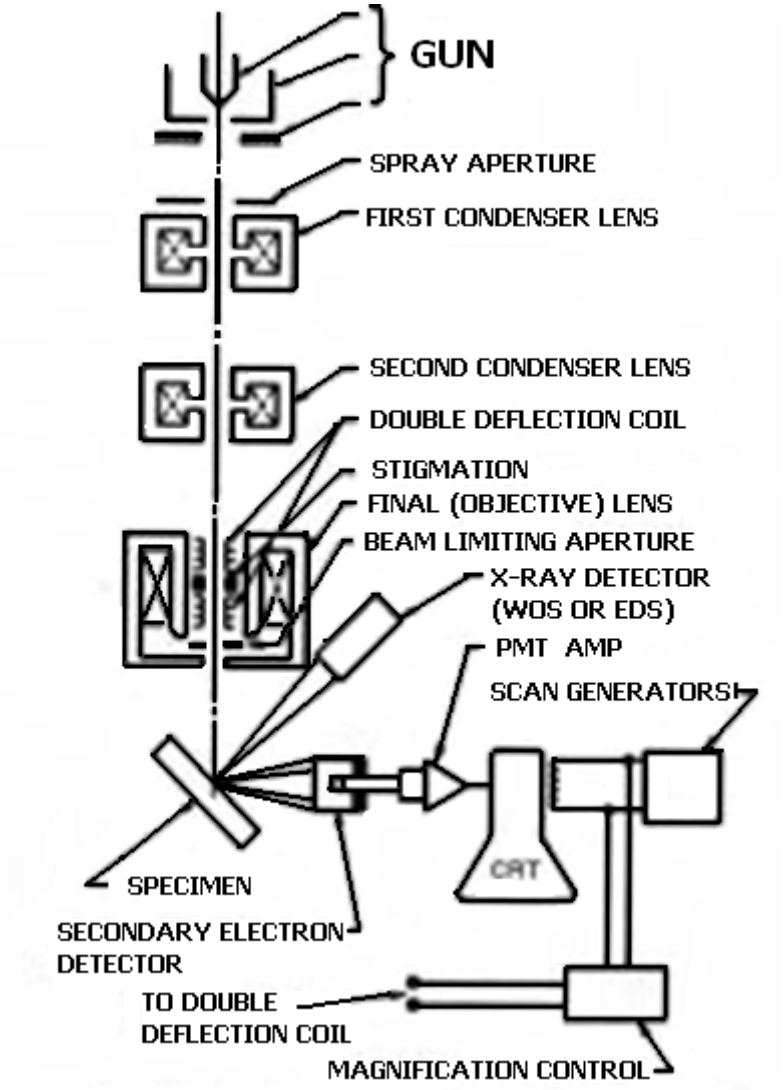

Figure 2.34: Schematic representation of SEM (http://serc.carleton.edu/ research_education/geochemsheets/techniques/SEM.html).

Examples of application of SEM

SEM is used by multitude of industry sectors including electronics and semiconductors, plastics and polymers, pharmaceutical, medical devices, petrochemicals, engineering, aerospace, automotive, chemicals, materials and metallurgy (Raper, 2011). However, in this study and other studies (Tables 2.4

and 2.5) SEM was used to gain information of the surface morphology of the imprinted polymer particles.

Other typical applications of SEM include (Raper, 2011)**:-**

- Identification of metals and materials
- Classification of materials
- Particle contamination identification and elimination
- Product and process failure and defect analysis
- Examination of surface morphology (including stereo imaging)
- Powder morphology, particle size and analysis
- Analysis and identification of surface and airborne contamination
- Cleaning problems and chemical etching
- Welding and joining technology quality evaluation and failure investigation
- Identification and elimination of corrosion and oxidisation problems
- Paint and coating failure and delamination investigation
- Contamination or stain investigation
- Reverse engineering of products and processes
- Structural analysis

2.12.2. Thermal gravimetric analysis (TGA) and differential scanning calorimetry (DSC)

Thermogravimetric analysis or thermal gravimetric analysis (TGA) is an analysis performed on samples for the determination percent weight change relative to change in temperature. The TGA measurements are more useful for determination of the thermal and/or oxidative stabilities of materials together with their compositional properties. High degree of precision in weight, temperature, and temperature change measurements is required in order for this technique to be reliable. However, due to similarities of many weight loss curves, transformation of the weight loss curve before results may be interpreted is necessary. In such

case, a derivative weight loss curve which shows exactly where the weight loss occurred is used although it may also need further refinement. The TGA technique can be used for various purposes such as in determining degradation temperatures for polymers, analysis of absorbed moisture content in materials, determination of the level of organic and inorganic components in materials, and estimation of corrosion kinetics in high temperature oxidation (Mansfield et al., 2010). The technique is especially useful for the study of polymeric materials, including thermoplastics, thermosets, elastomers, composites, films, fibres, coatings and paints. In most cases, TGA is used as a complementary technique to DSC.

TGA is particularly important for measurement of certain properties such as:

- Compositional analysis of multi-component materials or blends
- Oxidative stabilities
- Thermal stabilities
- Estimation of product lifetimes
- Effects of reactive atmospheres on materials
- Moisture and volatiles content
- Decomposition kinetics
- Filler content of materials

In principle, a pre-weighed sample in a sample pan is loaded in a furnace where the temperature is ramped to a desired degrees celsius usually in a 10°C min^{-1} for a certain duration of time in the presence or absence of oxygen. Change in weight percent of the sample as the temperature is increased is observed and recorded in the read-out device. Moreover, the instrument is also capable of supplying the derivative results which show exactly where those phase transitions/ changes had taken place. A schematic representation showing the possible components of a TGA is shown in Figure 2.35. The most important common parts in all TGA instruments are the furnace, the balance and the recorder.

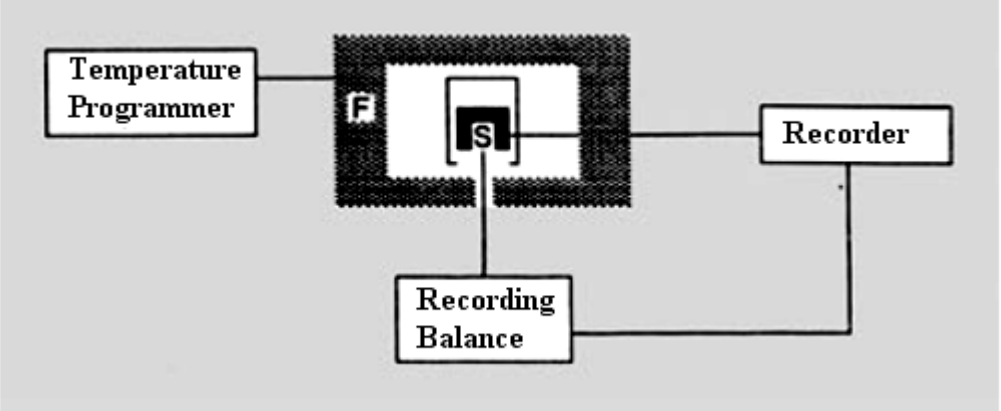

Figure 2.35: Schematic representation of TGA instrument.

A lot more information is obtained when TGA is coupled to DTA or DSC (TGA-DTA/DSC) as this technique allows for simultaneous determination of both heat flow and weight changes (TGA) in a material as a function of temperature or time in a controlled atmosphere (Mansfield et al., 2010). Information obtained from this technique allows for differentiation between endothermic and exothermic events with no associated weight loss (*e.g*., melting and crystallization) and those that involve a weight loss (*e.g.,* degradation) (Mansfield et al., 2010). High-precession balance capable of weighing micrograms which is sometimes built-in in the system is required for reliable results. The sample contained in a pan (usually platinum) is heated gradually in a small electrically heated oven with a thermocouple to accurately measure the temperature. The heating can either be performed under oxygen or under an inert gas such as nitrogen for prevention of oxidation or other side reactions. Weight loss is plotted against temperature. Data obtained is processed with the aid of a computer (Mansfield et al., 2010).

Differential Scanning Calorimetry (DSC) is a thermoanalytical technique in which the difference in the amount of heat required to increase the temperature of a sample and reference are measured as a function of temperature. A typical setup is shown in Figure 2.36. DSC is widely used for the characterization of *thermophysical* properties of polymers, where both the sample and reference are maintained at almost the same temperature throughout the experiment.

Thermoplastic properties that can be measured by DSC include (Fleming polymer testing and consultancy, http://www.flemingptc.co.uk/our-services/dsc-tga/):

- Melting temperature
- Tg or softening
- Heat of melting
- Plasticizers
- Presence of recyclates/regrinds
- Polymer blends (presence, composition and compatibility)
- Percent crystallinity
- Crystallization

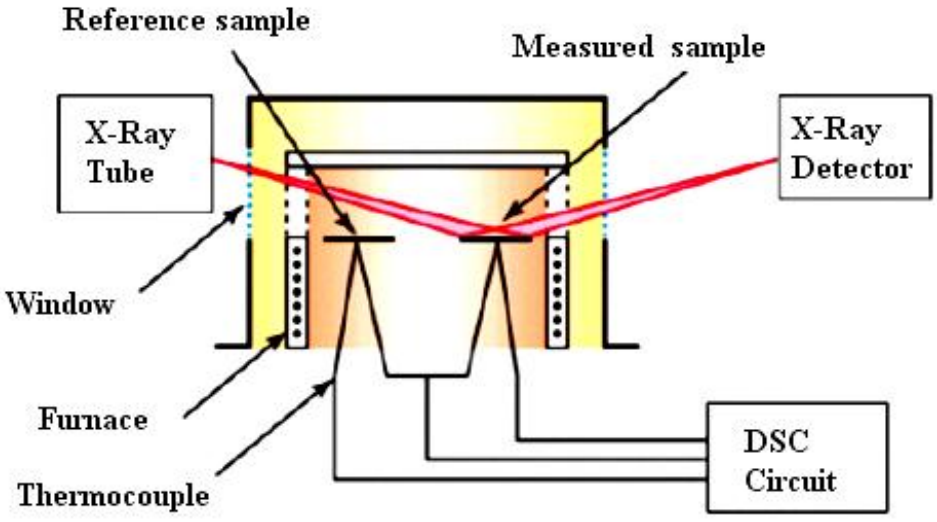

Figure 2.36: Schematic representation of DSC (Kishi and Toraya, 2004).

Principle

The basic principle for this technique underlies on the fact that, as the sample undergoes a physical transformation such as phase transitions, more (or less) heat will need to flow to the sample than the reference to maintain both at the same temperature. The amount of heat flowing to the sample depends on whether the process used is exothermic or endothermic. For example, more heat flow would be required for an endothermic phase transition due to absorption of heat by the sample. The opposite is true for an exothermic process like crystallization. DSC

measures the difference in heat flow between the sample and reference, and correlates this to the amount of heat absorbed or released during endothermic and exothermic transitions. Enthalpies of transitions can be calculated from the DSC curve by integration of peaks corresponding to a given transition. The enthalpy of transition can be expressed as:

$$\Delta H = KA \qquad (2.9)$$

where ΔH is the enthalpy of transition, K is the calorimetric constant, and A is the area under the curve. The calometric constant vary from instrument to instrument, and can be determined by analyzing a well-characterized sample with known enthalpies of transition. Below is a typical DSC curve representing possible transformations of a sample (Figure 2.37). Tg (glass transition), which may appear as a step in the baseline of the curve, is due to the sample undergoing a change in heat capacity but no formal phase change is happening in this transition. It is known that an amorphous solid become less viscous as the temperature is increased. Crystallization temperature (Tc) is the point where the molecules may have obtained enough freedom of motion to spontaneously arrange themselves into a crystalline form. A peak in the DSC curve is observed when the transition from amorphous solid to crystalline solid occurs as the process is exothermic. Eventually due to increased temperature the sample reaches its melting temperature (Tm) and this melting process results in an endothermic peak in the DSC curve, shown by the dip in Figure 2.37. The ability to determine transition temperatures and enthalpies makes DSC an invaluable tool in producing phase diagrams for various chemical systems.

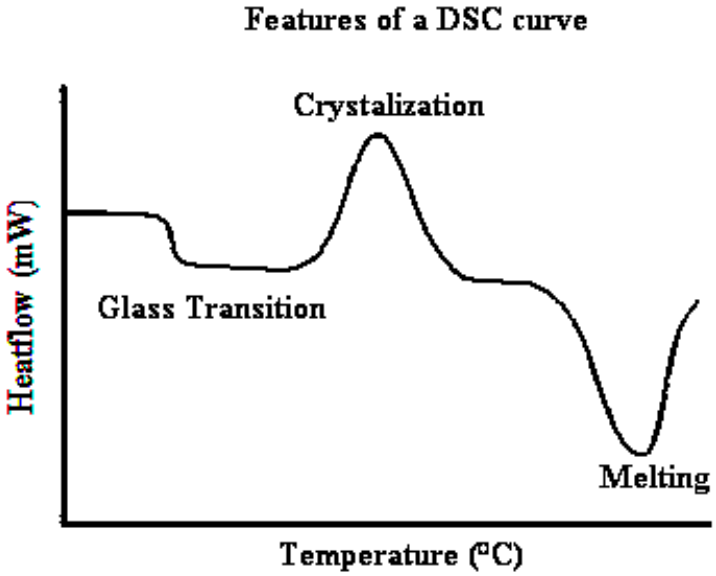

Figure 2.37: A schematic DSC curve demonstrating the appearance of several common features (Fleming polymer testing and consultancy).

Applications of TGA and DSC

Thermogravimetric techniques are used in many fields. Examples include use in forensic work for identification and comparison of various samples. Other applications include determination of the age of art treasures and stability of explosives. The techniques are also widely used in pharmaceutical industry for examination of the stability of drugs as well as investigating the rate of degradation of certain drugs when exposed to air. In MIPs, these methods are used to study the thermal behaviour of imprinted particles and to evaluate the impact of imprinting by comparing non-imprinted polymers to imprinted polymers before and after template removal.

2.12.3. The Brunauer-Emmett-Teller (BET)

The theory on the BET technique was published for the first time in a journal in 1938 and its name was derived from the initials of the family names of its pioneers, Stephen **B**runauer, Paul Hugh **E**mmett, and Edward **T**eller (Brunauer et al., 1938). The theory of this technique aims to explain the physical adsorption of gaseous molecules on a solid surface as well for measurement of the specific

surface area of a material. The concept of the BET theory is an extension of the monolayer Langmuir adsorption theory to multilayer adsorption with the following assumptions: (i) gas molecules physically adsorb on a solid in layers infinitely; (ii) there is no interaction between each adsorption layer; and (iii) the Langmuir theory can be applied to each layer. The BET equation is given as equation 2.10:

$$\frac{1}{v\left[(P_0/P)-1\right]} = \frac{c-1}{v_m c}\left(\frac{P}{P_0}\right) + \frac{1}{v_m c} \qquad (2.10)$$

where, P and P_0 are the equilibrium and the saturation pressure of adsorbates at the temperature of adsorption, v is the adsorbed gas quantity (for example, in volume units), and v_m is the monolayer adsorbed gas quantity. c is the BET constant, which is expressed by equation 2.11:

$$c = \exp\left(\frac{E_1 - E_L}{RT}\right) \qquad (2.11)$$

E_1 is the heat of adsorption for the first layer, and E_L is that for the second and higher layers and is equal to the heat of liquefaction.

BET plot

Equation (2.10) is an adsorption isotherm and can be plotted as a straight line with $1/v[(P_0 / P) - 1]$ on the y-axis and $\varphi = P / P_0$ on the x-axis according to experimental results. This plot is called a BET plot. The linear relationship of this equation is maintained only in the range of $0.05 < P / P_0 < 0.35$. The value of the slope A and the y-intercept I of the line are used to calculate the monolayer adsorbed gas quantity v_m and the BET constant c, using equations (2.12) and (2.13).

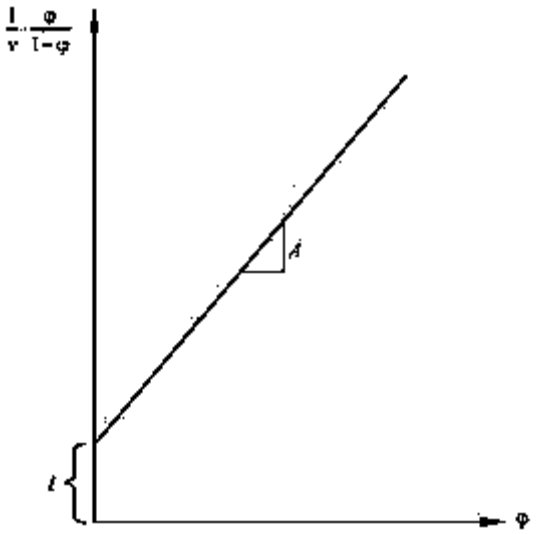

$$v_m = \frac{1}{A + I} \tag{2.12}$$

$$c = 1 + \frac{A}{I} \tag{2.13}$$

The BET method is widely used in surface science for the calculation of surface areas of solids by physical adsorption of gas molecules. A total surface area S_{total} and a specific surface area S are evaluated by the following equations:

$$S_{BET,total} = \frac{(v_m N s)}{V} \tag{2.14}$$

where v_m is in units of volume which are also the units of the molar volume of the adsorbate gas, N is Avogadro's number's is an adsorption cross section of the adsorbing species, a is a mass of adsorbent (in g), V is molar volume of adsorbate gas.

$$S_{BET} = \frac{S_{total}}{a} \tag{2.15}$$

Examples of applications include its use by catalyst manufacturers for monitoring the stability and activity of catalysts as well as measuring the total surface area. Similarly in MIPs, the technique is used for the latter function, that is, giving information on total surface area as this can be correlated with the adsorption potential of the imprinted polymers. Examples can be found in Tables 2.4 and 2.5.

2.12.4. The Fourier Transform InfraRed spectroscopy (FTIR)

Fourier Transform-InfraRed spectroscopy (FTIR) is an analytical technique that can be used for identification of organic (and to some extent inorganic) materials. FTIR technique measures the absorption of infrared radiation by the sample material against wavelength. Molecular components and structures can be identified from infrared absorption bands. This is because, following irradiation of a material with infrared radiation, molecules are excited to a higher vibrational state due to absorbed IR radiation. These absorbed wavelengths by the sample are characteristic of its molecular structure. The wavelength from a broadband infrared source is modulated with the aid of interferometer. Then, the intensity of transmitted or reflected light is recorded as a function of its wavelength on the detector. An interferogram signal is obtained from the detector and this is analyzed with a computer using Fourier transforms to obtain a single-beam infrared spectrum (Figure 2.38). FTIR allows for the identification of unknown materials; determination of the quality or consistency of a sample; quantification of components in a mixture. Basic operation of an ideal FTIR instrument is illustrated in Figure 2.39. Typically, FTIR consists of the following parts:

►***The Source*****:** Infrared energy is emitted from a glowing black-body source. This beam passes through an aperture which controls the amount of energy presented to the sample (and, ultimately, to the detector).

►***The Interferometer*****:** The beam enters the interferometer where the "spectral encoding" takes place. The resulting interferogram signal then exits the interferometer.

►***The Sample*:** The beam enters the sample compartment where it is transmitted through or reflected off of the surface of the sample, depending on the type of analysis being accomplished. This is where specific frequencies of energy, which are uniquely characteristic of the sample, are absorbed.

►***The Detector*:** The beam finally passes to the detector for final measurement. The detectors used are specially designed to measure the special interferogram signal.

►***The Computer*:** The measured signal is digitized and sent to the computer where the Fourier transformation takes place. The final infrared spectrum is then presented to the user for interpretation and any further manipulation.

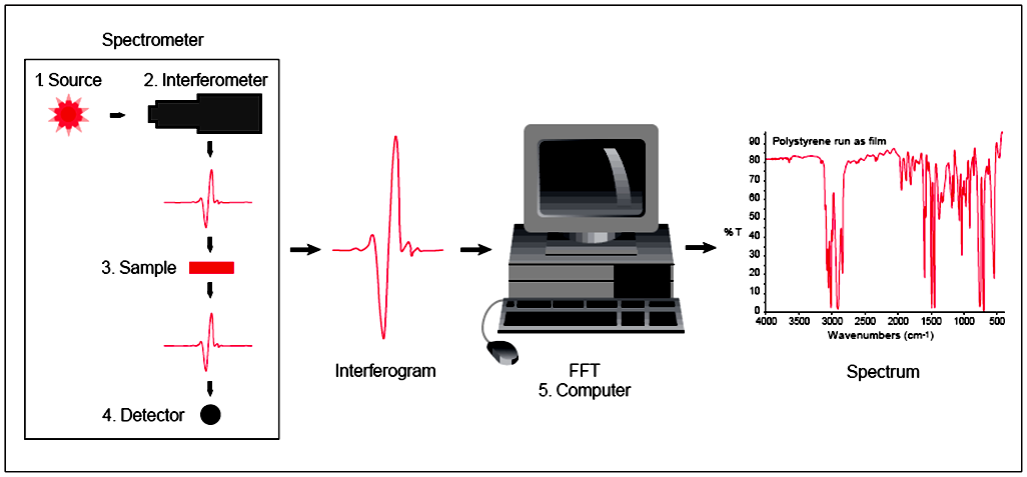

Figure 2.38: FTIR process illustration (ThermoNicolet, 2001).

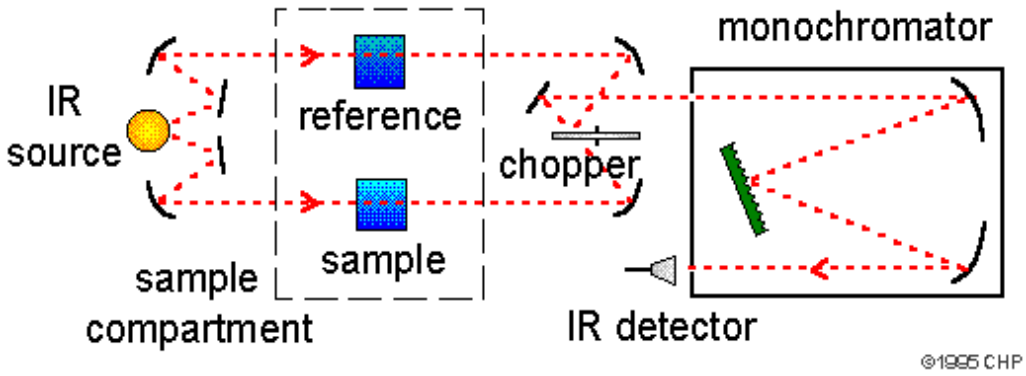

Figure 2.39: FTIR schematic representation (Chemicool).

This technique is extensively used in MIP/ IIP synthesis. Examples can be found in references listed in Tables 2.4 and 2.5. Other applications include polymer processing, in quality control, forensic *etc*. In fact, the technique is valuable to both industry and research.

2.13. Plant materials as samples for MIPs

Moringa plant description

Moringa belongs to the flowering plant family *Moringaceae* (Kwaambawa and Maikokera, 2007). There are 13 known species of *Moringa*, *viz*., *Moringa arborea* Verdc. (Kenya), *Moringa borziana* Mattei, *Moringa concanensis* Nimmo, *Moringa drouhardii* Jum. – Bottle Tree (southwestern Madagascar), *Moringa hildebrandtii* Engl. – Hildebrandt's *Moringa* (southwestern Madagascar), *Moringa longituba* Engl., *Moringa oleifera* Lam. (syn. *M. pterygosperma*) – Horseradish Tree (northwestern India), *Moringa ovalifolia* Dinter & Berger, *Moringa peregrina* (Forssk.) Fiori, *Moringa pygmaea* Verdc., *Moringa ruspoliana* Engl., *Moringa stenopetala* (Baker f.) Cufod. (Subordinate Taxa of *Moringa* Adans." (Tropicos.org, 2012). Of these, *Moringa oleifera* is the most commonly cultivated throughout the tropics. *Moringa stenopetala* is commonly grown in Africa but to a much lesser extent than M. *oleifera*.

M. *oleifera* has been called different names by different regions such as horseradish tree, clarifier tree, and drumstick tree (referring to the large drumstick shaped pods) and in East Africa it is called "mother's best friend" (Natural News). The species *Moringa oleifera* is native to the Himalayan Mountains of Northern India, now cultivated across Africa, Southeast Asia, and South America (Anwar et al., 2007; Bhuptawat et al., 2007; Rashid et al., 2008). The plant is known for its nutritional and medicinal value (stimulant, aphrodisiac, diuretic, and cholagogue) (Siddhuraju and Becker, 2003). The following are all present in excess in *Moringa* species; vitamin A (Beta Carotene), vitamin B1 (Thiamine), vitamin B2 (Riboflavin), vitamin B3 (Niacin), vitamin B6 (Pyrodixine), vitamin B7 (Biotin), vitamin C (Ascorbic Acid), vitamin D (Cholecalciferol), vitamin E (Tocopherol)

and vitamin K. Apart from these vitamins, the plant also contains the following minerals; calcium, copper, iron, potassium, magnesium, manganese and zinc. The importance of these minerals and vitamins in the body are well-known. For an example, vitamin A is most needed by the body to maintain a perfect vision and to maintain the cardiovascular health while calcium is one of the most important minerals for the growth, maintenance, and reproduction of the human body. Also, the interdependence of the minerals and vitamins is known just like as in case where calcium absorption by the body works well only in the presence of vitamin D (Moringa4Life, 2011). The importance of *Moringa* is clearly illustrated in Figure 2.40 below by a comparison of *Moringa* contents to some common foods.

Figure 2.40: Estimation of *Moringa* contents (http://www.*Moringa*.com/).

Besides the mentioned vitamins and minerals, the *Moringa* plant also contains an approximation of 46 antioxidants (Ezeike et al., 2011). This makes the plant one of the most powerful sources of natural anti-oxidants. Anti-oxidants are needed by human body to mitigate the effect of free radicals (Fridovich, 1978). It has been established that quercetin and kaempferol are the most prevalent flavonoids in *Moringa*. The other major antioxidants are ß-sitosterol, caffeoylquinic acid and zeatin (Moringa4Life, 2011). What's more intriguing about *Moringa* plant is that almost every part of the plant is usable. A summary of *Moringa* uses is given below, Figure 2.41, (Foidl et al., 2001). The seeds have also many bioactive compounds, which are used in anti-microbial, anti-genotoxic, anti-inflammatory and anti-tumour promoting activities (Dayrit et al., 1990; Villasenor, 1994; Makkar and Becker, 1997; Guevara et al., 1999).

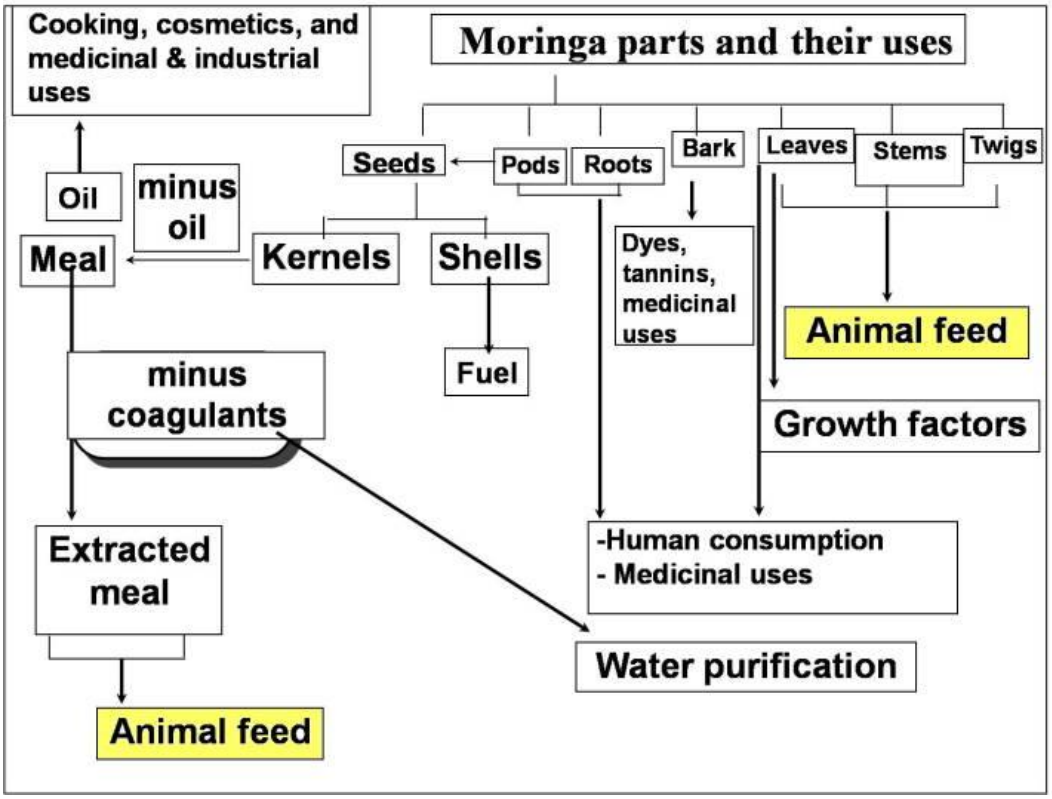

Figure 2.41: Summary of *Moringa* uses (Foidl et al., 2001).

Moringa species, particularly the leaves, are known to be rich in various forms of phytochemicals (Bennett et al., 2003; Fahey et al., 2001) as well as nitriles,

thiocarbamates and carbamates, with strong hypotensive and spasmolytic effects (Leuck and Kunz, 1998). Flavonoids are known for their antioxidant activity toward a variety of readily oxidizable compounds, and as such they are termed as radical scavengers. Consumption of pure or isolated forms of antioxidants is discouraged, these phytochemicals have to be taken together and in combination with other food components as it is only in this state where their nutraceutical value is realized (Dillard and German, 2000). Flavonoids are well distributed in the *Moringa* plant and are mostly found on leaves, flowering tissues, and pollens (Larson, 1988).

Extraction of polyphenols from Moringa

Various techniques for the extraction of these aglycones from the plant materials have been reported. These include, Soxhlet extraction, liquid-liquid extraction (LLE), partitioning, matrix solid-phase extraction (MSPD), solvent extraction (SE), solid-phase microextraction (SPME) etc and these are normally followed by a clean-up procedure using column chromatography or solid-phase extraction (SPE) (de Rijke et al., 2006). In most cases the common method used for extraction of flavonoids from plant materials is a solid-liquid extraction using aqueous methanol or ethanol at high temperature followed by hydrolysis of glycosillated forms to aglycones. Acetone, petroleum ether and hexane are also used for the extraction of *Moringa* seeds and in this case oil extracts are obtained after evaporation of the mentioned volatile organic solvents used (Mani et al., 2007). The oil extracts are normally passed through solid-phase extraction cartridges before injection into an HPLC system for separation, identification and quantification.

Furthermore, SPE offers the use of different solid sorbents, more recently molecular imprinted polymers (MIPs) have been used but the downfall of MIPs is that they are tailor made for a specific analyte and as such they cannot be used for screening purposes although MIPs are generally not specific but selective for a group of structurally related compounds to the template molecule (Molinelli et al., 2002; Ramström et al., 2001; de Rijke et al., 2006). In most cases for flavonoid

analysis the aim is to identify as many flavonoids from the plant extract as possible and hence MIPs limit this objective. However, MIPs can be used to get more purer compounds of the flavonoid family that have already been identified from plant materials. Natural antioxidants extracted from plants have higher potency and lower toxicity compared to synthetic compounds (Sun and Ho, 2005; Dillard and German, 2000). In our studies we are interested in extracting the medicinal compounds found from various parts of the plant, particularly, recovery of quercetin from plant waste. Most studies on *Moringa* have focussed on studying the nutriceutical and medicinal value of the plant (de Rijke et al., 2006) and as well as testing metabolism, taxonomy or antioxidant activity of various extracts of the plant (Siddhuraju and Becker, 2003; de Rijke et al., 2006; Bajpai et al., 2005).

Onion peels

Onion (scientific name, *Allium cepa* L.) belongs to the Liliaceae family and has been known for its therapeutic properties since antiquity. Onions are a good source of flavonoids in particular quercetin which is well known for its anticarcinogenic (eliminate free radicals in the human body) properties (Zill-e-Huma et al., 2011). Onions are an excellent source of vitamin B6, vitamin C, manganese, potassium chromium, folate, copper, phosphorus and fiber (World's Healthiest Foods: Onions). Quercetin and isorhamnetin are the most abundant aglycones in onions.

Besides the conventional SLE (Nuutila et al., 2002), a range of fascinating methods have been used for the extraction of quercetin from onion. These methods include, MHG (Zill-e-Huma et al., 2011), PHWE (Lindahl et al., 2010), SWE (Ko et al., 2011), PLE (SØltoft et al., 2009), SFE (Marino and Guyer, 2004) *etc*.

Chapter 3: Research objectives

The first main objective of the study was to develop novel high capacity selective trace metal removers based on molecularly imprinted polymers and to evaluate these molecularly imprinted polymers under laboratory conditions that simulate the environment where these trace metals occur and subsequently apply the developed MIPs on real samples.

The second main objective was to develop MIPs with high recognition and high capacity for selective recovery of quercetin from aqueous solutions of plant extracts. MIPs are cheaper to prepare and can be recycled for a substantial number of times with minimum loss of efficiency.

3.1. General objectives

The general aim of the project is to develop MIP particles for the extraction of Cr (VI), UO_2^{2+} (VI) and quercetin from complex samples.

3.2. Specific objectives

- To prepare independent MIPs particles with high specificity for Cr (VI), UO_2^{2+} (VI) or quercetin using bulk and precipitation polymerization.
- To compare the efficiency of the MIPs prepared from bulk polymerization and precipitation polymerization.
- To compare the adsorption efficiency of prepared MIPs to NIPs (non imprinted polymers).
- To prepare a water-compatible quercetin MIP.
- To optimize binding controlling parameters.
- To apply the developed and optimized MIPs to real samples such as wastewater and plant extracts.

3.3. Statement of the research

Hexavalent chromium and uranium (VI) are toxic, hence regulatory laws have been set for maximum allowance of these in the environment. Consequently, development of methods that can selectively remove these toxic substances from complex matrices are still needed. On the other hand, quercetin are known for their antioxidant properties and therefore methods that can specifically recover quercetin from complex samples like plant extracts are also desired. MIPs have shown in the past that they can be tailor-made for a specific target compound. Hence, in this study, MIPs were developed for selective removal of toxic substances (chromium VI and uranium VI) and for the recovery of high value compounds (quercetin).

3.4. Justification of research

It is known that South Africa is the largest chromite and ferrochromium producer, and the 6th largest stainless-steel producing country in the world with an estimate of about 70% of the world's chromium reserves in South Africa. In fact, in 2009 South Africa produced an estimated 9,600,000 t of chromium ore (Mbendi, 2011; http://countrystudies.us/south-africa/66-metals.htm). On the other hand, South Africa does not have any primary uranium producers, however, uranium oxide is produced as a by product in some of the Witwatersrand gold mines. Nonetheless, uranium is produced by AngloGold as a by-product at its Vaal River mines. According to statistics released in 2010 by the World Nuclear Association, South Africa produced 563 tonnes U in the year 2009 and in 2007 the Association estimated that South Africa had known recoverable resources of 435,000 tonnes U, which was 8% of the world total (Mbendi, 2011). Both the Witwatersrand basin and Vaal river are located in the Gauteng Province in South Africa with more than a quarter of the country's population. Vaal river supports the whole of Gauteng Province with water. It is obvious that if proper measures are not taken care off in the mining activities in the Witwatersrand basin and the Vaal river mines then South Africa might end up with the scarcity of clean water due to pollution from these activities. Therefore, methods for monitoring and removal of chromium and uranium from the environment are needed in South Africa and MIPs are potential materials which can be used by selectively binding the target analyte in the presence of a host others.

Onions in South Africa are produced in almost all the provinces with an estimation of 350 thousand tonnes a year and is used in almost every household (http://www.nda.agric.za/docs/Trends2000/onions.htm). Therefore, a few grams to kilograms of waste are generated. Waste onion can be used for animal feed and for heat generation but most of it is incinerated. Therefore, extraction of high value compounds before the waste is destroyed is a fascinating project, more so with methods that will allow the waste to be still used for its intended purpose even after extraction of those compounds. Due to complex nature of the matrix of

these plants, MIPs offer an opportune platform for selective extraction of desired compounds, quercetin in this particular case.

On the other hand, *Moringa* plant parts are highly perishable when harvested due to microbial spoilage so it needs to be stored in specific conditions (Mani et al., 2007). Hence, its long term storage is a challenge, therefore, recovery of specific high value compounds from the plant immediately after harvesting is of paramount importance. Currently, methods requiring total extraction are used but the challenge is that, the matrix of those extracts are complex giving difficulties in identification and quantification. MIPs on the other hand can reduce matrix interference as they are tailor-made for a particular compound. In this study, the antioxidant high value compounds quercetin will be recovered from *Moringa* plant or plant waste. To our knowledge no study has focussed on applying MIPs for the selective recovery of the high value compounds from the *Moringa* plant. Hence, the purpose of this study is to recover high value compounds like quercetin from the *Moringa* plant waste using highly selective material *i.e*. molecularly imprinted polymers.

Chapter 4: Materials and Methods

The focus in this chapter is on listing of chemicals and materials used in the study as well as elaborating on methods used for preparation of monomers, ion/ molecularly imprinted polymers and molecular imprinted solid-phase extraction (MISPE) cartridges. Furthermore, the preparation of buffers, real samples and sampling techniques are detailed.

4.1. Chemicals and reagents

Quercetin, kaempferol, disodium hydrogen phosphate, triethylamine and 1,1′-azobis(cyclohexanecarbonitrile) (ACCN) were purchased from Sigma-Aldrich (Steinheim, Germany). Quercetin-3,4′-diglucoside and quercetin-4′-glucoside were purchased from Polyphenols Laboratory AB (Sandnes, Norway) and morin was purchased from Extrasynthese (Genay, France). Methanol (Gradient grade) was purchased from B&J Brand (Honeywell, Germany) as well as from Sigma-Aldrich (Johannesburg, South Africa), formic acid and citric acid monohydrate were purchased from Merck (Darmstadt, Germany). 4-Vinylpyridine (4-VP) and ethylene glycol dimethacrylate (EDMA) were purchased from Acros Organics (Geel, Belgium) as well as from Sigma-Aldrich (Johannesburg, South Africa). 1,4-Dichlorobutane was purchased from Fluka (Buchs, Switzerland).

Uranyl nitrate ($UO_2(NO_3)_2 \cdot 6H_2O$) purchased from Sigma-Aldrich (Johannesburg, South Africa). Methacrylic acid (MAA), 2-vinylpyridine (2-VP), 2-picolylchloride hydroxide, allylpiperazine, formic acid, triethylamine and 1,1′-azobis(cyclohexanecarbonitrile) were all purchased from Sigma-Aldrich (Johannesburg, South Africa). Vinylpyridine was cleaned by vacuum distillation before use and stored in the freezer when not in use. Folin-Ciocalteu reagent, gallic acid, linoleic acid, ferrous chloride, ferric chloride, ammonium thiocyanate, 2,2-diphenyl-1-picrylhydrazyl free radical (DPPH'), nitro blue tetrazolium, phenazine methosulfate, nicotinamide adenine dinucleotide (NADH), potassium ferricyanide, trichloroacetic acid, 2,6-dichlorophenolindophenol dye, metaphosphoric acid, trifluoro acetic acid were all purchased from Sigma-Aldrich (Johannesburg, South Africa). HCl, KCl, CH_3COOH, CH_3COONa, borax, $K_2Cr_2O_7$, citric acid monohydrate, disodium hydrogen phosphate and H_3BO_3 were all AR reagents grade, mostly from Merck. Ultrapure water MilliQ (Molsheim, France) was used.

4.2. Instrumentation

Instruments used in this study for characterization of functional monomers and imprinted polymers, quantification and determination of analytes in solution, weighing of analytes *etc*. are listed in detail below.

4.2.1. High performance liquid chromatography (HPLC) and centrifuge

In this study the following HPLC systems were used:

* HPLC-UV, SRI 210D (LA, California, USA) equipped with UV/Vis detector (VUV-24) and a Phenomenex C_{18} (150 x 4.6 mm, 5 µm) column.
* HPLC-UV analysis chromatographic system, UltiMate-3000® from Dionex (Germering, Germany) equipped with an Agilent Zorbax SB-C_{18} column (100 x 2.1 mm, 3.5 µm) and an Agilent Zorbax SB-C_8 pre-column (12.5 x 2.1 mm, 5 µm).

Centrifugation was carried out using a Hettich Zentrifugen Rotofix 32A benchtop centrifuge from DJB Labcare (Buckingshire, England).

4.2.2. Ion chromatography

A Bischoff (Leonberg, Germany) LC-CaDI 22-14 ion chromatography system equipped with a Lambda 1010 UV-Vis absorbance detector was used for detection of chromium VI. The system consisted of an LC gradient mixer, 2 x HPLC compact pumps and a Variotherm. For system control and data collection an McDAcq32 Control chromatography workstation was used. An isocratic mode of elution was employed. A Dionex IonPac® AG 7 (50 x 4 mm) guard column and Dionex IonPac® AS7 (250 x 4 mm, 5 µm) analytical column, all from Dionex (Sunnyvale, CA, USA) were used for all separations. The injection volume was 500 µL. An eluent was prepared from a mixture of ammonium hydroxide (100 mM) and ammonium sulphate (250 mM), and this was pumped at a flow rate of 1.5 mL min^{-1}. The post-column derivatization reagent was a mixture of 1,5-

diphenylcarbazide reagent (2 mM), 10% methanol and 0.5 M H_2SO_4. The flow rate for post-column reagent was 0.7 mL min^{-1}. Detection of chromate was effected at 540 nm. Figure 4.1 shows a typical calibration curve obtained with the instrument. The calibration standards used were 1, 10, 50 and 100 µg L^{-1}. A good precision was obtained, as can be seen from the linearity constant in the Figure. Moreover, a typical chromatogram of a 100 µg L^{-1} standard solution is shown in Figure 4.2.

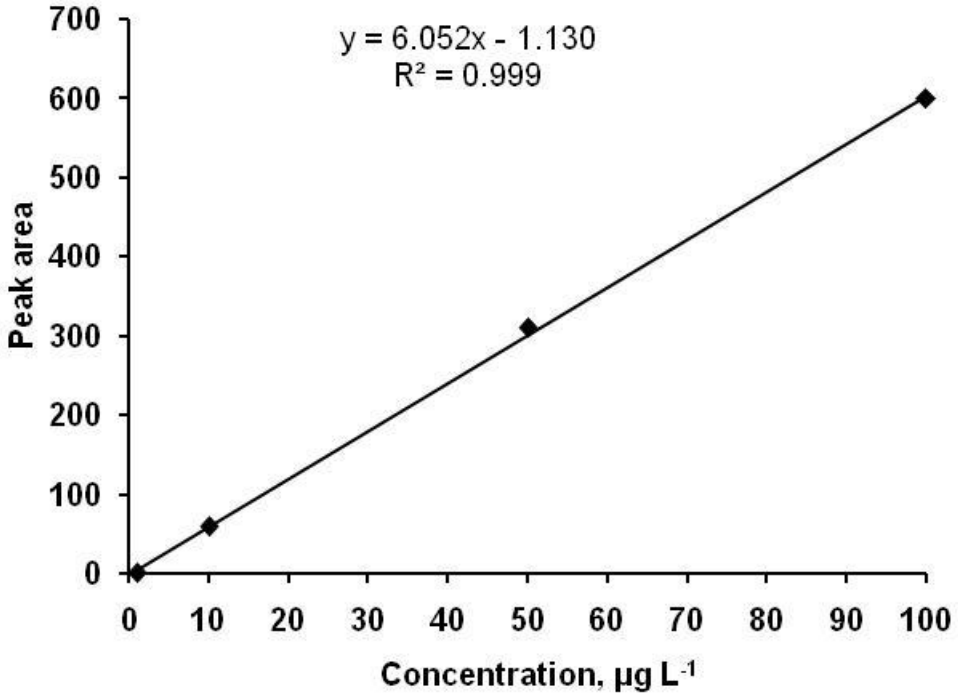

Figure 4.1: Typical calibration curve for chromium (VI) analysis using IC-HPLC with post-column derivatization.

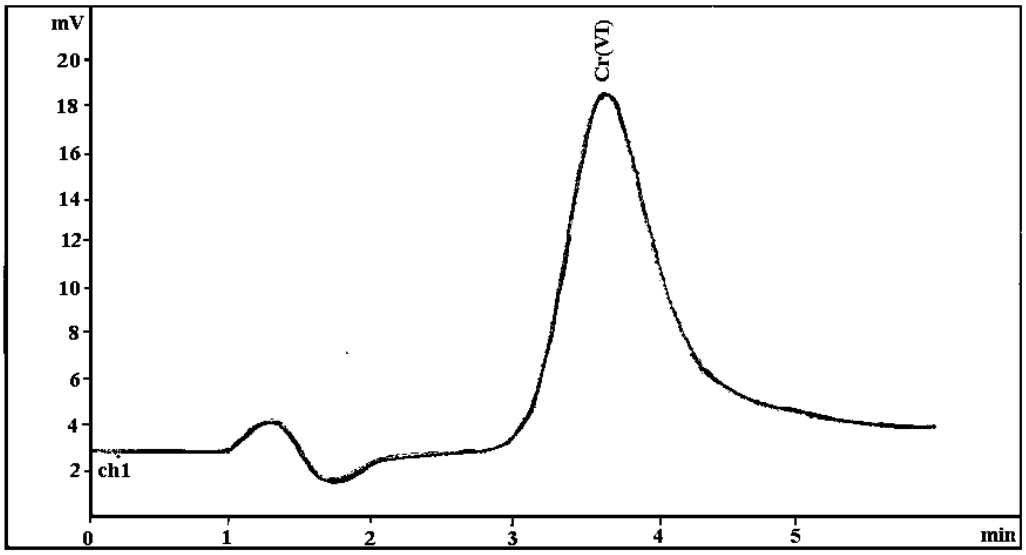

Figure 4.2: An example of a 100 µg L^{-1} calibration standard chromatogram.

Metrohm 762 Compact Ion Chromatograph with a Metrosep A Supp 5 (6.1006.520) 150 x 4.0 mm analytical column was used for the determination of sulphates and other important anions. The eluent was made from a solution of 1.0 mM $NaHCO_3$ and 3.2 mM Na_2CO_3. The eluent was pumped at 0.7 mL min^{-1}. The suppressor solution was 50 mM H_2SO_4 and Milli-Q water. Four point calibration standards were prepared from a mixture of seven anions, namely, Cl^-, F^-, Br^-, NO_3^-, NO_2^-, PO_4^{3-}, and SO_4^{2-}. Below are typical calibration curves obtained for the different salts (Figure 4.3) and the concentration used were 0.2, 5 and 10 mg L^{-1} for fluoride and chloride. For the rest of anions the concentration used were 1, 5, 15 and 50 mg L^{-1}. The calibration curve chromatograms are superimposed and shown in Figure 4.4. Again good precision was obtained. All the solutions used for chromatographic analysis including eluents and post-column reagents were degassed in ultrasonication and then filtered through a 0.45 µm filter paper before use.

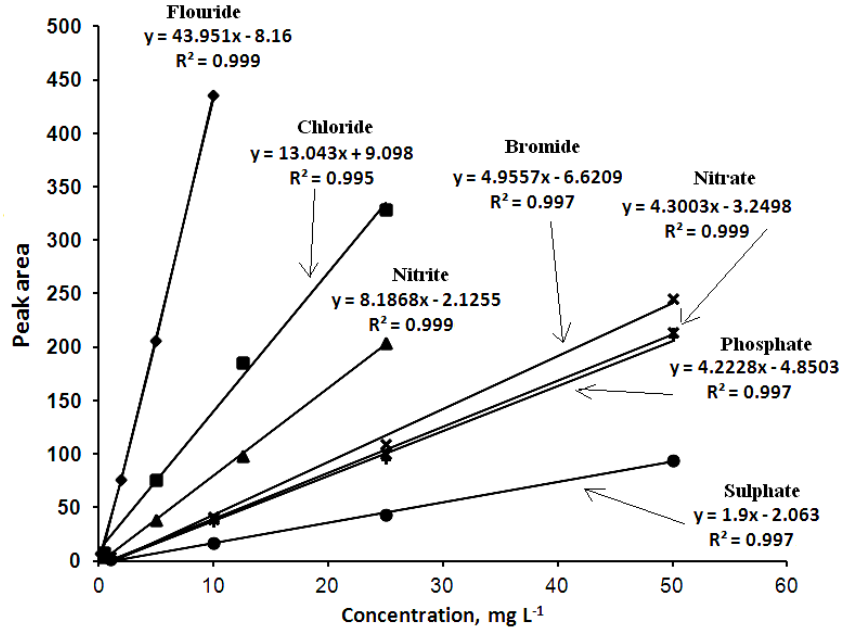

Figure 4.3: Typical calibration curves for anions.

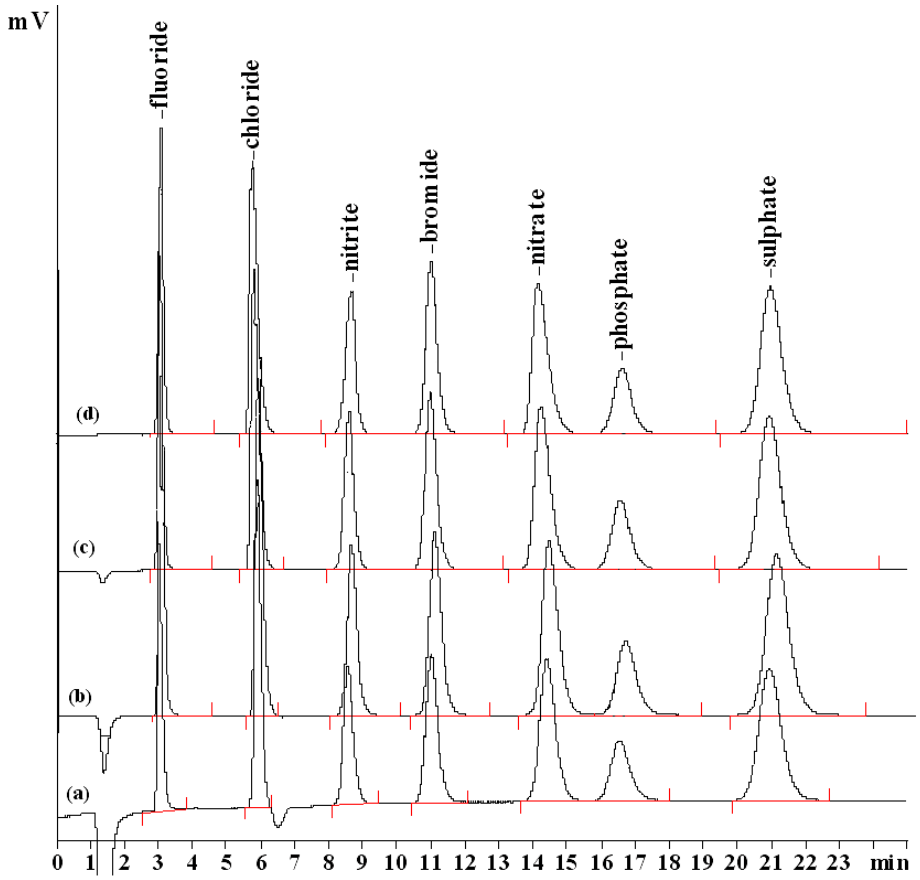

Figure 4.4: Superimposed chromatograms of calibration standards: (a) standard 1, (b) standard 2, (c) standard 3, and (d) standard 4.

4.2.3. Oil bath, ultrasonicator, electronic balances and pH meter

Ultrasonication was performed on the Transsonic 460 ultrasonic bath (Elma, Singen, Germany). Weights of samples were obtained using Precisa 180a (Oxfordshire, England) and Mettler Toledo PB303 (GmbH, Greinfensee, Switzerland) electronic balances. 766 Calimatic pH meter (Knick, Berlin, Germany) was used for pH measurements at 25.5°C.

4.2.4. Stirring and heating instruments

A multi-position magnetic stirrer RO 15 power IKA®-Werke from GmbH & Co (Staufen, Germany) with 15 stirring positions was used for stirring batch extraction experiments at room temperature. For experiments requiring higher temperature, Thermi Scientific, Pierce REACTI THERM III #18823 from Thermo Fisher Scientific (Rockford Illinois, USA) was used.

4.2.5. ICP-OES

Inductively coupled plasma-optical emission spectroscopy (Spectro Genesis, Spectro, Germany) was used for measuring uranium concentrations in solutions as well as for total metal analysis. Typical conditions used for the determination of uranium are illustrated in Table 4.1 below.

Table 4.1: Typical instrumental conditions used for the determination of UO_2^{2+} with ICP-OES

ICP source	27.12 MHz
Sample injection	
Nebulizer	Cross flow
Sample uptake	Peristaltic pump
Spectrometer	
Focal length, m	0.5
Grating grooves, mm^{-1}	2400
Slit width, um	100
Exposure time, s	5
Wavelength, nm	454.36
Experimental conditions	
Viewing height, mm	14
Outer Ar flow, L min^{-1}	14
Inner Ar flow, L min^{-1}	0.5
Auxiliary Ar flow, L min^{-1}	1.0
Sample flow rate, mL min^{-1}	1.0
Rf power, kW	1.25

4.2.6. UV-vis spectroscopy

UV/Vis spectroscopy (Varian, Cary 50 Conc, Germany) and a Varian Cary 1E double beam spectrophotometer (Palo Alto, CA, USA) scanning from 190 to 600 nm were utilised for obtaining UV-Vis absorption spectra.

4.2.7. FTIR

FTIR spectra were recorded in the frequency range of 4000-400 cm^{-1} using the Bruker FTIR spectrometer (Model Tensor 27, Germany) solid state method. However, some of the FTIR were recorded using a Bruker Alpha FTIR spectrometer in the frequency range of 4000-400 cm^{-1} (Ettlingen, Germany) with Attenuated Total Reflectance (ATR) solid state method with 24 scans.

4.2.8. SEM

Surface morphological information of molecularly imprinted polymers (MIPs) and non-imprinted polymers (NIPs) was obtained using a scanning electron microscope (SEM) JOEL Model JSM 6700F (Tokyo, Japan) while that of ion imprinted polymers (IIPs) and control polymers (CPs) was obtained from (SEM) JEOL Model JSM 840 (Tokyo, Japan).

4.2.9. BET

Brunauer-Emmett-Teller (BET) instrument (Micromeritics Tristar) was used for the surface area determinations. The protocol followed for analysis is given below:

At least about 200 mg of samples were degassed in N_2 at 150°C overnight prior to analysis using a Micromeritics Flow Prep 060, sample degas system. The surface areas and pore size distributions were then obtained at -196°C. The pore size distribution with specific surface areas of the samples, were determined *via* N_2 adsorption/desorption according to the BET method using a Micromeritics Tristar, surface area and porosity analyzer. In order to confirm the accuracy of the results, the analysis was repeated at least twice for all samples and the measurements were in good agreement.

4.2.10. Thermal gravimetric analysis

Thermal gravimetric analysis (TGA) was performed using a TA Instruments Q500 TGA in high-resolution dynamic mode (Sollentuna, Sweden) at a heating rate of 10°C min^{-1} up to 500°C under air atmosphere at 60 mL min^{-1}.

4.2.11. NMR

NMR characterization was conducted on Bruker 300MHz NMR.

4.2.12. Microwave

Samples of soils and leaves were totally digested using Multiwave 3000 SOLV Anton Par microwave (Österreich, Austria).

4.3. Conditions of HPLC and Quantification of Flavonoids

Quantification of analytes from *Moringa* and other selected vegetables before and after MISPE extraction was performed using an HPLC-UV, SRI 210D (LA, California, USA) equipped with UV/Vis detector (VUV-24). A Phenomenex C_{18} column (150 x 4.6 mm, 5 µm) was used for isocratic separation with a methanol–water (45:55) mobile phase containing formic acid (0.13 M, 0.5 *vol%*), at a flow rate of 1 mL min^{-1}. A column oven temperature of 40°C was maintained. The injection volume was 20 µl and detection for myricetin, quercetin and kaempferol, was accomplished at 370 nm. Quantification of quercetin and all other compounds tested was performed using a five-point calibration curve of standards at concentrations between 0.5 and 20 µg mL^{-1}.

For the analysis of flavonoids from onion samples the following HPLC-UV chromatographic system, UltiMate 3000® from Dionex (Germering, Germany) with an Agilent Zorbax SB-C_{18} column (100 x 2.1 mm, 3.5 µm) and an Agilent Zorbax SB-C_8 pre-column (12.5 x 2.1 mm, 5 µm) was used. The mode of separation was isocratic employing a methanol–water (50:50, *v/v*) mobile phase containing formic acid (0.13 M, 0.5 *vol%*), at a flow rate of 0.15 mL min^{-1}. The injection volume was 5 µL and detection was accomplished at 250 and 370 nm. Quantification of quercetin and all other compounds tested was performed using a five-point calibration curve of standards at concentrations between 1 and 75 µg mL^{-1}. This system employs an autosampler and analysis samples were placed on sample rack using 1 mL brown sample vials.

4.4. Preparations of stock and working solutions

***Chromium**:* A stock solution (1000 mg L^{-1}) of chromium (VI) was prepared by dissolving dried potassium dichromate, $K_2Cr_2O_7$ (analytical reagent grade) in Milli-Q water. Working solutions were prepared daily from the stock solution through serial dilutions. The stock solution was stored at 4°C when not in use. The pH was adjusted using dilute HCl or NaOH solutions.

***Uranium**:* A stock solution (1000 µg mL^{-1}) of uranyl ion was prepared by dissolving 2.109 g of uranyl nitrate ($UO_2(NO_3)_2 \cdot 6H_2O$) purchased from Sigma-Aldrich (Johannesburg, South Africa) in 20 mL of concentrated HCl and diluted to 1 litre with Milli-Q water. Similarly, working solutions were prepared every day from the stock solutions. Depending on the purpose of the experiment, the pH of working solution was adjusted with the following solutions: HCl/KCl for pH 1 and 2, CH_3COOH/CH_3COONa for pH 3–6, borax/H_3BO_3 for pH 7–8.

***Quercetin**:* Quercetin stock solution with concentration of 0.3 g L^{-1} was prepared in methanol and 0.5% formic acid. This stock solution was kept at -18°C when not in use. Ultrapure water (MilliQ) was used in all experiments and chemicals were used as received. For working solution dilutions the pH was adjusted with citric acid monohydrate (0.1 M) and disodium hydrogen phosphate (0.2 M) buffer solutions.

***Kaempferol, myricetin and quercetin**:* A stock solution (100 µg mL^{-1}) containing a mixture of kaempferol, myricetin and quercetin was prepared by dissolving an appropriate amount of each compound in 50 mL methanol. This stock solution was used to prepare the calibration standards and also for the breakthrough volume studies. When not in use the stock was stored at -18°C.

4.5. Preparation of buffers solutions

Preparation of 0.1 M citric acid-phosphate buffer was carried as follows; citric acid monohydrate $C_6H_8O_7 \cdot H_2O$, molecular weight is 210.14; 0.1 M solution contains 21.01 g L^{-1} Na_2HPO_4 molecular weight is 141.98, 0.2 M solution

contains 28.4 g L^{-1}. Similarly, other buffers were prepared by first preparing known concentrations of acids/ salt or bases in Table 4.2 then mixing as indicated in the Table. The ratios given in the Table are approximations and cannot be taken as true values.

Table 4.2: Approximate volumes used in citric acid-phosphate buffer used for quercetin study; and other buffers used for the adjustment of pH in the uranium studies

pH	**0.1 M citric acid (mL)**	**0.2 M Na_2HPO_4 (mL)**
4.0	61.45	38.55
5.5	43.12	56.88
7.0	17.65	82.35
	0.2 M HCl (mL)	**0.2 M KCl (mL)**
1.0	67.00	25.00
2.0	6.50	25.00
	0.1 M CH_3COOH (mL)	**0.1 M CH_3COONa (mL)**
3.0	98.23	1.77
4.0	84.70	15.30
5.0	35.70	64.30
6.0	52.20	47.80
	0.2 M Boric acid (mL)	**0.2 M Borax (mL)**
7.0	16.99	83.01
8.0	14.72	85.28

4.6. Preparation of MIP

MIPs for three different analytes were prepared in this study. The analytes of interest were chromium (VI), uranium (VI) and quercetin. It should be noted that due to lack of advanced technologies or software in our part, all MIPs were prepared using a trial-and-error method. In the case of chromium IIPs, for an example, one trial was that of the attempted synthesis using 1-vinylimidazole functional monomer and EDMA crosslinker. All polymers in this study were generated by the bulk polymerization method. However, in one case an attempt to prepare a quercetin MIP with precipitation method was also made.

4.6.1. Preparation of chromium MIP by bulk method

Preparation of a linear copolymer of 4-vinylpyridine and styrene

A linear polymer was prepared using a method reported by Li et al. (2005) with minor modifications. 4-Vinylpyridine (3.154 g, 30 mmol), styrene (4.262 g, 30 mmol) and 1,1′-azobis(cyclohexane carbonitrile) (50 mg) were dissolved in chloroform (12 mL) to form a homogeneous solution. The mixture was purged with a stream of nitrogen for 10 min then thermal polymerization was effected at 60°C for 12 hours. The resulting solution was diluted with chloroform and precipitated from petroleum ether (boiling point, 30–70°C), filtered and dried under vacuum to give a light orange product (3.384 g).

Preparation of ion imprinted quaternized polymer

A linear copolymer of 4-vinylpyridine and styrene (200 mg) prepared above, ammonium dichromate (3 mmol) and 1,4-dichlorobutane (18 mmol) were dissolved in aqueous methanol (15 mL) for 30 min. EDMA (18 mmol), 2-VP (2 mmol) and 1,1′- azobis(cyclohexane carbonitrile) (50 mg) were added while the solution was stirred under a stream of nitrogen on ice for 10 min. Polymerization was allowed to continue at 65°C for 48 hours. A black solid product was obtained. The product was washed with MeOH and water to remove unreacted reagents. Leaching of the chromate was afforded by using HNO_3. The product was ground, crushed and wet-sieved in dichloromethane through 53-90 µm. The CP was prepared in the same manner but omitting ammonium dichromate. The CP polymer was also treated with similar solutions used for treating IIP and both were dried overnight at 55°C. The prepared polymer was characterised by FTIR among other techniques. More details on leaching of the chromate anions from IIP are given in Section 4.7. This IIP will be referred to as P1 and CP will be referred to as P3.

Attempted preparation of chromium (VI) polymer with vinylimidazole

An ion imprinted polymer was prepared by first stirring potassium dichromate (0.588 g), pyridine (1 mmol) and 1-vinylimidazole (6 mmol) in aqueous methanol containing 0.1 M HCl for 6 hours at room temperature. This pre-polymerization

solution was placed on ice. EDMA (32 mmol), ACCN (100 mg) were added and the mixture was purged with nitrogen for 10 min. Following which, polymerization was initiated by stirring the sealed reaction vessel in an oil bath at 65°C for 2 hours. Then, the temperature was increased gradually until it reached 90°C and kept there for 6 hours. After the polymer has formed it was further dried in the oven at 55°C overnight. The resultant polymer was treated as above. Also in this case a CP was prepared for comparison.

4.6.2. Preparation of uranium IIP by bulk polymers

Synthesis of 1-(prop-2-en-1-yl)-4-(pyridin-2-ylmethyl)piperazine

40% aqueous NaOH (12 mL) was added to a mixture of 2-picolylchloride hydroxide (0.3960 g; 1 mmol) and allylpiperazine (140 µL; 1 mmol) in 40 mL benzene. Subsequently, 10 drops of 40% aqueous tetrabutylammonium bromide were added slowly and the mixture was refluxed for 24 hours. The organic layer was then separated and evaporated in *vacuo* to afford brown oil with white precipitation. The oil (yield = 0.4850 g, 85%) was separated from the solid. ^{1}H NMR, ^{13}C and DEPT 135 revealed that the oil was the intended product, 1-(prop-2-en-1-yl)-4-(pyridin-2-ylmethyl)piperazine (PPMP). ^{1}H NMR ($CDCl_3$, 300 MHz): δ 3.04 (d, *J*= 6.6Hz, 2H), 3.68 (s, 2H), 5.16 (t, *J*= 8.7Hz, 2H), 5.89 (m, 1H), 7.18 (t, *J*= 5.4Hz, 1H), 7.41 (d, *J*= 7.8Hz, 1H), 7.69 (t, *J*= 1.5Hz, 1H), 8.56 (d, *J*= 4.2Hz, 1H). ^{13}C NMR ($CDCl_3$, 300 MHz): 52.9, 53.0, 61.7, 64.4, 118.3, 122.0, 123.3, 134.6, 134.7, 136.7, 149.3, 158.3, 158.4.

Preparation of UO_2 (VI) IIP and control polymer

An ion-imprinted polymer was prepared by thermal polymerization using a method adapted from Singh and Mishra (2009b). The imprint ion (0.5021 g) was complexed with 1-(prop-2-en-1-yl)-4-(pyridin-2-ylmethyl)piperazine (1 mmol) prepared above and methacrylic acid (9 mmol) in 10 mL 3-methoxy ethanol for 30 min at room temperature. This pre-polymerization ternary complex solution was then mixed with ethylene glycol dimethacrylate (EDMA) (36 mmol) and 50

mg of 1,1′-azobis(cyclohexane carbonitrile) were added. During mixing, the reaction vessels containing pre-polymerization mixtures were kept on ice while continuously purged with N_2 for 10 min. The reaction vessel was then sealed and thermally polymerized in water bath at 80°C while stirring for 40 min. The bulk polymers were dried at 55°C overnight to remove the solvent (porogen). Unreacted monomers were removed by washing the polymers with acetone and subsequently they were washed with a mixture of acetone/water with increasing amounts of water until only water was used. Finally, the resulting polymer was then dried, ground and wet-sieved to obtain the ion-imprinted polymer. Control polymer (CP) was similarly prepared by omitting the imprint ion. The template molecule was removed as described in Section 4.7. The IIP will be referred to as P4 while the CP will be referred to as P5.

4.6.3. Preparation of quercetin MIP by bulk polymerization

The quercetin imprinted polymers were prepared according to published procedures but with slight modifications (Molinelli et al., 2002). The amounts used for each of the polymer reagents are summarized in Table 4.3. In Table 4.3, M1 and M2 refer to MIPs, and N1 and N2 refer to corresponding NIPs for the MIPs, respectively. M3 and M4 are MIPs that were used as references in order to see how MIPs prepared in pure MeOH and pure THF perform in for quercetin recognition from aqueous medium. In brief, quercetin (130 mg; 0.4 mmol) and 4-vinylpyridine (421 mg; 4 mmol) were stirred at room temperature in 50 mL round bottomed flask containing 10 mL THF:MeOH:H_2O (6:1:3, *v/v/v*) porogenic mixture for 30 min to establish weak van der Waals bonding. After which, the polymerization reaction vessels was placed on ice to prevent unwanted polymerization. EDMA (18.5 mmol) and ACCN initiator (100 mg) were added. The solution mixture was purged with nitrogen for 10 min to remove dissolved oxygen, sealed and stirred in an oil bath at 60°C (12 hours) to initiate polymerization. After 12 hours of polymerization, the temperature was increased to 80°C for 3 hours to achieve a solid monolith polymer. After polymerization, the polymers were ground and sieved through 88 µm sieves and finer particles were

removed by sedimentation over acetone decanting the solution every hourly interval for 3 cycles. The resulting polymer particles were dried in an oven at 60°C overnight. Non-imprinted polymer (NIP) was prepared in the same manner but quercetin was omitted and was subjected to the same washing steps. The quercetin template molecule was removed as detailed in Section 4.7.

Table 4.3: Composition of MIPs and NIPs for quercetin

Polymer	Quercetin, mmol	4-VP, mmol	EDMA, mmol	ACCN, mg	Solvent	Solvent volume, mL
M1	1	10	40	100	MeOH:H_2O (9:1, v/v)	10
N1	-	10	40	100	MeOH:H_2O (9:1, v/v)	10
M2	0.4	4	18.5	100	MeOH:THF:H_2O (1:6:3, v/v/v)	10
N2	-	4	18.5	100	MeOH:THF:H_2O (1:6:3, v/v/v)	10
M3	0.4	4	18.5	50	MeOH	5
M4	0.4	4	18.5	50	THF	5

Attempted preparation of quercetin MIP by precipitation polymerization

Precipitation polymer was prepared similar to bulk polymers except that larger volume of porogen was used. In brief, quercetin (670 mg; 2.2 mmol) and 4-vinylpyridine (10 mmol) were stirred at room temperature in 250 mL round bottomed flask containing 100 mL THF:MeOH:H_2O (6:1:3, *v/v/v*) porogenic mixture for 30 min. The pre-polymerization reaction mixture was placed on ice and EDMA (40 mmol) as well as ACCN initiator (100 mg) were added to the reaction flask. The solution mixture was sparged with nitrogen for 10 min to remove dissolved oxygen, sealed and stirred in an oil bath at 65°C (12 hours) to initiate polymerization. After 12 hours of polymerization, the temperature was increased to 80°C for 2 hours to achieve the polymer in powder form. Non-

imprinted polymer (NIP) was prepared likewise but quercetin was omitted. Similar to other polymers, the template was removed as specified in Section 4.7.

4.7. Removal of imprint ion/molecule from the polymers

Removal of chromium VI template: First the polymer was washed several times by stirring in methanol to remove unreacted monomers. The imprint anion (chromate) was removed by stirring 2 g of the polymer in 100 mL of 4 M HNO_3. After 6 hour intervals the IIP particles were filtered through a 0.45 μm filter paper and a fresh nitric acid solution was added, the process was continued until satisfactory removal of chromate was achieved as was determined by ICP OES as total chromium. The IIP particles were then collected and washed several times with distilled water until neutral pH was observed. After drying the particles were subjected to another leaching exactly the same as above but 1 M NaOH solution was used. Again the leachates of each step were collected and analysed for chromium with ICP-OES. After these treatments, the particles were further neutralized by washing with Milli-Q water. Similarly in this case, the CP particles were treated likewise.

Removal of uranyl ion template: To remove the imprint ion, the polymer (2 g) was stirred in 100 mL of 2 M HCl for 6 h after which the material was filtered through a 0.45 μm filter paper. This was repeated for about 9 cycles and then a stronger acid solution (5 M HCl) was used for about 3 cycles. The leachates/ filtrate were collected and analysed for uranium with ICP-OES. The IIP particles were collected and releached with a fresh hydrochloric acid solution. The process was continued until the collected leachates shown almost zero concentration of uranium. In order to ensure complete removal of the uranyl ions, the IIP particles were further stirred in a solution of sodium bicarbonate (1.0 mM) because carbonates for instance are known for their high affinity for uranium. The polymer was neutralised by washing off with doubly-distilled water to remove excess chloride ion (in the case after HCl use) and dried in an oven at 55°C to obtain leached ion-imprinted polymer for possible selective extraction of uranium (VI)

from dilute aqueous solution. The non-imprinted polymer or control polymer (CP) was subjected to the same pre-treatment as IIP. That is, CP was also stirred in 5 M HCl for 6 h and filtered when IIPs were filtered. This among other things serves to account for any swelling complications that the IIPs might be subjected to if they were to spend those hours in HCl solution alone.

Removal of quercetin template: After polymerization has ceased MIPs were crushed, ground and sieved to a desirable particle size. The particles were then washed in succession with methanol and acetone to remove unreacted monomers and weakly retained template. This procedure was carried out by stirring the polymer particles in the mentioned solvents followed by sedimentation for about an hour in order to remove finer particles. Following which the MIPs were dried in the oven at 55°C overnight and then these particles were placed in a Soxhlet extractor to remove the template using methanol-acetic acid (9:1, *v/v*). At identified time intervals, samples were withdrawn from the Soxhlet extractor and injected in the HPLC for quantification of quercetin in solution. The concentration of quercetin in solution increased until it reached a saturation point then the methanol-acetic acid solution was changed and a fresh one was poured in the extractor vessel. This was repeated until no quercetin could be detected from the extraction solution. After which the MIP particles were transferred to an Elernmeyer flask and stirred in a methanol-triethylamine (9:1, *v/v*) for 4 h in order to neutralize the acid. After filtration these particles were further treated by stirring them in pour methanol solution. After this the particles were dried in the oven overnight and hence were ready for use. Non-imprinted polymers (NIPs) were also subjected to the same pre-treatment procedures in order to ensure uniformity.

4.8. Binding constant: Equations used to treat the data

Batch adsorption studies for each experiment were performed by stirring specified amounts of IIP or CP or MIP or NIP in a reaction vial containing a certain concentration and volume of the analyte molecule (more data on this is given

under each specific experiment). After a specified experimental time has lapsed, some constants defining adsorption were calculated from such results. These adsorption binding constants include, adsorption capacity (Q, mg g^{-1}), the distribution coefficient (K_d , mL g^{-1}), selectivity coefficient (k), imprinting effect (k') as well as the percentage recovery (%R). Furthermore, the equation used for surface area determinations is described. The equations of these functions are supplied below.

Adsorption capacity of the imprinted polymers for a specific analyte was measured and calculated by the following equation (Birlik et al., 2007):

$$\boldsymbol{Q = \frac{(C_o - C_e)V}{W}} \qquad \textbf{(4.1)}$$

where C_o and C_e is the initial and final concentrations respectively, V is the volume of the solution used for the extraction and W is the mass of the polymer used for extraction. Percent recovery (R) was calculated using the following equation:

$$\%\boldsymbol{R} = \left(\frac{\boldsymbol{C_0 - C_e}}{\boldsymbol{C_0}}\right)\boldsymbol{x}\ \boldsymbol{100}\% \qquad \textbf{(4.2)}$$

where, all the terms have been previously described.

Distribution coefficients (K_d) were calculated as follows:

$$\boldsymbol{k_d = \frac{Q}{C_e}} \qquad \textbf{(4.3)}$$

where K_d is the distribution coefficient (mL g^{-1}) and the other variables are as already described. According to Birlik et al. (2007) equation 4.4 can be used to calculate the selectivity coefficient for the binding of a metal ion in the presence of other competitive species from equilibrium data:

$$\boldsymbol{k = \frac{k_d(\text{template})}{k_d(\text{B})}} \qquad \textbf{(4.4)}$$

where *k* is the selectivity coefficient and *B* represents any other analyte, but not template, that might have been used as a competitor to the template molecule during the experiment. The value of *k* gives an indication as to how much is the polymer selective for the template molecule with respect to its competitors present in solution. Furthermore, relative selectivity coefficient of MIP against NIP is calculated from the following equation (Birlik et al., 2007):

$$\boldsymbol{k' = \frac{k_{\text{MIP}}}{k_{\text{NIP}}}} \qquad \textbf{(4.5)}$$

where $K_{\text{imprinted}}$ and $K_{\text{non-imprinted}}$ are the selectivity coefficients of the MIP and NIP, respectively. The value of *k'* represents the enhanced effect of imprinting on selectivity and adsorption affinity for the template compared to the non-imprinted polymer. The same equation also applies for IIP and CP relationship.

The surface area of the polymers was measured using the BET technique but in some cases the methylene blue method was used. The equation describing this adsorption is described below.

$$\boldsymbol{A_S = \frac{GN_{AV}\emptyset\, X\, 10^{-20}}{MM_W}} \qquad \textbf{(4.6)}$$

where A_S is the polymer surface area in $m^2\ g^{-1}$, *G* is the amount of methylene blue adsorbed (g), N_{AV} is the Avogadro's number (6.02×10^{23} mol^{-1}), *Ø* is the methylene blue molecular cross section (197.2 $Å^2$), M_W is the molecular weight of methylene blue (373.9 g mol^{-1}) and *M* is the mass of adsorbent (g).

4.9. Optimization of parameters

Method development involves optimization of various parameters so that the developed materials can be applied on real samples. For this purpose parameters

such as the effect of pH on adsorption, optimum amount of polymer material required for maximum adsorption, effect of contact time on adsorption, effect of initial analyte concentration in solution as well as the volume of solution phase were all considered for optimization. Listed below are experimental details for the chromium imprinted polymer.

After the reaction time has lapsed, the stirring was stopped and the solution was equilibrated for 10 min. Following which, the polymer particles were filtered through a 0.45 µm filter paper and un-adsorbed chromium (VI) ions in solution were determined using an IC with diphenylcarbazide post-column derivatization. However, in some experiments the adsorbed chromium (VI) ions were stripped from the polymer particles using NaOH solution and the concentration of the stripped ions were determined.

4.9.1. Effect of amount of chromium

Different amounts of chromium (VI) imprinted polymer (25, 50, 75, 100 and 125 mg) were stirred for 1 h in various sample vials containing 25 mL aliquots of 1 µg mL^{-1} chromium (VI) spiked water at room temperature. The pH of the solution was adjusted to 3.0 using 0.1 M HCl. This pH was chosen based on the two preliminary batch studies, where the polymer showed maximum adsorption around pH 3. Concentration of un-adsorbed chromate ions was determined by IC-HPLC. All the experiments were conducted in triplicates and statistical methods were utilised to determine the mean values and standard deviations.

4.9.2. Effect of initial pH of solution on chromium (VI) adsorption

The effect of pH on the adsorption of chromium (VI) onto CP and IIP particles was investigated in the pH range of 1.0–4.0. This was achieved by stirring 20 mg of the polymer particles in a 25 mL solution of chromium (VI) with initial concentration of 1 µg mL^{-1} for 120 min at 25°C. After 120 min, the solution was

equilibrated for 10 min followed by filtration and un-adsorbed concentration was determined.

4.9.3. Effect of concentration/ retention capacity of chromium

The effect of the initial chromium (VI) concentration on the adsorption removal efficiency by IIP and CP was investigated by stirring the IIP or CP (20 mg) at room temperature for a duration of 120 min. The initial pH of the solutions was adjusted to 3.0 and the range of initial chromium (VI) concentrations studied was 20, 50, 80, 100, and 160 µg mL^{-1}. The solution volume was again fixed to 25 mL.

4.9.4. Effect of solution volume of chromium

Solution phase volume effect on adsorption of chromium (VI) by IIP and CP was investigated by stirring 20 mg of IIP or CP in solutions containing 1 µg mL^{-1} chromium (VI) concentration. The solution volumes investigated were in the range of 50-700 mL. The pH of the solutions was adjusted to pH 3.0 and the solutions were stirred for 120 min at room temperature. Un-adsorbed amounts were measured.

4.9.5. Effect of contact time on chromium (VI) adsorption

The effect of contact time on the extraction of chromium (VI) by IIP and CP was studied by stirring 20 mg of polymer materials at room temperature in a solution containing 1 µg mL^{-1} of chromium (VI) at pH 3.0. The time intervals investigated were 10, 30, 60 and 90 min. The solution volume used for such experiment was 25 mL. After each stirring time, the un-adsorbed amount was measured as described earlier.

4.9.6. Selectivity on adsorption of chromium (VI) by IIP

The selectivity of the prepared IIP for chromium (VI) among its competitors was investigated both in multi-element mixture analysis and in binary phase systems. The competitors examined were Cl^-, F^-, NO_2^-, NO_3^-, SO_4^{2-} and PO_4^{3-}. In multi-element analysis all the six anions together with the chromate were prepared in a single solution and the initial concentration of each analyte was 5 µg mL^{-1}. In binary analysis, competitive adsorption of chromate by IIP/CP against each competitor was investigated and again the initial concentrations of each analyte were maintained at 5 µg mL^{-1}. For each experiment 20 mg of IIP or CP in 25 mL of the abovementioned solutions were stirred for 1 h in reaction vials and the pH was adjusted to pH 3 using 0.1 M HCl. Initial solution concentration was 5 µg mL^{-1}. The experiments were performed in a batch mode at optimum conditions and the remaining concentrations of each anion were measured using ion chromatography and post-derivatization for the chromate.

4.9.7. Reusability of chromium (VI) IIP

The stability and reusability of the imprinted polymers was investigated by contacting 20 mg of polymer with chromium (VI) solution having an initial concentration of 1 µg mL^{-1} for 120 min. Optimum conditions obtained from other previous experiments were used for other variables. After extraction and equilibration, the aqueous solution was filtered and the polymer particles were transferred to another sample vial. To strip out the adsorbed chromium (VI) the polymer particles were stirred in a 20 mL solution of NaOH (0.1 M) for 15 min. This was followed by filtration and analysis of chromate anions in the filtrate. The imprinted polymer particles were used for the next rebinding without any conditioning.

4.9.8. Effect of ionic strength on chromium IIP

The influence of ionic strength on the adsorption of chromium (VI) was investigated by stirring 20 mg of IIP particles in 25 mL of chromium (VI) solution (1 µg mL^{-1}) containing different concentrations of NaCl (900 – 3500 µg mL^{-1}). The initial solution pH was adjusted to pH 3 and the stirring time was 120 min. After the contact time has lapsed, solutions were left to equilibrate for about 10 min then filtered and the concentration of chromium (VI) in the solution was determined by the diphenylcarbazide post-column derivatization method.

4.9.9. Application of chromium (VI) IIPs to real samples

The applicability of the prepared IIPs for the removal of chromium (VI) species on real-world samples was tested on three types of water samples, tapwater, dam water and wetland stream water samples. The samples were collected, treated and stored according to published procedures (Parks et al., 2004). The pH of these water samples was measured and subsequently adjusted to pH 3. The concentration of sulphate and chloride anions was measured using an ion chromatographic system while the post-column derivatization was used to measure the concentration of chromates from the samples before the application of IIPs. Following which, the pH of the samples was adjusted to 3.0. The extraction was carried out in batch mode in triplicates. Twenty mg of IIP was stirred in 25 mL of each real sample (spiked with 30 µg L^{-1} chromium (VI) of a certified reference material (CRM QCl-034-3) or unspiked) for 120 min. The solutions were filtered through a 0.45 µm filter paper and the particles were leached with 0.1 M NaOH as described previously. The concentration of chromium (VI) was determined in both unextracted and extracted solutions.

4.10. Optimization of various parameters for uranium IIP

The effect of amount of polymer (5–40 mg), pH (1-8) of solution, aqueous phase volume (25–1000 mL), stirring time (5–60 min) during the leaching step and

elution of bound uranium, eluent concentration (1– 6 M) and eluent volume (5–30 mL) for elution of bound uranium were studied. In all experiments, except binding capacity, 1 µg mL^{-1} of uranium (VI) present in buffered aqueous phase was stirred with 20 mg of IIP/ CP for 20 min. Unextracted concentration of uranium (VI) was measured by ICP-OES after filtration of the reaction sample solutions through a 0.45 µm filter paper. All the experiments were conducted in triplicates and statistical methods were utilised to determine the mean values and standard deviations. More details of each experiment are supplied below.

4.10.1. Effect of amount of uranium

In batch binding studies, 5–40 mg of IIP/ CP were stirred in a 25 mL uranium (VI) aqueous phase solution with an initial concentration of 1 µg mL^{-1}. CH_3COOH/CH_3COONa buffer was used to adjust the pH of the aqueous solution to pH 5.0 and the solutions were stirred at ambient temperatures for 20 min. The stirring speed was kept constant at 600 rpm. After equilibration, the concentration of unbound uranium in the filtrate was determined by ICP-OES.

4.10.2. Effect of pH of uranium

Similarly, the influence of pH on the extraction efficiency of uranium (VI) from aqueous solutions was investigated over the pH range of 1-8. To achieve this, 20 mg of IIP or CP were stirred in 30 mL aqueous solution containing uranium (VI) ions (1 µg mL^{-1}). The contact time was 20 min and the stirring speed was maintained at 600 rpm. Unbound uranium concentration was determined from the filtrate.

4.10.3. Effect of concentration/ retention capacity of uranium

To obtain the maximum amount of uranyl ions that can be pre-concentrated per gram of IIP, 20 mg of the IIP were added to aqueous solutions containing uranyl

ion. The concentrations investigated were 10, 132, 264, 396, 528 and 660 µg mL^{-1}. The aqueous phase solution volume was maintained at 30 mL and the stirring was uniformly maintained at 600 rpm. The adsorbed uranyl ion was eluted with 2 M HCl and the concentration of the uranyl ion in the eluent was measured by ICP-OES. The same experiment was performed also with a control polymer (CP). The amount adsorbed was worked out as per equation 4.1.

4.10.4. Effect of solution volume of uranium

Twenty mg of IIP and CP were stirred separately in solutions containing 1 µg mL^{-1} uranyl ion concentration in different volumes (25-1000 mL). The pH was adjusted to pH 5 using CH_3COOH-CH_3COONa buffer. The stirring time and stirring speed were kept constant at 20 min and 600 rpm, respectively. Unextracted uranium was measured from the solutions after filtration.

4.10.5. Effect of time of uranium

The effect of contact time on the extraction of IIP and CP was studied by stirring 20 mg of polymer with 1 µg mL^{-1} solution of uranium at pH 5. The range of contact time investigated was from 5–60 min. Other parameters such as solution volume, pH and stirring speed were maintained uniform at 30 mL, 5.0, and 600 rpm, respectively. Similarly, after equilibration the concentration of un-adsorbed uranyl ions in solution was determined with an ICP-OES.

4.10.6. Selectivity of uranium

To examine the selectivity of the prepared uranyl IIPs and CPs for uranium over the other inorganic ions which coexist with uranium in the environment, 20 mg of the polymers were stirred in reaction vials containing different ions in solution. Each vial contained 25 mL of solution of 1 µg mL^{-1} concentration for each metal ion. The studies were performed for each metal ion *versus* uranium, and as a

multi-element mixture. Similarly, the pH, contact time and stirring speed were kept constant at 5.0, 20 min, and 600 rpm. The metal ions investigated were Co^{2+}, Zn^{2+}, Cu^{2+}, Ni^{2+}, Mn^{2+}, Fe^{3+} and UO_2^{2+}. From such results, selectivity coefficient and distribution ratios were calculated.

4.10.7. Reusability of uranium

To test the polymer stability, the imprinted polymer was subjected to several loading and elution operations. The loading operations were carried out using an SPE format, where 50 mg of polymer were packed in the cartridge. The polymer particles were packed in-between two frits (bottom and top) so as not to disturb the particle bed during the introduction of sample. 25 mL of 1 μg mL^{-1} of uranium (VI) solution was then passed through cartridge at a constant flow rate of about 0.8 mL min^{-1}. The uranyl ion solution was introduced to the cartridges at 5 mL portions. The percolation solutions were collected and analyzed for uranyl ions. The elution was carried out by passing 10 mL of 2 M HCl. The polymer was then conditioned by passing deionised water to remove the excess chloride. The concentration of uranyl ion in the eluate was determined. The pH of the initial solution was maintained at pH 5.0. The flow rate was controlled with the aid of a vacuum pressure pump.

4.10.8. Application of uranium MIPs to real samples

Two hundred and fifty millilitres of each wastewater sample (pit water or stream water) was taken in a 500 mL beaker. From this, 10 mL of 0.1 M sodium acetate-acetic acid buffer was added to each wastewater sample to adjust the pH to 5.0. These samples were then divided into three equal portions, where the first portion of each sample was spiked with 0 μg mL^{-1}, the second with 1 μg mL^{-1} and the third with 3 μg mL^{-1} of UO_2^{2+} ion. In triplicates, twenty five millilitres of each sample were subjected to batch extraction with 20 mg IIP particles, stirring at room temperature for 1 hour. The uranium adsorbed on the IIP particles was leached out with 10 mL of 2 M HCl solution, stirring at room temperature for 20

min. Solutions were filtered through a 0.45 µm filter paper and analysed for uranium concentration using ICP-OES. However, before the IIP analysis the metal content of the wastewater samples was analyzed with ICP-OES as well as the pH and conductivity of such solutions was determined.

4.11. Optimization of various parameters for quercetin MIP

Similarly, to other imprinted polymer optimization experiments, the effect of sorbent dosage (5–100 mg), initial pH (4-7) of solution, breakthrough volume, stirring time (0.5–25 hours) during adsorption of quercetin, molecularly imprinted solid-phase extraction (MISPE) washing solution, effect of initial concentration and reusability were investigated. Bound quercetin was eluted with methanol-acetic acid solution. All experiments were performed in triplicates unless where stated statistical methods were used to determine the mean values and standard deviations. After filtration through a 0.45 µm filter paper, quercetin concentration was quantified using an HPLC-UV at 370 nm.

4.11.1 Effect of amount of quercetin

To investigate the effect of sorbent dosage on the adsorption of quercetin by the MIPs, different amounts of MIPs (5, 10, 20, 40, 75 and 100 mg) were contacted with a solution containing quercetin analyte. The pH of the solution was adjusted to pH 5.5. The initial concentration of quercetin in the solution was 66 µmol L^{-1} and the solution volume was maintained at 20 mL. After 8 hours of stirring and 30 min of equilibration the solutions were filtered and un-adsorbed quercetin in the solution was quantified.

4.11.2. Effect of pH of quercetin

The performance of the prepared MIPs was investigated at three different pH's (pH 4, 5.5 and 7). The MIP prepared in this study was to be used in an online extraction of quercetin from plant materials using an enzyme for hydrolysis. According to previous studies, pH 5.5 was the optimum for the performance of the enzyme (Lindahl et al., 2010). Hence, the aim here was to see how the binding capacity of MIPs was affected at pH 5.5, which is the optimum pH for enzyme catalysed hydrolysis of quercetin glucosides in onion extract. pH 4 and 7 were investigated just to get an idea how the polymer binding was on this range. MIP particles (8 mg) were stirred in buffered quercetin solutions (4 mL, 66 µmol L^{-1}) for 90 min at 25°C.

4.11.3. Effect of concentration/ retention capacity of quercetin

Binding capacity was evaluated at 25°C and 84°C using M2 and N2. The initial concentrations investigated were in the range of 10-400 µmol $L^{-1.}$ Other experimental conditions were kept the same for both temperatures, unless where stated, as follows; amount of polymer 8 mg, solution volume 4 mL, contact time 24 hours at 25°C, or 2 hours at 84°C, pH 5.5, solvent MeOH:H_2O, (7:3, *v/v*). Quantification of un-adsorbed quercetin concentration in after the extraction time has lapsed was carried out as mentioned previously.

4.11.4. Effect of solution volume of quercetin

The effect of solution volume was not investigated as it was done in the other polymers. In this case the breakthrough volume of the MIP sorbents was investigated by passing a solution mixture of myricetin, quercetin and kaempferol through MISPE cartridges. The details of such experiment are given in Section 4.12.

4.11.5. Effect of contact time of quercetin

The effect of contact time on the adsorption of quercetin to the imprinted polymers was explored at 25°C and 84°C. For the studies at 25°C an initial concentration of 218 µmol L^{-1} was used whereas 1 mmol L^{-1} initial concentration for the studies at 84°C was used. All experiments were conducted in triplicates. The solutions of quercetin were prepared in MeOH:H_2O (7:3, *v/v*) and pH adjusted to 5.5. That is, 8 mg of imprinted polymers were contacted with quercetin solutions (4 mL) with initial concentrations of 218 µmol L^{-1} and 1.0 mmol L^{-1}, for 25°C and 84°C experiments, respectively.

4.11.6. Selectivity for quercetin

In order to examine quercetin selectivity by M2 and N2, a solution containing morin, quercetin, quercetin-4'-glucoside, quercetin-3,4'-diglucoside and kaempferol was prepared. The concentration of each compound was 66 µmol L^{-1} prepared in MeOH:H_2O (7:3, *v/v*). The pH of the solution was adjusted to pH 5.5 with a citric acid-phosphate buffer. Experiment was done in a batch mode at 25°C and 84°C in triplicates. In short, 8 mg of the polymers were stirred in reaction vials containing 4 mL of the solution for 2 hours (at 84°C) and 6 hours (at 25°C), and un-adsorbed concentration of each substance was measured as previously described after the binding reached equilibrium.

In a separate experiment, the selectivity of the prepared MIPs (M2) was further tested using the MISPE extraction protocol. For this purpose, a mixture containing quercetin, kaempferol and myricetin was prepared in methanol. The concentration of each compound was 0.05 mg mL^{-1}. Ten mL of this mixture was loaded onto the MISPE cartridge. Following which, the cartridge was washed with 5 mL water-methanol (1:1, *v/v*) and finally eluted with 5 mL of methanol:acetic acid solution (9:1, *v/v*). Solutions collected from the percolation step, washing step and elution step were injected into the HPLC without reduction to a lesser volume due to larger concentrations of the analyte in solution. Mass of sorbent used was 150 mg

and the flow rate was maintained at 0.25 mL min^{-1}. The structures of the compounds investigated are supplied in Figure 4.5.

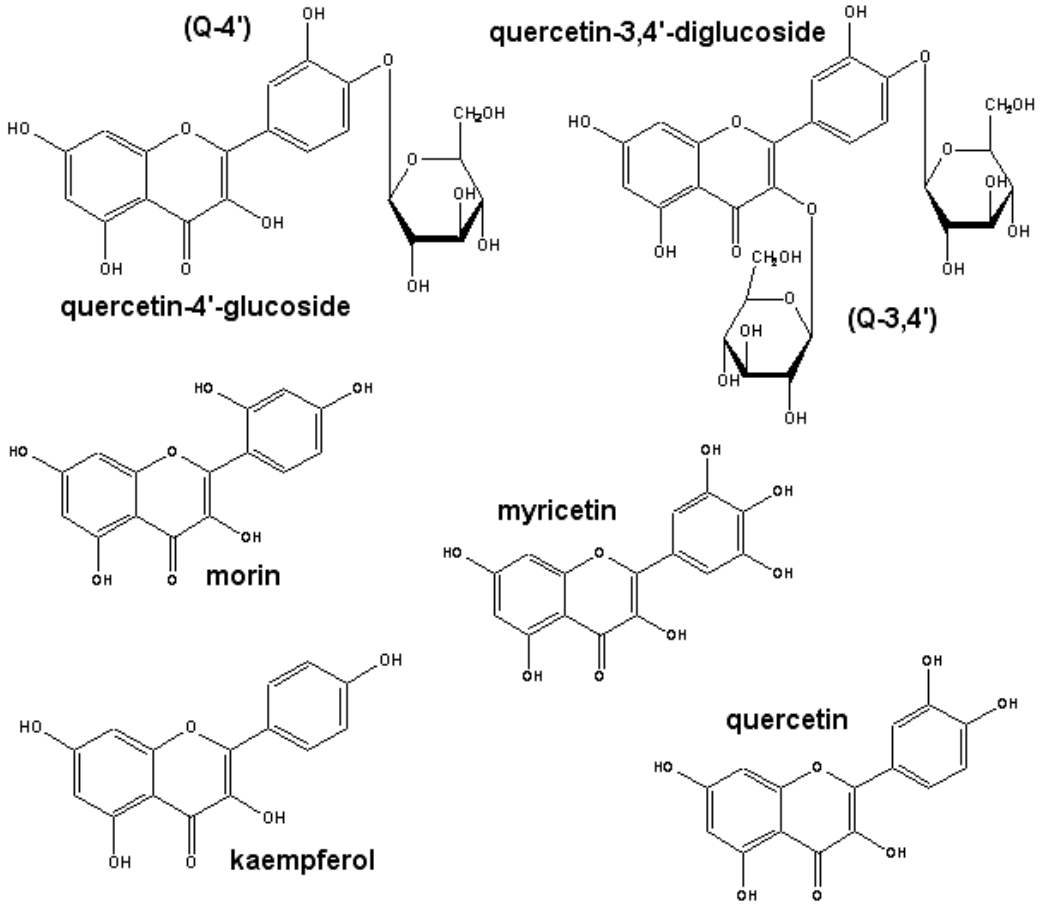

Figure 4.5: Chemical structures of compounds examined.

4.11.7. Reusability

In order to investigate the stability of the prepared MIPs, 3 mL of quercetin solution (20 µg mL^{-1}) was percolated on MISPE cartridges (150 mg) using a flow rate of 0.25 mL min^{-1}. Adsorbed quercetin was eluted from the MIP using methanol-acetic acid (9;1, *v/v*) solution (3 mL). Collected fractions were analyzed for quercetin using an HPLV-UV chromatographic system. The cartridges were regenerated by washing them with methanol-triethylamine (9;1, *v/v*) and methanol successively before the next percolation was done.

4.11.8. Application of quercetin MIPs to real samples

4.11.8.1. Onion water extracts

The potential of future application of the prepared MIPs was examined on aqueous yellow onion extracts in a batch mode. The pH of the onion extract solution was adjusted to pH 5.5 with the citric acid/phosphate buffer. In triplicates, 4 mL of pH 5.5 buffered yellow onion extract solution were extracted with 8 mg MIPs at 25 and 84°C for 8 and 2 hours, respectively. Concentration of quercetin before and after application of MIPs was quantified as described in previous sections. MIPs were first washed with 2 mL of MeOH in two portions of 1 mL and finally eluted with 2 mL of MeOH/acetic acid (9:1, *v/v*) in one portion by stirring the MIPs at room temperature for 20 minutes. To calculate the recovery, quercetin in the methanol extracts (washing solution) and in the methanol/acetic acid extracts were combined.

Aqueous yellow onion extracts were obtained from the extraction of onion with accelerated solvent extraction (ASE) (Turner et al., 2006). Known mass of chopped onion was placed in an ASE extraction cell, water was pumped through the cell for 5 min and extraction was carried out for 3 cycles. The temperature and pressure of water was maintained at 120°C and 50 bars, respectively. Once the extraction has finished, the extracts were collected and stored in dark bottles at -18°C when not in use. Onions were bought from a local supermarket.

4.11.8.2. Moringa

Moringa oleifera Lam. leaves and *Moringa* flowers investigated in this study were collected from the Limpopo farm near Polokwane and the Atteridgeville farm near Johannesburg in South Africa. Soon after collection, leaves were washed for a few minutes with drinking water. After this some leaves were freeze-dried and some were air-dried under a shade. Samples of *Moringa* from the Limpopo farm were taken from plants grown from different years, that is, 2006, 2009 and 2010. Whereas, in the Atteridgeville farm all the trees were grown from 2010, hence only 2010 samples were obtained. For differentiations, the samples were labelled 2006LF, 2009LF, 2010LF and 2010AF with LF indicating Limpopo farm while

AF is an abbreviation for Atteridgeville farm. Both sets of leaves were stored at -18°C when not in use because *Moringa* is a highly perishable plant. For experiments, dried leaves were ground to powder using a pulverizer.

(i) Dry matter determination

Due to the fact that fresh undried leaves were used for some experiments while in other freeze dried samples were used, therefore the varying water content can affect results. Hence, all calculations were made on dry mass basis. For this purpose, 1-3 g of all samples (in triplicates) were dried in an electric drying oven Labotec Model 321 (Umhlanga, South Africa) at 70°C for three days until a constant mass was achieved.

(ii) Optimization of extraction method for Moringa leaves

In order to optimize the extraction efficiency of polyphenols using our method, *Moringa* leaves were placed in the extraction cell and samples were taken periodically and analysed in HPLC. A modification of extraction method by Sultana and Anwar (2008), was used. In brief, 5.18 g of air-dried/freeze-dried *Moringa* leaves were placed in a round bottomed flask that was equipped with Soxhlet extractor and a condenser. 100 mL of acidified methanol (1% HCl) was added to the leaves, to this was added 50 mg of tetrachlorohydroquinone and 20 ml of 1.2 M HCl. The mixture was heated to 90°C to reflux using the Soxhlet technique. 500 µL samples were taken periodically using a syringe equipped with a 0.45 µm filtration head. The sampling times were 30 min intervals for the first 5 hours, 60 min for the next 3 hours and finally the samples were taken after 14, 24 and 30 hours. The samples were directly injected into the HPLC-UV and peak area of quercetin was monitored against time.

(iii) Extraction and hydrolysis of flavonols

Extraction and hydrolysis of flavonols was carried out using a method by Sultana and Anwar (2008) with slight modifications. Briefly, 100 mL of acidified methanol containing 1% (*v/v*) HCl was added to 5 g of dried leaves (or flowers) contained in a round-bottomed flask. The flask was fitted with a reflux condenser.

To this was added 20 mL of 1.2 M HCl and the mixture was heated at 90°C for 14 hours to obtain aglycones of flavonols and some phenolic acids. The extract was cooled to room temperature then sonicated for 5 min to remove air and then centrifuged at 5000 rpm for 10 min. Finally, the extract to be used for direct injection into the HPLC was further filtered through a 0.45 µm (Millipore) filter paper. The extract to be used for further analysis was stored at -18°C.

(iv) Conditions of HPLC and quantification of flavonoids

Quantification and identification of analytes on the extracts was achieved using an HPLC-UV, SRI 210D equipped with UV/Vis detector. More details on the conditions of the analysis are supplied in Section 4.3.

(v) Molecularly imprinted solid-phase extraction (MISPE)

Empty SPE cartridges were purchased from Anatech. A frit was inserted to the base of the tube. Then, the cartridges were packed by gravity using dry sorbent. However, when all the sorbet was entered inside the cartridge, conditioning solvent was run down the column. This ensured that there was nothing on the side of the tube. Lastly, a second frit was placed on top of the sorbent to prevent disturbing the sorbent bed during loading of sample and elution solvents. From this stage the cartridges were treated as detailed in the respective experiments.

Quercetin MIP prepared in this study was tested for its quercetin recognition from complex *Moringa* leaves and flowers extracts. In addition, one sample of *Moringa* flowers was also investigated. For selective extraction of quercetin form *Moringa* extracts, a molecularly imprinted solid-phase extraction (MISPE) method was used. Briefly, 3 mL of methanolic extracts obtained from Section 4.11.8.2 (iii) above were loaded onto MISPE cartridges packed with 150 mg MIP particles. Afterwards, the cartridges were washed with 3 mL water-methanol (1:1, *v/v*) solution and finally eluted with 3 mL of methanol:acetic acid solution (9:1, *v/v*). Effluents from the percolation step, washing step and elution step were collected and injected directly into the HPLC.

(vi) Optimization of quercetin washing solution in SPE

Various solvent systems were investigated as possibilities for the washing of the *Moringa* matrix during the application of MISPE technique for extraction of

quercetin. The solvents investigated were methanol, acetone, methanol-acetone, methanol-acetone-water, methanol-water, and acetone-water combinations. The experiment involved percolation with *Moringa* extracts through MIP cartridge, followed by washing it with each of the mentioned solvent system then lastly eluted with methanol-acetic acid (9:1, *v/v*). Experimental details were as follows, the column was packed as mentioned previously, the flow rate for percolation was 0.25 mL min^{-1} and that of washing and elution was 0.5 mL min^{-1}. Briefly, 5 mL of *Moringa* methanolic extract was loaded onto cartridges, the cartridges where washed with 5 mL of different solvents and finally eluted with 5 mL MeOH-acetic acid 9:1 (*v/v*).

4.12. Determination of breakthrough volume, adsorption capacity and selectivity

Breakthrough volume studies were conducted using a MISPE format. Briefly, 100 mL of methanol standard solution containing myricetin (initial concentration 5 µg mL^{-1}), quercetin and kaempferol (each with initial concentration of 10 µg mL^{-1}) was introduced into pre-conditioned MISPE cartridge in 10 mL portions at 0.25 mL min^{-1} flow rate. Sample effluents were collected individually from each aliquot and analyzed for myricetin, quercetin and kaempferol using HPLC-UV at 370 nm.

To get the amount adsorbed and capacity of the MIP used, once the equilibrium was reached the sorbent was first washed with 5 mL MeOH-water (4:6, *v/v*) to remove loosely bound compounds and finally eluted with 5 mL MeOH-acetic acid (9:1, *v/v*) solution. Both eluates were directly injected into an HPLC to quantify the amount of flavonols bound on the sorbent. To calculate the adsorption capacity (Q, µmol g^{-1}) of the MIP the following equation was used:

$$\boldsymbol{Q = \frac{n}{W}} \qquad \textbf{(4.7)}$$

where, *n* is the sum of the amount of compound adsorbed both in washing solution and in elution solution (µmol). *W* is the weight of the MIP sorbent in the cartridge (g).

The selectivity of the prepared MIP was tested using a mixture containing quercetin, kaempferol and myricetin prepared in methanol applied during breakthrough volume studies. The idea here is that if the MIP is super selective for the quercetin molecule among its structurally related compounds (kaempferol and myricetin) then the breakthrough curves might show a trend where quercetin will show higher breakthrough volume. That is, if the other compounds are not bound they will have low breakthrough volumes. The recoveries (%R) were calculated using equation 4.8.

$$\%\boldsymbol{R} = \frac{\mathbf{C_{extract}V_{extract}}}{\mathbf{C_{sample}V_{sample}}}\ \mathbf{x100} \qquad (\mathbf{4.8})$$

Chapter 5: Results and Discussion

This chapter is subdivided into three sections where in Section 5.1. the emphasis is on characterization, optimization of various parameters for the chromium six IIP as well as its application on real samples. Section 5.2. deals with uranium VI ion imprinted polymer. Again characterization, optimization of certain parameters and application to real samples were looked into. Section 5.3 deals with the preparation of quercetin MIP, study of monomer-template interaction in the methanol-water solvent, characterization, optimization of various parameters and application of the MIP on recovery of quercetin from onion extracts and *Moringa oleifera* methanolic extracts.

5.1. Preparation of ion imprinted polymer for chromium VI removal

An ion imprinted polymer that showed recognition abilities for chromium VI in the presence of competing ions such as sulphates was prepared from quaternized vinylpyridine functional monomer and ethylene glycol dimethacrylate crosslinker as described in Section 5.6.1. The schematic representation of the preparative method is supplied in Figure 5.1. As can be noted from the scheme, the aim was to quaternize the vinylpyridine so that it can have a permanent positive charge. Chromate ions were added in the form of $K_2Cr_2O_7$ to act as template. It is believed that the chromate can displace the smaller chloride anion in the polymer backbone resulting in micro cavities that will be specific for the chromate ion.

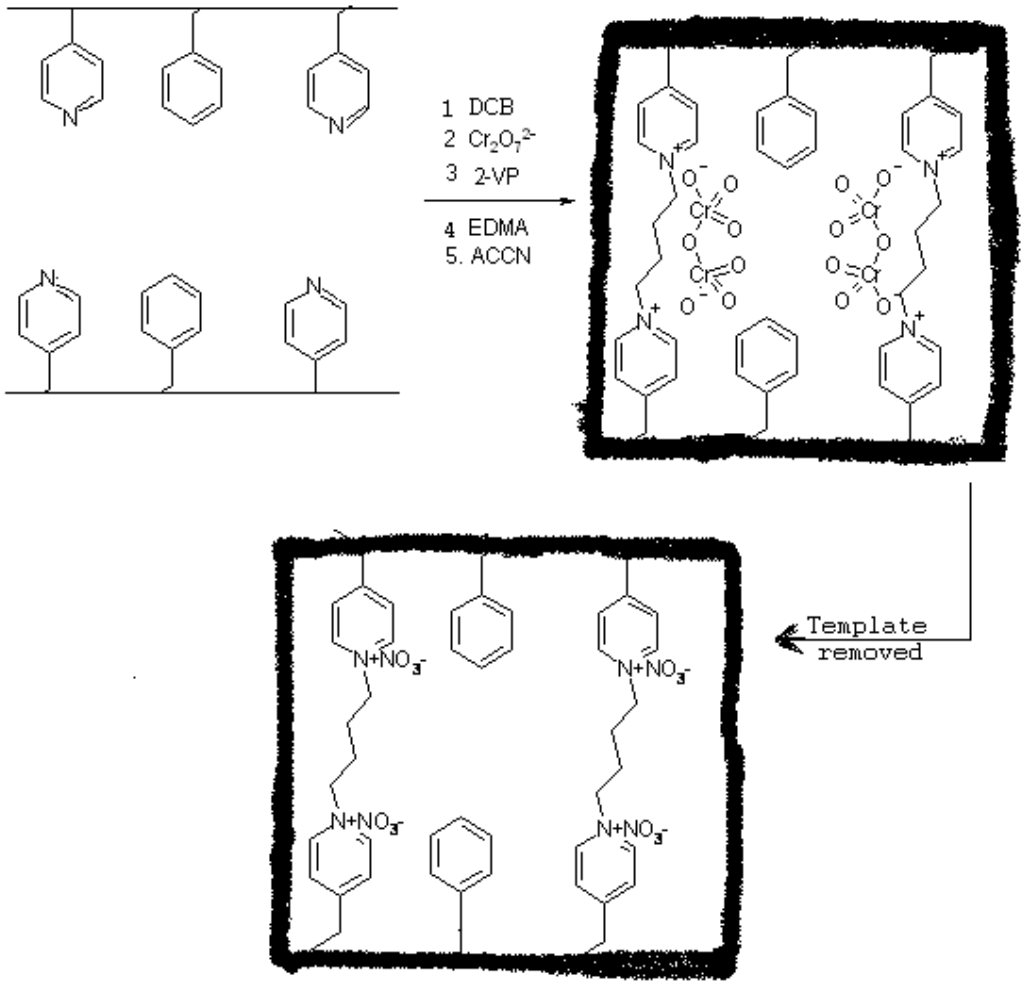

Figure 5.1: Diagrammatic representation of IIP preparation.

5.1.1. Characterization of chromium (VI) IIP

5.1.1.1. FTIR

A similar backbone for all the CP, leached and unleached IIP FTIR spectra (Figure 5.2) was observed for all polymers and this is indicative of the high level of the EDMA cross-linking reagent used. Characteristic absorption bands in the range between 2958 and 2852 cm^{-1} in all polymers could be ascribed to methyl (C-H) stretching vibration absorption peaks due to 1,4-dichlorobutane cross-linking agent. All three polymers show a strong vibration frequency at about 1720 cm^{-1} attributed to the C=O group of EDMA cross-linker and another distinctive vibration at 1150 cm^{-1} is associated with the C-O of EDMA. In agreement with studies by Li et al. (2005), the C=N band in pyridine usually at 1600 cm^{-1} was displaced to higher wave numbers (1636 cm^{-1}) due to quaternization. However, this band has a low intensity in the unleached IIP indicating the onset of nitrogen–metal coordination bonds which was in agreement with studies conducted by Ramos et al. (2000).

Other vibrations of interest were at 1454 cm^{-1} (CP and leached IIP) and 1438 cm^{-1} (unleached IIP) assigned to C-C/N-C. However, more interestingly was the presence of a broad band at 3198 cm^{-1} and the bands between 900 and 778 cm^{-1} in the unleached IIP only; these could all be attributed to the presence of Cr (VI) in the polymer as they were absent in both leached and control polymer. This was in agreement with studies by Goudarzian et al. (1996) who attributed bands at 938 and 790 cm^{-1} to the interaction of Cr (VI) with the adsorbent. Independently, Miller and Wilkins (1952) also observed chromate anion FTIR bands at 930 and 765 cm^{-1} in polyethyleneimine-supported silver dichromate oxidizing polymeric reagent. The FTIR spectrum of the quaternized polymer revealed the presence of two bands at 1630 and 1578 cm^{-1} which indicated the presence of the quaternized product as these were absent in the vinylpyridine spectrum.

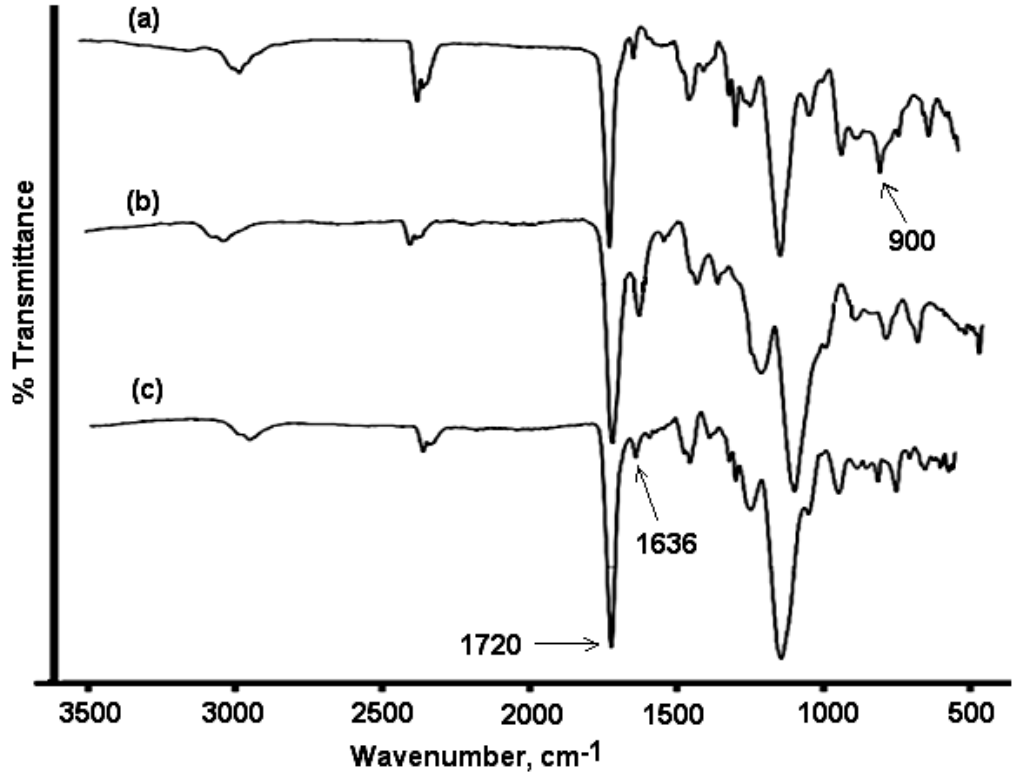

Figure 5.2: FTIR spectra of (a) CP, (b) leached IIP and (c) unleached IIP.

5.1.1.2. Scanning electron microscope

Surface morphology of the imprinted particles was evaluated by SEM images. IIP and CP images are shown in Figure 5.3(a) and 5.4(a), where 5.3(b) and 5.4(b) show magnifications of a single particle in Figures 5.3 and 5.4, respectively. The images revealed that both CP and IIP particles have irregular shapes and this is due to the method of preparation (bulk polymerization) as it requires grinding and crushing. It can also be observed that the surface of the produced particles have some degree of porous structure that will then help in adsorption. In fact, Figure 5.3(b) and 5.4(b), further revealed that the polymers have similar surface structures which also confirm other similarities observed in re-binding results for both polymers.

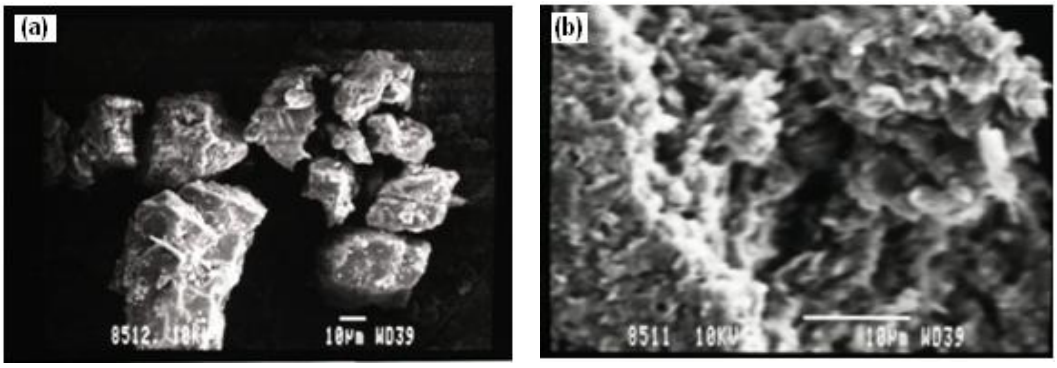

Figure 5.3: IIP particles (a), particle magnification (b).

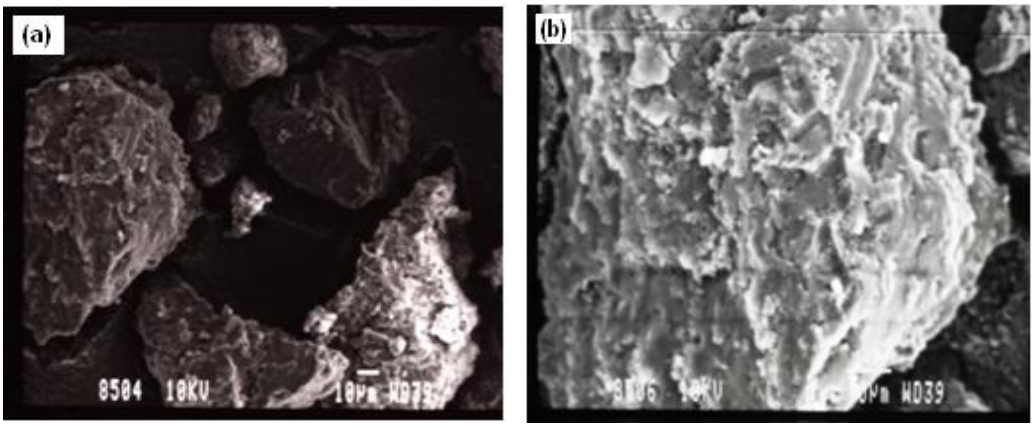

Figure 5.4: CP particles (a), particle magnification (b).

5.1.1.3. Surface area determinations

The surface area for all polymers was determined using the BET method. The values obtained were 61.7 and 5.9 m^2 g^{-1} for IIP (P1) and CP (P3), respectively. Therefore, it can be postulated that the IIP have higher surface area values due the imprinting effect. The surface area values obtained were compared to literature values for other uranium IIPs prepared by bulk polymerization. The surface area for P1 (61.7 m^2 g^{-1}) was found to be higher than the IIP (33.2 m^2 g^{-1}) prepared by Ahmadi et al. (2009) but much lower than IIPs (138.9 and 573.45 m^2 g^{-1}) prepared by James et al. (2009), and Singh and Mishra (2009), respectively. Many factors such as types of ligands, solvents, initiators, mechanical stirring *etc*. could contribute to these differences in surface area values.

5.1.2. Removal of the template

For optimum performance of the IIP/ MIP, it is imperative that the template molecule is removed successfully. Chromate anions were leached out in a batch mode as described in the experimental section. After timely intervals, the polymers were filtered and chromate concentrations were determined in the extracts. The results are given in Figure 5.5. It can be observed that after about 5 intervals of stirring and filtration, satisfactory amounts of chromium were removed from the polymer (Figure 5.5(a)). Also, changing the leaching solution to NaOH did not help that much, further emphasizing that nitric acid solution was enough (Figure 5.5(b)). However, it was paramount that NaOH is used for leaching as it was the leachant to be used for stripping re-bound chromate on imprinted polymers. Therefore, from these results it can be concluded that the prepared IIPs were washed successfully to be used for the subsequent binding studies.

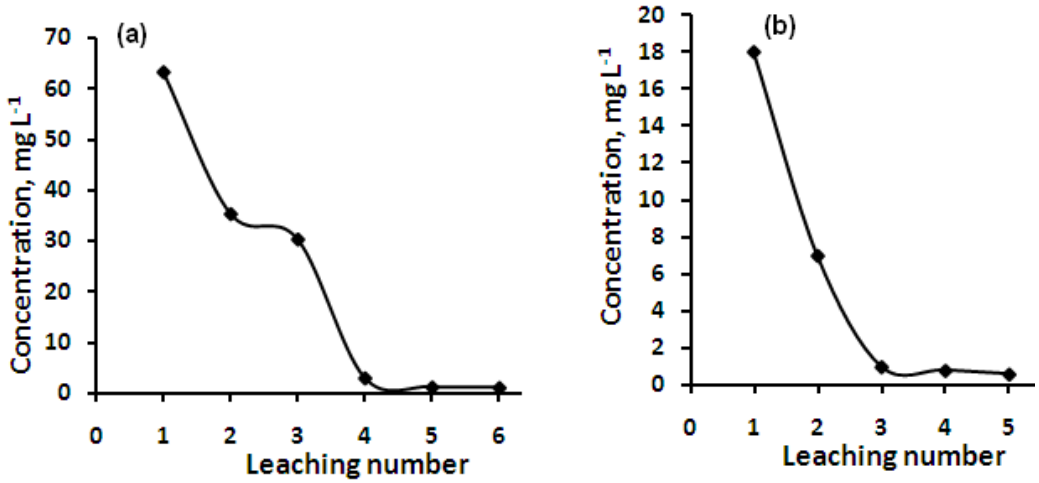

Figure 5.5: Leaching of the chromium (VI) template from IIP with HNO_3 (a), and NaOH (b).

Furthermore, the leaching of the chromium (VI) retained was optimized by performing simple experiment in SPE formats. An adsorption of chromium (VI) was performed by passing a solution containing known concentration on the IIPs in an SPE cartridge to get IIPs saturated with chromium six. The IIPs were dried

under vacuum and a solution of 0.1 M NaOH was passed through the IIPs in portions of 1 mL until a total volume of 10 mL was passed through. The solution was analyzed for chromate ions each time a 1 mL is passed and the results are depicted in the Figure 5.6 below. The results illustrated that 10 mL of 0.1 M NaOH was not enough to leach out all bound Cr (VI) on the polymer. Therefore, 20 mL was used as an optimum elution volume. Complete removal of chromate ions is important to avoid template bleeding by IIPs. Relatively large elution volume meant low analyte concentration enrichment but this did not pose any limitations because the IC-HPLC-UV method used is very sensitive with a detection limit below 1 µg L^{-1} with direct injection of pure standard.

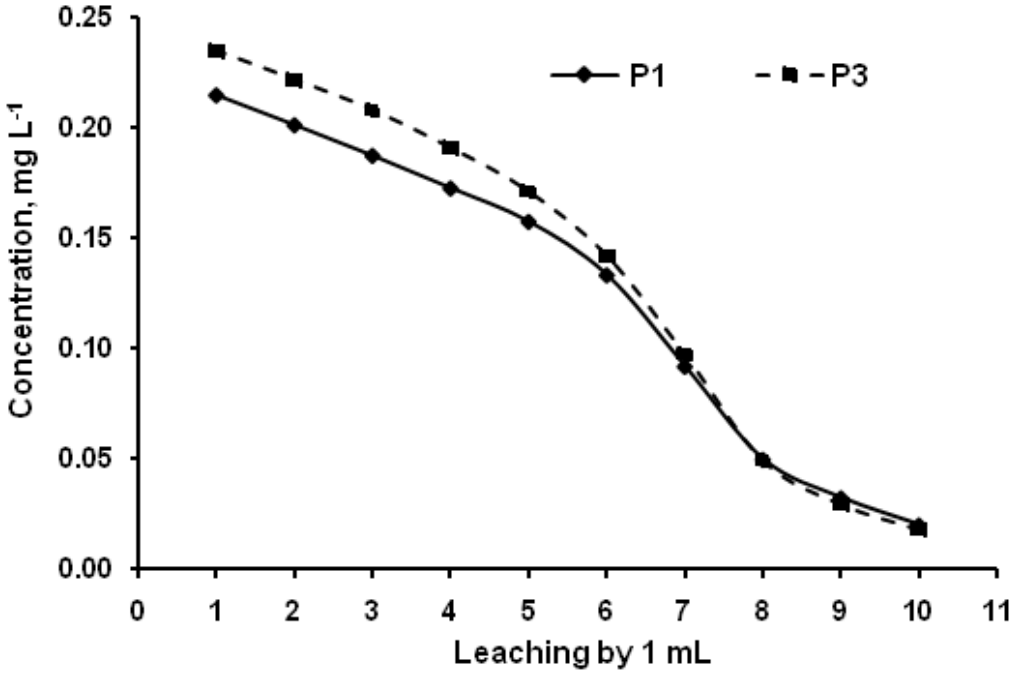

Figure 5.6: Leaching and washing of the retained chromate after rebinding. Amount of materials, 20 mg; solution pH 3; leaching solution, 1 mL of 0.1 M NaOH; material eluted from SPE cartridges. P1 and P3 are IIP and its corresponding CP, respectively.

5.1.3. Binding studies for chromium (VI) using chromium imprinted polymers (P1 and P3)

The chromium (VI) IIP prepared in this study was tested for chromium (VI) adsorption using two modes of extraction, namely, the batch mode and solid-phase extraction (SPE) method. Experimental parameters and recovery results are given in the Table 5.1 and the values reported are mean values. Percent recoveries obtained by both batch and SPE method showed that the IIP could be used successfully for extraction of chromium (VI) with either method of extraction. The idea here was to see if similar recoveries can be obtained with both methods as well as to investigate the reproducibility of the prepared IIPs as P1 and P2 are supposedly the same IIP polymer but prepared on different dates. From the high similar recoveries obtained from both P1 and P2 for batch extraction it can be concluded that the method of preparing these polymers is reproducible.

Table 5.1: Comparison of batch and SPE methods of adsorption using IIP and CP

	Batch			**SPE**	
	P1	P2	P3	P2	P3
Polymer (mg)	30	30	30	20	20
pH	3.0	3.0	3.0	3.0	3.0
Sample (mL)	25	25	25	25	25
Concentration added (µg L^{-1})	1000	1000	1000	1000	1000
Extraction time (min)	95	95	95	-	-
% Recovery	100 ± 0.05	98 ± 0.19	91 ± 2.48	96 ± 0.37	98 ± 0.52

P1 and P3 are IIP and its corresponding CP, respectively. P2 is the same as P1 but different batch production.

5.1.4. Optimization of MIP parameters

5.1.4.1. Effect of amount of chromium

Figure 5.7 shows the results obtained by varying the amounts of P1 and P3 particles during chromium (VI) adsorption studies. Different trends were observed for each polymer. In the particular case of CP, a maximum constant adsorption of

Cr (VI) of about 98% from 25 mg to 125 mg of the polymer observed. Hence, 30 mg can be regarded as optimum for this type of polymer. However, in the case of IIP particles the adsorption increased steadily going from 25 mg to reach maximum at 125 mg. Therefore, 130 mg was taken as an optimum for this polymer. The differences observed for these polymers can be attributed to the imprinting effect of P1 and the surface area. That is, due to imprinting effect the IIP can have different micro cavities (embedded in polymer matrix) compared to P3, which might have all surface micro cavities. Therefore, due to lower concentration of chromium (VI) in solution used and higher volume of surface area ratio it is possible for P3 to adsorb all chromium (VI) present even at lower amounts of P3.

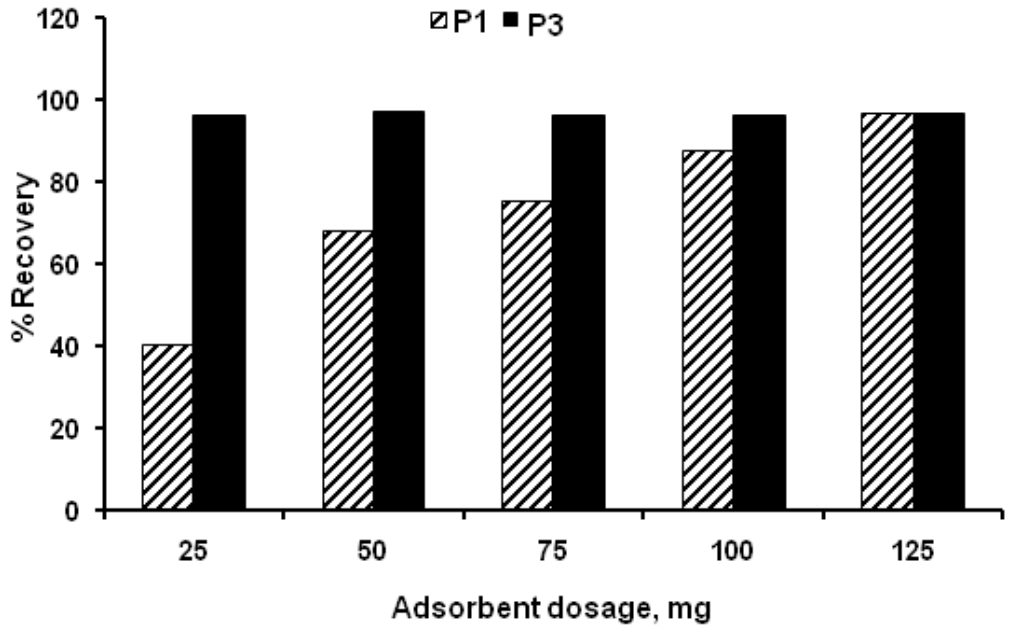

Figure 5.7: Effect of sorbent dosage of P1 and P3. Solution pH 3.0; concentration of solution, 1 mg L^{-1}; volume of solution, 25 mL; contact time, 120 min. P1 and P3 are IIP and its corresponding CP, respectively.

5.1.4.2. Effect of pH of chromium

The effect of pH on the removal of chromium (VI) ion by P1 and P3 was investigated by varying the pH from 1 to 4 and the results are shown in Figure 5.8. This pH range was chosen based on previous literature studies as can be seen in

Table 5.2 that the optimum pH for extraction of chromium (VI) was in this range. The chromate ion ($Cr_2O_7^{2-}$) from the salt used in the studies ($K_2Cr_2O_7$) is more predominant in the pH range of 2-6, hence the range studied. From Figure 5.8, one may note that there were no major differences in the influence of sample pH in the range studied. This similarity in Cr (VI) adsorption by P1 and P3 could be attributed to the nature of adsorbing polymer used. In this case, it is a quaternized polymer with a permanent positive charge that can attract negatively charged chromate species over the pH range investigated. Similar results where adsorption was independent of pH during the adsorption of Cr (VI) were reported by Neagu (2009) and Neagu and Mikhalovsky (2010) for their use of quaternized cross-linked pyridine polymers. Hence, for our studies pH 3 was used as optimal value.

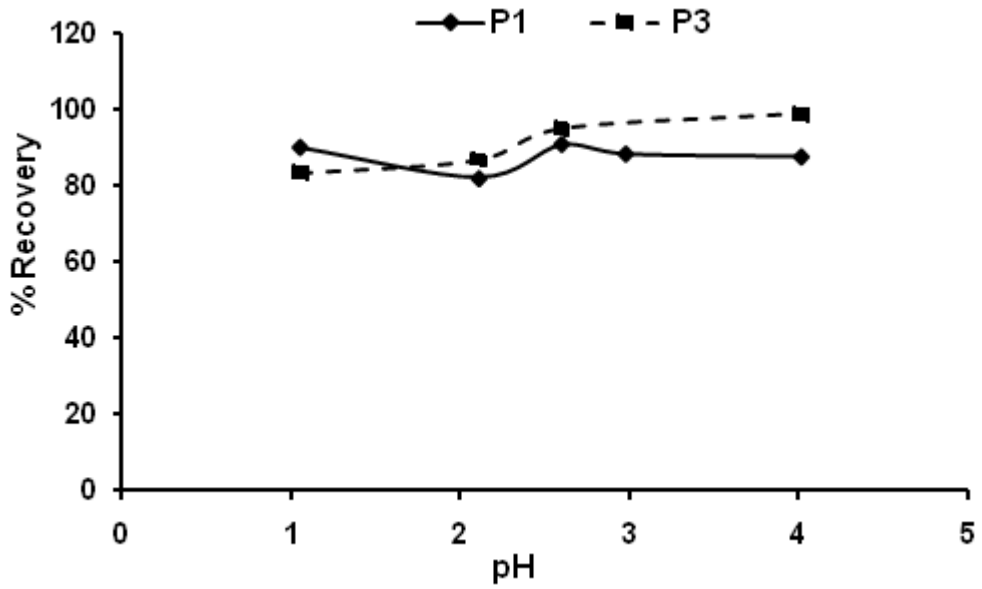

Figure 5.8: Effect of pH on the P3 and P1. Amount of materials, 20 mg; concentration of solution, 1 mg L^{-1}; volume of solution, 25 mL; contact time, 120 min. P1 and P3 are IIP and its corresponding CP, respectively.

Furthermore, Tunçeli and Türker (2002) obtained similar pH adsorption behaviour to the one obtained in this study where Cr (VI) adsorption was constant at about 75 % recovery from pH 2 to pH 8. It is known that Cr (VI) exists in different stable forms in aqueous solutions and the predominant species over the others is pH dependent. For an example, $Cr_2O_7^{2-}$ and $HCrO_4^{1-}$ more common in the pH

range 2.0-6.0, whereas CrO_4^{2-} predominates in basic solutions (Benhammou et al., 2007). The ionic strength of a solution increases with the decrease in pH and under such conditions one would expect that removal of Cr (VI) would be lower at low pH range (1.0-3.0) due to competition of the binding sites between Cr (VI) and Cl^- anions used pH adjustments. Furthermore, above pH 7, competition for the active binding sites from $–OH^-$ ions used for pH adjustments is expected to decrease the removal of Cr (VI). However, both these theoretical predictions were not observed either in this study or in a study by Tunçeli and Türker (2002). Both of the theoretical predictions are influenced by the selectivity of the polymer towards Cr (VI), the capacity of the polymer and amount of interfering ions.

5.1.4.3. Effect of initial concentration of chromium

The maximum adsorption capacity for the polymers was investigated and the results are shown in Figure 5.9. The results are presented in Figure 5.9 as retention capacity *versus* initial concentration of chromium (VI) in solution. From the graph it could be noted that, for the range of chromium (VI) concentration studied, the IIP reached a plateau around 38 mg g^{-1} while the CP seems to reach a plateau at 25 mg g^{-1}. These results illustrated that although the IIP (P1) and CP (P3) seem to have similar adsorption capability towards the chromate anion as indicated by the other experiments; actually the IIP has more binding sites due to imprinting effect. This means that the IIP can be deployed for environmental remediation for longer periods than the CP as it has higher binding capacity.

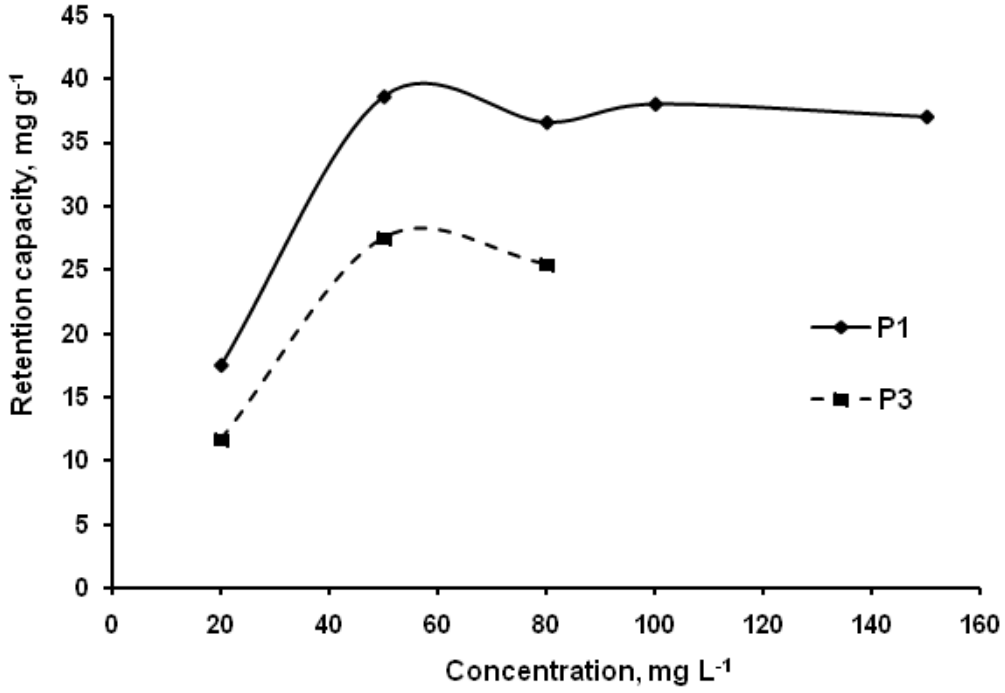

Figure 5.9: Retention capacity verses concentration of chromium (VI) in solution. The amount of IIP particles were 20 mg; solution pH 3; solution volume, 25 mL; contact time, 120 min. P1 and P3 are IIP and its corresponding CP, respectively.

The adsorption capacity values obtained in this study (38 and 25 mg g^{-1}) were compared to others values from literature. The data is presented in Table 5.2. It should be noted that the range obtained with the various adsorbents used for the removal of Cr (VI) is rather wide, *i.e.*, 1.88 – 200 mg g^{-1}. However, most of the listed adsorbents had a capacity between 20 and 60 mg g^{-1} of which our polymers fall under. This means that P1 and P3 could also be effective for removal of Cr (VI).

Table 5.2: Comparison of sorbent adsorption capacities

Sorbent	Binding capacity mg g^{-1}	Initial concentration mg L^{-1}	Initial pH	References
IIP 4-VP/MAA	37.58	60	3	*Present study*
CP 4-VP/MAA	25.44	60	3	*Present study*
IIP 4-VP/HEMA	(3.31)*	200	4	Bayramoglu and Arica, 2011
Chitosan coated with poly 3-methyl thiophene polymer	127.62	200	2	Hena, 2010
Chitosan	22.09	30	3	Aydin and Aksoy, 2009
Raw green alga *Oedogonium hatei*	31	100	2	Gupta and Rastogi, 2009
Acid-treated green alga *Oedogonium hatei*	35.2	100	2	Gupta and Rastogi, 2009
Bio-functional magnetic beads	6.73	40	1	Li et al., 2008v
Poly(methylacrylate) functionalized guar gum	29.67	400	1	Singh et al., 2009
Polyaniline-jute	4.66	20	3	Kumar and Chakraborty, 2009
Pre-boiled sunflower stem	4.9	50	2	Jain et al., 2009
Formaldehyde-treated sunflower stem	3.6	50	2	Jain et al., 2009
Synthesized CeO_2 nanoparticles	1.88	0.6	7	Recillas et al., 2010
Synthesized CeO_2 nanoparticles	83.33	37.5	7	Recillas et al., 2010
Synthesized CeO_2 nanoparticles	121.95	80	7	Recillas et al., 2010
Polyethyleneglycolmethacrylate-*co*-vinylimidazole (PEGMA-co-VI) microspheres	108.7	800	3	Uğuzdoğan et al., 2010
Spent cyanobacterial biomass from a hydrogen fermentor	39.2	50	3	Mona et al., 2011
Mercaptosilane functionalized sepiolites (acid-activated)	7.73	100	4.7	Marjanović et al., 2011

Mercaptosilane functionalized sepiolites (natural)	2.68	100	2.5	Marjanović et al., 2011
Powdered activated carbon	79.2	500	2	Anupam et al., 2011
Carbon nanotubes supported with activated carbon	9	0.5	2-4	Atieh, 2011
Poly [3-(acryloylamino) propyl] trimethylammonium chloride, P(ClAPTA)	164	30	9	Sánchez and Rivas, 2011
Poly (ar-vinyl benzyl) trimethylammonium chloride, P(ClVBTA)	152	30	9	Sánchez and Rivas, 2011
Poly[2-(acryloyloxy)ethyl] trimethylammonium methylsulfate, P(SAETA)	90	30	9	Sánchez and Rivas, 2011
Ethylenediamine (EDA)-functionalized magnetic polymers (EDA-MPs-2)	32.15	100	2.5	Zhao et al., 2010b
Ethylenediamine (EDA)-functionalized magnetic polymers (EDA-MPs-4)	36.63	100	2.5	Zhao et al., 2010b
Ethylenediamine (EDA)-functionalized magnetic polymers (EDA-MPs-6)	49.5	120	2.5	Zhao et al., 2010b
Ethylenediamine (EDA)-functionalized magnetic polymers (EDA-MPs-8)	60.98	140	2.5	Zhao et al., 2010b
Ethylenediamine (EDA)-functionalized magnetic polymers (EDA-MPs-10)	61.35	140	2.5	Zhao et al., 2010b
Quaternized poly(4-vinylpyridine)	33	138		Neagu and Mikhalovsky, 2010
Chitosan supported onto agave fiber – postconsumer HDPE composites	200	10-1000	4	Perez-Fonseca et al., 2011

* the value is in mmol g^{-1}. Authors did not name the source of Cr (VI) ions used to help with conversion

5.1.4.4. Effect of solution volume of chromium

Figure 5.10 depicts the results obtained from varying the solution phase volume during adsorption of Cr (VI) onto IIPs (P1) and CPs (P3). It can be noted from such results that both polymers showed similar trend, further emphasizing that these polymers are actually not very different. The slanting shape of the graph in Figure 5.10 can be explained in terms of the mass transfer of chromium from the bulk solution to the IIP and CP particles. The smaller the volume, the lesser the duration of contact time is needed for chromium in solution to come in contact with IIP particles as the distance between the IIP or CP particles and chromium in solution will be smaller compared to when the volume is larger. Hence, this explains the low recoveries in larger volumes of solution. The recovery generally is constant and independent of sample volume where the polymer is packed in a cartridge as in SPE until breakthrough volume is exceeded which is somewhat different from what is observed in Figure 5.10.

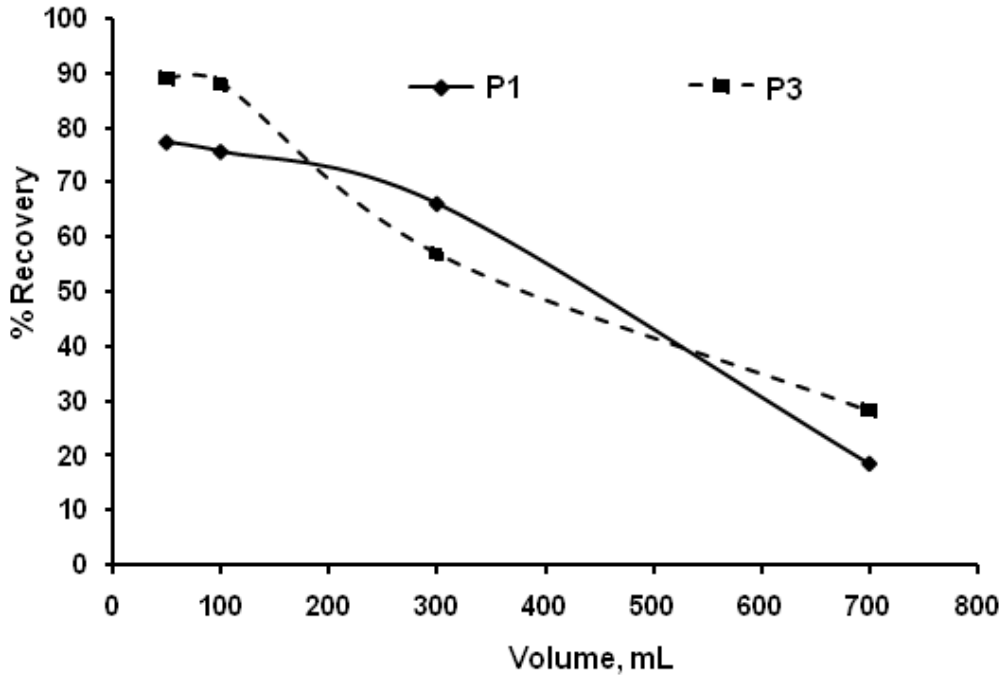

Figure 5.10: Effect of solution volume. Amount of materials, 20 mg; solution pH 3; concentration of solution, 1 mg L^{-1}; contact time, 120 min. P1 and P3 are IIP and its corresponding CP, respectively.

5.1.4.5. Effect of time on chromium (VI) adsorption

The effect of stirring time on extraction of chromium (VI) by IIP and CP was investigated and the results are shown in Figure 5.11. Both polymers showed greater than 85% recovery for the time intervals investigated. However, the IIP demonstrated somewhat faster binding kinetic as 92% recovery was obtained compared to 88% at just after 10 minutes of stirring. However, after 20 min of stirring it was the CP that showed higher recovery and seem to have reached a plateau after 60 min. The recovery for the IIP after 90 min was 97% and it was still on the rise, hence, 120 min was taken as an optimum stirring time for IIP and CP.

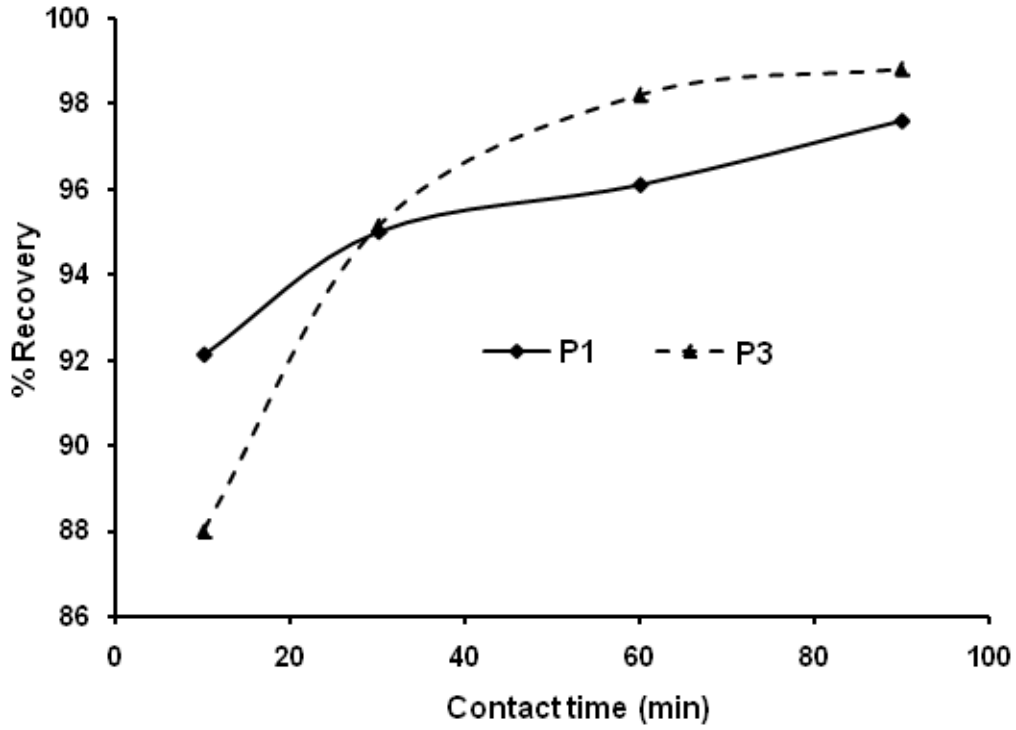

Figure 5.11: Effect of stirring time. Amount of materials, 20 mg; solution pH 3; concentration of solution, 1 mg L^{-1}; volume of solution, 25 mL. P1 and P3 are IIP and its corresponding CP, respectively.

5.1.4.6. Selectivity of chromium

Competitive adsorption of Cr (VI) / Cl^-, Cr (VI) / F^-, Cr (VI) / NO_2^-, Cr (VI) / NO_3^-, Cr (VI) / SO_4^{2-}, Cr (VI) / PO_4^{3-} and {Cr (VI) / Cl^-, F^-, NO_2^-, NO_3^-, SO_4^{2-} and PO_4^{3-}} were investigated and the results are summarized in Table 5.3. In terms of

recognition of the chromate anion the data is in agreement with that obtained previously (Table 5.1) in that the IIP and CP seem to adsorb chromate almost the same (Table 5.3). The distribution coefficients, K_D, and the selectivity coefficients *K*, for the IIP and CP are comparable further emphasizing that the polymers are similar. However, chloride anions (Cl^-) could not be quantified by IC because, firstly it was used to adjust pH (in the form of HCl) and secondly it was used during quaternization (as 1,4-dichlorobutane). Therefore, it was understandable that there would be a high concentration of the chloride ion from the samples.

The influence of the investigated co-existing anions on chromium (VI) sorption can be summarized to follow this order; $SO_4^{2-} > F^- > PO_4^{3-} > NO_2^- > NO_3^- > Cl^-$. The evaluated order is slightly off to what was reported by Fang et al., (2007) when they investigated the influence of SO_4^{2-}, PO_4^{3-} and NO_3^- on Cr (VI) sorption using 0.1, 1.0 and 10 mM concentrations of anions. The observed trend was $PO_4^{3-} > SO_4^{2-} > NO_3^-$ whereas our studies indicated that the sulphates compete more for binding sites than phosphates.

Table 5.3: Distribution coefficient and selectivity factor for IIP and CP

Adsorbent	*Kd*		*K*	*K'*	Adsorbent	*Kd*		*K*	*K'*
	Cr(VI)	Cl^-				Cr(VI)	SO_4^{2-}		
CP	423.6	N.D			CP	274.5	109.0	2.5	
IIP	442.7	N.D			IIP	347.0	249.9	1.4	0.55
Adsorbent	*Kd*		*K*	*K'*	Adsorbent	*Kd*		*K*	*K'*
	Cr(VI)	F^-				Cr(VI)	PO_4^{3-}		
CP	328.6	37.8	8.7		CP	379.2	127.5	3.0	
IIP	350.3	0.1	3503.0	403.0	IIP	383.6	138.4	2.8	0.93
Adsorbent	*Kd*		*K*	*K'*	Adsorbent	*Kd*		*K*	*K'*
	Cr(VI)	NO_3^-				Cr(VI)	NO_2^-		
CP	408.0	105.2	3.9		CP	434.2	69.3	6.3	
IIP	412.5	376.4	1.1	0.28	IIP	395.4	488.0	0.81	0.13

5.1.4.7. Reusability of chromium (VI) IIP (P1) and CP (P3)

The stability and reusability of the polymers was tested by stirring 20 mg of polymer in chromium (VI) solution (1 µg mL^{-1}). To achieve this, the prepared ion imprinted polymer sorbent was repeatedly used and regenerated for a number of times. The results are illustrated in Figure 5.12. It can be said that, no significant decrease was observed in the sorbent affinity over the number of cycles investigated. This clearly shows that the polymers are stable as there is no lose of affinity for chromium (VI) and polymer destruction. The polymers yielded greater than 96% extraction efficiency for up-to 5 cycles.

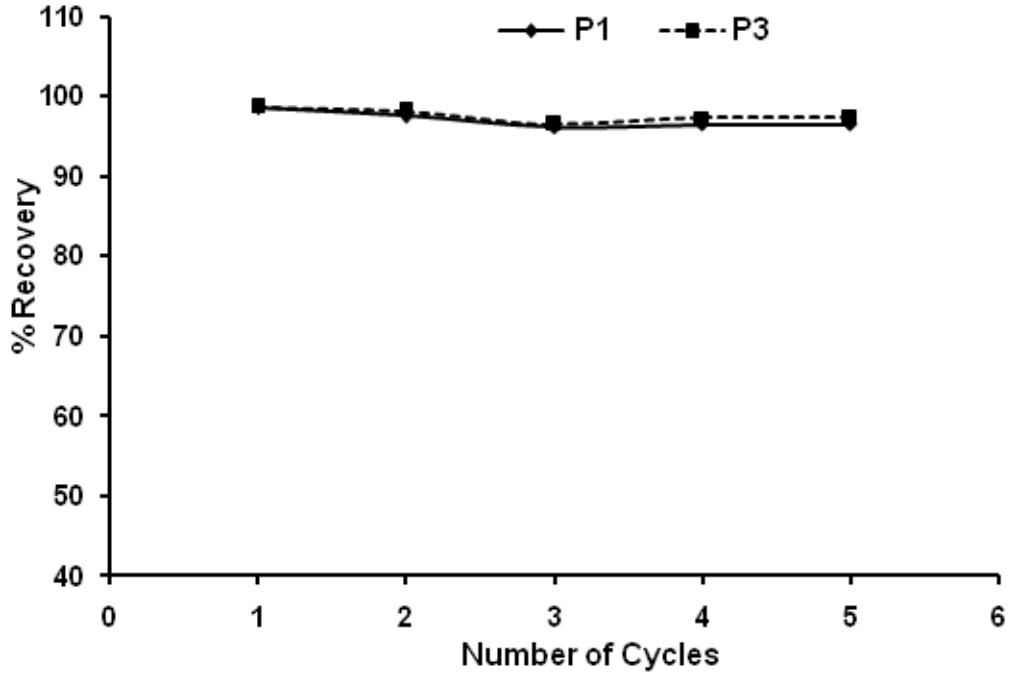

Figure 5.12: Reusability and stability of the polymers. Amount of materials, 20 mg; solution pH 3; solution volume, 25 mL; contact time, 120 min, concentration of solution, 1 mg L^{-1}. P1 and P3 are IIP and its corresponding CP, respectively.

5.1.5. Effect of ionic strength

The study of ionic strength influence is important on the adsorption of chromium (VI) by adsorbents as wastewater contains different ions (Anirudhan et al., 2009). The results from such studies are depicted in Figure 5.13. Consistent with the

literature (Li and Bowman, 2001; Fang et al., 2007), the sorption of chromium (VI) decreased with increasing ionic strength, meaning that chromium (VI) sorption is affected by exchange reactions (Fang et al., 2007). In fact, ion activity of chromium ions decreases with increase in ionic strength (Li and Bowman, 2001). The ion exchange process taking place on the surface of the polymer can be represented as:-

$$X\text{-}Cl + HCrO_4^- = X\text{-}HCrO_4 + Cl^- \qquad K_V\,(Cl\text{-}HCrO_4)$$

where, $K_V(Cl\text{-}HCrO_4)$ is the Vanselow selectivity coefficient (Fang et al., 2007).

According to Lee et al. (2005) if the change in ionic strength does not lead to any appreciable change in the removal of the chromate then the mechanism for removal might be due to precipitation and covalent bonding. Ions that form outer-sphere complexes show decreasing adsorption as the ionic strength is increased (McBride, 1997). The decrease in chromium (VI) adsorption with increase in ionic strength can be said to obey this theory.

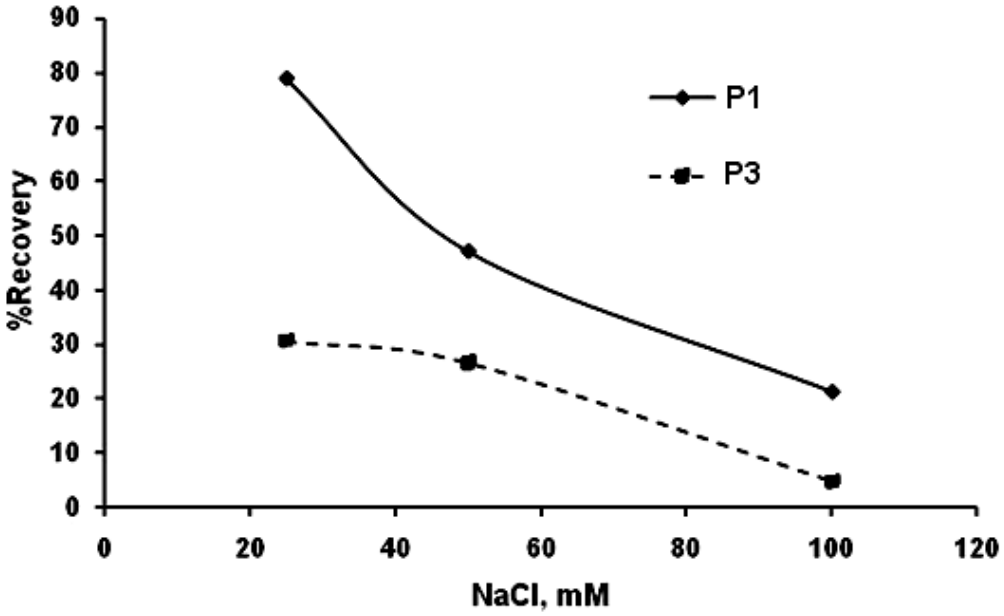

Figure 5.13 Effect of ionic strength. Twenty milligrams of polymers were stirred in 1 µg mL^{-1} concentration of chromium solution containing different concentrations of NaCl (25-300 mM, ~900 – 3500 µg mL^{-1}); solution pH 3; solution volume, 25 mL; contact time, 120 min. P1 and P3 are IIP and its corresponding CP, respectively.

This decrease is due to the competition for specific binding sites between the chromate and the chloride anions present in solution. For comparison between CP and IIP, the latter showed slightly higher recovery which is also a proof of the imprinting effect. IIP are therefore generally superior in selectivity compared to normal polymers with chelating functional groups.

5.1.6. Adsorption isotherms

The Langmuir and Freundlich models were used to study the adsorption of chromium (VI) on the IIP particles and the results are displayed on Table 5.4. The Langmuir model was first developed to describe the vapour adsorption on homogeneous surfaces. However, when used for solid-liquid systems several assumptions have to be made. These assumptions are: number of surface adsorption sites is fixed, adsorption involves a single monolayer, adsorption behaviour is independent of surface coverage and all adsorption sites are represented by similar types of functional groups. The Langmuir equation is given by:-

$$\boldsymbol{C_e/q_e = C_e/Q_o + 1/bQ_o} \qquad \textbf{(5.1)}$$

where, q_e is the amount of solute adsorbed on the surface of adsorbent (mg g^{-1}), C_e is the equilibrium chromium (VI) concentration (mg mL^{-1}), Q_o is the saturated monolayer adsorption capacity (mg g^{-1}), and b is the Langmuir adsorption constant (L mg^{-1}). A plot of C_e/q_e versus C_e gives the values of Q_o and b (Wang et al., 2009b). Freundlich adsorption isotherm which assumes a multilayer adsorption can be given by the linearized form:-

$$\boldsymbol{\ln q_e = \ln K_F + 1/n \ln C_e} \qquad \textbf{(5.2)}$$

where, K_F is the Freundlich constant, and n is the Freundlich exponent. The experimental values for q_{exp} and q_{max} are comparable. The initial solution concentrations used were in the range of 10 - 100 mg L^{-1}. In the Freundlich approach the values of n are both greater than 1 indicating favourable adsorption of chromium (VI) on the adsorbent (Candan et al., 2009).

The summary of the results obtained by fitting the experimental data to the 2 models, namely, the Langmuir and Freundlich adsorption isotherms is supplied in Table 5.4. It can be observed from the R^2 values that the results for the IIP fit both models, whereas results for the CP did not show a good fit for the Freundlich model. This unfavourable fit shown by CP data can be explained by the fact that the Freundlich model follows a multilayer mode of adsorption. The CP can be predicted to favour a monolayer mode of adsorption (surface adsorption), whereas in the IIP there are surface as well as some deep embedded cavities for adsorption due to imprinting effect. Thus, making IIP a multilayer adsorbent compared to the CP which is a single layer adsorbent due to lack of imprinting effect.

Table 5.4: Langmuir and Freundlich adsorption isotherm constant values determined for the IIP and CP

Polymers	Experimental	Langmuir Model			Freundlich Model		
	q_{exp} (mg g^{-1})	q_{max} (mg g^{-1})	b	R^2	K_F	n	R^2
IIP	38.43	45.23	7.8×10^{-3}	0.97	5.08	1.46	1.00
CP	25.44	34.31	3.6×10^{-2}	0.96	5.55	2.61	0.65

5.1.7. Application of prepared IIP to real samples

The IIPs prepared in this study were evaluated for adsorption of chromium (VI) from real-world samples. This screening experiment was performed using a batch mode of extraction. After batch experiments, un-adsorbed and adsorbed chromium (VI) were determined and the results are shown in Table 5.5. Unspiked tapwater and Bokkamp dam water were run as blank and chromium (VI) quantified was 0 and 2.24 µg L^{-1}, respectively (Table 5.5). In tap water both the CP and IIP showed high recoveries of about 95% which are in agreement with other previous results obtained in this study. What is worth noting is the results in acid mine drainage (AMD) water. The recovery of the control polymer in AMD collapsed because of high concentration of interfering sample matrix especially sulphate ions. This is not surprising since in IIP selectivity is based on size and shape besides ionic interaction.

Table 5.5: Analysis of Tapwater, Bokkamp dam 2 and acid mine drainage water spiked with 30 µg L^{-1} of reference material. Amount of materials used, 20 mg; solution pH 3; solution volume, 25 mL; contact time, 10 min; concentration, 30 µg L^{-1}

Samples	Direct analysis, µg/l			Concentration of Cr (VI) µg/l by IIP		% Recovery Cr (VI)	
	Cr (VI)	Cl^-	SO_4^{2-}	Added	Measured [a]	CP	IIP
Tapwater	-	0.87	1.03	0	-	-	-
	-	0.87	1.03	30.0		93.11	97.26
Bokkamp dam 2	2.26	4.61	19.41	30.0	33.74 ± 4.53 [b]	-	-
	2.26	4.61	19.41	30.0	15.70 ± 6.69	4.56	47.68
AMD wastewater	no peak			0	-	-	-
	no peak			30.0	25.87 ± 6.15	18.13	70.08

[a] Mean of triplicates ± RSD [b] Spiked sample before extraction

The selectivity was also compared by direct injection of the real sample (AMD) for both spiked and non-spiked to that after IIP selective extraction. Despite very low detection limit of direct injection of method (below 1 µg L^{-1}) no chromium (VI) was obtained in the spiked sample. After IIP extraction, spiked chromium (VI) was detected in the sample (Table 5.5).

5.1.8. Conclusions

A selective IIP for extraction of Cr (VI) was prepared and optimized. The prepared IIP showed superior selectivity towards Cr (VI) in acid mine drainage water, where the selectivity of the control collapsed due to high amounts of sulphate ions. The IIP backbone provides an opportunity to prepare Cr (VI) adsorbent materials with high stability and durability under different conditions (acidic, basic and common organic solvents). Maximum binding capacity of 38 mg g^{-1} polymer was obtained from an initial concentration of 60 mg L^{-1}, which was slightly higher than the amount obtained by Neagu and Mikhalovsky (2010), of 33 mg g^{-1}, from an initial concentration of 138 mg L^{-1}, and also comparable to the 50 mg g^{-1} binding capacity obtained by Fang et al. (2007) from an initial concentration of 98 mg mL^{-1}.

5.2. Preparation of ion imprinted polymer for uranium VI removal

For the preparation of the uranyl ion imprinted polymer, first the binding monomer 1-(prop-2-en-1-yl)-4-(pyridin-2-ylmethyl)piperazine (PPMP) was prepared as detailed in Section 3.6.2. ^{1}H NMR, ^{13}C and (Distortionless Enhancement by Polarization Transfer) DEPT 135 chemical shift results confirmed that ligand was successfully synthesized. The IIP was obtained from polymerization of the synthesized vinyl ligand in the presence of EDMA, MAA and azobis(bicyclohexane carbonitrile) (Figure 5.14). The active sites for the uranyl ion are the three amino atoms from the ligand (Figure 5.14) and the hydroxyl from the MAA. However, as per Donia et al. (2009), the mechanism of interaction between the amine active sites and positively charged uranyl ions is of the coordination type and this coordination is usually dominated by four, five or six donor atoms, all situated in the equatorial position. This is because the axial position is already occupied resulting in octahedral, pentagonal bipyramidal or hexagonal bipyramidal geometries, respectively (Meinrath, 1998; Sessler et al., 2006; van Horn et al., 2006). On the other hand, the hydroxyl groups and carbonyl groups bond to UO_2^{2+} ions through complexation (Anirudhan and Radhakrishnan, 2009). It was envisioned that the piperazine part of the vinyl ligand formed would be in a boat conformation meaning that the amino moieties of this ligand will be in a "C" shape with the methacrylic acid hydroxyl group closing the "C" in the process encapsulating the uranyl ion analyte, as illustrated in Figure 5.14.

The study by Manhas et al. (1993) demonstrated that piperazine ligands could form complexes with uranium (IV) when they are in either chair or boat conformations. Another possibility is the opening of the piperazine ring to yield with 1-(prop-2-en-1-yl)-4-(pyridin-2-ylmethyl)-*N*-2-hydroxylethane-ethylenediamine during complexation reaction. Similar observation was made (Albo et al., 2009) where complexation yielded the opening of the imidazoline ring in their use of *N,N'*-di(2-hydroxy-4,6-di-*tert*-butyl-benzyl)imidazoline as a complexing ligand for UO_2^{2+} ions. The authors demonstrated ligand transformation by studying the ^{13}C NMR of the ligand before and after leaching of the UO_2^{2+} ion. Differences in carbon chemical shifts due to the influence of the

ethylenediamine and hydroxyl groups were key for their proofs. The transformation is catalysed by the presence of a base in solution (*e.g.*, OH^- or $UO_2(OH)^+$). In our case, the presence of a broad band after leaching in Figure 5.15(b) at about 3400 cm^{-1} could be attributed to the opening of the ring, hence confirming presence of hydroxyl groups.

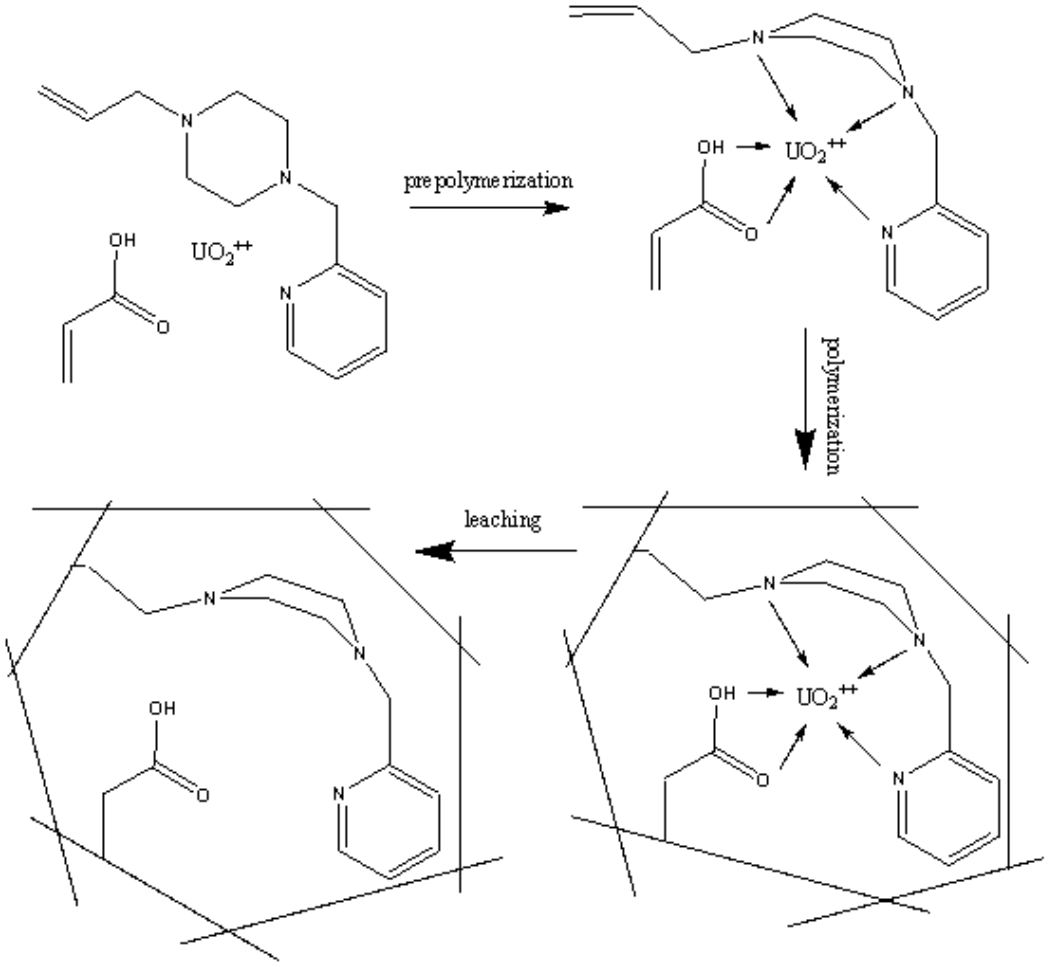

Figure 5.14: Schematic representation of the imprinting method.

5.2.1. Characterization of uranium IIP

5.2.1.1. FTIR

The FTIR spectra of the CP (P5), leached and unleached IIP (P4) show a similar backbone indicative of a high level of the EDMA cross linking reagent used (see Figure 5.15). All three spectra show strong vibration frequencies at about 1720

and 1141 cm^{-1} which could be respectively assigned to C=O and C-O functional groups of EDMA polymers. The band at 1637 cm^{-1} attributed to unpolymerized C=C of the monomer is almost diminished in all polymers indicating that almost all the monomers were reacted or washed out (Khajeh and Sanchooli, 2010). Normally pyridine has two strong vibration frequencies in the range 660-880 cm^{-1}. Notably here is the band at 814 cm^{-1} with the stronger intensity in the unleached IIP form. In both leached and control polymer, this band have equal intensity implying the absence of uranyl ion in CP and apt washing of uranyl ion from the leached polymer. The stronger intensity of the band at 814 cm^{-1} in unleached polymer can be attributed to the presence of UO_2^{2+} ion as it observed in the study by Singh and Mishra (2009b). Singh and Mishra (2009b) expressed that uranyl ion has a symmetric band at 815 cm^{-1} and an asymmetric band at 912 cm^{-1}. Also, notably was the shift and higher intensity of the band at 946 for (CP and leached) to 939 cm^{-1} (for unleached) also could be an indicative of the removal of uranyl ion.

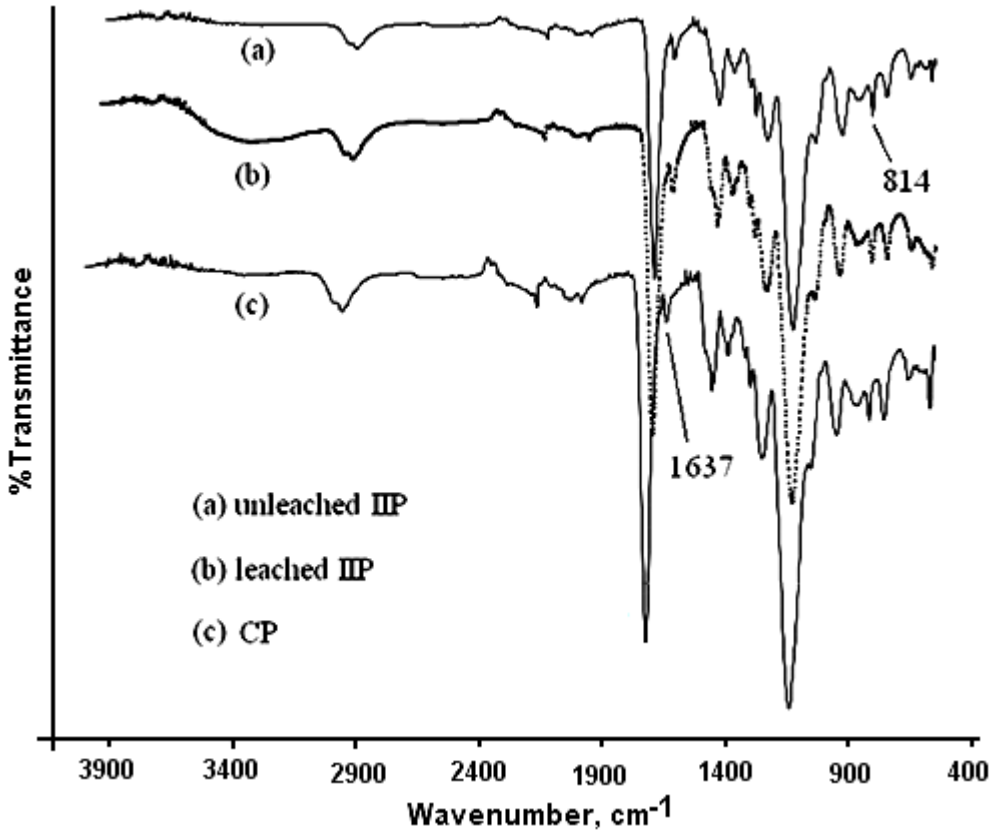

Figure 5.15: FTIR spectra of (leached and unleached) IIP (P4) and CP (P5).

5.2.1.2. Scanning electron microscopy

Figure 5.16 (a) depicts the SEM micrographs of P4 and it can be deduced that the particles have irregular shape due to crushing with mortar and a pestle. Further zooming in at some of the particles one can notice the pores created by the imprinting effect, Figure 5.16 (b).

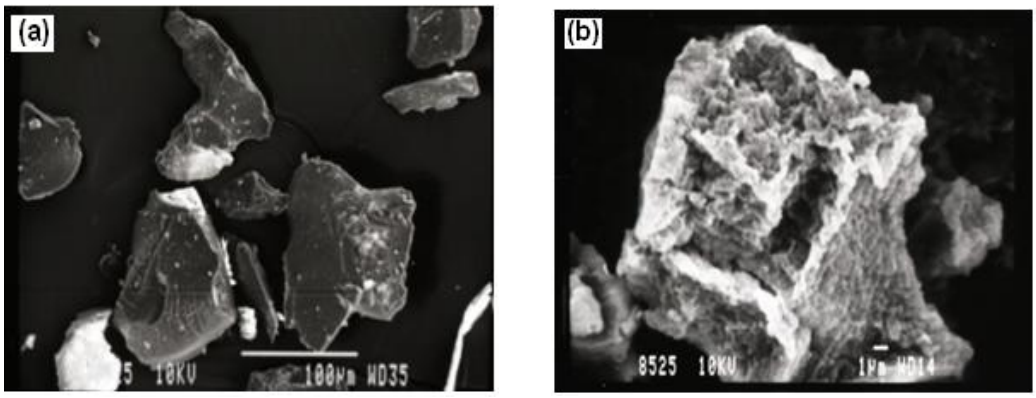

Figure 5.16: SEM micrograph of P4 (a), and one particle magnification (b).

5.2.1.3. Surface area determinations

Surface area measurements were obtained using two methods, namely, the BET instrument and methylene blue method. For P4 the values obtained using BET instrument and methylene blue method were 26.3 and 31.2 m^2 g^{-1}, respectively. While for P5, the values obtained 16.1 and 17.6 m^2 g^{-1} using BET and methylene blue method, respectively. It can be concluded that both methods gave similar values. This implies the accuracy of each method. It can be further observed that with both methods, the imprinted polymer (P4) exhibited higher surface area values and this could be attributed to micro cavity gaps created by the imprinting effect. In the case where methylene blue was used, three replicate experiments were conducted and for each experiment absorbance was recorded with UV spectrophotometry. The surface area was calculated from equation 4.6.

5.2.2. Removal of the uranyl ion template

The removal of the uranyl ion imprint was achieved by stirring the polymer particles in a solution of hydrochloric acid. This was because various researchers have successfully removed uranyl template ions from IIP using a solution of hydrochloric acid (Metilda et al., 2004; James et al., 2009; Singh and Mishra, 2009b). In this particular case, IIPs were first washed with 2 M HCl for about 9 cycles then a stronger acid solution (5 M HCl) was used to further certain the successful removal of uranyl imprint ion from IIPs. Figure 5.17 shows the analysis of such leaches at each and every cycle. After 14 cycles the IIP particles were conditioned with Milli-Q water to remove the excess chloride ions and dried in the oven overnight (55°C). However, during batch re-binding experiments of washed IIP, 10 mL of 2 M HCl was enough to remove the rebound uranyl ion. Re-bound uranium is not as tightly bound as uranium in un-leached polymers, hence the use of less concentrated acid. Further 1 M HCl was also tested but from the studies, it was found that 10 mL of 2 M HCl was the best for the removal of

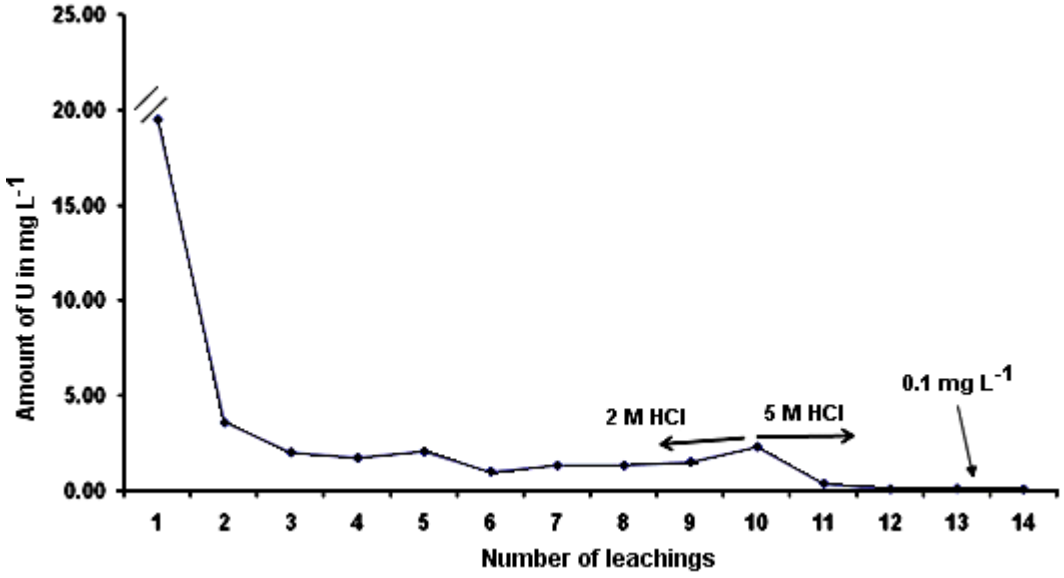

Figure 5.17: Leaching of the uranyl ion template.

bound uranyl ions from the polymer. The results were consistent with those of others (Preetha et al., 2006; Metilda et al., 2004; James et al., 2009; Singh and Mishra, 2009b) which demonstrated that hydrochloric acid alone is enough for the

quantitative removal of bound uranium from polymers bearing the amino moieties. These results are depicted in Figure 5.17.

5.2.3. Binding studies

Binding studies were conducted in a batch mode. However, a solid-phase extraction (SPE) method was also evaluated. Details of these methods are described in the experimental section. Both SPE and batch methods gave about 99% recovery of uranyl ion using P4 while the recovery with CP (P5) was about 50% (Table 5.6). The SPE method was used in the regeneration studies as it was easier eluting rebound uranyl ion from SPE cartridges than from a batch method. In a batch method there is a possibility of losing the IIP particles during the process, *e.g*., filtration. This study showed that the polymer could be used with either method (batch or SPE format) efficiently. However, only the batch method was used for further investigations in this study except for regeneration studies. Also, leaching of the SPE cartridges with 10 mL of 2 M HCl proved to be efficient for the removal of bound uranium.

Table 5.6: Binding studies of batch method versus SPE method

	SPE		**BATCH**	
	P4 (IIP)	**P5 (CP)**	**P4 (IIP)**	**P5 (CP)**
Amount (mg)	50	50	50	50
pH	5	5	5	5
Volume (mL)	25	25	25	25
Initial conc. (μg L^{-1})	1000	1000	1000	1000
% Removal	99	51	99	65

5.2.4. Optimization of IIP parameters

5.2.4.1. Effect of amount of uranium

Figure 5.18 shows the results obtained from the optimization of the amount of IIP (P4) particles for uranyl ion adsorption. From the results it can be observed that

IIP recorded higher % recoveries compared to CP (P5) for all the various amounts investigated. This is attributed to the imprinting effect in IIP. A constant extraction of 99.9% was achieved from 20 mg to 40 mg and hence, 20 mg was chosen as optimum IIP quantity needed for succeeding adsorptions.

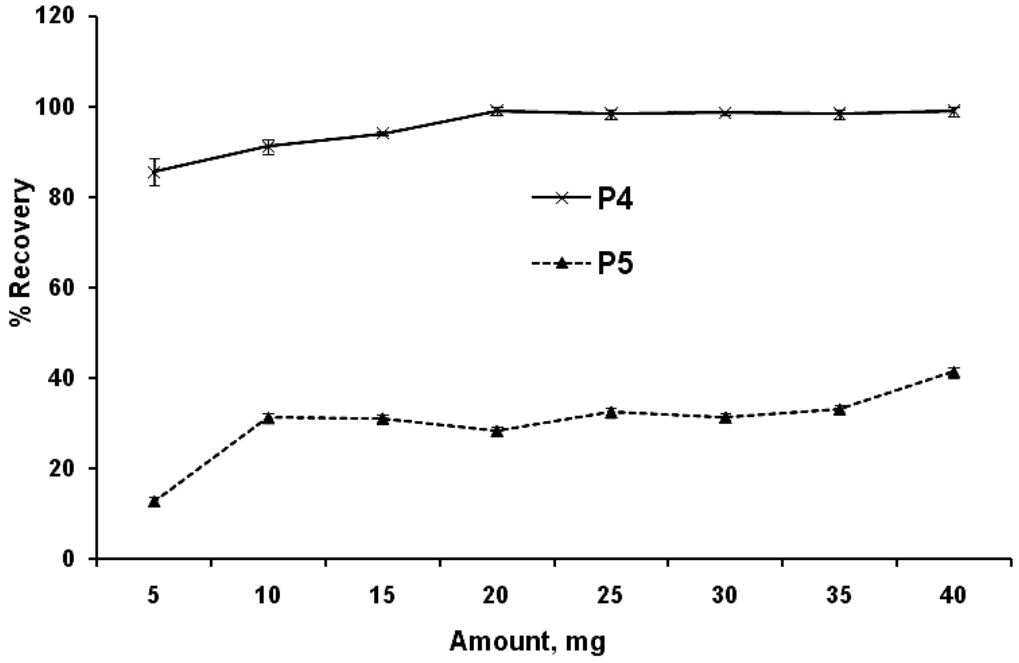

Figure 5.18: Quantity of IIP (P4) and CP (P5) optimization**.** Solution pH 5; solution volume, 25 mL; contact time, 20 min, concentration of solution, 1 µg mL^{-1}.

5.2.4.2. Effect of pH of uranium

The effect of pH on the extraction of uranium (VI) ion by P4 and P5 was investigated by varying the pH from 1 to 8 and the results are shown in Figure 5.19. From Figure 5.19, one may conclude that the IIP reached maximum extraction at pH 4-6 while the CP reached maximum at pH 7. Hence, pH 5 was used for subsequent experiments. Also, worth mentioning is the steady adsorption capacity demonstrated by the CP as the pH was increased and this resulted to about 95% adsorption. Not surprisingly, at lower pH values, the imprinting effect was expected to be lower due to protonation of the pyridine-N leading to repulsion of the uranyl ion. The pH studies suggested that this polymer could be successfully used for the pH range between 3.5 – 7.0. The CP showed unusual

high recovery at pH 6. The reason for this could not be fully explained. This unusual behaviour of the CP at pH 6 was further tested by repeating the whole experiment with CP but similar results were obtained.

In the absence of complexing ligands, the pentagonal bipyramidal $[UO_2(H_2O)_5]^{2+}$ is the most stable form of uranium in aqueous solutions with pH 0-4 (Cotton, 2006). At higher pH values where the uranyl ion might hydrolyse, UO_2OH^+, $(UO_2)_2(OH)_2^{2+}$, and $(UO_2)_3(OH)^{5+}$ species are present (Bae et al., 1999; Psareva et al., 2005). However, it is well documented that at lower pH values the uptake efficiency of the uranyl ion is limited by the competition from the H_3O^+ ion. From Figure 5.19, it can be observed that the uptake of UO_2^{2+} ion increases with pH and

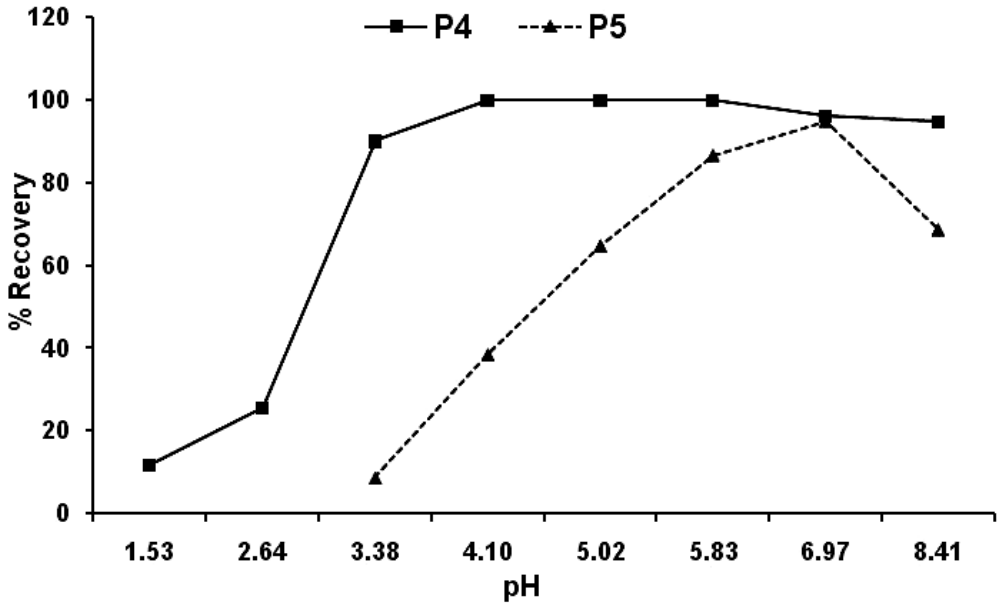

Figure 5.19: Effect of pH on IIP (P4) and CP (P5). Amount of materials, 20 mg; solution volume, 30 mL; contact time, 20 min, concentration of solution, 1 µg mL^{-1}.

then remained constant in the pH range 4-6. This suggests that the ligand binds these hydroxo complexes very well. At the same time literature (Shamsipur et al., 2007) reveals that the mechanisms for the removal of uranyl ion in the pH range 4-5.5 is believed to be that of ion exchange and complexation processes.

5.2.4.3. Effect of concentration of uranium

The retention capacity study was performed by equilibrating 20 mg of P4 or P5 particles with 30 mL uranium solution with concentrations ranging from 10–660 µg mL^{-1} under optimal conditions. The results are shown in Figure 5.20. It was observed that retention capacity of the IIP increased with increase in concentration until it reached a plateau at 120 mg g^{-1} when the concentration of the UO_2^{2+} ion in solution was about 528 µg mL^{-1} (Figure 5.20). At low concentrations, the IIP particles can take up all the uranium in solution without exhausting its binding sites hence, the increase of binding capacity with increase with increase in concentration.

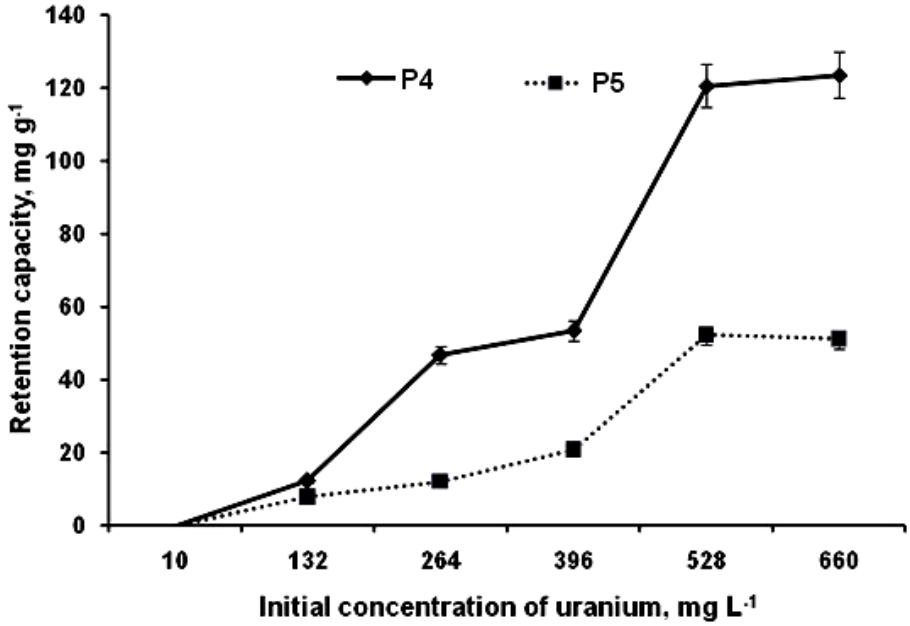

Figure 5.20: Retention capacity of IIP (P4) and CP (P5). Amount of materials, 20 mg; solution pH 5; contact time, 20 min; solution volume, 30 mL; stirring speed, 600 rpm.

The binding capacity demonstrated by the prepared IIP was compared to some of the literature values from the different sorbent as listed in Table 5.7. Some of these sorbents have relatively higher loading capacity (Sureshkumar et al., 2010; Lee et al., 2010) than the present IIP. This is because of larger surface area of

some natural polymers. However, the type of chelating ligand and cross-linker used also affect the capacity (Wang et al., 2009b). Lack of selectivity and swelling problems are some of the demerits of sorbents based on natural materials and on the other hand IIPs bring about the simplicity in preparation, low cost, selectivity, high thermal and mechanical strength.

Table 5.7: Comparison of retention capacity values for the uranyl ion with different sorbents

Metal ion	Sorbent	Binding capacity mg g^{-1}	Initial pH	Reference
UO_2^{2+}	Amberlite XAD-2000	3.6	3.0	Ghasemi and Zolfonoun, 2010
UO_2^{2+}	Cross-linked chitosan	72.46	3.0	Wang et al., 2009a
UO_2^{2+}	Cross-linked chitosan	239.9	5.0	Sureshkumar et al., 2010
UO_2^{2+}	Activated silica	153	4.0	Lee et al., 2010
UO_2^{2+}	Activated charcoal	82	4.5	Zhao et al., 2010
UO_2^{2+}	Date pits	10	5.5-6.5	Saad et al., 2008
UO_2^{2+}	Q-Amberlite XAD-4	37.4	4.5	Lee et al., 1997
UO_2^{2+}	IIP	98.5	3.5-5	Preetha et al., 2006
UO_2^{2+}	IIP	30.1	6.0	Gladis and Rao, 2003
UO_2^{2+}	IIP	38.58	6.0	Sadeghi and Mofrad, 2007
UO_2^{2+}	IIP	120	4.5-6	Present study

5.2.4.4. Effect of solution volume of uranium

The results obtained from the variation of solution phase volume during adsorption studies are shown in Figure 5.21. It can be observed from Figure 5.21 that more than 80% recovery was achieved from volumes less than 200 mL. At solution volumes higher than 200 mL, recoveries started to decrease. The shape of the graph in Figure 5.21 can be explained in terms of the mass transfer of uranium from the bulk solution to the IIP particles. Smaller sample volume gives high contact time of uranyl ions in solution with P4 particles. This explains the low recoveries in larger sample volumes. This observation is different to when the IIP is used in a SPE format due to pre-concentration effects. Then a decrease in

recovery at high sample volume could indicate that the capacity of the sorbent is exceeded.

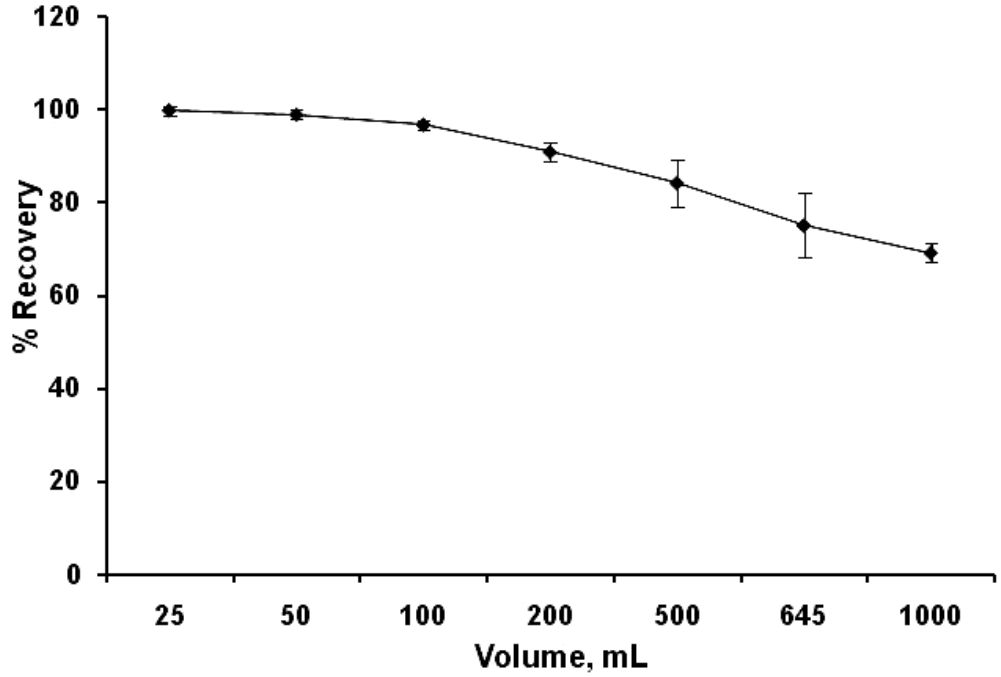

Figure 5.21: Effect of aqueous phase volume. Amount of materials 20 mg; solution pH 5; contact time, 20 min; concentration of solution, 1 µg mL^{-1}.

5.2.4.5. Effect of contact time of uranium

The results obtained from varying the time during uranyl ion adsorption by P4 and P5 are displayed in Figure 5.22. The trend observed for these kinds of experiments was similar to what was observed during the study of the effect of sorbent dosage (Section 5.2.1.1) in terms of the % recovery ratio between IIP and CP. That is, with IIP >99% extraction efficiency was attained while CP only achieved about 20% extraction efficiency. Both polymers seem to possess faster binding kinetics as they appear to reach saturation only after 5 min but for convenience 20 min was used as optimum in succeeding experiments.

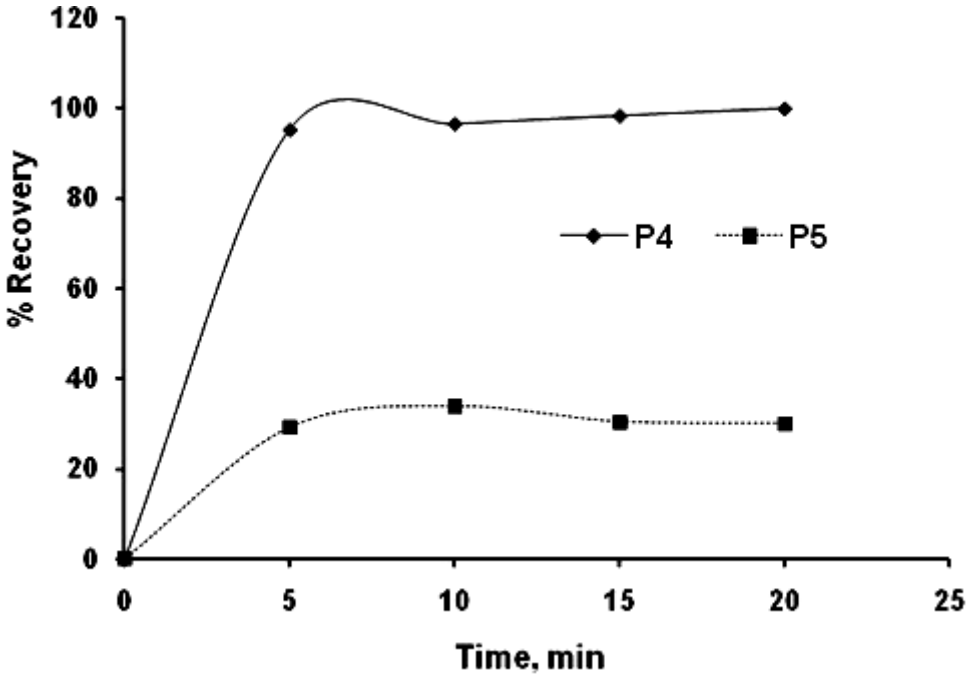

Figure 5.22: Effect of stirring time. Amount of materials 20 mg; Solution pH 5; solution volume, 30 mL; concentration of solution, 1 µg mL^{-1}. P4 and P5 are IIP and CP, respectively.

5.2.4.6. Selectivity of uranium

Inorganic ions with similar or less size as the uranyl ion were selected for selectivity studies. The ions were nickel (Ni^{2+}: A_w 58.69 g mol^{-1}: ionic radius 69 pm), zinc (Zn^{2+}: A_w 65.39 g mol^{-1}: ionic radius 74 pm), iron (Fe^{3+}: A_w 55.85 g mol^{-1}: ionic radius 64 pm), copper (Cu^{2+}: A_w 63.55 g mol^{-1}: ionic radius 72 pm), cobalt (Co^{2+}: A_w 58.93 g mol^{-1}: ionic radius 84 pm), manganese (Mn^{2+}: A_w 54.93 g mol^{-1}: ionic radius 89 pm), uranium (U^{6+}: A_w 238.03 g mol^{-1}: ionic radius 95 (+4) pm). The selected inorganic ions (which are likely to coexist with uranium in environmental samples) were equilibrated with 20 mg of P4 or P5 at optimum pre-concentration conditions. The selectivity of the IIP was tested using a mixture of 7 metal ions in solution as well as against each metal ion individually (binary mixtures). The concentration of the unextracted ions was determined by ICP-OES. The results of those experiments are shown in Table 5.8.

It can be observed that the selectivity coefficients of IIP are higher than those of CP. In fact, CP only reached about 17% extraction efficiency of uranium from the

multi-element mixture while IIP achieved 91% recovery of uranyl ion. This could be due to the specific shape, ionic charge and size of the binding cavity sites in IIP after removal of the template. Metals with higher ionic charge tend to bind more strongly to the ligands, as confirmed by high recoveries of such ions by the CP. It could be concluded that the prepared IIP can selectively remove uranyl ion from several other inorganic ions contained in dilute aqueous solutions. Based on this, it was observed that the bigger the charge on the central ion, the more attraction there will be for negatively charged ligands, however, at the same time, the bigger the charge the smaller the ion becomes which then limits the number of groups able to coordinate. In simple terms, the coordination number of a complex is influenced by the relative sizes of the metal ion and the ligands and by electronic factors, such as charge which is dependent on the electronic configuration of the metal ion. These competing effects are described by the term ionic potential which is defined as the charge to radius ratio (q/r).

It can be deduced that, from the examined selective sorption of heavy metals, the relative order of magnitude of metal sorption follows the order; $UO_2^{2+} > Fe^{3+} >> Cu^{2+} > Co^{2+} > Mn^{2+} > Zn^{2+} \sim Ni^{2+}$. Therefore it can be concluded that this polymer takes up far larger amounts of uranium and iron ions than other metals ions investigated in this study implying that the polymer can be used to recover uranyl ion from wastewater. The selectivity factor for P4 (Fe^{3+}) is close to unity. This could imply that P4 was not selective for Fe^{3+}, however, when one considers that the solutions were buffered to pH 5 and the pH of hydrolysis of Fe^{3+} is 3.0 (Britton, 1965). Therefore, the decrease of Fe^{3+} in solution after IIP extraction can be attributed to precipitation through formation iron hydroxide species. Hence, the concentration of Fe^{3+} measured in solution was less and this should not be mistaken with adsorption.

Table 5.8: Selectivity coefficients and distribution ratio using IIP. Initial concentration, 1 µg mL^{-1}; solution pH 5; solution volume, 25 mL; sorbent mass, 20 mg. P4 and P5 are IIP and CP, respectively

Metal ion	Distribution ratio (k_d, mL g^{-1})	Selectivity factor (α)		pH of hydrolysis*
		P4	P5	
UO_2^{2+}	453500	-	-	
Mn^{2+}	12000	37.8	0.5	8.5-8.8
Co^{2+}	7500	60.5	1.6	6.8
Cu^{2+}	73000	6.2	0.2	5.3
Ni^{2+}	500	907.0	0.2	6.7
Fe^{3+}	395000	1.2	0.2	2.0
Zn^{2+}	500	907.0	0.2	7.0

* Britton, 1965

5.2.4.7. Reusability of uranium

The results obtained from the investigation on IIP reusability potential are displayed in Figure 5.23. From the Figure it can be observed that almost 100% extraction efficiency was achieved in about 8 cycles. Therefore, it can be said that this polymer showed good stability and reusability towards uranium (VI) cation adsorption.

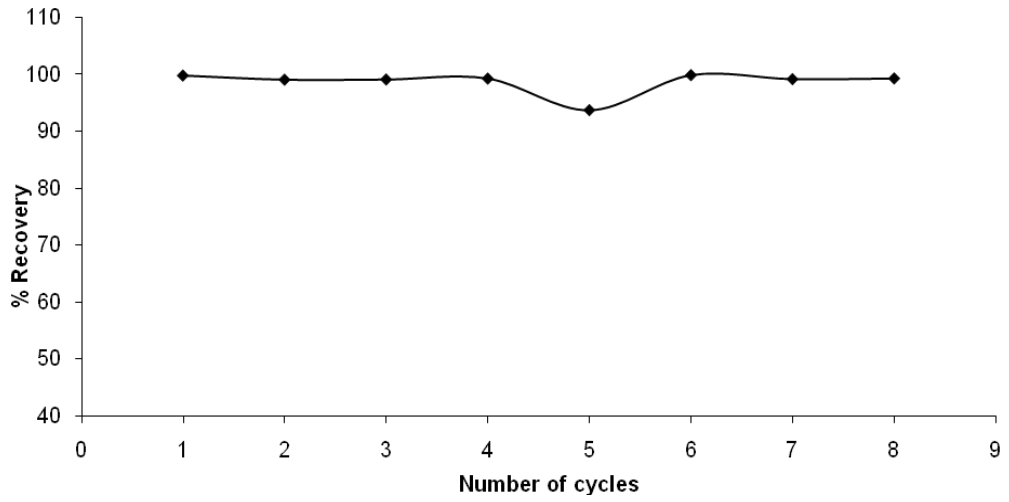

Figure 5.23: Regeneration and reusability**.** Amount of IIP, 50 mg; solution pH 5; solution volume, 25 mL; concentration of solution, 1 µg mL^{-1}; SPE, flow rate 0.8 mL min^{-1}.

5.2.5. Fitting of data into adsorption isotherms

Kinetic data obtained from contact time batch experiments were analyzed using a pseudo-second-order rate equation 5.3 to study the sorption mechanism and potential rate controlling steps. However, to do that an assumption that the adsorption capacity of adsorbent is proportional to the number of active sites on its surface was made (Ho and McKay, 1998).

$$\frac{1}{q_t} = \frac{1}{k_2 q_e^2} + \frac{1}{q_e} t \qquad (5.3)$$

where q_e and q_t are the amounts of UO_2^{2+} adsorbed onto adsorbent at equilibrium and any time t, respectively (mg g^{-1}) and k_2 is the second order rate constant at the equilibrium [(g mg^{-1})/ min]. It follows that by plotting t/q_t against t, will allow the determination of the values such as k_2 (slope^2/intercept), q_e (1/slope) and $k_2 q_e^2$ [the initial adsorption rate (mg g^{-1} min), 1/intercept] graphically from the slope and intercept of the plots (Figure 5.24).

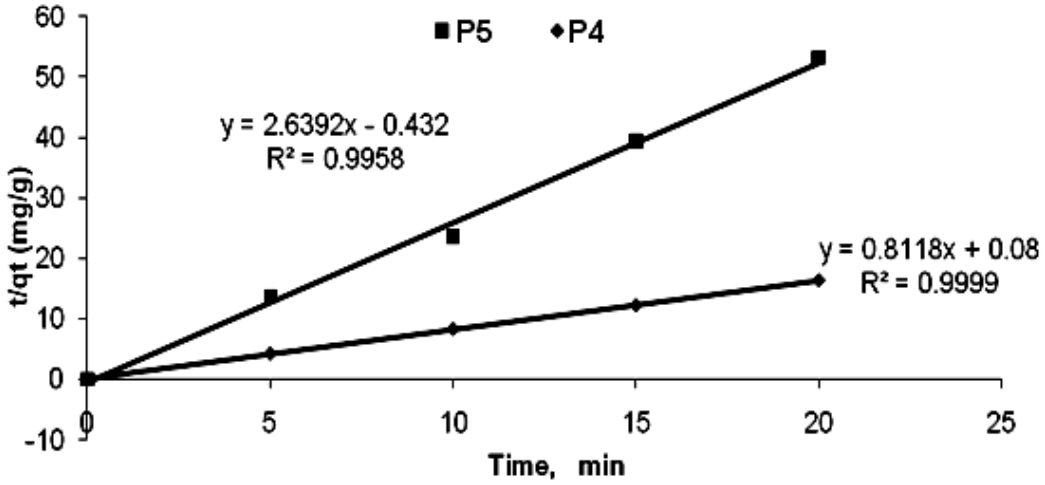

Figure 5.24: Fitting curves. Linear plot of t/q_t *vs*. t for UO_2^{2+} IIP and CP. P4 and P5 are IIP and CP, respectively.

The fitting and the linearity of the data could be confirmed by the r^2 values of 0.996 and 0.999 for CP and IIP, respectively (Table 2.9). Equilibrium adsorption capacity ($q_e.c$) values calculated from the pseudo-second-order model (1.23 mg g^{-1} and 0.38 mg g^{-1}) were close to the experimental q_e (1.13 mg g^{-1} and 0.20 mg g^{-1}) values for IIP and CP, respectively. Hence, the data fits the model and it can be applied to predict the adsorption kinetics. This suggested that the mechanism that controls the rate constant was chemisorptions (Taty-Costodes et al., 2003).

Table 5.9: Kinetic parameters of the pseudo-order rate equation for UO_2^{2+} adsorption on IIP and CP

	P4 (IIP)	P5 (CP)
k_2 [(g mg^{-1})min^{-1}]	8.24	16.1
q_e (mg g^{-1})	1.23	0.379
$k_2 q^2_2$ (mg $g^{-1}min^{-1}$)	12.5	2.31
r^2	0.999	0.996

However, k_2 value (adsorption velocity) for the CP was twice as bigger as for IIP implying faster adsorption kinetics for the CP as there were no defined cavities.

5.2.6. Application to real samples

Wastewater samples were collected from the Natalspruit wetland that is part of the Witwatersrand Basin in Johannesburg, South Africa. Pitwater and stream water was collected using polypropylene bottles. ICP-OES was used to determine the total metal content of the samples and the results are shown in Table 5.10. Generally, the concentration of all the metals, including uranium, was higher in pit water (Table 5.10). The higher concentrations of total sulphur were supported by high concentrations of sulphates obtained from ion chromatography results (750 and 210 µg mL^{-1} for pit water and stream water, respectively). The pH of the pit water was measured at 3.5 while that of stream water was 6.6. The evidence of uranium leaching from gold tailings dumps in the Witwatersrand Basin was extensively studied before using geochemical modelling and radioactive disequilibrium (Tutu et al., 2009).

Table 5.10: Composition of wastewater samples as determined by ICP-OES. Concentrations are in µg mL^{-1}, inside parenthesis are the %RSD values

	Ce	Co	Cu	Cr	Fe	Mn	Ni	S	Zn	Th
Streamwater	$4.30x10^{-2}$ (1.99)	0.45 (2.02)	-	-	$2.80x10^{-2}$ (3.94)	5.91 (1.48)	0.44 (1.91)	86 (1.50)	0.44 (1.61)	-
Pitwater	0.38 (1.28)	1.28 (1.29)	0.60 (1.27)	$3.20x10^{-2}$ (2.07)	0.23 (1.15)	9.06 (1.27)	2.37 (1.66)	315 (0.94)	4.18 (1.50)	$2.90x10^{-2}$ (3.59)

The pH of both water samples was adjusted to pH 5 using sodium acetate-acetic acid buffer and the extraction of uranium was carried out in a batch mode in triplicates. After batch extraction, the bound uranium was leached out from the IIPs using 10 mL of 2 M HCl solution stirring at room temperature for 20 min. The concentration of uranium in the leachate was quantified using ICP-OES. The results obtained are shown in Table 5.11. It can be seen that the IIPs successfully pre-concentrated the uranyl ion in the presence of the complex matrix (shown in Table 5.11). The effect of competing ions did not have a pronounced consequence on the removal of uranyl ion. However, the amounts recovered were slightly higher than what was spiked in due to template bleeding. Nonetheless, the developed method proved to be suitable for quantitative monitoring of uranium in wastewaters.

Table 5.11: Application of IIPs on waste water samples. Initial concentration, 1 µg mL^{-1}, 3 µg mL^{-1} spiked samples; solution pH 5; solution volume, 25 mL; sorbent mass, 20 mg. In brackets are the %RSD values

Sample No.	Sample	Uranium found (µg mL^{-1}) Present Method[a]		Direct[c] Analysis µg mL^{-1}	% Recovery
		Added	Found		
1	Pit water	-	0.55 (9.97)	0.52 (1.82)	104
		1.00	1.47 (8.42)		95
		3.00	3.60 (4.61)		102
2	Stream water	-	0.22 (5.92)	B.D.L[b]	100
		1.00	1.37 (7.06)		100
		3.00	3.36 (4.88)		105

[a]Average of three determinations [b]Below detection limit

[c] analysis of water prior to any extraction

5.2.7. Conclusions

It can be concluded that an IIP which can successfully remove uranium from other similar cations was prepared successfully from 1-(prop-2-en-1-yl)-4-(pyridin-2-ylmethyl)piperazine and methacrylic acid. Influence of various parameters such as pH, contact time *etc*. were studied and optimum values were used for the successive experiments. Due to high selectivity shown by this IIP and high uranyl ion removal efficiency at pH 5-8, then the IIP was successfully applied for the removal of uranium from wastewaters.

5.3. Molecularly imprinted polymer for quercetin recovery

MIPs with high recognition for quercetin from complex samples were prepared by bulk polymerization using 4-vinylpyridine as a functional monomer, EDMA as a cross-linking agent and ACCN as the initiator. A three-phase solvent system of MeOH:THF:H_2O was used as a porogen. A schematic representation showing how the MIP was prepared is depicted in Figure 5.25. The vinylpyridine functional monomer used may interact with the quercetin in two ways, *i.e.*, *via* hydrogen bonding and hydrophobic interactions. However, it was essential that hydrogen bonding would be much stronger than hydrophobic bonding as this would translate to a production of a polymer with no unspecific bonding.

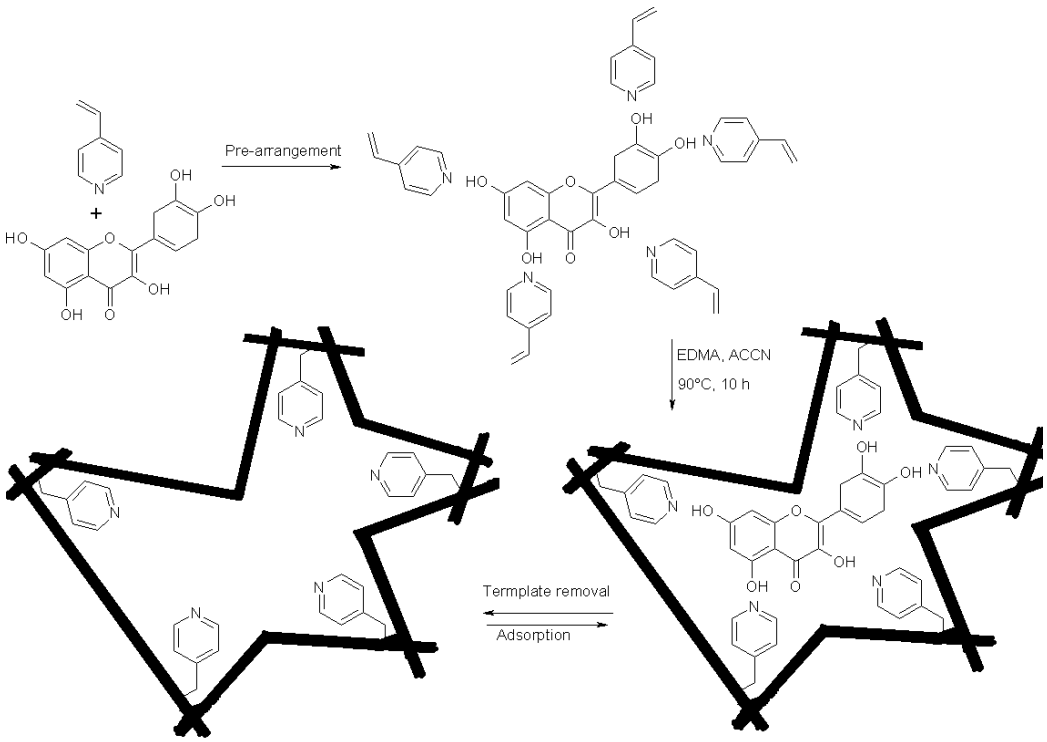

Figure 5.25: Quercetin MIP preparation.

One of the challenges that face MIPs today is their incompatibility with aqueous media. In order to address this limitation researchers have used hydrophilic monomers such as HEMA or imprint in aqueous media. In our study we attempted to use the latter where we made MIPs with high recognition for quercetin using a

three-phase aqueous solvent system. Because the target template molecule (quercetin) can have both hydrophobic and hydrogen bonding, therefore it was important to do tests to prove whether the monomer-template interactions would prevail under such circumstances. Two techniques were used for such studies, namely, UV/Vis and FTIR. However, it can be expressed that developed world use advanced computational models for such studies.

5.3.1. UV/vis spectroscopy

5.3.1.1. UV/vis studies of monomer-template interactions

The effect of the solvent on the monomer-template strength was investigated by stirring the following ratios, 1:1, 1:4, 1:8, 1:12, 1:16 and 1:20 of quercetin-to-4-vinylpyridine (Q:V) in THF:MeOH:H_2O (6:1:3, *v/v/v*) for 2 hours at room temperature. The resulting solution mixtures were scanned using the UV/vis spectrophotometer from 190 to 600 nm and the results are depicted in Figure 5.26. It could be observed in Figure 5.26 that quercetin absorbs at two different wavelengths, *i.e.*, ~250 and 370 nm, where the band at 250 nm was attributed to the benzoyl chromophore and the band at 370 nm was assigned to the cinnamoyl chromophore of the quercetin molecule (Shan and Wang, 2011). The benzoyl and cinnamoyl chromophores are the rings labelled A and B in the quercetin molecule (in insert quercetin structure to show A and B). No significant shift of the wavelength for all the quercetin:4-vinylpyridine (Q:V) ratios for the band at 370 nm, except that the ratio of 1:8 and 1:12 (Q:V) have the highest absorbencies in that order. However, there's a noticeable change for the bands at ~250 nm wavelength. With the increase of the ratio of 4-vinylpyridine, lambda max shifts to the longer wavelength gradually. This shift can be said it obeys Einstein shift phenomenon, which is defined as a shift toward longer wavelengths of spectral lines emitted by atoms in strong gravitational field resulting in molecules with less energy and lower frequency. In this case, the Einstein shifts are a result of the formation of hydrogen bonding and π-π interactions between the template molecule quercetin and the 4-vinylpyridine resulting in the formation of a self-assembled complex of Q:V.

Based on these observations, it can be said that strong monomer-template for the pre-polymerization complex can be achieved under the porogen conditions used. A 1:10 (Q:V) ratio which is a compromise for the benzoyl and cinnamoyl chromophore intensity and shifts was regarded as the optimum ratio, hence, this ratio was used for polymer fabrication (Table 4.43). This is slight different to the 1:8 ratio previously used by Molinelli et al. (2002) for the preparation of quercetin MIPs with 4-vinyl pyridine in acetone. Furthermore, the ratio of 1:10 was chosen as a compromise as it is known that excess of vinylpyridine will lead to the formation of unspecific binding sites. The failure of the 1:4 ratio to give stable template-monomer interactions further illustrate the negative effect of water in 4-vinylpyridine-quercetin systems. Hence, excess of monomer is needed to create

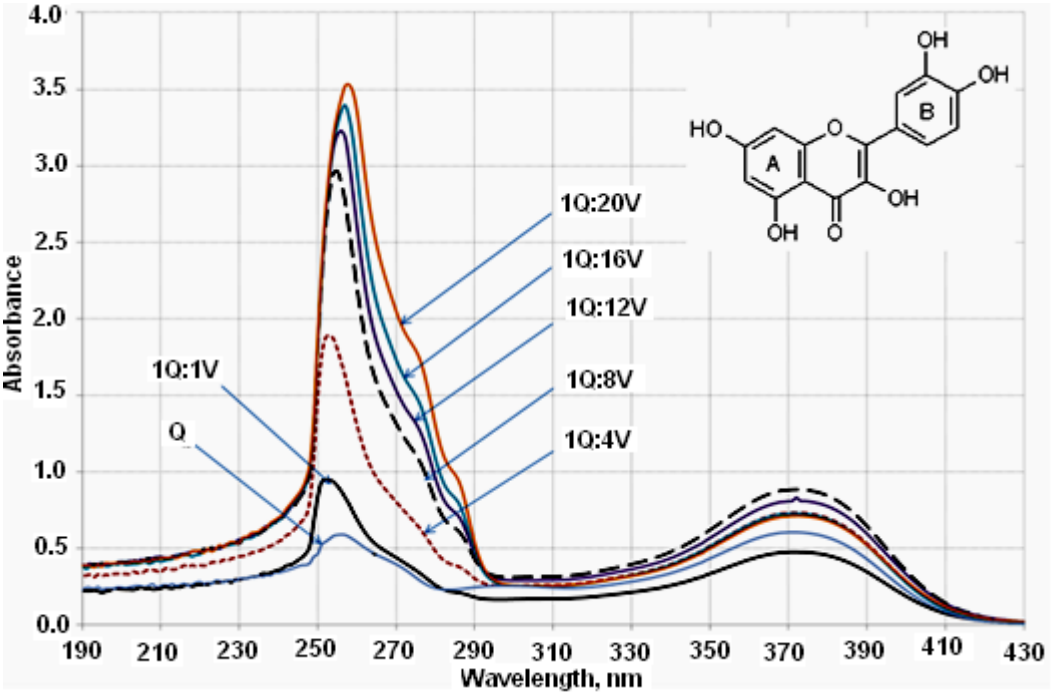

Figure 5.26: The UV spectrogram of different ratios of quercetin:4-VP (Q:V) in THF:MeOH:H_2O (6:1:3, v/v/v), three times scan.

strong interactions between monomer and template but one has to be careful as this can lead to creation of single-point attachment which then lead to nonspecific binding. Therefore, a compromise has to be made in order to form that desired multipoint interaction. A similar result where an excess of monomers was used was reported by Sun et al. (2008) in their study on methacrylic acid:ofloxacin

imprinted polymers under methanol:water (9:1, *v/v*) conditions. The optimum ratio of ofloxacin-to-methacrylic acid was 1:10 (Sun et al., 2008).

5.3.1.2. FTIR studies of monomer-template interaction

Figure 5.27 shows different FTIR spectra for vinylpyridine-quercetin complex (a), vinylpyridine (b), and quercetin (c). It can be noted from Figure 5.27 (a) that vibration bands that corresponds to both quercetin and vinylpyridine are present. More interestingly was the fact that these bands have shifted (1594 to 1598 cm^{-1}, 829 to 833 cm^{-1}) in terms of the frequency signalling both compounds were involved in the complex formation through bonding. Notably, there was no real shift on the quercetin C=O band (1657 to 1656 cm^{-1}) because this functional group did not participate in hydrogen bonding with vinylpyridine.

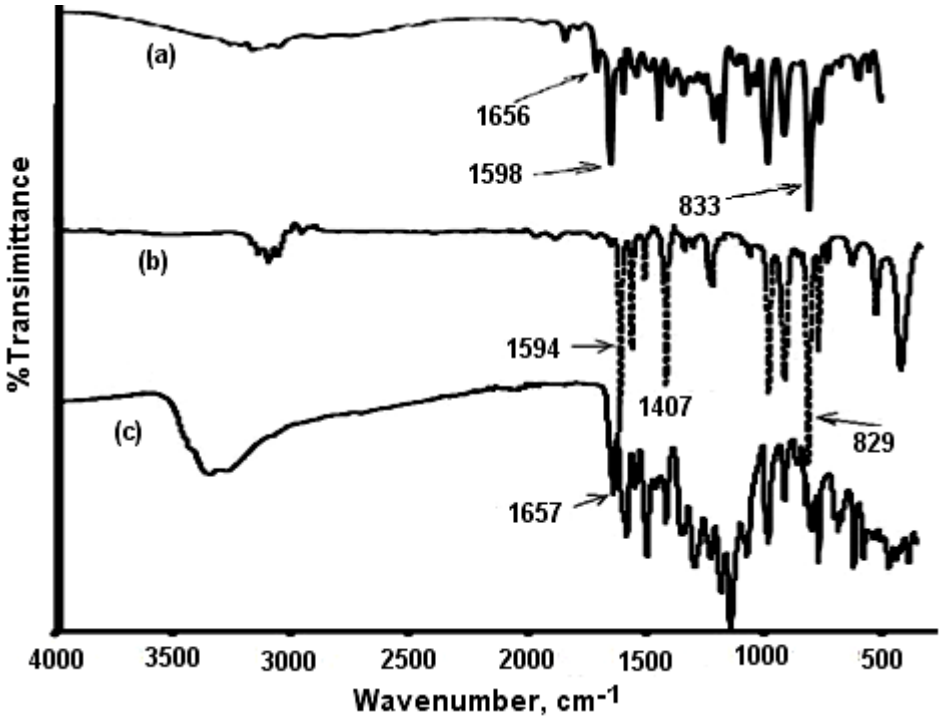

Figure 5.27: FTIR spectra of quercetin-4-vinylpyridine complexes (a), 4-vinylpyridine (b) and quercetin (c).

Furthermore, quercetin characteristic bands have also disappeared in the complex. These characteristic bands are the C-OH stretch bend at 1160-1030 cm^{-1}, C-OH

in-plane bend at 1440-1260 cm^{-1} as well as C-OH wag at 700-600 cm^{-1} (Figure 5.27(b)). This disappearance can be attributed to the result of the lowering in energy of these bands due to complexation with vinylpyridine molecules as this will limit movement of the bonds resulting in molecules with lower energy and this was supported by the redshifts observed in UV-vis spectra.

5.3.2. Characterization of quercetin MIP

5.3.2.1. FTIR analysis

Similarly to other imprinted polymers prepared in this study, the FTIR spectra of unwashed, washed MIP and NIP showed similar backbone structure. This was again attributed to the presence of high degree of cross-linking (EDMA) agent used (Figure 5.28). These structural attributes were the strong vibration bands at 1720 and 1140 cm^{-1} assigned to the C=O and C-O functional groups of EDMA,

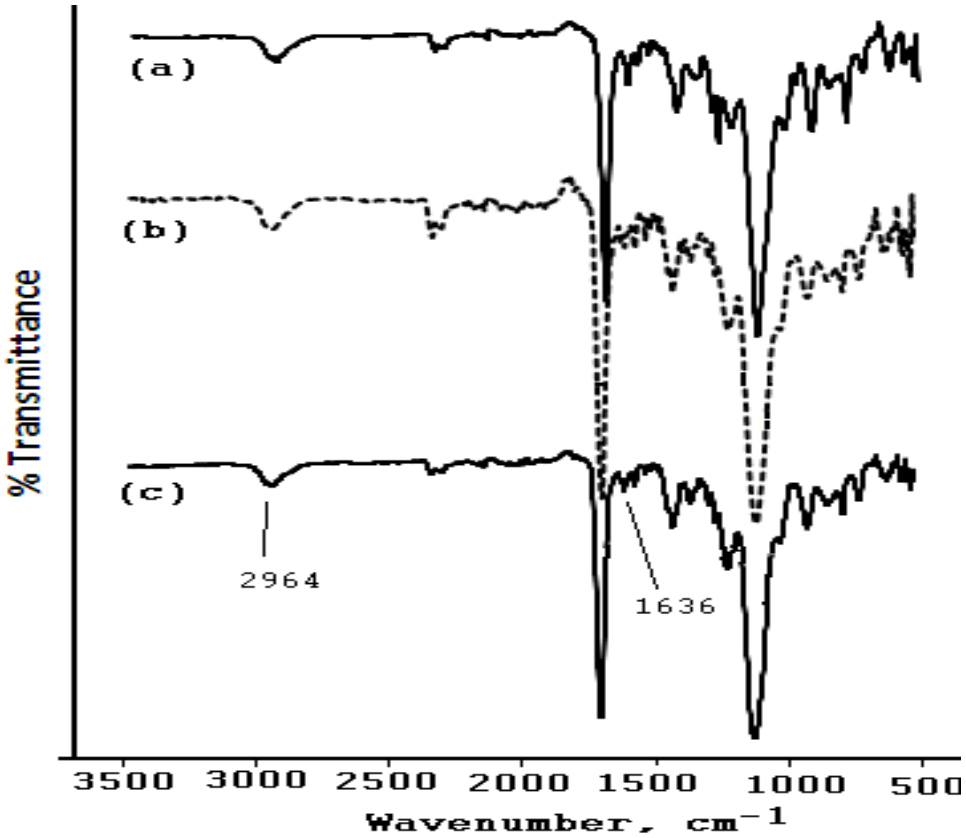

Figure 5.28: FTIR of the MIPs, unwashed (a), washed (b), and NIP (c).

respectively. Again the vibration band at 1736 cm^{-1} was almost diminished in all imprinted polymers indicating that very few 4-VP functional monomers were left as unpolymerized double bonds (Li et al., 2005).

5.3.2.2. Scanning electron microscopy

The morphology of the imprinted polymer particles was investigated using SEM analysis and the SEM images of MIP and NIP are shown in Figure 5.29 and 5.30, respectively. Under the detector resolution used no distinct pores due to imprinting and removal of template could be observed. However, notably was the irregular shape of the particles due to crushing and the particle size distribution looked similar (Figure 5.29 and 5.30).

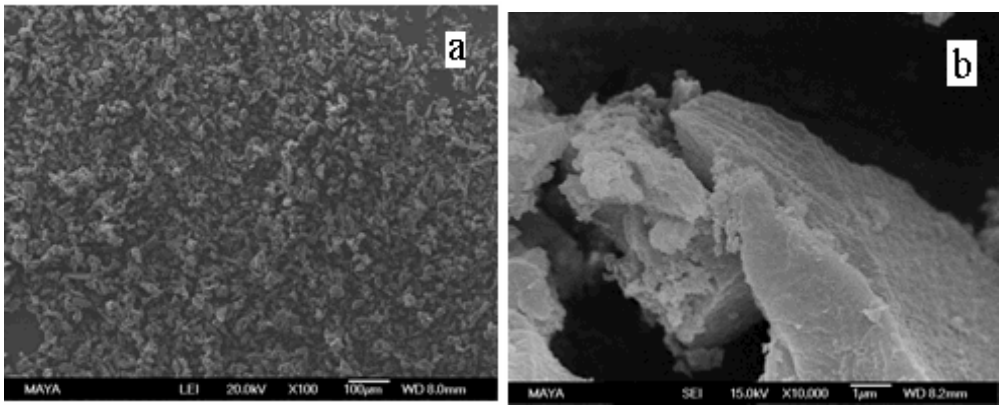

Figure 5.29: MIP particles (a), and magnification (b).

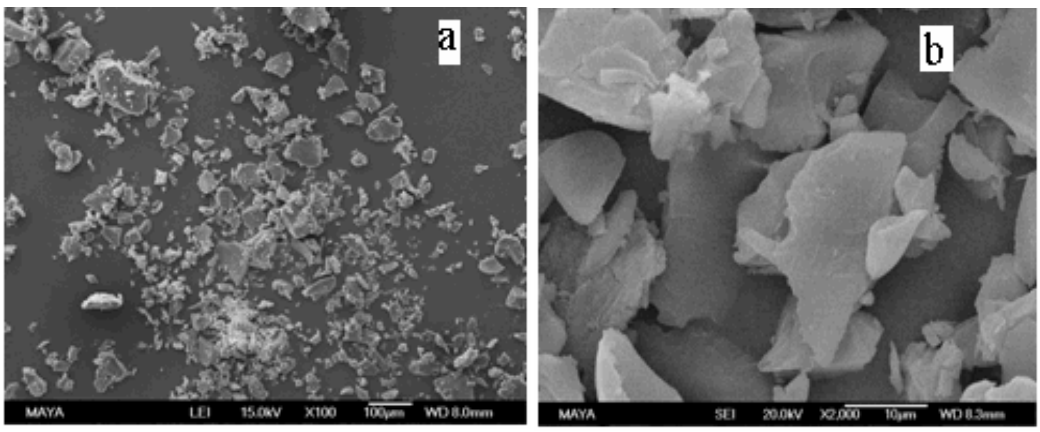

Figure 5.30: NIP particles (a), and magnification (b).

5.3.2.3. Surface area measurement

Table 5.12 summarizes the surface area and average pore diameter values obtained from the BET method for quercetin imprinted polymers. The range of surface area values for the imprinted and non-imprinted polymers varied by a great margin. This could be attributed to the influence of different porogenic solvents used, the imprinting nature, the level of incomplete removal of the template from the imprinted polymers, swelling ratio etc. The imprinted polymer which was mostly used in the study is M2 (334 m^2 g^{-1}) together with its corresponding non-imprinted polymer N2 (69 m^2 g^{-1}). MIP particles exhibited higher surface area (334 m^2 g^{-1}) and pore size diameter (6.7 nm) than NIP (69 m^2 g^{-1} and 5.5 nm, respectively).

Table 5.12: Pore size diameter and surface area summary results for other polymers

	M1	N1	M2	N2	M3	M4
Average pore diameter, nm	10.2	19.7	6.7	5.3	17.6	12.9
Surface area, m^2 g^{-1}	222	71	334	69	5.5	1.7

5.3.2.4. TGA

TGA plots of M1 (washed and unwashed), M2 (washed and unwashed), N1 and N2 are presented in Figure 5.31. It can be observed that there are differences in decomposition between washed and unwashed MIPs and between MIPs and NIPs. There are two decomposition steps for washed and unwashed M1 and unwashed M2, but in the case of N1, N2 and washed M2, there seem to be one decomposition step (the experiment was only allowed to run up to 500°C and at this temperature not everything has decomposed). For washed M1, almost 15% weight loss is seen up to 90-100°C and for unwashed M1 there is almost 30% weight loss up to 150°C. For unwashed M2 the first weight loss up to 150°C is approximately 10%. The weight loss percent below 150°C is normally attributed to water loss, decomposition of free monomer, cross-linker and monomer-template decomposition (Azodi-Deilami et al., 2010; Khajeh et al., 2007; Arabzadeh and Abdouss, 2010).

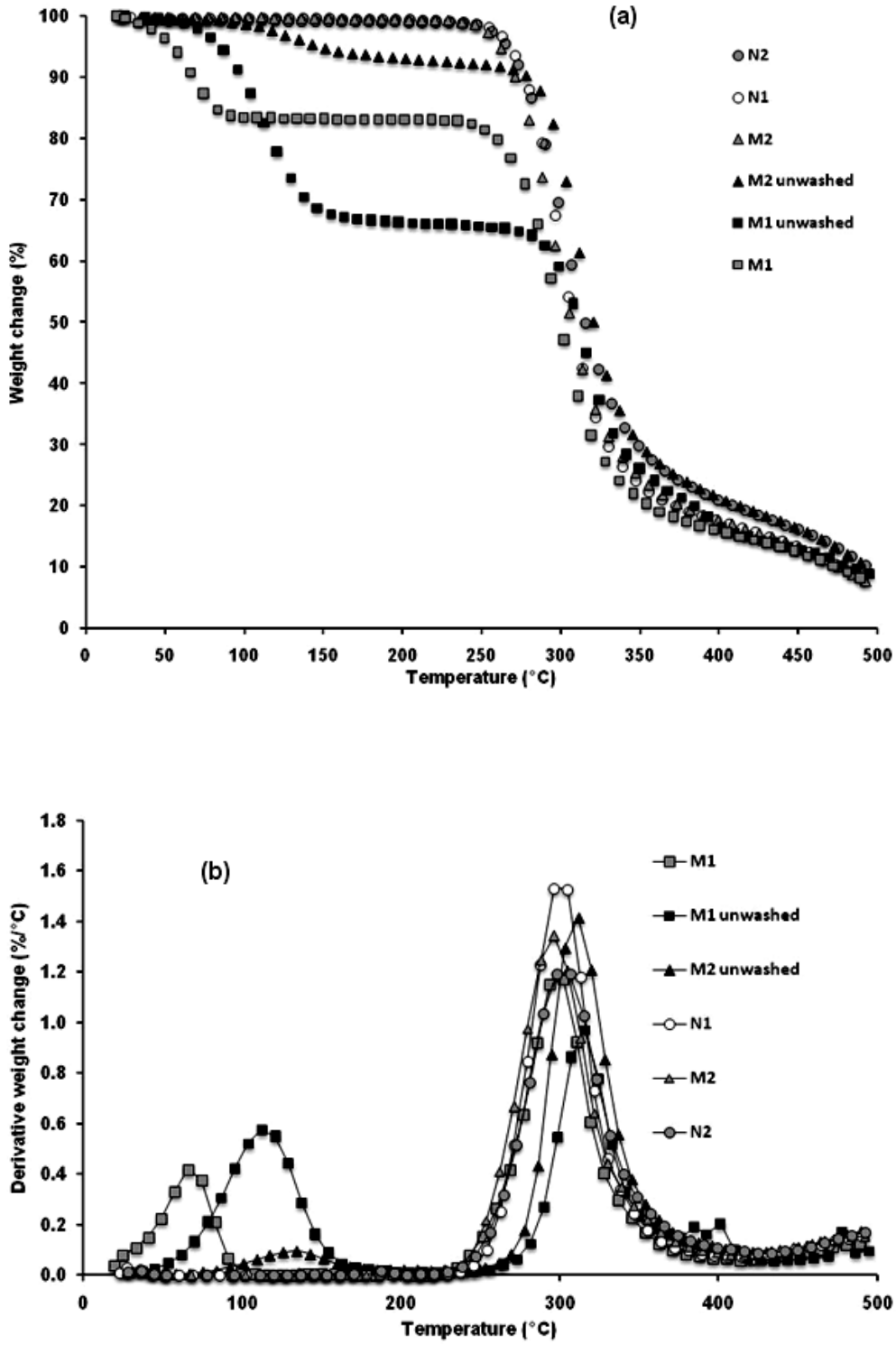

Figure 5.31: TGA curves of M1 (washed and unwashed), M2 (washed and unwashed), N1 and N2. TGA curves in (a) and second derivative weight (%) loss in (b).

All the polymers started to disintegrate after 250°C. Larger weight loss on M1 suggests high volumes of free monomer and cross-linker on the surface of the polymer. Interestingly, N1, N2, and M2 have the same rigidity.

Also, noteworthy mentioning is that both M1 and M2 show no other decomposition step compared to N1 and N2 which might be attributed to unleached quercetin. Therefore, M2 showed that is can withstand up to 250°C. M2 unwashed showed a slightly higher thermal stability than M2 washed and its corresponding NIP, N2. This is attributed to the presence of quercetin in the unwashed MIP as the melting point of quercetin is around 320°C. Also, because there are no exposed cavities on the surface of unwashed MIP particles this implies less surface area. Therefore, the stability of the polymer might increase.

5.3.3. Polymerization of quercetin water-compatible MIPs

As mentioned earlier that aqueous media is a challenge in MIPs, hence, the aim was to form quercetin water-compatible MIPs. Water was used as part of the porogen because it is known that MIPs perform better in the re-binding evaluations if the analyte was present in the same solvent as was used for imprinting as this imparts less influence on the monomer-template complex binding strength (Wu and Li, 2004). An ideal situation would be to use water as porogen but due to limited solubility of quercetin in water (Srinivas et al., 2010) and its potential to disrupt hydrogen bonding between the template and the monomer, therefore, water alone could not be used as a porogen. In this study, MIPs were prepared in two different aqueous environments, namely, using MeOH:H_2O (9:1, *v/v*) as porogen (M1) or usingTHF-MeOH-H_2O (6:1:3, *v/v/v*) as a porogen (M2). As references, two other polymers were made in pure methanol and pure tetrahydrofuran solvents (M3 and M4, respectively) (Table 3.3).

In addition, solvent for rebinding experiments containing maximum amount of water was to be found as this would mimic the aqueous environments of the extracts for the ultimate application. Figure 5.32 shows the results obtained by

studying the effect re-binding solvents on different MIPs and NIPs. These re-binding studies were performed using water-methanol systems that contain 0, 10, 30 and 50% MeOH. Known equal amounts of quercetin were added to equal volumes of 9:1, 7:3 and 5:5 methanol:water systems. Each of these solutions was divided into equal portions. One part was stirred for the duration of the experiment without the addition of MIPs, that is, were used as controls and they are referred to as "Stds" in Figure 4.33. After the duration of the experiment quercetin concentration was measured with HPLC and it was found that it decreased with increase in water content. This could be attributed to the lower solubility of quercetin in water, probably due to precipitation of quercetin. MIPs and NIPs were added on the second solutions and these were stirred the same way as the "Stds" solutions and the results are shown in Figure 5.32.

The results revealed that the higher recoveries by MIPs and NIPs at 5:5 (methanol:water) ratio was not due to adsorption of quercetin to MIPs or NIPs but rather to loss of quercetin. Another portion of the sets of standards was stored at -18°C for the duration of the experiment and the results were comparable to the stirred standards (Stds). Moreover, monomer-template binding strength could be affected by dielectric constant of the solvent as well as other solvent parameters and this result in MIPs with poor recognition capabilities (Wu and Li, 2004). Particularly, in the studies by Mikhail and Kimel (1961), and Kurata et al. (1971) it was demonstrated that the viscosity of methanol-water systems increased as the amount of water was increased. With this in mind, lower recoveries of quercetin were expected with 5:5 solvent mixture due to greater viscosity as this impart less impact on penetrating the binding sites of polymers. Higher recoveries at this ratio could also be attributed to pure hydrophobic mode of recognition. From the results in Figure 5.32, it was concluded to proceed with the 7:3 solvent mixture for the next adsorption experiments.

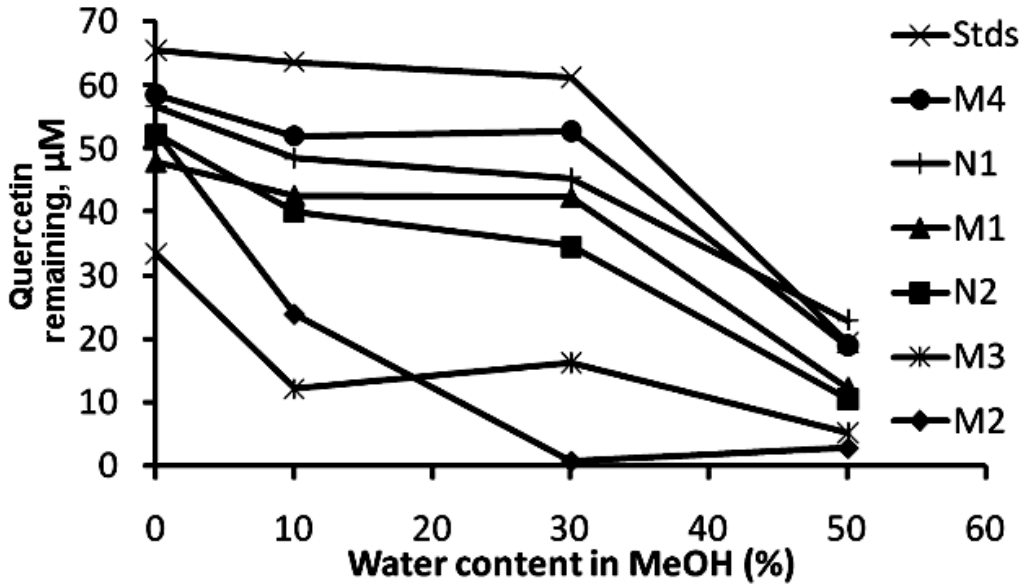

Figure 5.32: Effect of water content on quercetin MIPs and NIPs. Amount polymer 8 mg, solution volume 4 mL, contact time 24 hours, temperature 25°C, pH not controlled (MeOH:H_2O), n = 2. See Table 4.3 for explanations**.**

Quercetin possesses phenolic hydroxyl groups that behave as weak acids, as such; strong hydrogen bonding interaction can be established with the vinylpyridine. Therefore, these interactions could be said to be stronger in the case of M2 compared to other polymers under the tested conditions when the water content was 30% (Figure 5.32). Consequently, a MeOH:H_2O ratio of 7:3 *v/v* was found optimal for M2 and hence, all the other re-binding studies were conducted using this solvent mixture (Figure 5.32). However, the higher recoveries achieved by the NIP of this polymer denote that the strength of nonspecific binding (*e.g.*, hydrophobic interactions) could be stronger as well due to the presence of water in the porogen. Similar results were reported by Chen et al. (2005) where hydrophobic interactions were suggested as a mode of recognition when the water content was greater than 65% but when water content was lower than 10% hydrogen bonding was predicted as the mode of recognition (Sun and Qiao, 2008; Chen et al., 2005).

It has been previously demonstrated that a medium polar solvent such as THF gives better imprinting factor for quercetin MIPs involving hydrogen bonding (Song et al., 2009a). However, the authors reported lower imprinting factor when

more polar solvents than THF were used. In our studies we increased the polarity by adding water and methanol to THF to form a tertiary solvent mixture with a ratio of 6:3:1 (THF:H_2O:MeOH) (porogen used to make M2 and N2) due to the miscibility of the three. With this porogenic solvent mixture, MIPs with recognition properties of quercetin in polar medium were produced although it was expected that the presence of water would diminish the interaction of 4-VP and quercetin as water could form strong interaction with both 4-VP and quercetin resulting in less chances of the 4-VP and quercetin to interact with each other (Song et al., 2009a). The successful imprinting of quercetin MIP in this solvent mixture revealed that the 4-VP and quercetin interactions were stronger than the counter action induced by the solvent mixture. The reason behind this could that, in our case, the porogenic solvent and the re-binding solution have the same water content (30%). That is, MIPs made from THF-MeOH-H_2O (6:1:3, *v/v/v*) porogen were found to perform better in rebinding of quercetin under studied conditions.

5.3.4. Template removal studies

After crushing, grinding and sieving MIPs were subjected to Soxhlet extraction in order to remove the quercetin template molecules. Known amounts of MIP particles were placed in Soxhlet thimbles and extracted with 100 mL of methanol-acetic acid (9:1, *v/v*). Samples were taken periodically from the Soxhlet extractor and injected into the HPLC to determine the concentration of quercetin in solution (Figure 5.33). When the solution has reached saturation, the solution was changed and a fresh one was used. This was continued until the peak area of quercetin in the extract solution was almost zero and hence, it was found that almost all quercetin could be extracted from the MIP within 96 hours of continuous Soxhlet extraction (Figure 5.33). Therefore, all other MIPs were extracted for 96 hours changing the methanol-acetic acid solution after every 24 hours.

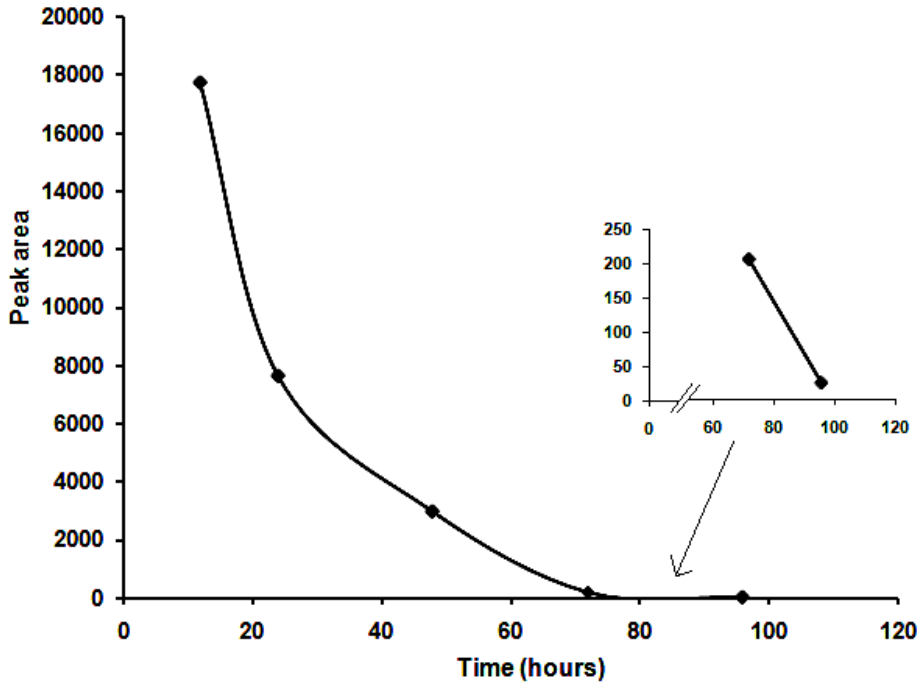

Figure 5.33: Extraction of quercetin from the MIPs.

5.3.5. Re-binding studies for quercetin MIP/ NIP

Similarly with other imprinted polymers in this study, the re-binding studies were conducted using the batch mode and in some cases the SPE method. The prepared MIP showed that it can be used successfully well with both methods.

5.3.6. Optimization of MIP parameters

5.3.6.1. Effect of amount of quercetin

Figure 5.34 shows the results obtained from the optimization of MIP/ NIP sorbent dosage for quercetin adsorption. Figure 5.34 shows a plot of sorbent amount *versus* the peak area of quercetin obtained from the eluates obtained after eluting the adsorbed quercetin from MIPs/ NIPs using methanol-acetic acid mixture. It can be observed that the amount of quercetin adsorbed on MIP and NIP increased with the increase in the amount of imprinted particles used. However, in the case of MIP this increase was observed up to 40 mg then afterwards the polymer seemed to have attained saturation. The plateau was due to the initial

concentration of quercetin used. That is, it required 40 mg of MIP to extract all the quercetin from the solution not that MIP capacity was exceeded. Therefore, 40 mg were regarded as optimum sorbent dosage for MIP. However, in the succeeding studies only 8 mg of MIP/NIP were used. In this case, instead of using 40 mg MIP for each extraction a sorbent-solution volume ratio was kept constant namely, 40 mg-to-20 mL and 8 mg-to-4 mL. The difference in the amounts of quercetin adsorbed by MIP and NIP could be attributed to the influence of the imprinting effect in MIP.

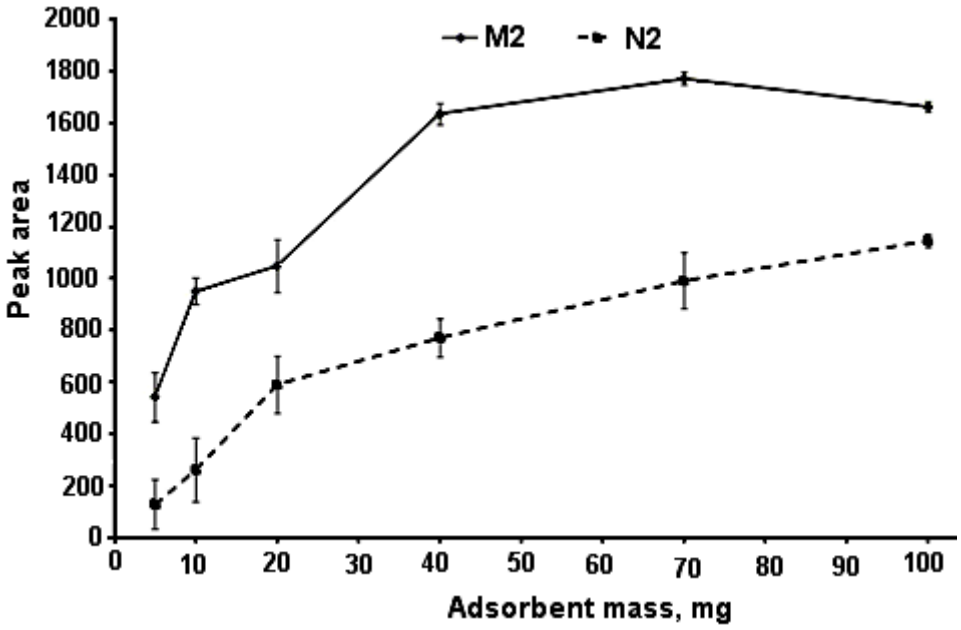

Figure 5.34: Effect of amount on quercetin MIP. Solution pH 5.5; solution volume, 20 mL; contact time, 24 h, initial concentration of solution, 20 µM; temperature, 25°C.

5.3.6.2. Effect of pH of quercetin

The results obtained from variation of pH during quercetin adsorption onto MIP and NIP is shown in Figure 5.35. It can be observed that the amount of quercetin adsorbed at pH 5.5 was similar to that adsorbed at pH 7 but both were much higher compared to amount adsorbed at pH 4. Also the performance of the prepared MIPs was better than NIPs under the conditions investigated,

particularly pH 5.5 and 7. These differences in adsorption capacities can be explained in terms of pKa values for quercetin and vinylpyridine. Quercetin is slightly acidic with a pKa of 6.74 (Arshad et al., 2009) whereas vinylpyridine is slightly basic with pKa 5.39 (Pinkrah et al., 2003) meaning that it will most likely exist as a protonated form in acidic solutions. So the pH plays a crucial role in the affinity of the two compounds. This is the same pH effect that is used to wash-out quercetin template molecules from the MIP as an acidified methanol solution is mostly used.

This is believed to charge the amino group of the vinylpyridine resulting in the release of the quercetin molecule from MIP to the solution. In re-binding, one has to avoid this as it was shown that both MIP and NIP exhibited lower binding capacities at pH 4. M2 seemed to work well at the desired pH 5.5 (Figure 5.35) and this was a good sign that these MIPs could be used for selective extraction of quercetin from yellow onion aqueous extracts at this pH.

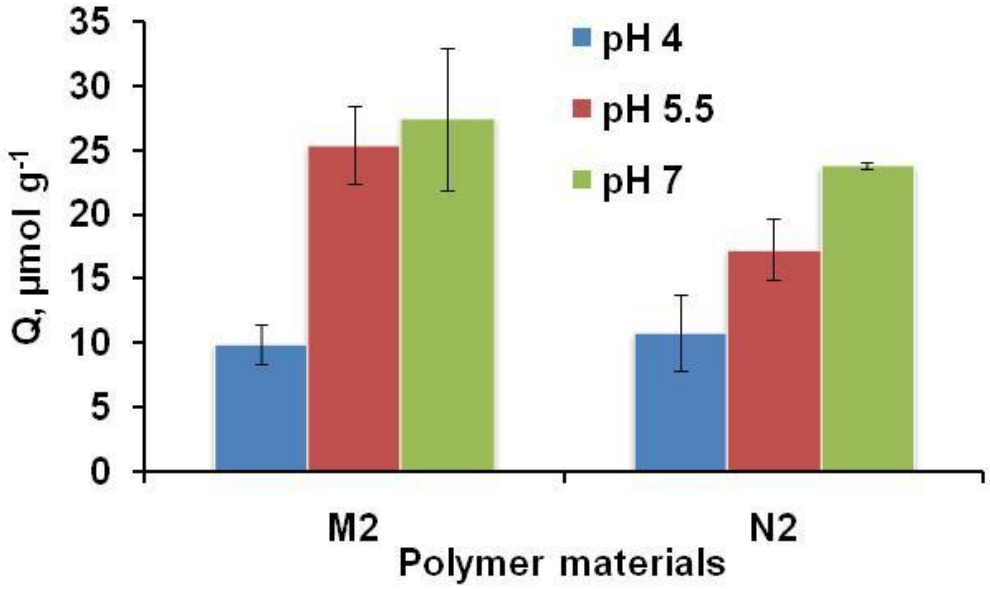

Figure 5.35: Effect of pH**.** Initial concentration of quercetin 20 µg mL^{-1}, amount of polymer 8 mg, solution volume 4 mL, contact time 90 min, temperature 25°C.

5.3.6.3. Effect of concentration of quercetin

Binding capacity of the MIPs at different temperatures

Binding capacity was evaluated at 25°C and 84°C using M2 and N2. The initial concentration was varied between 10-400 µM and the results are depicted in Figure 5.36(a) and (b). When the experiments were done at room temperature, in Figure 5.36(a), it could be observed that M2 reached equilibrium at about 270 µM of about 28 µmol g^{-1} whereas N2 at about the same concentration had a loading capacity of 16 µmol g^{-1}. This difference in loading capacity was attributed to predefined imprinting cavities present in the MIP and absent in the NIP in addition to shape and size, and unspecific binding. Therefore, the MIP (M2) had higher degree of quercetin recognition than its corresponding NIP (N2). However, for the same initial concentration range the binding capacity of both M2 and N2 increased by 4-folds when the experiments were conducted at higher temperature, Figure 5.36(b). As discussed before, this was attributed to faster diffusion rates at higher temperature and also the changes in properties of water as water will become less polar as the temperature was increased.

Moreover, to test whether the quercetin was actually adsorbed on the polymer particles or was just the effect of degradation, reaction vials containing the different initial concentrations of quercetin solution were also subjected to the same temperature for the duration of the experiments. The concentration of quercetin before and after exposure to the temperature was determined and it showed that indeed that quercetin was adsorbed on the particles as the concentration was the same. The observed results are in agreement with the theory that MIPs prepared at higher temperature tend to work better at higher temperatures (Piletska et al., 2009), and our MIP was prepared at higher temperature (80°C) due to the use of the ACCN initiator which requires higher temperature to form radicals.

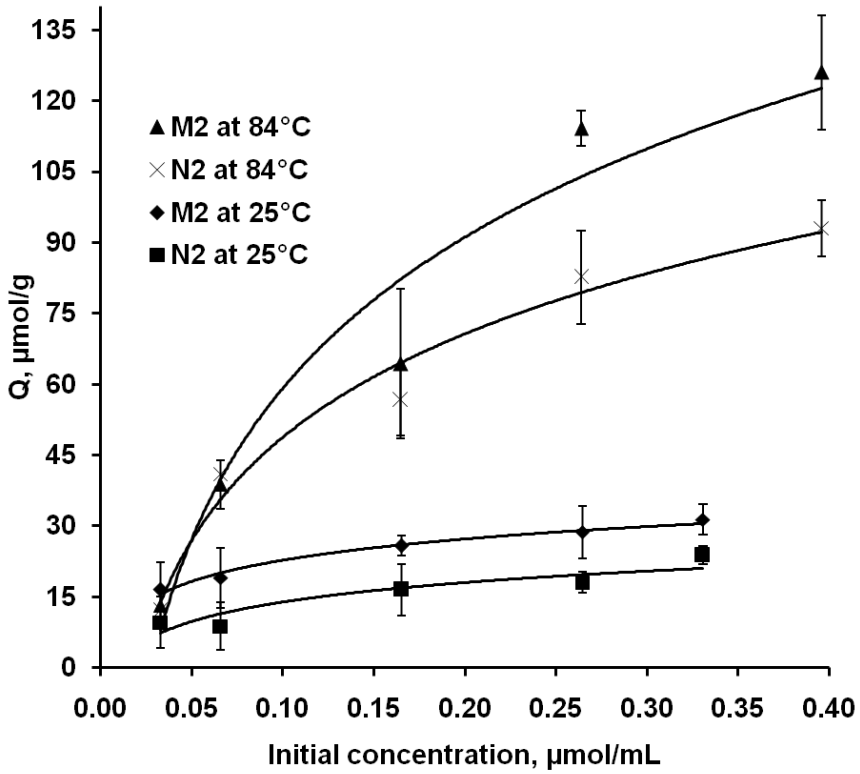

Figure 5.36: Effect of concentration on binding capacity of polymers. Amount of polymer 8 mg, solution volume 4 mL, contact time 24 hours at 25°C, or 2 hours at 84°C, pH 5.5, solvent MeOH:H_2O, (7:3, v/v).

Furthermore, the results from the saturation experiments were fitted in Scatchard plots. It can be argued that M2 shows two independent binding mechanisms as demonstrated by linear lines in Figure 5.37. These could be ascribed to hydrophobic and hydrogen bonding interactions. N2 displays a different pattern which might be due to unspecific binding. Binding constant K_D and maximum adsorption Q_{max} for M2 can be easily obtained from the straight lines of the fitting. Where K_D is the reciprocal of the negative slope and Q_{max} is the y-intercept.

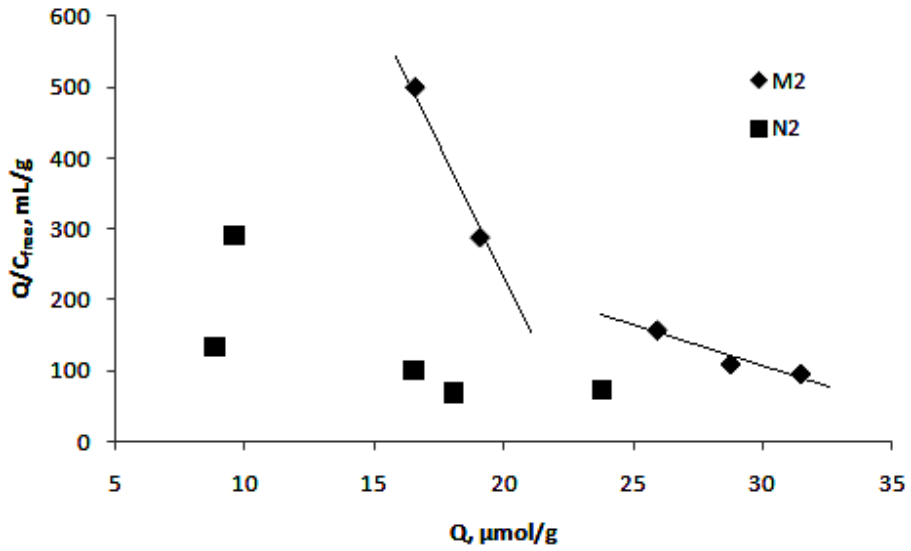

Figure 5.37: Scatchard plots of binding results.

5.3.6.4. Effect of solution volume of quercetin (Breakthrough volume studies)

Unlike in other polymers, uranium and chromium, where the effect of solution volume was investigated by stirring certain amounts of imprinted polymer particles in different solution volumes containing the analyte molecules, in this case, breakthrough volume studies were conducted. Breakthrough volume curves resulting from frontal analysis are plotted in Figure 5.38 and the parameters that were deduced from such curves are listed in Table 5.14. It could be observed from Figure 5.38 that the breakthrough volumes of quercetin and kaempferol from the MIP particles were almost similar. As explained before this was due to cross reactivity of the two compounds as kaempferol can fit the quercetin micro cavity perfectly. In the case of myricetin, the breakthrough volume was a bit lower than the two other compounds. Myricetin though similar to quercetin has an extra hydroxyl group which might act as a hindrance for it to fit perfectly in the pocket created by the quercetin template. However, it has to be taken into account that the cause of the rather low breakthrough volume of quercetin might be due to the fact that a mixture of similar compounds (myricetin, quercetin and kaempferol) was used in this investigation. Therefore, it can be presumed if quercetin was used alone the breakthrough volume might even be higher as the adsorption sites in the polymer were occupied by the other compounds in this instance.

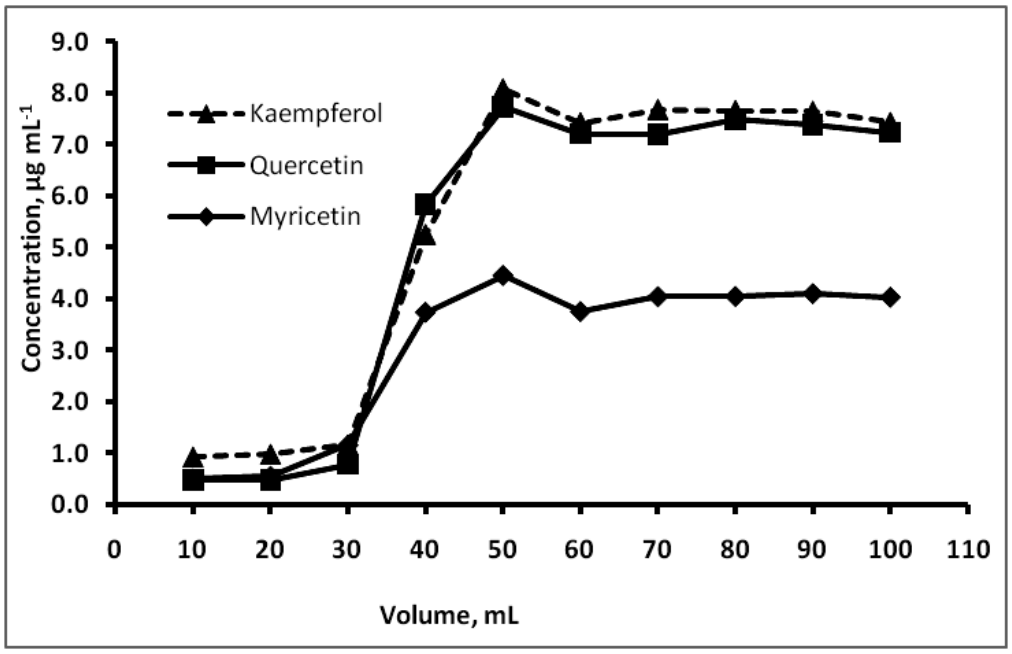

Figure 5.38: Showing selectivity of MIPs.

Table 5.13 presents parameters determined from breakthrough volume curves. V_B and N were calculated as given in equation 2.1 and 2.2, respectively. The breakthrough volumes (V_B) were 8, 22 and 27 for myricetin, quercetin and kaempferol, respectively. These values indicated that myricetin was less bound to the MIP compared to the other compounds. Kaempferol had a slightly higher V_B due to cross-reactivity of quercetin and kaempferol for the same binding sites. The number of theoretical plates, which is a function of retention volume (V_R), determined for each compound also revealed that the value was lower for myricetin (Table 5.14). Furthermore, the theoretical number of plates (N) obtained were in the range of MISPE cartridge.

Table 5.13: Parameters determined for different flavonols using frontal analysis

	V_B (mL)	V_R (mL)	σ_V (mL)	C_E	$0.159C_E$	$0.841C_E$	V_E (mL)	$0.159C_E$ (mL)	N
Myricetin	8	32	12	4.0	0.6	3.4	50	20	4
Quercetin	22	38	8	7.2	1.1	6.1	50	30	18
Kaempferol	27	37	5	7.4	1.2	6.2	50	32	47

Using the same data generated from the breakthrough curves, the amount of each compound that was adsorbed on the MIP sorbent was calculated and the results are listed in Table 5.14. This was achieved on the basis that the sorbents have reached maximum capacity when the loading analytes were passing without being adsorbed onto sorbent (plateau). Therefore, the MISPE was first washed with methanol-water (4:6, *v/v*) (5 mL) to remove unbound/ loosely bound analytes and finally the analytes were eluted with 5 mL of methanol:acetic acid solution (9:1, *v/v*). The amount of flavonols in these effluents was quantified to obtain the maximum adsorption capacity of the MIPs in this case. Maximum adsorption for quercetin, calculated using equation 3, was 2.54 µmol g^{-1}, for myricetin was 1.27 µmol g^{-1} and 2.92 µmol g^{-1} for kaempferol. Total adsorption capacity for this MIP was 6.73 µmol g^{-1}. These values, specifically for quercetin, are acceptable considering that in most studies adsorption capacities are determined with only one analyte in the solution. These adsorption capacities were compared to those in literature (Table 5.15) and indeed the MIP prepared in this study showed good adsorption capacity for the quercetin molecule.

Table 5.14: Adsorption capacity of the MISPE column

Sample	**Myricetin**	**Quercetin**	**Kaempferol**	**Total**
Amount in wash solution (µmol)	0.02	0.03	0.04	0.08
Amount in elution solution (µmol)	0.23	0.48	0.55	1.26
Total compound weight (µmol)	0.25	0.51	0.58	1.35
Weight of MIP (g)	0.20	0.20	0.20	0.20
Amount adsorbed, *Q* (µmol g^{-1})	1.27	2.54	2.92	6.73

Table 5.15: Selected adsorption capacities on MIPs for myricetin, quercetin and kaempferol

Amount adsorbed	**Myricetin**	**Quercetin**	**Kaempferol**	**Reference**
Q (µmol g^{-1})	1.27	2.54	2.92	Present study
Q (µmol g^{-1})	-	1.6	-	Song et al., 2009a
Q (µmol g^{-1})	-	1.32	-	Xia et al., 2006
Q (µmol g^{-1})	0.26	-	-	Tian et al., 2011

SPE specificity of the MIPs for quercetin

Again using the results obtained from the breakthrough volume curves because three different compounds were applied in the same mixture, the selectivity of the MIP for quercetin was investigated. Super specificity of the MIP for quercetin would have resulted in much lower breakthrough volumes for myricetin and kaempferol. This was never the case as the polymer showed cross-reactivity for the three compounds. The breakthrough volumes are similar and all the compounds were bound sufficiently on the MIP (*Q* values in Table 5.16). The cross-reactivity of the MIP towards these types of compounds is not unknown as Xie et al. (2001) also reported that kaempferol displayed stronger affinity to their quercetin-imprinted polymer than was to the non-imprinted polymer. This was attributed to the fact that kaempferol could almost match the micro cavity created by quercetin in terms of shape, size and functionalities (Xie et al., 2001). Similar results were obtained for triazine MIPs, where one template could be used for the extraction of a group of compounds (Chapuis et al., 2004, Mhaka et al., 2009, Carabias-Martínez et al., 2005). Therefore, the cross-reactivity demonstrated by the MIP prepared in this study for these types of compounds was acceptable.

5.3.6.5. Effect of time of quercetin

The influence of contact time on the adsorption of quercetin to the polymers was investigated at 25°C and 84°C, and the results of these investigations are depicted in Figure 5.39(a) and (b), respectively. For the studies at 25°C, an initial

concentration of 66 µg mL^{-1} was used whereas 1 mM quercetin initial concentration for the studies at 84°C was used. All experiments were conducted in triplicates but due to overlap of the adsorption curves error bars were included only for the M2 and N2. Notably in Figure 5.39(a) is that M2 exhibited higher binding capacity at about 55 µmol g^{-1} after 6 hours closely followed by its corresponding NIP, N2, at 42 µmol g^{-1} after 6 hours. All the other polymers were either below or on level with N2. These results revealed that M2 had better imprinting capabilities compared to other polymers. Figure 5.39(b) showed that after 2 hours M2 and N2 had the same imprinting capability as they both reached saturation at the same time. However, this was not the case as in this experiment only 20 µg mL^{-1} was used as the initial concentration and after 2 hours for both M2 and N2 there was no free quercetin left in the reaction solution meaning everything has been adsorbed on the polymers. The decrease observed on M1 and M3 in Figure 5.39(b) may be attributed to the fact that in these polymers the binding with time was less than the imposing disrupting effect of the polar solvent and hence quercetin molecules were released back into solution.

From Figure 5.39(a) one may notice that N2 reached saturation at about 44 µmol g^{-1} of which this binding capacity was enough to consume everything from a 66 µM initial concentration solution. The claim that levelling of the graphs in Figure 5.39(b) was just a matter having less amount of quercetin in solution to the binding capacity of the NIP, (N2) is further emphasized when one look at the effect of concentration graph, Figure 5.39(b), which clearly shows that the MIP, M2, still has higher binding capacity than the NIP, N2. Nonetheless, the effect of temperature seem to lead to faster reaction rates as it only required about 2 hours to reach saturation at 84°C compared to 10 hours at 25°C. This is due to a well known phenomenon that molecules diffuse faster when the temperature is increased. In addition, viscosity is lower at higher temperatures. As it is shown from the figures below that other polymers M1, N1, M3 and M4 were not better than the NIP, N2 in both experiments at 25 and 84°C, therefore they were not investigated further.

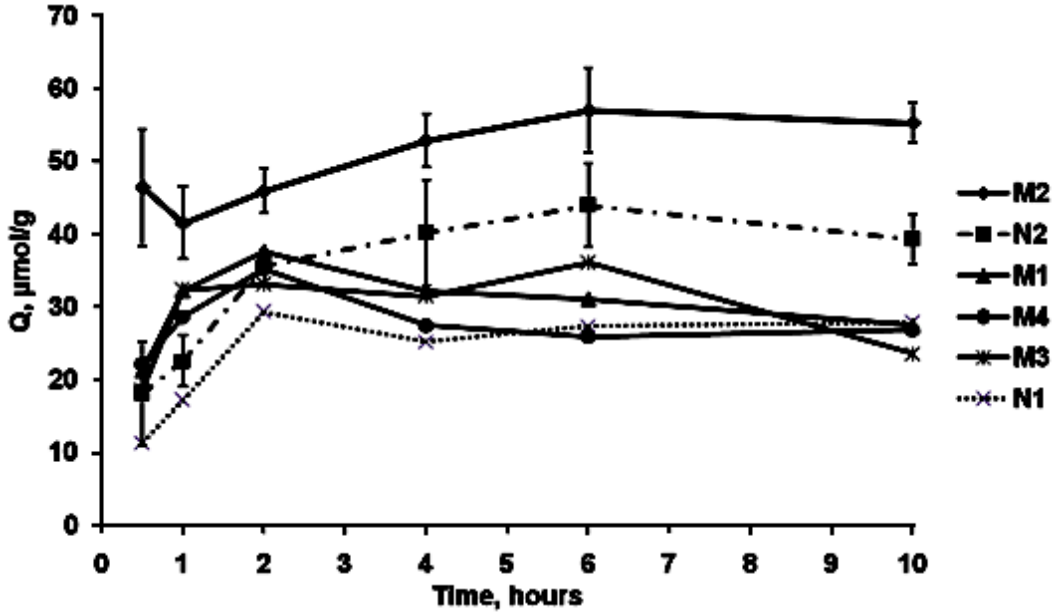

Figure 5.39(a): Effect of contact time on binding capacity of polymers**.** Amount polymer 8 mg, solution volume 4 mL, initial concentration 66 µg mL^{-1}, temperature 25°C, pH 5.5, solvent (MeOH:H_2O, 7:3, v/v).

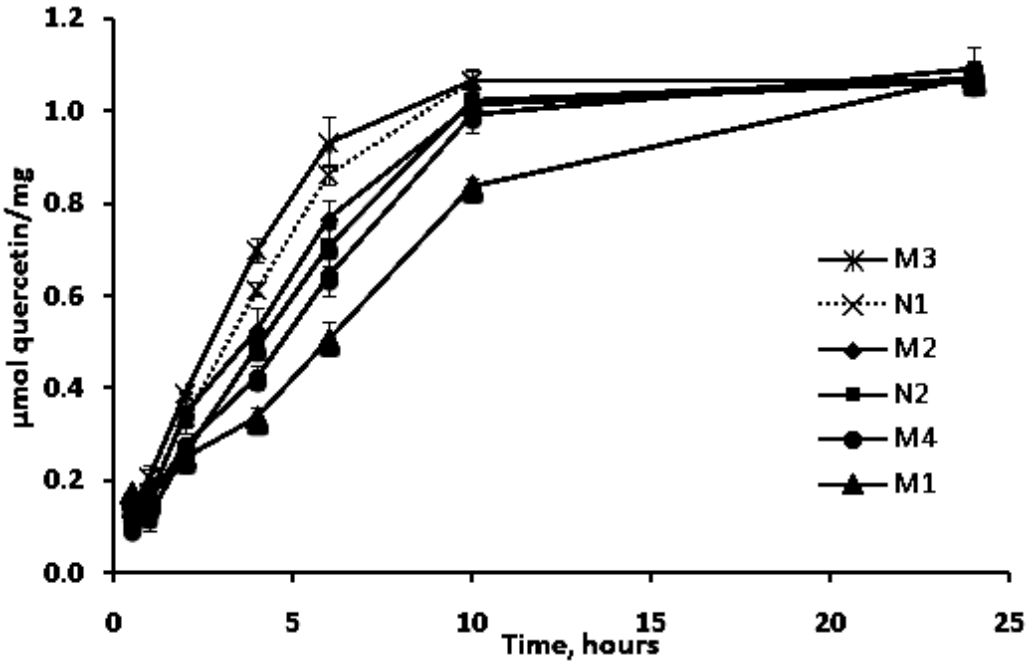

Figure 5.39 (b): Effect of contact time on binding capacity of polymers. Amount polymer 4 mg, solution volume 4 mL, initial concentration 1.0 mmol L^{-1}, temperature 84°C, pH 5.5, solvent (MeOH:H_2O, 7:3, *v/v*).

5.3.6.6. Selectivity of quercetin

The selectivity of the MIP, M2, to quercetin amongst some of its structural related compounds, kaempferol and morin, was evaluated at the selected processing temperature 84°C (Lindahl et al., 2011) in triplicates. Distribution coefficient (k_d), selectivity coefficient (k) and the relative selectivity coefficient (k') were calculated as described in Equations 3.3, 3.4 and 3.5, respectively. The results are illustrated in Table 5.16. As shown in Table 5.16, M2 and N2 have the same binding capacity as demonstrated by the k_d values tabulated. Both M2 and N2 showed highest k_d values for quercetin (14260 mL g^{-1}). This implied that both adsorbed quercetin equally well. Hence, the expected higher binding capacity of MIP was not seen in Table 5.16 because all the dissolved quercetin was adsorbed, even though the solution was nearly saturated.

Table 5.16: Selectivity and binding capacity amounts

	Analyte	k_d (mL g^{-1})	k	k'
M2	quercetin	14260	-	-
	kaempferol	388	37	1.19
	morin	148	97	1.07
N2	quercetin	14260	-	-
	kaempferol	452	31	-
	morin	156	91	-

Another explanation to the similar binding capacity is that MIPs are less selective in binding target compounds when a polar solvent is used. Instead, the selectivity of the MIPs is demonstrated from washing and elution steps, as described further below for a real sample. However, as discussed above, the imprinting effect of M2 prevailed over N2 when the concentration of the analyte was higher (Figure 5.39). Because of the high cost of the other compounds tested for selectivity we have only been able to work with relatively low concentrations. Moreover, as mentioned above, quercetin is a radical scavenger so during the polymerization process some amount of quercetin could be transformed to another form, leading to formation of more unspecific binding (something close to NIP; hence explaining similar behaviour). The higher k_d values of kaempferol and morin for

N2 can be explained as due to the lack of imprinting effect on NIP. That is, the polymer can adsorb anything as long as there are sites available that can interact with the analyte.

As mentioned earlier, quercetin-4´-glucoside and quercetin-3,4´-diglucoside are commonly hydrolyzed to quercetin aglycone, therefore these were not included in Table 5.16 for calculations of selectivity and distribution factors. The selectivity factor and distribution coefficient values summarized in Table 5.16 further emphasize that both M2 and N2 can bind the quercetin substantially well. The imprinting effect of M2 over N2 is demonstrated by the *k* and *k´* values, which show that M2 is better than N2. However, *k´* is just above 1, implying closeness in binding the quercetin molecule by M2 and N2. Hydrogen bonding and π-π interactions are most likely the main recognition sites, as explained by the structure of the quercetin molecule. The presence of water in these experiments might disrupt hydrogen bonding resulting in more π-π interactions (aromaticity of quercetin and vinylpyridine monomer). Future studies will be carried out to further improve the selectivity of quercetin MIPs in pure aqueous environments.

Figure 5.40 shows a typical chromatogram of the selectivity standard solution mixture before the application of MIP (M2) and Figure 5.41 is a typical chromatogram obtained after MIP application as described above. It can be seen that the MIP was able to selectively remove all the quercetin from the mixture of compounds containing kaempferol, morin, quercetin-4´-glucoside and quercetin-3,4´-diglucoside. Both quercetin-4´-glucoside and quercetin-3,4´-diglucoside are relatively "bulky" molecules due to attached glucose moieties and hence unable to fit in the quercetin cavities created by imprinting. Therefore, almost none of these were selectively adsorbed, particularly the diglucoside, whereas to some extent morin and kaempferol were adsorbed on the polymer (Figure 5.41). This shows that MIPs can be selective but they still suffer from unspecific binding.

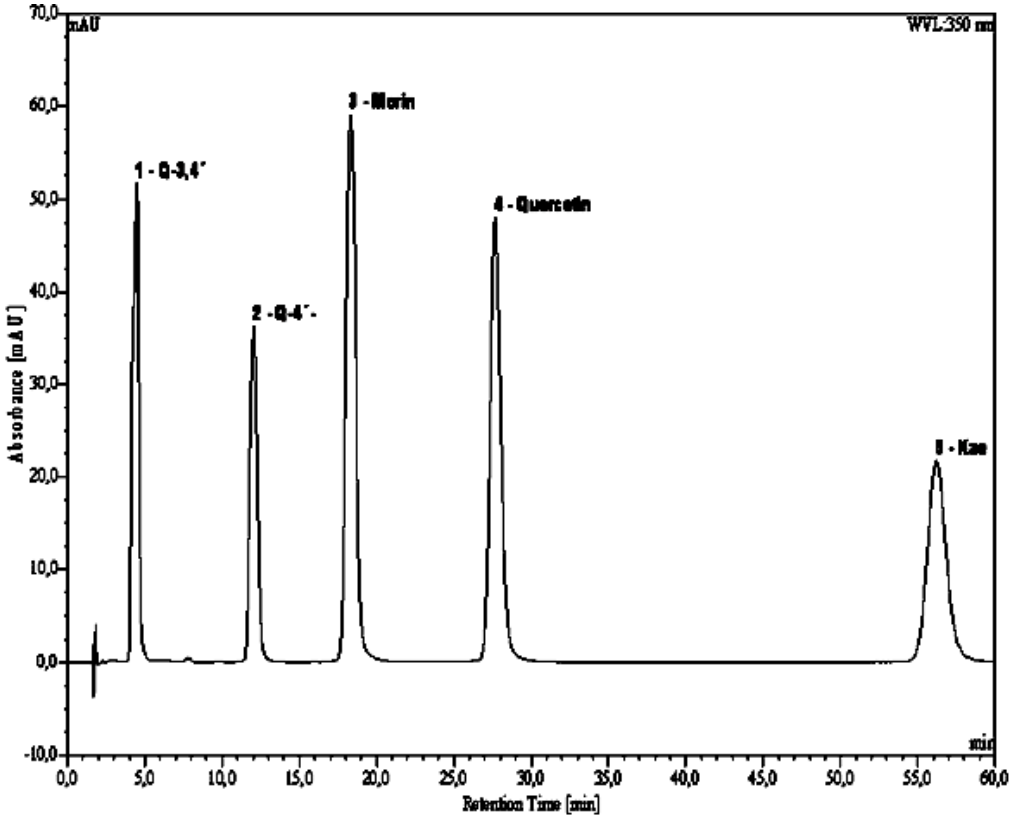

Figure 5.40: Chromatogram of selectivity solution before M2 application.

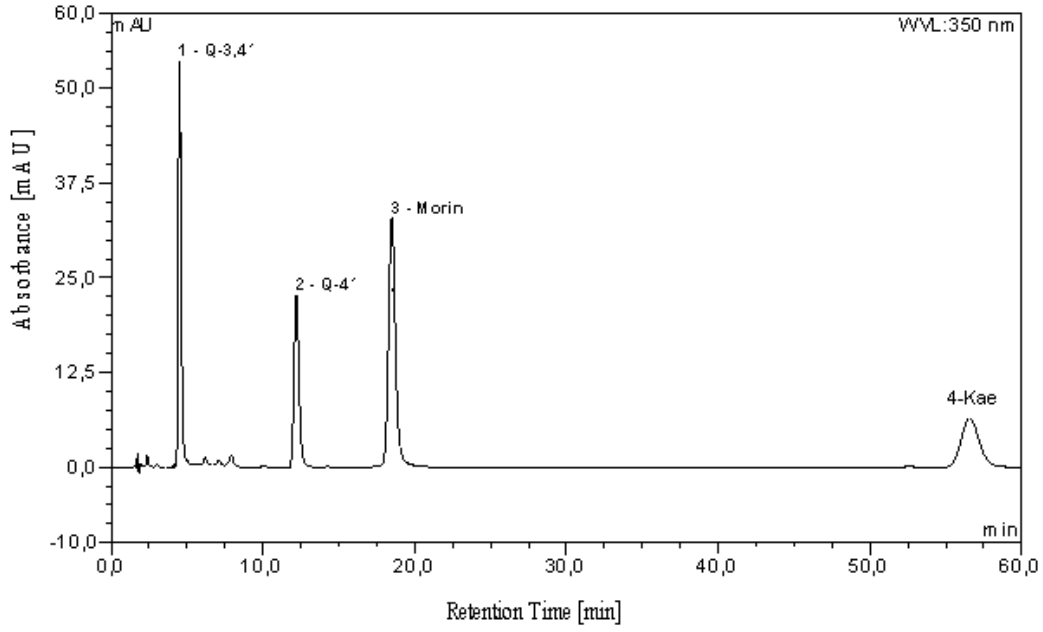

Figure 5.41: Chromatogram of selectivity solution after M2 application.

5.3.6.7. Reusability of quercetin

Figure 5.42 shows the results obtained from the reusability studies of the quercetin imprinted polymer (M2). It can be observed from the graph that the polymer demonstrated good stability and reusability as it showed that it could be used for more than 10 cycles without loosing its adsorption efficiency. Almost 99% of quercetin recovery was obtained in all 10 cycles. However, it should be noted that the concentration and volume of the analyte used during these studies could affect the recovery.

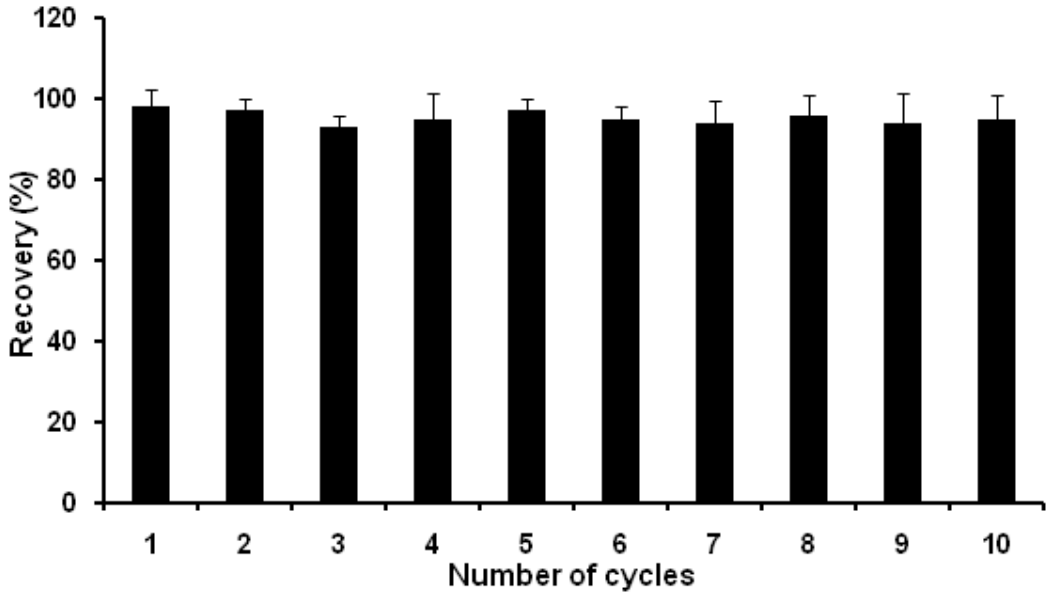

Figure 5.42: Reusability of quercetin MIP. 3 mL, 150 mg MIP, pH 5.5, 20 µg mL^{-1}

5.3.7. Application of quercetin MIPs to real samples

5.3.7.1. Onion

Yellow onion extraction batch mode with MIPs

The yellow onion extract solution was applied in its aqueous form, no organic solvents were used. Aqueous onion extracts were obtained from extraction of chopped onion materials using an accelerated solvent extraction unit (ASE) (Turner et al., 2006). The conditions of the ASE were as follows; water at 120°C and 50 bars of pressure pumped for 5 min in 3 cycles. The chromatogram of the

‘as received’ onion extract in 10 times dilution in the mobile phase is shown in Figure 5.43(a). Figure 5.43(b) is the chromatogram of the unextracted onion solution after MIP application. Figure 5.43(c) shows a chromatogram of M2 particles washed with pure methanol solution (2 mL) for 75 min and Figure 5.43(d) shows M2 particles washed with MeOH:acetic acid (9:1, *v/v*) after the MeOH wash. It is known that in onion quercetin-4’-glucoside is the most abundant form and hence in the application of MIP particles in batch form on the onion extract solution it proved that quercetin-4’-glucoside was the most abundant and hence it competed fairly with quercetin for the binding sites. The prepared polymer seemed to work well under the tested conditions, in that, in Figure 5.43(b) almost no quercetin peak was observed implying a possible adsorption to the polymer and of further notable is the substantial decrease of the quercetin-4’-glucoside peak meaning it has been also adsorbed fairly well on the polymer particles.

However, when the MIP particles were washed with MeOH it showed that a substantial amount of the quercetin-4’-glucoside was washed out compared to the quercetin molecule meaning that the quercetin-4’-glucoside was unspecifically bound to the polymer material. When stronger acidified methanol was used almost equal amounts of quercetin and quercetin-4’-glucoside were washed out but the amount of quercetin-4’-glucoside was lower (5 times less) in this case than with MeOH wash. However, quercetin from the MeOH and MeOH-acetic acid mixture was the same amount implying that the equal amount of unspecifically bound quercetin to specifically bound quercetin. The quercetin-4’-glucoside that was still left after MeOH wash was not a problem as in the ultimate application of the prepared MIPs, this glucoside will be hydrolyzed to aglycone thereby increasing the amount of quercetin in the sample.

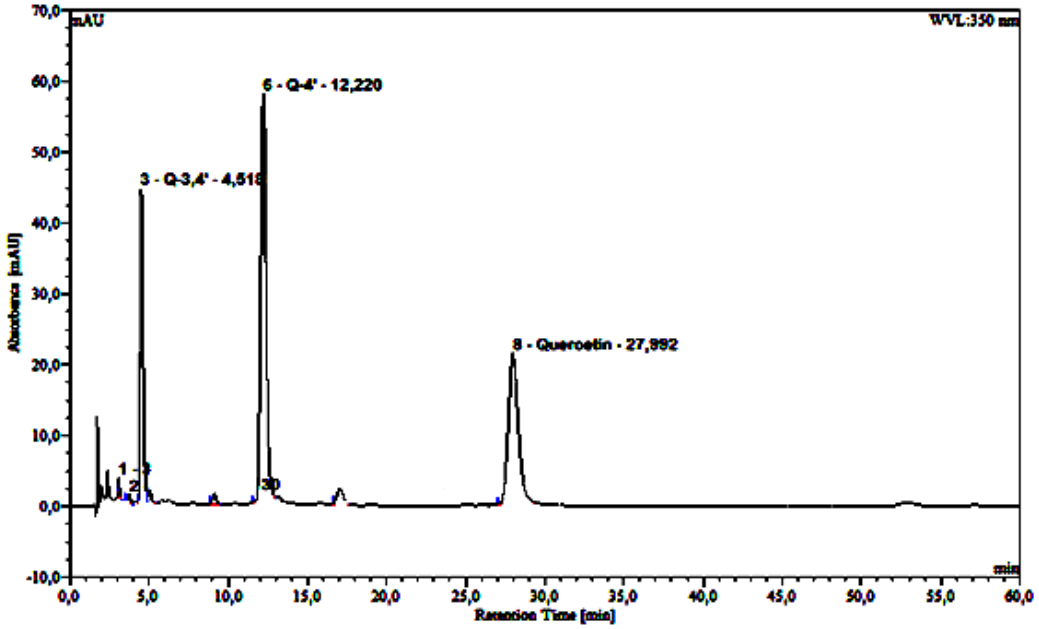

Figure 5.43(a): Chromatogram of a diluted aqueous yellow onion extract solution from ASE.

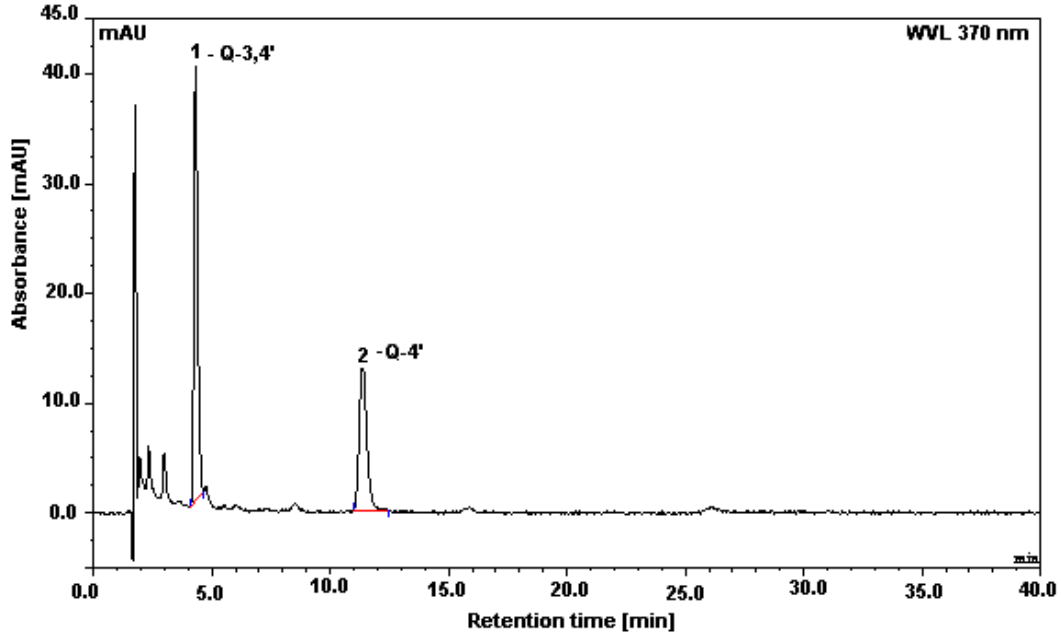

Figure 5.43(b): Chromatogram after MIP application.

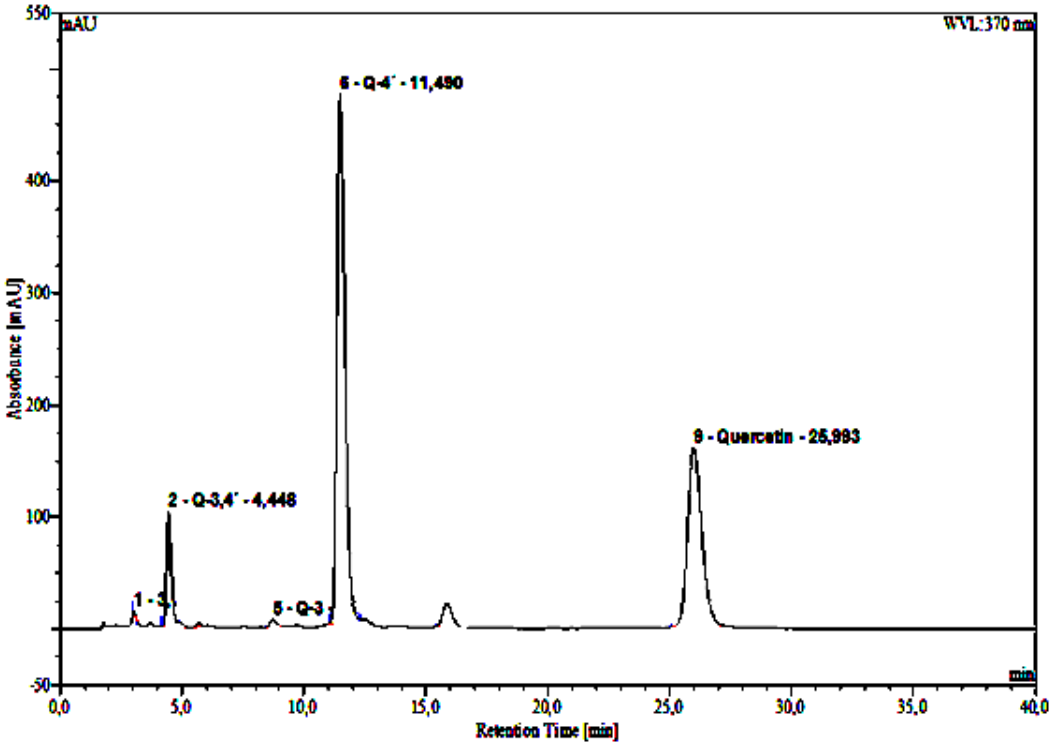

Figure 5.43(c): Chromatogram of MIP MeOH wash.

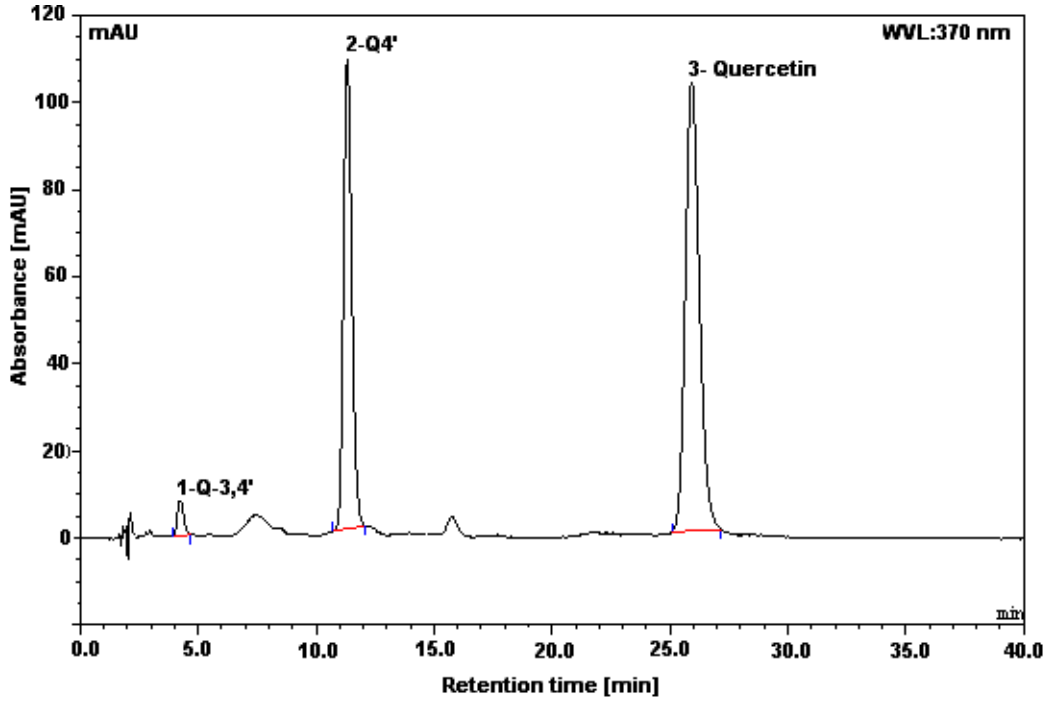

Figure 5.43(d): Chromatogram of MIP MeOH-acetic acid wash.

5.3.7.2. Moringa – optimization of extraction and MISPE washing solution

(i) Optimization of extraction method for Moringa leaves

The extraction efficiency of quercetin was optimized by putting a known amount of *Moringa* leaves in a Soxhlet extractor and the extraction was carried out for 30 hours at 90°C. The results of such experiment are depicted in Figure 5.44. These results are important as they show total extraction quercetin from the leaves. From the graph it can be observed that during the first few hours (up to 3.5 hours) the extraction was fast and from there it slowed down to about 8 hours. Maximum extraction was achieved between 8 and 14 hours, after 14 hours the peak area of quercetin tend to decrease which might indicated signs of degradation. Hence, 14 hours were used as optimum extraction time of quercetin from the *Moringa* plant.

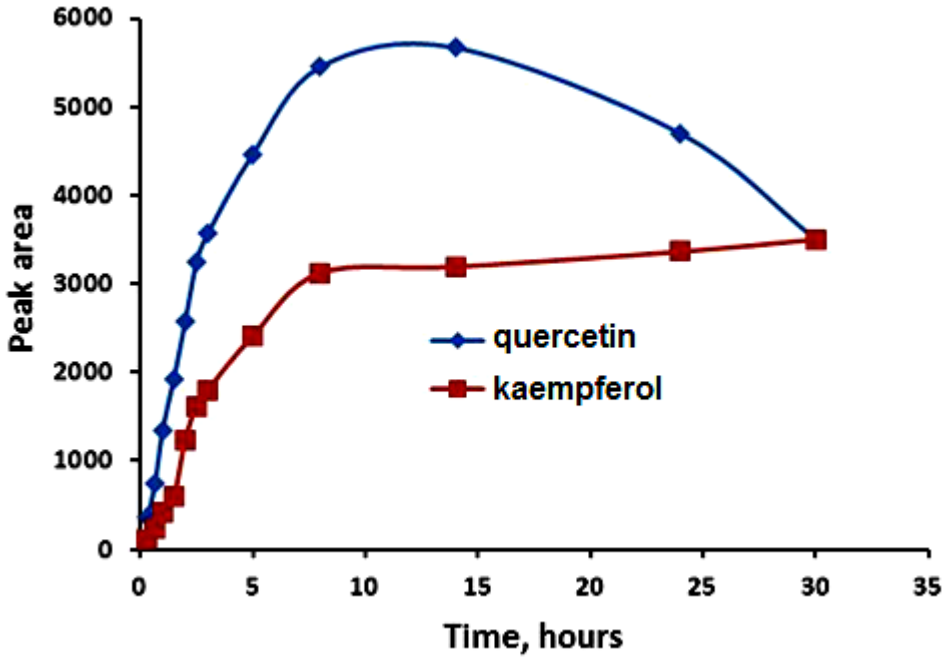

Figure 5.44: Quercetin extraction efficiency optimization. n = 3.

Figure 5.45 shows typical calibration curves obtained in the study for myricetin, quercetin and kaempferol while Figure 5.46 is showing typical chromatograms for the three compounds mentioned. In Figure 5.45 it can be observed that good correlation coefficients were obtained during the quantification of the three

flavonols. The chromatograms in Figure 5.46 demonstrated that a good separation and baseline was obtained for these flavonols implying that the mobile phase system used was optimal. However, due to the presence of matrix peaks from the real samples sometimes it was required that the solvent system be changed. This was done by using less percentage of organic solvent in order to push the myricetin peak further down (greater retention time).

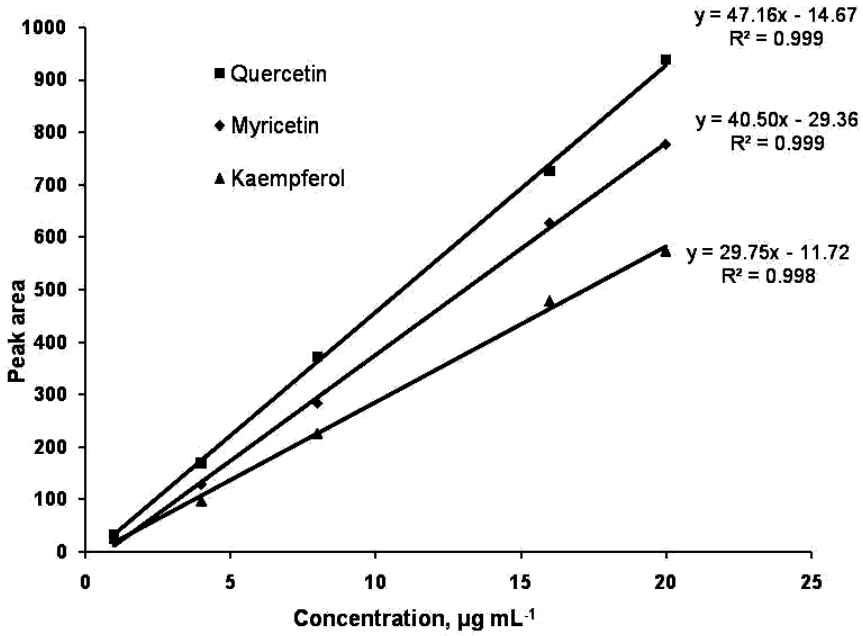

Figure 5.45: Typical calibration curve for the flavonols.

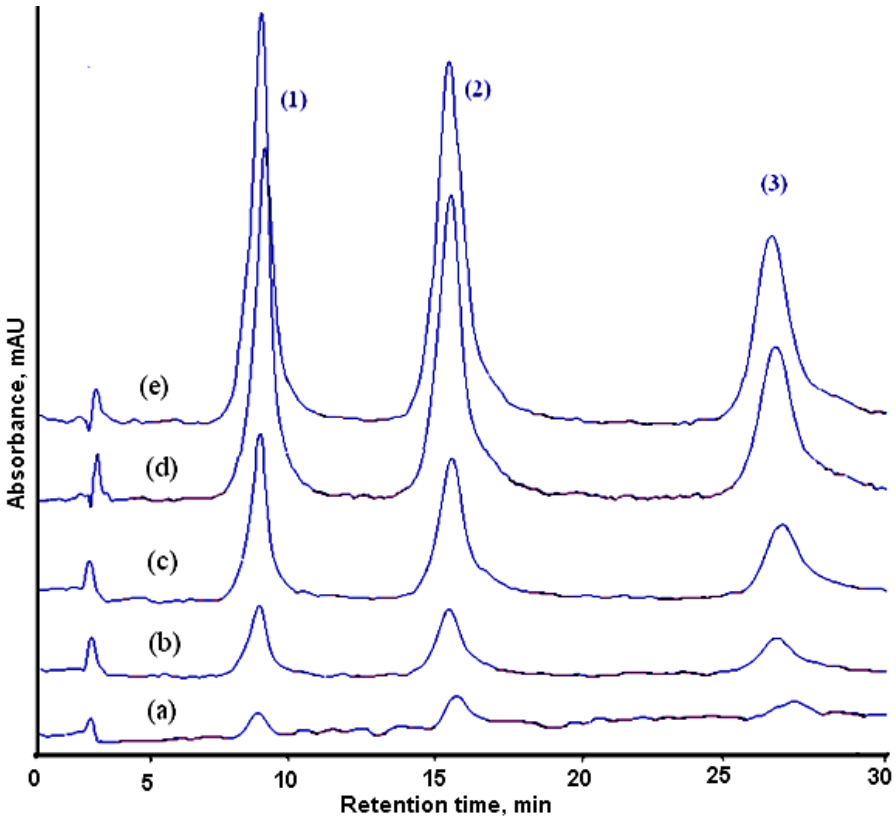

Figure 5.46: Chromatograms of standards solution, (a) 1, (b) 4, (c) 8, (d) 16 and (e) 20 µg mL^{-1}. Peak (1) is myricetin, peak (2) is quercetin and peak (3) is kaempferol. Mobile phase MeOH:H_2O (45:55, v/v) with 0.5% formic acid. Flow rate 1 mL min^{-1}.

(ii) Selection of washing solvent for the application of MISPE technique on Moringa extracts

It is well known that the MISPE technique consists of five stages. These include, in this order, conditioning, equilibration, percolation, washing and elution. For the optimum performance of the technique all stages have to be performed in a careful manner including the choice of solvents used for rinsing and elution. During rinsing, a less stronger solvent capable of removing the matrix while leaving the analyte on the solid sorbent for elution step is used. Therefore, the choice of this solvent is important. Various solvents were investigated for the removal of the matrix during the rinsing step of the MISPE method. The solvents investigated are methanol, acetone, methanol:acetone (1:1, *v/v*), acetone:water (1:1, *v/v*), methanol:water:acetone (1:1:1, *v/v/v*) and methanol:water (1:1, *v/v*). The flow rate

during percolation was 0.25 mL min^{-1} and that of washing and elution was 0.5 mL min^{-1}. 3 mL of *Moringa* extract was loaded onto cartridges, the cartridges were washed with 3 mL of different solvents mentioned above and finally the cartridges were eluted with 3 mL methanol:acetic acid (9:1, *v/v*). From the results, it was found that the optimum rinsing solvent for this case was methanol:water (1:1, *v/v*) and was used for rinsing in all experiments.

Figure 5.47 and 5.48 show chromatograms obtained from using different solvent systems during the selection and optimization of washing solvent for *Moringa* extracts. In this case, all the chromatograms from percolation, washing and elution are shown. Figure 5.47 shows results where (c) - acetone-water (1:1, *v/v*), (f) - acetone-water-methanol (1:1:1, *v/v/v*) and (i) - acetone-methanol (1:1, *v/v*) were used as washing solvents. In all cases the cartridges were finally eluted with 5 mL MeOH-acetic acid (9:1, *v/v*) (Figure 5.47 d, g and j). Figure 5.47 b, e and h are the solutions collected from the percolation step. It was observed that with all these tested washing solvents, very little quercetin was eluted during the final elution stage because most of it was washed out by the washing solvents. Therefore, these were not good washing solvents and other solvents were investigated (Figure 5.48).

Figure 5.48 shows chromatograms obtained from an experiment where methanolic *Moringa* extracts where passed through MIP in an SPE mode. The conditions were as exactly as reported above but washing solvents were (c) – 1:1 methanol-water, (f) – methanol and (i)– acetone. Figure 5.48 b, e and h are eluents collected during percolation and Figure 5.48 d, g and j show elute chromatograms. It can be observed from the chromatograms during the percolation step that the MIPs prepared were very selective for the quercetin and related compounds as all the matrix passed through but retained quercetin. It can also be observed in Figure 5.48 g and j that very little quercetin was obtained during elution step and is because much of the quercetin was washed away as part of matrix during washing step. This meant that (f) and (i) were not good washing solvent for this particular MIP. The optimum solvent was methanol-water (1:1, *v/v*) Figure 5.48 c.

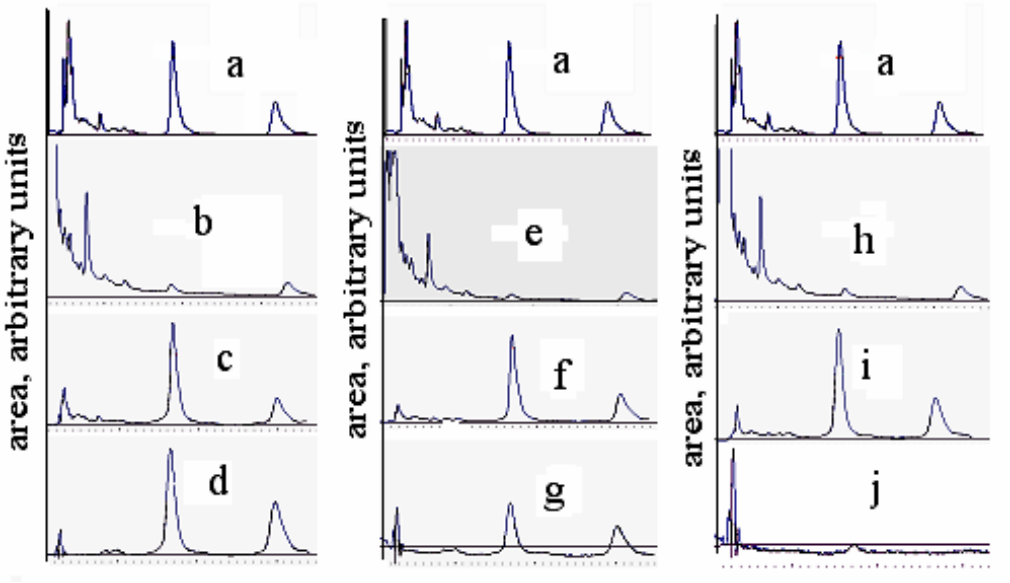

Figure 5.47: Optimization of washing solvent. (a) is the *Moringa* extract before passing through MIP; (b), (e), (h) are solutions after passing through MIP; (c), (f), (i) are solution from washing with different solvents; (d), (g), (j) are solutions after elution with MeOH-acetic acid 9:1 (v/v). Washing solvents were (c) - acetone-water (1:1, *v/v*), (f) - acetone-water-methanol (1:1:1, *v/v/v*) and (i) - acetone-methanol (1:1, *v/v*).

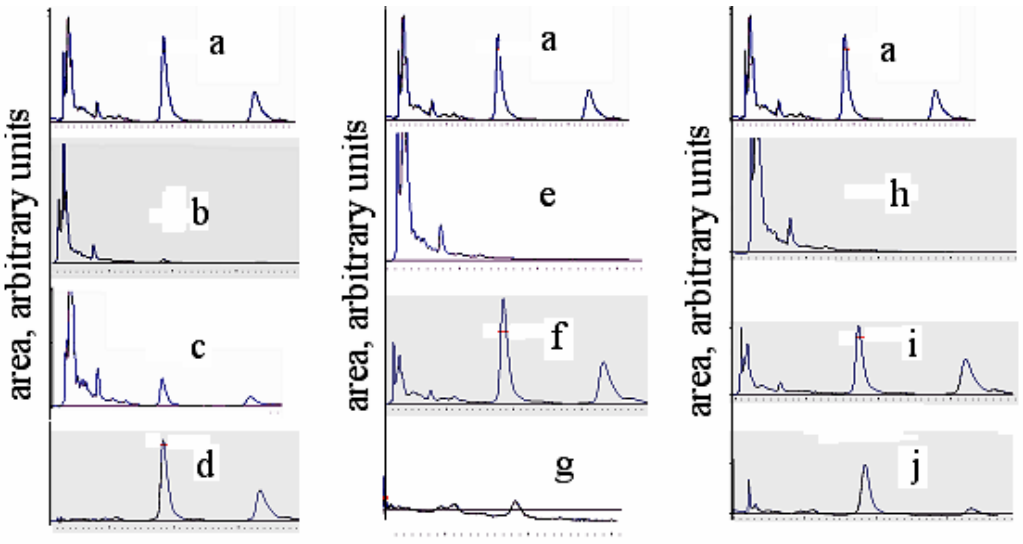

Figure 5.48: Optimization of washing solvent. (a) is the *Moringa* extract before passing through MIP; (b), (e), (h) are solutions after passing through MIP; (c), (f), (i) are solution from washing with different solvents; (d), (g), (j) are solutions after elution with MeOH-acetic acid 9:1 (*v/v*). Washing solvents were (c) – 1:1 methanol-water, (f) – methanol and (i)– acetone.

The above results were summarized in a chart. Figure 5.49 shows the influent of matrix removal and quercetin removal by the rinsing solvent as explained above. It can be observed from Figure 5.49 that the solvents investigated removed the matrix almost in a similar manner. However, methanol:water (1:1, *v/v*) was chosen as optimum because other solvents as much as they removed matrix they also removed more quercetin from the MIPs. That is, methanol:water (1:1, *v/v*) rinsing solvent removed less quercetin. For elution, a methanol:acetic acid (9:1, *v/v*) solution was used as it has been demonstrated in several studies (Xie et al., 2001; Song et al., 2009b; Xia et al., 2006) including this work during elution of template in MIP synthesis that this solution can be used successfully for removal of quercetin molecules.

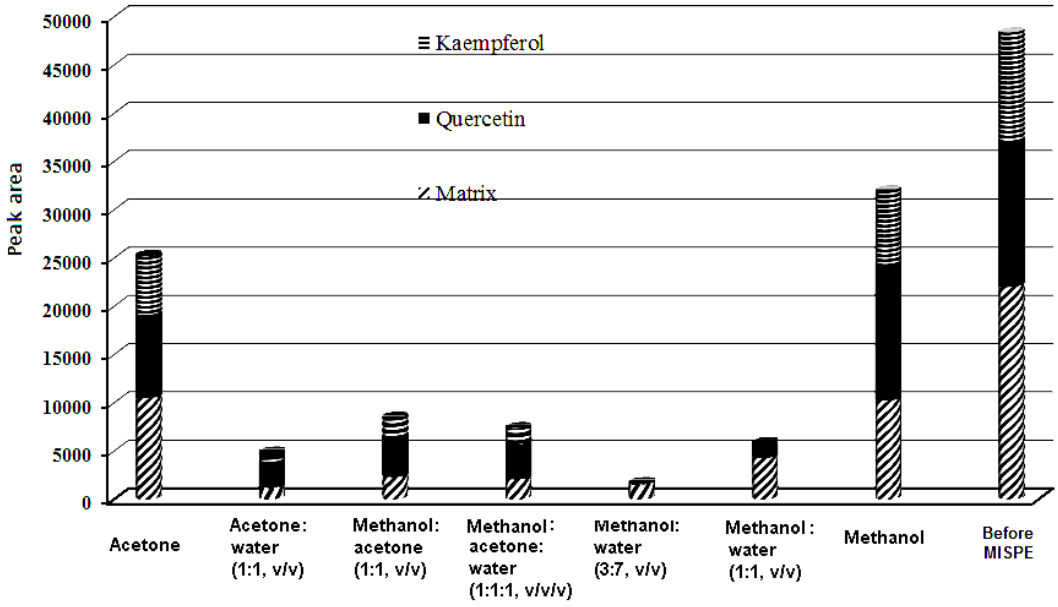

Figure 5.49: Estimated matrix removal and quercetin removal by the rinsing solvents using area under the peaks of the different chromatograms obtained.

5.3.7.3. MISPE versus direct injection

Using the optimized washing solvent, this work was aimed at providing a simple method of using MISPE for separation and determination of quercetin from *Moringa* extract samples. For this purpose, different aged *Moringa* leaves were directly extracted using acidified methanol in a round-bottomed flask for 14 hours (80°C). These extracts were passed through MISPE for sample clean-up,

separation and quantification. Figure 5.50 shows chromatograms obtained from these solutions depicting clearly the effect of imprinting. Therefore, the MIP can be used for selective extraction of quercetin and kaempferol. Contrary to breakthrough volume studies, no myricetin peak was observed from elution effluents. This could mean that *Moringa* does not contain myricetin or its concentration was too low to be detected. The recovery of quercetin from these samples is illustrated in Table 5.17. Recoveries greater than 83% were obtained for all samples. Also the results obtained from quantification using recoveries for method development are in agreement with the direct analysis implying that the MISPE method is well optimized and can be used for the recovery of quercetin in *Moringa* leaves (Table 5.18). All values for quantification of flavonols from *Moringa* are based on dry-mass basis.

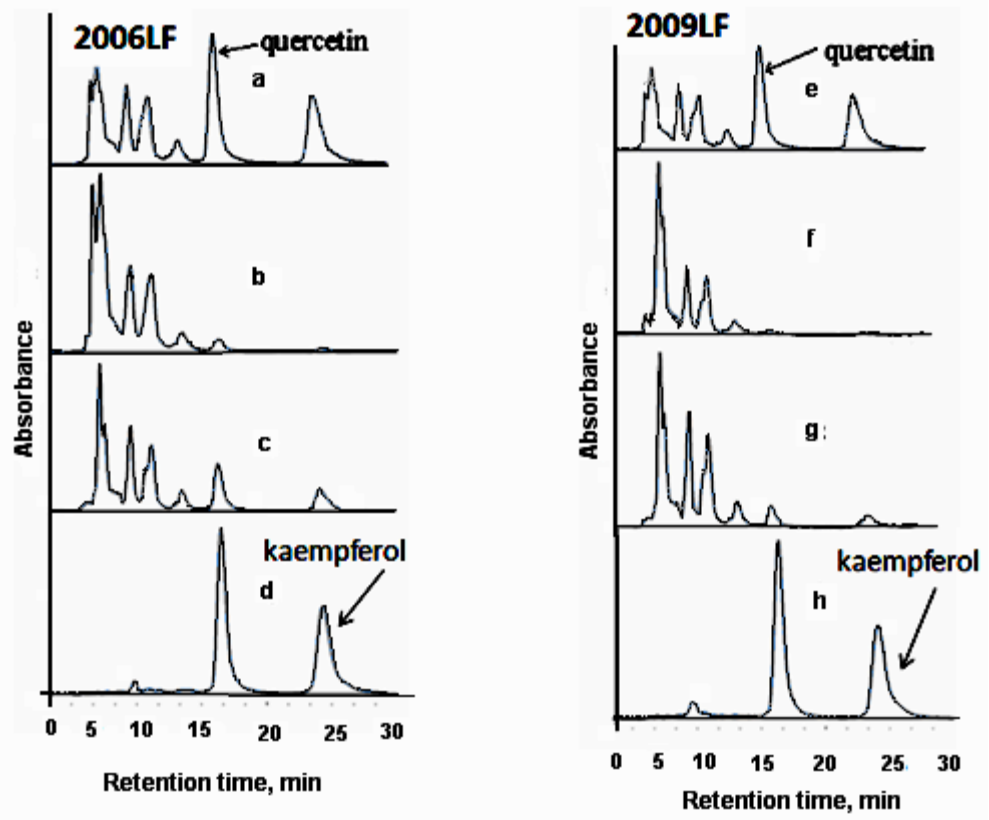

Figure 5.50: Chromatograms of *Moringa* leaf extracts. (a) and (e) Initial solutions before MISPE. (b) and (f) Solutions after MISPE. (c) and (g) Solutions after rinsing with MeOH-H_2O (1:1, *v/v*). (d) and (h) Eluates after rinsing with MeOH-acetic acid (9:1, *v/v*). (a)-(d) 2006LF sample. (e)-(h) 2009LF sample.

Table 5.17: Recovery of quercetin from loading, rinsing and elution solutions (n=3)

Fractions	Mean recovery (%)		
	Freeze-dried leaves	Air-dried leaves	Flower
Percolation (3 mL, MeOH)	1.0	1.9	5.3
Washing (3 mL, MeOH:H_2O, 1:1, v/v)	4.8	4.5	9.9
Elution (3 mL, MeOH:acetic acid, 9:1, v/v)	85.1	80.2	76.8
Total	90.9	86.6	92.0
Amount of quercetin in extracts before MIP application ($\mu g\ mL^{-1}$)	23.7	64.8	59.6

Table 5.18: Quantification quercetin amounts in *Moringa* using MIPs recovery percentage

	Freeze-dried leaves	Air-dried leaves	Flower
Quercetin amount from 5 mg extracted with 120 mL ($mg\ kg^{-1}$)[1]	569	1555	1430
Concentration of eluate with calibration curve ($\mu g\ mL^{-1}$)	20.22	51.95	45.77
C_{sample} (quercetin concentration using recovery, $\mu g\ mL^{-1}$)	23.73	64.78	59.59
Quecertin amonunt 5 mg using C_{sample} ($mg\ kg^{-1}$)[2]	570	1555	1430

Note: C_{sample} is the concentration of quercetin obtained by MISPE quantification

[1] direct injection

[2] after MISPE application

However, it should be emphasized that the extraction yield of these flavonols is not only affected by MISPE but also by the type of extraction method used prior MISPE (i.e. heated reflux extraction in this case). The conditions employed for extraction such as temperature, time and acidity could have negative effects on extraction yields. Turner group has specifically studied the extraction and degradation rates of flavonoids using PFE (which is viewed as a milder extraction technique than heated-reflux extraction) (Petersson et al., 2010; Co et al., 2012). Their results showed that degradation of such compounds happen as early as the initial extractions (Petersson et al., 2010). However, in this study the effect of degradation was not studied but cannot be ruled out. The emphasis was using

MISPE on *Moringa* methanolic extracts for selectivity not quantifying these compounds directly from *Moringa* methanolic extracts.

5.3.8. Attempted precipitation polymerization of quercetin MIP

The quercetin MIPs prepared by precipitation polymerization exhibited very low binding capacity than the bulk polymerization polymers (M2). This was despite the fact that others have reported out-performance of bulk polymers by precipitation polymers (Beltran et al., 2007; Beltran et al., 2009). The authors stated that the out-performance was not only due to synthetic issues such as polymerization yield and particle uniformity but also due to sorbent capacities. So in the present study, it was also anticipated that the precipitation polymers would be better but it was not the case. However, it should be stated that the precipitation polymerization was attempted only once in the current study. In addition, because there are many parameters that can influence polymer performance, therefore it can not be generalized that for quercetin template this will always be the case. Nevertheless, bulk polymers were used through out the study.

5.3.9. Conclusions

MIP showed slightly higher breakthrough volume of kaempferol than quercetin and this could be attributed to cross-reactivity because kaempferol has one less hydroxyl group than quercetin. All the other groups are similar and positioned as exactly as in quercetin. This means that kaempferol can fit perfectly in the micro cavity created by quercetin template molecule. Methanol:water (1:1, *v/v*) solvent mixture was found optimum for the removal of matrix during MISPE application to *Moringa* extracts. Considering that recoveries of 87 to 92% of quercetin from *Moringa* extracts were achieved, then it can be said that the method can be successfully applied for the analysis of *Moringa* extracts. Studies of MIP at high temperature showed some positive results but further studies are still necessary in order to fully understand the mechanism.

Chapter 6: Additional work – studies on *Moringa*

This chapter focuses on the work done on *Moringa*. This work was divided into two sections. In Section 6.1, the focus of the studies is on comparing the contents of three flavonols, *i.e*., quercetin, kaempferol and myricetin in *Moringa* samples and some selected vegetables like cabbage, spinach, peas, cauliflower, and broccoli. Furthermore, the contents of metals from *Moringa* and the aforementioned selected vegetables were also compared. In Section 6.2, the focus of the study was to compare the antioxidant activity of *Moringa* and the mentioned vegetables. This was achieved by measuring the total phenolic content, total flavonoid content, reducing power and by using the DPPH radical generating method. This work did not include MIPs and hence it was separated from the main study. In the main study for example the *Moringa* plant was used as a matrix to test the applicability of the prepared MIPs for quercetin recognition in such matrix.

6.1. Metal and flavonol contents from *Moringa oleifera* grown in South Africa

This study was motivated by the recent interest in Moringa growing in South Africa. The study was aimed at helping the growers and consumers of Moringa in South Africa. Flavonol background is already covered in the main study, hence, it's only metal covered below.

6.1.1. Heavy metals

Heavy metal pollution of the soil is known worldwide and the source of these metals are different ranging from mining activities, smelting, coal burning, urban composts, paint pigment and battery manufacturing, municipal wastewater sludges, leather tanning, metal finishing, phosphate fertilizers, atmospheric depositions, or pesticides (Adriano, 1986; Kabata-Pendias and Pendias, 1992). In fact, soil is known to act as a reservoir for these heavy metals (Boularbah et al., 2006). However, there are also some other natural sources of heavy metals. Unlike organic compounds, inorganics are not degradable that makes them have longer half-lives in both terrestrial and aquatic environments. When these heavy metals are present in higher concentrations than would be recommended they become toxic to the ecosystem and eventually humans (Olowoyo et al., 2010). This is because the plants which are consumed by humans may accumulate these heavy metals and as a result by the time people consume the plants or any animal that have consumed such plants may feel sick. Nonetheless, trace elements are needed as they play an important role in biological, chemical, enzymatic, and metabolic reactions in the living cells of plants, animals and human beings (Hashmi et al., 2007).The *Moringa* plants studied in the present study were grown in Johannesburg which is one of the leading industrialized region of South Africa (Naicker et al., 2003). Therefore, it was imperative that heavy metal concentrations on the *Moringa* plants grown in Johannesburg as well as the soil from which the plants are being grown be investigated. This knowledge is important for the community because *Moringa* is being used by the disadvantaged and poor as a supplement for nutrients and vitamins in their daily diet. Other

Moringa plant samples were investigated from a *Moringa* farm based in Limpopo Province in a village known as Tooseng.

6.1.2. Experiments

6.1.2.1. Chemicals and reagents

Quercetin, kaempferol, myricetin, methanol (HPLC grade), formic acid, nitric acid, and hydrogen peroxide were purchased from Sigma-Aldrich (Johannesburg, South Africa). Stock solutions of quercetin (0.3 g L^{-1}), kaempferol and myricetin (50 µg mL^{-1}) in methanol and 1.0% formic acid were prepared in the laboratory and kept at -18°C when not in use. Ultrapure water (MilliQ) was used in all experiments and chemicals were used as received. The pH was adjusted with citric acid monohydrate (0.1 M) and disodium hydrogen phosphate (0.2 M). The flavonols monitored are given in Figure 6.1.

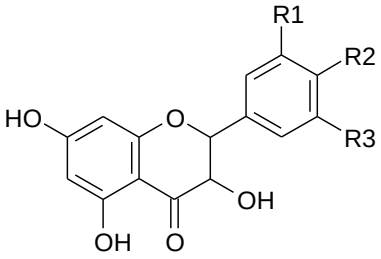

	R1	R2	R3
quercetin	OH	OH	H
myricetin	OH	OH	OH
kaempferol	H	OH	H

Figure 6.1: Chemical structures of quercetin, myricetin and kaempferol.

6.1.2.2. Leaf samples

Fresh M. *oleifera* leaves were collected in April 2011 from two growing areas (Limpopo and Atteridgeville) in Johannesburg. A total of four *Moringa* leaves samples were investigated. The samples were labelled 2006LF, 2009LF, 2010LF and 2010AF. The number denotes the year the plant was grown, *e.g.*, 2006 whereas LF and AF stands for Limpopo farm and Atteridgeville farm, respectively. The leaves were immersed in a container with deionised water for a minute to remove surface contaminants. Following which, the leaves were lyophilized for few days. After freeze-drying the samples were homogenized and ground into a fine powder and kept in the dark under a cool place until further use.

Moringa flowers were processed exactly the same as leaves, but sampling was only conducted for 2010 trees in LF.

6.1.2.3. Vegetable samples

Vegetable samples were bought from a local supermarket. The inedible parts were removed with a sharp steel knife, thereafter, about 1.0 kg of the edible part of each vegetable sample was washed with tap water. A sharp knife was used to cut the washed parts into small pieces of approximately 1x1 cm. After this, they were processed as *Moringa* leaves above. These vegetables were selected based on common knowledge that they are mostly used by South Africans.

6.1.2.4. Soil samples

Soil samples were collected next to the tree-trunk where the leaves were collected and these were labelled clearly to correspond with the leaf samples. That is, a spade was used to dig about 10–15 cm next to plant roots and soil was collected. The soil was air-dried, homogenized and passed through a 1 mm sieve to remove big particles and possibly some stones. The soils were then milled to a fine powder using a commercial pulverizer, Fritsch pulverisette 6 (Fritsch GmbH, Idar-Oberstein, Germany).

6.1.2.5. Extraction and hydrolysis of flavonols

Extraction and hydrolysis of flavonols was carried out as detailed in the main study Section 4.11.8.2 (iii).

6.1.2.6. Dry matter determination

Similarly, the same drying method adopted in the main study was used, Section 4.11.8.2 (i).

6.1.2.7. Total digestion

0.1 g of freeze-dried leaf samples were placed in microwave digestion vessels. To this was added 8 mL concentrated nitric acid and 2 mL hydrogen peroxide. Digestion was carried out for about 30 min in the microwave. After digestion the samples were transferred to 25 mL volumetric flasks and made up to the volume with deionised water. The solutions were directly analyzed for metal content using

inductively coupled plasma-optical emission spectroscopy (ICP-OES) (Spectro Genesis, Spectro, Germany). All digestions were carried out in triplicates.

Similar protocol was followed for total digestion of soils samples. 0.1 g of dried soil samples were placed in microwave digestion vessels. However, 6 mL of concentrated hydrochloric acid, 2 mL concentrated nitric acid and 1 mL hydrofluoric acid were added to the vessel. When the digestion was finished (about 50 min) 6 mL boric acid was added to each vessel to neutralize the HF acid. The solutions were transferred into 25 mL volumetric flasks and made up to the volume with deionised water. All solutions were measured for metal content using ICP-OES. All digestions were carried out in triplicates.

6.1.2.8. Conditions of HPLC and quantification of flavonols

Identification and quantification of flavonols from methanolic extracts was performed as detailed in Section 4.3 of the main study.

6.1.3. Results and discussion

6.1.3.1. Flavonols in Moringa grown in SA

The flavonols content in the investigated *Moringa oleifera* leaves is reported in Table 6.1 as the concentration of quercetin, myricetin and kaempferol. The results showed that the sample from *Moringa* leaves taken from plants grown since 2009, have the highest concentration of flavonol content (5121.9 mg kg^{-1}). This is closely followed by 2010 sample which has a total concentration of 4535.7 mg kg^{-1} whereas 2006 sample has the lowest concentration of total flavonols (4447.1 mg kg^{-1}). However, looking at individual concentrations of the three different flavonols assayed from these plant samples one may pick up that 2009 has the highest concentration of quercetin and kaempferol (1972.8 and 2145.2 mg kg^{-1} respectively). Myricetin was found to be ranging from 1004–1809 mg kg^{-1} from the investigated samples. Interestingly, the total flavonols content in the investigated M. *oleifera* samples was comparable to that obtained by Sultana and Anwar (2008) (6125.6 mg kg^{-1}) for *Moringa* grown in Pakistan. However, the distributions are different as they found that the *Moringa* contained 5804.4, 281.0

and 40.2 mg kg^{-1} of myricetin, quercetin and kaempferol, respectively. Particularly, the three flavonols (kaempferol, quercetin, and myricetin) were investigated in detail and found to reduce the risk of pancreatic cancer by 23 percent (Nöthlings et al., 2007). Hence, consumption of *Moringa* leave products is very important.

In another study (Siddhuraju and Becker, 2003), it was reported that the quercetin concentration from the M. *oleifera* leaves investigated ranged from 6340–27490 mg kg^{-1} while kaempferol levels were from 1050–6470 mg kg^{-1}. It is clear that the quercetin levels obtained from these studies was higher than the concentrations obtained in the present study whilst some kaempferol levels were much similar to present study at about 1200 mg kg^{-1}. Such differences are largely attributed to various factors such as agroclimatic regions, postharvest handling, genetic variability as well as the stage of the leaf development (Anwar et al., 2005; Siddhuraju and Becker, 2003). It was shown in the same study (Siddhuraju and Becker, 2003) that flavonol content was different from samples obtained from India, Niger and Nicaragua.

Table 6.1: Contents of flavonols (mg kg^{-1} dry matter) of different *Moringa oleifera* leaves materials

	Myricetin	Quercetin	Kaempferol	Total flavonols
Vegetables				
Cabbage	nd	nd	nd	nd
Spinach	620.0 (±5.1)	17.9 (±0.1)	215.3 (±0.3)	853.1 (±2.3)
Peas	nd	nd	nd	nd
Cauliflower	nd	nd	nd	nd
Brocolli	nd	nd	nd	nd
Moringa leaves				
2006 LF	1443.3 (±12.5)	1084.7 (±4.2)	1919.1 (±3.5)	4447.1 (±4.5)
2009 LF	1004.0 (±8.5)	1972.8 (±2.1)	2145.2 (±3.3)	5121.9 (±3.7)
2010 LF	1809.1 (±2.4)	1097.1 (±1.1)	1629.5 (±3.4)	4535.7 (±2.6)
2010 AF	929.8 (±12.6)	1295.6 (±10.7)	2040.8 (±11.8)	4266.1 (±5.9)
Moringa flowers	27.6 (±11.3)	4244.6 (±5.2)	6535.8 (±3.9)	10807.9 (±4.5)

± RSD nd - not detected

6.1.3.2. Properties of the soil

In order to understand the relationships between the metal concentrations in soils and plants selected properties of the soils from the sites where the *Moringa* was grown were investigated and the results are given in Table 6.2. Properties measured were conductivity, pH and redox potential. The pH was measured using two methods, the first involve using a suspension of soil and deionised water in a 1:2 ratio, the second involves using a suspension of soil in a solution of $CaCl_2$ (0.01 M) also in a 1:2.5 ratio (Nicholls and Evans, 1991). When deionised water was used, the pH of the soil was found to be in the range of 7.32–8.24. While when $CaCl_2$ solution was used the soil pH recorded was in the range 4.62–7.85. Due to high pH level of the soils from which these plants were grown, it can be said that to a certain extent some trace metals may not be available for plant uptake. This is because low pH (acid level) increase the mobility of trace metals due to possibility of cation exchange reactions taking place. The optimum soil pH

required for *Moringa* plant growth is pH 5.0 – 9.0 (Palada and Chang, 2003). The soil pH values reported above are within this range.

The electrical conductivity of soil is related to the presence of cations and anions. Higher electrical conductivity value indicates high concentration of such ions in soil. However, similar values of electrical conductivity between two soils do not mean that the ions present in the soil are the same. Some slight variation between the soils might be possible. The electrical conductivity values obtained from the study are presented in Table 6.2. It can be observed that the older the plant (2006LF) the higher is the electrical conductivity value. This can be explained by the fact that all soil samples were taken near the proximity of the plant stem at almost similar distances for all plants. So the older the plant the farther its roots grow and hence the farther its metal uptake. This means that newly grown plants still take their nutrients near the proximity of the plant stem. Therefore, soil closer to the newly grown plant stem will have lower metal and/ or nutrients content hence lower conductivity values (*e.g.*, 2010AF and 2010LF). Whereas, for older plants (2006LF and 2009LF) the conductivity of the soil close to the plant might be higher due to presence of nutrients and other metal ions as the plant takes its metals from far.

The redox potential (E_h) shows that the condition of all the soils in under basic reducing conditions which further illustrate the poor ability of releasing heavy metals to the plants (Krauskopf, 1967). Hence, this could be the reason that no toxic heavy metals were detected from *Moringa* samples. Generally, positive E_h values are characteristic of bottom deposits which are poor in organic matter, or which are well oxygenated whereas negative E_h values are associated with bottom deposits which are rich in organic matter (ZoBell, 1946).

Table 6.2: Properties of the soil from which the *Moringa* plants were grown

Sample	Conductivity, $\mu S\ cm^{-1}$	pH ($CaCl_2$)	pH ($D\text{-}H_2O$)	Redox potential, mV
2009 LF	26	7.65	8.03	281
2010 LF	14	7.55	8.24	286
2006 LF	59	7.86	7.32	240
2010 AF	14	4.62	7.87	370

Where AF= Atteridgeville farm, LF = Limpopo farm. Years denote when the plants were planted. The years represent when the plants were planted.

6.1.3.3. Metal content is soil

Metal content on the soils where the plants were grown was determined from total digestion solutions using ICP-OES. The investigation is important as it gives the relative concentrations of metals in soil and in plants. The results obtained from such investigations are reported in Figures 6.2-6.4. These results give an indication of whether there is any source of contamination of the soil or the metals are just a result of natural abundance. Since the *Moringa* leaves are consumed by people it is imperative to know the concentration of toxic heavy metals from the soil as these can be uptaken by plants and cause injuries, even deaths.

The results of metal concentrations are spread into two categories, major nutrients and trace elements. Major nutrients (K, Na, Ca, Mg, P) are needed by both plants and humans in large quantities and these results are presented in Figure 6.2. On the other hand, trace elements (Zn, Mn, Cu, Cr, Co, Ni) are only needed in small quantities by both plants and humans (Figure 6.3). However, due to pollution the soil might contain some toxic heavy metals such as Pb, Hg, or U. These toxic heavy metals were not detected from the soil samples investigated in this study. Generally, the Limpopo farm soils contain the highest concentration of major nutrients than the soils from the Atteridgeville farm (Figure 6.2). Limpopo farm soil contains the highest concentration of K, Ca and Mg at 15000, 3200 and 3000 mg kg^{-1}, respectively. However, the Atteridgeville farm slightly edges out

Limpopo farm on the concentration of Na at 7000 mg kg^{-1} compared to 5800 mg kg^{-1}. Phosphorus concentration is similar in both soils (Figure 6.2).

Figure 6.3 displays the minor nutrient elements found in both farms. Both farms contain high concentrations of Mn relative to other trace elements. In Limpopo farm, the Mn concentration found was 650 mg kg^{-1} while in the Atteridgeville farm this concentration was 550 mg kg^{-1}. All other minor elements investigated were below 100 mg kg^{-1} except Cr in the Atteridgeville farm (about 240 mg kg^{-1}). High concentrations of these trace metals (particularly, Fe and Mn) in Urban soils and soils from waste dump sites with special reference to the top soil were also reported by Gonzalez and Gonzalez-Chavez (2006). It was noted in the study that the effect of anthropogenic sources for these elements could not be separated from the rest of the other elements (Gonzalez and Gonzalez-Chavez, 2006).

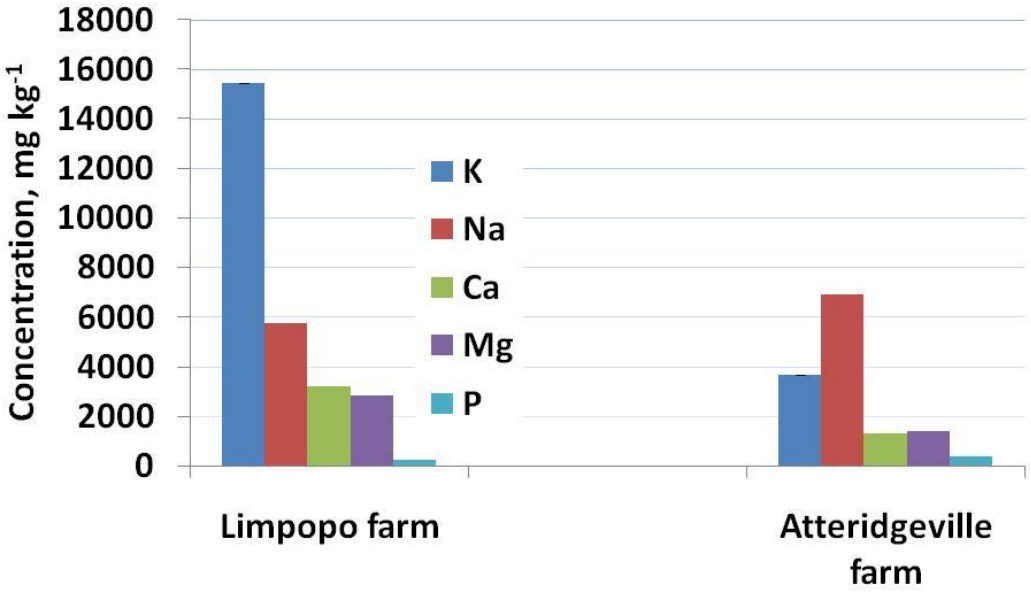

Figure 6.2: Averages of major nutrients in soils from Limpopo farm and Atteridgeville farm. All results are mean of triplicates but error bars (%RSD) are omitted as they are meaningless because of the scale in the y-axis.

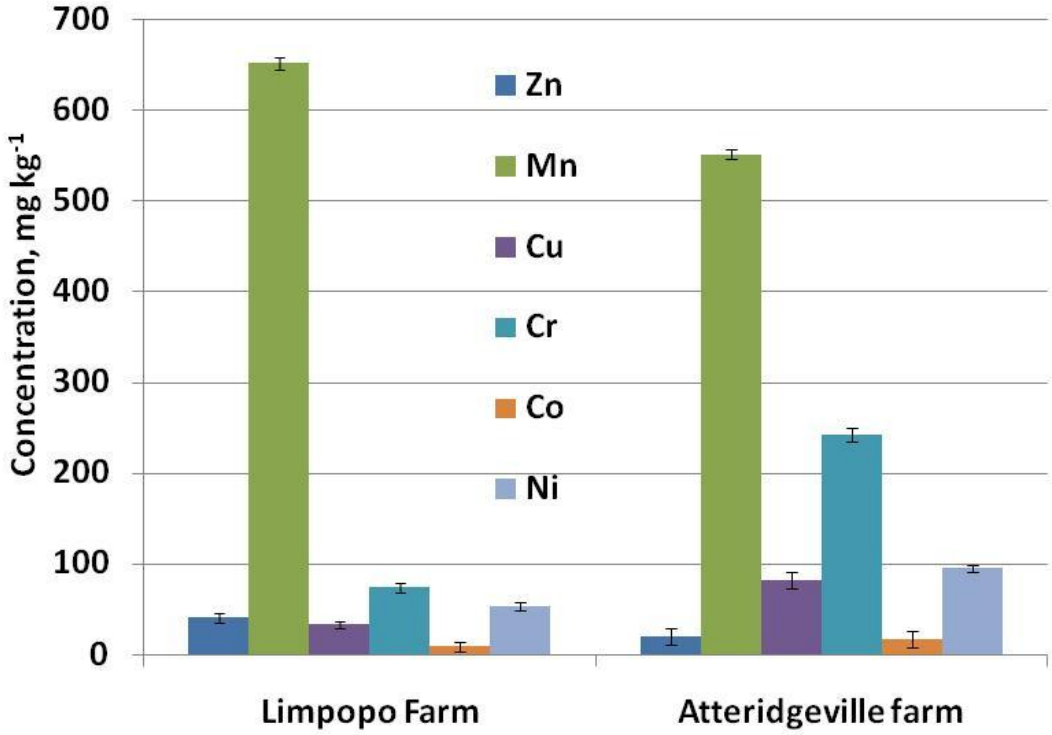

Figure 6.3: Averages of minor elements in soils from Limpopo farm and Atteridgeville farm.

Concentrations of trace elements found in this study were compared to standards from Germany, UK and Canada. The trace elements compared were Cr, Cu, Zn as well as Pb and the results are depicted in Figure 6.4. The Cr from the Limpopo farm was well lower than (80 mg kg^{-1}) that from the standard in Germany (200 mg kg^{-1}) and within range with the standard from UK and Canada. However, Cr from the Atteridgeville farm was highest at about 240 mg kg^{-1}. For the other trace elements, their concentrations were either well below the standards (Zn) or within range (Pb and Cu). Higher concentrations of Cr in the Atteridgeville farm could mean possible contamination of the soil with some kind of anthropogenic source. However, this is difficult to pin-point as there is no previous data of metal concentration studies on the soil of that site. Hence, this makes it difficult to conclude whether the source is present or the concentrations are actually going down now.

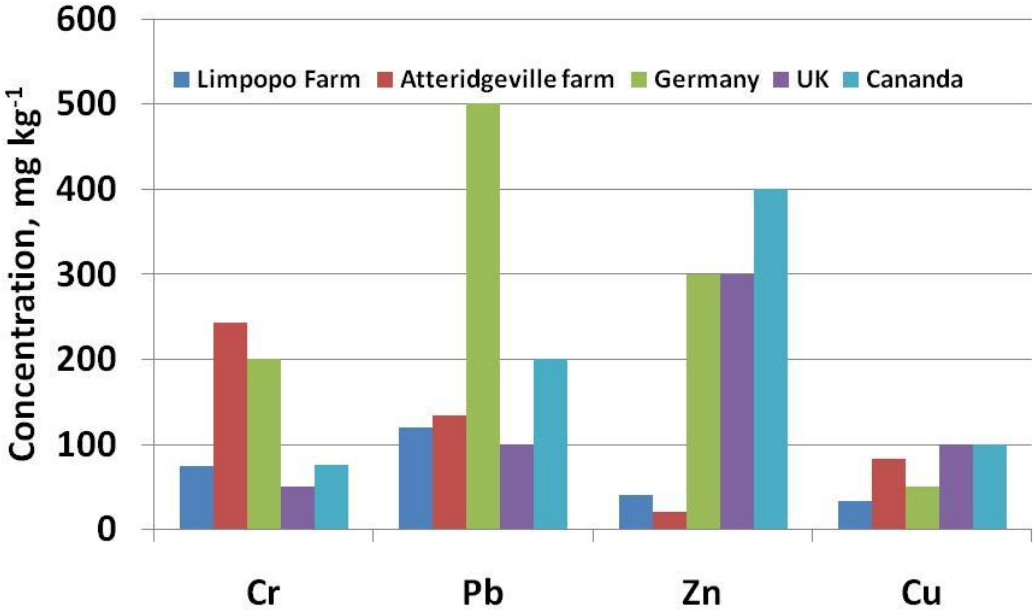

Figure 6.4: Comparison of trace nutrient elements in soils from two farms with standards from other countries.

6.1.3.4. Metal content in Moringa leaves

Metal content on *Moringa* leaves, flowers and some vegetables such as spinach, cabbage, peas, broccoli and cauliflower were determined. The results of these investigations are reported in Figure 6.5 and 6.6. Like in the soils, these are grouped into major nutrients (Figure 6.5) and trace elements (Figure 6.6). *Moringa* leaves obtained from plants grown from the years 2006, 2009 and 2010 in Limpopo farm are labelled as 2006LF, 2009LF and 2010LF respectively. *Moringa* leaves from plants grown at Atteridgeville farm are labelled 2010AF. Crushed *Moringa* in the figures refer to *Moringa* leaves which were already in packets for selling. The concentrations of these metals were compared between the plants and this will be related to the soil content in the case of *Moringa* samples to see if there is any correlation. It is known that use of agrochemicals and amendments may result in accumulation of heavy metals due to intensification of agriculture.

In Figure 6.6, it can be seen that *Moringa* contain higher concentration on Ca than other vegetables. However, spinach, broccoli and cauliflower have higher

concentration of K than *Moringa*. *Moringa* contain more Mg (average 6000 mg kg^{-1}) than all other vegetables tested except spinach (9000 mg kg^{-1}). Other nutrients tested were more similar between the plants. Moreover, *Moringa* is more comparable to spinach as per this study in terms of major nutrient concentrations. Other trace elements such as Cd, Cu, and Pb were not detected in the present study and there the plants can be said to be deficient of these metals or occur at very low levels (Pugh et al., 2002).

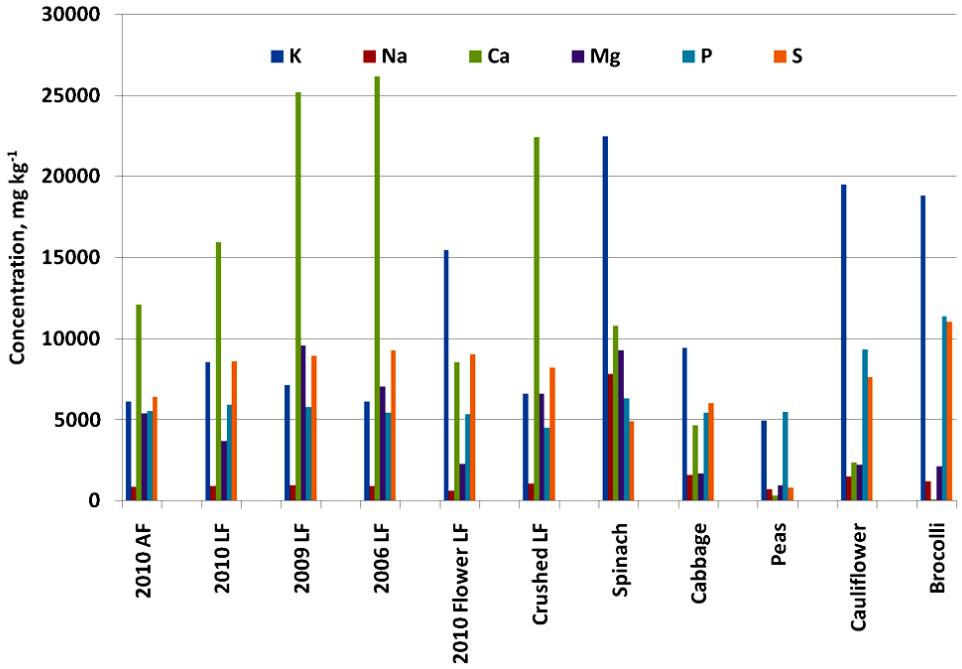

Figure 6.5: Major nutrient elements in *Moringa* trees and comparison with other vegetables. Where AF= Atteridgeville farm, LF = Limpopo farm.

Results showing Cr and Zn trace nutrient analysis is shown in Figure 6.6 and these were interpreted using Table 6.3 (Pugh et al. (2002). Zn concentrations from the *Moringa* were in the range of 10–150 mg kg^{-1} which is regarded as normal (Table 6.3). Therefore, it can be observed that all Zn concentrations were in the range of 10–150 mg kg^{-1} which is regarded as normal (Table 6.3). Therefore, the *Moringa* plants investigated in this study are safe for human consumption as far as the level of trace elements is concerned. By comparing the levels of trace metals in *Moringa* leaves and the soils, it can be said that *Moringa* plant is not able to take up trace metals. Hence, the source of trace metals in the leaves might not be

particularly from the soils (Olowoyo et al., 2010) but rather other factors such atmospheric deposition of heavy metals and absorption capacities of heavy metals by plants (Zurera et al., 1989). Other numerous environmental factors that can affect metal uptake by *Moringa* plant include wind velocity, temperature, moisture and the nature of the vegetables (*e.g.*, leaves, roots, fruit exposed surface area, smooth or hairy exposed parts) (Zurera et al., 1989). However, since it is only the leaves that were investigated here therefore the accumulation by roots is not known. Nonetheless, if the roots are accumulating the heavy metals then it is good as they are not transferring them to the leaves in this particular case.

Table 6.3: Typical levels for heavy metals in plants

Status	Metal concentration (mg kg^{-1})			
	Cd	Cu	Pb	Zn
Deficient	-	<1-5	-	<10
Normal	0.05-2	3-30	0.5-10	10-150
Phytotoxic	5-700	20-100	30-300	>100

Adapted from Pugh et al. (2002)

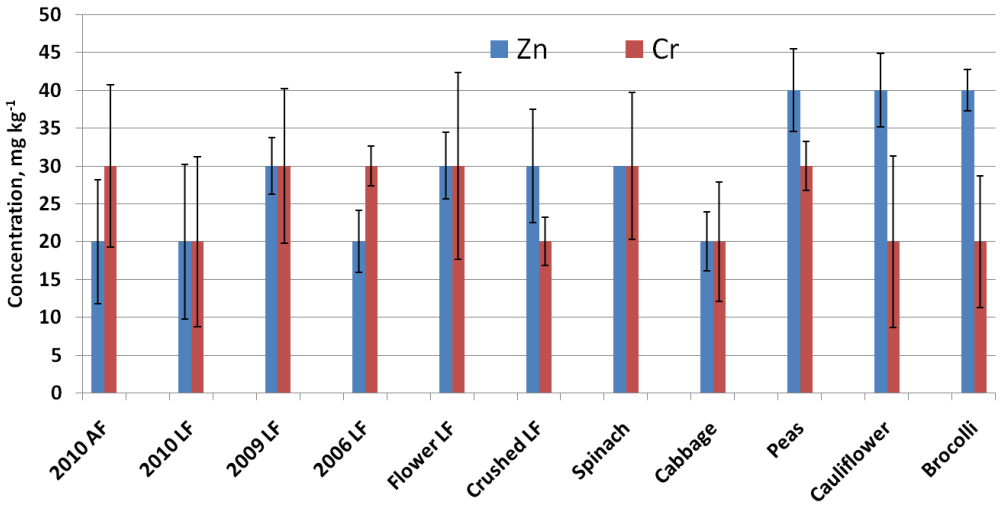

Figure 6.6: Trace nutrient elements in *Moringa* trees and comparison with other vegetables. Where AF= Atteridgeville farm, LF = Limpopo farm.

Iron is one of the most essential trace minerals required by human body as it plays an important role in the formation of hemoglobin. It is known that the body would shut down if hemoglobin was absent as red blood cells would not be able to transport oxygen and nutrients to various cells. Furthermore, the body needs iron to perform certain redox reactions. Iron is present in two forms, the heme and non-heme. Usually the heme is found from red meat and chicken whereas non-heme is found in green leafy vegetables (Cook et al., 1991). Of the two forms heme is the most easily absorbed by the body. On the other hand, non-heme is much harder to be adsorbed by the intestines, however, presence of vitamin C in the diet facilitate absorption of non-heme by the intestines. For this to happen, it is recommended that green leafy vegetables be taken together with vitamin C containing foods like orange juice, broccoli and tomato (Hurrell and Egli, 2010).

Due to relative abundance of Fe compared to other minor nutrients in Figure 6.6, therefore the results showing Fe concentrations of the investigated materials is depicted separately in Figure 6.7.

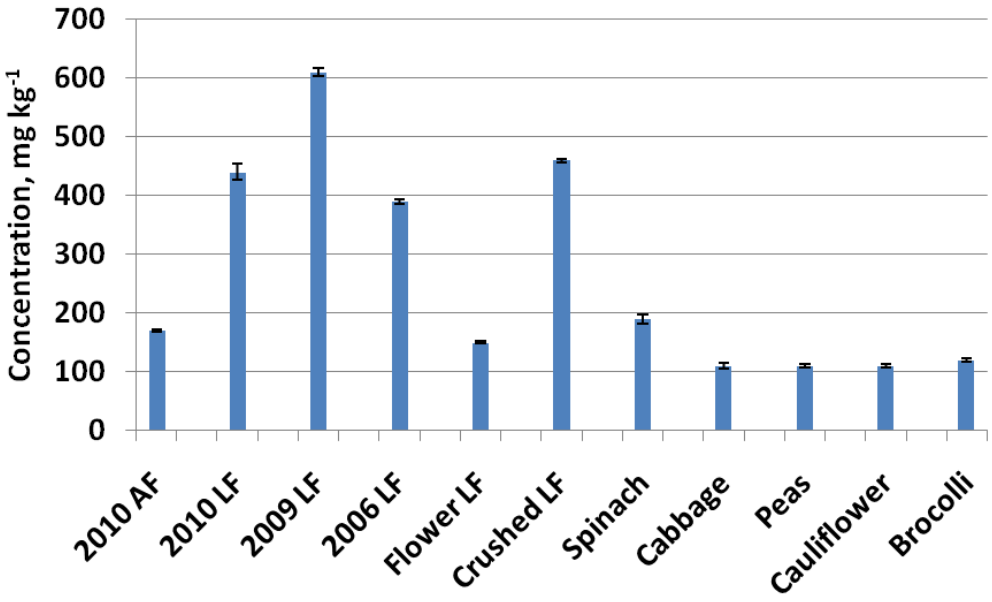

Figure 6.7: Concentration of iron in vegetables and *Moringa* samples. Where AF= Atteridgeville farm, LF = Limpopo farm.

The results revealed that *Moringa* contained more Fe than the selected vegetables. *Moringa* 2006LF sample showed the highest levels of iron at about 600 mg kg^{-1}. Vegetables like cabbage, peas, cauliflower and broccoli contained the lowest iron levels of about 100 mg kg^{-1} each. It can be generalized that *Moringa*, on average, contained about 2.5 to 4 times more the amount of iron than the vegetables under investigation. Therefore, in this case it might be enough to consume *Moringa* alone as this will have both vitamin C and iron.

6.2. Antioxidant activity studies of *Moringa* and selected vegetables in South Africa

6.2.1. Background

Humans are exposed to the harmful effects of free radicals almost all the time. The sources of these free radicals can be both endogenous and exogenous. Endogenous sources of free radicals arise due to the impact of several metabolic pathways in cells. Particularly, the oxidative species that can be produced this way are the reactive oxygen species (ROS), hydroxyl ($HO^{\cdot}$), reactive nitrogen species (RNS) and hydrogen peroxide (H_2O_2). Exposure to cigarette smoke, UV light, ionizing radiation, certain organic solvents, pollutants and industrial waste are all causes of exogenous sources of free radicals (Boonchum et al., 2011). The presence of these free radicals in human bodies might lead to degenerative diseases such as coronary heart disease, cancer and Alzheimer's disease (Ames et al., 1993; Razali et al., 1997; Pezzuto and Park 2002). Therefore, to protect the body against these diseases it is advised to consume antioxidants as part of the diet. The dietary in take of antioxidants could be in the form of beverages that are rich in flavonoids and phenolic acids, for example, a cup of coffee may contain 200-550 mg of polyphenols, while a cup of tea may contain about 150-200 mg of polyphenols and glass of wine may contain about 200-800 mg of polyphenols (Bravo 1998; Lakenbrink et al., 2000). Antioxidants are also available as supplements as well as from natural products such as fruits and vegetables (Wilson 1999; Ramathnam et al., 2001; Ismail et al., 2004; Moon and Shibamoto, 2009). Natural antioxidants come very highly recommended than their synthetic counterparts (butylated hydroxyanisole BHA and butylated hydroxytoluene BHT) because they are viewed as less toxic and more potent compared to synthetic antioxidants (Sun et al., 2005; Shahidi et al., 2009; Boonchum et al., 2011; Sun and Ho, 2005; Diallard and German, 2000).

It is known that certain plants may contain natural antioxidants such as vitamin C, tocopherols, flavonoids and other phenolic compounds (Yen et al., 1996; Yen et

al., 2000; Ramarathnam et al., 1995; Laandrault et al., 2001). *Moringa oleifera* is one such plant that has been identified to contain natural antioxidants (Larson, 1988; Siddhuraju and Becker, 2003; Iqbal and Bhanger 2006).

Although it is known that *Moringa* can resist drought and tolerate a wide range of rainfall and soil conditions (Iqbal and Bhanger, 2006), but the contents of certain chemicals in the plant might be influenced by agroclimatic conditions. Consequently, the antioxidant activity of the plant extracts can also be influenced by these same conditions. Siddhuraju and Becker (2003) analyzed the antioxidant activity of *Moringa* from India, Nicaragua and Niger. Also, Makkar and Becker (1997) assayed the antioxidant activity of *Moringa* from Nicaragua and the values obtained were actually higher than those of Siddhuraju and Becker (2003). However, the values reported by Becker were lower than those obtained by Iqbal and Bhanger (2006) for *Moringa* from Pakistan. Therefore, it was important to investigate these variables on *Moringa* grown in South Africa.

The aim of the present study was to evaluate the antioxidant activity of *Moringa* grown in South Africa and compare it to selected vegetables such as spinach, cabbage, peas, cauliflower and broccoli. The comparison of antioxidant activity was achieved by using five methods, *viz*., 2,2-diphenyl-1-picrylhydrazyl ($DPPH^{\cdot}$), Folin- Ciocalteu, ferric reducing power, total phenolics, total flavonoids, and superperoxide free radical scavenging. Furthermore, the correlation between these methods was investigated.

6.2.2. Materials and Methods

6.2.2.1. Chemicals and reagents

Linoleic acid, dihydronicotinamide adenine dinucleotide phosphate (NADPH), adenosine 5′-phosphate (ADP), 2,2-diphenyl-1-picrylhydrazyl free radical (DPPH•), nitro blue tetrazolium, phenazine methosulfate, ammonium thiocyanate, and stable free radical were purchased from Sigma-Aldrich (Johannesburg, South Africa). Ascorbic acid, trifluoro acetic, 2,6-dichlorophenolindophenol, gallic acid,

metaphosphoric acid, sodium acetate, ferric chloride, sodium dihydrogen phosphate, disodium hydrogen phosphate, potassium dihydrogen phosphate, dipotassium hydrogen phosphate and potassium chloride were also purchased from Sigma-Aldrich (Johannesburg, South Africa). Kaempferol, myricetin, quercetin, methanol (HPLC grade), formic acid, nitric acid, and hydrogen peroxide were purchased from Sigma-Aldrich (Johannesburg, South Africa). Stock solutions of quercetin (0.3 g L^{-1}), kaempferol and myricetin (50 µg mL^{-1}) in methanol and 1.0% formic acid were prepared in the laboratory and kept at -18 °C when not in use. Ultrapure water (MilliQ) was used in all experiments and chemicals were used as received. The pH was adjusted with citric acid monohydrate (0.1 M) and disodium hydrogen phosphate (0.2 M).

6.2.2.2. Leaf samples collection

Fresh M. *oleifera* leaves were collected in April 2011 from two growing areas (Limpopo and Atteridgeville) in South Africa. The leaf samples were collected from trees that were grown in different years (2006, 2009 and 2010) and labelled as such. That is, the samples were labelled 2006LF, 2009LF, 2010LF and 2010AF. The number denotes the year the plant was grown, *e.g.*, 2006 whereas LF and AF stands for Limpopo farm and Atteridgeville farm, respectively. A total of four *Moringa* leaf samples were investigated. Immediately after collection, the leaves were immersed in a container with deionised water for about a minute to remove surface contaminants. After freeze-drying for a few days the samples were homogenized, ground into a fine powder and kept in a dark-cool place until further use. *Moringa* flowers were treated exactly the same as leaves but were only collected from 2010LF trees.

6.2.2.3. Vegetable samples.

Vegetable samples were bought from a local supermarket. The inedible parts were removed with a sharp steel knife, thereafter, about 1.0 kg of the edible part of each vegetable sample was washed with tap water. A sharp knife was used to cut the washed parts into small pieces of approximately 1x1 cm. After lyophilisation the samples were mixed well, homogenized and ground to a fine powder using a commercial pulverizer, Fritsch pulverisette 6 (Fritsch GmbH, Idar-Oberstein,

Germany). The material that passed through 53 µm sieve was used for extraction purposes.

6.2.2.4. Dry matter determination

Dry matter determined as explained previously.

6.2.2.5. Extraction of total flavonoids

Total flavonoids extraction was conducted as per Siddhuraju and Becker (2003). Powdered freeze-dried *Moringa* leaf or vegetables (1 g) samples were extracted in an apparatus containing a round-bottom flask and reflux condenser with 100 mL of 80% methanol for 3 h. After cooling the extracts were centrifuged at 3000 g for 15 min, and filtered through 0.45 µm filter paper. Finally the volume of the extract was made up to 100 mL with 80% methanol. These extracts were used for the estimation of total flavonoids.

6.2.2.6. Estimation of total flavonoids

A method from Siddhuraju and Becker (2003) was followed with some modifications. A known volume of extract (0.30 mL) was placed in a 10 mL volumetric flask, and distilled water was added to make 4 mL. To this was added 0.3 mL of $NaNO_2$ (5 g 100 mL^{-1}) and mixed well. Three millilitres of $AlCl_3$ solution (1:100) was added 5 min later. After 6 min, 2 mL of 1 M NaOH solution was added, and the total volume was made up to 10 mL with distilled water. The solution was mixed well again, and the absorbance was measured against a blank at 510 nm with a UV-visible spectrophotometer (Varian, Cary 50 Conc, Germany). Quercetin (Sigma-Aldrich) was used as the standard for the calibration curve. The following linear equation based on the calibration curve was used to calculate the flavonoid content in the different methanol extracts of the samples.

$$\boldsymbol{y = 171.2x + 176.6, \quad r^2 = 0.998} \qquad \textbf{(6.1)}$$

6.2.2.7. Extraction of total phenolics

Extraction of *Moringa* leaves and vegetable samples was carried out following the method reported by Siddhuraju and Becker, 2003 with modifications. Freeze-dried *Moringa* leaf samples and vegetable samples (0.25 g) were ground so as to

pass 1 mm sieve size and extracted with 20 mL of 80% acetone (80 mL of acetone plus 20 mL of distilled water) under a sonication bath for 25 min. The resultant solution was centrifuged for 10 min at 3800 g and the supernatant saved. The residue was re-extracted as above, both supernatants were combined and total volume made up to 50 mL with 80% acetone solution. The total phenolic contents were estimated according to the Folin-Ciocalteu method using gallic acid as standard Makkar et al. (1997).

6.2.2.8. Determination of total phenolic content

Total phenolic content (TPC) in the acetone extracts of M. *oleifera* leaves and vegetable samples was measured using Folin–Ciocalteu reagent assay (Folin and Ciocalteu, 1927; Singleton and Rossi, 1965). 200 µL of extract was added to a solution mixture of 750 µL Folin–Ciocalteu reagent (1:10) freshly prepared and 2 mL of 7.5% sodium carbonate. The final mixture was diluted to 7 mL with deionized water. The reaction mixtures were incubated at ambient conditions in the dark for 2 h to complete the reaction. Then the absorbance at 765 nm was measured on a 6300 Jenway Spectrophotometer, with a 1cm cell. All the experiments were conducted in triplicates using gallic acid as a calibration standard, and results were recorded as gallic acid equivalents (g/100 g of extract).

6.2.2.9. DPPH (2,2'-diphenyl-2-picryl-hydrazyl) radical scavenging assay

The DPPH radical-scavenging activity assay was performed using a method adapted from Brand-Williams et al. (1995) with some modifications. Briefly, methanolic extracts of *Moringa* leaves or vegetables samples (0.1 mL) were added to 3.9 mL of 0.025 g L^{-1} DPPH in MeOH prepared daily. The decrease in absorbance was measured at 0, 5, 15, 30, 60 and 120 minutes at 515 nm. In between measurements, the reaction mixtures were kept in the dark at room temperature. Furthermore, 50% and 75% dilution methanolic extracts of each sample were prepared. These were treated as above however the absorbance was measured after 60 minutes of incubation only. The results are reported as percentage of DPPH concentration left in solution.

6.2.2.10. Superoxide radical scavenging activity

Superoxide radical scavenging activity was carried out by the method of Nikishimi et al. (1972) as described in Boochum et al. (2011). Superoxide radicals were determined by the phenazine methosulphate (PMS)–NADH superoxide generating system containing a 0.5 mL of *Moringa* or vegetable extract, 0.5 mL of 2.52 mM nitroblue tetrazolium (NBT), 0.5 mL of 624 µM b-nicotinamide adenine dinucleotide (NADH) and 0.5 mL of 120 µM PMS were added. The NBT, NADH and PMS solutions were prepared in 0.1 M sodium phosphate buffer (pH 7.4). The mixtures were incubated at room temperature for 5 min and the absorbance measured at 560 nm. The decrease of absorbance at 560 nm was calculated as percentage of inhibition of NBT using equation 6.2 below expressed as gallic acid equivalent (GAE), that is, mg of gallic acid equivalents per 1 g of sample.

$$\%\ \boldsymbol{inhibition} = \left[\frac{\boldsymbol{A_0 - A_1}}{\boldsymbol{A_0}}\right] \boldsymbol{x}\ \mathbf{100} \qquad \textbf{(6.2)}$$

Where A_0 is the absorbance of blank and A_1 is the absorbance of sample after time t.

6.2.2.11. Reducing power

The reducing power of different *Moringa* leaf or vegetable samples was determined according to the method of Oyaizu (1986) as described by Yen et al. (1993) and, Sidhhuraju and Becker (2003). Lyophilized extracts of each sample (0, 1.0, 2.0, 5.0, 7.5, 10.0 and 15.0 mg) in 1 mL of methanol were mixed with a 0.2 M phosphate buffer (5 mL, pH 6.6) and 1.0% potassium ferricyanide (5.0 mL); the mixture was incubated at 50°C for 20 min. 10% trichloroacetic acid (5 mL) was added to each mixture, which was then centrifuged at 5000 rpm for 10 min. The upper layer of the solution (5.0 mL) was mixed with distilled water (5.0 mL) and 0.1% ferric chloride (1.0 mL), and then the absorbance was read spectrophotometrically at 700 nm. A higher absorbance of the reaction mixture indicated greater reducing power.

6.2.3. Results and discussion

6.2.3.1. Total Phenolics and total flavonoids

Total phenolics (TPC) and total flavonoid contents (TFC) of dried M. *oleifera* leaf samples from two different farms in South Africa are given in Table 6.4 and 6.5, respectively. The *Moringa* leaf samples were compared to selected vegetables as well as to some literature values. The samples from Limpopo farm were collected from trees grown in three different years, that is, 2006, 2009 and 2010. The contents between these were compared in order to rationalize whether the age of the plant has any contribution on the TPC and TFC. However, the trees from Atteridgeville farm were only grown from 2010 because this was a new farm. Nonetheless, the TFC and TPC from *Moringa* flowers from the Limpopo farm were also profiled. No real correlation was observed on the TPC and TFC of the *Moringa* leaves with respect to the age of the plant. This could be due to the fact that there are many factors that influence the contents of these variables in plants other than the age. These factors could be genetic variability, leaf age development and postharvest handling of the leaf samples (Siddhuraju and Becker, 2003).

It was observed that TPC of *Moringa* samples was almost twice that of selected vegetables, whilst TFC of *Moringa* were almost three times more than those of selected vegetables were. These results revealed that *Moringa* has more TPC and TFC than the selected vegetables. It is known that the phenolics and flavonoids are directly linked to the antioxidant properties. Therefore, in this case it can be said that *Moringa* shows higher antioxidant activity than the selected vegetables due to the higher concentrations of TFC and TPC. However, the TPC of the *Moringa* investigated in this study was similar to *Moringa* samples studied by Siddhuraju and Becker (2003), particularly, the samples from India and Niger (Table 6.4). Nonetheless, the TPC of *Moringa* investigated in this study were much less than those of *Moringa* from the Pakistani, Table 6.4, (Iqbal and Bhanger, 2006). A similar trend was observed for the TFC where the *Moringa* in this study was similar to the values reported by Siddhuraju and Becker (2003) but

much less to values reported by Iqbal and Bhanger, (2006). This could further substantiate that the contents of plants are affected by agroclimatic conditions.

Table 6.4a: Total phenolic content (g kg^{-1} dry matter) of different vegetables and *Moringa* plant

Sample	Present study g/kg	Literature g/ 100 g	Literature g/ 100 g	Literature g/ 100 g	Literature g/ 100 g	Literature g/ 100 g	Reference
Vegetables							
Cabbage	11.8 (±6.0)						
Spinach	14.4 (±2.6)						
Peas	10.4 (±7.9)						
Cauliflower	14.7 (±3.9)						
Brocolli	17.6 (±2.9)	1.61-2.36					Cieslik et al., 2006
Moringa leaves							
2006LF	28.7 (±4.0)	4.25±0.14[a]	2.94±0.17[b]	3.66±0.21[c]			Siddhuraju and Becker,2003
2009LF	31.9 (±4.9)	33.82 - 336.95*					Verma et al., 2009
2010LF	30.4 (±5.9)	8.82±0.34[d]	8.99±0.33[e]	12.79±0.29[f]	10.54±0.38[g]	11.94±0.31[h]	Iqbal and Bhanger, 2006
crushed	24.4 (±8.7)	3.0 - 3.5					Kunyanga et al., 2012
2010AF	19.5 (±3.5)						
Moringa flowers	29.7 (±2.9)						

a Nicaragua d Nawabshah g Chakwal
b India e Jamshoro h Balakot
c Niger f Mardaan * India (mg/g)

Table 6.4b: Total flavonoids content (TFC) of different vegetables and *Moringa* plant

Sample	Present study g/kg	Literature g/ 100 g	Literature g/ 100 g	Literature g/ 100 g	Literature g/ 100 g	Literature g/ 100 g	Reference
Vegetables							
Cabbage	9.8 (±6.1)						
Spinach	12.5 (±3.1)						
Peas	6.4 (±5.8)						
Cauliflower	4.6 (±4.4)						
Brocolli	15.7 (±2.2)						
Moringa leaves							
2006LF	33.8 (±5.2)	4.43±0.21[a]	2.10±0.18[b]	3.81±0.25[c]			Siddhuraju and Becker,2003
2009LF	40.8 (±5.2)						
2010LF	24.0 (±5.9)	6.93±0.25[d]	7.38±0.28[e]	12.53±0.28[f]	9.32±0.21[g]	11.90±0.31[h]	Iqbal and Bhanger, 2006
crushed	58.7 (±3.0)						
2010AF	35.8 (±4.4)						
Moringa flowers	36.1 (±2.9)						
a Nicaragua	d Nawabshah	g Chakwal					
b India	e Jamshoro	h Balakot					
c Niger	f Mardaan						

6.2.3.2. Antioxidant activity by DPPH method

Figure 6.8 shows the results obtained from measuring the antioxidant activity using the DPPH assay. What is measured in this method is the scavenging activity of phenolic extracts of different selected vegetables and *Moringa* leaves obtained from different farms in South Africa. DPPH is a free radical generation system and so in this case the ability of the various solvent extracts to scavenge these free radials is monitored. The lesser the concentration of DPPH free radicals in solution the higher is the ability of that particular extract to scavenge free radicals. In the results shown in Figure 6.8 it can be observed that the order in which high concentration of DPPH radicals remained after 120 min is peas ≥ cabbage > cauliflower ≥ spinach > broccoli >> 2010AF > 2006LF > 2010LF > 2009LF > *Moringa* flower > powdered *Moringa*. From this conclusions can be drawn that *Moringa* samples showed high scavenging activity that the selected vegetables.

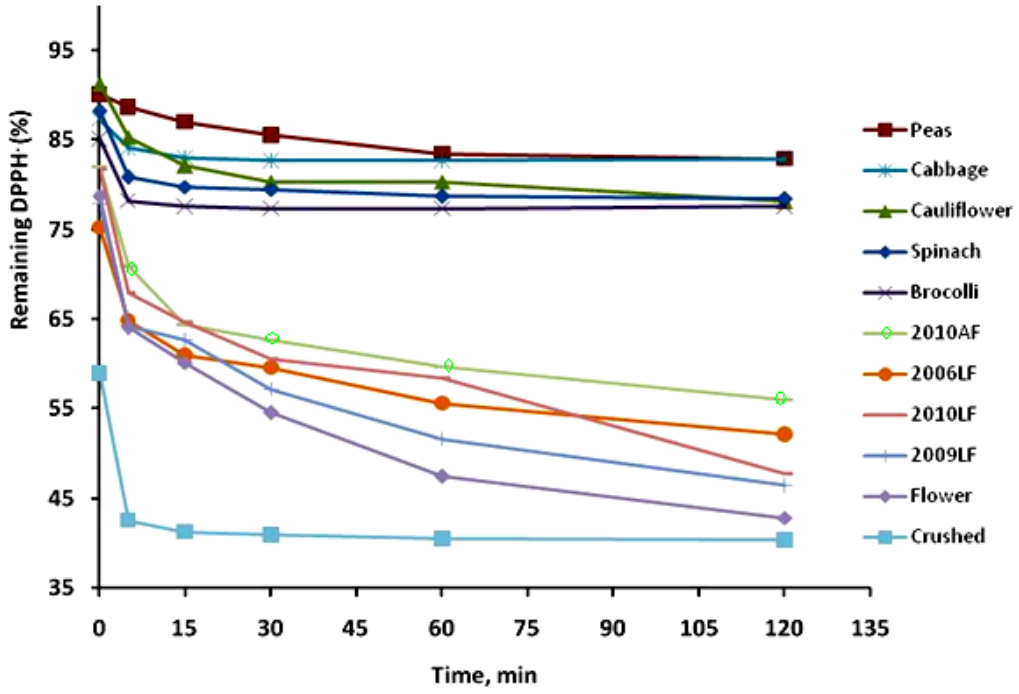

Figure 6.8. Percentage DPPH· radicals remaining after 120 min of incubation of undiluted methanol extracts.

Table 6.5: Percentage DPPH$^{\cdot}$ Radicals remaining after 60 min of incubation of three different concentration

Sample	Undilute MeOH extract (%)	1:2 dilution, (%)	1:4 dilution, (%)
Vegetables			
Cabbage	82.7 (±0.1)	90.0 (±3.2)	98.7 (±0.7)
Spinach	78.5 (±0.5)	90.1 (±0.6)	97.4 (±1.2)
Peas	83.5 (±1.7)	93.5 (±2.5)	95.3 (±1.6)
Cauliflower	79.6 (±0.8)	80.4 (±2.8)	97.9 (±1.5)
Brocolli	71.4 (±1.1)	88.7 (±2.3)	96.3 (±1.1)
Moringa leaves			
2006LF	55.6 (±4.1)	51.2(±3.0)	89.6 (±1.0)
2009LF	51.6 (±15.2)	42.3 (±2.5)	88.2 (±1.4)
2010LF	58.4 (±1.0)	50.5 (±5.8)	89.9 (±0.4)
crushed	40.4 (±1.2)	38.2 (±6.2)	64.4 (±2.1)
2010AF	59.8 (±1.7)	62.7 (±1.1)	88.8 (±2.1)
Moringa flowers	47.5 (±12.5)	41.7 (±3.6)	83.4 (±1.7)

6.2.3.3. Reducing power of different solvent extracts from Moringa leaves

The reducing power of the extracts was measured by the ability of the extracts to put forth electrons in order to facilitate the reduction of the ferric ion to ferrous ion and the results are depicted in Figure 6.9. Different concentration of sample extracts were charged with solutions containing the Fe^{3+} ions and the absorbance was monitored at 700 nm. This absorbance was actually the concentration of Fe^{2+} ions in solution. So the higher was this absorbance the higher is the concentration of Fe^{2+} and the higher is the ability of that particular extract to donate electrons which implies higher reducing power. The higher the reducing power, the higher is the antioxidant activity as it has been reported that the reducing power of bioactive compounds was related to the antioxidant activity (Yen and Duh (1993) and Siddhuraju et al. (2002). However, *Moringa* extracts had higher reducing power than the vegetable samples. The order of samples ranked from lowest to highest reducing power is as follows, peas < cabbage < spinach < broccoli < cauliflower < 2010AF < 2006LF < 2010AF 2009LF < *Moringa* powder <

Moringa flower. The order is very much the same with the results obtained from the DPPH studies except that *Moringa* flower and *Moringa* powder have exchange places as well as cauliflower and spinach have also exchanged positions. In both results peas and cabbage showed the lowest antioxidant activity. Similarly, TFC and TPC results were also in good agreement with the DPPH and reducing power results in showing that *Moringa* samples have a higher antioxidant activity than vegetable samples. It could be said that the amount of phenolics is related with the reducing power and the DPPH method (Siddhuraju and Becker, 2003).

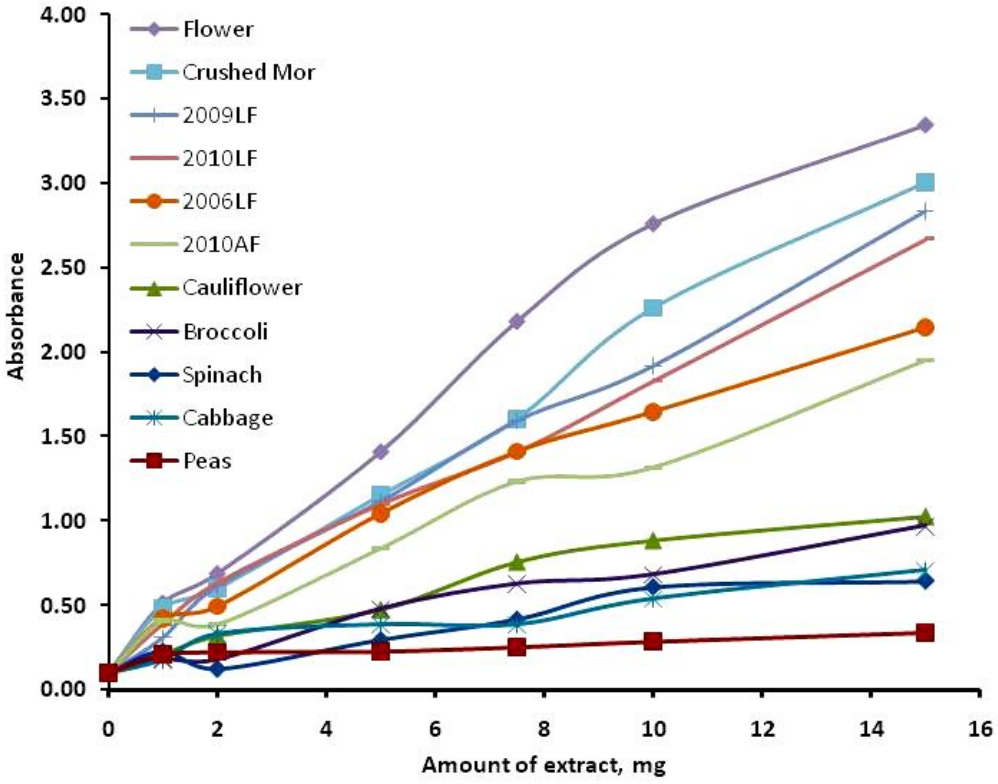

Figure 6.9: Reducing power of different *Moringa* extracts and vegetable extracts.

Chapter 7: Conclusions and recommendations

7.1. Conclusions

This study demonstrated successful preparation of three imprinted polymers for trapping three analytes individually, that is, chromium (VI), uranium (VI) and quercetin. These imprinted polymers were successfully applied for the selective extraction of the respective analytes from various complex samples. Chromium (VI) imprinted polymer was prepared *via* quaternization of linear vinylpyridine copolymer and dichromate salt as template. Several parameters like effect of pH, amount of sorbent, concentration *etc*. were optimized for all polymers. The optimized polymer showed potential as sorbent for the extraction of chromium from aqueous samples. However, the presence of higher amounts of sulphates seemed to affect the polymer selectivity and loading capacity. This is due to cross-reactivity of polymer sites with sulphate anion.

Uranyl ion imprinted polymer prepared in the study also showed good selectivity for uranium against competing ions. When the polymer was applied on wastewater samples, good recoveries of uranium were obtained, *i.e.* 85%. This demonstrated that the prepared polymer could be potentially applied for removal of uranyl ion from such matrix. Also, the higher loading capacity (120 mg g^{-1}) demonstrated by the polymer could allow for longer exposure to the environment as normally the concentrations of uranium in the environment are quite low.

Quercetin imprinted polymers were successfully prepared, optimized and used for selective recovery of quercetin from onion and *Moringa* extracts. Again, the polymer demonstrated high specificity for quercetin from aqueous onion extracts and from methanolic *Moringa* extracts. Solid liquid extraction was used in the form of batch (onion) and cartridge (*Moringa*). However, kaempferol was also co-extracted with quercetin from *Moringa* samples. This was understandable due to

similarities of quercetin and kaempferol, since it is well known that MIPs can extract a group of structurally related compounds as was demonstrated by the examples of triazines (Cacho et al., 2006; Carabias-Martinez et al., 2005; Chapuis et al., 2004). Recoveries of no less than 83% were obtained for quercetin extraction from *Moringa* extracts.

In concluding, all the polymers prepared in this study shown high efficiency in terms of extraction of their respective template, hence implying successful fabrication and optimization of such polymers.

The concentrations of the metals from the soils were in the range of those published as maximum allowable concentration in Germany, Canada and UK. This implies that the soils from which the *Moringa* trees are being grown in South Africa are not polluted by heavy metals and as such the *Moringa* grown there is fit for consumption. Also, the *Moringa* plant was found to not accumulating the metals on its leaves. On average *Moringa* leaves contained more mineral nutrients than the vegetables compared with (Figure 6.1.5 and 6.1.7). *Moringa* leaves also showed to contain substantial amount of flavonols hence justifying its use as a natural supplement for antioxidants (Table 6.1.2).

Moringa leaves showed to contain almost twice the amount of TPC of vegetables and 3-fold more TFC than vegetables. Reducing power, DPPH radical scavenging ability of *Moringa* leaves were much higher than those of vegetables. This proved that *Moringa* is a good antioxidant source than common vegetables. Also, it was shown that *Moringa* grown in South Africa contain almost similar TPC as *Moringa* from Niger and India (Siddhuraju and Becker, 2003) but much less than *Moringa* from Pakistan (Iqbal and Bhanger, 2006). These differences are attributed, among other things, to agroclimatic conditions. Nonetheless, the antioxidant activity results shown from other methods proved that *Moringa* studied is as good as those from other countries. Meaning that the South African agroclimatic conditions did not impact the *Moringa* that much.

7.2. Recommendations

- ***The future work emanating from this study, include studying of MIP fundamentals at high temperature and also application of MIPs on PHWE online extraction of quercetin from various plant materials.***

Part of the future work emanating from this study include studying of MIP fundamentals at high temperature as well as application of such MIPs at high temperature. What stimulated this research is that the authors plan to use MIPs for selective extraction of high value compounds from plant materials following the total extraction of such plant materials using "green" extraction technologies such as PHWE, PLE, or ASE. These "green" technologies are known to employ water at elevated temperature and pressure. Therefore, it is very important to do MIP fundamental studies first before these polymers can be applied. Currently, in MIP literature not many studies have focussed on the use of MIPs at high temperature particularly in pure aqueous environments. A study by Theodoridis et al., (2006) dealt with using MIPs at 60°C. In their case MIP was packed in a minicolumn, a mobile phase consisting of methanol-water ratios was pumped through the column, and adsorption capacity of the MIPs was monitored at various temperatures, *i.e.*, 25 and 60°C. The authors noticed a decrease in retention of quercetin and rutin at 60°C and the reasons for this decrease were not discussed. This further implies that higher temperature studies in MIP are still necessary.

In the presents study, the authors plan to study the effect of change of adsorption time, change in pH, change in concentration, change in sorbent dosage *etc*., might have on MIPs adsorption capacity at high temperature (84°C).

- ***Improving the retention and selectivity of chromium (VI) IIP by using other functional ligands during preparation of IIPs.***

In the present study, it was noted that the selectivity of the prepared Cr (VI) IIP was greatly influenced by the presence of other anions such as SO_4^{2-}. However, it should be noted that Bayramoglu and Arica (2011) prepared Cr (VI) IIP using 4-

vinylpyridine and HEMA as functional monomers. Competitive adsorption was only done between Cr (VI) and Cr (III) or Cr (VI) and Ni^{2+}. Both Cr (III) and NI (II) are cations and their effect on MIP might be less than say SO_4^{2-} or PO_4^{3-}. Therefore, from this one might see that Cr (VI) IIPs which are selective in the presence of anions are still necessary to be found. Several functional ligands which can form strong bonds with Cr (VI) will be investigated. The investigation will include making MIPs using different functional monomers and different polymerization methods. The shape and size of anions is different to cations therefore it could be more interesting to test the selectivity and efficiency of prepared MIPs using anions such as SO_4^{2-}, PO_4^{3-}, NO_3^- *etc* rather than cations.

- ***Use of other methods for preparation of ion imprinted polymers; these include use of magnetite to ease with separation of sorbent after extraction. Separation in this case is usually effected by using external magnet, meaning that the filtration step will be eliminated.***

Preparation of magnetic imprinted polymers is one of the recent advances in the imprinting technology field. An example is shown in Figure 7.1.

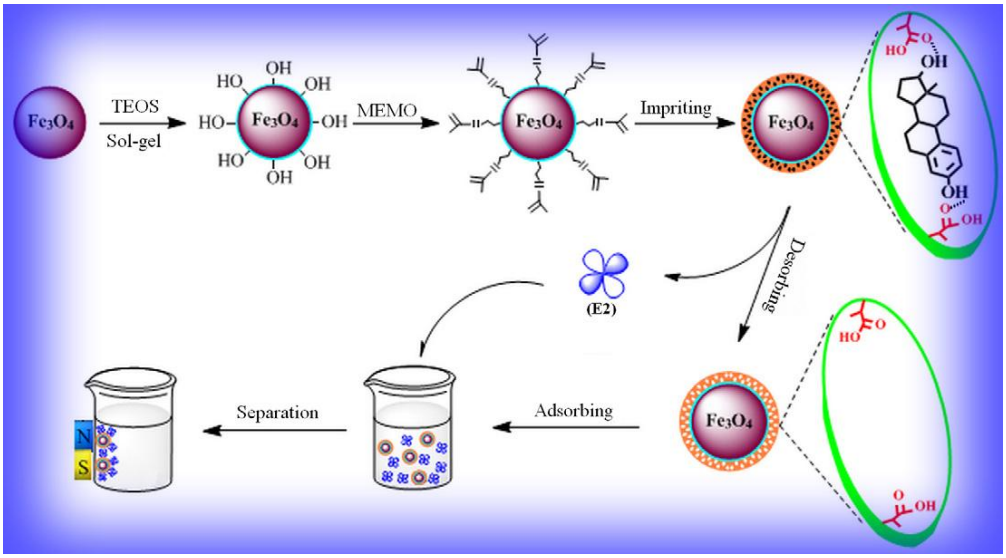

Figure 7.1: Use of external magnet for removal of magnetic imprinted 17-β-estradiol (Wang et al., 2011).

This method has been said to have numerous advantages over the traditional imprinting approaches. In the traditional imprinting approaches the binding sites are imbedded deep within the polymer matrix and as such, some binding sites become inaccessible during rebinding of the template due to highly cross-linked nature of such polymers. In contrast, using magnetic particles (Fe_3O_4) allows the binding sites to be imprinted on the surface or near the proximity of the surface. This is because during the use of this method, Fe_3O_4 particles are normally coated with the material that contains active sites for the template. Magnetic imprinted polymers are more ideal for scale up purposes for use in removal of pollutants by industries as application of external magnet instead of filtration for traditional imprinting approaches. Below is a schematic representation diagram showing how magnetic MIPs are prepared (Wang et al., 2011). Literature have reported successful preparation of magnetic polymers for Cr (VI) (Webster et al., 2007) and UO_2^{2+} (Zhou et al., 2011) using chitosan as a chelating polymer. The future study might look at using other natural polymers or synthetic functional monomers. However, in the case of Cr (VI) it should be noted that although the literature have reported several magnetic polymers using different polymers for chelation, however, no imprinting was used. Therefore, to improve selectivity one might look at imprinting.

List of conference and seminar presentations

1. Pakade V., Cukrowska E., Darkwa J., Torto N., Chimuka L. Simple and efficient ion imprinted polymers for recovery of uranyl ion and chromium (VI) from environmental samples, 15th International Conference of Heavy Metals in the Environment, ICHMET2010, 19th-23rd September, Gdańsk Poland, *poster presentation.*

2. Pakade V., Lindahl S., Chimuka L., Turner C. Pre-concentration and clean-up of quercetin from yellow onion extract using molecularly imprinted polymers, SACI2011, 16th-21st January. University of the Witwatersrand, Johannesburg, South Africa, *poster presentation.*

3. Pakade V., Lindahl S., Cukrowska E., Turner C., Darkwa J., Torto N., Chimuka L. Novel imprinted polymers for selective extraction of metal ions and organic compounds from wastewater and waste plant materials, Analitika2010, 5th – 9th December. University of Stellenbosch, Cape Town, South Africa, *poster presentation.*

4. Pakade V., Cukrowska E., Chimuka L. Flavonols (myricetin, quercetin, kaempferol) contents and antioxidant properties of selected vegetables and *Moringa oleifera*, ChromSA Students Chromatographer Seminars2011, 22nd September. University of Pretoria, Pretoria, South Africa, *oral presentation.*

5. Pakade V.E., Cukrowska E.M., Darkwa J., Darko G., Torto N., L. Chimuka, Simple and efficient ion imprinted polymer for recovery of uranium from environmental samples, 2nd Regional Conference of the Southern African young water professionals 2011, 3rd-5th July. CSIR International Convention Centre, Pretoria, South Africa, *poster presentation.*

6. Pakade V.E., Cukrowska E., Chimuka L. Synthesis and application of molecular imprinting on extraction of quercetin from plant materials and studies on *Moringa* plant, Students PhD Seminars 2011, 21st September. University of the Witwatersrand, Johannesburg, South Africa, *oral presentation.*

List of publications emanating from the study

1. **Pakade, V.,** Cukrowska, E., Darkwa, J., Torto, N., Chimuka, L. (2011), Selective removal of chromium (VI) from sulphates and other metal anions using an ion-imprinted polymer, *Water SA*, 37(4), pp. 529-537. (Appendix I)

2. **V. E. Pakade,** E. M. Cukrowska, J. Darkwa, G. Darko, N. Torto and L. Chimuka, (2012), Simple and efficient ion imprinted polymer for recovery of uranium from environmental samples, *Water Science and Technology*, 65.4, pp. 728-736. (Appendix II)

3. **Vusumzi Pakade,** Sofia Lindahl, Luke Chimuka, Charlotta Turner, (2012), Molecularly imprinted polymers targeting quercetin in high-temperature aqueous solutions, *Journal of Chromatography A* 1230, pp. 15– 23. (Appendix III)

4. **Vusumzi Pakade,** Ewa Cukrowska, Luke Chimuka, Metal and flavonol contents from *Moringa oleifera* grown in various regions of South Africa, *South African Journal of Science* (submitted – revision stage).

5. **Vusumzi Pakade,** Ewa Cukrowska, Sofia Lindahl, Charlotta Turner and Luke Chimuka, Molecular imprinted polymer for solid-phase extraction of flavonol aglycones from *Moringa oleifera* leaf extracts, *Journal of Separation Science* (manuscript in preparation).

Other publications during the course of study

1. Vrana, B., Tolgyessy, P., Silharova, K., Krascsenits, Z., **Pakade, V.E.,** Chimuka, L. (2011), Validation of passive sampling devices for organic priority pollutants in surface waters, *Vodohospodarsky spravodajca*, 54, pp. 30-34 (in Slovak).

2. Idahosa, K.C., Molefe, D.M., **Pakade, V.E**., Brown, M.E., Kaye, P.T. (2011), Elucidation of the complex Baylis-Hillman reaction of 3-methoxy-2-nitrobenzaldehyde with methyl vinyl ketone, *South African Journal of Chemistry*, 64, pp. 144-150.

References

Acar, F.N., Malkoc, E. (2004), The removal of chromium (VI) from aqueous solutions by *Fagus orientalis L*., *Bioresour. Technol.,* 94, pp. 13-15.

Adriano D.C. (1998), Trace elements in the terrestrial environment, New York, Springer-Verlag.

Ahmadi, S.J., Noori-Kalkhoran, O., Shirvani-Arani, S. (2010), Synthesis and characterization of new ion-imprinted polymer for separation and pre-concentration of uranyl (UO(2)(2+)) ions, *J. Hazard. Mater.,* 175, pp. 193-197.

Albo, Y., Saphier, M., Maimon, E., Zilbermann, I., Meyerstein, D. (2009), A new chelate ligand designed for the uranyl ion, *Coord. Chem. Rev.,* 153(15-16), pp. 2049-2055.

Alexander, C., Andersson, H.S., Andersson, L.I., Ansell, R.J., Kirsch, N., Nicholls, I.A., O'Mahony, J., Whitcombe, M.J. (2006), Molecular imprinting science and technology: a survey of the literature for the years up to and including 2003, *J. Mol. Recognit*., 19, pp. 106–180.

Allender, C.J. (2005), Molecularly imprinted polymers: technology and applications – Preface, *Adv. Drug Delivery Rev.,* 57(12), pp. 1731-1732.

Ames, B.N., Shigenga, M.K., Hagen, T.M. (1993), Oxidants, antioxidants and degenerative diseases of aging. Proceedings of the National Academy of Sciences of the United States of America, 90, pp. 7915–7922.

An, F., Gao, B. (2009), Adsorption characteristics of Cr (III) ionic imprinting polyamine on silica gel surface, *Desalination*, 249, pp. 1390–1396.

An, Z., Shi, Q., Tang, W., Tsung, C., Hawker, C.J., Stucky, G.D. (2007), Facile RAFT precipitation polymerization for the microwave-assisted synthesis of well-defined, double hydrophilic block copolymers and nanostructured hydrogels, *J. Am. Chem. Soc*., 129, pp. 14493–14499.

Andersson, L.I., Müller, R., Vlatakis, G., Mosbach, K. (1995), Mimics of the binding sites of opioid receptors obtained by molecular imprinting of enkephalin and morphine, *Proc. Natl. Acad. Sci*. U.S.A., 92, pp. 4788-4792**.**

Anirudhan, T.S., Divya, L., Suchithra, P.S. (2009), Kinetic and equilibrium characterization of uranium (VI) adsorption onto carboxylate-functionalized

poly(hydroxyethylmethacrylate)-grafted lignocellulosics, *J. Environ. Manage.*, 90, pp. 549-560.

Anirudhan, T.S., Radhakrishnan, P.G. (2009), Improved performance of a biomaterial-based cation exchanger for the adsorption of uranium (VI) from water and nuclear industry wastewater, *J. Environ. Radioact.*, 100, pp. 250-257.

Ansell, R.J., Wang, D. (2009), Imprinted polymers for chiral resolution of (+/-)-ephedrine. Part 3: NMR predictions and HPLC results with alternative functional monomers, *Analyst*, 134, pp. 564–576.

Anupam, K., Duttab, S., Bhattacharjee, C., Datta, S. (2011), Adsorptive removal of chromium (VI) from aqueous solution over powdered activated carbon: Optimisation through response surface methodology, *Chem. Eng. J.*, 173, pp. 135– 143

Anwar, F., Ashraf, M., Bhanger, M.I. (2005), Interprovenance variation in the composition of *Moringa oleifera* from Pakistan, *J. Am. Oil Chemists Soc.*, 82, pp. 45-51.

Anwar, F., Latif, S., Ashraf, M., Gilani, A.H. (2007), *Moringa oleifera*: A food plant with multiple medicinal uses, *Phytother. Res.*, 21, pp. 17–25.

Arabzadeh, N., Abdouss, M. (2010), Synthesis and characterization of molecularly imprinted polymers for selective solid-phase extraction of pseudoephedrine, *Colloid J.*, 72(4), pp. 446–455.

Araki, K., Maruyama, T., Kamiya, N., Goto, M. (2005), Metal ion-selective membrane prepared by surface molecular imprinting, *J. Chromatogr. B*, 818, pp. 141–145.

Arshad, N., Janjua, N.K., Ahmed, S., Khan, A.Y., Skibsted, L.H. (2009), Electrochemical investigations of antioxidant interactions with radical anion and dianion of 1,3-dinitrobenzene, *Electrochim. Acta*., 54(26), pp. 6184-6189.

Arshady, R., Mosbach, K. (1981), Synthesis of substrate-selective polymers by host-guest polymerization, *Makromol. Chem*., 182, pp. 687-692.

Atieh, M.A. (2011), Removal of Chromium (VI) from polluted water using carbon nanotubes supported with activated carbon, *Proc. Environ. Sci.*, 4, pp. 281–293.

Aydin, Y.A., Aksoy, N.D. (2009), Adsorption of chromium on chitosan: Optimization, kinetics and thermodynamics, *Chem. Eng. J.*, 151, pp. 188–194.

Azenha, M., Kathirvel, P., Nogueira, P., Fernando-Silva, A. (2008), The requisite level of theory for the computational design of molecularly imprinted silica xerogels, *Biosens. Bioelectron.*, 23, pp. 1843–1849.

Azodi-Deilami, S., Abdouss, M., Seyedi, S.R. (2010), Synthesis and characterization of molecularly imprinted polymer for controlled release of tramadol, *Cent. Eur. J. Chem.*, 8(3), pp. 687-695.

Bae, S.Y., Southard, G.L., Murray, G.M. (1999), Molecularly imprinted ion exchange resin for purification preconcentration and determination of UO_2^{2+} by spectrophotometry and plasma spectrometry, *Anal. Chim. Acta*, 397, pp. 173-181.

Baggiani, **C.,** Giraudi, G., Giovannoli, C., Tozzi, C., Anfossi, L. (2004), Adsorption isotherms of a molecular imprinted polymer prepared in the presence of a polymerizable template - Indirect evidence of the formation of template clusters in the binding site, *Anal. Chim. Acta*, 504, pp. 43-52.

Bajpai, **M.,** Pande, A., Tewari, S.K., Prakash, D. (2005), Phenolic contents and antioxidant activity of some food and medicinal plants, *Int. J. Food Sci. Nutr.*, 56, pp. 287–291.

Banks, **M.K.,** Schwab, A.P., Henderson, C. (2006), Leaching and reduction of chromium in soil as affected by soil organic content and plants, *Chemosphere*, 62, pp. 255–264.

Barahona, F., Turiel, E., Cormack, P.A.G. (2011), Synthesis of core-shell molecularly imprinted polymer microspheres by precipitation polymerization for the inline molecularly imprinted solid-phase extraction of thiabendazole from citrus fruits and orange juice samples, *J. Sep. Sci.*, 34, pp. 217-224.

Bartlett, **R.J.,** Kimble, J.M. (1976), Behavior of chromium in soils. II. Hexavalent forms, *J. Environ. Qual.* 5, pp. 383–386.

Bartsch, **R.A.,** Maeda, M. (1998), Molecular and ionic recognition with imprinted polymers, American Chemical Society, Washington, DC.

Batlokwa, B.S., Mokgadi, J., Nyokong, T., Torto, N. (2011), Optimal template removal from molecularly imprinted polymers by pressurized hot water extraction, *Chromatographia*, 73, pp. 589–593.

Bayramoglu, G., Yakup Arica, M. (2011), Synthesis of Cr (VI)-imprinted poly(4-vinyl pyridine-co-hydroxyethyl methacrylate) particles: Its adsorption propensity to Cr (VI), *J. Hazard. Mater*., 187, pp. 213–221.

Becke, A.D. (1993), Density-functional thermochemistry.3. The role of exact exchange, *J. Chem. Phys.*, 98, pp. 5648-5652.

Beek, T.A., Tetala, K.K.R., Koleva, I.I., Dapkevicius, A., Exarchou, V., Jeurissen, S.M.F., Claassen, F.W., Klift E.J.C. (2009), Recent developments in the rapid analysis of plants and tracking their bioactive constituents, *Phytochem. Rev*., 8, pp. 387-399.

Beltran, A., Caro, E., Marcé, R.M., Cormack, P.A.G., Sherrington, D.C., Borrull, F. (2007), Synthesis and application of a carbamazepine-imprinted polymer for solid-phase extraction from urine and wastewater, *Anal. Chim. Acta*, 597, pp. 6-11.

Beltran, A., Borrull, F., Cormack, P.A.G., Marcé, R.M. (2010), Molecularly-imprinted polymers: useful sorbents for selective extractions, *Trends Anal. Chem*., 29(11), pp. 1363–1375.

Beltran, A., Marcé, R.M., Cormack, P.A.G., Borrull, F. (2009), Synthesis by precipitation polymerization of molecularly imprinted polymer microspheres for the selective extraction of carbamazepine and oxcarbazepine from human urine, *J. Chromatogr. A,* 1216, pp. 2248-2253.

Benhammou, A., Yaacoubi, A., Nibou, L., Tanouti B. (2007), Chromium (VI) adsorption from aqueous solution onto Moroccan Al-pillared and cationic surfactant stevensite, *J. Hazard. Mater*. 140, pp. 104-109.

Bennett, R.N., Rosa, E.A.S., Mellon, F.A., Kroon, P.A. (2006), Ontogenic profiling of glucosinolates, phenolics, flavonoids and other secondary metabolites in Eruca sativa (salad rocket), Diplotaxis erucoides (wall rocket), Diplotaxis tenuifolia (wild rocket), and Bunias orientalis (Turkish rocket), *J. Agric. Food Chem*., 54, pp. 4005–4015.

Berggren, C., Bayoudh, S., Sherrington, D., Ensing, K. (2000), Use of molecularly imprinted solid-phase extraction for the selective clean-up of clenbuterol from calf urine, *J. Chromatogr., A,* ,889, pp. 105–110.

Bhattacharyya, **A.,** Mohapatra, P.K., Gadly, T., Raut, D.R., Ghosh, S.K., Manchanda, V.K. (2011), Liquid-liquid extraction and flat sheet supported liquid membrane studies on Am (III) and Eu (III) separation using 2,6-bis(5,6-dipropyl-1,2,4-triazin-3-yl)pyridine as the extractant, *J. Hazard. Mater.*, 195, pp. 238-44.

Bhuptawat, **H.,** Folkard, G.K., Chaudhari, S. (2007), Innovative physic-chemical treatment of wastewater incorporating *Moringa* oleifera seed coagulant, *J. Hazard. Mater.*, 142, pp. 477–482.

Bianchi, F., Mangia, A., Mattarozzi, M., Musci, M. (2011), Characterization of the volatile profile of thistle honey using headspace solid-phase microextraction and gas chromatography–mass spectrometry, *Food Chem.*, 129(3), pp. 1030-1036.

Bielicka-Daszkiewicz, K., Voelkel, A. (2009), Theoretical and experimental methods of determination of the breakthrough volume of SPE sorbents, *Talanta*, 80(2), pp. 614-621.

Biesaga, M., Pyrzynska, K. (2009), Analytical procedures for determination of quercetin and its glycosides in plant material, *Crit. Rev. Anal. Chem.*, 39(2), pp. 95-107.

Biju, V.M., Gladis, J.M., Prasada Rao, T. (2003a), Ion imprinted polymer particles: synthesis, characterization and dysprosium ion uptake properties suitable for analytical applications, *Anal. Chim. Acta*, 478, pp. 43–51.

Biju, V.M., Gladis, J.M., Prasada Rao, T. (2003b), Effect of gamma-irradiation of ion imprinted polymer (IIP) particles for the preconcentrative separation of dysprosium from other selected lanthanides, *Talanta*, 60, pp. 747–754.

Birlik, E., Ersöz, A., Açykkalp, E., Denizli, A., Say, R. (2007), Cr (III)-imprinted polymeric beads: Sorption and preconcentration studies, *J. Hazard. Mater*., B140, pp. 110–116.

Bonaccorsi, **P.,** Caristi, C., Gargiulli, C., Leuzzi, U. (2005), Flavonol glucoside profile of southern Italian red onion (*Allium cepa L.*), *J. Agric. Food Chem.*, 53, pp. 2733–2740.

Boonchum, W., Peerapornpisal, Y. Vacharapiyasophon, P. Pekkoh, J. Pumas, C. Jamjai, U., Amornlerdpison, D., Noiraksar, T., Kanjanapothi, D. (2011), Antioxidant activity of some seaweed from the gulf of Thailand, *Int. J. Agric. Biol.*, 13, pp. 95-99.

Borges, **F.,** Guimaraẽs, C., Lima, J.L.F.C., Pinto, I., Reis, S. (2005), Potentiometric studies on the complexation of copper (II) by phenolic acids as discrete ligand models of humic substances, *Talanta*, 66, pp. 670–673.

Boss, C.B., Fredeen, K.J. (1997), "Concepts, Instrumentation and Techniques in Inductively Coupled Plasma Optical Emission Spectrometry", 2nd edition, 1997 by The Perkin-Elmer Corporation.

Bossi, A., Piletsky, S.A., Piletska, E.V., Righetti, P.G., Turner, A.P.F. (2001), Surface-grafted molecularly imprinted polymers for protein recognition, *Anal. Chem.*, 73, pp. 5281–5286.

Boularbah, A., Schwartz, C., Bitton, G., Aboudrar, W., Ouhammou, A., Morel, J.L. (2006), Heavy metal contamination from mining sites in South Morocco: 2. Assessment of metal accumulation and toxicity in plants, *Chemosphere*, 63, pp. 811–817.

Brand-Williams, W., Cuvelier, M.E., Berset, C. (1995), Use of a free radical method to evaluate antioxidant activity, *Lebensm. Wiss. Technol.*, 28, pp. 25-30.

Bratkowska, **D.,** Marce, R.M., Cormack, P.A.G., Borrull, F., Fontanals, N. (2011), Development and application of a polar coating for stir bar sorptive extraction of emerging pollutants from environmental water samples, *Anal. Chim. Acta*, 706(1), pp. 135-42.

Bravo, L. (1998), Polyphenols: chemistry, dietary sources, metabolism and nutritional significance, *Nutr. Rev.*, 56, pp. 317-333.

Breton, F., Rouillon, R., Piletska, E.V., Karim, K., Guerreiro, A., Chianella, I., Piletsky, S. A. (2007), Virtual imprinting as a tool to design efficient MIPs for photosynthesis-inhibiting herbicides, *Biosens. Bioelectron.*, 22, pp. 1948–1954.

Britannica encyclopedia, http://www.britannica.com/EBchecked/topic/624185/Nicolas-Louis-Vauquelin, accessed 18 February 2011.

Britton, H.T.S. (1965), Hydrogen ions, 4th ed, Chapmen and Hill, London.

Brookins, D.G. (1988), Eh-pH diagrams for Geochemistry, Springer-Verlag, Berlin-Heidelberg-New York.

Brower, J.B., Ryan, R.L., Pazirandeh, M. (1997), Comparison of ion-exchange resins and biosorbents for the removal of heavy metals from plating factory wastewater, *Environ. Sci. Technol.*, 31(10), pp. 2910-2914.

Brunauer, **S.,** Emmett, P.H., Teller, E. (1938), Adsorption of gases in multimolecular layers, *J. Am. Chem. Soc., 60,* pp. 309-319.

Byun, H.–S., Youn, Y.–N., Yun, Y.–H., Yoon, S.–D. (2010), Selective separation of aspirin using molecularly imprinted polymers, *Sep. Purif. Technol.,* 74, pp. 144-153.

Caceres, A., Saravia, A., Rizzo, S., Zabala, L., Leon, E.D., Nave, F. (1992), Pharmacologic properties of *Moringa oleifera*: 2: Screening for antispasmodic, anti-inflammatory and diuretic activity, *J. Ethnopharmacol.,* 36, pp. 233–237.

Cacho, C., Turiel, E., Martın-Esteban, A., Ayala, D., Perez-Conde, C. (2006), Semi-covalent imprinted polymer using propazine methacrylate as template molecule for the clean-up of triazines in soil and vegetable samples, *J. Chromatogr. A,* 1114, pp. 255–262.

Cacho, C., Turiel, E., Pérez-Conde, C. (2009), Molecularly imprinted polymers: An analytical tool for the determination of benzimidazole compounds in water samples, *Talanta*, 78, pp. 1029–1035.

Camel, V. (2003), Solid phase extraction of trace elements, *Spectrochim. Acta Part B*, 58(7), pp. 1177-1233.

Campitelli, **P.A.,** Velasco, M.I., Ceppi, S.B. (2006), Chemical and physicochemical characteristics of Humic acids extracted from compost, soil and amended soil, *Talanta*, 69, pp. 1234–1239.

Candan, N., Tüzmen, N., Andac, M., Andac, C.A., Say, R., Denizli, A. (2009), Cadmium removal out of human plasma using ion-imprinted beads in a magnetic column, *Mater. Sci. Eng. C,* 29, pp. 144-152.

Cannon, F.S., Parette, R.B., Na, C, Chen, W., Hagerup, B. (2005), A method for perchlorate removal from ground water. *US Patent 6881348*.

Carabias-Martínez, R., Rodríguez-Gonzalo, E., Herrero-Hernández, E. (2005), Determination of triazines and dealkylated and hydroxylated metabolites in river water using a propazine-imprinted polymer, *J. Chromatogr. A*, ,1085, pp. 199–206.

Caro, E., Marcé, R.M., Cormack, P.A.G., Sherrington, D.C., Borrull, F. (2006), Novel enrofloxacin imprinted polymer applied to the solid-phase extraction of

fluorinated quinolones from urine and tissue samples, *Anal. Chim. Acta,* 562, pp. 145–151.

Caro, E., Masque, N., Marcé, R.M, Borrull, F., Cormack, P.A.G., Sherrington, D.C, (2002), Non-covalent and semi-covalent molecularly imprinted polymers for selective on-line solid-phase extraction of 4-nitrophenol from water samples, *J. Chromatogr. A,* 963, pp. 169–178.

Chakraborty, S., Kumar, P.A. (2009), Fixed-bed column study for hexavalent chromium removal and recovery by short-chain polyaniline synthesized on jute fiber, *J. Hazard. Mater*. 162, pp. 1086-1098.

Chandrasekaran, K., Karunasagar, D., Arunachalam, J. (2011), Dispersive liquid–liquid micro extraction of uranium (VI) from groundwater and seawater samples and determination by inductively coupled plasma–optical emission spectrometry and flow injection–inductively coupled plasma mass spectrometry, *Anal. Methods*, 3, pp. 2140-2147

Chang, X.J., Jiang, N., Zheng, H., He, Q., Hu, Z., Zhai, Y.H., Cui, Y.M. (2007), Solid-phase extraction of iron(III) with an ion- imprinted functionalized silica gel sorbent prepared by a surface imprinting technique, *Talanta*, 71, pp. 38-43.

Chapuis, F., Pichon, V., Lanza, F., Sellergren, B., Hennion, M.-C. (2004), Retention mechanism of analytes in the solid-phase extraction process using molecularly imprinted polymers Application to the extraction of triazines from complex matrices, *J. Chromatogr. B,* 804, pp. 93–101.

Chemicool, http://www.chemicool.com/definition/fourier_transform_infrared_spectrometer_ftir.htm, accessed 21 September 2011.

Chen, L., Xua, S., Li, J. (2010), Recent advances in molecular imprinting technology: current status, *Chem. Soc. Rev.,* 40, pp. 2922-2942.

Chianella, I., Karim, K., Piletska, E.V., Preston, C., Piletsky, S.A. (2006), Computational design and synthesis of molecularly imprinted polymers with high binding capacity for pharmaceutical applications-model case: Adsorbent for abacavir, *Anal. Chim. Acta*, 559, pp. 73-78.

Cieślik, E., Anna Gręda, A., Adamus, W. (2006), Contents of polyphenols in fruit and vegetables, *Food Chem.,* 94, pp. 135–142.

Clark, J. (2007), http://www.chemguide.co.uk/analysis/chromatography/hplc.html, accessed 01 May 2011.

Claude, B., Morin, P., Lafosse, M., Belmont, A., Haupt, K. (2008), Selective solid-phase extraction of a triterpene acid from a plant extract by molecularly imprinted polymer, *Talanta*, 75(2), pp. 344-350.

Co, M., Zettersten, C., Nyholm, L., Sjöberg, Per J.R., Turner, C. (2012), Degradation effects in the extraction of antioxidants from birch bark using water at elevated temperature and pressure, *Anal. Chim. Acta*, 716, pp. 40– 48.

Cook, J.D., Dassenko, S.A., Lynch, S.R. (1991), Assessment of the role of nonheme-iron availability in iron balance, *Am. J. Clin. Nutr.*, 54, pp. 717–722.

Cotton, S. (2010), Lanthanide and actinide chemistry. John Wiley and Sons. ISBN 0470010061. Retrieved 2010-02-07. 2006.

Courtois, J., Fischer, G., Schauff, S., Albert, K., Irgum, K. (2006). Interactions of bupivacaine with a molecularly imprinted polymer in a monolithic format studied by NMR, *Anal. Chem.*, 78, pp. 580–584.

Covelo, E.F., Vega, F.A., Andrade, M.L. (2007), Competitive sorption and desorption of heavy metals by individual soil components, *J. Hazard. Mater.*, 140, pp. 308-315.

Criado, M.R., Fernandez, D.H., Pereiro, I.R., Torrijos, R.C. (2004), Application of matrix solid-phase dispersion to the determination of polychlorinated biphenyls in fat by gas chromatography with electron-capture and mass spectrometric detection, *J. Chromatogr. A.*, 1056, pp. 187-194.

Croll, L.M., Stöver, H.D.H., Hitchcock, A.P. (2005), Composite tectocapsules containing porous polymer microspheres as release gates, *Macromolecules*, 38, pp. 2903-2910.

Dai, S., Barleigh, M.C., Shin, Y. (2001), Imprint-coating synthesis of selective functionalized ordered mesoporous sorbents for separation and sensors US Patent 6,251,280.

Dai, S., Shin, Y.S., Barnes, C.E., Toth, I.M. (1997), Enhancement of uranyl adsorption capacity and selectivity on silica sol-gel glasses via molecular imprinting, *Chem. Mater*., 9, pp. 2521–2525.

Daniel, S., Prabhakara Rao, P., Prasada Rao, T. (2005), Investigation of different polymerization methods on the analytical performance of palladium (II) ion imprinted polymer materials, *Anal. Chim. Acta*, 536, pp. 197–206.

Day, A.J., Williamson, G. (1999), Human metabolism of dietary quercetin glycosides. In: Gross, G.G., Hemingway, R.W., Yoshida, T. (Eds.). Plant Polyphenols 2: Chemistry, Biology, Pharmacology, Ecology. Kluwer Academic / Plenum Publishers, New York. Basic Life Sciences, Vol. 66, pp. 415-434.

Davis, J.M., Murphy, E.A., Carmichael, M.D., Davis, B. (2009), Quercetin increases brain and muscle mitochondrial biogenesis and exercise tolerance, *Am. J. Physiol. Regul. Integ.r Comp. Physiol..*, 296 (4), pp. R1071–7.

Dayrit, **F.,** Alcantara, A., Villasenor, I. (1990), The antibiotic compound and its deactivation in aqueous solutions, *Phil J. Sci.*, 119, pp. 23–26.

Das, K., Penelle, J., Rotello, V.M. (2003), Selective picomolar detection of hexachlorobenzene in water using a quartz crystal microbalance coated with a molecularly imprinted polymer thin film, *Langmuir*, 19, pp. 3921-3925.

Deng, S., Bai, R. (2004), Removal of trivalent and hexavalent chromium with aminated polyacrylonitrile fibers: performance and mechanisms, *Water Res*., 38, pp. 2423-2431.

de Barros, L.A, Martins, I., Rath, S. (2010), A selective molecularly imprinted polymer-solid phase extraction for the determination of fenitrothion in tomatoes, *Anal. Bioanal. Chem*., 397(3), pp. 1355-1361.

de Rijke, E., Out, P., Niessen, W.M.A., Ariese, F., Gooijer, C., Brinkman, U.A.Th. (2006) Analytical separation and detection methods for flavonoids, *J. Chromatogr. A,* 1112, pp. 31-63.

Deutsch, W.J., Serne, R.J. (1984), Uranium mobility in the natural environment: evidence from sedimentary roll-front deposits, *Geochemical Behavior of Disposed Radioactive Waste*, Chapter 17, pp. 287-302.

Diallo, M.S., Arasho, W., Johnson, Jr. J.H., Goddard, W.A. (2008), Dendritic chelating agents. 2. U (VI) binding to poly(amidoamine) and poly(propyleneimine) dendrimers in aqueous solutions, *Envin. Sci. Technol.,* 42, pp. 1572-1579.

Dillard, C.J., German, J.B. (2000), Phytochemicals: nutraceuticals and human health, Review. *J. Sci. Food Agric*., 80, pp. 1744–1756.

Ding, L., Li, H., Tang, F., Yao, S. (2006), Molecularly imprinted solid-phase extraction of epicatechin from tea beverage, *Anal. Lett*., 39(12), pp. 2373-2385.

Diňeiro, Y., Menéndez, M.I., Blanco-López, M.C., Lobo-Castañón, M.J., Miranda-Ordieres, A.J., Tuňón-Blanco, P. (2005), Computational approach to the rational design of molecularly imprinted polymers for voltammetric sensing of homovanillic acid, *Anal. Chem.,* 77, pp. 6741-6746.

Diňeiro, Y., Menéndez, M.I., Blanco-López, M.C., Lobo-Castañón, M.J., Miranda-Ordieres, A.J., Tuňón-Blanco, P. (2006), Computational predictions and experimental affinity distributions for a homovanillic acid molecularly imprinted polymer, *Biosens. Bioelectron*., 22, pp. 364-371.

Dirion, B., Cobb, Z., Schillinger, E., Andersson, L.I., Sellergren, B. (2003), Water-compatible molecularly imprinted polymers obtained via high-throughput synthesis and experimental design, *J. Am. Chem. Soc*., 125 (49), pp. 15101-15109.

Djozan, D., Ibrahimi, B. (2008), Preparation of new solid phase micro extraction fiber on the basis of atrazine-molecular imprinted polymer: Application for GC and GC/MS screening of triazine herbicides in water, rice and onion, *Anal. Chim. Acta*, 616(2), pp. 152-159.

Donia, A.M., Atia, A.A., Moussa, E.M.M., El-Sherif, A.M., Mahmoud, O.A. (2009), Removal of uranium (VI) from aqueous solutions using glycidyl methacrylate chelating resins, *Hydrometallurgy*, 95, pp. 183-189.

Dopico-García, M.S., Valentão, P., Jagodziñska, A., Klepczyñska, J., Guerra, L., Andrade, P.B., Seabra, R.M. (2007), Solid-phase extractionversus matrix solid-phase dispersion: Application to white grapes, *Talanta*, 74, pp. 20–31.

Dżygiel, P., O'Donnell, E., Fraiera, D., Chassainga, C., Cormack, P.A.G. (2007), Evaluation of water-compatible molecularly imprinted polymers as solid-phase extraction sorbents for the selective extraction of sildenafil and its desmethyl metabolite from plasma samples, *J. Chromatogr. B*, 853, pp. 346–353.

Ebarvia, B.S., Binag, C.A., Sevilla, F. (2004), Biomimetic piezoelectric quartz sensor for caffeine based on a molecularly imprinted polymer, *Anal. Bioanal. Chem*., 378(5), pp. 1331-1337.

Ellwanger, A., Berggren, C., Bayoudh, S., Crecenzi, C., Karlsson, L., Owens, P. K., Ensing, K., Cormack, P., Sherrington, D., Sellergren, B. (2001), Evaluation of methods aimed at complete removal of template from molecularly imprinted polymers, *Analyst*, 126, pp. 784–792.

El-Shahawi, M.S., Al-Saidi, H.M., Bashammakh, A.S., Al-Sibaai, A.A., Abdelfadeel, M.A. (2011), Spectrofluorometric determination and chemical speciation of trace concentrations of chromium (III & VI) species in water using the ion pairing reagent tetraphenyl-phosphonium bromide, *Talanta*, 84, pp. 175–179.

EPA radionuclides, http://www.epa.gov/radiation/radionuclides/uranium.html, accessed 13 Feb 2011.

Ersóz, A., Say, R., Denizli, A. (2004), Ni (II) ion-imprinted solid-phase extraction and preconcentration in aqueous solutions by packed-bed columns, *Anal. Chim. Acta*, 502, pp. 91-97.

Ezeike, C.O., Aguzue, O.C, Thomas, S.A. (2011), Effect of brewing time and temperature on the release of manganese and oxalate from lipton tea and *Azadirachta Indica* (Neem), *Phyllanthus Amarus* and *Moringa oleifera* blended Leaves, *J. Appl. Sci. Environ. Manage*. 15(1), pp. 175 – 177.

Fahey, J.W., Zalcmann, A.T., Talalay, P. (2001), The chemical diversity and distribution of glucosinolates and isothiocyanates among plants, *Phytochemistry*, 56, pp. 5–51.

Fang, G.Z., Tan, J., Yan, X.P. (2005), An ion- imprinted functionalized silica gel sorbent prepared by a surface imprinting technique combined with a sol-gel process for selective solid-phase extraction of cadmium (II), *Anal. Chem.*, 77, pp. 1734-1739.

Fang, J., Gu, Z., Gang, D., Liu, C., Iiton, E.S., Deng, B. (2007), Cr (VI) removal from aqueous solution by activated carbon coated with quaternized poly(4-vinylpyridine), *Environ. Sci. Technol*. 41, pp. 4748-4753.

Farrington, K., Regan, F. (2007), Investigation of the nature of MIP recognition: The development and characterization of a MIP for Ibuprofen, *Biosens. Bioelectron.*, 22, pp. 1138–1146.

Feas, X., Seijas, J.A., Vazquez-Tato, M.P., Regal, P., Cepeda, A., Fente, C. (2009), Syntheses of molecularly imprinted polymers: Molecular recognition of cyproheptadine using original print molecules and azatadine as dummy templates, *Anal. Chim. Acta*, 631, pp. 237–244.

Ferrer, R., Beltran, J.L., Guiteras, J. (1997), Mathematical procedure for the determination of the breakthrough volumes of polycyclic aromatic hydrocarbons (PAHs), *Anal. Chim. Acta*, 346, pp. 253-258.

Fleming polymer testing and consultancy, http://www.flemingptc.co.uk/our-services/dsc-tga/, accessed 19 March 2011.

Foidl, **N.,** Makkar, H.P.S., Becker, K. (2001), The Potential use of *Moringa oleifera* for Agriculture and Industrial uses. In: The Miracle Tree/The Multiple Attributes of *Moringa oleifera*. Fuglie, L.J. (Ed.). CTA, USA.

Folin, O., Ciocalteu, V. (1927), On tyrosine and tryptophane determination in proteins, *J. Biol. Chem*., 27, pp. 627–650.

Foy, G.P., Pacey, G.E. (2000), Specific extraction of chromium (VI) using supercritical fluid extraction, *Talanta*, 51, pp. 339–347.

FOSS, (2006), www.foss.dk, P/N99990307, Issue 2 GB.

Fridovich, I. (1978), The biology of oxygen radicals, *Science*, 201, pp. 875–880.

Frisch M.J., et al., Gaussian Development Version, Revision A.03, Gaussian, Inc, Pittsburgh, PA (2003).

Fujiwara, I., Uchiyama, A., Sasaki, Y., Maeda, M., Takagi, M. (2003). Preparation of Cu-II-imprinted microspheres with imidazole groups at the surfaces by surface imprinting polymerization, *Bunseki Kagaku*, 52, pp. 147-150.

Gallego-Gallegos, M., Muňoz-Olivas, R., Cámara, C. (2009), Different formats of imprinted polymers for determining organotin compounds in environmental samples, *J. Environ. Manage.*, 90, pp. S69–S76.

Gam-Derouich, S., Nguyen, M.N., Madani, A., Maouche, N., Lang, P., Perruchot, C., Chehimi, M.M. Aryl diazonium salt surface chemistry and ATRP for the preparation of molecularly imprinted polymer grafts on gold substrates, *Surface Interface Analysis*, 42(6-7), pp. 1050-1056.

Gavrilescu, M., Pavel, L.V., Cretescu, I. (2009), Characterization and remediation of soils contaminated with uranium, *J. Hazard. Mater.*, 163, pp. 475–510.

Genera Nutrients Ltd, (2011), http://www.*Moringa*.com/, accessed 13 May 2011.

Ghasemi, J.B., Zolfonoun, E. (2010), Simultaneous spectrophotometric determination of trace amounts of uranium, thorium, and zirconium using the partial least squares method after their preconcentration by α-benzoin oxime modified Amberlite XAD-2000 resin, *Talanta*, 80, pp. 1191–1197.

Gilman, A.P., Villencuve, D.C., Seccours, V.E., Yagminas, A.P., Tracy, B.L., Quinn, J.M., Valli, V.E., Willes, R.J., Moss, M.A. (1998), Uranyl nitrate: 28-day and 91-day toxicity studies in the sprague-dawley rat, *Toxicol Sci.*, 41, pp. 117-128.

Glad, M., Reinholdsson, P., Mosbach, K. (1995), Molecularly imprinted composite polymers based on trimethylolpropane trimethacrylate (TRIM) Particles for efficient enantiomeric separations, *React. Polym.*, 25 (1), pp. 47-54.

Gladis, J.M., Prasada Rao, T. (2004). Effect of progen type on the synthesis of uranium ion imprinted polymer materials for the preconcentration/separation of traces of uranium, *Microchim. Acta*, 146, pp. 251–258.

Gladis, J.M., Prasada Rao, T. (2002), Preconcentration techniques for uranium (VI) and thorium (IV) prior to analytical determination-an overview, IPA516 DEL, 28, pp. 303–320.

Gladis, J.M., Prasada Rao, T. (2003), Synthesis and analytical application of uranyl ion imprinted polymer particles, *Anal. Lett.*, 36, pp. 2107–2121.

Goldstein, **G.I.,** Newbury, D.E., Echlin, P., Joy, D.C., Fiori, C., Lifshin, E. (1981), Scanning electron microscopy and X-ray microanalysis, New York, Plenum Press. ISBN 030640768X).

Gonzalez-Nunez, L., Canizares-Macias, N., Maria, P. (2011), Focused microwaves-assisted extraction of theobromine and caffeine from cacao, *Food Chem.*, 4, pp. 1819-1824.

Gonzalez, R.C., Gonzalez-Chavez, M.C.A. (2006), Metal accumulation in wild plants surrounding mining wastes, *Environ. Pollut.*, 144, pp. 84–92.

Goyal, N., Jain, S.C., Banerjee, U.C. (2003), Comparative studies on the microbial adsorption of heavy metals, *Adv. Environ. Res.,* 7, pp. 311–319.

Gu, **B.,** Yan, H., Zhou, P., Watson, D., Park, M., Istok, J.D. (2005), Humics impact uranium bioreduction and oxidation, *Environ. Sci. Technol*. 39, pp. 5268–5275.

Gu, X.-h., Xu, R., Yuan, G.-l., Lu, H., Gu, B.-r, Xie, H.-p. (2010), Preparation of chlorogenic acid surface-imprinted magnetic nanoparticles and their usage in separation of Traditional Chinese Medicine, *Anal. Chim. Acta*, 675, pp. 64–70

Guevara, **A.P.,** Vargas, C., Sakurai, H., Fujiwara, Y., Hashimoto, K., Maoka, T., Kozuka, M., Ito, Y., Tokuda, H. and Nishino, H. (1999), An antitumor promoter from *Moringa oleifera* Lam, *Mutat. Res.*, 440, pp. 181–188.

Gupta, S.N., Neckers, D.C. (1982), Template effects in chelating polymers, *J. Polym. Sci. Polym. Chem. Ed*., 20, pp. 1609-1622.

Gupta, V.K., Rastogi, A. (2009), Biosorption of hexavalent chromium by raw and acid-treated green alga *Oedogonium hatei* from aqueous solutions, *J. Hazard. Mater.,* 163, pp. 396–402

Hantash, J., Bartlett, A., Oldfield, P., D0en0es, G., O'Rielly, R., Roudiere, D., Menduni, S. (2006), Use of an on-line imprinted polymer pre-column, for the liquid chromatographic-UV absorbance determination of carbaryl and its metabolite in complex matrices *J. Chromatogr. A*, 1125, pp. 104–111.

Hashmi, D.S., Ismail, S., Shaikh, G.H. (2007), Assessment of the level of trace metals in commonly edible vegetables locally available in the markets of Karachi city. *Pak. J. Bot.*, 39, pp. 747–751.

Hawthorne, S.B., Yang, Y., Miller, D.J. (1994), Extraction of organic pollutants from environmental solids with subcritical and supercritical water, *Anal. Chem*., 66, pp. 2912-2920.

He, C., Long, Y., Pan, J., Li K., Liu, F. (2008). Molecularly imprinted silica prepared with immiscible ionic liquid as solvent and porogen for selective recognition of testosterone *Talanta*, 74, pp. 1126–1131.

He, Q., Chang, X.J. Zheng, H., Jiang, N., Hu, Z., Zhai, Y.H. (2006), Preconcentration and separation of Zn^{2+} using surface zinc (II) imprinted functionalized silica gel sorbent *Chem. Anal.*, 51, pp. 715-725 (Warsaw, Poland).

Hena, S. (2010), Removal of chromium hexavalent ion from aqueous solutions using biopolymer chitosan coated with poly 3-methyl thiophene polymer, *J. Hazard. Mater.*, 181, pp. 474–479

Hennion, M.-C. (1999), Solid-phase extraction: method development, sorbents, and coupling with liquid chromatography, *J. Chromatogr. A,* 856, pp. 3–54.

Herdes, C., Sarkisov, L. (2009), Computer simulation of volatile organic compound adsorption in atomistic models of molecularly imprinted polymers, *Langmuir*, 25, pp. 5352–5359.

Hjertén, S., Liao, J.L., Nakazato, K., Wang, Y., Zamaratskaia, G., Zhang, H.X. (1997), Gels mimicking antibodies in their selective recognition of proteins, *Chromatographia*, 44, pp. 227–234.

Hoai, N.T., Yoo, D.-K., Kim, D. (2010), Batch and column separation characteristics of copper imprinted porous polymer micro-beads synthesized by a direct imprinting method, *J. Hazard. Mater*. 173, pp. 462–467.

Hollman, P.C.H., Arts, I.C.W. (2000), Flavonols, flavones and flavanols - nature, occurrence and dietary burden, *J. Sci. Food Agric.*, 80(7), pp. 1081-1093.

Hoshina, K., Horiyama, S., Matsunaga, H., Haginaka, J. (2009). Molecularly imprinted polymers for simultaneous determination of antiepileptics in river water samples by liquid chromatography-tandem mass spectrometry, *J. Chromatogr. A*, 1216, pp. 4957–4962.

Hosoya, K., Yoshizako, K., Tanaka, N., Kimata, K., Araki, T., Haginaka, J. (1994). Uniform-size macroporous polymer-based stationary-phase for HPLC prepared through molecular imprinting technique, *Chem. Lett.*, 0, pp. 1437–1438.

Hu, S.-G., Li, L., He, X.-W. (2005), Comparison of trimethoprim molecularly imprinted polymers in bulk and in sphere as the sorbent for solid-phase extraction and extraction of trimethoprim from human urine and pharmaceutical tablet and their determination by high-performance liquid chromatography, *Anal. Chim. Acta*, 537, pp. 215–222.

Hu, X., Dai, G., Huang, J., Jin, H.J., Yu, Y., Liang, Y. (2011), Preparation and characterization of metolachlor molecularly imprinted polymer coating on stainless steel fibers for solid-phase microextraction, *Anal. Lett.*. 44(7), pp. 1358-1370.

Hu, X., Dai, G., Huang, J., Ye, T., Fan, H., Youwen, T., Yu, Y., Liang, Y. (2010), Molecularly imprinted polymer coated on stainless steel fiber for solid-phase microextraction of chloroacetanilide herbicides in soybean and corn, *J. Chromatogr. A*, 1217, pp. 5875–5882.

Hu, Y., Liu, R., Zhang, Y., Li, G. (2009), Improvement of extraction capability of magnetic molecularly imprinted polymer beads in aqueous media *via* dual-phase solvent system, *Talanta*, 79, pp. 576–582.

Huang, C.P., Wu, M.H. (1977), The removal of chromium (VI) from dilute aqueous solution by activated carbon, *Water Res.* 11(8), pp. 673-679.

Huang, J.W., Blaylock, M.J., Kapulnik, Y., Ensley, B.D. (1998), Phytoremediation of uranium-contaminated soils: role of organic acids in triggering uranium hyperaccumulation in plants, *Environ. Sci. Technol.*, 32(13), pp. 2004–2008.

Hunt, I. University of Calgary**,** http://www.chem.ucalgary.ca/courses/ 351/Carey/ Ch13/ch13-uvvis.html, 12 March 2011.

Hurrell, R., Egli, I. (2010), Iron bioavailability and dietary reference values, *Am. J. Clin. Nutr.*, 91, pp. 1461S–1467S.

http://serc.carleton.edu/research_education/geochemsheets/techniques/SEM.html, accessed 14 March 2011.

http://www2.chemistry.msu.edu/faculty/reusch/VirtTxtJml/Spectrpy/nmr/nmr1.htm,accessed 14 May 2011.

http://www.epa.gov/radiation/radionuclides/uranium.html, accessed 13 Feb 2011

Igwe, J.C., Nnorom, I.C., Gbaruko, B.C. (2005), Kinetics of radionuclides and heavy metals behavior in soils: Implications for plant growth, *Afr. J. Biotechnol.*, 4, pp. 1541-1547.

Ingle, Jr. J.D., Crouch, S.R. (1988), Spectrochemical analysis, Upper Saddle River, NJ, Prentice-Hall, pp. 34-35.

Iqbal, S., Bhanger, M.I. (2006), Effect of season and production location on antioxidant activity of *Moringa oleifera* leaves grown in Pakistan,. *J. Food Comp. Anal.*, 19, pp. 544–551.

Ishii, K., Furuta, T., Kasuya, Y. (2003), High-performance liquid chromatographic determination of quercetin in human plasma and urine utilizing solid-phase extraction and ultraviolet detection, *J. Chromatogr. B*, 794, pp. 49–56.

Ismail, A., Marjan, Z.M., Foong, C.W. (2004), Total antioxidant activity and phenolic content in selected vegetables, *Food Chem.*, 87, pp. 581–586.

Jain, S., Garg, V.K., Kadirvelu, K. (2009), Chromium (VI) removal from aqueous system using *Helianthus annuus* (sunflower) stem waste, *J. Hazard. Mater*., 162, pp. 365–372

James, D., Venkateswaran, G., Prasada Rao, T. (2009), Removal of uranium from mining industry feed simulant solutions using trapped amidoxime functionality within a mesoporous imprinted polymer material, *Microporous Mesoporous Mater.*, 119, pp. 165-170.

Jardine, **P.M.,** Fendorf, S.E., Mayes, M.A., Larsen, I.L., Brooks, S.C., Bailey , W.B. (1999), Fate and transport of hexavalent chromium in undisturbed heterogeneous soil, *Environ. Sci. Technol.*, 33, pp. 2939–2944.

Jiang, N., Chang, X.J., Zheng, H., He, Q., Hu, Z. (2006), Selective solid-phase extraction of nickel (II) using a surface- imprinted silica gel sorbent, *Anal. Chim. Acta*, 577, pp. 225-231.

Jin, Y., Ming, J., Yun, S., Yi, L., Yan, P., Kang, D., Bin, L. (2008), Narrowly dispersed molecularly imprinted microspheres Prepared by a modified precipitation polymerization method, *Anal. Chim. Acta*, 612, pp. 105–113.

Jing, T., Gao, X., Wang, P., Wang, Y., Lin, Y., Hu, X., Hao, Q., Zhou, Y., Mei, S. (2009), Determination of trace tetracycline antibiotics in foodstuffs by liquid chromatography–tandem mass spectrometry coupled with selective molecular-imprinted solid-phase extraction, *Anal. Bioanal. Chem*., 393, pp. 2009–2018.

John, J.M., Nigel, P.S., Saunders, G.D., Walton, P.H. (1998), European Patent 10 19555, WO9915707.

Johnson, R., Smith, K.P., Quinn, J. (1999), The application of adaptive sampling and analysis program (ASAP) techniques to NORM Sites, Rep. DOE/BC/W-31-109-ENG-38-9, OSTI No. 14169, 1999. United States Department of Energy, Washington DC.

Kabanov, V.A., Efendiev, A.A., Orujev, D.D. (1979), Complex-forming polymeric sorbents with macromolecular arrangement favorable for ion sorption, *J. Appl. Polym. Sci*., 24, pp. 259–267.

Kabata-Pendias, A., Pendias, H. (1992), Trace elements in soils and plants. 2nd ed. Boca Raton: CRC Press.

Kala, R., Biju, V.M., Prasada Rao, T. (2005), Synthesis, characterization, and analytical applications of erbium (III) ion imprinted polymer particles prepared *via* gamma-irradiation with different functional and crosslinking monomers, *Anal. Chim. Acta*, 549, pp. 51–58.

Kala, R., Gladis, J.M., Prasada Rao, T. (2004), Preconcentrative separation of erbium from Y, Dy, Ho, Tb and Tm by using ion imprinted polymer particles *via* solid phase extraction, *Anal. Chim. Acta*, 518, pp. 143–150.

Kala, R., Prasada Rao, T. (2006), Ion imprinted polymer solid phase extraction (IIP-SPE) for preconcentrative separation of erbium (III) from adjacent lanthanides and yttrium, *Sep. Sci. Technol*., 41, pp. 233–246.

Karim, K., Breton, F., Rouillon, R., Piletska, E.V., Guerreiro, A., Chianella, I., Piletsky, S.A. (2005), How to find effective functional monomers for effective molecularly imprinted polymers? *Adv. Drug Deliv. Rev.*, 57(12), pp. 1795-1808.

Katz, S.A., Salem, H. (1994), The biological and environmental chemistry of chromium, VCH, New York.

Kawaguchi, M., Hayatsu, Y., Nakata, H., Ishii, Y., Ito, R., Saito, K., Nakazawa, H. (2005), Molecularly imprinted solid phase extraction using stable isotope labeled compounds as template and liquid chromatography-mass spectrometry for trace analysis of bisphenol A in water sample, *Anal. Chim. Acta*, 539, pp. 83–89.

Kempe, M., Glad, M., Mosbach, K. (1995), An approach towards surface imprinting using the enzyme ribonuclease A, *J. Mol. Recogn.* 8, pp. 35–39.

Kempe, H., Kempe, M. (2006), Development and evaluation of spherical molecularly imprinted polymer beads, *Anal. Chem.*, 78, pp. 3659–3666.

Kempe, M., Mosbach, K. (1995), Separation of amino-acids, peptides and proteins on molecularly imprinted stationary phases, *J. Chromatogr. A*, 691, pp. 317–23.

Khajeh, M., Sanchooli, E. (2010), Development of a selective molecularly imprinted polymer-based solid-phase extraction for copper from food samples, *Biol. Trace Elem. Res*., 135, pp. 325-333.

Khajeh, M., Yamini, Y., Ghasemi, E., Fasihia, J., Shamsipur, M. (2007), Imprinted polymer particles for selenium uptake: Synthesis, characterization and analytical applications, *Anal. Chim. Acta*, 581, pp. 208-213.

Ki, C.D., Oh, C., Oh, S., Chang, J.Y. (2002), The use of a thermally reversible bond for molecular imprinting of silica spheres, *J. Am. Chem. Soc.*, 124, pp. 14838–14839.

Kim, H., Spivak, D.A. (2003), New insight into modeling non-covalently imprinted polymers, *J. Am. Chem. Soc.*, 125, pp.11269–11275.

Kim, J.S., Choi, Y.R., Kim, Y.S., Lee, Y.J., Ko, J.H., Kwon, S.Y., Heo, S.B. (2011), Determination of hexavalent chromium (Cr (VI)) in plastics using organic-assisted alkaline extraction, *Anal. Chim. Acta*, 690, pp. 182–189.

Kimaro, A., Kelly, L.A., Murray, G.M. (2005), Synthesis and characterization of molecularly imprinted uranyl ion exchange resins, *Sep. Sci. Technol.*, 40: 10, pp. 2035-2052.

Kirsch, N., Alexander, C., Davies, S., Whitcombe, M.J. (2004), Sacrificial spacer and non-covalent routes toward the molecular imprinting of "poorly-functionalized" N-heterocycles, *Anal. Chim. Acta*, 504, pp. 63–71.

Kishi, A., Toraya, H. (2004), Simultaneous measurements of x-ray diffraction (XRD) and Differential scanning calorimetry (DSC) data under Controlled humidity condition: instrumentation and Application to studies on hydration, dehydration, and Re-hydration processes of pharmaceutical compounds; copyright ©jcpds - international centre for diffraction data 2004, advances in x-ray analysis, volume 47, pp. 240-248.

Klein, J.U., Whitcombe, M.U., Mulholland, F., Vulfson, E.N. (1999), Template-mediated synthesis of a polymeric receptor specific to amino acid sequences, *Angew. Chem., Int. Ed.*, 38 (13-14), pp. 2057–2060.

Ko, M-J., Cheigh, C.-I., Cho, S.-W., Chung, M.-S. (2011), Subcritical water extraction of flavonol quercetin from onion skin, *J. Food Eng.*, 102, pp. 327–333.

Koohpaei, A.R., Shahtaheri, S.J., Ganjali, M.R., Rahimi Forushani, A., Golbabaei, F. (2008), Application of multivariate analysis to the screening of molecularly imprinted polymers (MIPS) for ametryn, *Talanta*, 75, pp. 978–986.

Kratochvil, D., Pimentel, P., Volesky, B. (1998), Removal of trivalent and hexavalent chromium by seaweed biosorbent, *Environ. Sci. Technol.*, 32(18), pp. 2693-2698.

Krauskopf, K.B. (1967), Introduction to geochemistry, New York, NY McGraw Hill.

Krishna, P.G., Gladis, J.M., Prasada Rao, T. (2005), Selective recognition of neodymium (III) using ion imprinted polymer particles, *J. Mol. Recognit*., 18, pp. 109–116.

Kronholm, J., Hartonen, K., Riekkola, M.L. (2007), Analytical extractions with water at elevated temperatures and pressures, *Trends Anal. Chem*. 26, pp. 396-412.

Krska, R., Welzig, E., Berthiller, F., Molinelli, A., Mizaikoff, B. (2005), Advances in the analysis of mycotoxins and its quality assurance, *Food Addit. Contam. Part A*, 22(4), pp. 345-353.

Kubo, T., Matsumoto, H., Shiriaishi, F., Nomachi, M., Nemoto, K., Hosoya, K., Kaya, K. (2007), Selective separation of hydroxy polychlorinated biphenyls (HO-PCBs) by the structural recognition on the molecularly imprinted polymers: Direct separation of the thyroid hormone active analogues from mixtures, *Anal. Chim. Acta*, 589, pp. 180–185.

Kubo, T., Hosoya, K., Nomachi, M., Tanaka, N., Kaya, K. (2005b), Preparation of a novel molecularly imprinted polymer using a water-soluble crosslinking agent, *Anal. Bioanal. Chem*., 382, pp. 1698–1701.

Kubo, T., Hosoya, K., Sano, T., Nomachi, M., Tanaka, N., Kaya, K. (2005a), Selective separation of brominated bisphenol A homologues using a polymer-based medium prepared by the fragment imprinting technique, *Anal. Chim. Acta*, 549, pp. 45–50.

Kubo, T., Tanaka, N., Hosoya, K. (2004), Target-selective ion-exchange media for highly hydrophilic compounds: a possible solution by use of the "interval immobilization technique" *Anal. Bioanal. Chem.*, 378, pp. 84–88.

Kuchen, W., Schram, J. (1988), Metal-ion-selective exchange resins by matrix imprint with methacrylates, *Angew. Chem. Int. Engl*., 27, pp. 1695-1697.

Kudrinskaya, V.A., Dmitrienko, S.G., Zolotov, YuA. (2009), Synthesis and study of sorption properties of molecularly imprinted polymers for quercetin, Moscow University Chemistry Bulletin, 64(3), pp. 124-129.

Kugimiya, A., Takei, H. (2008), Selectivity and recovery performance of phosphate-selective molecularly imprinted polymer, *Anal. Chim. Acta*, 606, pp. 252–256.

Kumar, A., Rout, S., Narayanan, U., Mishra, M.K., Tripathi, R.M., Singh, J., Kumar, S., Kushwaha, H.S. (2011a), Geochemical modelling of uranium speciation in the subsurface aquatic environment of Punjab State in India, *J. Geol. Mining Res.*, 3(5), pp. 137-146.

Kumar, M.S.Y., Dutta, R., Prasad, D., Misra, K. (2011b), Subcritical water extraction of antioxidant compounds from Seabuckthorn (*Hippophae rhamnoides*) leaves for the comparative evaluation of antioxidant activity, *Food Chem.*, 127(3), pp. 1309-1316.

Kumar, P.A., Chakraborty, S. (2009), Fixed-bed column study for hexavalent chromium removal and recovery by short-chain polyaniline synthesized on jute fiber, *J. Hazard. Mater.*, 162, pp. 1086–1098.

Kumbasar, R.A. (2010), Selective extraction of chromium (VI) from multicomponent acidic solutions by emulsion liquid membranes using tributhylphosphate as carrier, *J. Hazard. Mater.*, 178, pp. 875–882.

Kunyanga C.N., Imungi J.K., Okoth W.M., Biesalski H.K., Vadivel V. (2012), Total phenolic content, antioxidant and antidiabetic properties of methanolic extract of raw and traditionally processed Kenyan indigenous food ingredients, *LWT- Food Sci. Technol*., 45, pp. 269-276.

Kurata, F., Yergovich, T.W., Swift, G.W. (1971), Density and viscosity of aqueous solutions of methanol and acetone from freezing point to 10 degrees C. *J. Chem. Eng. Data*, 16(2), pp. 222-226.

Kwaambwa, H.M., Maikokera, R. (2007), A fluorescence spectroscopic study of a coagulating protein extracted from *Moringa oleifera* seeds, *Colloids Surf. B.*, 60(2), pp. 213-220.

Laandrault, N., Pouchert, P., Ravel, P., Gase, F., Cros, G., Teissedro, P.-L. (2001), Antioxidant activities and phenolic level of French wines from different varities and vintages. *J. Agric. Food Chem*. 49, pp. 3341–3343.

Lakenbrink, C., Lapczynski, S., Maiwald, B., Engelhardt, U.H. (2000), Flavonoids and other polyphenols in consumer brews of tea and other caffeinated beverages, *J. Agric. Food Chem*. 48, pp. 2848-2852.

Lambropoulou, D.A., Albanis, T.A. (2007), Liquid-phase micro-extraction techniques in pesticide residue analysis, *J. Biochem. Biophys. Meth*., 70, pp. 195-228.

Langmuir, D. (1978), Uranium solution-mineral equilibria at low temperatures with applications to sedimentary ore deposits, *Geochim. Cosmochim. Acta*, 42, pp. 547–569.

Larson, R.A. (1988), The antioxidants of higher plants. *Phytochemistry.*27, pp. 969–978.

Lee, C.H., Suh, M.Y., Joe, K.S., Eom, T.Y., Lee, W. (1997), A chelating resin containing 4-(2-thiazolylazo)resorcinol as the functional group. Chromatographic application to the preconcentration and separation of some trace metal ions including uranium, *Anal. Chim. Acta,* 35(1), pp. 57-63.

Lee, H.I., Kim, J.H., Kim, J.M., Kim, S., Park, J.-N., Hwang, J.S., Yeon, J.-W., Jung, Y. (2010), Application of ordered nanoporous silica for removal of uranium ions from aqueous solutions, *J. Nanosci. Nanotechnol.*, 10(1), pp. 217-221.

Lee, M.Y., Hong, K.J., Shin, A.Y., Kajiuchi, T. (2005), Adsorption of hexavalent chromium by chitosan-based polymeric surfactants, *J. Appl. Polym. Sci*., 96, pp. 47-50.

Leita, L., Margon, A., Pastrello, A., Arcŏn, I., Contin, M., Mosett, D. (2009), Soil humic acids may favour the persistence of hexavalent chromium in soil. *Environ. Pollut.*, 157, pp. 1862–1866.

Leuck, M., Kunz, H. (1998), Synthesis of active principles from the leaves of *Moringa oleifera* using *S*-pent-4-enyl thioglucosides, *Carbohydr Res.*, 312, pp. 33–44.

Li, F., Jiang, H.Q., Zhang, S.S. (2007), An ion- imprinted silica-supported organic-inorganic hybrid sorbent prepared by a surface imprinting technique

combined with a polysaccharide incorporated sol-gel process for selective separation of cadmium (II) from aqueous solution, *Talanta*, 71, pp. 1487-1493.

Li, H., Li, Z., Liu, T., Xiao, X., Peng, Z., Deng, L. (2008), A novel technology for biosorption and recovery hexavalent chromium in wastewater by bio-functional magnetic beads, *Bioresour. Technol.*, 99, pp. 6271–6279.

Li, M., Zhang, L., Meng, Z., Wang, Z., Wu, H. (2010), Molecularly-imprinted microspheres for selective extraction and determination of melamine in milk and feed using gas chromatography–mass spectrometry, *J. Chromatogr. B*, 878, pp. 2333–2338.

Li, Y., Yang, H., You, Q., Zhuang, Z., Wang, X., (2006a), Protein recognition via surface molecularly imprinted polymer nanowires, *Anal. Chem.*, 78, pp. 317–320.

Li, Y., Yang, T., Qi, X., Qiao, Y., Deng, A. (2008), Development of a group selective molecularly imprinted polymers based solid phase extraction of malachite green from fish water and fish feed samples, *Anal. Chim. Acta*, 624, pp. 317–325.

Li, Z., Bowman, R.S. (2001), Retention of inorganic oxyanions by organo-kaolinite, *Water. Res.*, 35, pp. 3771-3776.

Lindahl, S., Ekman, A., Khan, S., Wennerberg, C., Börjesson, P., Sjöberg, P.J.R., Karlsson, E.N., Turner, C. (2010), Exploring the possibility of using a thermostable mutant of beta-glucosidase for rapid hydrolysis of quercetin glucosides in hot water, *Green Chem.*, 12(1), pp. 159-168.

Lindahl, S., Liu, J., Khan, S., Nordberg, Karlsson, E., Turner, C., manuscript in preparation (November 2011).

Liska, I. (2000), Fifty years of solid-phase extraction in water analysis - historical development and overview, *J. Chromatogr. A*, 885, pp. 3-16.

Liu, L., Hoshina, K., Haginaka, J. (2010a), Monodispersed, molecularly imprinted polymers for cinchonidine by precipitation polymerization, *Talanta*, 80, pp. 1713–1718.

Liu, Y., Cao**,** X., Le**,** Z., Luo**,** M., Xu, W., Huang, G. (2010b), Pre-concentration and determination of trace uranium (VI) in environments using ion-imprinted chitosan resin *via* solid phase extraction, *J. Braz. Chem. Soc.*, 21(3), pp. 533-540.

Liu, Y., Cao, X., Hua, R., Wang, Y., Liu, Y., Pang, C., Wang, Y. (2010c), Selective adsorption of uranyl ion on ion-imprinted chitosan/PVA cross-linked hydrogel, *Hydrometallurgy*, 104, pp. 150–155.

Liu, Y., Liu, Y., Cao, X., Hua, R., Wang, Y., Pang, C., Hua, M., Li, X. (2011), Biosorption studies of uranium (VI) on cross-linked chitosan: isotherm, kinetic and thermodynamic aspects, *J. Radioanal. Nucl. Chem.,* 290, pp. 231–239

Liu, Y., Zai, Y., Chang, X., Guo, Y., Meng, S., Feng, F. (2006), Highly selective determination of methylmercury with methylmercury-imprinted polymers, *Anal. Chim. Acta* 575, pp. 159–165.

Lopez, C., Claude, B., Morin, Ph., Max, J.-P., Pena, R., Ribet, J.-P. (2011), Synthesis and study of a molecularly imprinted polymer for the specific extraction of indole alkaloids from Catharanthus roseus extracts, *Anal. Chim. Acta,* 683, pp. 198–205.

López, P., Batlle, R., Nerín, C., Cacho, J., Ferreira, V. (2007), Use of new generation poly(styrene-divinylbenzene) resins for gas-phase trapping-thermal desorption - Application to the retention of seven volatile organic compounds, *J. Chromatogr. A,* 1139, pp. 36-44.

Lu, Y.K., Yan, X.P. (2004), An imprinted organic-inorganic hybrid sorbent for selective separation of cadmium from aqueous solution, *Anal. Chem.*, 76(2), pp. 453-457.

Lubal, P., Široky, D., Fetsch, D., Havel, J. (1998), The acidobasic and complexation properties of humic acids.Study of complexation of Czech humic acids with metal ions, *Talanta, 4* 7, pp. 401–412.

Luo, W., Gu, B. (2009), Dissolution and mobilization of uranium in a reduced sediment by natural humic substances under anaerobic conditions, *Environ. Sci. Technol., 43*(1), pp. 152–156.

Luo, W., Zhu, L., Yu, C., Tang, H., Yu, H., Li, X., Zhang, X. (2008), Synthesis of surface molecularly imprinted silica micro-particles in aqueous solution and the usage for selective off-line solid-phase extraction of 2,4-dinitrophenol from water matrixes, *Anal. Chim. Acta*, 618, pp. 147–156.

Lv, Y., Lin, Z., Feng, W., Tan, T. (2007), Evaluation of the polymerization and recognition mechanism for phenol imprinting SPE, *Chromatographia*, 66, pp. 339–347.

Madane, N.S., Nikam, G.H., Mahanwar, K.R., Mohite, B.S. (2011), Liquid–liquid extraction of uranium (VI) using cyanex 272 in toluene from sodium salicylate medium, *J. Radioanal. Nucl. Chem.*, 288, pp. 285–290

Majors, **R.E,** (2008), The role of polymers in solid-phase extraction and sample preparation, *Lc Gc North America*, 26(11), pp. 1074-1090.

Makkar, **H.P.S.,** Becker, K. (1997), Nutrient and antiquality factors in different morphological parts of *Moringa oleifera* tree, *J. Agric. Sci.* (Cambridge), 128, pp. 311–322.

Mallik, **S.,** Johnson, R.D., Arnold, F.H. (1994), Synthetic bis-metal ion receptors for bis-imidazole protein analogs, *J. Am. Chem. Soc*., 116, pp. 8902–8911.

Mallik, S., Plunkett, S.D., Dhal, P.K., Johnson, R.D., Pack, D., Shnek, D., Arnodl, F.H. (1994), Towards materials for the specific recognition and separation of proteins, *New J. Chem.*, 18, pp. 299–304.

Malosse, L., Palmas, P., Buvat, P., Ades, D., Siove, A. (2008), Novel stoichiometric, noncovalent pinacolyl methylphosphonate imprinted polymers: A Rational Design by NMR Spectroscopy, *Macromolecules*, 41, pp. 7834–7842.

Mandiwana, K.L., Panichev, N., Panicheva, S. (2011), Determination of chromium (VI) in black, green and herbal teas, *Food Chem.*, 129, pp. 1839–184.

Manhas, B.S., Pal, S., Trikka, A.K. (1993), Synthesis and characterization of uranium (IV) compounds with piperazines, *Polyhedron.*, 12, pp. 241-246.

Mani, S., Jaya, S., Vadivambal, R. (2007), Optimization of solvent extraction of *Moringa* (*Moringa oleifera*) seed kernel oil using response surface methodology, Trans Institution of Chemical Engineers Part C, *Food Bioprod. Process.*, 85 (C4), pp. 328–335.

Mansfield, **E.,** Kar, A., Quinn, T.P., Hooker, S.A. (2010), "Quartz Crystal Microbalances for Microscale Thermogravimetric Analysis", *Anal. Chem.*. 101116152615035.

Marjanović, V., Lazarević, S., Jankovíč-Castvan, I., Potkonjakc, B., Janaćkovićb, Đ., Petrović, R. (2011), Chromium (VI) removal from aqueous solutions using mercaptosilane functionalized sepiolites, *Chem. Eng. J.*, 166, pp. 198–206.

Martino, **K.G.,** Guyer, D. (2004), Supercritical fluid extraction of quercetin from onion skins, *J. Food Process Eng.*, 27, pp. 17–28.

Mason, **C.F.V.,** Turney, W.R.J.R., Thomson, B.M., Lu, N., Longmire, P.A., Chisholm-Brause, C.J. (1997), Carbonate leaching of uranium from contaminated soils, *Environ. Sci. Technol.* 31, pp. 2707–2711.

Mayes, A.G., Mosbach, K. (1996), Molecularly imprinted polymer beads: Suspension polymerization using a liquid perfluorocarbon as the dispersing phase, *Anal. Chem*., 68, pp. 3769–3674.

Mayes, A.G., Whitcombe, M.J. (2005), Synthetic strategies for the generation of molecularly imprinted organic polymers, *Adv. Drug Delivery Rev.*, 57, pp. 1742–1778.

Mbendi, (2011), http://www.mbendi.com/indy/ming/chrm/af/sa/p0005.htm, accessed 18 February 2011.

Mcbride, M.B. (1997), A critique of diffuse double layer models applied to colloid and surface chemistry, *Clays Clay Miner.*, 45(4), pp. 598-608.

Meinrath, G. (1998), Chemometric analysis: Uranium (VI) hydrolysis by UV-Vis spectroscopy, *J. Alloys Compd.*, 275, pp. 777-781.

Meng, **Z.,** Yamazaki, T., Sode, K. (2004), A molecularly imprinted catalyst designed by a computational approach in catalysing a transesterification process, *Biosens. Bioelectron*., 20, pp. 1068–1075.

Mermet, **J.M.** (2005), "Is it still possible, necessary and beneficial to perform research in ICP-atomic emission spectrometry?", *J. Anal. At. Spectrom.*, 20, pp. 11–16.

Metilda, P., Gladis, J.M., Prasada Rao, T. (2004), Influence of binary/ternary complex of imprint ion on the preconcentration of uranium (IV) using ion imprinted polymer materials, *Anal. Chim. Acta*, 512, pp. 63–69.

Metilda, P., Gladis, J.M., Venkateswaran, G., Prasada Rao, T. (2007a), Investigation of the role of chelating ligand in the synthesis of ion-imprinted

polymeric resins on the selective enrichment of uranium (VI), *Anal. Chim. Acta*, 587, pp. 263–271.

Metilda, P., Prasada, K., Kala, R., Gladis, J.M., Prasada Rao, T., Naidu, G.R.K. (2007b), Ion imprinted polymer based sensor for monitoring toxic uranium in environmental samples, *Anal. Chim. Acta,* 582, pp. 147–153.

Meyer, C.A. (1993), Steam Tables: Thermodynamics and transport properties of steam, American Society of Mechanical Engineers, New York.

Mhaka, B., Cukrowska, E., Bui Bernadette T.S., Ramström, O., Haupt, K., Tutu, H., Chimuka, L. (2009), Selective extraction of triazine herbicides from food samples based on a combination of a liquid membrane and molecularly imprinted polymers, *J. Chromatogr. A*, 1216, pp. 6796-6801.

Michalkiewicz, A., Biesaga, M., Pyrzynska, K. (2008), Solid-phase extraction procedure for determination of phenolic acids and some flavonols in honey, *J. Chromatogr. A*, 1187, pp. 18–24.

Michel, T., Destandau, E., Elfakir, C. (2011), Evaluation of a simple and promising method for extraction of antioxidants from sea buckthorn (*Hippophaë rhamnoides* L.) berries: Pressurised solvent-free microwave assisted extraction, *Food Chem.*, 126(3), pp. 1380-1386.

Mikhail, S.Z., Kimel, W.R. (1961), Densities and viscosities of methanol-water mixtures, *J. Chem. Eng. Data*, 6 (4), pp. 533-537.

Milja, T.E., Prathish, P.K., Prasada Rao, T. (2011), Synthesis of surface imprinted nanospheres for selective removal of uranium from simulants of Sambhar salt lake and ground water, *J. Hazard. Mater.,* 188, pp. 384–390.

Miller, F.A., Wilkins, C.H. (1952), Infrared spectra and characteristic frequencies of inorganic ions, *Anal. Chem*., 24, pp. 1253-1294.

Mitchell, M.D., Collias, D.I., Bjorkquist, D.W., Zaveri, P.N., Woolley, M.M. (2004), Water filter materials, water filters and kits containing particles coated with cationic polymer and processes for using the same. *U.S. Pat. Appl. Publ*. (2004164018) 30 pp. Cont.-in-part of U.S. Ser. No. 464,210.

Mohajeri, **S.A.,** Hosseinzadeh, H., Keyhanfar, F., Aghamohammadian, J. (2010), Extraction of crocin from saffron (Crocus sativus) using molecularly imprinted polymer solid-phase extraction, *J. Sep. Sci.*, 33 (15), pp. 2302-2309.

Molinelli, A., O'Mahony, J., Nolan, K., Smyth, M.R., Jakusch, M., Mizaikoff, B. (2005), Analyzing the mechanisms of selectivity in biomimetic self-assemblies *via* IR and NMR spectroscopy of prepolymerization solutions and molecular dynamics simulations, *Anal. Chem.*, ,77, pp. 5196–5204.

Molinelli, A., Weiss, R., Mizaikoff, B. (2002), Advanced solid phase extraction using molecularly imprinted polymers for the determination of quercetin in red wine, *J. Agric. Food Chem.*, 50(7), pp. 1804-1808.

Mona, S., Kaushik, A., Kaushik, C.P. (2011), Biosorption of chromium (VI) by spent cyanobacterial biomass from a hydrogen fermentor using Box-Behnken model, *Int. Deter. Biodegr.*, 65, pp. 656-663.

Moon, J., Shibamoto, T. (2009), Antioxidant assays for plant and food components. *J. Agric. Food Chem*., 57, pp. 1655–1666.

Moon, Y.J., Wang, L., DiCenzo, R., Morris, M.E. (2008), Quercetin pharmacokinetics in humans, *Biopharm. Drug Dispos.*, 29, pp. 205-217.

Moringa4Life, (2011), www.Moringa4life.co.za, accessed 12 August 2011.

Mosbach, K., Ramström, O. (1996), The emerging technique of molecular imprinting and its future impact on biotechnology, *Biotechnology*, 14, pp. 163–170.

Mosbach, K. (1994), Molecular imprinting, *Trends Biochem. Sci*., 19, pp. 9–14.

Moullec, S.L., Begos, A., Pichon, V., Bellier, B. (2006), Selective extraction of organophosphorus nerve agent degradation products by molecularly imprinted solid-phase extraction, *J. Chromatogr. A,* 1108, pp. 7–13.

Naicker, K., Cukrowska, E., McCarthy, T.S. (2003), Acid mine drainage arising from gold mining activity in Johannesburg, South Africa and environs, *Environ Pollut*., 22, pp. 29–40.

National Department of Agriculture, (2000), Trends in agricultural sector, http://www.nda.agric.za/docs/Trends2000/onions.htm, accessed 14 November 2010.

Natural News, http://www.naturalnews.com/022272.html#ixzz1MKFQlKWe, accessed 14 May 2011.

Neagu, V. (2009), Removal of Cr (VI) onto functionalised pyridine copolymer with amide groups, *J. Hazard. Mater.*, 171, pp. 410-416.

Neagu, V., Mikhalovsky, S. (2010), Removal of hexavalent chromium by new quaternized crosslinked poly(4-vinylpyridines). *J. Hazard. Mater.,* 183, pp. 533-540.

Nemulenzi, O., Mhaka, B., Cukrowska, E., Ramström, O., Tutu, H., Chimuka, L. (2009), Potential of combining of liquid membranes and molecularly imprinted polymers in extraction of 17 beta-estradiol from aqueous samples, *J. Sep. Sci*.. 32, pp. 1941 – 1948.

Nemoto, K., Kubo, T., Nomachi, M., Sano, T., Matsumoto, T., Hosoya, K., Hattori, T., Kaya, K. (2007), Simple and effective *3D* recognition of domoic acid using a molecularly imprinted polymer, *J. Am. Chem. Soc.*, 129, pp. 13626–13632.

Nicholls, I.A. (1995), Thermodynamic considerations for the design of and ligand recognition by molecularly imprinted polymers, *Chem. Lett.,* 0, pp. 1035–1036.

Nicholls, P.H, Evans, A.A. (1991), Sorption of organic compounds by field soils. Part one: *Acids Pesticide Sci.,* 33, pp. 319–330.

Nikishimi, M., Rao N., Yagi, K. (1972), The occurrence of superoxide anion in the reaction of reduced phenazine methosulphate and molecular oxygen, *Biochem. Biophys. Res. Commun.,* 46, pp. 849–854

Nishide, H., Deguchi, J. (1976), Selective adsorption of metal-ions on crosslinked poly(vinylpyridine) resin prepared with a metal-ion as a template, *Chem. Lett*., 5, pp. 169–174.

Norrlow, O., Glad, M., Mosbach, K. (1984), Acrylic polymer preparations containing recognition sites obtained by imprinting with substrates, *J. Chromatogr.,* 299, pp. 29–41.

Nuutila, A.M., Kammiovirta, K., Oksman-Caldentey, K.M. (2002), Comparison of methods for the hydrolysis of flavonoids and phenolic acids from onion and spinach for HPLC analysis, *Food Chem.,* 76(4), pp. 519-525.

Nöthlings, U., Murphy, S.P., Wilkens, L.R., Henderson, B.E., Kolonel, L.N. (2007), Flavonols and pancreatic cancer risk: the multiethnic cohort study, *Am. J. Epidemiol*. 166, pp. 924–931.

Olowoyo, J.O., van Heerden, E., Fischer, J.L., Baker, C. (2010), Trace metals in soil and leaves of Jacaranda mimosifolia in Tshwane area, South Africa, *Atmos. Environ.,* 44, pp. 1826–1830.

Olszewska, M. (2008), Separation of quercetin, sexangularetin, kaempferol and isorhamnetin for simultaneous HPLC determination of flavonoid aglycones in inflorescences, leaves and fruits of three Sorbus species, *J. Pharmaceut. Biomed.,* 48(3), pp. 629-635.

O'Mahony, J., Molinelli, A., Nolan, K., Smyth, M.R., Mizaikoff, B. (2006a), Anatomy of a successful imprint: Analysing the recognition mechanisms of a molecularly imprinted polymer for quercetin, *Biosens. Bioelectron.*, 21, pp.1383–1392.

O′Mahony, J., Wei, S., Molinelli, A., Mizaikoff, B. (2006b), Imprinted Polymeric Materials. Insight into the Nature of Prepolymerization Complexes of Quercetin Imprinted Polymers, *Anal. Chem.*, 78, pp. 6187-6190.

Ong, E.S., Cheong, J.S.H., Goh, D. (2006), Pressurized hot water extraction of bioactive or marker compounds in botanicals and medicinal plant materials, *J. Chromatogr. A,* 1112, pp. 92-102.

Ong, E.S. (2004), Extraction methods and chemical standardization of botanicals and herbal preparations, *J. Chromatogr. B,* 812, pp. 23-33.

Ong, E.S., Len, S.M. (2003a), Pressurized hot water extraction of berberine, baicalein and glycyrrhizin in medicinal plants, *Anal. Chim. Acta*, 482, pp. 81-89.

Ong, E.S., Len, S.M. (2003b), Evaluation of surfactant-assisted pressurized hot water extraction for marker compounds in Radix Codonopsis pilosula using liquid chromatography and liquid chromatography/electrospray ionization mass spectrometry, *J. Sep. Sci*. 26, pp. 1533-1540.

Ong, E.S., Len, S.M. (2004), Evaluation of pressurized liquid extraction and pressurized hot water extraction for tanshinone I and IIA in Salvia miltiorrhiza using LC and LC-ESI-MS, *J. Chromatogr. Sci*., 42, pp. 211-216.

Ong, E.S., Woo, S.O., Yong, Y.L. (2000), Pressurized liquid extraction of berberine and aristolochic acids in medicinal plants, *J. Chromatogr. A,* 22, pp. 57-64.

Ortega, L., López, R., Cacho, J., Ferreira, V. (2001), Use of solid-liquid distribution coefficients to determine retention properties of Porapak-Q resins - Determination of optimal conditions to isolate alkyl-methoxypyrazines and beta-damascenone from wine, *J. Chromatogr. A*, 931, pp. 31-39.

Oyaizu, M. (1986), Studies on products of browning reaction: antioxidative activity of products browning reaction prepared from glucosamine. *Jpn. J. Nutr*., 44, pp. 307-315.

Ozcan, A.A., Say, R., Denizli, A., Ersoz, A. (2006), L-histidine imprinted synthetic receptor for biochromatography applications, *Anal. Chem*. 78, pp. 7253–7258.

Pakade, V., Cukrowska, E., Darkwa, J., Torto, N., Chimuka, L. (2011), Selective removal of chromium (VI) from sulphates and other metal anions using an ion-imprinted polymer, *Water SA*, 37(4), pp. 529-537.

Palada, M.C., Chang, L.C. (2003), Suggested cultural practices for *Moringa*, International Cooperators' Guide AVRDC, pub # 03-545, pp. 1-5.

Palmer, **C.D.,** Wittbrodt, P.R. (1991), Processes affecting the remediation of chromium-contaminated sites, *Environ. Health Perspect.*, 92, pp. 25–40.

Pan, G., Zhang, Y., Guo, X., Li, C., Zhang, H. (2010), An efficient approach to obtaining water-compatible and stimuli-responsive molecularly imprinted polymers by the facile surface-grafting of functional polymer brushes via RAFT polymerization, *Biosens. Bioelectron.*, 26, pp. 976–982.

Pan, J., Xue, X., Wang, J., Xie, H., Wu, Z. (2009), Recognition property and preparation of Staphylococcus aureus protein A-imprinted polyacrylamide polymers by inverse-phase suspension and bulk polymerization, *Polymer*, 50, pp. 2365–2372.

Papelis, C., Hayes, K.F., Leckie, J.O. (1988), HYDRAQL: a program for the computation of chemical equilibrium composition of aqueous batch systems, Technical Report No. 306, 1988. Department of Civil Engineering, Stanford University, Stanford, CA, USA.

Parks, J.L., McNeill, L., Frey, M., Eaton, A.D., Haghani, A., Ramirez, L., Edwards, M. (2004), Determination of total chromium in environmental water samples, *Water Res.*, 38, pp. 2827–2838.

Patterson, J.W. (1985), Industrial wastewater treatment technology, 2nd ed., Butterworth-Heinemann, London.

Pavel, L.V., Cretescu, I., Gavrilescu, M. (2009), Characterization and remediation of soils contaminated with uranium, *J. Hazard. Mater.*, 163, pp. 475–510.

Pavel, D., Lagowski, J. (2005), Computationally designed monomers and polymers for molecular imprinting of theophylline and its derivatives. Part I , *Polymer*, 46, pp. 7528-7542.

Pavel, D., Lagowski, J., Lepage, C.J. (2006), Computationally designed monomers for molecular imprinting of chemical warfare agents - Part V, *Polymer*, 47, pp. 8389-8399.

Pehlivan, E., Cetin, S. (2009), Sorption of Cr (VI) ions on two Lewatit-anion exchange resins and their quantitative determination using UV-visible spectrophotometer, *J. Hazard. Mater.*, 163, pp. 448–453.

Peng, J., Fan, G., Chai, Y., Wu, Y. (2006), Efficient new method for extraction and isolation of three flavonoids from *Patrinia villosa* Juss. by supercritical fluid extraction and high-speed counter-current chromatography, *J. Chromatogr. A.*, 1102, pp. 44-50.

Perez-Moral, N., Mayes, A.G. (2001), Novel MIP formats, *Bioseparation*, 10, pp. 287–299.

Perez-Fonseca, A.A., Gomez Hermosillo, C., Davila, H., Gonzalez Nunez, R., Robledo-Ortiz, J., Vazquez-Lepe, M.O., Herrera-Gomez, A. (2011), Chitosan supported onto Agave fiber – postconsumer HDPE composites for Cr (VI) adsorption, *Ind. Eng. Chem. Res*., DOI: 10.1021/ie201242x.

Petersson, E.V., Liu, J., Sjöberg Per, J.R., Danielsson, R., Turner, C. (2010), Pressurized Hot Water Extraction of anthocyanins from red onion: A study on extraction and degradation rates, *Anal. Chim. Acta*, 663, pp. 27–32.

Pezzuto, J.M., Park, E.J. (2002), Autooxidation and antioxidants. In: Swarbrick J. and Boylan J.C. (Eds) Encyclopedia of Pharmaceuticals Technology. Vol. 1. 2nd ed New York: Marcel Dekker Inc., pp. 97–113.

Piletska, E.V., Guerreiro, A.R., Whitcombe, M.J., Piletsky, S.A. (2009), Influence of the polymerization conditions on the performance of molecularly imprinted polymers, *Macromolecules*, 42(14), pp. 4921-4928.

Piletska, E.V., Guerreiro, A.R., Romero-Guerra, M., Chianella, I., Turner, A.P.F., Piletsky, S.A. (2008), Design of molecular imprinted polymers compatible with aqueous environment, *Anal. Chim. Acta,* 607, pp. 54–60**.**

Piletska, E.V., Turner, N.W., Turner, A.P.F., Piletsky, S.A. (2005), Controlled release of the herbicide simazine from computationally designed molecularly imprinted polymers, *J. Controlled Release,* 108, pp. 132– 139.

Piletsky, S.A., Andersson, H.S., Nicholls, I.A. (1999), Combined hydrophobic and electrostatic interaction-based recognition in molecularly imprinted polymers, *Macromolecules*, *32*, pp. 633–636.

Piletsky, S.A., Karim, K., Piletska, E.V., Day, C.J., Freebairn, K.W., Legge, C., Turner, A.P.F. (2001), Recognition of ephedrine enantiomers by molecularly imprinted polymers designed using a computational approach, *Analyst*, 126, pp. 1826-1830.

Pinkrah, V.T., Snowden, M.J., Mitchell, J.C., Seidel, J., Chowdhry, B.Z., Fern, G.R. (2003), Physicochemical properties of poly(N-isopropylacrylamide-co-4-vinylpyridine) cationic polyelectrolyte colloidal microgels, *Langmuir*, 19, pp. 585-590.

Plunkett, S.D., Arnold, F.H. (1995), molecularly imprinted polymers on silica - selective supports for high-performance ligand-exchange chromatography, *J. Chromatogr. A,* 708, pp. 19–29.

Polyakov, M.V. (1931), *Zh. Fiz. Khim*, 2, pp. 799-805.

Poole, C.F. (2003), New trends in solid-phase extraction, *Trends Anal. Chem*., 22, pp. 362-373.

Prasada Rao, T., Kala, R., Daniel, S. (2006), Metal ion-imprinted polymers—Novel materialsfor selective recognition of inorganics, *Anal. Chim. Acta,* 578, pp. 105–116.

Preetha, C.R., Gladis, J.M., Prasada Rao, T., Venkateswaran, G. (2006), Removal of toxic uranium from synthetic nuclear power reactor effluents using uranyl ion imprinted polymer particles, *Environ. Sci. Technol*., 40, pp. 3070–3074.

Price, K.R, Rhodes, M.J.C. (1997), Analysis of the major flavonol glycosides present in four varieties of onion (*Allium cepa*) and changes in composition resulting from autolysis, *J. Sci. Food Agric.*, 74(3), pp. 331-339.

Psareva, T.S., Zakutevskyy, O.I., Chubar, N.I., Strelko, V.V., Shaposhnikova, T.O., Carvalho, J.R., Correia, M.J.N. (2005), Uranium sorption on cork biomass, *Colloids Surf. A.*, 252, pp. 231-236.

Pugh, R.E., Dick, D.G., Fredeen, A.L. (2002), Heavy metal (Pb, Zn, Cd, Fe and Cu) contents of plant foliage near the Anvil Range Lead/Zinc mine, Faro, Yukon Territory, *Ecotoxicol. Environ. Saf.*, 52, pp. 273–279.

Qian, S., Huang, C., Jiang, J., He, F., Wang, Y. (2000), Studies of adsorption behaviour of crosslinked chitosan for Cr (VI) and Se (VI), *J. Appl. Polym. Sci.*, 77, pp. 3216-3219.

Qiao, F., Sun, H. (2010), Simultaneous extraction of enrofloxacin and ciprofloxacin from chicken tissue by molecularly imprinted matrix solid-phase dispersion, *J. Pharmaceut. Biomed.*, 53, pp. 795–798.

Quaglia, M., De, L.E., Sulitzky, C., Massolini, G., Sellergren, B. (2001), Surface initiated molecularly imprinted polymer films: a new approach in chiral capillary electrochromatography, *Analyst*, 126 (9), pp. 1495-1498.

Rajesh, N., Deepthi, B., Subramaniam, ,A. (2007), Solid phase extraction of chromium (VI) from aqueous solutions by adsorption of its ion-association complex with cetyltrimethylammoniumbromide on an alumina column, *J. Hazard. Mater.*, 144, pp. 464–469.

Raji, C., Anirudhan, T.S. (1998), Batch Cr (VI) removal by polyacrylamide-grafted sawdust: Kinetics and thermodynamics, *Water Res.*, 32, pp. 3772-3780.

Ramarathnam, N., Osawa, T., Namiki, M., Kawakishi, S. (1988), Chemical studies on novel rice hull antioxidants. I. Isolation, fractionation, and partial characterization, *J. Agric. Food Chem., 36*, pp. 732-737.

Ramarathnam, N., Osawa, T., Ochi, H., Kawakishi, S. (1995), The contribution of plant food antioxidants to human health, *Trends Food Sci. Technol.*, 6, pp. 75–82.

Ramnani, S.P., Sabharwal, S. (2006), Adsorption behaviour of Cr (VI) onto radiation crosslinked chitosan and its possible application for the treatment of wastewater containing Cr(VI), *React. Funct. Polym.*, 66, pp. 902–909.

Ramos, J., Millán, A., Palacio, F. (2000), Production of magnetic nanoparticles in a polyvinylpyridine matrix, *Polymer*, 41, pp. 8461–8464.

Ramström, J., Skudar, K., Haines, J., Patel, P., Brüggemann, O. (2001), Food analyses using molecularly imprinted polymers, *J. Agric. Food Chem*., 49, pp. 2105-2114.

Ramström, O. (2005), Book chapter, Synthesis and selection of functional and structural monomers, In: Molecularly Imprinted Materials: Science and Technology, Yan M, Ramström O (Eds.) Marcel Dekker: New York, Ch. 7, pp. 181-224.

Raper, K. (2011), http://www.lpdlabservices.co.uk/analytical_techniques/sem/index.php, accessed 10 November 2011.

Rashid, U., Anwar, F., Moser, B.R., Knothe, G. (2008), *Moringa oleifera* oil: A possible source of biodiesel, *Bioresour. Technol.*, 99, pp. 8175–8179.

Razali, I., Norhaya, H., Norasimah, A.S. (1997), Determination of antioxidants in palm oil products by HPLC, *Elaeis*, 9(1), pp. 25–31.

Recillas, S., Colón, J., Casals, E., González, E., Puntes, V., Sánchez, A., Font, X. (2010), Chromium VI adsorption on cerium oxide nanoparticles and morphology changes during the process, *J. Hazard. Mater.*, 184(1-3), pp. 425-431.

Ren, Y., Zhang, M., Zhao, D. (2008), Synthesis and properties of magnetic Cu (II) ion imprinted composite adsorbent for selective removal of copper, *Desalination*, 228, pp. 135–149.

Richard, J., Ansell, I., Mosbach, K. (1997), Molecularly imprinted polymers by suspension polymerization in perfluorocarbon liquids, with emphasis on the influence of the porogenic solvent, *J. Chromatogr. A*, 787, pp. 55-66.

Richter, B.E., Jones, B.A., Ezzell, J.L., Porter, N.L., Avdalovic, N., Pohl, C. (1996), Accelerated solvent extraction: A technique for sample preparation, *Anal. Chem*., 68, pp. 1033-1039.

Robinson, T. (1959), "Michael Tswett" *J. Chem. Educ.*, 36(3), pp. 144-147.

Rosatzin, T., Andersson, L.I., Simon, W., Mosbach, K. (1991), Preparation of Ca^{2+} selective sorbents by molecular imprinting using polymerizable ionophores, *J. Chem. Soc. Perkin Trans*., 2, pp. 1261-1265.

Roudsari, M.H., Chang, P.R., Pegg, R.B., Tyler, R.T. (2009), Antioxidant capacity of bioactives extracted from canola meal by subcritical water, ethanolic and hot water extraction, *Food Chem.*, 114, pp. 717-726.

Rubio, M.G., Medina, A.R., Reguera, M.I.P., de Cordova, M.L.F. (2007), Multiresidue analysis of three groups of pesticides in washing waters from olive processing by solid-phase extraction-gas chromatography with electron capture and thermionic specific detection, *Microchem, J.*, 85, pp. 257-264.

Rufyikiri, G., Wannijn, J., Wang, L., Thiry, Y. (2006), Effects of phosphorus fertilization on the availability and uptake of uranium and nutrients by plants grown on soil derived from uranium mining debris, *Environ. Pollut.*, 141, pp. 420-427.

Russo, N., Toscano, M., Uccella, N. (2000), Semiempirical molecular modeling into quercetin reactive site: Structural, conformational, and electronic features, *J. Agric. Food Chem*., 48, pp. 3232-3237.

Saad, E.M., Mansour, R.A., El-Asmy, A., El-Shahawi, M.S. (2008), Sorption profile and chromatographic separation of uranium (VI) ions from aqueous solutions onto date pits solid sorbent, *Talanta*, 76, pp. 1041–1046.

Sadeghi, S, Mofrad, A.K. (2007), Synthesis of a new ion imprinted polymer material for separation and preconcentration of traces of uranyl ions, *React. Funct. Polym.*, 67, pp. 966–976.

Sambe, H., Hoshina, K., Haginaka, J. (2007), Molecularly imprinted polymers for triazine herbicides prepared by multi-step swelling and polymerization method - Their application to the determination of methylthiotriazine herbicides in river water, *J. Chromatogr. A*, 1152, pp. 130–137.

Sambe, H., Hoshina, K., Moaddel, R., Wainer, I.W., Haginaka, J. (2006), Uniformly-sized, molecularly imprinted polymers for nicotine by precipitation polymerization, *J. Chromatogr. A*, 1134, pp. 88–94.

Sani, **R.K.,** Peyton, B.M., Dohnalkova, A., Amonette, J.E. (2005), Reoxidation of biologically reduced uranium with Fe (III)(hydr)oxides under sulfate-reducing conditions, *Geochim. Cosmochim. Acta*, 69, pp. A471-A471.

Saunders, G.D., Foxon, S.P., Walton, P.H., Joyce, M.J., Port, S.N. (2000), A selective uranium extraction agent prepared by polymer imprinting, *Chem. Commun*., pp. 273–274.

Say, R., Birlik, E., Ersöz, A., Yilmaz, F., Gedibey, T., Denizli, A. (2003), Preconcentration of copper on ion-selective imprinted polymer microbeads, *Anal. Chim. Acta*, 480, pp. 251-258.

Say, R., Ersöz, A., Denizli, A. (2003), Selective separation of uranium containing glutamic acid molecular-imprinted polymeric microbeads, *Sep. Sci. Technol.*, 38 (14), pp. 3431-3447.

Santiago, I., Worland, V.P., Cazares-Rivera, E., Cadena, F. (1992), Removal of hexavalent chromium from water using tailored zeolites, *Met. Finish.*, 90(11), pp. 37-43.

Sarin, V., Pant, M.M. (2006), Removal of chromium from industrial waste by using eucalyptus bark, *Bioresour. Technol*., 97(1), pp. 15–20.

Schantz, M.M. (2006), Pressurized liquid extraction in environmental analysis, *Anal. Bioanal. Chem.*, 386, pp. 1043-1047.

Scott, R.P.W. (2008), http://www.chromatography-online.org/HPLC-Detectors/Electrical-Conductivity/rs85.html, accessed 5 November 2011.

Sellergren, B. (1994), Imprinted dispersion polymers - a new class of easily accessible affinity stationary phases, *J. Chromatogr. A*, 673, pp. 133–141.

Sellergren, B. (1997), Noncovalent molecular imprinting: antibody-like molecular recognition in polymeric network materials, *Trends Anal. Chem.*, 16, pp. 310-320.

Sellergren, **B.** (1999), Polymer- and template-related factors influencing the efficiency in molecularly imprinted solid-phase extractions, *Trends Anal. Chem*., 18, pp. 164–174.

Sengupta, A., Gupta, M.P. (1970), Studies on seed fat composition of *Moringaceae* family, *Fette, Seifen, Anstrichm*, 72, pp. 6-10.

Senko, **J.M.,** Istok, J.D., Suflita, J.M., Krumholz, L.R. (2002), *In situ* evidence for uranium immobilization and remobilization, *Environ. Sci. Technol*., 36, pp. 1491–1496.

Sessler, J.L., Melfi, J.P., Pantos, G.D. (2006), Uranium complexes of multidentate N-donor ligands, *Coord. Chem. Rev.*, 250, pp. 816-843.

Settle, F. (1997), Handbook of instrumental techniques for analytical chemistry, Ed. Upper Saddle River, NJ: Prentice-Hall.

Shahidi, F. (2009), Nutraceuticals and functional foods: whole versus processed foods, *Trends Food Sci. Technol*., 20, pp. 376–387.

Shamsipur, M., Fasihi, J., Khanchi, A., Hassani, R., Alizadeh, K., Shamsipur, H. (2007), A stoichiometric imprinted chelating resin for selective recognition of copper(II) ions in aqueous media, *Anal. Chim. Acta,* 599, pp. 294–301.

Shan, J., Wang, B. (2011), Preparation and characterization of a metal-complexing imprinted polymer for improved quercetin recognition, *Sep. Sci. Technol.*, 46(1), pp. 164-171.

Sharma, N., Sharma, U.K., Gupta, A.P., Sinha, A.K. (2010), Simultaneous determination of epicatechin, syringic acid, quercetin-3-*O*-galactoside and quercitrin in the leaves of *Rhododendron* species by using a validated HPTLC method, *J. Food Compos. Anal.*, 23(3), pp. 214-219

She, Y., Cao, W., Shi, X., Lv, X.-l., Liu, J.-j, Wang, R.-y., Jin, F., Wang, J., Xiao, H. (2010), Class-specific molecularly imprinted polymers for the selective extraction and determination of sulfonylurea herbicides in maize samples by high-performance liquid chromatography–tandem mass spectrometry, *J. Chromatogr. B,* 878, pp. 2047–2053

Shea, **K.J.,** Sasaki, D.Y. (1989), On the control of microenvironment shape of functionalized network polymers prepared by template polymerization, *J. Am. Chem. Soc*., 111, pp. 3442–3444.

Shea, **K.J.,** Sasaki, D.Y. (1991), An analysis of small-molecule binding to functionalized synthetic polymers by ^{13}C CP/MAS NMR and FT-IR spectroscopy, *J. Am. Chem. Soc*., 113, pp. 4109–4120.

Shea, K.J. (1994), Molecular imprinting of synthetic network polymers: The de novo synthesis of macromolecular binding and catalytic sites, *Trends Polym. Sci*., 2, pp. 166–173.

Shen, S., Sudol, E.D., El-Aasser, M.S. (1993), Control of particle-size in dispersion polymerization of methyl-methacrylate, *J. Polym. Sci: Part A: Polym. Chem*., 31, pp. 1393-1402.

Shen, X., Ye, L. (2011), Molecular imprinting in Pickering emulsions: a new insight into molecular recognition in water, *Chem. Commun*., 47, 10359-10361.

Shen, Y., Tan, X., Wang, L., Wu, W. (2011), Extraction of the uranyl ion from the aqueous phase into an ionic liquid by diglycolamide, *Sep. Purif. Technol*., 78, pp. 298–302.

Sheppard, M.I., Thibault, D.H. (1992), Desorption and extraction of selected heavy metals from soils, *Soil Sci. Soc. Am. J*., 56, pp. 415–423.

Siddhuraju, P., Becker, K. (2003), Antioxidant properties of various solvent extracts of total phenolic constituents from three different agroclimatic origins of drumstick tree (*Moringa oleifera* Lam.) leaves, *J. Agric. Food Chem.*, 51, pp. 2144–2155.

Siemann, M., Andersson, L.I., Mosbach, K. (1996), Selective recognition of the herbicide atrazine by noncovalent molecularly imprinted polymers, *J. Agric. Food Chem*. 44, pp. 141-145.

Singh, D.K., Mishra, S. (2009a), Synthesis, characterization and removal of Cd (II) using Cd(II)-ion imprinted polymer, *J. Hazard. Mater*., 164, pp. 1547–1551.

Singh, D.K., Mishra, S. (2009b), Synthesis and characterization of UO_2^{2+}-ion imprinted polymer for selective extraction of UO_2^{2+}, *Anal. Chim. Acta,* 644, pp. 42–47

Singh, V., Kumari, P., Pandey, S., Narayan, T. (2009), Removal of chromium (VI) using poly(methylacrylate) functionalized guar gum, *Bioresour. Technol.*, 100, pp. 1977–1982.

Singleton, Y.L., Rossi, J.A. (1965), Colorimetry of total phenolics with phosphomolybdic-phosphotungestic acid reagent, *Am. J. Enol. Viticult.*, 16, pp. 144–158.

Skoog, D.A., Leary, J.J. (1992), Principles of instrumental analysis, 4th edition, Harcourt Brace College Publisher, pp. 233-244.

Smith, C., Lombard, K.A., Peffley, E.B., Liu, W. (2003), "Genetic Analysis of Quercetin in Onion (*Allium cepa L.*) *Lady Raider*", *Tex. J. Agric. Nat. Res.*, 16, pp. 24–28.

Smith, K. (1990), Soil analysis, morden instrumental techniques, 2nd edition, Marcel Dekker Inc., New York, pp. 63-96.

Smith, R.M. (2002), Extractions with superheated water, *J. Chromatogr. A*, 975, pp. 31-46.

Southard, **G.E.** (2009), Molecularly imprinted polymers (MIPS) for the selective removal of inorganic contaminants from liquids, Patent number US7, 476, 316

SØltoft, **M.,** Christensen, J.H., Nielsen, J., Knuthsen, P. (2009), Pressurized liquid extraction of flavonoids in onions. Method development and validation. *Talanta*, 80, pp. 269–278.

Song, X., Li, J., Wang, J., Chen, L. (2009a), Quercetin molecularly imprinted polymers: Preparation, recognition characteristics and properties as sorbent for solid-phase extraction, *Talanta*, 80(2), pp. 694-702.

Song, X., Wang, J., Zhu J., (2009b), Effect of porogenic solvent on selective performance of molecularly imprinted polymer for quercetin, *Mater. Res.*, 12(3), pp. 299-304.

Srinivas, K., King, J.W., Howard, L.R., Monrad, J.K. (2010), Solubility and solution thermodynamic properties of quercetin and quercetin dihydrate in subcritical water, *J. Food Eng.*, 100, pp. 208-218.

Srinivasan, K., Balasubramanian, N., Ramakrishan, T.V. (1988), Studies on chromium removal by rise husk carbon, *Ind. J. Environ. Health*, 30(40), pp. 376-387.

Stahl, E. (1959), Thin-layer chromatography. IV. Insertion scheme, marginal effect, "acid and base" layers, gradation technic, *Arch . Pharm*., 292, pp. 411-416.

Stefánsson, A., Gunnarsson, I., Giroud, N. (2007), New methods for the direct determination of dissolved inorganic, organic and total carbon in natural waters by Reagent-Free Ion Chromatography and inductively coupled plasma atomic emission spectrometry, *Anal. Chim. Acta*, 582(1), pp. 69–74.

Stoob, K., Singer, H.P., Stettler, S., Hartmann, N., Mueller, S.R., Stamm, C.H. (2006), Exhaustive extraction of sulfonamide antibiotics from aged agricultural soils using pressurized liquid extraction, *J. Chromatogr. A*, 1128 (1-2), pp. 1-9.

Su, H., Li J., Tan, T. (2008), Adsorption mechanism for imprinted ion (Ni^{2+}) of the surface molecular imprinting adsorbent (SMIA), *Biochem. Eng. J.*, 39, pp. 503-509.

Suedee, R., Seechamnanturakit, V., Canyuk, B., Ovatlarnporn, C., Martin, G. P. (2006), Temperature sensitive dopamine-imprinted (*N*,*N*-methylene-bis-acrylamide cross-linked) polymer and its potential application to the selective extraction of adrenergic drugs from urine, *J. Chromatogr., A*, 1114, pp. 239–249.

Sultana, B., Anwar, F. (2008), Flavonols (kaempeferol, quercetin, myricetin) contents of selected fruits, vegetables and medicinal plants, *Food Chem.*, 108, pp. 879–884.

Sun, H.–w., Qiao, F.–x. (2008), Recognition mechanism of water-compatible molecularly imprinted solid-phase extraction and determination of nine quinolones in urine by high performance liquid chromatography, *J. Chromatogr. A*, 1212, pp. 1-9.

Sun, T., Ho, C.-T. (2005), Antioxidant activities of buckwheat extracts, *Food Chem.*, 90, pp. 743–749.

Sun, Z., Schussler, W., Sengl, M., Niessner, R., Knopp, D. (2008), Selective trace analysis of diclofenac in surface and wastewater samples using solid-phase extraction with a new molecularly imprinted polymer, *Anal. Chim. Acta*, 620, pp. 73–81.

Sureshkumar, M.K., Das, D., Mallia, M.B., Gupta, P.C. (2010), Adsorption of uranium from aqueous solution using chitosan-tripolyphosphate (CTPP) beads, *J. Hazard. Mater.*, 184, pp. 65–72.

Svenson, **J.,** Karlsson, J.G., Nicholls, I.A. (2004), H^{-1} nuclear magnetic resonance study of the molecular imprinting of (-)-nicotine: template self-association, a molecular basis for cooperative ligand binding, *J. Chromatogr. A*, 1024, pp. 39-44.

Tamayo, F.G., Casillas, J.L., Martin-Esteban, A. (2005), Evaluation of new selective molecularly imprinted polymers prepared by precipitation

polymerization for the extraction of phenylurea herbicides, *J. Chromatogr. A*, 1069, pp. 173–181.

Tamayo, F.G., Martín-Esteban, A. (2005), Selective high performance liquid chromatography imprinted-stationary phases for the screening of phenylurea herbicides in vegetable samples, *J. Chromatogr. A,* 1098, pp. 116–122.

Tamayo, F.G., Turiel, E., Martin-Esteban, A. (2007), Molecularly imprinted polymers for solid-phase extraction and solid-phase microextraction: recent developments and future trends, *J. Chromatogr. A*, 1152, pp. 32–40.

Tan, C.J., Chua, H. G., Ker, K.H., Tong, Y.W. (2008), Preparation of bovine serum albumin surface-imprinted submicrometer particles with magnetic susceptibility through core-shell miniemulsion polymerization, *Anal. Chem.*, 80, pp. 683–692.

Tan, C.J., Tong, Y.W. (2007), Preparation of superparamagnetic ribonuclease A surface-imprinted submicrometer particles for protein recognition in aqueous media, *Anal. Chem.*, 79, pp. 299–306.

Takekoh, R., Li, W.-H., Burke, N.A.D., Stöver, H.D.H. (2006), Multilayered polymer microspheres by thermal imprinting during microsphere growth, *J. Am. Chem. Soc*. 128, pp. 240-244.

Taty-Costodes, V.C., Fauduet, H., Porte, C., Delacroix, A. (2003), Removal of Cd (II) and Pb (II) ions, from aqueous solutions, by adsorption onto sawdust of Pinus sylvestris, *J. Hazard. Mater.*, B105, pp.121-142.

Teo, C.C., Tan, S.N., Hong Yong, J.W., Hew, C.S., Ong, E.S. (2010), Pressurized hot water extraction (PHWE), *J. Chromatogr. A,* 1217, pp. 2484–2494.

Theodoridis, G., Lasáková, M., Škeříková, V., Tegou, A., Giantsiou, N., Jandera, P. (2006), Molecular imprinting of natural flavonoid antioxidants: Application in solid-phase extraction for the sample pretreatment of natural products prior to HPLC analysis, *J. Sep. Sci*. 29, pp. 2310–2321.

ThermoNicolet Corporation, (2001), Introduction to fourier transform spectrometry, http://mmrc.caltech.edu/FTIR/FTIRintro.pdf., accessed 18 August 2011.

Thomas, D.H., Rohrer, J.S., Jackson, P.E., Pak, T., Scott, J.N. (2002), Determination of hexavalent chromium at the level of the California Public Health Goal by ion chromatography, *J. Chromatogr. A*, 956, pp. 255–259,

Tian, M., Dandan, H., Ho, R.K. (2011), Preparation of molecularly imprinted polymer for extracting flavones from *chamaecyparis obtusa, Anal. Lett.,* 44(5), pp. 737-746.

Tominaga, Y., Kuto, T., Kaya, K., Hosoya, K. (2009), Effective recognition on the surface of a polymer prepared by molecular imprinting using ionic complex, *Macromolecules*, 42, pp. 2911–2915.

Tropicos.org., 2012, Missouri Botanical Garden, http://www.tropicos.org/Name/4002223, accessed 18 January 2012.

Truchado, P., Vit, P., Ferreres, F., Tomas-Barberan, F. (2011), Liquid chromatography–tandem mass spectrometry analysis allows the simultaneous characterization of C-glycosyl and O-glycosyl flavonoids in stingless bee honeys, *J. Chromatogr. A,* 1218, pp. 7601– 7607.

Tunçeli, A., Türker, A.R. (2002), Speciation of Cr (III) and Cr (VI) in water after preconcentration of its 1,5-diphenylcarbazone complex on amberlite XAD-16 resin and determination by FAAS, *Talanta*, 57, pp. 1199-1204.

Turiel, E., Martin-Esteban, A., Tadeo, J.L. (2007), Molecular imprinting-based separation methods for selective analysis of fluoroquinolones in soils, *J. Chromatogr. A,* 1172, pp. 97–104.

Turner, C., Turner, P., Jacobson, G., Almgren, K., Waldeback, M., Sjöberg, P., Nordberg Karlsson, E., Markides, K.E. (2006), Subcritical water extraction and *b*-glucosidase-catalyzed hydrolysis of quercetin glycosides in onion waste, *Green Chem.*, 8, pp. 949–959.

Tutu, **H.,** Cukrowska, E.M., McCarthy, T.S., Hart, R., Chimuka, L. (2009), Radioactive disequilibrium and geochemical modeling as evidence of uranium leching from tailings dumps in the Witwatersrand Basin, *Intern. J. Environ. Anal. Chem.*, 89, pp. 687-703.

Uezu, K., Nakamura, H., Goto, M., Murata, M., Maeda, M., Takagi, M., F. Nakashio, F. (1994) Novel metal ion-imprinted resins prepared by surface template polymerization with W/O emulsion, *J. Chem. Eng. Jpn*. 27, pp. 436-438.

Uğuzdoğan, E., Denkbas, E.B., Kabasakal, O.S. (2010), The use of polyethyleneglycolmethacrylate-co-vinylimidazole (PEGMA-co-VI) microspheres for the removal of nickel (II) and chromium (VI) ions, *J. Hazard. Mater.*, 177, pp. 119–125

Um, W., Icenhower, J.P., Brown, C.F., Serne, R.J., Wang, Z., Dodge, C.J., Francis, A. J. (2010), Characterization of uranium-contaminated sediments from beneath a nuclear waste storage tank from Hanford, Washington: Implications for contaminant transport and fate, *Geochim. Cosmochim. Acta,* 74, pp. 1363–1380.

Unnithan, M.R., Anirudhan, T.S. (2001), The kinetics and thermodynamics of sorption of chromium (VI) onto the iron (III) complex of a carboxylated polyacrylamide-grafted sawdust, *Ind. Eng. Chem. Res*. 40 (12), pp. 2693-2701.

U.S. Environmental Protection Agency. (1999). *Integrated Risk Information System (IRIS) on Chromium VI*. National Center for Environmental Assessment, Office of Research and Development, Washington, DC.

U.S. Library of Congress, http://countrystudies.us/south-africa/66-metals.htm, accesed 23 March 2009.

Vallverdu-Queralt, A., Olga, J., Di Lecce, G., Andrés-Lacueva, C., Lamuela-Raventós, R.M., (2011), Screening of the polyphenol content of tomato-based products through accurate-mass spectrometry (HPLC-ESI-QTOF), *Food Chem*., 29(3), pp. 877-883.

van Horn, J.D., Huang, H. (2006), Uranium (VI) bio-coordination chemistry from biochemical, solution and protein structural data, *Coord. Chem. Rev*., 250, pp. 765-775.

Vasapollo, G., Del Sole, R., Mergola, L., Rosaria Lazzoi, M., Scardino, A., Scorrano, S., Mele, G. (2011), Molecularly imprinted polymers: Present and future prospective, *Int. J. Mol. Sci*. 12, pp. 5908-5945.

Verma, A.R., Vijayakumar, M., Mathela, C.S., Rao, C.V. (2009), In vitro and in vivo antioxidant properties of different fractions of *Moringa oleifera* leaves, *Food Chem. Toxicol.*, 47, pp. 2196–2201

Villasenor, **I.** (1994), Bioactive metabolites from *Moringa oleifera* Lam, *Kimika*, 10, pp. 47–52.

Vincent, T., Guibalf, E. (2001), Cr (VI) extraction using Aliquat 336 in a hollow fiber module made of chitosan, *Ind. Eng. Chem. Res.* 40, pp. 1406-1411.

Wach, A., Pyrzynska, K., Biesaga, M. (2007), Quercetin content in some food and herbal samples, *Food Chem.*, 100(2), pp. 699-704**.**

Walle, T., Walle, U.K., Halushka, P.V. (2001), Carbon dioxide is the major metabolite of quercetin in humans, *J. Nutr*., 131(10), pp. 2648-2652.

Walker, N.R., Linman, M.J., Timmers, M.M., Dean, S.L., Burkett, C.M., Lloyd, J.A., Keelor, J.D., Baughman, B.M., Edmiston, P.L. (2007), Selective detection of gas-phase TNT by integrated optical waveguide spectrometry using molecularly imprinted sol-gel sensing films, *Anal. Chim. Acta*, 593, pp. 82–91.

Wan, **J.M.,** Tokunaga, T.K., Brodie, E., Wang, Z.M., Zheng, Z.P., Herman, D., Hazen, T.C., Firestone, M.K., Sutton, S.R. (2005), Reoxidation of bioreduced uranium under reducing conditions, *Environ. Sci. Technol.*, 39, pp. 6162–6169.

Wang, G., Liu, J., Wang, X., Xie, Z., Deng, N. (2009a), Adsorption of uranium (VI) from aqueous solution onto cross-linked chitosan, *J. Hazard. Mater*., 168, pp. 1053–1058.

Wang, J., Cormack, P.A.G., Sherrington, D.C., Khoshdel, E. (2003), Monodisperse, molecularly imprinted polymer microspheres prepared by precipitation polymerization for affinity separation applications, *Angew. Chem. Int. Ed. Engl.*, 42, pp. 5336–5338.

Wang, L.-L., Wang, J.-Q., Zheng, Z.-X., Xiao, P. (2010), Cloud point extraction combined with high-performance liquid chromatography for speciation of chromium (III) and chromium (VI) in environmental sediment samples, *J. Hazard. Mater*., 177, pp. 114–118.

Wang, S., Li, Y., Ding, M., Wu, X., Xu, J., Wang, R., Wen, T., Huang, W., Zhou, P., Ma, K., Zhou, X., Du, S. (2011), Self-assembly molecularly imprinted polymers of 17 β-estradiol on the surface of magnetic nanoparticles for selective separation and detection of estrogenic hormones in feeds, *J. Chromatogr. B,* 879, pp. 2595– 2600.

Wang, X., Wang, L., He, X., Zhang, Y., Chen, L. (2009b), A molecularly imprinted polymer-coated nanocomposite of magnetic nanoparticles for estrone recognition, *Talanta*, 78, pp. 327–332.

Wei, S., Jakusch, M., Mizaikoff, B. (2007), Investigating the mechanisms of 17 beta-estradiol imprinting by computational prediction and spectroscopic analysis, *Anal. Bioanal. Chem.,* 389(2), pp. 423-431.

Weiss, J., Weiss, T. (2005). Handbook of Ion Chromatography, Third, Completely Revised and Enlarged Edition. John Wiley and Sons, Inc. 931p. ISBN: 3-527-28701-9, pp. 6.

Weiss, R., Molinelli, A., Jakusch, A.M., Mizaikoff, B. (2002), Molecular imprinting and solid phase extraction of flavonoid compounds, *Bioseparation,* 10, pp. 379–387.

Whitcombe, M.J., Rodriguez, M.E., Villar, P., Vulfson, E.N. (1995), A new method for the introduction of recognition site functionality into polymers prepared by molecular imprinting - synthesis and characterization of polymeric receptors for cholesterol, *J. Am. Chem. Soc.* 117, pp. 7105-7114.

WHO, 1998, http://www.who.int/water_sanitation_health/dwq/chemicals/ uranium290605. pdf, accessed 07 April, 2009.

Willis, R.C. (2002), Today's Chemist at work, Historica chromatographica, *Am. Chem. Soc*., February 2002.

Wilson, T. (1999), Whole foods, antioxidants and health. In Antioxidants, Human Health and Diseases, pp. 141–150.

Winnik, M.A., Lukas, R., Chen, W.F., Furlong, P., Croucher, M.D. (1987), Studies of the dispersion polymerization of methyl-methacrylate in nonaqueous media, *Makromol. Chem., Macromol. Symp*., 10, pp. 483-501.

Wu, L.Q., Li, Y.Z. (2004), Study on the recognition of templates and their analogues on molecularly imprinted polymer using computational and conformational analysis approaches, *J. Mol. Recognit.,* 17(6), pp. 567-574.

Wu, **L.,** Sun, B., Li, Y., Chang, W. (2003), Study properties of molecular imprinting polymer using a computational approach, *Analyst*, 128, pp. 944–949.

Wu, S., Xu, Z., Yuan, Q., Tang, Y., Zuo, X., Lai, J. (2011), Recognition characteristics of molecularly imprinted microspheres for triazine herbicides using hydrogen-bond array strategy and their analytical applications for corn and soil samples, *J. Chromatogr. A*, 1218, pp. 1340–1346.

Wulff, G., Sarhan, A. (1972), Use of polymers with enzyme-analogous structures for resolution of racemates, Angew. *Chem. Int. Ed.*, 11, pp. 341-341.

Wulff, G. (2002), Enzyme-like catalysis by molecular imprinted polymers, *Chem. Rev*. 102 (1), pp. 1-27.

www.epa.gov/radiation/radionuclides/uranium.html, accessed 12 September 2009.

www.pembina.org/pub/1503, accessed 14 September 2009.

Xia, Y.-q., Guo, T.-y., Song, M.-d., Zhang, B.-h., Zhang, B.-l. (2006), Selective separation of quercetin by molecular imprinting using chitosan beads as functional matrix, *React. Funct. Polym.*, 66, pp. 1734–1740.

Xie, J., Chen, L., Li, C., Xu, X. (2003), Selective extraction of functional components derived from herb in plasma by using a molecularly imprinted polymer based on 2,2-bis(hydroxymethyl)butanol trimethacrylate, *J. Chromatogr. B*, 788, pp. 233–242.

Xie, **J.,** Zhu, L., Luo, H., Zhou, L., Li, C., Xu, X. (2001), Direct extraction of specific pharmacophoric flavonoids from gingko leaves using a molecularly imprinted polymer for quercetin, *J. Chromatogr. A*, 934, pp. 1-11.

Xu, X., Kuang, D., Liu, L., Deng, Q. (2007), Selective adsorption of norfloxacin in aqueous media by an imprinted polymer based on hydrophobic and electrostatic interactions, *J. Pharmaceut. Biomed.*, 45, pp. 54–61.

Yan, H., Qiao, F., Row, K.H. (2007), Molecularly imprinted-matrix solid-phase dispersion for selective extraction of five fluoroquinolones in eggs and tissue, *Anal. Chem.* 79, pp. 8242–8248.

Yan, H., Row, K.H., Yang, G. (2008), Water-compatible molecularly imprinted polymers for selective extraction of ciprofloxacin from human urine, *Talanta*, 75, pp. 227–232.

Yan, H., Tian M., Row K.H. (2009), Selective solid-phase extraction of glabridin from licorice root using molecularly imprinted polymer, *Sep. Sci. Technol.* 44(2), pp. 359-369

Yao, J., Li, X., Qin, W. (2008), Computational design and synthesis of molecular imprinted polymers with high selectivity for removal of aniline from contaminated water, *Anal. Chim. Acta*, 610, pp. 282–288.

Ye, **L.,** Cormack, P.A.G., Mosbach, K. (1999), Molecularly imprinted monodisperse microspheres for competitive radioassay, *Anal. Commun.,* 36, pp. 35–38.

Ye, **L.,** Cormack, P.A.G., Mosbach, K. (2001), Molecular imprinting on microgel spheres, *Anal. Chim. Acta,* 435, pp. 187–196.

Ye, L., Mosbach, K. (2001a), The technique of molecular imprinting –principle, state of art, and future aspects, *J. Incl. Phenom. Macromol.,* 41, pp. 107-113.

Ye, L., Mosbach, K. (2001b), Molecularly imprinted microspheres as antibody binding mimics, *React. Funct. Polym*. 48(12), pp. 149-157.

Yen, G.C., Chuang, D.Y. (2000), Antioxidant properties of water extracts from *Cassia tora* L. in relation to the degree of roasting, *J. Agric. Food Chem.,* 48, pp. 2760-2765.

Yen, G.C., Duh, P.D., Tsai, C.L. (1993), Relationship between antioxidant activity and maturity of peanut hulls, *J. Agric. Food Chem.,* 41, pp. 67-70.

Yen, G.C., Wu, S.C., Duh, P.D. (1996), Extraction and identification of antioxidant components from the leaves of mulberry (*Morus alba* L.). *J. Agric. Food Chem.,* 44, pp. 1687-1690.

Yeung, E.S., Synovec, R.E. (1986), Detectors for liquid-chromatography, *Anal Chem.,* 58, pp. 1237A-1256A.

Yilmaz, E., Adali, T., Yilmaz, O., Bengisu, M. (2007), Grafting of poly(triethylene glycol dimethacrylate) onto chitosan by ceric ion initiation, *React. Funct. Polym.,* 67, pp. 10–18.

Ying, L-Y., Jiang, H.-L., Zhou, S.-c., Zhou, Y. (2011), Ionic liquid as a complexation and extraction medium combined with high-performance liquid chromatography in the evaluation of chromium (VI) and chromium (III) speciation in wastewater samples, *Microchem. J.,* 98, pp. 200–203.

Yoshimatsu, K., Reimhult, K., Krozer, A., Mosbach, K., Sode, K., Ye, L. (2007), Uniform molecularly imprinted microspheres and nanoparticles prepared by precipitation polymerization: The control of particle size suitable for different analytical applications, *Anal. Chim. Acta*, 584, pp. 112–121.

Yu, C., Ramström, O., Mosbach, K. (1997), Enantiomeric recognition by molecularly imprinted polymers using hydrophobic interactions, *Anal. Lett.*, 30:12, pp. 2123-2140.

Yu, K.Y., Tsukaghoshi, K., Maeda, M., Takagi, M. (1992), Metal ion-imprinted microspheres prepared by reorganization of the coordinating groups of the surface, *Anal. Sci.* 8, pp. 701–703.

Zaibunnisa, **A.H.,** Norashikin, S., Mamot, S., Osman, H. (2009), An experimental design approach for the extraction of volatile compounds from turmeric leaves (Curcuma domestica) using pressurised liquid extraction (PLE), *LWT Food Sci. Technol.*, 42, pp. 233-238.

Zbiral, J., Nemec, P., (2009), Comparison of some soil extractants for determination of boron, *Commun. Soil Sci. Plant Anal.*, 40, pp. 96-105.

Zhai, C., Lu, Q., Chen, X., Peng, Y., Chen, L., Du, S. (2009), Molecularly imprinted layer-coated silica nanoparticles toward highly selective separation of active diosgenin from Dioscorea nipponica Makino, *J. Chromatogr., A*, 1216, pp. 2254–2262.

Zhang, H., Ye, L., Mosbach, K. (2006), Non-covalent molecular imprinting with emphasis on its application in separation and drug development, *J. Mol. Recognit*. 19(4), pp. 248–259.

Zhang, H.T., Song, T., Zong, F.L., Chen, T.C., Pan, C.P. (2008a), Synthesis and characterization of molecularly imprinted polymers for phenoxyacetic acids, *Int. J. Mol. Sci*., 9, pp. 98–106.

Zhang, M.L., Me, J.P., Zhou, Q., Chen, G.Q., Liu, Z. (2003), Online solid-phase extraction of ceramides from yeast with ceramide III imprinted monolith, *J. Chromatogr. A,* 984, pp. 173-183.

Zhang, N., Hu, B., Huang, C.Z. (2007), A new ion- imprinted silica gel sorbent for on-line selective solid-phase extraction of dysprosium (III) with detection by inductively coupled plasma-atomic emission spectrometry, *Anal. Chim. Acta*, 597, pp. 12-18.

Zhang, N., Suleiman, J.S., He, M., Hu, B. (2008b), Chromium (III)-imprinted silica gel for speciation analysis of chromium in environmental water samples with ICP-MS detection, *Talanta*, 75, pp. 536–543.

Zhang, Y., Li, Y., Hu, Y., Li, G., Chen, Y. (2010a), Preparation of magnetic indole-3-acetic acid imprinted polymer beads with 4-vinylpyridine and β-cyclodextrin as binary monomer *via* microwave heating initiated polymerization and their application to trace analysis of auxins in plant tissues, *J. Chromatogr. A*, 1217, pp. 7337–7344

Zhang, Z., Zhang, Y., Tan, W., Li, G., Hu, Y. (2010b), Preparation of styrene-co-4-vinylpyridine magnetic polymer beads by microwave irradiation for analysis of trace 24-epibrassinolide in plant samples using high performance liquid chromatography, *J. Chromatogr. A*, 1217, pp. 6455–6461.

Zhao, Y., Liu, C., Feng, M., Chen, Z., Li, S., Tian, G., Wang, L., Huang, J., Li, S. (2010a), Solid phase extraction of uranium (VI) onto benzoylthiourea-anchored activated carbon, *J. Hazard. Mater.*, 176, pp. 119–124

Zhao, Y.-G., Shen, H.-Y., Pan, S.-D., Hu, M.-Q. (2010b), Synthesis, characterization and properties of ethylenediamine-functionalized Fe_3O_4 magnetic polymers for removal of Cr (VI) in wastewater, *J. Hazard. Mater.*, 182, pp. 295–302.

Zheng, H., Zhang, D., Wang, W.Y., Fan, Y.Q., Li J., Han, H.P. (2007), Highly selective determination of palladium (II) after preconcentration using Pd(II)-imprinted functionalized silica gel sorbent prepared by a surface imprinting technique, *Microchim. Acta* 157, pp. 7-11.

Zhong, **L.R.L.,** Liui, C.X., Zachara, J.M., Kennedy, D.W., Szecsody, J.E., Wood, B. (2005), Oxidative remobilization of biogenic uranium (IV) precipitates: Effects of iron (II) and pH, *J. Environ. Qual.*, 34, pp. 1763–1771.

Zhou, J., Ma, C., Zhou, S., Ma, P., Chen, F., Qi, Y., Chen, H. (2010), Preparation, evaluation and application of molecularly imprinted solid-phase microextraction monolith for selective extraction of pirimicarb in tomato and pear, *J. Chromatogr. A*, 1217, pp. 7478–7483

Zhou, L., Shang, C., Liu, Z., Huang, G., Adesina, A.A. (2011), Selective adsorption of uranium (VI) from aqueous solutions using the ion-imprinted magnetic chitosan resins. *J. Colloid. Interf. Sci.*, 366**,** pp. 165-72.

Zhu, L., Chen, L., Xu, X. (2003), Application of a molecularly imprinted polymer for the effective recognition of different anti-epidermal growth factor receptor inhibitors, *Anal.Chem*., 75, pp. 6381-7.

Zhu, L., Duan, W., Xu, J., Zhu, Y. (2011a), Extraction of actinides and lanthanides by supercritical fluid, *J. Eng. Gas Turb. Power*, 33, pp. 052903-8.

Zhu, L., Xu, X. (2003), Selective separation of active inhibitors of epidermal growth factor receptor from Caragana Jubata by molecularly imprinted solid-phase extraction, *J. Chromatogr. A*, 991, pp. 151–158.

Zhu, Q.H., Huang, D.D., Li, L., Yin, Y.G. (2010), Synthesis of molecularly imprinted polymers for the application of selective clean-up vinblastine from *Catharanthus roseus* extract, *Sci. China-Chem.*, 53(12), pp. 2587-2592.

Zhu, Q.-h., He, J.-f., Feng, J.-y. (2007), Optimization of the process parameters of synthesis of vinblastine imprinted polymer, *Eur. Polym. J.*, 43, pp. 4043–4051

Zhu, T., Row, K.H. (2011), Preparation of amino-modified active carbon cartridges and their use in the extraction of quercetin from Oldenlandia diffusa, *J. Pharmaceut. Biomed.*, 56, pp. 713– 720.

Zhu, T., Li, S., Row, K.H. (2011b), Molecularly imprinted monolithic material for the extraction of three organic acids from Salicornia *herbacea* L., *J. Appl. Polym. Sci.*, 121 (3), pp. 1691-1696.

Zhu, Y.-G., Chen, B.-D. (2009), Principles and technologies for remediation of uranium-contaminated environments. in: Radioactivity in the Environment, vol. 14, Remediation of Contaminated Environments, (G. Voigt and S. Fesenko, Eds), pp. 357-375.

Zill-e-Huma, Vian, M.A., Fabiano-Tixier, A., Elmaataoui, M., Dangles, O., Chemat, F., (2011) A remarkable influence of microwave extraction: Enhancement of antioxidant activity of extracted onion varieties, *Food Chem.*, 127, pp. 1472–148.

Zimmerman, S.C., Lemcoff, N.G. (2004), Synthetic hosts via molecular imprinting - are universal synthetic antibodies realistically possible? *Chem. Commun*., 1, pp. 5–14.

ZoBell, C.E. (1946), Studies on redox potential of marine sediments. AAPG Bulletin**.** 1946; no. 30: DOI: 10.1306/3D933808-16B1-11D7-8645000102C1865D.

Zu, Y., Li, C., Fu, Y., Zhao, C. (2006), Simultaneous determination of catechin, rutin, quercetin kaempferol and isorhamnetin in the extract of sea buckthorn (*Hippophae rhamnoides* L.) leaves by RP-HPLC with DAD, *J. Pharmaceut. Biomed.*, 41, pp. 714–719.

Zurera, G., Moreno, R., Salmeron, J., Pozo, R. (1989), Heavy metal uptake from greenhouse border soils for edible vegetables, *J. Food Sci. Agric.*, 49, pp. 307–314.

APPENDIX I

Selective removal of chromium (VI) from sulphates and other metal anions using an ion-imprinted polymer

V Pakade[1], E Cukrowska[1], J Darkwa[2], N Torto[3] and L Chimuka[1]*

[1]*School of Chemistry, University of the Witwatersrand, P/Bag 3, WITS 2050, Johannesburg, South Africa*
[2]*Department of Chemistry, University of Johannesburg, PO Box 524, Auckland Park 2006, South Africa*
[3]*Department of Chemistry, Rhodes University, PO Box 94, Grahamstown, 6140, South Africa*

Abstract

A linear copolymer was prepared from 4-vinylpyridine and styrene. An ion-imprinted polymer (IIP) specific for Cr (VI) adsorption was prepared by copolymerisation of the quaternised linear copolymer (quaternised with 1,4-chlorobutane), 2-vinylpyridine functional monomer and ethylene glycol dimethacrylate (EGDMA), as the cross-linking monomer, in the presence of 1,1'-azobis(cyclohexanecarbonitrile) as initiator. Ammonium dichromate and aqueous methanol were used as a template and porogenic solvent, respectively. Leaching of the chromate template from the polymer particles was achieved with successive stirring of the ion-imprinted polymer (IIP) particles in 4 M HNO_3 solutions to obtain leached materials, which were then used for selective rebinding of Cr (VI) ions from aqueous solutions. Similarly, the non-imprinted polymer/control polymer (NIP/CP) material was also prepared under exactly the same conditions as the IIP but without the chromate anion template. Various parameters, such as solution pH, initial concentration, aqueous phase volume, sorbent dosage, contact time and leaching solution volumes, were investigated. Scanning electron microscopy (SEM), Fourier Transform Infrared (FTIR) spectroscopy, BET surface area and pore size analysis were used for the characterisation of IIP (both unleached and leached) and CP materials. Optimal parameters were as follows: solution pH, 3; contact time, 120 min; eluent, 20 mℓ of 0.1 M NaOH; and sorbent amount, 125 mg. Maximum retention capacity of IIP and CP was 37.58 and 25.44 $mg \cdot g^{-1}$, respectively. The extraction efficiencies of the IIP and CP were compared using a batch and SPE mode of extraction. In the absence of high concentrations of ions, especially sulphate ions, both CP and IIP demonstrated no differences in binding of Cr (VI), which was almost 100%. However, in the presence of high concentrations of sulphate ions, the selectivity on the CP completely collapsed. The study clearly demonstrates the suitably of the developed IIP for selective extraction of Cr (VI) in complex samples such as those from acid mine drainage. The selectivity was also compared by direct injection of the real-world sample, both spiked and non-spiked, into that obtained after IIP selective extraction. Despite the method's very low detection limits for direct injection (below 1 $\mu g \cdot \ell^{-1}$), no Cr (VI) was obtained. However, after IIP selective extraction, spiked Cr (VI) was detected in the spiked sample.

Keywords: Ion-imprinted polymer, chromium (VI), acid mine drainage, selectivity

Introduction

Hexavalent chromium Cr (VI)), the most toxic and carcinogenic form of chromium, exists in most aquatic environments as water soluble oxyanions, $HCrO_4^{1-}$ or CrO_4^{2-}. Pulmonary congestion, liver damage, vomiting, and severe diarrhoea are some of the known health problems associated with Cr (VI) (Raji and Anirudhan, 1998). Chromium is mostly present in the +3 oxidation state in chromite, but can also exist in other oxidation states, ranging from -2 to +6 in different samples. Of these various oxidation states that chromium can exhibit, only the hexavalent and trivalent forms are known to have environmental importance (Goyal et al., 2003).

Chromium in the +6 oxidation state is regarded as a genotoxic, mutagenic and carcinogenic to humans and ecosystems (Chakraborty and Kumar, 2009) due to its solubility and a mobility which is 500 times (Sarin and Pant, 2006) and toxicity which is 100 times more than that of Cr (III) (Unnithan et al., 2001). Furthermore, Cr (VI) is declared as a Group 1 carcinogen by the US Environmental Protection Agency (US EPA, 1999), while Cr (III) is known to be important for mammalian functions as it helps to maintain glucose, lipid and protein metabolism (Ramnani and Sabharwal, 2006). Due to its toxicity, hexavalent chromium has to be strictly regulated and as such the maximum permissible levels set out by the US EPA for both drinking water and wastewater are 0.05 $mg \cdot \ell^{-1}$ for Cr (VI) and 5 $mg \cdot \ell^{-1}$ for Cr (III), respectively (Acar and Malkoc, 2004). Anthropogenic sources, such as mining operations, leather tanning, metal plating, water cooling and pigment manufacturing, are responsible for water and soil contamination by chromium (Katz and Salem, 1994).

Various technologies, have been used for the removal of Cr (VI) including: reduction of Cr (VI) to Cr (III), followed by Cr (III) precipitation under alkaline conditions (Kratochvil et al., 1998); membrane separation, extraction, and sorption (Patterson, 1985); and sorption by activated carbon (Huang and Wu, 1977), ion exchangers (Santiago et al., 1992) and biosorbents (Brower et al., 1997). However, adsorption and ion exchange are the most common techniques used for the removal of Cr (VI) from aqueous environments (Neagu and Mikhalovsky, 2010). A range of natural and synthetic sorbents have been used (Srinivasan et al., 1988; Fang et al., 2007; Qian et al., 2000; Ramnani and Sabharwal, 2006; Deng and Bai, 2004; Raji and Anirudhan, 1998). Similarly, the use of ion exchangers for the removal of Cr (VI) has been reported in the literature, including the use of the commercial Aliquat

* To whom all correspondence should be addressed.
☎ +27 11 717-6703; fax: +27 11 717-6749;;
e-mail: luke.chimuka@wits.ac.za
Received 13 January 2011; accepted in revised form 6 October 2011.

http://dx.doi.org/10.4314/wsa.v37i4.11
Available on website http://www.wrc.org.za
ISSN 0378-4738 (Print) = Water SA Vol. 37 No. 4 October 2011
ISSN 1816-7950 (On-line) = Water SA Vol. 37 No. 4 October 2011

336 (Vincent and Guibalf, 2001) and Lewatit-anion exchangers (Pehlivan and Cetin, 2009). Incomplete metal removal, expense, swelling (in case of resins), etc., are some of the drawbacks associated with some of the techniques. Ion-imprinted polymers (IIPs) offer several advantages, including high thermal stability and mechanical strength, over other polymeric materials.

The use of quaternised poly-(4-vinylpyridine) polymers for the removal of anionic species such as chromate, arsenate and perchlorate has been documented (Mitchell et al., 2004; Cannon et al., 2005). The quaternised polymeric molecules are known to possess both the hydrophobic groups and ionic moieties capable of undergoing ion exchange and ion pairing reactions, in aqueous environments, with the anionic species present (Fang et al., 2007). The reason for this is that, after quaternisation, the electron-deficient pyridine ring renders the pyridyl-N more attractive to anions than amine-N (Fang et al., 2007). Of particular interest to this study is the removal Cr (VI) from aqueous environmental samples using quaternised poly(4-vinylpyridine) incorporated in a molecular imprinted polymer backbone. This work is different from the studies reported by Fang et al. (2007) and Gang et al. (2000), who also used quaternised poly(4-vinylpyridine) for the removal of Cr (VI) from aqueous solutions – in the case reported by the former, the polymer was coated on activated carbon and in the case reported by the latter, the polymer was coated on silica gel particles. Ion-imprinted polymer backbones offer the sorbent stability in both alkaline and acidic conditions, as it is known that chromate can exist as $HCrO_4^-$ and CrO_4^{2-} depending on concentration and pH. Also, imprinting will improve the selectivity and pre-concentration effect, as compared to non-imprinted resins.

Experiments

Instrumentation

An ion chromatography system LC-CaDI 22-14 from Bischoff (Leonberg, Germany) equipped with a Lambda 1010 UV-Vis absorbance detector was used for this work. The system consisted of an LC gradient mixer, 2 x HPLC compact pumps and a Variotherm. For system control and data collection a McDAcq32 Control chromatography workstation was used. An isocratic mode of elution was employed. A Dionex IonPac® AG 7 (4 x 50 mm) guard column and Dionex IonPac® AS7 (4 x 250 mm) analytical column, all from Dionex (Sunnyvale, CA, USA) were used for all separations.

766 Calimatic pH meter from Knick (Berlin, Germany) was used for pH measurements. FTIR spectra were recorded in the frequency range of 4 000 to400 cm^{-1} using a Bruker FTIR spectrometer, Model Tensor 27 (Ettlingen, Germany) and spectra were recorded in the solid state.

Materials and reagents

A stock solution (1 000 $mg \cdot \ell^{-1}$) of Cr (VI) was prepared by dissolving dried potassium dichromate, $K_2Cr_2O_7$ (analytical reagent grade) in Milli-Q water. Working solutions were prepared daily from the stock solution through serial dilutions. The stock solution was stored at 4°C when not in use. The pH was adjusted using dilute HCl or NaOH solutions. 1,4-Dichlorobutane from Fluka (Buchs, Switzerland), 1,5-diphenylcarbazide, 2-vinylpyridine (2-VP), 4-vinylpyridine (4-VP), ethylene glycol dimethacrylate (EGDMA), styrene and 1,1'-azobis(cyclohexanecarbonitrile) were used (all from Aldrich). Vinylpyridines were vacuum distilled prior to use. All other reagents were of AR grade, mostly from Merck. All HPLC solutions were filtered through a 0.45 µm filter paper.

Preparation of a linear copolymer of 4-vinylpyridine and styrene

A linear polymer was prepared using a method reported by Li et al. (2005) with minor modifications. 4-vinylpyridine (3.154 g, 30 mmol), styrene (4.262 g, 30 mmol) and 1,1'-azobis(cyclohexane carbonitrile) (50 mg) were dissolved in chloroform (12 mℓ) to form a homogeneous solution. The mixture was purged with N_2 for 10 min; then thermal polymerisation was effected at 60°C for 12 h. The resulting solution was diluted with chloroform and precipitated from petroleum ether (boiling point, 30-70°C), filtered and dried under vacuum to give a light orange product (3.384 g).

Preparation of ion-imprinted quaternised polymer

A linear copolymer of 4-vinylpyridine and styrene (200 mg), ammonium dichromate (3 mmol) and 1,4-dichlorobutane (DCB) (18 mmol) were dissolved in methanol (15 mℓ) for 30 min. EGDMA (18 mmol), 2-VP (2 mmol) and 50 mg 1,1'- azobis(cyclohexane carbonitrile) were added while the solution was stirred under a stream of N_2 in ice for 10 min. Polymerisation was allowed to continue at 65°C for 48 h. A black solid product was obtained, which was then washed with MeOH and water to remove unreacted reagents. Leaching of the chromate was afforded by the use of 4 M HNO_3. The product was ground, crushed and wet-sieved in dichloromethane through 53-90 µm. The CP was prepared in the same manner but omitting ammonium dichromate. The CP polymer was also treated with similar solutions to those used for treating the IIP and both were dried overnight at 55°C. The prepared polymer was characterised by FTIR, among other techniques (Li et al., 2005). Schematic representation of IIP preparation is show in Scheme 1.

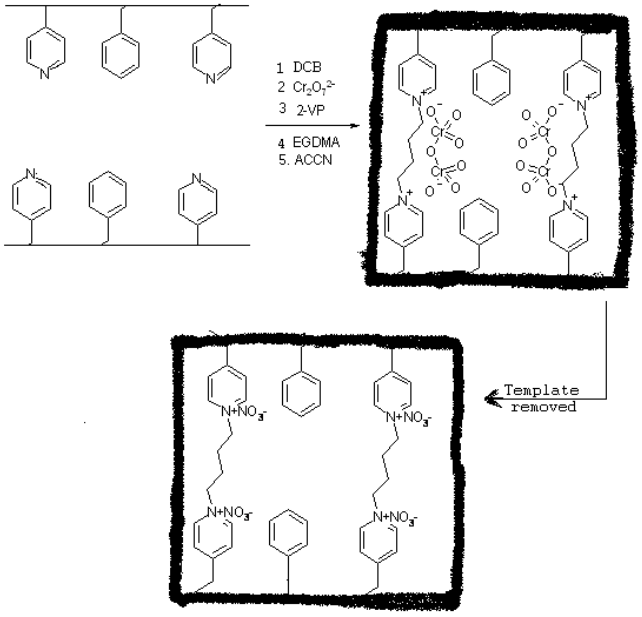

Scheme 1
Diagrammatic representation of IIP preparation.

http://dx.doi.org/10.4314/wsa.v37i4.11
Available on website http://www.wrc.org.za
ISSN 0378-4738 (Print) = Water SA Vol. 37 No. 4 October 2011
ISSN 1816-7950 (On-line) = Water SA Vol. 37 No. 4 October 2011

Adsorption studies

Batch adsorption studies were performed by stirring 20 mg of IIP or CP in a reaction vial containing 25 mℓ metal ion solution for 1 h at pH 2.6 and at a temperature of 25.5°C. The pH of the solutions was adjusted using dilute HCl and NaOH solutions. The concentration of unextracted Cr (VI) ions in solution was determined by IC-HPLC with post-column derivatisation. Adsorption equilibrium data obtained by varying Cr (VI) initial concentration (0-300 mg·ℓ$^{-1}$) were used to calculate maximum adsorption capacity for the IIP and CP at optimum conditions. Adsorption capacity of each metal was measured and calculated by the following equation (Birlik et al., 2007):

$$Q = \frac{(C_o - C_e)V}{W} \quad (1)$$

where:

C_o and C_e are the initial and final concentrations, respectively
V is the volume of the solution used for the extraction
W is the mass of the polymer used for extraction.

Per cent recovery (R) was calculated using the following equation:

$$\% R = \left[\frac{C_o - C_e}{C_o}\right] \text{x } 100\% \quad (2)$$

Optimisation studies

The effect of amount of polymer (20-125 mg), solution phase volume (25-700 mℓ), contact time (10-90 min) and pH (1-4) of solution was studied. In all experiments 1.00 mg·ℓ$^{-1}$ of chromium (VI) present in aqueous phase was stirred with the appropriate amount of polymer, typically 20 mg of IIP/ CP. The pH of the solution was controlled using 0.1 M HCl and 0.1 M NaOH.

Surface area measurements

The surface area of leached IIP and CP was measured using BET instrument (Micromeritics Tristar). At least 0.3 g of sample was degassed in N_2 at 150°C for 4 h prior to analysis, using a Micromeritics Flow Prep 060 sample degas system. The surface areas and pore size distributions were then obtained at −196°C. The pore size distribution for specific surface areas of the sample was determined via N_2 adsorption/desorption according to the BET method, using a Micromeritics Tristar surface area and porosity analyser. In order to confirm the accuracy of the results, the analysis was repeated at least twice for all samples and the measurements were in good agreement. The specific surface area was calculated from the experimental values obtained from the desorption step.

Selectivity studies

In order to examine the selectivity of the prepared IIP, competitive adsorption of Cl^-, F^-, NO_2^-, NO_3^-, SO_4^{2-} and PO_4^{3-} with respect to Cr (VI) was studied. The studies were conducted in a multi-element mixture and in binary phases involving Cr (VI) and the respective anions. For each experiment, 20 mg of IIP or CP in 25 mℓ of the abovementioned solutions was stirred for 1 h in reaction vials and the pH was adjusted to pH 2.63 using 0.1 M HCl. Initial solution concentration was 5 mg·ℓ$^{-1}$. The experiments were performed in a batch mode at optimum conditions and the remaining concentrations of each anion were measured.

Distribution coefficients (K_d) of Cl^-, F^-, NO_2^-, NO_3^-, SO_4^{2-}, PO_4^{3-} and Cr (VI) were calculated as:

$$K_d = \frac{(C_o - C_e)V}{C_o W} \quad (3)$$

where:

K_d is the distribution coefficient (mℓ·g^{-1}) and the other variables are as described for Eqs. (1) and (2).

According to Birlik et al. (2007) Eq. (3) can be used to calculate the selectivity coefficient for the binding of a metal ion in the presence of other competitive ions, from equilibrium binding data:

$$K = \frac{K_d(\text{Cr(VI)})}{K_d(B)} \quad (4)$$

where:

K is the selectivity coefficient and
B represents Cl^-, F^-, NO_2^-, NO_3^-, SO_4^{2-} and PO_4^{3-} anions.

The value of K gives an indication as to how selective the polymer is for Cr (VI) ions in the presence of other anionic species in solution. Furthermore, the relative selectivity coefficient of IIP against CP was calculated from the following equation (Birlik et al., 2007):

$$K' = \frac{K_{imprinted}}{K_{non\text{-}imprinted}} \quad (5)$$

where:

$K_{imprinted}$ and $K_{non\text{-}imprinted}$ are the selectivity coefficients of the IIP and CP, respectively. The value of K' represents the enhanced effect of imprinting on selectivity and adsorption affinity for the template compared to the non-imprinted polymer.

Results and discussion

Characterisation

FTIR analysis

The FTIR spectra of CP leached and unleached IIP (Fig. 1) all show a similar backbone indicative of the high levels of EGDMA cross-linking reagent used. The characteristic absorption bands in the range between 2 958 and 2852 cm^{-1} in all polymers could be ascribed to methyl (C-H) stretching vibration absorption peaks, due to 1,4-dichlorobetane cross-linking agent. All 3 polymers show a strong vibration frequency at about 1 720 cm^{-1}, attributed to the carbonyl group of EGDMA polymers, and another distinctive vibration at 1 150 cm^{-1} assigned to C-O of EGDMA. In all spectra, a C=N band in pyridine, usually at 1 600 cm^{-1}, is displaced to higher wave numbers (1 636 cm^{-1}) due to quaternisation (Li et al., 2005). However, this band has low intensity in the unleached IIP indicating the onset of nitrogen–metal coordination bonds, which is in agreement with studies conducted by Ramos et al. (2000).

Other vibrations of interest are at 1 454 cm^{-1} (CP and leached IIP) and 1 438 cm^{-1} (unleached IIP) assigned to C-C/ N-C. More important is the presence of a broad band at 3 198 cm^{-1} , and the bands between 900 and 778 cm^{-1} in the unleached IIP only; these could all be linked to the presence of Cr (VI) in the polymer as they are absent for both the leached and control polymer. This is in agreement with Goudarzian et al. (1996)

http://dx.doi.org/10.4314/wsa.v37i4.11
Available on website http://www.wrc.org.za
ISSN 0378-4738 (Print) = Water SA Vol. 37 No. 4 October 2011
ISSN 1816-7950 (On-line) = Water SA Vol. 37 No. 4 October 2011

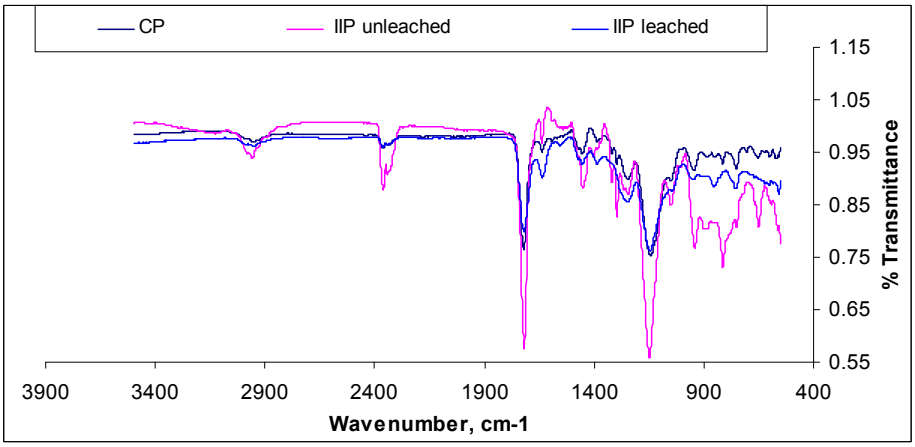

Figure 1
FTIR spectra of CP, leached IIP and unleached IIP

(a) IIP particles

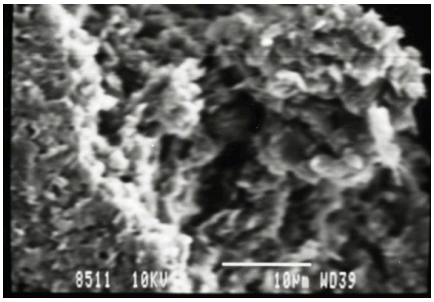

(b) IIP particle, zoomed in

Figure 2
SEM images for IIP particles

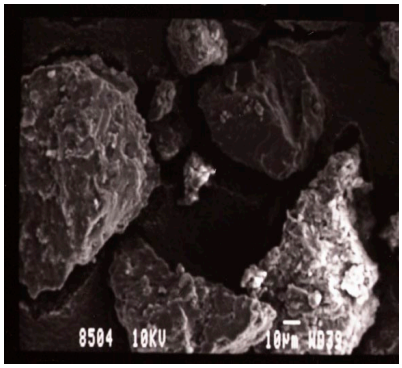

(a) CP particles

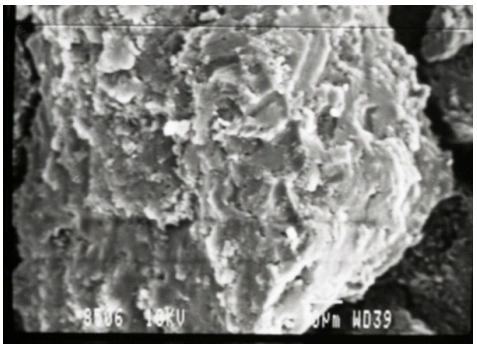

(b) CP particle, zoomed in

Figure 3
SEM images for CP particles

who attributed bands at 938 and 790 cm^{-1} to the interaction of Cr (VI) with the adsorbent, and also with Miller and Wilkins (1952), who observed chromate anion FTIR bands at 930 and 765 cm^{-1} in polyethyleneimine-supported silver dichromate oxidising polymeric reagent. The FTIR spectrum of the quaternised polymer revealed the presence of 2 bands, at 1 630 and 1 578 cm^{-1}, which indicate the presence of the quaternised product as these were absent in the vinylpyridine spectrum.

Surface area measurements

The surface area was determined using the BET method and values of 61.7 and 5.9 $m^2 \cdot g^{-1}$ were obtained for IIP and CP, respectively. Although the ratios of IIP to CP surface areas are similar for both methods, there is a huge difference in the surface area values obtained. Three replicate experiments were conducted and for each experiment absorbance was measured in triplicate. The morphology of the particles was evaluated from SEM images. Images for IIP and CP are shown in Figs. 2(a) and 3(a); Figs. 2(b) and 3(b) show zoomed-in images for a single particle. From the images it can be concluded that the particles produced for both CP and IIP have irregular shapes with some degree of porous surface that will aid in adsorption. In fact, Figs. 2(b) and 3(b) reveal that the polymers have similar surface structures, which further confirms the similarities in binding results obtained for both polymers.

Optimisation studies

For the optimisation studies discussed below for the IIP and CP only the batch method was employed.

Optimisation of leaching

Leaching and washing of the retained Cr (VI) from the polymers was performed using 0.1 M NaOH (Fig. 4). The results indicate that 10 mℓ of 0.1 M NaOH was not enough to leach out any Cr (VI) on the polymer. 20 mℓ was therefore taken as optimum. This is important to avoid IIP bleeding as well as to achieve complete recovery of bound Cr (VI). A relatively large

http://dx.doi.org/10.4314/wsa.v37i4.11
Available on website http://www.wrc.org.za
ISSN 0378-4738 (Print) = Water SA Vol. 37 No. 4 October 2011
ISSN 1816-7950 (On-line) = Water SA Vol. 37 No. 4 October 2011

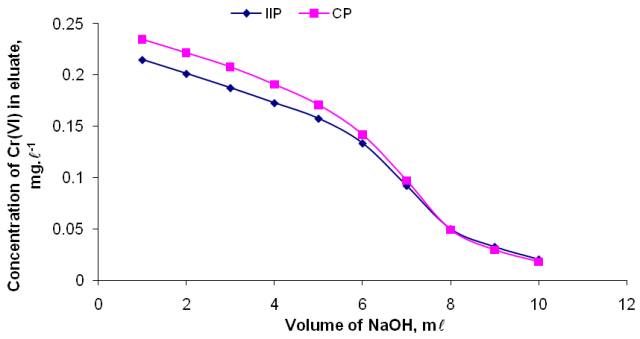

Figure 4
Leaching and washing of the retained chromate after rebinding. Amount of material, 20 mg; solution pH, 3; leaching solution, 1 mℓ of 0.1 M NaOH; material eluted from SPE cartridges.

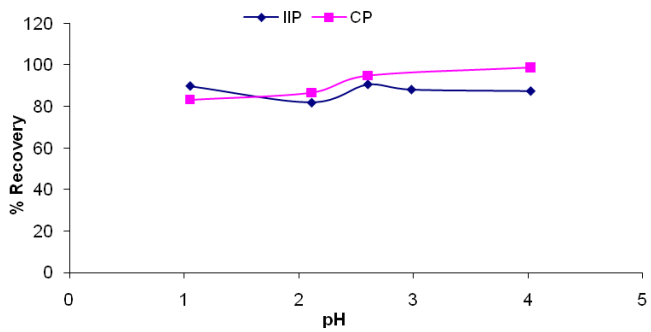

Figure 6
Effect of pH on the extraction of chromium (VI) ions by CP and IIP. Amount of materials, 20 mg; concentration of solution, 1 mg·ℓ-1; volume of solution, 25 mℓ; contact time, 120 min.

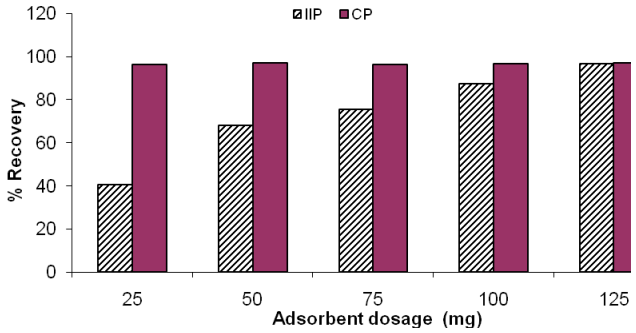

Figure 5
Effect of sorbent dosage of IIP and CP. Solution pH, 3.0; concentration of solution, 1 mg·ℓ-1; volume of solution, 25 mℓ; contact time, 120 min.

elution volume meant low analyte concentration enrichment but this did not pose any limitations because the HPLC-UV method is very sensitive, with a detection limit below 1 µg·ℓ$^{-1}$ with direct injection of pure standard.

Optimisation of IIP quantity needed for maximum extraction of Cr (VI)

Different amounts of Cr (VI) imprinted polymer (25, 50, 75, 100 and 125 mg) were stirred for 1 h in various sample vials containing 25 mℓ aliquots of 1 µg·mℓ$^{-1}$ Cr (VI) spiked water and the pH was adjusted to 3.0. This pH was chosen based on the 2 earlier batch studies, where maximum adsorption occurred around pH 3. All of the experiments were conducted in triplicate and the mean values and standard deviations were determined.

From Fig. 5, CP showed a maximum constant adsorption of Cr (VI) of about 98%, where 25-125 mg of the polymer was used. Hence, 30 mg can be regarded as optimum for this type of polymer. However, the adsorption increases steadily for the IIP and seem to reach maximum at 125 mg. Therefore, 130 mg was taken as an optimum for this polymer.

Effect of pH

The effect of pH on the extraction of chromium (VI) ions by IIP and CP was investigated by varying the pH from 1 to 4; results are shown in Fig. 6. From Fig. 6, it can be noted that there was no major variation in the influence of sample pH, within the range studied. Similar results where adsorption was independent of pH were reported by Neagu (2009) and Neagu and Mikhalovsky (2010) for their use of quaternised crosslinked pyridine polymers.

Tunçeli and Türker (2002) obtained a similar relationship between pH and adsorption behaviour, where Cr (VI) adsorption was constant at about 75% recovery from pH 2 to pH 8. It is known that Cr (VI) exists in different stable forms in aqueous solutions and that the predominance of various species is pH dependent. For example, $Cr_2O_7^{2-}$ and $HCrO_4^{1-}$ are more common in the pH range 2.0-6.0, whereas CrO_4^{2-} predominates in basic solutions (Benhammou et al., 2007). The ionic strength of a solution increases with the decrease in pH and under such conditions one would expect that removal of Cr (VI) would be lower at low pH ranges (1.0-3.0) due to competition for binding sites between Cr (VI) and the Cl^- anions used for pH adjustments. Furthermore, above pH 7, competition for the active binding sites from OH^- ions used for pH adjustments is expected to decrease the removal of Cr (VI). However, both these theoretical predictions were not observed, in this study or in a study by Tunçeli and Türker (2002). Both of the theoretical predictions are influenced by the selectivity of the polymer towards Cr (VI), the capacity of the polymer and the amount of interfering ions.

Effect of contact time

The effect of contact time on the extraction of chromium (VI) ions by IIP and CP was studied by stirring 20 mg of polymer with 1 mg·ℓ$^{-1}$ solution of chromium at pH 3.0 for 10, 30, 60 and 90 min (Fig. 7). Although both polymers showed greater than 85% recovery for all of the contact times investigated, the IIP was shown to have a faster binding kinetic, as 92% recovery was obtained, compared to 88% after the first 10 minutes of stirring. However, after 20 min of stirring it was the CP that showed higher recovery and seemed to have reached a plateau after 60 min. The recovery for the IIP after 90 min was 97% and was still on the rise; hence, 120 min was taken as an optimum stirring time for IIP and CP.

Effect of solution volume

Twenty mg of IIP and CP were stirred in solutions containing 1 mg·ℓ$^{-1}$ chromium, of different volumes (50-700 mℓ). The results for both polymers show a similar trend, further emphasising that these (polymers) are actually the same (Fig. 8). The shape of the graph in Fig. 8 can be explained in terms of the mass transfer of chromium from the bulk solution to the IIP and CP particles. The smaller the volume, the shorter the contact time needed for chromium in solution to come into contact with IIP particles, as the distance between the IIP or CP particles

http://dx.doi.org/10.4314/wsa.v37i4.11
Available on website http://www.wrc.org.za
ISSN 0378-4738 (Print) = Water SA Vol. 37 No. 4 October 2011
ISSN 1816-7950 (On-line) = Water SA Vol. 37 No. 4 October 2011

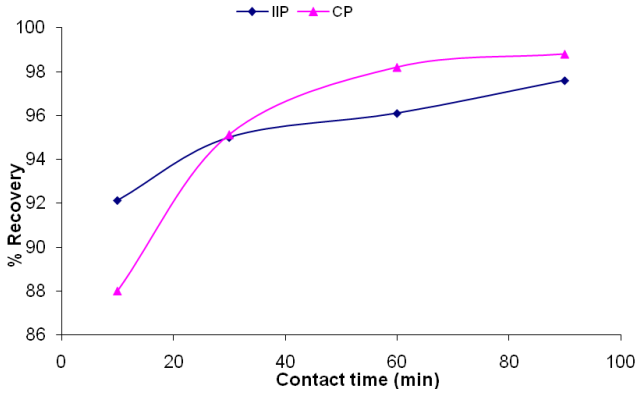

Figure 7
Effect of contact time on extraction of chromium (VI) ion by IIP and CP. Amount of materials, 20 mg; solution pH, 3; concentration of solution, 1 mg·ℓ⁻¹; volume of solution, 25 mℓ.

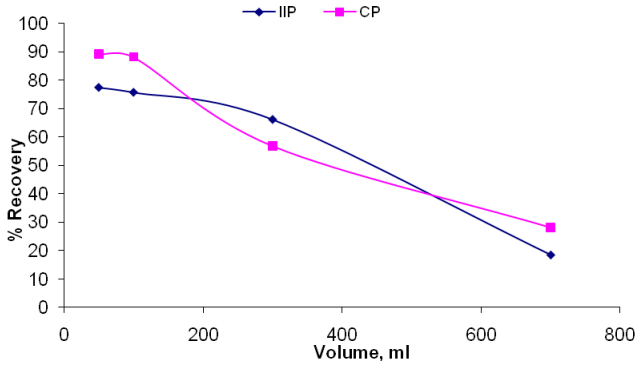

Figure 8
Effect of solution volume on extraction of chromium (VI) ion by IIP and CP. Amount of materials, 20 mg; solution pH, 3; concentration of solution, 1 mg·ℓ⁻¹; contact time, 120 min.

and chromium in solution will be smaller than it will be in larger volumes.. This explains the low recoveries obtained for larger volumes of solution. The recovery is generally constant and independent of sample volume when the polymer is packed in a cartridge, as in SPE, until the breakthrough volume is exceeded; this is somewhat different from what is observed in Fig. 8.

Retention capacity

The maximum adsorption capacity for the polymer was investigated and the results are shown in Fig. 9. For the range of concentrations studied, the IIP reached a plateau around 38 mg·g^{-1}, while the CP seems to reach a plateau at 25 mg·g^{-1}. This result illustrates that, although the IIP and CP seem to have similar adsorption capabilities towards the chromate anion, as

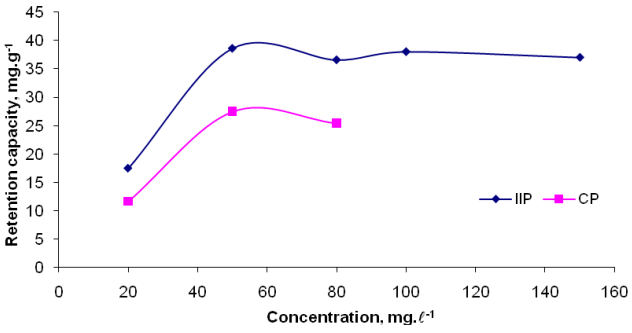

Figure 9
Retention capacity verses concentration of Cr (VI) in solution. Amount of IIP particles, 20 mg; solution pH, 3; solution volume, 25 mℓ; contact time, 120 min.

indicated by the other experiments, the IIP actually has more binding sites due to imprinting. This means that the IIP can be deployed for environmental remediation for longer periods than the CP as it has higher binding capacity.

Binding studies

Binding studies using batch and solid-phase extraction methods (SPE) were compared and the results are presented in Table 1. Experimental parameters are given in the Table and the values reported are mean values. Percent recoveries obtained by both batch and SPE method show that the IIP can be used succefully for extraction of chromium (VI) with either method of extraction. %RSD values are given in brackets.

Adsorption isotherms

The Langmuir and Freundlich models were used to study the adsorption of Cr (VI) on the IIP particles. The Langmuir model was first developed to describe the vapour adsorption on homogeneous surfaces. However, when used for solid-liquid systems several assumptions are made. These assumptions are: number of surface adsorption sites is fixed; adsorption involves a single monolayer; adsorption behaviour is independent of surface coverage; and all adsorption sites are represented by similar types of functional groups. The Langmuir equation is given by:

$$C_e/q_e = C_e/Q_o + 1/bQ_o \quad (6)$$

where:

q_e is the amount of solute adsorbed on the surface of adsorbent (mg·g^{-1})
C_e is the equilibrium Cr (VI) concentration (mg·mℓ$^{-1}$)
Q_o is the saturated monolayer adsorption capacity (mg·g^{-1})
b is the Langmuir adsorption constant (ℓ·mg^{-1})

Table 1
Comparison of batch and SPE methods of adsorption using IIP and CP

	Batch		SPE	
	IIP	CP	IIP	CP
Polymer (mg)	30	20	20	20
pH	3	3	3	3
Sample (mℓ)	30	25	25	25
Concentration added (µg·ℓ$^{-1}$)	1 000	1 000	1 000	1 000
Extraction time (min)	95	30	-	-
% Recovery	98 ± 0.19	91 ± 2.48	96 ± 0.37	98 ± 0.52

http://dx.doi.org/10.4314/wsa.v37i4.11
Available on website http://www.wrc.org.za
ISSN 0378-4738 (Print) = Water SA Vol. 37 No. 4 October 2011
ISSN 1816-7950 (On-line) = Water SA Vol. 37 No. 4 October 2011

Table 2
Langmuir and Freundlich adsorption isotherm constant values determined for the IIP and CP

Polymers	Experimental	Langmuir Model			Freundlich Model		
	q_{exp} (mg·g^{-1})	q_{max} (mg·g^{-1})	b	R^2	K_F	N	R^2
IIP	38.43	45.23	7.8 x 10^{-3}	0.97	5.08	1.46	1.00
CP	25.44	34.31	3.6 x 10^{-2}	0.96	5.55	2.61	0.65

A plot of C_e/q_e versus Ce gives the values of Q_o and b (Wang et al., 2009). The Freundlich adsorption isotherm which assumes a multilayer adsorption can be given by the linearised form:

$$\ln q_e = \ln K_F + 1/n \ln C_e \quad (7)$$

where:
K_F is the Freundlich constant
n is the Freundlich exponent

The experimental values for q_{exp} and q_{max} are comparable. The initial solution concentrations used were in the range of 10-100 mg·ℓ$^{-1}$. In the Freundlich approach the values of n are both greater than 1 indicating favourable adsorption of Cr (VI) on the adsorbent (Candan et al., 2009).

Table 2 summarises the results obtained by fitting the experimental data to the 2 models, namely, the Langmuir and Freundlich adsorption isotherms. Results for the IIP fit both models, whereas results for the CP did not show a good fit for the Freundlich model. This can be explained by the fact that the Freundlich model follows a multilayer mode of adsorption. The CP can be predicted to favour a single layer mode of adsorption (surface adsorption), whereas in the IIP there are surface as well as some deep embedded cavities for adsorption, making IIP a multilayer adsorbent.

Effect of ionic strength

The study of the influence of ionic strength is important for the adsorption of Cr (VI) as wastewater contains different ions (Anirudhan et al., 2009). The results are depicted in Fig. 10. Consistent with the literature (Li and Bowman, 2001; Fang et al., 2007), the sorption of Cr (VI) decreased with increasing ionic strength, meaning that Cr (VI) sorption is affected by exchange reactions (Fang et al., 2007). In fact, ion activity of chromium ions decreases with increase in ionic strength (Li and Bowman, 2001). The ion exchange process taking place on the surface of the polymer can be represented as:

$$X\text{-}Cl + HCrO_4^- = X\text{-}HCrO_4 + Cl^- \qquad K_V(Cl\text{-}HCrO_4)$$

where:
K_V(Cl-HCrO$_4$) is the Vanselow selectivity coefficient (Fang et al., 2007).

According to Lee et al. (2005), if the change in ionic strength does not lead to any appreciable change in the removal of the chromate then the mechanism for removal might be due to precipitation and covalent bonding. Ions that form outer-sphere complexes show decreasing adsorption as the ionic strength is increased (McBride, 1997). The decrease in Cr (VI) adsorption with increase in ionic strength can be said to obey this theory. This decrease is due to the competition for specific binding sites between the chromate and the chloride anions present in solution. The IIP showed slightly higher recovery than the CP, which is also evidence of the imprinting effect. IIPs are therefore generally superior in selectivity compared to normal polymers with chelating functional groups.

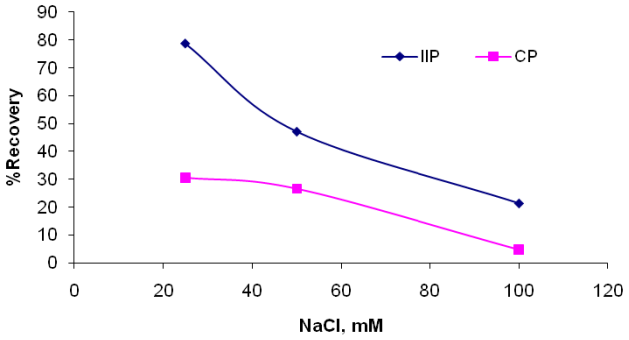

Figure 10
Effect of ionic strength. 20 mg of polymer was stirred in a 1 mg·ℓ$^{-1}$ chromium solution containing different concentrations of NaCl (25-300 mM, ~900-3 500 mg·ℓ$^{-1}$); solution pH. 3; solution volume, 25 mℓ; contact time, 120 min.

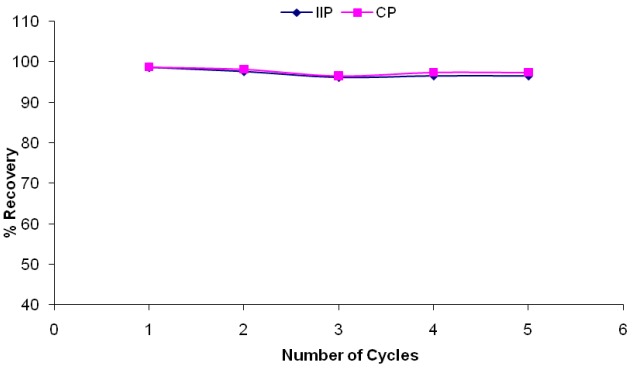

Figure 11
Reusability and stability of the polymers. Amount of polymer, 20 mg; solution pH, 3; solution volume, 25 mℓ; contact time, 120 min, concentration of solution, 1 mg·ℓ$^{-1}$.

Stability and reusability

The effect of reusability and stability of the polymers was studied by stirring 20 mg of polymer in 1 mg·ℓ$^{-1}$ solution of chromium for 60 min. Optimum conditions were used for other variables. After leaching with 0.1 M NaOH the polymers were used for the next rebinding without conditioning. The results are illustrated in Fig. 11. The polymers yielded greater than 96% extraction efficiency for up to 5 cycles.

Effect of co-existing anions

Competitive adsorption of Cr (VI) / Cl^-, Cr (VI) / F^-, Cr (VI) / NO_2^-, Cr (VI) / NO_3^-, Cr (VI) / SO_4^{2-}, Cr (VI) / PO_4^{3-} and

http://dx.doi.org/10.4314/wsa.v37i4.11
Available on website http://www.wrc.org.za
ISSN 0378-4738 (Print) = Water SA Vol. 37 No. 4 October 2011
ISSN 1816-7950 (On-line) = Water SA Vol. 37 No. 4 October 2011

Table 3
Distribution coefficient and selectivity factor for IIP and CP

Adsorbent	*Kd*		*K*	*K'*	Adsorbent	*Kd*		*K*	*K'*
	Cr(VI)	Cl^-				Cr(VI)	SO_4^{2-}		
CP	423.6	N.D			CP	274.5	109	2.5	
IIP	442.7	N.D			IIP	347	249.9	1.4	0.55
Adsorbent	*Kd*		*K*	*K'*	Adsorbent	*Kd*		*K*	*K'*
	Cr(VI)	F^-				Cr(VI)	PO_4^{3-}		
CP	328.6	37.8	8.7		CP	379.2	127.5	3.0	
IIP	350.3	0.1	3503.0	403.0	IIP	383.6	138.4	2.8	0.93
Adsorbent	*Kd*		*K*	*K'*	Adsorbent	*Kd*		*K*	*K'*
	Cr(VI)	NO_3^-				Cr(VI)	NO_2^-		
CP	408	105.2	3.9		CP	434.2	69.3	6.3	
IIP	412.5	376.4	1.1	0.28	IIP	395.4	488	0.81	0.13

Table 4
Analysis of tap-water, Bokkamp Dam 2 and acid mine drainage water spiked with 30 µg·ℓ$^{-1}$ of reference material. Amount of polymer used, 20 mg; solution pH, 3; solution volume, 25 mℓ; contact time, 10 min; concentration, 30 µg·ℓ$^{-1}$

Samples	Direct analysis			Concentration of Cr (VI) by IIP		% Recovery Cr (VI)	
	µg·ℓ$^{-1}$ Cr (VI)	mg·ℓ$^{-1}$ Cl^-	mg·ℓ$^{-1}$ SO_4^{2-}	µg·ℓ$^{-1}$			
				Added	Measured [a]	CP	IIP
Tap-water	-	0.87	1.03	0.00	-	-	-
	-	0.87	1.03	30.00	29.19 ± 7.44	93.11	97.26
Bokkamp Dam 2	2.26	4.61	19.41	30.00	33.74 ± 4.53[b]	-	-
	2.26	4.61	19.41	30.00	15.70 ± 6.69	4.56	47.68
AMD wastewater	no peak			0.00	-	-	-
	no peak			30.00	25.87 ± 6.15	18.13	70.08

[a] Mean of triplicates ± RSD [b] Spiked sample before extraction

Cr (VI) / {Cl^-, F^-, NO_2^-, NO_3^-, SO_4^{2-} and PO_4^{3-}} was investigated; the results are summarised in Table 3. In terms of recognition of the chromate anion the data are in agreement with those obtained previously (Table 1), in that the IIP and CP seem to adsorb chromate to the same extent (Table 3). The distribution coefficients, K_D, and the selectivity coefficients, K, for the IIP and CP are comparable, further emphasising that the polymers are similar. However, chloride anions could not be quantified by IC because: Cl^- was used to adjust pH (in the form of HCl); and Cl^- was used during quaternisation (as 1,4-dichlorobutane). Therefore, it was understandable that there would be a high concentration of the chloride ions in the samples.

The influence of the investigated co-existing anions on Cr (VI) sorption can be summarised as following the order: $SO_4^{2-} > F^- > PO_4^{3-} > NO_2^- > NO_3^- > Cl^-$. The evaluated order is slightly different to that reported by Fang et al. (2007), who investigated the influence of SO_4^{2-}, PO_4^{3-} and NO_3^- on Cr (VI) sorption using 0.1, 1.0 and 10 mM concentrations of anions. The observed trend was $PO_4^{3-} > SO_4^{2-} > NO_3^-$ whereas our studies indicated that sulphates compete more for binding sites than phosphates.

Application to real samples

A screening experiment was performed using a batch mode of extraction. The experiment was done to explore the application of the prepared polymers to real-world samples. Samples from Bokkamp Dam 2, acid mine drainage water and tap-water were adjusted to pH 3.0 and spiked with 30 µg·ℓ$^{-1}$ Cr (VI) of a certified reference material (CRM QCl-034-3). The CRM value was below 50 µg·ℓ$^{-1}$ which is the maximum allowable limit of Cr (VI) in drinking water. After batch experiments were conducted, unextracted and extracted concentrations of Cr (VI) were determined; results are shown in Table 4. Unspiked tap-water and Bokkamp Dam 2 water were run as a blank, and Cr (VI) quantified was zero and 2.24 µg·ℓ$^{-1}$, respectively (Table 4). For tap-water both the CP and IIP showed high recoveries, of about 95%, which is in agreement with previous results. The results for acid mine drainage (AMD) water are worth noting. The recovery of the control polymer in AMD collapsed due to high concentrations of interfering sample matrix, especially sulphate ions. This is not surprising since in IIP selectivity is based on size and shape in addition to ionic interaction.

The selectivity was also compared, by direct injection of the real-world sample (AMD) for both spiked and non-spiked samples into that obtained after IIP selective extraction. Despite a very low detection limit of the method for direct injection (below 1 µg·ℓ$^{-1}$) no Cr (VI) was obtained in the spiked sample. After IIP extraction, spiked Cr (VI) was detected in the sample (Table 4).

Conclusion

A selective IIP for extraction of Cr (VI) was prepared and optimised. The prepared IIP showed superior selectivity towards Cr (VI) in acid mine drainage water, where the selectivity of the control collapsed due to high amounts of sulphate ions. The MIP backbone provides an opportunity to prepare Cr (VI) adsorbent materials with high stability and durability under different conditions (acidic, basic and common organic solvents). Maximum binding capacity of 38 mg·g^{-1} polymer was obtained from an initial concentration of 50 mg·ℓ$^{-1}$, which

http://dx.doi.org/10.4314/wsa.v37i4.11
Available on website http://www.wrc.org.za
ISSN 0378-4738 (Print) = Water SA Vol. 37 No. 4 October 2011
ISSN 1816-7950 (On-line) = Water SA Vol. 37 No. 4 October 2011

was slightly higher than the amount obtained by Neagu and Mikhalovsky (2010), 33 $mg \cdot g^{-1}$, from an initial concentration of 138 $mg \cdot \ell^{-1}$, and also comparable to the 50 $mg \cdot g^{-1}$ binding capacity obtained by Fang et al. (2007) from an initial concentration of 98 $mg \cdot m\ell^{-1}$.

Acknowledgements

This work was supported by the National Research Foundation of South Africa and the Swedish Foundation for International Cooperation in Research and Higher Education (STINT, YR2009-7015).

References

ACAR FN and MALKOC E (2004) The removal of chromium(VI) from aqueous solutions by *Fagus orientalis L*. *Bioresour. Technol.* **94** 13-15.

ANIRUDHAN TS, DIVYA L and SUCHITHRA PS (2009) Kinetic and equilibrium characterization of uranium(VI) adsorption onto carboxylate-functionalized poly(hydroxyethylmethacrylate)-grafted lignocellulosics. *J. Environ. Manage.* **90** 549-560.

BENHAMMOU A, YAACOUBI A, NIBOU L and TANOUTI B (2007) Chromium(VI) adsorption from aqueous solution onto Moroccan Al-pillared and cationic surfactant stevensite. *J. Hazard. Mater.* **140** 104-109.

BIRLIK E, ERSÖZ A, AÇIKKALP E, DENIZLI A and SAY R (2007) Cr(III)-imprinted polymeric beads: Sorption and preconcentration studies. *J. Hazard. Mater.* **B140** 110-116.

BROWER JB, RYAN RL and PAZIRANDEH M (1997) Comparison of ion-exchange resins and biosorbents for the removal of heavy metals from plating factory wastewater. *Environ. Sci. Technol.* **31** (10) 2910-2914.

CANDAN N, TÜZMEN N, ANDAC M, ANDAC CA, SAY R and DENIZLI A (2009) Cadmium removal out of human plasma using ion-imprinted beads in a magnetic column. *Mater. Sci. Eng. C* **29** 144-152.

CANNON FS, PARETTE RB, NA C, CHEN W and HAGERUP B (2005) A method for perchlorate removal from ground water. *US Patent 6881348*.

CHAKRABORTY S and KUMAR PA (2009) Fixed-bed column study for hexavalent chromium removal and recovery by short-chain polyaniline synthesized on jute fiber. *J. Hazard. Mater.* **162** 1086-1098.

DENG S and BAI R (2004) Removal of trivalent and hexavalent chromium with aminated polyacrylonitrile fibers: performance and mechanisms. *Water Res.* **38** 2423-2431.

FANG J, GU Z, GANG D, LIU C, IITON ES and DENG B (2007) Cr(VI) removal from aqueous solution by activated carbon coated with quaternised poly(4-vinylpyridine). *Environ. Sci. Technol.* **41** 4748-4753.

GANG D, BANERJI SK and CLEVENGER TE (2000) Chromium(VI) removal by modified PVP-coated silica gel. *Pract. Period. Hazard. Toxic Radioact. Waste Manage.* **4** (3) 105-110.

GOUDARZIAN N, GHAHRAMANI P and HOSSINI S (1996) Polymeric reagent (I): Polyethyleneimine-supported silver dichromate as a new oxidizing agent. *Polym. Int.* **39** 61-62.

GOYAL N, JAIN SC and BANERJEE UC (2003) Comparative studies on the microbial adsorption of heavy metals. *Adv. Environ. Res.* **7** 311–319.

HUANG CP and WU MH (1977) The removal of chromium(VI) from dilute aqueous solution by activated carbon. *Water Res.* **11** (8) 673-679.

KATZ SA and SALEM H (1994) *The Biological and Environmental Chemistry of Chromium*. VCH, New York.

KRATOCHVIL D, PIMENTEL P and VOLESKY B (1998) Removal of trivalent and hexavalent chromium by seaweed biosorbent. *Environ. Sci. Technol.* **32** (18) 2693-2698.

LEE MY, HONG KJ, SHIN-Y AY and KAJIUCHI T (2005) Adsorption of hexavalent chromium by chitosan-based polymeric surfactants. *J. Appl. Polym. Sci.* **96** 47-50.

LI Y, YANG MJ and SHE Y (2005) Humidity sensitive properties of crosslinked and quaternized poly(4-vinylpyridine-co-butyl methacrylate). *Sensor Actuat. B* **107** 252-257.

LI Z and BOWMAN RS (2001) Retention of inorganic oxyanions by organo-kaolinite. *Water Res.* **35** 3771-3776.

NEAGU V, UNTEA I, TUDERACHE E and ORBECI C (2004) Sorption equilibrium of Cr(VI) ions by strong base anion exchangers with pyridine structures. *J. Appl. Polym. Sci.* **93** 1957-1963.

NEAGU V (2009) Removal of Cr(VI) onto functionalised pyridine copolymer with amide groups. *J. Hazard. Mater.* **171** 410-416.

NEAGU V and MIKHALOVSKY S (2010) Removal of hexavalent chromium by new quaternized crosslinked poly(4-vinylpyridines). *J. Hazard. Mater.* **183** 533-540.

McBRIDE MB (1997) A critique of diffuse double layer models applied to colloid and surface chemistry. *Clays Clay Miner.* **45** (4) 598-608.

MILLER FA and WILKINS CH (1952) Infrared spectra and characteristic frequencies of inorganic ions. *Anal. Chem.* **24** 1253-1294.

MITCHELL MD, COLLIAS DI, BJORKQUIST DW, ZAVERI PN and WOOLLEY MM (2004) Water filter materials, water filters and kits containing particles coated with cationic polymer and processes for using the same. *U.S. Pat. Appl. Publ.* (2004164018) Cont.-in-part of U.S. Ser. No. 464, 210. 30 pp.

PATTERSON JW (1985) *Industrial Wastewater Treatment Technology* (2nd edn.) Butterworth-Heinemann, London.

QIAN S, HUANG C, JIANG J, HE F and WANG Y (2000) Studies of adsorption behaviour of crosslinked chitosan for Cr(VI) and Se(VI). *J. Appl. Polym. Sci.* **77** 3216-3219.

RAJI C and ANIRUDHAN TS (1998) Batch Cr(VI) removal by polyacrylamide-grafted sawdust: Kinetics and thermodynamics. *Water Res.* **32** 3772-3780.

RAMNANI SP and SABHARWAL S (2006) Adsorption behaviour of Cr(VI) onto radiation crosslinked chitosan and its possible application for the treatment of wastewater containing Cr(VI). *React. Funct. Polym.* **66** 902-909.

RAMOS J, MILLÁNA and PALACIO F (2000) Production of magnetic nanoparticles in a polyvinylpyridine matrix. *Polymer* **41** 8461-8464.

SANTIAGO I, WORLAND VP, CAZARES-RIVERA E and CADENA F (1992) Removal of hexavalent chromium from water using tailored zeolites. *Met. Finish.* **90** (11) 37-43.

SARIN V and PANT MM (2006) Removal of chromium from industrial waste by using eucalyptus bark. *Bioresour. Technol.* **97** (1) 15-20.

SRINIVASAN K, BALASUBRAMANIAN N and RAMAKRISHAN TV (1988) Studies on chromium removal by rise husk carbon. *Ind. J. Environ. Health* **30** (40) 376-387.

TUNÇELI A and TÜRKER AR (2002) Speciation of Cr(III) and Cr(VI) in water after preconcentration of its 1,5-diphenylcarbazone complex on amberlite XAD-16 resin and determination by FAAS. *Talanta* **57** 1199-1204.

UNNITHAN MR and ANIRUDHAN TS (2001) The kinetics and thermodynamics of sorption of chromium (VI) onto the iron (III) complex of a carboxylated polyacrylamide-grafted sawdust. *Ind. Eng. Chem. Res.* **40** (12) 2693-2701.

VINCENT T and GUIBALF E (2001) Cr(VI) extraction using Aliquat 336 in a hollow fiber module made of chitosan. *Ind. Eng. Chem. Res.* **40** 1406-1411.

http://dx.doi.org/10.4314/wsa.v37i4.11
Available on website http://www.wrc.org.za
ISSN 0378-4738 (Print) = Water SA Vol. 37 No. 4 October 2011
ISSN 1816-7950 (On-line) = Water SA Vol. 37 No. 4 October 2011

http://dx.doi.org/10.4314/wsa.v37i4.11
Available on website http://www.wrc.org.za
ISSN 0378-4738 (Print) = Water SA Vol. 37 No. 4 October 2011
ISSN 1816-7950 (On-line) = Water SA Vol. 37 No. 4 October 2011

APPENDIX II

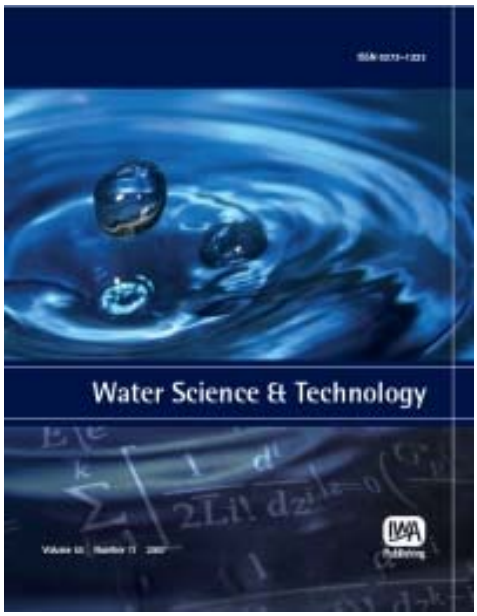

Simple and efficient ion imprinted polymer for recovery of uranium from environmental samples

V. E. Pakade, E. M. Cukrowska, J. Darkwa, G. Darko, N. Torto and L. Chimuka

ABSTRACT

Ion imprinted polymer material (IIP) was prepared by forming ternary complexes of uranyl imprint ion with 1-(prop-2-en-1-yl)-4-(pyridin-2-ylmethyl)piperazine and methacrylic acid followed by thermal copolymerization with ethylene glycol dimethacrylate as the cross-linking monomer in the presence of 1,1′-azobis(cyclohexanecarbonitrile) initiator and 2-methoxy ethanol porogenic solvent. HCl solution (5 mol/L) was used to leach out the uranyl template ion from the IIP particles. Similarly, the control polymer (CP) material was also prepared exactly under the same conditions as the IIP but without the uranyl ion template. Various parameters such as solution pH, initial concentration, aqueous phase volume, sorbent dosage, contact time and leaching solution volumes were investigated. SEM, IR and BET-surface area and pore size analysis were used for the characterization of IIP and CP materials. The extraction efficiency of the IIP and CP was compared using a batch and SPE mode of extraction. The optimal pH for quantitative removal is 4.0–8.0, sorbent amount is 20 mg, contact time is 20 min and the retention capacity is 120 mg of uranyl ion per g of IIP. The IIP prepared demonstrated superior selectivity towards coexisting cations and therefore it can be used for selective removal of uranium from complex matrices.

Key words | complex samples, ion imprinted polymer, piperazine, uranyl ion

V. E. Pakade
E. M. Cukrowska
L. Chimuka (corresponding author)
School of Chemistry,
University of the Witwatersrand. P/Bag 3,
WITS 2050,
Johannesburg,
South Africa
E-mail: *luke.chimuka@wits.ac.za*

J. Darkwa
Department of Chemistry,
University of Johannesburg,
P.O. Box 524,
Auckland Park 2006,
South Africa

G. Darko
N. Torto
Department of Chemistry,
Rhodes University,
P.O. Box 94,
Grahamstown, 6140,
South Africa

INTRODUCTION

Recently, there has been an increased demand for developing methods that are suitable for separation and trace level determination of uranium from various types of samples including rocks, sea water and industrial effluents. This demand is two-fold, firstly, because of the large requirement for uranium in the atomic energy programme and secondly due to the toxicity of uranium in the environment and hence the need for its removal (Agrawal *et al.* 2006). Uranium may cause irreversible renal injuries or even death if consumed at high concentrations. Maximum allowable concentration of uranium in drinking water as per WHO is 20 $\mu g\,L^{-1}$ (WHO 1998). Both groundwater and surface water can be polluted by uranium, which gets seeped from the mining and milling leachates as well as from the normal run-off associated with mining sites (Winfield 2007).

Different methods including chemical precipitation, micellar ultrafiltration, solvent extraction, organic and inorganic ion exchange and adsorption processes, have been used for the removal of UO_2^{2+} ion from aqueous solutions. Many of these methods suffer from environmental, economic, health and technical problems such as long processing time, high energy consumption, low efficiency, and larger quantities of hazardous materials used (Preetha *et al.* 2006). However, the use of adsorption methods has proved to be the most efficient, more specifically for effluents with moderate and low concentrations. Ion imprinted polymers (IIPs) are an example of such adsorbents and hence the recent focus on using IIPs for the recovery of uranium from aqueous media (Preetha *et al.* 2006).

Chemical immobilization, trapping and surface imprinting approaches are the most used methods for preparing IIPs (Rao *et al.* 2006). Nevertheless, IIP for pre-concentration and/or extraction of UO_2^{2+} ion from different samples have been successfully developed (Gladis & Rao 2003; Preetha *et al.* 2006; Singh & Mishra 2009; Ahmadi

doi: 10.2166/wst.2012.911

et al. 2010). Also, in this study an IIP for the preconcentration and removal of UO_2^{2+} ion from complex samples was developed using a simple synthesized ligand 1-(prop-2-en-1-yl)-4-(pyridin-2-ylmethyl)piperazine (PPMP) which showed high recognition for uranyl ions. To our best knowledge, this study is the first report on the use of PPMP for uranium removal. The uranium ion imprinted polymer prepared in this study was found to have a much higher capacity and showed very high selectivity towards UO_2^{2+} ions than those previously reported by Preetha *et al.* (2006), Singh & Mishra (2009), and Gladis & Rao (2003). The prepared IIP was applied to real environmental water samples for the extraction and determination of uranium.

EXPERIMENTS

Materials

A stock solution (1,000 μg mL^{-1}) of uranium was prepared from uranyl nitrate ($UO_2(NO_3)_2{\cdot}6H_2O$) purchased from Sigma-Aldrich (Johannesburg, South Africa). The pH was adjusted with the following solutions: HCl/KCl for pH 1–2, CH_3COOH/CH_3COONa for pH 3–6, borax/H_3BO_3 for pH 7–8. Methacrylic acid (MAA), 2-vinylpyridine (2-VP), ethylene glycol dimethacrylate (EGDMA), 2-picolylchloride hydroxide, allylpiperazine and 1,1′-azobis(cyclohexanecarbonitrile) (ACCN) were used, and all purchased from Sigma-Aldrich (Johannesburg, South Africa). Vinylpyridine was cleaned by vacuum distillation before use. All other reagents were of AR grade.

Instrumentation

Inductively coupled plasma-optical emission spectroscopy ICP-OES (Spectro Genesis, Germany) was used for measuring uranium concentrations in solutions. FTIR spectra (4,000–400 cm^{-1}) were recorded using the Bruker FTIR spectrometer (Model Tensor 27, Germany). A scanning electron microscope (SEM) Model JSM 840 (JEOL, Tokyo, Japan) was used to study the surface morphology of IIP and CP particles. A Brunauer–Emmett–Teller (BET) instrument (Micromeritics Tristar) was used for surface area determinations and UV/Vis absorption spectra were collected using UV/Vis spectroscopy (Varian, Cary 50 Conc, Germany).

Synthesis of 1-(prop-2-en-1-yl)-4-(pyridin-2-ylmethyl) piperazine

40% aqueous NaOH (12 mL) was added to a mixture of 2-picolylchloride hydroxide (0.3960 g; 1 mmol) and allylpiperazine (140 μL; 1 mmol) in 40 mL benzene. Subsequently, 10 drops of 40% aqueous tetrabutylammonium bromide were added slowly and the mixture was refluxed for 24 h. The organic layer was then separated and evaporated *in vacuo* to afford brown oil with white precipitation. The oil (yield = 0.4850 g, 85%) was separated from the solid. ^1H NMR, ^{13}C and DEPT 135 revealed that the oil was the intended product, 1-(prop-2-en-1-yl)-4-(pyridin-2-ylmethyl)piperazine (PPMP).

^1H NMR ($CDCl_3$, 300 MHz): δ 3.04 (d, $J = 6.6$ Hz, 2 H), 3.68 (s, 2 H), 5.16 (t, $J = 8.7$ Hz, 2 H), 5.89 (m, 1 H), 7.18 (t, $J = 5.4$ Hz, 1 H), 7.41 (d, $J = 7.8$ Hz, 1 H), 7.69 (t, $J = 1.5$ Hz, 1 H), 8.56 (d, $J = 4.2$ Hz, 1 H). ^{13}C NMR ($CDCl_3$, 300 MHz): 52.9, 53.0, 61.7, 64.4, 118.3, 122.0, 123.3, 134.6, 134.7, 136.7, 149.3, 158.3, 158.4.

Preparation of UO_2^{2+} IIP and control polymer (CP)

The imprint ion (1 mmol) was stirred with PPMP (1 mmol) and MAA (9 mmol) in 10 mL 2-methoxy ethanol for 30 min at room temperature. EGDMA (36 mmol) and 50 mg of ACCN were added while the reaction vessel was kept on ice and purged with N_2 for 10 min. Polymerization was initiated thermally in a water bath at 80 °C while stirring for 40 min. Bulk polymers were ground and sieved between 90 and 53 μm. Unreacted monomers were removed by stirring the particles in acetone and the imprint ion was leached using successive stirring of particles in 5 mol/L HCl. CP was similarly prepared by omitting the imprint ion. Figure 1 shows the schematic diagram of IIP preparation.

Characterization

Both the CP and IIP were characterized by FTIR for absence and presence of functional groups, BET for surface area measurements and SEM for surface morphologies.

Optimization studies

The effect of amount of polymer (5–40 mg), pH (1–8) of solution, aqueous phase volume (25–1,000 mL), stirring time (0–20 min), and eluent volume (5–30 mL) for elution of bound uranium were studied. After adsorption, polymers were filtered through a 0.45 μm filter paper and unextracted

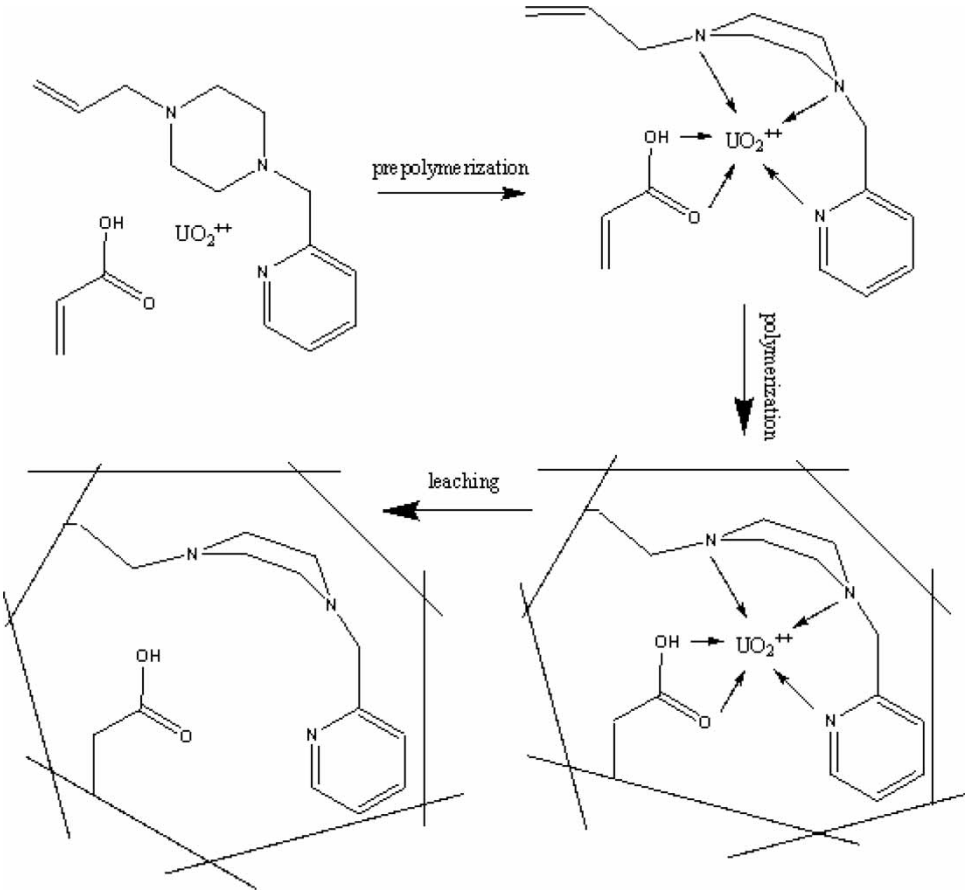

Figure 1 | Schematic representation of the imprinting method.

concentration of uranium(VI) was measured unless stated otherwise.

Retention capacity studies

To obtain the maximum amount of preconcentrated UO_2^{2+} ion per gram of IIP or CP, 20 mg of the IIP and CP were added to solutions containing UO_2^{2+} ion in the range of 0–660 μg mL^{-1} in 25 mL of deionized water under optimal conditions. The adsorbed UO_2^{2+} ion was eluted with 2 mol/L HCl. The concentration of the UO_2^{2+} ion in the eluent was measured by ICP-OES.

Binding studies

All experiments were carried out in a batch format except for the regeneration studies in which the SPE format was used. For SPE, the sample was introduced in portions of 5 mL (total volume was 25 mL) to fill up the cartridge. The polymer particles (50 mg) were packed in-between two frits (bottom and top) so as not to disturb the particle bed during the introduction of sample. Using a vacuum pressure pump, the elution flow rate was maintained to approximately 0.8 mL min^{-1}.

Selectivity studies and other constants

To examine the selectivity of the prepared IIP and CP for uranium over the other inorganic ions which coexist with uranium in the environment, 20 mg of the polymers were stirred in reaction vials containing different ions in solution. Each vial contained 25 mL of solution of 1 μg mL^{-1} concentration for each metal ion. The studies were performed for each metal ion versus uranium, and as a multi-element mixture. Adsorption capacity of each metal was measured and calculated using Equation (1) (Birlik *et al.* 2007):

$$Q = \frac{(C_o - C_e)V}{W} \quad (1)$$

where C_o and C_e are the initial and final concentrations respectively, V is the volume of the solution used for the

extraction and W is the mass of the polymer used for extraction. Per cent recovery (R) was calculated using Equation (2):

$$\%\ R = \frac{C_o - C_e}{C_o} \times 100\% \quad (2)$$

Distribution coefficients (K_d) of Co^{2+}, Zn^{2+}, Cu^{2+}, Ni^{2+}, Mn^{2+}, Fe^{3+} and UO_2^{2+} were calculated as:

$$K_d = \frac{(C_o - C_e)V}{C_o W} \quad (3)$$

where K_d is the distribution coefficient (mL g^{-1}) and the other variables are as already described. According to Birlik *et al.* (2007), Equation (4) can be used to calculate the selectivity coefficient for the binding of a metal ion in the presence of other competitive ions from equilibrium data:

$$K = \frac{K_d(UO_2^{2+})}{K_d(B)} \quad (4)$$

where K is the selectivity coefficient and B represents Co^{2+}, Zn^{2+}, Cu^{2+}, Ni^{2+}, Mn^{2+} and Fe^{3+} cations. The value of K gives an indication as to how much the polymer is selective for UO_2^{2+} ions in the presence of other cationic species in solution. Furthermore, the relative selectivity coefficient of IIP against CP is calculated from Equation (5):

$$K' = \frac{K_{imprinted}}{K_{non\text{-}imprinted}} \quad (5)$$

where $K_{imprinted}$ and $K_{non\text{-}imprinted}$ are the selectivity coefficients of the IIPs and CPs, respectively. The value of K' represents the enhanced effect of imprinting on selectivity and adsorption affinity for the template compared to the non-imprinted polymer.

Analysis of wastewater samples

Two-hundred-and-fifty millilitres of each wastewater sample were taken in a 500 mL beaker. 10 mL of 0.1 mol/L CH_3COOH/CH_3COONa buffer (pH 5.0) was added to each wastewater sample. These samples were divided into three equal portions, in which the first portion of each sample was spiked with 0 μg mL^{-1}, the second with 1 μg mL^{-1} and the third with 3 μg mL^{-1} of UO_2^{2+} ion. In triplicate, 25 mL of each sample were subjected to batch extraction with 20 mg IIP particles, stirring at room temperature for 1 h. The uranium adsorbed on the IIP particles was leached out with 2 mol/L HCl solution (10 mL), stirring at room temperature for 20 min. Concentration of uranium was determined by ICP-OES.

RESULTS AND DISCUSSION

Ligand and IIP preparation

^1H NMR, ^{13}C and DEPT 135 results revealed that the ligand used in this study (PPMP) was successfully synthesized. The active sites for the UO_2^{2+} ion are the three amino atoms from the ligand (Figure 1) and the hydroxyl from the MAA, giving a coordination type of bonding. Another possibility is the opening of the piperazine ring to yield 1-(prop-2-en-1-yl)-4-(pyridin-2-ylmethyl)-*N*-2-hydroxylethane-ethylenediamine during the complexation reaction. Albo *et al.* (2009) made a similar observation in which complexation yielded the opening of the imidazoline ring when using *N,N′*-di(2-hydroxy-4,6-di-*tert*-butyl-benzyl)imidazoline as a complexing ligand for UO_2^{2+} ions. The transformation was catalysed by the presence of a base in solution (e.g. OH^- or $UO_2(OH)^+$) (Albo *et al.* 2009). In our case, the presence of a broad band after leaching in Figure 2(b) at about 3,400 cm^{-1} could be attributed to the opening of the ring, hence the presence of hydroxyl groups.

Characterization

FTIR spectra

The FTIR spectra of the CP, leached and unleached IIP show a similar backbone indicative of a high level of the EGDMA cross linking reagent used (see Figure 2). All three spectra show a strong vibration frequency at about 1,720 cm^{-1} attributed to the C=O group of EGDMA polymers and another distinctive vibration at 1,141 cm^{-1} assigned to the C–O bond of EGDMA. The band at 1,637 cm^{-1} attributed to unpolymerized C=C of the monomer is almost diminished in all polymers indicating that almost all the monomers were reacted (Khajeh & Sanchooli 2010). Higher intensity of the band at 814 cm^{-1} in unleached polymer can be attributed to the presence of UO_2^{2+} ion as observed in the study by Singh & Mishra (2009).

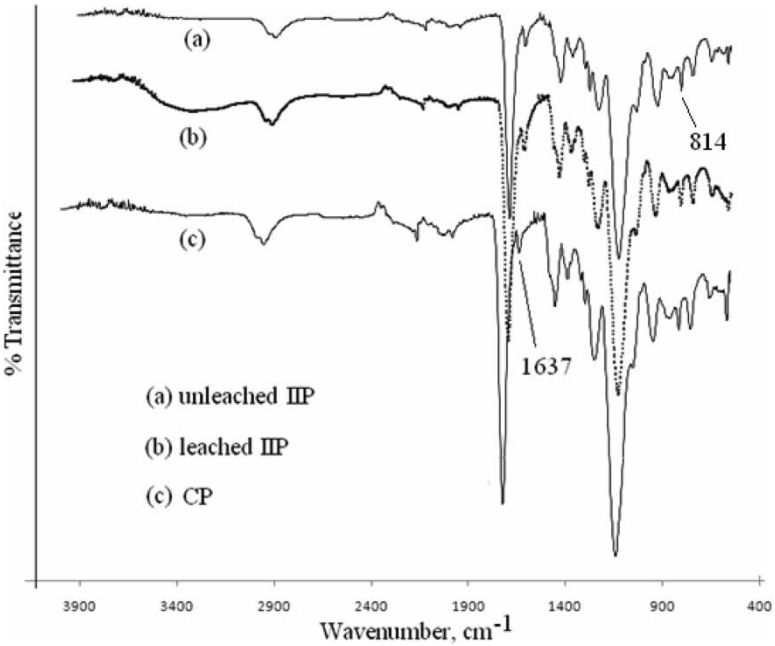

Figure 2 | FTIR spectra of (leached and unleached) IIP and CP.

Surface morphology and surface area determination

BET surface area values obtained for the IIP and CP were 26.3 and 16.1 $m^2 g^{-1}$, respectively. SEM micrographs of the IIP revealed that the particles have irregular shape due to crushing with mortar and pestle (Figure not shown).

Optimization studies

Various parameters optimized in the study are listed in Table 1.

Optimization of IIP quantity needed for maximum extraction of UO_2^{2+}

Table 1 No. 1 shows the results in the optimization of the amount of IIP particles varied from 20 to 40 mg. Optimum was achieved with 20 mg (%$R = 99.9\%$). Results also indicate that the IIP particles had a much higher recovery compared with CP.

Effect of pH

The effect of pH on the extraction of UO_2^{2+} ion IIP and CP are shown in Table 1 No. 2. IIP reached maximum extraction at pH 4–6 while the CP reached maximum at pH 7. Hence, pH 5 was used for subsequent experiments. Also, worth mentioning is the steady adsorption capacity demonstrated by the CP as the pH was increased and this situation resulted in about 95% adsorption. Not surprisingly, at lower pH values, the imprinting effect was lower due to protonation of the pyridine-N leading to repulsion of the UO_2^{2+} ion. The pH studies suggest that this polymer can be used successfully for the pH range 3.5–7.0. The CP showed unusually high recovery at pH 7. The reason for this finding cannot be fully explained. The mechanism for the removal of UO_2^{2+} ion in the pH range 4–5.5 is ion exchange and complexation processes (Shamsipur *et al*. 2007).

Effect of contact time

Results for the effect of contact time are shown in Table 1 No. 3. Within 20 min the extraction efficiency was >99%, hence, 20 min was used for all other experiments. The short time required to reach close to 100% recovery shows that the kinetics of UO_2^{2+} ion rebinding on IIP were fast.

Effect of aqueous phase volume

More than 90% recovery was achieved from volumes less than 200 mL (Table 1 No. 4), hence 30 mL was taken as optimum volume. At a sample volume higher than 200 mL, recoveries started to decrease. The decrease in %R as solution volume increased could be explained in

Table 1 | Influence of various parameters on per cent recovery of uranyl ion using IIP and CP particles

No.	Parameters	% Recovery IIP	CP
1	[a]Amount of sorbent, mg		
	5	86 ± 4	13 ± 1
	10	91 ± 2	31 ± 1
	15	94 ± 1	31 ± 3
	20	99 ± 1	28 ± 2
	25	98 ± 1	32 ± 2
	30	99 ± 1	31 ± 1
	35	98 ± 2	33 ± 1
	40	99 ± 1	41 ± 4
2	[b]pH of sample		
	1.53	12	1
	2.64	26	3
	3.38	90	9
	4.10	99	39
	5.02	99	65
	5.83	99	87
	6.97	96	95
	8.41	95	67
3	[c]Contact time, min		
	0	0	0
	5	95	29
	10	97	34
	15	99	31
	20	99	30
4	[d]Sample volume, mL		
	25	99 ± 1	–
	50	99 ± 1	–
	100	98 ± 1	–
	200	91 ± 2	–
	500	84 ± 5	–
	645	75 ± 7	–
	1,000	69 ± 2	–
5	[e]Regeneration		
	Cycle 1	99	–
	Cycle 2	99	–
	Cycle 3	99	–
	Cycle 4	99	–
	Cycle 5	94	–
	Cycle 6	99	–
	Cycle 7	99	–
	Cycle 8	99	–

[a]Solution pH 5; sample volume 25 mL; contact time, 20 min; initial concentration 1 μg mL^{-1}; stirring speed, 600 rpm.
[b]Sorbent mass, 20 mg; sample volume 30 mL; contact time, 20 min; initial concentration 1 μg mL^{-1}; stirring speed, 600 rpm.
[c]Sorbent mass, 20 mg; solution pH 5; sample volume 30 mL; initial concentration 1 μg mL^{-1}; stirring speed, 600 rpm.
[d]IIP quantity, 20 mg; solution pH 5; contact time, 20 min; initial concentration 1 μg mL^{-1}; stirring speed, 600 rpm.
[e]Amount of IIP, 50 mg; solution pH 5; sample volume 30 mL; initial concentration 1 μg mL^{-1}; SPE, flow rate 0.8 mL min^{-1}.

terms of the mass transfer of uranium from the bulk solution to the IIP particles. Smaller sample volume gives high contact time of UO_2^{2+} ions in solution with IIP particles. This observation is different to when IIP is used in SPE format. Then a decrease in recovery at high sample volume could indicate that the capacity of the sorbent is exceeded.

Retention capacity

The retention capacity study was performed by equilibrating 20 mg of IIP or CP particles with 30 mL uranium solution with concentrations ranging from 10 to 660 μg mL^{-1} under optimal conditions. It was observed that retention capacity of the IIP increases with increase in concentration until it reaches a plateau at 120 mg g^{-1} when the concentration of the UO_2^{2+} ion in solution was about 528 μg mL^{-1} (figure not shown). At low concentrations, the IIP particles can take up all the uranium in solution without exhausting its binding sites; hence the increase of binding capacity with increase in concentration. The binding capacity demonstrated by the prepared IIP was compared with some of the literature values from the different sorbent as listed in Table 2. Some of these sorbents have relatively higher loading capacity (Sureshkumar *et al.* 2010) than the present IIP. This situation is because of the larger surface area of some natural polymers. However, the type of chelating ligand and cross-linker used also affect the capacity. On the other hand IIPs bring about simplicity in preparation, low cost, selectivity, high thermal and mechanical strength.

Selectivity studies

The inorganic ions investigated for selectivity studies were Ni^{2+}, Zn^{2+}, Fe^{3+}, Cu^{2+}, Co^{2+}, and Mn^{2+}. The selected

Table 2 | Comparison of retention capacity values for the UO_2^{2+} ion with different sorbents

Metal ion	Sorbent	Binding capacity mg g^{-1}	Initial pH	Reference
UO_2^{2+}	Amberlite XAD-2000	3.6	3.0	Ghasemi & Zolfonoun 2010
UO_2^{2+}	Cross-linked chitosan	72.46	3.0	Wang *et al.* 2009
UO_2^{2+}	Cross-linked chitosan	239.9	5.0	Sureshkumar *et al.* 2010
UO_2^{2+}	Activated silica	153	4.0	Lee *et al.* 2010
UO_2^{2+}	Activated charcoal	82	4.5	Zhao *et al.* 2010
UO_2^{2+}	Date pits	10	5.5–6.5	Saad *et al.* 2008
UO_2^{2+}	Q-Amberlite XAD-4	37.4	4.5	Lee *et al.* 1997
UO_2^{2+}	IIP	98.5	3.5–5	Preetha *et al.* 2006
UO_2^{2+}	IIP	38.58	6.0	Sadeghi & Mofrad 2007
UO_2^{2+}	IIP	30.10	6.0	Gladis & Rao 2003
UO_2^{2+}	IIP	120	4.5–6	Present study

inorganic ions were equilibrated with 20 mg of IIP or CP at optimum pre-concentration conditions. The selectivity of the IIP was tested using a mixture of seven metal ions in solution as well as against each metal ion individually (binary mixtures). The concentration of the unextracted ions was determined by ICP-OES. Table 3 shows the results of such an experiment.

Extraction efficiencies of 17 and 91% were obtained for CP and IIP, respectively. This finding is due to the specific

Table 3 | Selectivity coefficients and distribution ratio using IIP. $C_o = 1\ \mu g\ mL^{-1}$; pH 5; $V = 25$ mL; sorbent mass, 20 mg

Metal ion	Distribution ratio (k_d, mL g^{-1})	Selectivity factor (α) IIP	CP
UO_2^{2+}	453,500	–	–
Mn^{2+}	12,000	37.8	0.5
Co^{2+}	7,500	60.5	1.6
Cu^{2+}	73,000	6.2	0.2
Ni^{2+}	500	907.0	0.2
Fe^{3+}	395,000	1.2	0.2
Zn^{2+}	500	907.0	0.2

shape, ionic charge and size of the binding cavity sites in IIP after removal of the template. It can be concluded that the prepared IIP can selectively remove UO_2^{2+} ion from several other inorganic ions contained in dilute aqueous solutions. The observed trend for selectivity was $UO_2^{2+} > Fe^{3+} \gg Cu^{2+} > Co^{2+} > Mn^{2+} > Zn^{2+} \sim Ni^{2+}$. Therefore it can be concluded that this polymer takes up far larger amounts of uranium and iron ions than other metal ions investigated in this study, implying that the polymer can be used to recover UO_2^{2+} ion from wastewater.

Elution and regeneration

Reusability of the IIP was tested using the SPE format, where 50 mg of polymer was packed in the cartridge and 25 mL of 1 $\mu g\ mL^{-1}$ of uranium(VI) solution was then passed through the cartridge as described in the experimental. The results show good stability and reusability of the polymer as %R of above 98% for up-to eight cycles in 95% confidence limits were obtained (Table 1 No. 5).

Table 4 | Application of IIPs on wastewater samples. $C_o = 1\ \mu g\ mL^{-1}$, 3 $\mu g\ mL^{-1}$ spiked samples; pH 5; $V = 25$ mL; sorbent mass, 20 mg. In brackets are the %RSD values

Sample No.	Sample	Uranium found ($\mu g\ mL^{-1}$) Present method[a] Added	Found	Direct analysis $\mu g\ mL^{-1}$	% Recovery
1	Pit water	–	0.55 (9.97)	0.52 (1.82)	104
		1.00	1.47 (8.42)		95
		3.00	3.60 (4.61)		102
2	Stream water	–	0.22 (5.92)	B.D.L.[b]	100
		1.00	1.37 (7.06)		100
		3.00	3.36 (4.88)		105

[a]Average of three determinations.
[b]Below detection limit.

Application of wastewater samples using IIPs

Pitwater and streamwater wastewater samples were collected from the Natalspruit wetland part of the Witswatersrand Basin in Johannesburg, South Africa. The extent of uranium leaching from gold tailings dumps in the Witwatersrand Basin was extensively studied using geochemical modelling and radioactive disequilibrium (Tutu *et al*. 2009).

The pH of both water samples was adjusted to pH 5 using CH_3COOH/CH_3COONa buffer and the extraction of uranium was carried out in a batch mode in triplicate and 2 mol/L HCl (10 mL) was used for leaching. The developed method proved to be suitable for quantitative monitoring of uranium in wastewaters (Table 4). The direct analysis column in Table 4 refers to analysis of water prior to any extraction.

CONCLUSIONS

It can be concluded that an IIP which can successfully remove uranium from other similar cations was prepared successfully from 1-(prop-2-en-1-yl)-4-(pyridin-2-ylmethyl) piperazine and methacrylic acid. Influence of various parameters such as pH, contact time, etc. were studied and optimum values were used for the successive experiments. Due to high selectivity shown by this IIP and high uranyl ion removal efficiency at pH 5–8, the prepared IIP can be applied for the removal of uranium from wastewaters.

ACKNOWLEDGEMENTS

The authors gratefully appreciate the financial support from National Research Foundation (NRF) of South Africa and The Swedish Foundation for International Cooperation in Research and Higher Education (STINT) Sweden–South Africa.

REFERENCES

Agrawal, Y. K., Shah, G. & Vora, S. B. 2006 Solvent extraction, speciation, separation and recovery of uranium(VI) from nuclear fuel, phosphate rocks and monazite sand with N-phenylbenzo-18-crown-6-hydroxamic acid. *J. Radioanal. Nucl. Chem.* **270** (2), 453–459.

Ahmadi, S. J., Noori-Kalkhoran, O. & Shirvani-Arani, S. 2010 Synthesis and characterization of new ion-imprinted polymer for separation and preconcentration of uranyl (UO_2^{2+}) ions. *J. Hazard. Mater.* **175**, 193–197.

Albo, Y., Saphier, M., Maimon, E., Zilbermann, I. & Meyerstein, D. 2009 A new chelate ligand designed for the uranyl ion. *Coord. Chem. Rev.* **153**, 2049–2055.

Birlik, E., Ersöz, A., Açykkalp, E., Denizli, A. & Say, R. 2007 Cr(III)-imprinted polymeric beads: sorption and preconcentration studies. *J. Hazard. Mater.* **B140**, 110–116.

Ghasemi, J. B. & Zolfonoun, E. 2010 Simultaneous spectrophotometric determination of trace amounts of uranium, thorium, and zirconium using the partial least squares method after their preconcentration by α-benzoin oxime modified Amberlite XAD-2000 resin. *Talanta* **80**, 1191–1197.

Gladis, J. M. & Rao, T. P. 2003 Synthesis and analytical applications of uranyl ion imprinted polymer particles. *Anal. Lett.* **36** (10), 2107–2121.

Khajeh, M. & Sanchooli, E. 2010 Development of a selective molecularly imprinted polymer-based solid-phase extraction for copper from food samples. *Biol. Trace Elem. Res.* **135**, 325–333.

Lee, C. H., Suh, M. Y., Joe, K. S., Eom, T. Y. & Lee, W. 1997 A chelating resin containing 4-(2-thiazolylazo)resorcinol as the functional group. Chromatographic application to the preconcentration and separation of some trace metal ions including uranium. *Anal. Chim. Acta* **35**, 57–63.

Lee, H. I., Kim, J. H., Kim, J. M., Kim, S., Park, J. N., Hwang, J. S., Yeon, J. W. & Jung, Y. 2010 Application of ordered nanoporous silica for removal of uranium ions from aqueous solutions. *J. Nanosc. Nanotech.* **10**, 217–221.

Preetha, C. R., Gladis, J. M., Rao, T. P. & Venkateswaran, G. 2006 Removal of toxic uranium from synthetic nuclear power reactor effluents using uranyl ion imprinted polymer particles. *Environ. Sci. Technol.* **40**, 3070–3074.

Rao, T. P., Kala, R. & Daniel, S. 2006 Metal ion-imprinted polymers – novel materials for selective recognition of inorganics. *Anal. Chim. Acta* **578**, 105–116.

Saad, E. M., Mansour, R. A., El-Asmy, A. & El-Shahawi, M. S. 2008 Sorption profile and chromatographic separation of uranium (VI) ions from aqueous solutions onto date pits solid sorbent. *Talanta* **76**, 1041–1046.

Sadeghi, S. & Mofrad, A. A. 2007 Synthesis of a new ion imprinted polymer material for separation and preconcentration of traces of uranyl ions. *React. Funct. Polym.* **67**, 966–976.

Shamsipur, M., Fasihi, J. & Ashtari, K. 2007 Grafting of ion-imprinted polymers on the surface of silica gel particles through covalently surface-bound initiators: a selective sorbent for uranyl ion. *Anal. Chem.* **79**, 7116–7123.

Singh, D. K. & Mishra, S. 2009 Synthesis and characterization of UO_2^{2+}-ion imprinted polymer for selective extraction of UO_2^{2+}. *Anal. Chim. Acta* **644**, 42–47.

Sureshkumar, M. K., Das, D., Mallia, M. B. & Gupta, P. C. 2010 Adsorption of uranium from aqueous solution using chitosan-tripolyphosphate (CTPP) beads. *J. Hazard. Mater.* **184**, 65–72.

Tutu, H., Cukrowska, E. M., McCarthy, T. S., Hart, R. & Chimuka, L. 2009 Radioactive disequilibrium and geochemical modeling as evidence of uranium leaching from tailings dumps in the Witwatersrand Basin. *Intern. J. Environ. Anal. Chem.* **89**, 687–703.

Wang, G., Liu, J., Wang, X., Xie, Z. & Deng, N. 2009 Adsorption of uranium (VI) from aqueous solution onto cross-linked chitosan. *J. Hazard. Mater.* **168**, 1053–1058.

WHO 1998 Available from: http://www.who.int/water_sanitation_health/dwq/chemicals/uranium290605.pdf (accessed 7 April 2009).

Winfield, M. S. 2007 *Clearing the Air: Uranium Mining: Nuclear Power's Dirty Secret.* Available from: www.pembina.org/pub/1503 (accessed 14 September 2009).

Zhao, Y., Liu, C., Feng, M., Chen, Z., Li, S., Tian, G., Wang, L., Huang, J. & Li, S. 2010 Solid phase extraction of uranium(VI) onto benzoylthiourea-anchored activated carbon. *J. Hazard. Mater.* **176**, 119–124.

First received 22 July 2011; accepted in revised form 12 October 2011

APPENDIX III

Journal of Chromatography A, 1230 (2012) 15–23

Contents lists available at SciVerse ScienceDirect

Journal of Chromatography A

journal homepage: www.elsevier.com/locate/chroma

Molecularly imprinted polymers targeting quercetin in high-temperature aqueous solutions

Vusumzi Pakade[a], Sofia Lindahl[b], Luke Chimuka[a], Charlotta Turner[b,*]

[a] School of Chemistry, University of the Witwatersrand, P/Bag 3, WITS 2050, Johannesburg, South Africa
[b] Department of Chemistry, Centre for Analysis and Synthesis, Lund University, P.O. Box 124, SE-221 00 Lund, Sweden

ARTICLE INFO

Article history:
Received 16 August 2011
Received in revised form 14 January 2012
Accepted 19 January 2012
Available online 25 January 2012

Keywords:
Extraction
High temperature
Molecular imprinting
Quercetin
Water
Yellow onion

ABSTRACT

Molecularly imprinted polymers (MIPs) targeting quercetin were prepared from 4-vinylpyridine and ethylene dimethacrylate (EDMA) under various solvent systems with the aim to form MIPs with high recognition for the quercetin molecule in aqueous systems at high temperature. A MIP prepared from the three-component solvent mixture of THF/H_2O/MeOH showed potential in its application for the determination of quercetin in plants (onion). The polymer particles before and after washing were characterized by infrared spectroscopy and thermogravimetric analysis. Surface morphology was recorded by scanning electron microscopy. The binding capacity of the MIPs was investigated at 25 and 84 °C, respectively, in batch mode. Parameters, including the influence of pH, extraction time and binding capacity, were evaluated. The slopes for the effect of extraction time revealed that the mass transfer of the analytes was higher at 84 °C than at 25 °C. Also, the binding capacity for the most promising MIP and its corresponding NIP was higher at 84 °C. The binding capacity for the MIP was ~30 μmol g^{-1} at 25 °C and ~120 μmol g^{-1} at 84 °C, while for the corresponding NIP, it was ~15 and ~90 μmol g^{-1}, at 25 and 84 °C, respectively. A demonstration of MIP selectivity at higher temperature using standard solutions of selected flavonols showed that the MIP still retained its selectivity for quercetin. Similar selectivity was observed when preliminary application studies on aqueous yellow onion extracts were investigated.

1. Introduction

The technique of molecular imprinting has, over the years, gained a lot of applications in biology and in chemistry, and it continues to attract interest in various fields. These include, but are not limited to, biosensors [1], antibody simulation [2], chiral resolution [3], enzyme catalysis simulation [4], and biochemical separation [5]. Molecular imprinting technique mimics natural molecular recognition [6–8], in that, macromolecules possessing high affinity and selectivity for the imprint/target compounds are produced through formation of predefined interaction between the template molecule and the ligand system. The most widely used technique for preparing molecularly imprinted polymers (MIPs) is the non-covalent imprinting approach, which is based on physical interaction of the template molecule and the functional monomer through, for example, hydrogen bonding, hydrophobic, electrostatic bonding and/or dispersion interactions [9,10]. The less usage of the covalent imprinting approach is due to the bottleneck of polymerizable functional units that possess reversible covalent bonds [11]. Mostly, MIPs are used as sorbents for the solid-phase extraction (MISPE) technique, as this offers both pre-concentration and removal of interferences [12]. However, Nemulenzi et al. [13] also demonstrated the potential of combining MIPs with liquid membrane for the extraction of β-estradiol from aqueous samples.

Although MIPs offer several advantages (high thermal stability and mechanical strength) over other polymeric materials there has been a general concern on the applicability of MIPs in polar solvents such as water [14]. In the non-covalent imprinting approach, the presence of polar solvents such as water disrupts the interaction of the template and the monomer resulting in polymers with poor level of recognition [15]. Several studies about preparation of MIPs in aqueous environments have been reported [16–23]. The successful imprinting in these studies was achieved by using hydrophilic monomers [18,20], a two-step extraction method [21], and surface imprinting [19] and it has also been noted that the template molecule can offer specific solutions [22]. Templates that can form ionic interactions are much better to be extracted by MIPs in aqueous media than those possessing hydrogen bonding. Recently, Shen and Ye [23] reported a new technique for producing water-compatible MIPs for propranolol using Pickering emulsion

* Corresponding author. Tel.: +46 46 222 8125; fax: +46 46 222 8209.
E-mail address: charlotta.turner@organic.lu.se (C. Turner).

0021-9673/$ – see front matter © 2012 Elsevier B.V. All rights reserved.
doi:10.1016/j.chroma.2012.01.051

polymerization in which a combination of hydrophobic and electrostatic interactions was the mode of recognition. However, in the above examples the MIPs were not used at high temperature.

In this study, the aim was to prepare quercetin MIPs in aqueous environments for selective recovery of quercetin from aqueous yellow onion extracts at high temperature. To our knowledge, this is the first time MIPs have been prepared in aqueous medium and used at higher temperature. The selectivity of the prepared MIPs was investigated in adsorption studies with structurally related compounds, and evaluated by high performance liquid chromatography (HPLC).

However, MIPs are not immune to drawbacks as the issue of batch-to-batch reproducibility in surface area and particle size distribution is yet to be satisfactorily resolved [24]. Also, the post-treatment of crushing and grinding has a potential of increasing non-specific binding due to the possibility of destroying the binding active sites thereby reducing batch-to-batch reproducibility. Although there have been substantial efforts in using other polymerization techniques such as emulsion polymerization [25] and precipitation polymerization [26] instead of bulk polymerization, bulk polymerization is still being widely used owing to its simplicity, robustness, compatibility with a variety of templates and because it requires limited organic chemistry [27–29]. Hence, in this study, bulk polymerization was used.

Quercetin, the most active antioxidant of the flavonol family, is present in vegetables and fruits, such as onions, apples and grapes in low amounts [30]. Besides antioxidant properties, quercetin possesses antitumor and antiviral properties as well as aiding in adjusting the immune system [31]. In fruits and vegetables, quercetin is present as glycosides, where glucose and rhamnose are the two most common sugar groups [32]. In yellow onion, quercetin-3,4′-diglucoside and quercetin-4′-glucoside are the main abundant glucosides [32]. Nonetheless, the aglycone and other quercetin glucosides are also present but in lower amounts. Quercetin species can be extracted from onion using solid–liquid extraction with aqueous methanol, which normally involves the use of high concentrations of HCl to catalyze the hydrolysis of glucosides to aglycones [33,34]. However, a more sustainable alternative method to methanol–HCl extraction/hydrolysis has been proposed and it involves the use of pressurized hot water as extraction solvent and enzyme-catalyzed hydrolysis [35,36]. Chromatographic methods have been widely used for the isolation of quercetin from plants employing a variety of solvent combinations [37–39]. However, MIPs offer much improved selectivity for a particular solute group than the mentioned chromatographic methods [40–42].

2. Materials and methods

2.1. Chemicals

Quercetin, kaempferol, disodium hydrogen phosphate, triethylamine and 1,1′-azobis(cyclohexanecarbonitrile) (ACCN) were purchased from Sigma–Aldrich (Steinheim, Germany). Quercetin-3,4′-diglucoside and quercetin-4′-glucoside were purchased from Polyphenols Laboratory AB (Sandnes, Norway) and morin was purchased from Extrasynthese (Genay, France). Methanol (Gradient grade) was purchased from B&J Brand (Honeywell, Germany), formic acid and citric acid monohydrate were purchased from Merck (Darmstadt, Germany). 4-Vinylpyridine (4-VP) and ethylene dimethacrylate (EDMA) were purchased from Acros Organics (Geel, Belgium). A stock solution of quercetin (0.3 g L^{-1}) in methanol and 0.5% formic acid was prepared in the laboratory and kept at −18 °C when not in use. Ultrapure water (MilliQ) was used in all experiments and chemicals were used as received. The pH was adjusted with citric acid monohydrate (0.1 M) and disodium hydrogen phosphate (0.2 M). The structurally related compounds tested are given in Fig. 1.

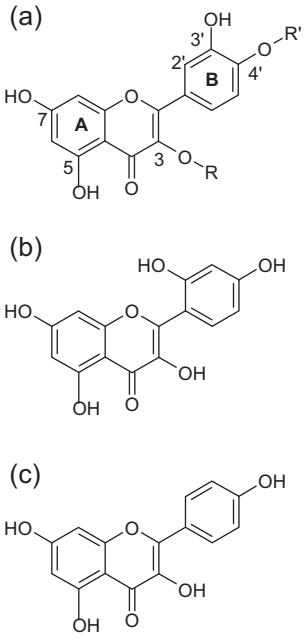

Fig. 1. Chemical structures of (a) quercetin (R, R′ = H), quercetin-4′-glucoside (R = H, R′ = glucose), quercetin-3,4′-diglucoside (R, R′ = glucose), (b) morin and (c) kaempferol.

2.2. Monomer–template interaction as studied by FTIR and UV/vis

Quercetin and 4-VP were stirred in THF/H_2O/MeOH (6:3:1, v/v/v) for 2 h at room temperature. Thereafter, this complex solution was passed through a solid-phase extraction (SPE) cartridge containing anhydrous $MgSO_4$ for drying out water, and then the eluate was bubbled with nitrogen to remove the organic solvent. The remains of this were then placed in the FTIR on a diamond plate using a liquid dispenser to acquire the spectrum. Fourier transform infrared spectroscopy (FTIR) spectra were recorded in the frequency range of 4000–400 cm^{-1} using a Bruker Alpha FTIR spectrometer (Ettlingen, Germany) with Attenuated Total Reflectance (ATR) solid state method with 24 scans. UV–vis absorption spectra were obtained using a Varian Cary 1E double beam spectrophotometer (Palo Alto, CA, USA) scanning from 190 to 600 nm.

2.3. MIP preparation

The quercetin imprinted polymers were prepared according to published procedures but with slight modifications [41]. The amounts of reagents used for each polymer are summarized in Table 1. In Table 1, M1 and M2 refer to MIPs, and N1 and N2 refer to corresponding NIPs for the MIPs, respectively. M3 and M4 are MIPs that were used as references in order to see how MIPs prepared in pure MeOH and THF perform in the recognition of quercetin compared to those prepared in aqueous medium, M1 and M2. In brief, for M2 and N2, a mixture of quercetin (0.4 mmol) and 4-VP (4 mmol) was stirred at room temperature in a 50 mL round bottomed flask containing 10 mL THF/H_2O/MeOH (6:3:1, v/v/v) porogenic mixture for 30 min to establish monomer–template interactions. After which, the polymerization reaction vessels were placed on ice to prevent unwanted polymerization. EDMA (18.5 mmol) and ACCN initiator (100 mg) were added. The solution mixture was purged with nitrogen for 10 min to remove dissolved oxygen, sealed and stirred in an oil bath at 60 °C (12 h) to initiate polymerization. After

Table 1
Composition of MIPs and NIPs.

Polymer	Quercetin (mmol)	4-VP (mmol)	EGDMA (mmol)	ACCN (mg)	Solvent	Solvent volume (mL)
M1	1.0	10.0	40.0	100	MeOH/H_2O (9:1, v/v)	10
N1	–	10.0	40.0	100	MeOH/H_2O (9:1, v/v)	10
M2	0.4	4.0	18.5	100	THF/H_2O/MeOH (6:3:1, v/v/v)	10
N2	–	4.0	18.5	100	THF/H_2O/MeOH (6:3:1, v/v/v)	10
M3	0.4	4.0	18.5	50	MeOH	5
M4	0.4	4.0	18.5	50	THF	5

12 h of polymerization, the temperature was increased to 80 °C for 3 h to achieve a solid monolith polymer. After polymerization, the polymers were crushed, ground and sieved through 88 μm sieves and finer particles were removed by sedimentation over acetone, decanting the solution in hourly intervals for 3 cycles. The resulting polymer particles were dried in an oven at 60 °C overnight, thereafter, the template was washed off by Soxhlet extraction for 24 h with MeOH/acetic acid (9:1, v/v). Following which, the particles were in addition washed with MeOH, MeOH/triethylamine (9:1, v/v) and MeOH in that order, and finally the polymers were dried in an oven at 55 °C overnight to give the final MIPs. Non-imprinted polymer (NIP) was prepared and washed in the same manner but quercetin was omitted. MIPs and NIPs prepared in other porogens used a similar preparation and washing procedure, and they were also subjected to the same treatment process in terms of template removal.

2.4. Characterization of MIPs and NIPs

Surface morphological information of MIP and NIP was obtained using a scanning electron microscope (SEM) JOEL Model JSM 6700F (Tokyo, Japan). Brunauer–Emmett–Teller (BET) instrument (MicromeriticsTristar) was used for the surface area determinations. Thermal gravimetric analysis (TGA) was performed using a TA Instruments Q500 TGA in high-resolution dynamic heating mode (New Castle, US) at a heating rate of 10 °C min^{-1} up to 500 °C under air atmosphere at 60 mL min^{-1}.

2.5. Determination of binding capacity

Several experiments were conducted at 25 °C and 84 °C in order to evaluate the binding capacity of the MIPs and NIPs. These experiments include adsorption as a function of time and concentration of quercetin, effect of pH, effect of initial temperature, and the selectivity of MIP for quercetin from structurally related compounds. All experiments were conducted in triplicates unless otherwise stated. Experiments on adsorption as a function of quercetin concentration for the MIP and NIP were investigated in static adsorption mode where 8 mg polymer particles were stirred in 4 mL MeOH/H_2O (7:3, v/v) solutions containing five different concentrations of quercetin at room temperature or 84 °C for pre-determined time intervals. Adsorption rate studies were conducted at pH 5.5 both at 25 °C and 84 °C and samples were drawn at 0.5; 1.0; 2.0; 4.0; 6.0; 10.0 h intervals. For experiments conducted at 25 °C, 4 mL of 218 μmol L^{-1} quercetin solution and 8 mg of polymer were used and for experiments conducted at 84 °C, 4 mL of 1.0 mmol L^{-1} quercetin solution and 4 mg of polymers were used. The influence of pH was studied at pH 4, 5.5 and 7, although the desired pH in a combined extraction/biocatalysis/MIP-based clean-up targeting quercetin in onion is pH 5.5, because this is the pH at which the enzyme hydrolysis of quercetin glucosides is performed. For the influence of pH, 8 mg of MIPs was stirred in 4 mL MeOH/H_2O (7:3, v/v) mixture containing quercetin (initial concentration 66 μmol L^{-1}) at 25 °C for 24 h. In all experiments, after the reaction time, samples were withdrawn from the reaction vials at suitable time intervals and placed in 1.5-mL centrifuge tubes and the solid material was spin down in a bench-top centrifuge. The supernatant was transferred into an HPLC vial containing MilliQ water with 0.5% formic acid for the determination of un-extracted concentration of quercetin. The quercetin concentration was measured as described in Section 2.6.

For investigations on binding as a function of quercetin concentration, initial concentrations in the range of 30–400 μmol L^{-1} were used. The experiments were conducted at 25 °C and stirred for 24 h whereas experiments at 84 °C were stirred only for 2 h. The amount adsorbed (Q, μmol g^{-1}) was calculated from Eq. (1):

$$Q = (C_0 - C_e)\frac{V}{W} \quad (1)$$

where C_0 and C_e (μmol mL^{-1}) are the initial and final concentrations respectively, V (mL) is the volume of the solution used for the extraction and W (g) is the mass of the polymer used for extraction.

2.6. HPLC analysis

HPLC–UV analysis was performed using a chromatographic system, UltiMate-3000® from Thermo Fisher (former Dionex, Germering, Germany). An Agilent Zorbax SB-C_{18} column (100 mm × 2.1 mm, 3.5 μm) with an Agilent Zorbax SB-C_8 pre-column (12.5 mm × 2.1 mm, 5 μm) was used for isocratic separation with a methanol/water (50:50, v/v) mobile phase containing formic acid (0.13 M), at a flow rate of 0.15 mL min^{-1}. The injection volume was 5 μL and detection was accomplished at 350 and 370 nm, respectively. Quantification of quercetin and all other compounds tested was performed using a five-point calibration curve of standards at concentrations between 1 and 75 μmol L^{-1}. Each vial taken to analysis had a total volume of 1.00 mL.

2.7. Selectivity studies

In order to examine quercetin selectivity by M2 and N2, a solution containing morin, quercetin, quercetin-4′-glucoside, quercetin-3,4′-diglucoside and kaempferol was used. The concentration of each compound was 66 μmol L^{-1} prepared in MeOH/H_2O (7:3, v/v). The pH of the solution was adjusted to 5.5 with a citric acid-phosphate buffer. Experiment was done in batch mode at 25 °C and 84 °C in triplicates. In short, 8 mg of the polymers were stirred in reaction vials containing 4 mL of the solution for 2 h (at 84 °C) and 6 h (at 25 °C), and non-adsorbed concentration of each substance was measured as previously described (see Section 2.6) after the binding reached equilibrium.

The distribution constant (k_d, mL g^{-1}) for each substance was calculated using Eq. (2):

$$k_d = \frac{Q}{C_e} \quad (2)$$

where Q (μmol g^{-1}) and C_e (μmol L^{-1}) are as described previously.

The selectivity coefficient (k) of MIP for quercetin with respect to the competitor species (quercetin-4′-glucoside, quercetin-3,

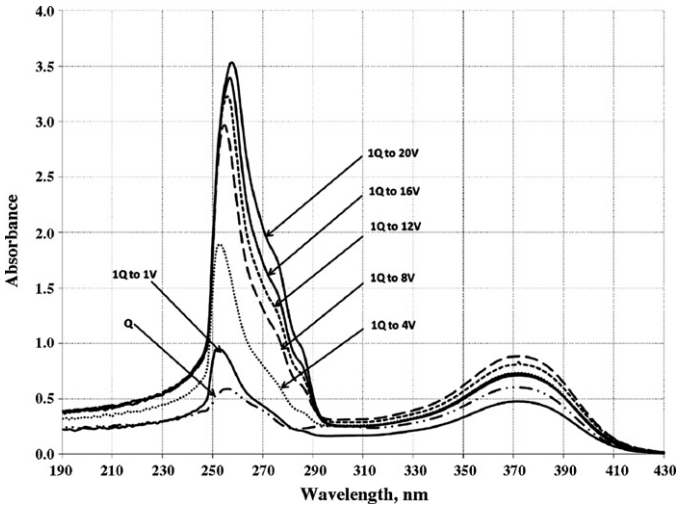

Fig. 2. The UV/vis spectra of different ratios of quercetin:4-VP (Q:V) in THF/H_2O/MeOH (6:3:1, v/v/v), three times scan.

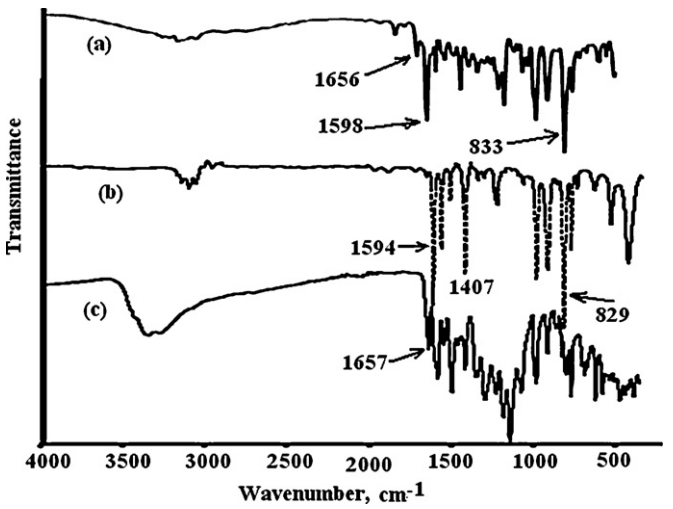

Fig. 3. FTIR spectra of quercetin-4–vinylpyridine complexes (a), 4-vinylpyridine (b) and quercetin (c).

4′-diglucoside, kaempferol or morin), referred to as B in Eq. (3) was calculated from the distribution constant as indicated in Eq. (3):

$$k = \frac{k_{d,(quercetin)}}{k_{d,B}} \quad (3)$$

The value of k gives an indication on the recognition ability and selectiveness of the MIP for quercetin with respect to other similar compounds. Similarly, a relative selectivity coefficient k' can be calculated as illustrated in Eq. (4), where the value of k' shows the imprinting effect on binding affinity and selectivity of MIP for quercetin over NIP [43].

$$k' = \frac{k_{MIP}}{k_{NIP}} \quad (4)$$

2.8. Application to aqueous yellow onion extract

The potential of future application of the prepared MIPs was tested on aqueous yellow onion extracts in batch mode. Yellow onion extract was prepared using pressurized hot water extraction as described by Turner et al. [35]. The pH of the aqueous onion extract solution was adjusted to pH 5.5 with the citric acid/phosphate buffer. In triplicates, 4 mL of pH 5.5 buffered yellow onion extract solution were extracted with 8 mg MIPs at 25 and 84 °C for 24 and 2 h, respectively. Concentration of quercetin before and after application of MIPs was quantified as described in Section 2.6. MIPs were first washed with 2 mL of MeOH in two portions of 1 mL and finally washed with 2 mL of MeOH/acetic acid (9:1, v/v) in one portion by stirring the MIPs at room temperature for 20 min. To calculate the recovery, quercetin in the methanol extracts (washing solution) and in the methanol/acetic acid extracts were combined.

3. Results and discussion

3.1. UV/vis studies of monomer–template interactions

The effect of the solvent on the monomer–template strength was investigated by stirring the following ratios: 1:1, 1:4, 1:8, 1:12, 1:16 and 1:20 of quercetin-to-4-VP (Q:V) in THF/H_2O/MeOH (6:3:1, v/v/v) for 2 h at room temperature. The resulting solution mixtures were scanned using the UV/vis spectrophotometer from 190 to 600 nm and the results are depicted in Fig. 2. It can be observed that quercetin absorbs light at two different wavelengths, i.e. at ~250 and 370 nm, where the band at 250 nm is attributed to the benzoyl chromophore and the band at 370 nm is assigned to the cinnamoyl chromophore of the quercetin molecule [44]. The benzoyl and cinnamoyl chromophores are the rings labeled A and B in the quercetin molecule in Fig. 1. There is no significant shift of the wavelength for any of the quercetin:4-VP (Q:V) ratios at 370 nm, except that the ratio of 1:8 and 1:12 (Q:V) have the highest absorbencies in that order. However, there is a noticeable change for the bands at ~250 nm wavelength. With the increase in the ratio of 4-VP, lambda max (λ_{max}) shifts to the longer wavelength gradually. This shift can be said to obey Einstein shift phenomenon, which is defined as a shift toward longer wavelengths of spectral lines emitted by atoms in strong gravitational field resulting in molecules with less energy and lower frequency. In this case the Einstein shifts are a result of the formation of hydrogen bonding and π–π interactions between the template molecule quercetin and the 4-VP resulting in the formation of a self-assembled complex of quercetin:4-VP.

Based on these observations, it can be said that strong monomer–template for the pre-polymerization complex can be achieved under the porogen conditions used. A 1:10 (quercetin:4-VP) ratio which is a compromise for the benzoyl and cinnamoyl chromophore intensity and shifts was regarded as the optimum ratio, hence, this ratio was used for polymer fabrication (Table 1). This is slightly different from the 1:8 ratio previously used by Molinelli et al. [41] for the preparation of quercetin MIPs with 4-VP in acetone. Excess of monomer is needed to create strong interactions between monomer and template but one has to be careful as this can lead to the creation of single-point attachments, which then lead to non-specific binding. Therefore, a compromise was made in order to form the desired multipoint interaction, i.e. a 1:10 ratio was chosen. Similar results in which an excess of monomers was used was reported by Sun and Qiao [17] in their study on methacrylic acid:ofloxacin imprinted polymers under MeOH/water (9:1, v/v) conditions. The optimum ratio of ofloxacin-to-methacrylic acid was 1:10 [17].

3.2. FTIR studies of monomer–template interaction

The spectra for quercetin:4-VP complex, 4-VP, and quercetin are shown in Fig. 3. Vibrational bands corresponding to both quercetin and 4-VP are present in Fig. 3(a) (although the frequency was shifted from 1594 to 1598 cm^{-1}, and from 829 to 833 cm^{-1}) implying their involvement in complex formation. No real shift of the quercetin C=O band (1657–1656 cm^{-1}) was observed because this functional group is not involved in hydrogen bonding with 4-VP. Furthermore, quercetin hydroxyl characteristic

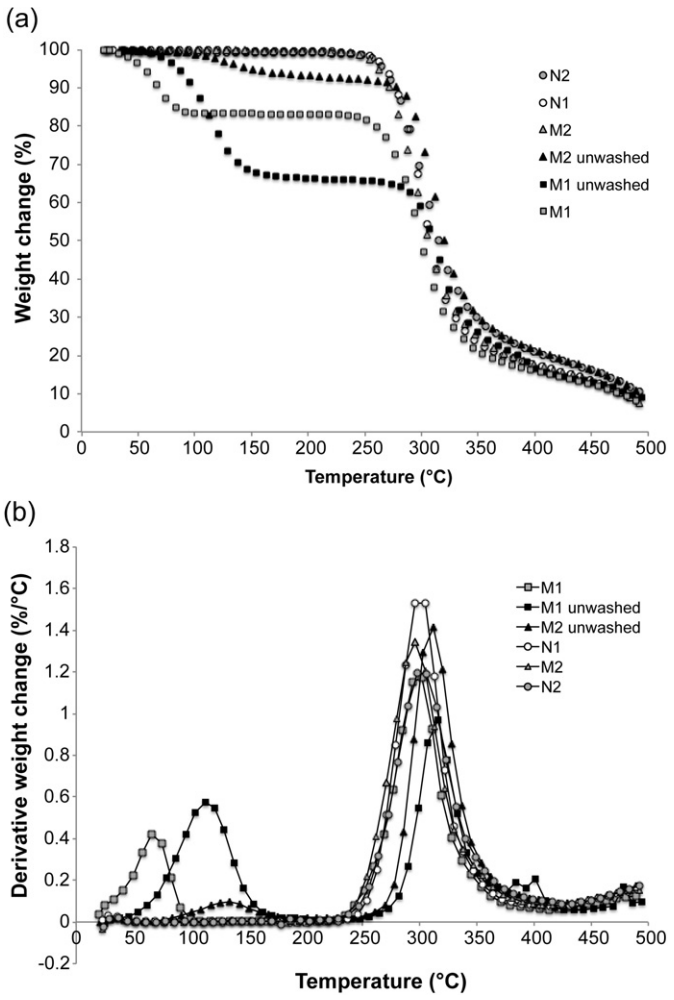

Fig. 4. TGA curves of M1 (washed and unwashed), M2 (washed and unwashed), N1 and N2. (a) The weight change in % as function of temperature (°C), and (b) the derivative of the weight change as function of temperature (°C).

bands C—OH stretch bend at 1160–1030 cm^{-1}, C—OH in-plane bend at 1440–1260 cm^{-1} as well as C—OH wag at 700–600 cm^{-1} (Fig. 3(b)) have also disappeared. Also, the hydroxyl broad band of quercetin (Fig. 3(c)) is slightly flattened out on the complex (Fig. 3(a)). Both these changes are attributed to the involvement of quercetin to complexation with 4-VP molecules. Furthermore, complexation might result in molecules of lower energy due to limited movement of the resulting bonds, which is supported by the redshifts observed in UV–vis spectra.

3.3. Characterization of MIPs and NIPs

The FTIR spectra of unwashed MIPs and washed MIPs and NIPs showed similar backbone structure indicative of the high degree of cross-linking (EDMA) agent used (data not shown), characterized by strong vibration bands at 1720 and 1140 cm^{-1} attributed to the C=O and C—O functional groups of EDMA, respectively. All polymers exhibited an almost diminished vibration band at 1736 cm^{-1}, indicating that almost all the monomer 4-VP was polymerized as this peak is normally attributed to unpolymerized double bonds of the monomer [45]. The presence of quercetin in unwashed MIPs was characterized by a broad band at around 3300 cm^{-1}, whose intensity diminished in washed MIPs.

TGA plots of M1 (washed and unwashed), M2 (washed and unwashed), N1 and N2 are presented in Fig. 4. It can be observed

Table 2
Pore size diameter and surface area summary results for the studied polymers ($n = 1$).

Polymer	Average pore diameter (nm)	Surface area ($m^2\ g^{-1}$)
M1	10.2	222
N1	19.7	71
M2	6.7	334
N2	5.3	69
M3	17.6	6
M4	12.9	2

that there are differences in decomposition patterns between washed and unwashed MIPs, and between MIPs and NIPs. There are two decomposition steps for washed and unwashed M1 and unwashed M2, but in the case of N1, N2 and washed M2, there seem to be only one decomposition step. However, the experiment was only allowed to run up to 500 °C and at this temperature the polymers have not completely decomposed. For washed M1, almost 15% weight loss is seen up to 90–100 °C and for unwashed M1 there is almost 30% weight loss up to 150 °C. For unwashed M2 the first weight loss up to 150 °C is approximately 10%. Weight losses at temperatures below 150 °C are normally attributed to water loss and decomposition of free monomer, cross-linker and monomer–template complex [46–48]. Larger weight loss for M1 suggests that more of free monomer and cross-linker were remaining in this polymer. Most importantly, all the polymers appear to be rigid up to 250 °C, and beyond that temperature they started to disintegrate.

SEM analysis was performed to observe the morphology of the particles. Although no pores were observed under the detector resolution used in SEM, however, the particles exhibited irregular shape due to crushing and the particle size distribution look similar (images not shown). Further, it was proved by BET that M2 particles exhibited higher surface area (334 $m^2\ g^{-1}$) than N2 (69 $m^2\ g^{-1}$) as well as higher pore size diameter. Results are summarized in Table 2.

3.4. Polymerization of quercetin water-compatible MIPs

MIPs were prepared in two different aqueous environments, that is, using MeOH/H_2O (9:1, v/v) (M1) and THF/H_2O/MeOH (6:3:1, v/v/v) (M2) as porogens, respectively. As references, two other polymers were made in pure methanol and pure THF solvents (M3 and M4, respectively, see Table 1). It is well known that MIPs perform better if the same solvent for preparation is used for re-binding [49]. Therefore, solvent for re-binding experiments containing maximum amount of water was investigated, as this would mimic the aqueous environments of the extracts for the ultimate application. MIPs and NIPs were stirred in different proportions of methanol/water mixtures (9:1, 7:3 and 5:5) and adsorption of quercetin was investigated (Fig. 5). Control samples were also included, labeled "Stds", which refers to quercetin standard solutions used in each adsorption experiment, but without the addition of MIPs/NIPs. Maximum re-binding solvent was found to be methanol/water (7:3) for M2, hence this was used for all subsequent experiments. Monomer–template binding strength can be affected by the relative permittivity of the solvent as well as other solvent parameters, which could result in MIPs with poor recognition capabilities [49].

In the case of M2, the porogenic solvent and the re-binding solution have the same water content. Quercetin possesses phenolic hydroxyl groups that behave as weak acids, as such strong hydrogen-bonding interaction can be established with the vinylpyridine. Therefore, these interactions can be said to be stronger in the case of M2 compared to other polymers under the tested conditions when the water content was 30% (Fig. 5). Chen et al. [50] reported hydrophobic interactions as a mode of

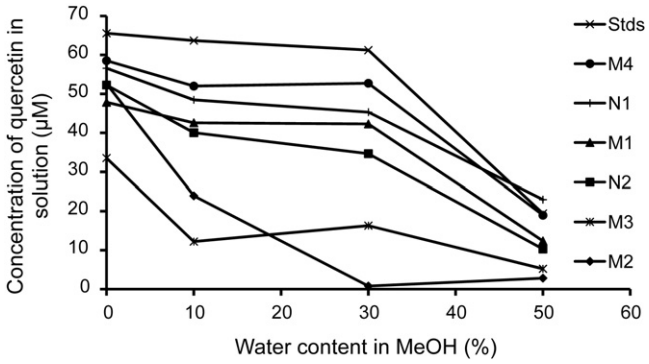

Fig. 5. Effect of water content on quercetin removal by MIPs and NIPs. Amount polymer 8 mg, solution volume 4 mL, contact time 24 h, temperature 25 °C, initial concentration 66 μM, pH not controlled (MeOH/H_2O), $n = 2$. See Table 1 for explanations on MIPs and NIPs.

recognition when the water content was greater than 65%. When water content was lower than 10%, hydrogen bonding was predicted as the main mode of recognition [17,50].

It has been previously demonstrated that a medium polar aprotic solvent such as THF gives better imprinting factor for quercetin MIPs involving hydrogen bonding [42]. However, the authors reported lower imprinting factor when more polar solvents than THF were used. In our studies we increased the polarity by adding water and methanol to THF to form a ternary solvent mixture with a ratio of 6:3:1 (THF/H_2O/MeOH, the porogen used to make M2 and N2) due to the miscibility of the three. MeOH is expected to impart the porogenic effect while higher volumes of THF will balance the disturbing effect of water while providing higher chances of hydrogen bond formation.

3.5. The effect of pH

The performance of the prepared MIPs at three different pHs (pH 4, 5.5 and 7) was investigated (Fig. 6). The aim here was to see if the binding capacity was better or worse at pH 5.5, which is the optimum pH for enzyme-catalyzed hydrolysis of quercetin glucosides in onion extract.

Obviously, the pH plays a crucial role in the affinity between quercetin and the MIP. This is the same pH effect that is used to washout quercetin template molecules from the MIP, i.e. an acidified methanol solution is commonly used. A low pH is believed to charge the amino groups of the MIP resulting in the release of quercetin molecules to the solution. In re-binding, one has to avoid low pH as it is shown that both MIP and NIP exhibited lower binding capacities at pH 4, see Fig. 6. M2 seems to work well at the desired

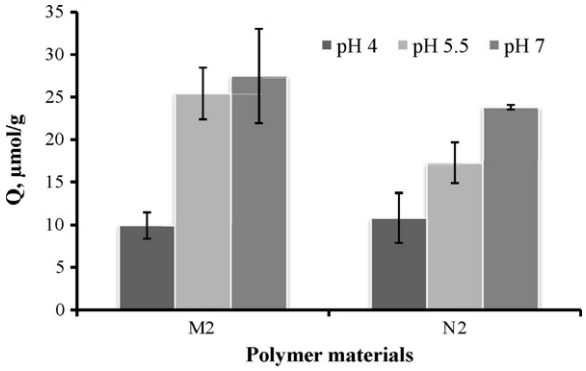

Fig. 6. Effect of pH on binding capacity. Initial concentration of quercetin 66 μmol L^{-1}, amount of polymer 8 mg, solution volume 4 mL, contact time 90 min, temperature 25 °C.

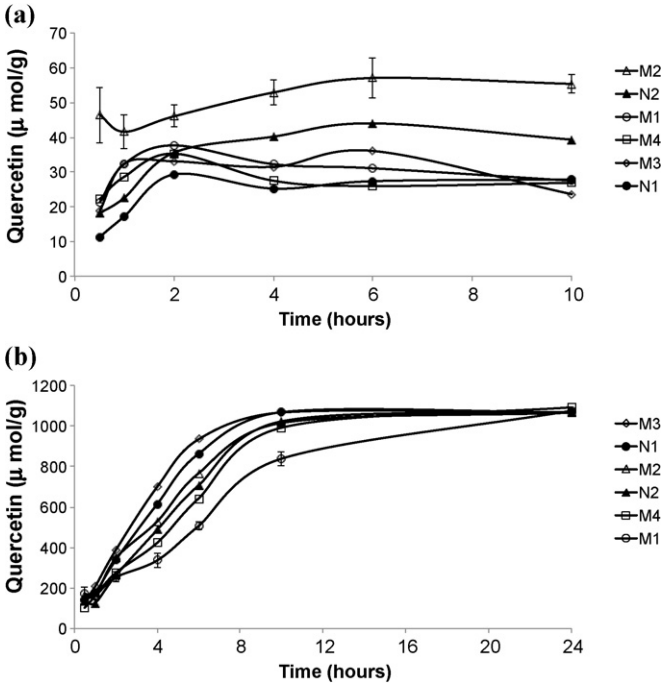

Fig. 7. Effect of contact time on binding capacity of polymers at 25 °C (a) and 84 °C (b). pH was 5.5 and solvent was MeOH/H_2O, 7:3 (v/v). Error bars showing standard deviation are only displayed for one of the curves in each figure, due to limited space. $n = 3$.

pH 5.5 (Fig. 6) and this is a good sign that these MIPs can be used for selective extraction of quercetin from yellow onion extracts.

3.6. Adsorption as a function of time

The influence of contact time on the adsorption of quercetin to the polymers was investigated at 25 °C and 84 °C, and the results of these investigations are depicted in Fig. 7(a) and (b), respectively. For the studies at 25 °C, an initial concentration of 218 μmol L^{-1} was used whereas 1000 μmol L^{-1} initial concentration was used for the studies at 84 °C. All experiments were conducted in triplicates but due to overlap of the adsorption curves, error bars were included only for one of the MIPs in Fig. 7. Notably in this figure is that M2 exhibited a higher binding capacity at about 55 μmol g^{-1} after 6 h closely followed by its corresponding NIP, N2, at 42 μmol g^{-1} after 6 h. All the other polymers were either below or in level with N2. These results reveal that M2 had better imprinting capabilities compared to other polymers. The graphs of the tested MIPs and NIPs in Fig. 7(b) reach a plateau after 24 h, possibly with the exception of M1. This plateau was not reached because the polymers had reached saturation but rather because all the quercetin present in the initial solution was adsorbed to the polymers. Hence, since all quercetin in the solution was adsorbed it is not possible to evaluate if there is any difference in binding capacity between the different MIPs and NIPs. The fastest adsorption at 84 °C (Fig. 7(b)) is seen for M3 and N1, then followed by M2, N2 and M4 and the slowest adsorption was seen for M1. When the slopes of Fig. 7(a) and (b) for the first 5 h are compared, it reveals that the influence of higher temperature (84 °C) leads to faster mass transfer. It is also clear that a higher temperature leads to a larger magnitude of binding capacity (Fig. 7(a)). The effect of higher binding capacity at higher temperature can be explained by the lower viscosity and surface tension of the solvent, enabling improved wetting of the MIPs and NIPs. A higher temperature also leads to lower relative permittivity, i.e. weakened hydrogen bonding, which could also result in higher binding capacity. A follow up detailed study

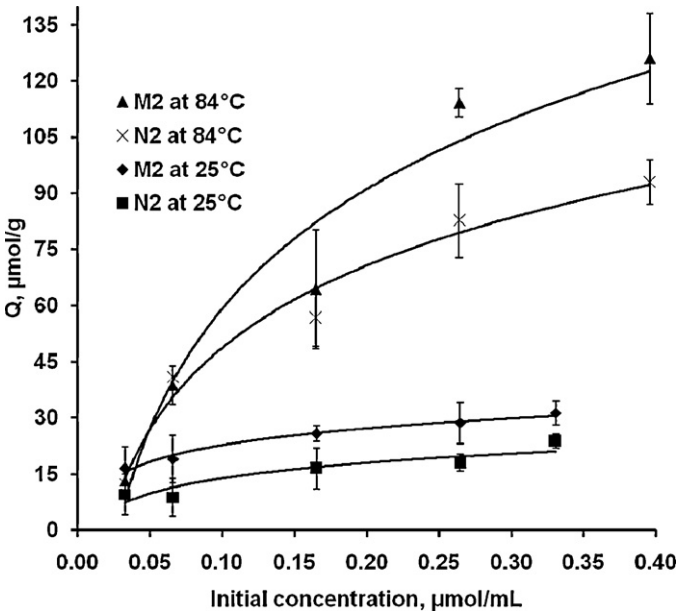

Fig. 8. Effect of initial quercetin concentration on binding capacity of polymers M2 and N2. Amount of polymer 8 mg, solution volume 4 mL, contact time 24 h at 25 °C, or 2 h at 84 °C, pH 5.5, solvent MeOH/H_2O (7:3, v/v).

on the effects of temperature on binding capacity is planned in the nearest future.

3.7. Binding capacity of the MIPs at different temperatures

Binding capacity was evaluated at 25 °C and 84 °C using M2 and N2. The initial concentration was varied between 10 and 400 μM and the results are depicted in Fig. 8. When the experiments were done at room temperature, 25 °C, it can be observed that M2 is approaching steady state at about 270 μmol L^{-1} of about 28 μmol g^{-1} whereas N2 at about the same concentration had a binding capacity of 16 μmol g^{-1}. This difference in binding capacity is attributed to predefined imprinting cavities present in the MIP and absent in the NIP in addition to shape and size, and unspecific binding. Therefore, the MIP (M2) has slightly higher degree of quercetin recognition than its corresponding NIP (N2). However, for the same initial concentration range the binding capacity of both M2 and N2 increased by 4-folds when the experiments were conducted at higher temperature, 84 °C, confirming the results in Fig. 7 as discussed above. To test whether the quercetin was actually adsorbed on the polymer particles or it was just an effect of degradation, reaction vials containing the different initial concentrations of quercetin solution were also subjected to the same temperature for the duration of the experiments. No MIPs/NIPs were added in these solutions. Indeed it showed that there was no degradation involved as concentrations before and after exposure were similar (data not shown). The observed results are in agreement with the theory that MIPs prepared at higher temperature tend to work better at higher temperatures [22,51], and our MIP was prepared at 80 °C due to the use of the ACCN initiator which requires higher temperature to form radicals.

3.8. Selectivity

The selectivity of the MIP, M2, to quercetin amongst some of its structural related compounds, morin and kampferol (Fig. 1(b) and (c)), was evaluated at the selected processing temperature of 84 °C in triplicates. Distribution constant (k_d), selectivity coefficient (k) and the relative selectivity coefficient (k') were calculated as described in Eqs. (2)–(4), respectively. The results are illustrated in Table 3. As shown in Table 3, M2 and N2 have the same binding capacity as demonstrated by the Q and k_d values tabulated. Although the capacity of the MIP is expected to be higher than that of the NIP, this is not demonstrated in Table 3 because all the dissolved quercetin was adsorbed, even though the solution was nearly saturated. Another explanation to the similar binding capacity is that MIPs are less selective in binding target compounds when a polar solvent is used. Instead, the selectivity of the MIPs is demonstrated from washing and elution steps, as described further below for a real sample. However, as discussed above, the imprinting effect of M2 prevailed over N2 when the concentration of the analyte was higher (Fig. 8). Because of the high cost of the other compounds tested for selectivity we have only been able to work with relatively low concentrations as mentioned already.

Table 3
Distribution coefficient (k_d), selectivity coefficient (k) and relative selectivity coefficient (k') of the MIP (M2) and NIP (N2) taken from results conducted at 84 °C.

Polymer	Analyte	k_d (mL g^{-1})	k	k'
M2	Quercetin	14,260	–	–
	Kaempferol	388	37	1.19
	Morin	148	97	1.07
N2	Quercetin	14,260	–	–
	Kaempferol	452	31	–
	Morin	156	91	–

Fig. 9(a) shows a typical chromatogram of the selectivity standard solution mixture before the application of MIP (M2) and Fig. 9(b) is a typical chromatogram obtained after MIP application as described above. It can be seen that the MIP was able to selectively remove all the quercetin from the mixture of compounds containing kaempferol, morin, quercetin-4′-glucoside and quercetin-3,4′-diglucoside. Both quercetin-4′-glucoside and quercetin-3,4′-diglucoside are relatively "bulky" molecules due to attached glucose moieties and hence unable to fit in the quercetin cavities created by imprinting. Therefore, almost none of these were selectively adsorbed, particularly not the diglucoside,

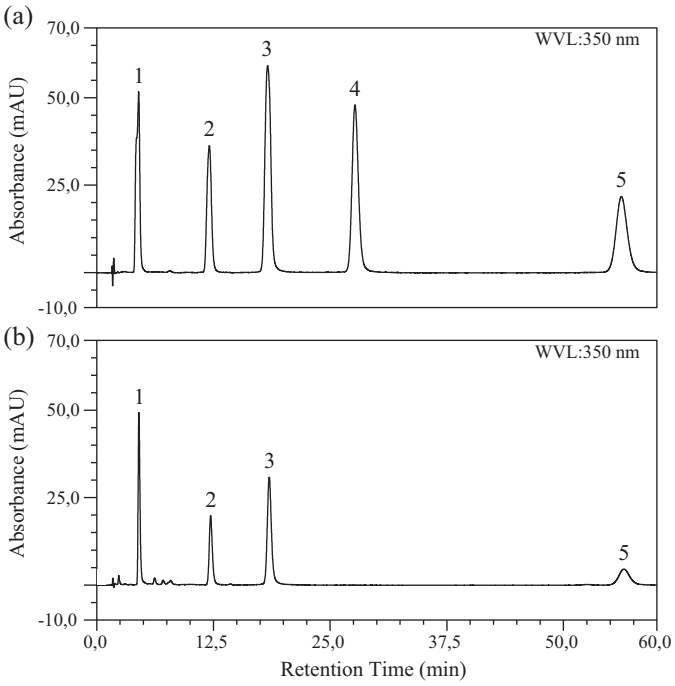

Fig. 9. HPLC chromatograms of a standard solution of Q-3,4′ (1), Q-4′ (2), morin (3), quercetin (4) and kaempferol (5), before (a) and after (b) the addition of M2 MIPs.

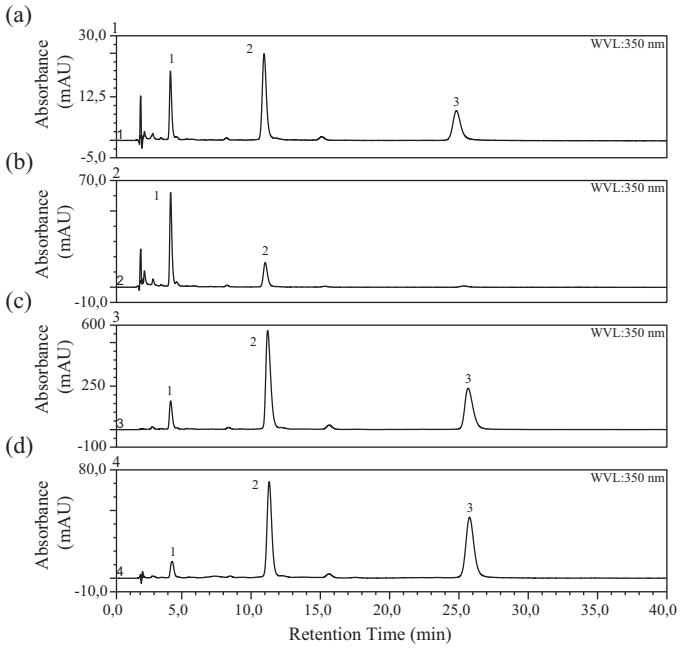

Fig. 10. HPLC chromatograms of (a) onion extract before addition of M2 MIP, (b) onion extract after addition of M2 MIP, (c) collected MeOH washing solution and (d) collected MeOH/acetic acid washing solution. 1 = Q-3,4′, 2 = Q-4′, 3 = Q.

whereas to some extent morin and kaempferol were adsorbed on the polymer (Fig. 9). This shows that MIPs can be selective but they still suffer from unspecific binding.

As mentioned earlier, quercetin-4′-glucoside and quercetin-3,4′-diglucoside are commonly hydrolyzed to quercetin aglycone, therefore these are not included in Table 3 for calculations of selectivity and distribution factors. The selectivity factor and distribution constant values summarized in Table 3 further emphasize that both M2 and N2 can bind the quercetin substantially well. The imprinting effect of M2 over N2 is demonstrated by the k and k' values, which show that M2 is better than N2. However, k' is just above 1, implying closeness in binding the quercetin molecule by M2 and N2. Hydrogen bonding and π–π interactions are most likely the main recognition sites, as explained by the structure of the quercetin molecule. The presence of water in these experiments might disrupt hydrogen bonding resulting in more π–π interactions (aromaticity of quercetin and 4-VP monomer). Studies are underway to further improve the selectivity of quercetin MIPs in pure aqueous environments.

3.9. Application to a yellow onion extract

Fig. 10(a) shows an aqueous yellow onion extract (ten times dilution) obtained from pressurized hot water extraction of yellow onion. Fig. 10(b) shows the chromatogram of the onion extract after MIP application, Fig. 10(c) shows a chromatogram of M2 particles washed with pure methanol solution (2 mL) for 75 min and Fig. 10(d) shows M2 particles washed with MeOH/acetic acid (9:1, v/v) after the MeOH wash. The prepared polymer seemed to work well under the tested conditions, in that almost no quercetin peak was observed in Fig. 10(b) compared to in Fig. 10(a), implying a possible adsorption to the polymer. A similar trend was observed when N2 was applied to the aqueous onion extract (data not shown). However, since quercetin was found both in the MeOH and MeOH/acetic acid wash solutions, and this trend was the same for N2, it is hard to draw any conclusions on the ratio between unspecifically and specifically bound quercetin. For future studies, it needs to be investigated further the choice of washing solution for unspecifically bound quercetin.

4. Conclusion

Novel quercetin MIPs that can be used at high temperatures under aqueous conditions were produced using a THF/H_2O/MeOH porogenic mixture. All MIPs and NIPs produced were intact at temperatures of up to 250 °C as determined by TGA. The most promising MIP worked well at pH 5.5 and with the re-binding solution methanol/water (7:3), demonstrating a significantly higher binding capacity of the MIP compared to its corresponding NIP. Furthermore, our results demonstrate that a higher temperature (84 °C compared to 25 °C) can beneficially be used to obtain faster adsorption kinetics as well as higher binding capacity and more research in this direction is planned. Finally, the MIP demonstrated good affinity and selectivity to the quercetin from yellow onion extract solution. No conclusive remark on the type of bonding (unspecific or specific) could be made on experiments conducted at 84 °C for 24 h as all the quercetin was adsorbed on both MIP and NIP. However, the influence of the imprinting effect under these conditions was observed when adsorption of structurally related analogs was tested. Other monomers that can have adequate hydrogen bonding under aqueous conditions are currently being explored.

Acknowledgments

The financial support from National Research Foundation (NRF) of South Africa, the Swedish Research Council Formas (209-2006-1346, 229-2009-1527), the Swedish Foundation for International Cooperation in Research and Higher Education (STINT, YR2009-7015) and the Swedish Research Council (VR, 2010-333) is gratefully appreciated. Prof. Patric Jannasch and Carlos Rodriguez Arza (Centre for Analysis and Synthesis, Department of Chemistry, Lund University) are thanked for help with TGA instrument, Prof. Reine Wallenberg (*ditto*) is thanked for SEM analysis and Prof. Ola Wendt (*ditto*) is acknowledged for usage of FTIR instrumentation.

References

[1] B.S. Ebarvia, C.A. Binag, F. Sevilla, Anal. Bioanal. Chem. 378 (2004) 1331.
[2] L. Ye, K. Mosbach, React. Funct. Polym. 48 (2001) 149.
[3] M. Quaglia, L.E. De, C. Sulitzky, G. Massolini, B. Sellergren, Analyst 126 (2001) 1495.
[4] G. Wulff, Chem. Rev. 102 (2002) 1.
[5] M.L. Zhang, J.P. Me, Q. Zhou, G.Q. Chen, Z. Liu, J. Chromatogr. A 984 (2003) 173.
[6] K.J. Shea, Trends Polym. Sci. 2 (1994) 166.
[7] K. Mosbach, O. Ramstrom, Biotechnology 14 (1996) 163.
[8] H. Zhang, L. Ye, K. Mosbach, J. Mol. Recogn. 19 (2006) 248.
[9] B. Sellergren, M. Lepisto, K. Mosbach, J. Am. Chem. Soc. 110 (1988) 5853.
[10] R. Arshady, K. Mosbach, Makromol. Chem. 182 (1981) 687.
[11] J. O'Mahony, A. Molinelli, K. Nolan, M.R. Smyth, B. Mizaikoff, Biosens. Bioelectron. 21 (2006) 1383.
[12] E. Caro, N. Masque, R.M. Marce, F. Borrull, P.A.G. Cormack, D.C. Sherrington, J. Chromatogr. A 963 (2002) 169.
[13] O. Nemulenzi, B. Mhaka, E. Cukrowska, O. Ramström, H. Tutu, L. Chimuka, J. Sep. Sci. 32 (2009) 1941.
[14] B. Dirion, Z. Cobb, E. Schillinger, L.I. Andersson, B. Sellergren, J. Am. Chem. Soc. 125 (2003) 15101.
[15] P.A.G. Cormack, A.Z. Elorza, J. Chromatogr. B 804 (2004) 173.
[16] J.L. Urraca, M.C. Moreno-Bondi, A.J. Hall, B. Sellergren, Anal. Chem. 79 (2007) 695.
[17] H.W. Sun, F.X. Qiao, J. Chromatogr. A 1212 (2008) 1.
[18] F. Qiao, H. Sun, J. Pharmaceut. Biomed. 53 (2010) 795.
[19] G. Pan, Y. Zhang, X. Guo, C. Li, H. Zhang, Biosens. Bioelectron. 26 (2010) 976.
[20] H. Yan, K.H. Row, G. Yang, Talanta 75 (2008) 227.
[21] Y. Hu, R. Liu, Y. Zhang, G. Li, Talanta 79 (2009) 576.
[22] E.V. Piletska, A.R. Guerreiro, M.J. Whitcombe, S.A. Piletsky, Macromolecules 42 (2009) 4921.
[23] X. Shen, L. Ye, Chem. Commun. 47 (2011) 10359.
[24] K. Booker, M.C. Bowyer, C.I. Holdsworth, A. McCluskey, Chem. Commun. (2006) 1730.
[25] N. Perez-Moral, A.G. Mayes, Anal. Chim. Acta 504 (2004) 15.

[26] A. Beltran, R.M. Marce, P.A.G. Comack, F. Borrull, J. Chromatogr. A 1216 (2009) 2248.
[27] M. Gallego-Gallegos, R. Muñoz-Olivas, C. Cámara, J. Environ. Manage. 90 (2009) S69.
[28] L. Chen, S. Xu, J. Li, J. Chem. Soc. Rev. 40 (2011) 2922.
[29] A. Beltran, F. Borrull, P.A.G. Cormack, R.M. Marcé, Trends Anal. Chem. 29 (2010) 1363.
[30] P.C.H. Hollman, I.C.W. Arts, J. Sci. Food Agric. 80 (2000) 1081.
[31] N. Russo, M. Toscano, N. Uccella, J. Agric. Food Chem. 48 (2000) 3232.
[32] M. Biesaga, K. Pyrzynska, Crit. Rev. Anal. Chem. 39 (2009) 95.
[33] K.R. Price, M.J.C. Rhodes, J. Sci. Food Agric. 74 (1997) 331.
[34] A.M. Nuutila, K. Kammiovirta, K.M. Oksman-Caldentey, Food Chem. 76 (2002) 519.
[35] C. Turner, P. Turner, G. Jacobson, K. Almgren, M. Waldebäck, P. Sjöberg, E. Nordberg-Karlsson, K.E. Markides, Green Chem. 8 (2006) 949.
[36] S. Lindahl, A. Ekman, S. Khan, C. Wennerberg, P. Börjesson, P.J.R. Sjöberg, E. Nordberg-Karlsson, C. Turner, Green Chem. 12 (2010) 159.
[37] Y. Wei, Q. Xie, D. Fisher, I.A. Sutherland, J. Chromatogr. A 1218 (2011) 6206.
[38] E. Gikas, F.N. Bazoti, N. Papadopoulos, A. Alesta, G. Economou, A. Tsarbopoulos, Anal. Lett. 44 (2011) 1463.
[39] S.M. Tzouwara-Karayanni', S.M. Philianos, Microchem. J. 27 (1982) 155.
[40] L. Zhu, X. Xu, J. Chromatogr. A 991 (2003) 151.
[41] A. Molinelli, R. Weiss, B. Mizaikoff, J. Agric. Food Chem. 50 (2002) 1804.
[42] X. Song, J. Li, J. Wang, L. Chen, Talanta 80 (2009) 694.
[43] Z. Yuan, Y. Liu, F. An, Microchim. Acta 172 (2011) 89.
[44] J. Shan, B. Wang, Sep. Sci. Technol. 46 (2011) 164.
[45] Z. Li, M. Day, J.F. Ding, K. Faid, Macromolecules 38 (2005) 2620.
[46] S. Azodi-Deilami, M. Abdouss, S.R. Seyedi, Cent. Eur. J. Chem. 8 (2010) 687.
[47] M. Khajeh, Y. Yamini, E. Ghasemi, J. Fasihia, M. Shamsipur, Anal. Chim. Acta 581 (2007) 208.
[48] N. Arabzadeh, M. Abdouss, Colloid J. 72 (2010) 446.
[49] L.Q. Wu, Y.Z. Li, J. Mol. Recogn. 17 (2004) 567.
[50] Z.Y. Chen, R. Zhao, D. Shangguan, G.Q. Liu, Biomed. Chromatogr. 19 (2005) 533.
[51] S. Li, X. Huang, M. Zheng, W. Li, K. Tong, Sensors 8 (2008) 2854.